JOURNAL OF THE MYANMAR ACADEMY OF ARTS AND SCIENCE

Chemistry

Vol. XVII, No.1A, August 2019

Myanmar Academy of Arts and Science

Journal of the Myanmar Academy of Arts and Science

Vol. XVII, No.1A

Contents

Section (i) Chemistry

SYNTHESIS, CHARACTERIZATION AND BIOCOMPATIBILITY STUDY OF HYDROXYAPATITE-MAGNESIUM OXIDE NANOCOMPOSITES FOR *IN VIVO* AND *IN VITRO* ORTHOPAEDIC APPLICATIONS*

Cho Lwin Lwin Khine[1], San Nwe Zin[2], Aye Win Oo[3], Ni Ni Sein[4]

Abstract

Hydroxyapatite (HAp) materials are very popular for bone restoration. The application of pure hydroxyapatite are restricted to non load-bearing implants due to the poor mechanical properties of hydroxyapatite. To improve the mechanical properties of hydroxyapatite prepared from cow bone, incorporation of magnesium oxide was conducted in this research. Hydroxyapatite-Magnesium oxide nanocomposites (5 % and 10 %) were prepared at 1000 °C and 1100 °C. Crystal structures of all HAp-MgO nanocomposites and HAp were indexed as hexagonal. FT IR spectral data revealed the characteristic peaks of both HAp and MgO in the prepared nanocomposites. HAp-10 % MgO nanocomposites calcined at 1100 °C was found to have the highest hardness value of 53 N. HAp and HAp-MgO nanocomposites prepared at 1000 °C and 1100 °C showed no cytotoxic effect according to brine shrimp lethality bioassay. *In vitro* protein adsorption test and *in vitro* hemolysis test indicated that the prepared HAp and HAp-MgO nanocomposites were biocompatible. Orthopaedic application of HAp and HAp-MgO nanocomposites were conducted by *in vivo* study using Wistar rats. X-ray diagnosis showed that HAp-MgO nanocomposites were suitable for treatment of bone defect. *In vitro* study for repairing the non-living broken bones by HAp-MgO nanocomposites was also conducted using chicken femur bone and it was found that the composites could be used as bioglue.

Keywords: cow bone, hydroxyapatite, HAp-MgO nanocomposites, protein adsorption, hemolysis, orthopaedic application

[1]. Dr, Demonstrator, Department of Chemistry, University of Yangon
[2]. Dr, Associate Professor, Department of Chemistry, Bago University
[3]. Dr, Head of Research Officer, Laboratory Animal Services Division, Department of Medical Research (Lower Myanmar)
[4]. Dr, Professor (Retd.), Department of Chemistry, University of Yangon
* Best Paper Award Winning Paper in Chemistry, (2018)

Introduction

Hydroxyapatite is a significant biomaterial in the health care industry. Its chemical and mineral phases are analogous to those of natural bone and hence, its usage in the field of dentistry and orthopedics has been explored (Hornez *et al.*, 2007). Properties like osteoconductivity and osteoinductivity enhance bone regeneration and make hydroxyapatite an important material in tissue engineering (Burg *et al*., 2000), and its biocompatibility leads to its use as bioactive coating over implants (Ye and Wang, 2007). However, the brittleness and poor performance of mechanical stability of pure hydroxyapatite limit its use for the regeneration of non-load-bearing bone defects and tissue engineering applications (Rajkumar *et al*., 2010). Composite biomaterials like metal and polymer matrix are used to improve the mechanical compatibility of nano hydroxyapatite. Generally, composite biomaterials are prepared by using biocompatible/biodegradable and synthetic/natural polymers (Wang *et al.,* 2007). Inorganic minerals such as hydroxyapatite, bioactive glasses metal oxides and carbon nanotube are incorporated into polymer matrixes to impart bioactivity (Dhanalakshmi *et al.*, 2012). The addition of nanosized particles is desirable to develop composite with a good mechanical strength similar to the natural bone which contains mineral crystals at the nanometer scale and embedded in the collagen matrix (Joseph and Tanner, 2005).

The natural-biological origin hydroxyapatite has several important advantages: worldwide availability in almost unlimited supply, very low cost of raw materials, utilization of very simple and inexpensive apparatus, rapid, uncomplicated and very efficient transformation from raw materials into hydroxyapatite. Therefore, it seems to be an alternative for numerous products based on synthetic hydroxyapatite.

MgO is one of the most successful candidates of reinforcement oxides. The mechanical and biodegradable properties of MgO added composites and alloys are especially attractive for bone and teeth implant applications due to its excellent biocompatibility, high degradability, low weight and density similar to natural bones. MgO included HAp are widely used as bone graft materials due to faster recovery of host material (bone) by gradually releasing Mg ions from implanted materials. The MgO inclusion into the pure HAp

powder is strongly expected to affect the grain growth in HAp and improves the mechanical properties of HAp significantly (Gautam *et al*., 2016).

This research is aimed to synthesize biocompatible HAp-MgO nanocomposites from waste cow bone for orthopaedic application.

Materials and Methods

Sample Collection

Waste cow bone samples were collected from Mingalar Taung Nyunt retail market in Yangon Region.

Synthesis of HAp-MgO Nanocomposites

HAp powder was prepared by using readily affordable biowaste cow bone employing simple unit operations and acid-alkali processes (Cho Lwin Lwin Khine *et al*., 2017). For HAp-MgO, firstly MgO (5 g) was dispersed in 20 mL of distilled water with the help of a magnetic stirrer for 1 h. The hydroxyapatite suspension was also prepared using the ratio of 1:1 for powder (100 g) and water (100 mL) by means of magnetic stirring for 1 h to get homogeneity of the dispersion. To prepare HAp-5 % MgO nanocomposite, the prepared suspension was poured into the HAp solution and then was thoroughly mixed using stirrer at 80-90 °C for 1 h. The suspension was cooled to room temperature for 12 h and kept undisturbed for aging. It was then filtered and the residues were washed 2 to 3 times with distilled water. Then, it was transferred into porcelain basin and placed in an oven at 120 °C for 4 h. The resulting products were annealed at 1000 °C and 1100 °C for 4 h.

Characterization Techniques

Phase analysis and purity of prepared HAp-MgO nanocomposites were investigated by X-ray analysis. X-ray diffraction patterns of the samples were recorded on X-ray diffractometer (Rigaku, Tokyo, Japan), using CuK_{α} radiatio (λ= 1.54 Å) at 40 kV and 40 mA. The diffraction angle ranged from 10^{o} to 70^{o} of 2θ. The crystallite size was calculated by Scherrer method. Fourier transform infrared (FT IR) spectra of the samples was recorded on a FT IR

spectrometer (FT IR-8400 SHIMADZU, Japan). FT IR analysis was in a range of wavenumber from 4000 to 440 cm^{-1}.

pH and Hardness of the Prepared HAp-MgO Nanocomposites

pH values of HAp-MgO nanocomposites were determined by a pH meter (Jenway 4330, England) and the hardness of prepared HAp-MgO nanocomposites were determined by hardness tester (PHAMA Test, PTB 302).

Cytotoxicity Test

The brine shrimp (*Artemia salina*, fairy shrimp or sea monkeys) was used in this study for cytotoxicity bioassay of the prepared HAp-MgO nanocomposites (Ali *et al*., 2013). The toxicity of samples were tested at various concentrations *viz.* 1,10, 100 and 1000 µg/mL in seawater. Ten nauplii were used in each test. Three replications were used for each concentration. A parallel series of tests with the standard potassium dichromate solution and caffeine were conducted. After 24 h, the number of dead brine shrimps was counted and 50 % lethality dose (LD_{50}) was calculated (Sahgal *et al*., 2010).

Biocompatibility Tests
Protein adsorption test

Protein adsorption test was conducted according to Mishra (2013) with some modifications. Adsorbate used was Bovine Serum Albumin (BSA) from Sigma. Firstly,1 mL each of HAp-MgO nanocomposites samples with concentrations of 10 mg/mL was added to 1mL of aqueous solution of BSA (1200 µ g/mL) in respective test tubes. The mixtures were then shaken and incubated at the physiological temperature (37 ^{o}C) for 24 h. After 24 h of incubation, the samples were centrifuged at 3000 rpm for 10 min. The supernatants were removed and the residual protein concentration was determined using Biuret assay at 550 nm (Holme and Peck, 1998). Sample solution (1 mL) and 4 mL of Biuret reagent were thoroughly mixed and kept at room temperature for 30 min. After that, the absorbance value was measured at 550 nm. Hence, by difference the residual protein amount from the total protein amount, the protein adsorbed (µ g) was determined.

Hemolysis test

Hemolysis test was conducted according to Mishra (2013) with some modifications. Blood was collected from central ear artery of two white rabbits by needle. The rabbits were provided by Laboratory Animal Service, Department of Medical Research, Yangon. Trisodium citrate as anticoagulant was immediately added. The noncoagulant blood was diluted with normal saline (10 mL of normal saline per 8 mL of blood) and stored at 4 °C till use. Following this, the test specimens (10 mg each) were placed in test tubes with phosphate buffered saline (1 mL each) and agitated and incubated for 24 h at 37 °C before being exposed to blood. After that, 0.5 mL of blood was added to each test tube and the volume made up to 10 mL with saline. Hydrochloric acid was used as positive control and phosphate buffer saline (PBS) solution was used as negative control. The samples and controls were placed in contact with blood for 1 h in incubator at 37 °C. After centrifugation at 4000 rpm for 10 min, the absorbance of the supernatant was measured at 545 nm. The percentage of hemolysis was determined by the following formula.

$$\text{Percent hemolysis} = \frac{\left(A_{\text{sample}} - A_{\text{negative control}}\right)}{\left(A_{\text{positive control}} - A_{\text{negative control}}\right)} \times 100$$

***In Vivo* Test for Orthopaedic Application of HAp-MgO Nanocomposites**

HAp-MgO nanocomposites were conducted for orthopaedic application employing Wistar rats (male with 250-300 g body weight). The animals were obtained from Laboratory Animal Service Division, Department of Medical Research, Yangon. All of the rats were kept in standard rat cages. The animals were facilitated with standard environmental condition of photoperiod (12:12 h dark: light cycle) and temperature (24 °C). They were provided with standard laboratory pellets and water was given *ad libitum*. Animals were divided into two individual groups in this experiment as follows;

Group I, after surgery procedure, left side of skull defect was not filled any materials. Group I, after surgery procedure, right side of skull defect was filled with HAp. Group II, after surgery procedure, left side of skull defect was filled with HAp-5 % MgO nanocomposite at 1100 ºC. Group II, after

surgery procedure, right side of skull defect was filled with HAp-10 % MgO nanocomposite at 1100 ºC.

Wistar rats were injected with Ketamine hydrochloride (50 mg/kg) before the surgery. The dorsal area of each rats skull was shaved before the surgery, and the surgical field was prepared with septidine solution. A 3 cm midline scalp incision was made, and underlying musculature and periosteum were elevated, exposing the parietal bones. Identical 0.3 cm diameter (left side and right side) round bony defect was then created in the parietal bone using stainless steel hand drill carefully. Care was then taken to avoid injury to the dura or midsagittal sinus. The nanocomposite powder was taken in a watch glass and distilled water added drop wise till the powder got fully wet and got paste. The paste was molded in the skull bone cavity before suturing. Defects were gently packed with HAp paste for right side of test (I) animal and left side was left unfilled (control) and HAp-10 % MgO nanocomposite at 1100 ºC paste for right side of test (II) animal and HAp-5 % MgO nanocomposite at 1100 ºC paste for left side of test (II) animal. External examination of the skull bone defects was conducted after 15 days and 30 days surgery by taking photos of the skull bone. Test animals of groups (I) and (II) were post-tested by X-ray radiography. The Wistar rats were observed (a) immediately on operation day (b) 15 days after surgery and (c) 30 days after surgery at Crown Veterinary Resources, Yankin Township, Yangon. Skull bone lesion samples were used for histological examination in Pathology Research Division, Department of Medical Research (Lower Myanmar).

In Vitro Test for Orthopaedic Application (as Bone Glue) of HAp-MgO Nanocomposites

Chicken femur bones were also used *in vitro* bone glue experiment. With a manual bone saw shaft, femur bones of some of the chicken were horizontally and completely cut and some were almost completely. Bone glue made of HAp-MgO nanocomposites and polyethylene glycol (1:1) were then applied to stick the broken dried chicken femur bones and kept for 24 h.

Results and Discussion

Characterization of HAp-MgO Nanocomposites

XRD analysis

HAp-MgO nanocomposites was prepared using HAp calcined at 900 ^{o}C and MgO obtained by heating $Mg(OH)_2$ at 600 ^{o}C. Two different weight percentages of 5 % and 10 % magnesium oxide were added into HAp sample in this study.

HAp calcined at 900 ^{o}C showed well-resolved XRD pattern (Figure 1) which could be easily indexed on the basis of hexagonal crystal system with equal length of a and b axes (9.4009 Å) and shorter length of c axis (6.8757 Å). When the prepared magnesium oxide sample obtained at 600 ^{o}C was subjected to XRD analysis three well-defined diffraction peaks were observed at Miller indices of (111), (220) and (200) (Figure 2). After incorporation of magnesium oxide to HAp, the XRD patterns of HAp-MgO nanocomposites showed two new peaks corresponding to magnesium oxide peaks at (200) and (220) in addition to HAp peaks (Figure 3).

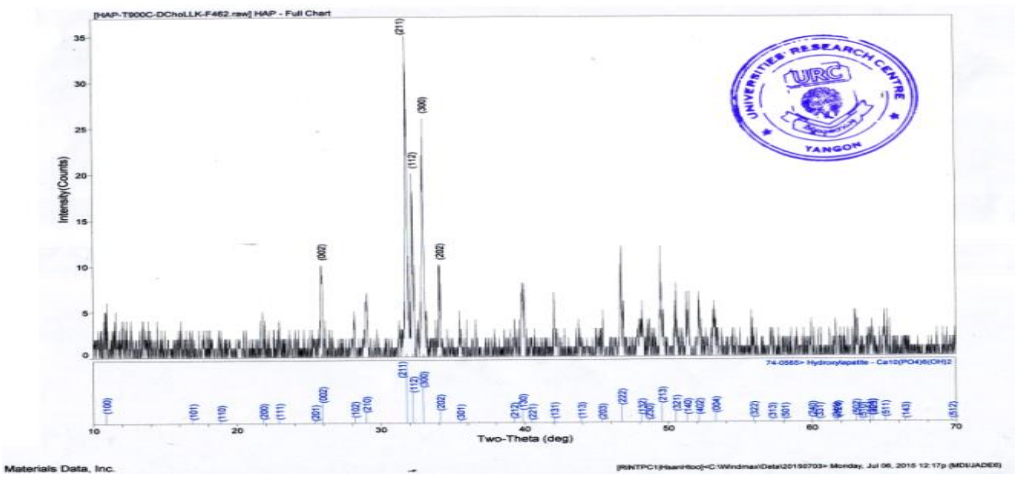

Figure 1: X-ray diffractogram of hydroxyapatite

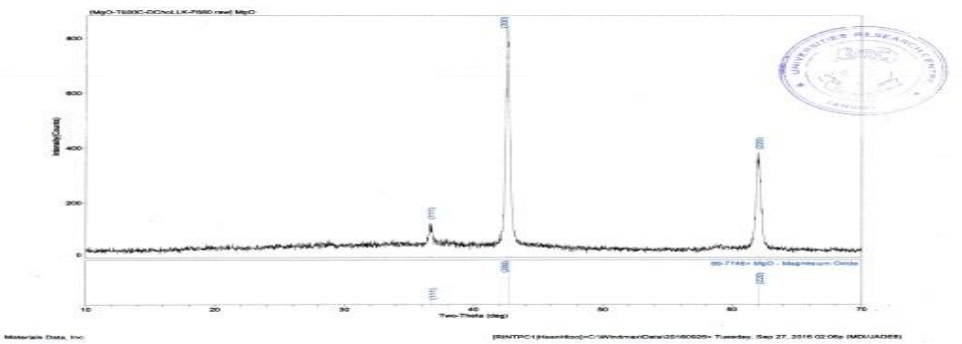

Figure 2: X-ray diffractogram of magnesium oxide obtained at 600 °C

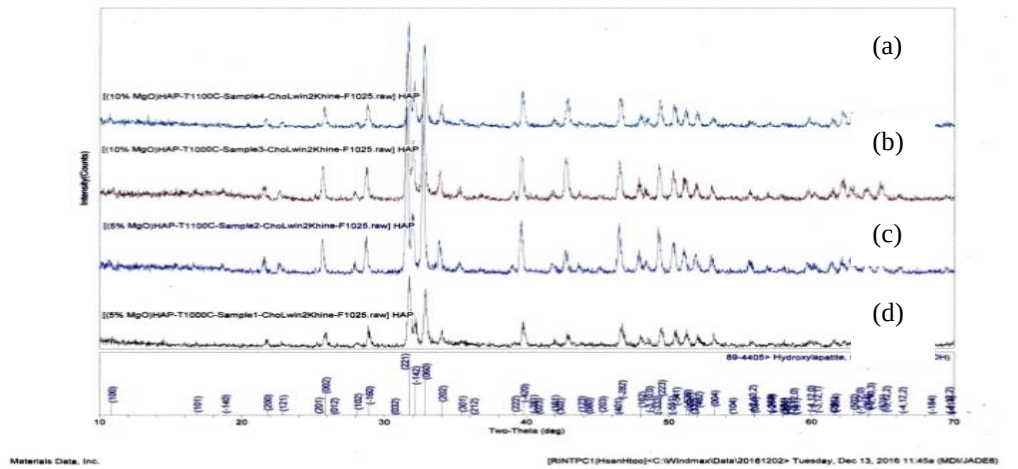

Figure 3: X-ray diffractograms of HAp-MgO nanocomposites
(a) HAp-10 % MgO (1100 ^{o}C) (b) HAp-10 % MgO (1000 ^{o}C)
(c) HAp-5 % MgO (1100 ^{o}C) (d) HAp-5 % MgO (1000 ^{o}C)

With increase in temperature the crystallite size of HAp-MgO nanocomposites were found to increase. However, the results were reversed as the amount of magnesium oxide was increased (Table 1). For HAp, the crystallite size was 69.92 nm. Crystallite sizes of HAp-MgO nanocomposites were 32.17 nm and 37.87 nm for HAp-5 % MgO nanocomposites calcined at 1000 °C and 1100 °C, respectively. For HAp-10 % MgO nanocomposites the crystallite sizes were 31.46 nm and 36.70 nm, respectively for calcination temperature of 1000 °C and 1100 °C.

Table 1: Average Crystallite Sizes, Lattice Constant and Crystal Structure of HAp-MgO Nanocomposites

No.	Sample	Average crystallite size (nm)	Lattice constant (Å)		Crystal structure
			a=b	c	
1	HAp	69.92	9.4009	6.8757	Hexagonal
2	HAp-5 % MgO nanocomposite (1000 ^{o}C)	32.17	9.5469	6.8434	Hexagonal
3	HAp-5 % MgO nanocomposite (1100 ^{o}C)	37.87	9.5998	6.9544	Hexagonal
4	HAp-10 % MgO nanocomposite (1000 ^{o}C)	31.46	9.5650	6.7985	Hexagonal
5	HAp-10 % MgO nanocomposite (1100 ^{o}C)	36.70	9.5295	6.8878	Hexagonal

Crystal structures of HAp and all of the HAp-MgO nanocomposites were hexagonal. The lattice constants of HAp-MgO nanocomposites noticeably changed from those of HAp indicating the formation of composites. Among the HAp-MgO nanocomposites, the lattice constants changed slightly with change in temperature and amount of magnesium oxide.

FT IR analysis

FT IR spectral data revealed the assignment of the vibration bands of HAp-MgO nanocomposites together with the characteristic peaks of both HAp and MgO (Table 2). The characteristic peaks of HAp in nanocomposites were observed between 700-500 cm^{-1} due to P-O bending vibration and between 1200-900 cm^{-1} due to P-O stretching vibration (Karthikeyan *et al.*, 2016). Similarly, the characteristic peaks of MgO in HAp-MgO nanocomposites were observed at 474 cm^{-1} (Nakamoto, 1970).

pH and Hardness of HAp-MgO Nanocomposites

HAp calcined at 900 ^{o}C was found to have pH value of 9.6 (Table 3). Addition of MgO nanoparticles in HAp caused slight decrease in pH values. All of the HAp-MgO nanocomposites samples and HAp sample were found to have alkaline in nature.

Hardness of HAp prepared from cow bone was found to be 12 N. Hardness increased as the amount of the addition of MgO increased in the range of 19 N to 53 N. With same composition of MgO, hardness increased as the temperature was increased. HAp- 10 % MgO at 1100 ^{o}C was found to have the highest hardness value of 53 N.

Table 2: FT IR Spectral Data of HAp, MgO and HAp-MgO Nanocomposites

No.	Wavenumber (cm^{-1})						Reported values (cm^{-1})	Remark
			HAp-MgO Nanocomposites					
	HAp (900°C)	MgO (600°C)	5 % (1000°C)	5 % (1100°C)	10 % (1000°C)	10 % (1100°C)		
1.	3697		3570	3570	3510	3568	3500-3100*	Vibration of O-H
2.	3443	3440	3427	3419	3479	3443	3444**	O-H stretching vibration of physically absorbed water molecules
3.	1456		1460	1462	1460	1462	1629-1400*	Carbonate group
4.	1413		1413	1413	1413	1413		
5.	1089		1091	1089	1091	1091	1200-900*	P-O stretching of phosphate
6.	1047		1047	1047	1047	1047		
7.	962		960	960	960	960		
8.	877						871*	Carbonate group
9.		653					650-450**	Mg-O deformation vibration
10.	632		632	632	632	634	700-500*	P-O bending of phosphate
11.	601		601	601	601	601		
12.	570		569	570	569	569		
13.		474	472	474	474	474	650-450**	Mg-O deformation vibration

***** Nakamoto, 1970 ** Karthikeyan *et al.*, 2016

Table 3: pH and Hardness of HAp and HAp-MgO Nanocomposites

No.	Samples	pH	Hardness(N)
1	HAp	9.0	12
2	HAp-5 % MgO Nanocomposite (1000 °C)	9.3	19
3	HAp-5 % MgO Nanocomposite (1100 °C)	9.5	31
4	HAp-10 % MgO Nanocomposite (1000 °C)	9.5	42
5	HAp-10 % MgO Nanocomposite (1100 °C)	9.4	53

Cytotoxicity

Brine shrimp cytotoxicity bioassay was used for the cytotoxicity test of HAp-MgO nanocomposites. Brine shrimp was used for this assay (Tawhawa, 2006). This was expressed in terms of mean ± SEM (standard error mean) and LD_{50} (50 % Lethality Dose). The data are described in Table 4. According to Meyer's toxicity index, the sample with LD_{50}<1000 μ g/mL are considered as toxic, while the sample with LD_{50} > 1000 μ g/mL are considered as non-toxic (Meyer *et al*., 1982). The prepared HAp-MgO nanocomposites were found to be noncytotoxic in the brine shrimp bioassay so they can be used as biomaterial.

Table 4: Cytotoxicity of HAp and HAp-MgO Nanocomposites

Samples	Percentage of dead brine shrimp (Mean ± SEM) in various concentrations (μg/mL)				LD_{50} (μg / mL)
	1	10	100	1000	
HAp	0 ± 0	0 ± 0	3.3 ± 1.90	6.7 ± 11.54	> 1000
A 1	0 ± 0	0 ± 0	3.3 ± 1.90	3.3 ± 1.90	> 1000
A 2	0 ± 0	0 ± 0	3.3 ± 1.90	3.3 ± 1.90	> 1000
B 1	0 ± 0	0 ± 0	6.7 ± 11.54	6.7 ± 11.54	> 1000
B 2	0 ± 0	0 ± 0	3.3 ± 1.90	6.7 ± 11.54	> 1000
*Caffeine	0 ± 0	0 ± 0	9.58 ± 0.92	12.73 ± 4.10	> 1000
*$K_2Cr_2O_7$	48.63±19.19	73.13 ±4.08	74.67 ±11.8	100 ± 0	1.5

* = used as cytotoxic standard

A 1 = HAp-5 % MgO nanocomposite (1000 °C)

A 2 = HAp-5 % MgO nanocomposite (1100 °C)

B 1 = HAp-10 % MgO nanocomposite (1000 °C)

B 2 = HAp-10 % MgO nanocomposite (1100 °C)

Protein adsorption

Cellular response on the implant after implantation depends on the initial amount of serum proteins that get adsorb to the implant.

Among the HAp-MgO nanocomposites, protein adsorption capacity increased and found to be in the range of 72.07 μg/10 mg to 90.09 μg/10 mg (Table 5). It may be due to the decrease of the crystallite size and hence, increase of surface area of the nanocomposites. In other words protein adsorption increases with increase in surface area of the samples where the crystal size is small (Feng *et al*., 2002).

Table 5: Protein Adsorption Capacities of HAp Prepared from Cow Bone (900^{o}C) and HAp-MgO Nanocomposites with Different Concentrations of MgO at Different Temperatures*

No.	Samples	Residual protein (μg/10 mg)	Protein adsorption (μg/10 mg)	Mean (μg/10 mg)
1.	HAp	1145.95	54.05	
		1167.57	32.43	54.05 ± 21.63
		1124.32	75.68	
2.	HAp-5 % MgO	1124.32	75.68	
	nanocomposite (1000 ^{o}C)	1145.95	54.05	75. 68 ± 21.63
		1102.70	97.30	
3.	HAp-5 % MgO	1102.70	97.30	
	nanocomposite (1100 ^{o}C)	1145.95	54.05	72. 07 ± 22.50
		1135.13	64.87	
4.	HAp-10 % MgO	1091.89	108.11	
	nanocomposite (1000 ^{o}C)	1113.51	86.49	90.09 ± 16.52
		1124.32	75.67	
5.	HAp-10 % MgO	1102.70	97.30	
	nanocomposite (1100 ^{o}C)	1135.13	64.87	82. 88 ± 16.53
		1113.51	86.49	

*Initial protein in 1 mL sample = 1200 μg/10 mg

Hemolysis

The prepared composites were tested for hemolytic activity and the results obtained were quite satisfactory (Table 6). The results obtained clearly indicated that, with incorporation of MgO content, the extent of hemolysis slightly increased. The observed results may be attributed to the reason that, with the incorporation of MgO in the composite, the surface composition favorably changes, which increased the hemolytic property of the material. Among the composites the hemolysis percentages did not change appreciably. If hemolysis percentage is below 2 % the material is considered non-hemolytic, between 2 % and 5 % slightly hemolytic, and above 5 % it is considered hemolytic (Laranjeiraa *et al.,* 2016). All the samples were found to have hemolysis percentages less than 5 %. Thus, these samples exhibit good biocompatibility and may be suitable biomaterials for clinical implant purposes.

Table 6: Hemolysis Percentage of HAp Prepared from Cow Bone (900 ^{o}C) and HAp-MgO Nanocomposites with Different Concentrations of MgO at Different Temperatures*

No.	Samples	Absorbance of test sample	Hemolysis (%)	Mean (%)
1.	HAp	0.096	1.61	
		0.099	1.91	1.71 ±0.17
		0.096	1.61	
2.	HAp-5 % MgO nanocomposite (1000 ^{o}C)	0.099	1.91	
		0.101	2.11	1.94 ±0.15
		0.098	1.81	
3.	HAp-5 % MgO nanocomposite (1100 ^{o}C)	0.102	2.21	
		0.099	1.91	1.98 ±0.21
		0.098	1.81	
4.	HAp-10 % MgO nanocomposite (1000 ^{o}C)	0.097	1.71	
		0.101	2.11	1.94 ±0.21
		0.100	2.00	
5.	HAp-10 % MgO nanocomposite (1100 ^{o}C)	0.099	1.91	
		0.103	2.31	2.11 ±0.20
		0.101	2.11	

*Absorbance of negative control = 0.080
Absorbance of positive control = 1.077

In Vivo Orthopaedic Application of the Prepared HAp-MgO Nanocomposites

HAp, HAp-5 % MgO (1100 ^{o}C) and HAp-10 % MgO (1100 ^{o}C) nanocomposites were separately applied as bone cement on skull bones of Wistar rats (Figure 4). The progress of these operation skull bone were recorded by the photos at specified time interval and the recorded photographs are shown in Figure 5. After 15 days, the hairs of the Wistar rats were started to grow and after 30 days it was found to be normal.

The Wistar rats were radiographed on the operation day, after 15 days and 30 days of operation (Figure 6). Bone gap were found to be 0.28 cm for control, 0.30 cm each for HAp and HAp-10 % MgO nanocomposite (1100 ^{o}C) and 0.32 cm for HAp-5 % MgO nanocomposite (1100 ^{o}C) (Table 7). After 15 days of operation, bone gap was found to decrease to 0.10 cm in control and 0.08 cm in Wistar rat filled with HAp (Table 8). This means that tiny bony defects were still observed in these rats. However, complete bone healing was observed for Wistar rats filled with nanocomposites. The composites bridged the defects and new bonds were formed. After 30 days of operation the defects were completely filled in all Wistar rats whether unfilled or filled with HAp and HAp-MgO nanocomposites (Table 9). It was found that application of HAp-MgO nanocomposites for bone defect enhanced bone healing effect compared to control and HAp only. Due to histological findings (Tables 10 and 11), HAp-10 % MgO nanocomposite at 1100 °C group is the best in the good scoring within 30 days after application.

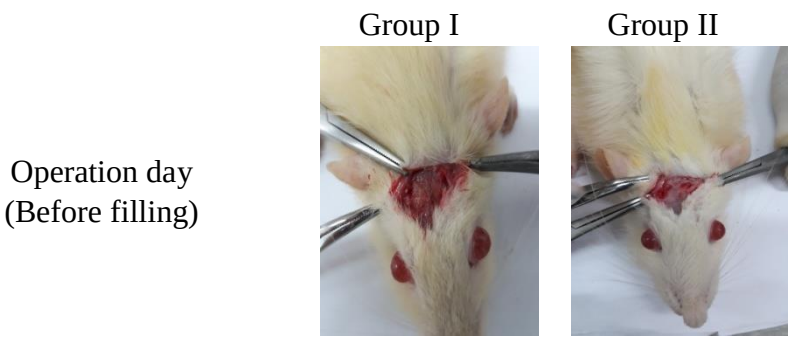

(a)

Filling
(After surgery)

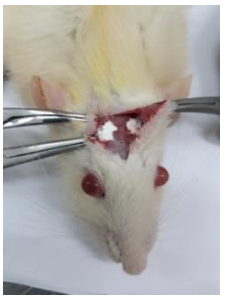

(b)

Suturing and dressing
(After filling)

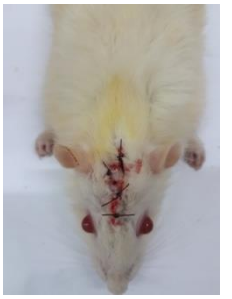

(c)

Figure 4 : Surgical procedure (a) skin incision in the dorsal portion of skull bone with surgical knife (b) filling the skull bone cavity (c) closing with suturing cat gut continuously and dressing with septidine solution

Group I

(a)

(b)

(c)

Group II

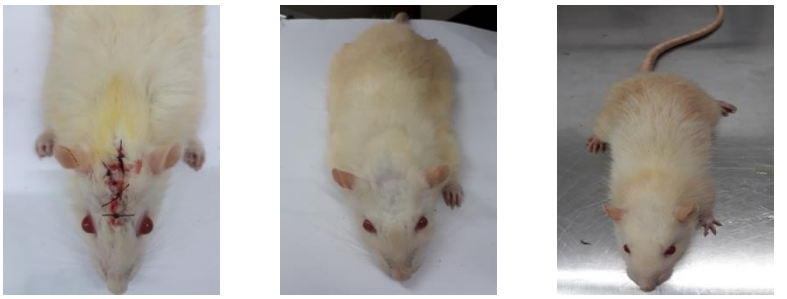

(a) (b) **(c)**

Figure 5: External feature of the skull bone defect healing progressiveness of Wistar rats
(a) Operation day
(b) 15 days after surgery
(c) 30 days after surgery

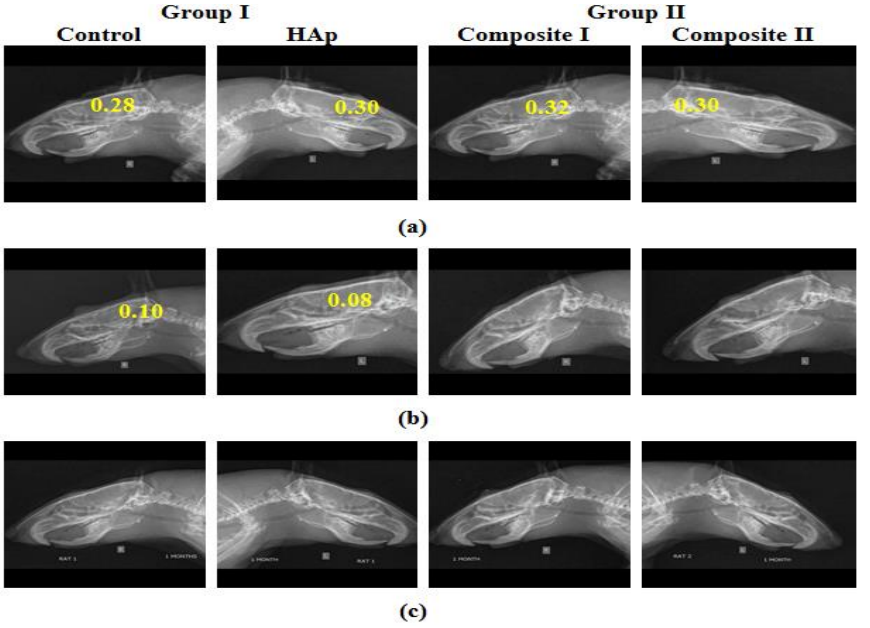

Figure 6 : Progressiveness of skull bone defect healing in X-ray view of Wistar rats
(a) Operation day
(b) 15 days after surgery
(c) 30 days after surgery

Composite I = HAp-5 % MgO nanocomposite (1100 ^{o}C)
Composite II = HAp-10 % MgO nanocomposite (1100 ^{o}C)

Table 7: Examination of Skull Bone Defect by X-ray Radiography (Operation day)

Samples	Condition	X-ray diagnosis	X-ray picture
Control	Unfilled defect	Incomplete filling (Bone cavity gap = 0.28 cm)	
HAp	HAp (900 ºC)	Incomplete filling (Bone cavity gap = 0.30 cm)	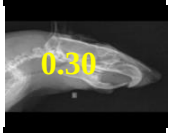
Composite I	HAp-5 % MgO nanocomposite (1100 ºC)	Incomplete filling (Bone cavity gap = 0.32 cm)	
Composite II	HAp-10 % MgO nanocomposite (1100 ºC)	Incomplete filling (Bone cavity gap = 0.30 cm)	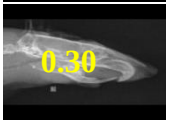

Table 8: Examination of Skull Bone Defect by X-ray Radiography (15 days after Surgery)

Samples	Condition	X-ray diagnosis	X-ray picture
Control	Unfilled defect	A tiny hole bone defect remaining (Bone cavity gap = 0.10 cm)	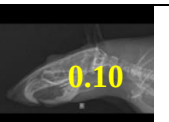
HAp	HAp (900 ºC)	Remaining very little pointed bony defect to become completely (Bone cavity gap = 0.08 cm)	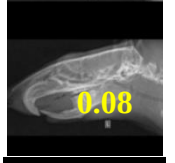
Composite I	HAp-5 %MgO nanocomposite (1100 ºC)	Complete bone healing bridge the defect (No bone cavity gap)	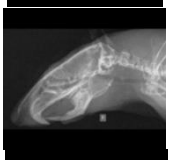
Composite II	HAp-10 %MgO nanocomposite (1100 ºC)	Complete bone healing bridge the defect (No bone cavity gap)	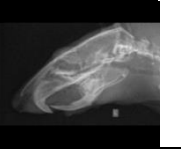

Table 9: Examination of Skull Bone Defect by X-ray Radiography (30 days after Surgery)

Samples	Condition	X-ray diagnosis	X-ray picture
Control	Unfilled defect	Complete bone healing bridge the defect (No bone cavity gap)	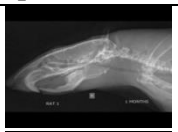
HAp	HAp (900 ºC)	Complete bone healing bridge the defect (No bone cavity gap)	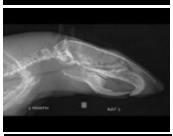
Composite I	HAp-5 % MgO nanocomposite (1100 ºC)	Complete bone healingbridge the defect (No bone cavity gap)	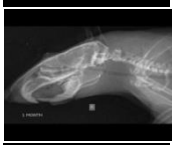
Composite II	HAp-10 % MgO nanocomposite (1100 ºC)	Complete bone healing bridge the defect (No bone cavity gap)	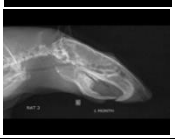

Histopathological report of 15 days and 30 days skull bone healing of the Wistar rats using prepared HAp and HAp-MgO nanocomposites

Histology features of bony healing (15 days after operation) are shown in Table 10.

Table 10: Histological Report of Bone Healing (15 Days after Operation)

No.	Slide Image	Histology Description	Bony Healing Results
1.	Control 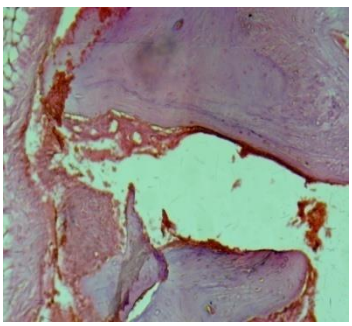	Histology of fracture skull bone revealed that connective tissue was occupied especially fibroblast and admixed with net work of delicate bone trabeculae lined with osteoblast and formed from inner surface of wall of skull bone. Blood clot remnants were observed.	Score - 0 Non-union of skull bone

2.	HAp 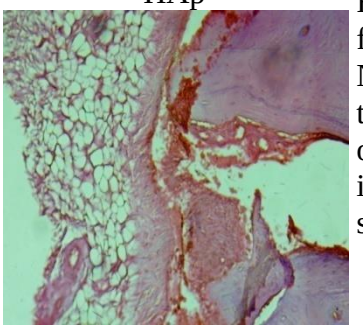	Fracture site was filled with fibroblast and blood clots. Net work of delicate bone trabeculae lined with osteoblast and formed from inner surface of wall of skull bone.	Score- 1 Incomplete cartilage union
3.	Composite I 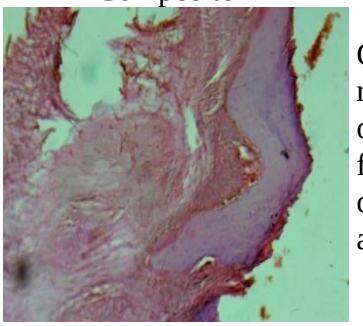	Coagulum (blood clot) was reduced in size and observed woven bone formation composed of few osteoblast and increased amount of chondrocytes.	Score- 2 Complete with cartilage union
4.	Composite II 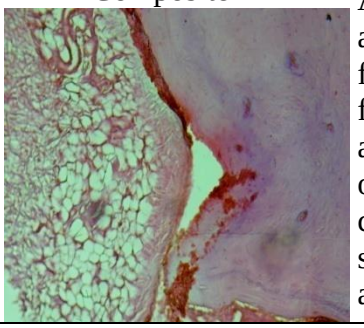	A few coagulum was found and mixed with few fibroblast. Woven formation was noted and accompanied with increased osteoblast and chondrocytes. A fracture site was replaced by few amount of trabecular bone.	Score -3 Predorminantly cartilage with some trabecular bone

Histology features of bony healing (30 days after operation) are shown in Table 11.

Table 11: Histological Report of Bone Healing (30 Days after Operation)

No.	Slide Image	Histology Description	Bony Healing Results
1.	Control 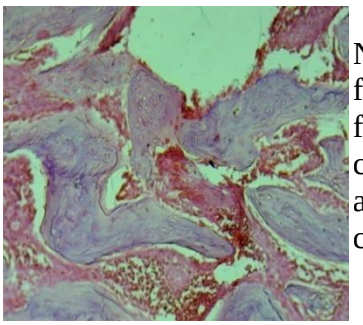	New trabecular bone formation was started from fracture site and composed of osteoblast and increased amount of chondrocytes.	Score - 3 Predorminantly cartilage with some trabecular bone
2.	HAp 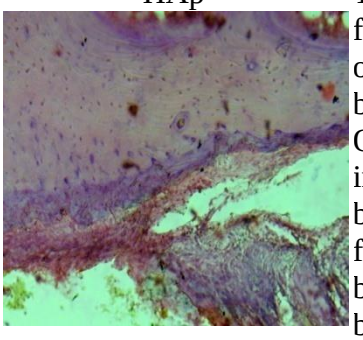	Trabecular bone formation was well organized and absence of blood clots and fibroblast. Osteoblast was seen in inner layer of fracture bone. Chrondrocytes were filled in some trabecular bone areas. Incomplete bony union with intermediate ossification was observed.	Score-4 Equal amounts of cartilage and trabecular bone
3.	Composite I 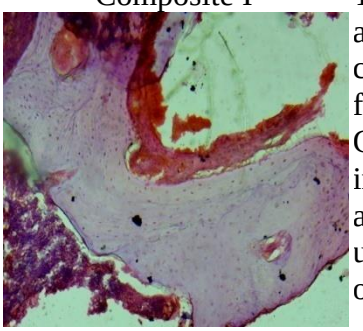	There was increased amount of osteocytes in centre area of bony fracture site. Chrondrocytes were filled in some trabecular bone areas. Incomplete bony union with late ossification was observed.	Score-5 Predorminantly trabecular bone with some cartilage

4.	Composite II		
	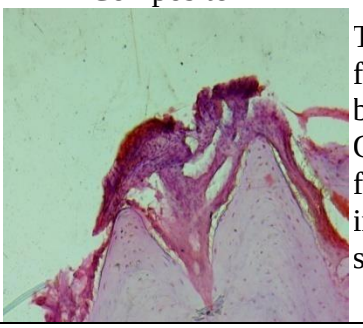	There was complete new formation of trabecular bone in fracture site. Complete union of fracture area was observed in entire bony fracture site.	Score-6 Complete union of fractured bone

***In Vitro* Orthopaedic Application of the Prepared HAp-MgO Nanocomposites (Bone Glue)**

Since HAp-MgO nanocomposites has low adhesive property of non-living bone, addition of polyethylene glycol to HAp-MgO nanocomposites with ratio of 1:1 (w/w) was prepared and the paste was used as bone glue for the broken non-living chicken femur bone in this study. After application of the prepared bone glue on the intentionally broken femur bone, it was observed that HAp-MgO nanocomposites and polyethylene glycol particles adhered to the bone.

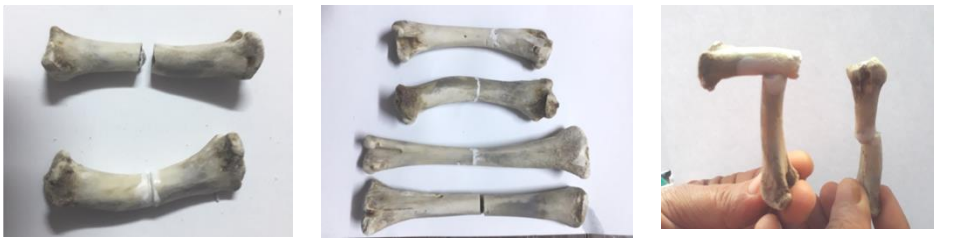

(a) (b) (c)

Figure 7: HAp-10 % MgO nanocomposite (1100 °C) as bone glue for broken chicken femur bone
(a) completely cut bone (broken straight across)
(b) almost completely cut bone
(c) connection of two pieces of bone

Conclusion

HAp-MgO nanocomposites were successfully prepared using natural HAp from waste cow femur bone in order to enhance the bioactivity of the HAp, to improve the mechanical properties and to increase its potential use as scaffold for bone tissue engineering application in this research. Increase in hardness was observed after incorporation with magnesium oxide. Brine shrimp cytotoxic assay showed that the composites were noncytotoxic. Protein adsorption test and hemolysis test revealed that HAp-MgO nanocomposites were found to be biocompatible with living tissue. HAp-MgO nanocomposites promoted the bone healing activity of HAp. *In vitro* study of HAp-MgO nanocomposites as bioglue showed a good adherence between the two non-living broken bones. Thus, the composites can be used as bioglue in museums for repairing the broken bones. These results indicate that the prepared HAp-MgO nanocomposites has demonstrated better osteoconductive and osteopromotive abilities with faster proliferation of new bone tissue formation than HAp.

Acknowledgements

The authors would like to express their profound gratitude to the Department of Higher Education, Ministry of Education, Myanmar for provision of opportunity to do this research. Professor Dr Hnin Hnin Aye (Head of the Chemistry Department) for her support and staff members from Department of Medical Research (Lower Myanmar) for their cooperation.

References

Ali, N., Allen, U., Shaha, S. W. A., Shaha, I., Junaid, M., Ahmed, G., Ali, W. and Ghias, M. (2013). "Acute Toxicity, Brine Shrimp Cytotoxicity, Anthelmintic and Relaxant of Fruits of *Rubus fruiticosis* Agg". *BMC Complement. Alter. Med.*, vol. 13, pp. 138-143

Burg, K. J. L., Porter, S. and Kellam, J. F. (2000). "Biomaterial Developments in Bone Tissue Engineering". *Biomaterials*, vol. 21, pp. 2347-2359

Cho Lwin Lwin Khine, San Nwe Zin and Ni Ni Sein. (2017). **"**Effect of Calcination on Morphological, Structural and Thermal Properties of Hydroxyapatite (HAp) Prepared from Cow Bone". *J. Myan. Acad. Tech*., vol. 17(1), pp. 68-81

Dhanalakshmi, C. P., Vijayalakshmi L. and Narayanan. V. (2012). "Synthesis and Preliminary Characterization of Polyethylene Glycol (PEG)/ Hydroxyapatite (HAp) Nanocomposite for Biomedical Applications". *International Journal of Physical Sciences*, vol. 7(13), pp. 2093-2101

Feng, B., Chen, J. and Zhang, X. (2002). "Interaction of Calcium and Phosphate in Apatite Coating on Titanium with Serum Albumin". *Biomaterials*, vol. 23, pp. 2499-2507

Gautam, C. R., Kumar, S., Biradar, S., Jose, S., and Mishra, V. K. (2016). "Synthesis and Enhanced Mechanical Properties of MgO Substituted Hydroxyapatite: A Bone Substitute Material". *Royal Society of Chemistry Adv.*, vol. 6(72), pp. 67565-67574

Holme, J. D. and Peck, H. (1998). *Analytical Biochemistry*. London : 3rd Ed., Longman, pp. 390-391

Hornez, J. C., Chai, F., Monchau, F., Blanchemain, N., Descamps, N. and Hildebrand, H. F. (2007). "Biological and Physico-chemical Assessment of Hydroxyapatite (HA) with Different Porosity". *Biomol. Eng*., vol. 24, pp. 505-509

Joseph, R. and Tanner, K. E. (2005). "Effect of Morphological Features and Surface Area of Hydroxyapatite on the Fatigue Behavior of Hydroxyapatite-Polyethylene Composites".*Biomacromolecules*, vol. 6, pp.1021-1026

Karthikeyan, V., Dhanapandian, S. and Manoharan, C. (2016). "Characterization and Antibacterial Behavior of MgO Nanoparticles Synthesized via Co-precipitation Method". *International Journal for Scientific Research and Development*, vol. 10(1), pp. 2321-2323

Laranjeiraa, M. S., Moc, A., Ferreira, J., Coimbra, S., Costa, E., Santos-Silva, A., Ferreira, P. J. and Monteiro, F. J. (2016). "Different Hydroxyapatite Magnetic Nanoparticles for Medical Imaging: Its Effects on Hemostatic, Hemolytic Activity and Cellular Cytotoxicity". *Colloids and Surfaces B: Biointerfaces*, vol.146, 363–374

Meyer, B. N., Ferrigni, N. R., Putnam, J. E., Jacobsen, L. B., Nichols, D. E., and McLaughlin, J. L. (1982). "Brine Shrimp: A Convenient General Bioassay for Active Plant Constituents". *Planta Medica*., vol. 45, pp. 31-34

Mishra, U. (2013). *Development of Cobalt-Magnesium Doped Hydroxyapatite for Bone Tissue Engineering Application.* Rourkela: A Project Report Submitted to National Institute of Technology, Department of Biotechnology and Medical Engineering National Institute of Technology, Rourkela

Nakamoto, K. (1970). *Infrared Spectra of Inorganic and Coordination Compounds*. New York: 2nd Edition, Wiley Interscience Publication, pp. 233-235

Rajkumar, M., Sundaram, N. M. and Rajendran, V. (2010). "In-situ Preparation of Hydroxyapatite Nanorod Embedded Poly (Vinyl Alcohol) Composite and its Characterization". *International Journal of Engineering Science and Technology*, vol. 2(6), pp. 2437-2444

Sahgal, G., Ramanathan, S., Sasidlharan, S., Mordi, M. S., Ismail, S. and Mansor, S. M. (2010). "Brine Shrimp Lethality and Acute Oral Toxicity Studies on *Swietenia mahagoni* (Linn.) Jacq. Seed Methanolic Extract". *Pharmacognosy Research*, vol. 2, pp. 215-220

Tawaha, K. A. (2006). "Cytotoxicity Evaluation of Jordanian Wild Plants using Brine Shrimp Lethality Test". *J Appl Sci*., vol. 8(1), pp. 12-17

Wang, H., Li, Y., Zuo, Y., Li, J., Ma, S. and Cheng, L. (2007). "Biocompatibility and Osteogenesis of Biomimetic Nanohydroxyapatite/Polyamide Composite Scaffolds for Bone Tissue Engineering". *Biomaterials*, vol. 28, pp. 3338-3348

Ye, W. and Wang, X. X. (2007). "Ribbon-Like and Rod-Like Hydroxyapatite Crystals Deposited on Titanium Surface with Electrochemical Method". *Mater. Lett*., vol. 61, pp. 4062-4065

SCREENING OF SOME BIOACTIVE CONSTITUENTS FROM THE BARK OF *Cinchona succirubra* PAV. (KWI-NEING)

Mie Mie Aye[1], Wyine Myat Noe Oo[2]

Abstract

Cinchona succirubra Pav. (Kwi-neing in Myanmar) has been used in traditional medicine due to the presence of alkaloids such as quinine, quinidine, cinchonine and cinchonidine. The alkaloids contained in cinchona bark are powerful drugs and so *C. succirubra* has remarkable biological activities. The present study focuses on screening of some bioactive constituents from the bark of *C. succirubra* Pav. (Kwi-Neing). Preliminary phytochemical investigation was carried out by the reported chemical methods. The extractable matters of the bark of *C. succirubra* were prepared by extracting powdered sample with polar solvents such as ethanol and water using WHO standard method. Some organic constituents, compound 1 (terpenoid), compound 2 (phenolic compound) and compound 3 (alkaloid) were isolated from EtOH crude extract by column chromatographic separation technique. The isolated compounds were identified by treating with specified reagent on TLC and by UV and FT IR spectroscopic methods. The antimicrobial activity of crude extracts and isolated compounds 2 and 3 was determined by agar well diffusion method against six species of microorganisms namely *Bacillus subtilis*, *Staphylococcus aureus*, *Pseudomonas aeruginosa*, *Bacillus pumilus*, *Candida albicans* and *E.coli*. Both extracts showed the pronounced antimicrobial activity against *Bacillus subtilis* (inhibition zone diameter = 30 mm). In addition, compound 3 showed the strong antimicrobial activity against *E.coli* (inhibition zone diameter = 33 mm). Antioxidant activity of crude extracts and compounds 2 and 3 was also screened by Dot-Blot and DPPH staining method. It was found that the violet colour of DPPH disappeared from 400 μg up to minimum concentration of 100 μg for EtOH extract and 200 μg for H_2O extract. In addition, compound 2 showed potent antioxidant activity with sample concentration 25 μg (31.25 μg/mL). The mineral contents of bark of *C. succirubra* were quantitatively determined by AAS method. Calcium (Ca) was found to be the principal element.

Keywords: *Cinchona succirubra* Pav., antimicrobial activity, antioxidant activity, AAS

[1] Dr, Associate Professor, Department of Chemistry, Taungoo University
[2] Demonstrator, Department of Chemistry, Taungoo University

Introduction

In the developing countries, large numbers of the world's population are unable to afford pharmaceutical drugs and they continue to use their own systems of indigenous medicine that are mainly plant based. There is an increasing awareness of the potential of natural products, which may lead to the development of much-needed new drugs. *Cinchona succirubra* Pav. is known to be native to south America and was long used and its alkaloids, quinine, quinidine, cinchonine and cinchonidine, as herbal medicine (Pelletier and Caventou, 2015). Quinine has remarkable biological activities such as anti-inflammatory, anti-aging, anti-tumor, anti-bacterial and astringent activity (Skogman, 2012). At the start of world war II, cinchona production became a military objective. The development of synthetic drugs replaced the widespread use of quinine to treat malaria, and as a result its plantations decreased (Achan, 2011). In Myanmar, cinchona plant is cultivated in Thantaung Gyi and Laketho township, Kayin state. The photographs of *C. succirubra* Pav. is described in Figure 1.The present research has focused on screening of some bioactive constituents from the bark of *C. succirubra* Pav. (Kwi-neing).

Botanical Aspects of *Cinchona succirubra* Pav. (Kwi-neing)

Family	:	Rubiaceae
Botanical name	:	*Cinchona succirubra* Pav.
English name	:	Quinine
Myanmar name	:	Kwi-neing
Genus	:	*Cinchona*
Species	:	*succirubra*
Past used	:	Bark

Leaves Flowers Barks

Figure 1: Photographs of *Cinchona succirubra* Pav.

Materials and Methods

In this research work, the bark of *Cinchona succirubra* Pav. (Kwi-neing) was collected from Thantaung Gyi Township, Kayin State during August, 2015 and then identified at Botany Department, Taungoo University. The sample was made to fine powder and stored in air tight container. All chemicals used in this work were reagent grade (BDH) and the instruments consisted of a UV - visible Spectrophotometer (Shimadzu UV-240), Shimadzu FT IR- 8400 Spectrophotometer and AAS (A.Analyst-300 Spectrophotometer: Perkin Elmer).

Preliminary Phytochemical Investigation on Sample

In order to find out the types of phytochemical constituents present in sample, preliminary phytochemical investigation was carried out by using the reported chemical methods (Harborne, 1984) (Robinson, 1983) (Vogel, 1966).

Determination of Extractable Matter Contents of Sample

Dried powdered sample (100 g) was percolated with ethanol (400 mL) for four days and then filtered. The same procedure was repeated three times. The combined filtrate was concentrated under vacuum rotatory evaporator. The dried filtrate was transferred to a weighed porcelain basin and evaporated to dryness on water-bath to obtain ethanol extract.

For water soluble extractable matter, dried powdered sample (100 g) was boiled with distilled water (300 mL) for 2 h. The extract was then filtered and transferred to a weighed porcelain basin and evaporated to dryness on water-bath. The dried filtrate was placed in oven, maintained till constant weight, at 100 °C. The two extracts were stored in a desiccator containing dry silica gel prior using in each experiment.

Isolation and Identification of some Phytoconstituents from the Ethanol Crude Extract

The ethanol crude extract was subjected to chromatography over a silica gel column. The column was initially eluted with pet-ether:ethyl acetate (9:1 v/v)solvent system and the fractions were collected at the rate of one drop per second. The polarity of eluting solvent was gradiently increased by addition of increasing amount of ethyl acetate in petroleum ether, ethyl acetate, and ethanol in ethyl acetate. A quantity of 20 mL was collected for

each fraction and chromatographic separation was monitored by TLC. Spots on TLC were examined under UV lamp (254 and 365 nm). Fractions that showed similar TLC pattern were combined to provide six main fractions. Fraction F_2 provided compound 1 as colourless crystals, fraction F_3 provided compound 2 as pale yellow powder and fraction F_5 provided compound 3 as colourless crystals.

The isolated compounds were characterized by determining R_f values, by treating with 1 % $FeCl_3$ solution, 5 % H_2SO_4, Vanillin-HCl, I_2 vapour and Dragendorff, and by their spectral data, Shimadzu UV-240 UV–visible Spectrophotometer and Shimadzu FT IR-8400 Fourier Transform Infrared Spectrophotometer.

Investigation of Biological Activities of *Cinchona succirubra* Pav. Bark

Investigation of Antimicrobial Activity by Agar Well Diffusion Method

Agar well diffusion method was employed for determining antimicrobial activity of the ethanol and water extracts, and compounds 2 and 3. Two small holes of 10 mm diameter each were cut out in the inoculated agar to place samples to be tested. The volume of each sample placed in each hole was 0.1 mL. The petri dish was then incubated at 27 ºC for 24 h, and the diameter of clear inhibition zone appeared around the hole were measured.

Screening of Antioxidant Activity by Dot-Blot and DPPH Staining Method

The antioxidant activity of ethanol and water extracts, and compounds 2 and 3 was screened by Dot-Blot and DPPH staining method. 5 mg each of the sample was dissolved in 10 mL of corresponding solvent. Test amounts were 400 μg to 1.5625 μg. The samples were carefully loaded on 1×1 cm TLC plate (Silica gel 60 GF_{254}, Merck) by using microliter syringes and dried for 3 min. Loaded samples gave 1 cm diameter (area 78mm^2). Drop of each sample was loaded in order of decreasing concentration along the row. The staining of the silica plate was based on the procedure of Soler-Rives *et al*., 2000. The sheet bearing the dry spot was placed upside down for 10 s in 60 μM DPPH solution. Then, the excess solution was removed with a dryer blowing cold air. The stained silica gel layer revealed a purple background with white spots at the location of the drops, which showed radical scavenger

capacity. The intensity of the white colour depends upon the amount and nature of radical scavenger present in sample.

Determination of Elements in *Cinchona succirubra* Pav. Bark by AAS

The elemental contents in cinchona bark was determined by Atomic Absorption Spectroscopy (AAS) at the Universities' Research Centre (URC).

Results and Discussion

Preliminary Phytochemical Investigation of *Cinchona succirubra* Pav. Bark

The phytochemical tests showed that alkaloids, α-amino acids, flavonoids, glycosides, organic acids, phenolic compounds, saponins, tannins, steroids and terpenoids were present in sample. However, carbohydrates, cyanogenic glycosides, reducing sugars and starch were not detected.

Extractable Matter Contents of *Cinchona succirubra* Pav. Bark

After performing the preliminary phytochemical tests, it is required to investigate some organic constituents present in sample. Ethanol and water crude extracts were prepared and the percentage of crude extract yield was derived from the weight of dried and ground plant material. According to the results, it was observed that the yield of ethanol extract (15.2 %) was higher than that of water extract (12.3 %).

Identification of the Isolated Compounds

Compound 1

Compound 1 (0.002 %) was isolated as colourless crystals from fraction F_2 of the ethanol extract on silica gel by column chromatography using PE:EtOAc (4:1) solvent system. Its R_f value was 0.56 in this solvent system. It provided pink colour on TLC with 5 % H_2SO_4 and also brown colour with vanillin-HCl. Compound 1 may be terpenoid compound since it gave pink colour with acetic anhydride and H_2SO_4 (conc.).

In the FT IR spectrum of compound 1 (Figure 2), the absorption band appeared at 3419 cm^{-1} was attributed to O-H stretching vibration. A strong absorption bands appeared at 2931 cm^{-1} and 2850 cm^{-1} were attributed to asymmetric and symmetric C-H stretching vibration respectively. The C=O stretching vibration was observed at 1734 cm^{-1}. A band in medium intensity at

1641 cm^{-1} was due to the C=C stretching vibration. The absorption band at 1465 cm^{-1} was attributed to C-H bending vibration. The O-H bending vibration appeared at 1377 cm^{-1} and stretching vibration of C-O group was observed at 1092 cm^{-1} and 1022 cm^{-1} (Silverstein and Webster, 1998).

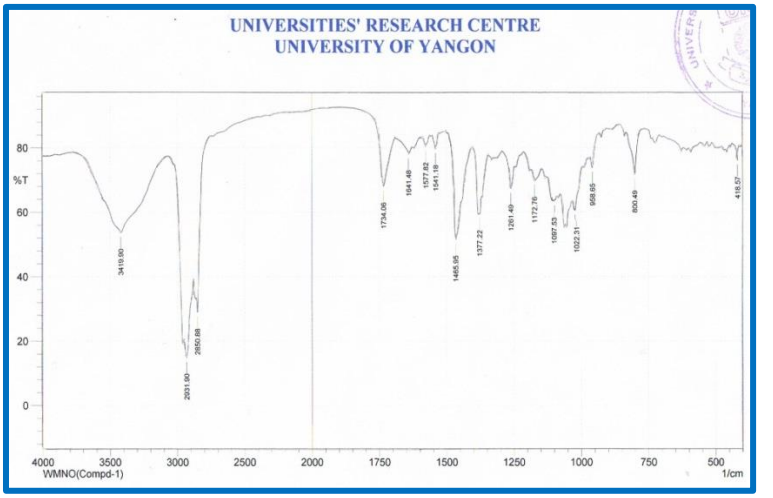

Figure 2: FT IR spectrum of compound 1 (KBr)

Compound 2

Compound 2 (0.0036 %) was isolated as a pale yellow powder from fraction F_3 of the ethanol extract on silica gel by column chromatography using PE:EtOAc (1:4) solvent system. Its R_f value was 0.45 in this solvent system. Compound 2 provided pink colour on TLC with 5 % H_2SO_4 and also with vanillin-HCl. It provided deep blue colour on TLC when treated with 1 % $FeCl_3$ solution suggested that compound 2 may be phenolic compound.

The ultraviolet spectra of the isolated compound 2 in methanol solvent and in methanolic NaOH solution are illustrated in Figure 3. The wavelengths of maximum absorption were found to be 215 nm (K-band) and 292 nm (R-band). Since the bathochromic shift was observed by adding NaOH, the compound may contain phenolic –OH groups. The shift of R band (292 nm) to longer wavelength (317 nm) by addition of NaOH indicating the presence of phenolic OH group in isolated compound 2.

In FT IR spectrum of compound 2 (Figure 4), the broad absorption band appeared at 3350 cm^{-1} was attributed to O-H stretching of phenolic –OH group. The absorption band at 3143 cm^{-1} was due to the aromatic C-H

stretching and the absorption band at 2948 cm^{-1} was assigned as aliphatic C-H stretching. The stretching vibration of aromatic C=C ring was observed at 1691 cm^{-1}, 1610 cm^{-1}, 1519 cm^{-1} and 1465 cm^{-1}. The O-H bending vibration was observed at 1334 cm^{-1} and C-O stretching vibration was observed at 1234 cm^{-1}, 1139 cm^{-1} and 1031 cm^{-1}. The absorption bands at 825 cm^{-1} and 763cm^{-1} were assigned as aromatic C-H out of plane bending (Silverstein and Webster, 1998).

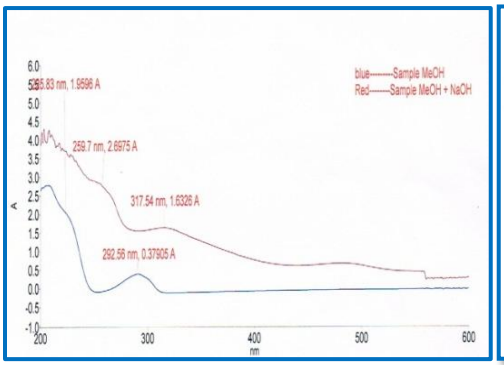

Figure 3:UV spectra of compound 2

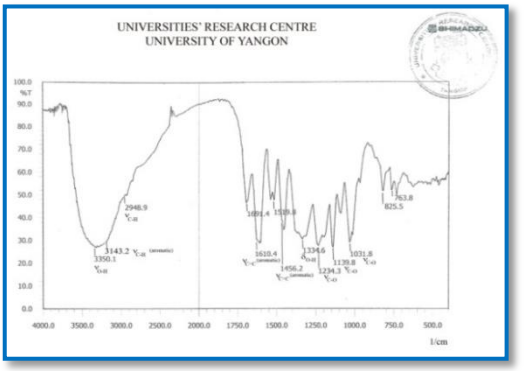

Figure 4: FT IR spectrum of compound 2 (KBr)

Compound 3

Compound 3 (0.061 %) was isolated as colourless crystals form fraction F_5 of the ethanol extract on silica gel column by eluting with EtOAc:EtOH:HOAc (9:1:0.5) solvent system. Its R_f value was 0.31 in this solvent system. Compound 3 may be an alkaloid compound since it gave yellow colour on TLC when treated with iodine vapour and also orange colour with Dragendorff"s reagent.

The ultraviolet spectrum in ethanol of compound 3 (Figure 5) showed wavelengths of maximum absorption (λ_{max}) at 241, 270, and 392 nm due to $\pi \rightarrow \pi^*$ transition.

In FT IR spectrum of compound 3 (Figure 6), a band appeared at 3375 cm^{-1} was interpreted as O-H stretching vibration. The presence of asymmetric and symmetric C-H stretching vibration were also confirmed by the bands at 2932 cm^{-1} and 2867 cm^{-1} respectively. Absorption bands at 1620cm^{-1} was due to the presence of C=C stretching of olefinic group. Aromatic C=C ring stretching appeared at 1486 cm^{-1}, 1450 $cm^{-1}$and 1431cm^{-1}.

Absorption bands at 1239 cm^{-1} and 1227 cm^{-1} were due to the presence of C-O stretching vibration. C-N stretching vibration was observed at 1077 and 1028 cm^{-1}. C-H out of plane bending vibration was appeared at 821 cm^{-1} (Silverstein and Webster, 1998). Photographs of the isolated compounds 1, 2 and 3 are illustrated in Figure 7.

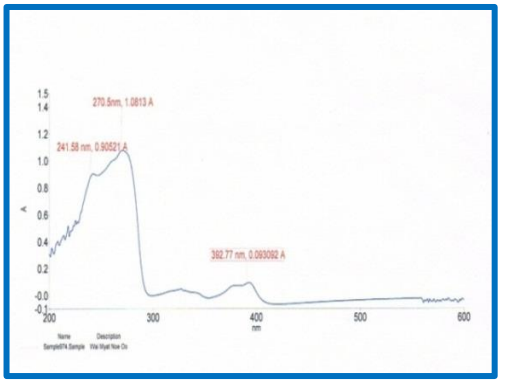

Figure 5: UV spectrum of compound 3 (EtOH)

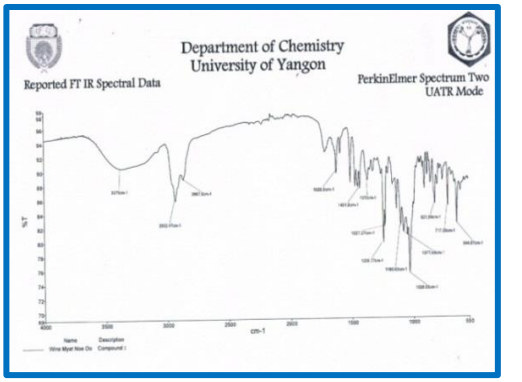

Figure 6: FT IR spectrum of compound 3 (KBr)

Compound 1 Compound 2 Compound 3

Figure 7: Photographs of the isolated compounds 1, 2 and 3

Biological Activities of *Cinchona succirubra* Pav. Bark

Antimicrobial Activity by Agar Well Diffusion Method

The antimicrobial activity of ethanol and water extracts, and compounds 2 and 3 was screened by agar well diffusion method on *Bacillus subtilis*, *Staphylococcus aureus*, *Pseudomonas aeruginosa*, *Bacillus pumilus*, *Candida albicans* and *Escherichia coli* (Figures 8 and 9). Both extracts exhibited antimicrobial activity against all test species with inhibition zone diameters ranged between 20-30 mm. Compound 2 showed antimicrobial

activity with inhibition zone diameter range between 13-20 mm and compound 3 exhibited inhibition zone diameter between 30-33 mm. The results indicated that compound 3 of *C. succirubra* bark showed strong antimicrobial activity against *E.coli* (inhibition zone diameter = 33 mm). Therefore, cinchona bark may be effectively used for the treatment of diseases infected by the microorganisms such as diarrhoea, dysentery, skin infection and wound infections.

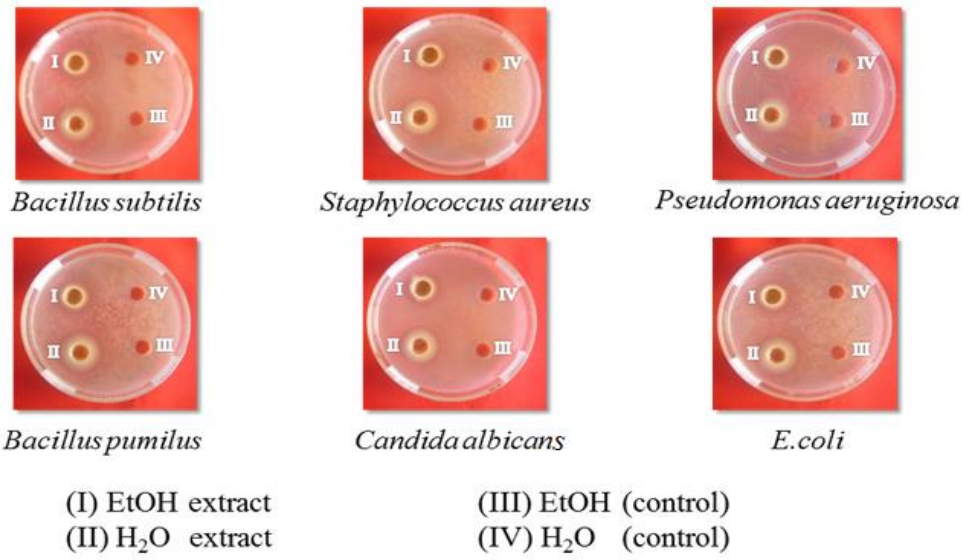

Figure 8: Antimicrobial activity of crude extracts of *Cinchona succirubra* Pav. bark

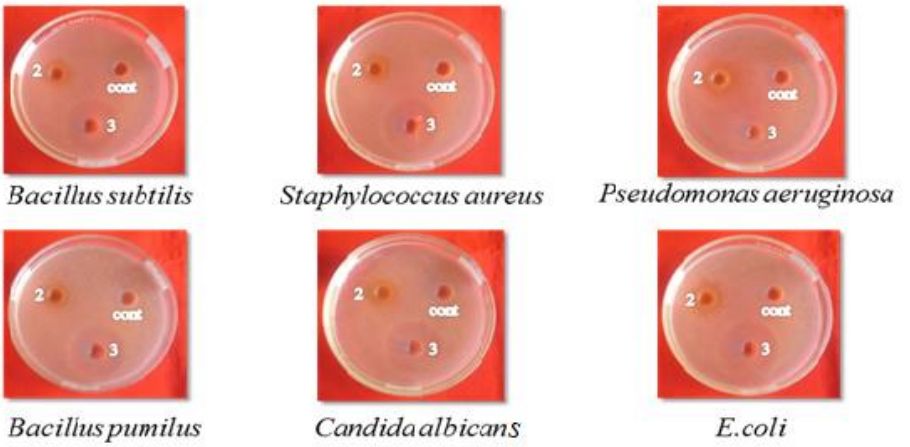

(2) compound 2
(3) compound 3

Figure 9: Antimicrobial activity of isolated compounds of *Cinchona succirubra* Pav. bark

Antioxidant Activity by Dot-Blot and DPPH Staining Method

The 2, 2-diphenyl-1-picryl hydrazyl (DPPH) radical was widely used in the model system to investigate the scavenging activity of several natural compounds such as phenolic compounds and anthocyanins or crude mixtures such as the alcohol extracts of plants. DPPH radical is scavenged by antioxidants through the donation of a proton forming the reduced DPPH.

To make a semi-quantitative visualization possible, the antioxidant activity of the EtOH and H_2O extracts, compounds 2 and 3 of cinchona bark sample was detected on the TLC plates by DPPH staining method. The appearance of yellow colour in the spots has a potential value for indirect evaluation of test samples in the dot blot (Solar-Rives *et al*., 2000).

When the antioxidant activity was screened by DPPH staining, white spots with strong intensity appeared from 400 μg to minimum concentration of 100 μg for EtOH extract, 200 μg for H_2O extract and 25 μg for compound 2. Antioxidant activity of compound 3 was not detected in concentration range between 200 μg-1.5625 μg. The results indicated that isolated compound 2 contains phenolic – OH group and it is responsible for antioxidant property by

free radical scavenging. Therefore, the bark of *C. succirubra* may be used for the cure of oxidative stress related diseases in Myanmar traditional medicine.

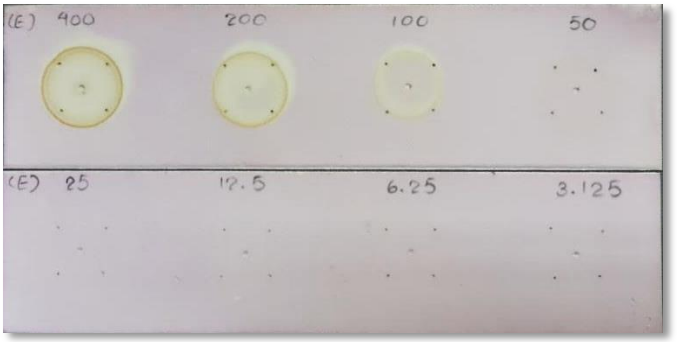

Figure 10: Antioxidant activity of EtOH extract by Dot-Blot and DPPH staining method

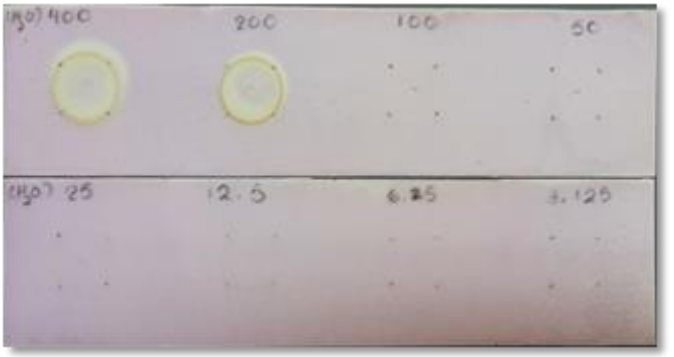

Figure 11: Antioxidant activity of H_2O extract by Dot-Blot and DPPH staining method

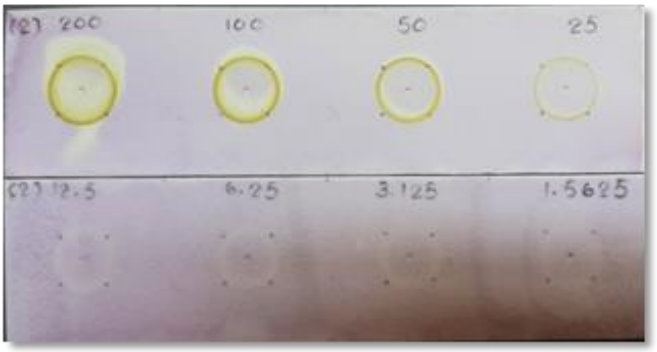

Figure 12: Antioxidant activity of compound 2 by Dot-Blot and DPPH staining method

Quantitative Analysis of Some Elements in *Cinchona succirubra* Pav. Bark by AAS

Quantitative analysis of 8 elements (Fe, Mn, Cu, Cd, Mg, Pb, Zn and Ca) in cinchona bark was carried by AAS and the data are described in Table 1. AAS method has high sensitivity and several elements are easily analyzed and measured in the range between ppm and ppb. Among these elements, calcium content in cinchona bark is significant. In the human body, Ca ranks fifth after oxygen, carbon, hydrogen and nitrogen and make up 1.9 % of the body by weight. Ca is an essential nutrient that plays a vital role in neuromuscular function, many enzyme mediated processes in blood clotting and providing rigidity to the skeleton by virtue of its phosphate salts. Therefore, cinchona bark may be used in Myanmar traditional medicine.

Table 1: Elemental contents in C*inchona succirubra* Pav. Bark by AAS

No.	Elements	Content (ppm)
1	Fe	3.978
2	Mn	1.551
3	Cu	0.233
4	Cd	0.06
5	Mg	8.802
6	Pb	0.492
7	Zn	0.266
8	Ca	115.6

Conclusion

The preliminary phytochemical tests on bark of *C. succirubra* revealed the presence of alkaloids, α-amino acids, flavonoids, glycosides, organic acids, phenolic compounds, saponins, tannins, steroids and terpenoids in it. In extractable matter contents, ethanol extract (15.2 %) was found to be higher than water extract (12.3 %). On silica gel column chromatographic separation, compound 1 (terpenoid, 0.002 %), compound 2 (phenolic compound, 0.0036 %) and compound 3 (alkaloid, 0.061 %) were isolated from ethanol crude extract and then identified by UV and FTIR spectroscopic methods. Antimicrobial activity of ethanol and water extracts, compounds 2 and 3 was screened by agar well diffusion method. Among the tested samples, compound 3 showed the pronounced antimicrobial activity with inhibition

zone diameter range between 30-33 mm. In addition antioxidant activity was also screened by Dot-Blot and DPPH staining method. Among the tested samples, compound 2 exhibited the potent antioxidant activity. In the elemental analysis of plant sample by AAS, Ca is more predominant than other elements such as Fe, Mn, Cu, Cd, Mg, Pb and Zn. Therefore, the bark of *C. succirubra* may be effectively used for the treatment of diseases infected by the microorganisms such as diarrhoea, dysentery, skin infection and wound infection and also as antioxidant in the cure of oxidative stress related diseases.

Acknowledgements

The authors would like to thank the Department of Higher Education, Ministry of Education, Yangon, Myanmar, for the permission of doing this research. I would like to express my deepest gratitude to Dr Tin Tun, Rector and Dr Mar Lar, Pro-rector, Taungoo University, for their permission to do this research. Special thanks are extended to Professor and Head, Dr Mi Mi Kyaing and Professor Dr Nay Mar Soe, Department of Chemistry, Taungoo University, for their valuable advices and kind encouragement and for providing research facilities.

References

Achan, J., Talisuna, A. O. and Tibenderana, J. K. (2011). "Quinine, An Old Anti-malarial Drug in a Modern World: Role in the Treatment of Malaria". *Malaria Journal*, vol 10, p. 144

Harborne, J. B. (1984). *Phytochemical Methods; A Guide to Modern Techniques of Plant Analysis*. New York: 2nd Ed., Chapman and Hall, p. 154

Pelletier, P. and Caventou, J . (2015). "History of Quinine". *Journal of the Association of Physicians of India*, vol 63, p. 58

Robinson, T. (1983). *The Organic Constituents of Higher Plants*. North America: 5th Ed., Cordus Press, pp. 63-68

Silverstein, R. M. and Webster, F. X. (1998). *Spectrometric Identification of Organic Compounds*. New York: 6th Ed., John Wiley and Sons Inc., pp. 12-28, 81-98

Skogman, M. E. (2012)."Evaluation of Antibacterial and Anti-biofilm Activities of Cinchona Alkaloid Derivatives against *Staphylococcus aureus*". *Nat. Prod. Commun*., vol **7**(9), pp. 1173-1176

Soler – Rives, C., Espin, J. C. and Wishers, H. J. (2000). "An Easy and Fast Test to Compare Total Free Radical Scavenger Capacity of Foodstuffs". *Phytochem. Anal*., vol 11, p. 330

Vogel, A. I. (1966). *The Textbook of Practical Organic Chemistry*. London: 3rd Ed., Longmans, Green and Co., Ltd., p. 453

A STUDY ON SOME BIOLOGICAL ACTIVITIES AND IDENFTIFICATION OF AN ISOLATED COMPOUND FROMTHE LEAVES OF*Eupatorium odoratum* L.

Nwe Thin Ni[1], Ma Hla Ngwe[2], Khin Ohnmar Kyaing[3]

Abstract

In this study, leaves of a Myanmar indigenous medicinal plant, *Eupatorium odoratum* L. (Taw-bizat) were chosen for the investigation of phytochemical constituents andsome of the biological activities such as antitumor, antimicrobial, antioxidant and acute toxic properties. The phytochemical constituents, nutritional values and elemental contents were analyzed on the leaves sample by using appropriate reported methods. The methanol extract (25 μg/disc) of the leaves sample was found to possess the antitumor activity against the tumor producing bacteria: *Agrobacterium tumefaciens* isolated from gall tissues of leaves of *Sandoricum koetjape* Merr. (Thitto). The crude extracts such as pet-ether, ethanol, methanol and ethyl acetate extracts were observed to be more potent than watery extract in antimicrobial activity against *Bacillus subtilis*, *Staphylococus aureus*, *Pesudomonas aeruginosa*, *Bacillus pumilus*, *Candida albicans* and *Escherichia coli*. However, the watery showed the antioxidant activity (IC_{50}= 13.07 μg/mL) higher than ethanol extract (IC_{50}= 56.14 μg/mL), determined by DPPH radical scavenging assay method. Both of watery and ethanol extracts did not show acute toxic effect up to 5000 mg/kg body weight dose on albino mice. From the separation of silica gel column chromatographic method, a bioflavonoid compound, 2´-hydroxy-4,4´,5´,6´-tetramethoxy chalcone(143-144 °C, 0.12 %) was isolated from the active pet-ether extract of *E. odoratum* leaves. It was identified by UV-Visible, FT IR, ^{1}HNMR, ^{13}C NMR, and EI-MS spectroscopic methods and also by comparing with the reported data. This isolated chalcone compound was observed to exhibit higher antioxidant activity (IC_{50}= 9.69 μg/mL) than the watery and ethanol extracts.

Keywords*: Eupatorium odoratum* L., bioflavonoid, 2´- hydroxy 4,4´,5´,6´ tetramethoxy chalcone, antitumor activity, antioxidant activity, acute toxicity

Introduction

Eupatorium odoratum L. belongs to the family Asteraceae and it is (up to 9 feet) shrubby with rather large, lanceolate, leaf blades coarsely

1. Dr, Associate Professor, Department of Chemistry, Taungoo University
2. Dr, Professor and Head (Retired), Department of Chemistry, University of Yangon
3. Dr, Professor and Head, Department of Pharmacology, Defense Service Medical Academy

toothed, especially near the base on long leaf less branches which spreading from the axils. These flowers are white, flowering time from August to October. It is distributed throughout Indian, Indochina and common in open country. In Myanmar, it can be widely distributed throughout the country (Ahmad and Nabi, 1969). The part of leaves are used externally in traditional medicine as a wound healing, skin abscess, diuretic, cathartic, intermittent fever, ulcers, bilious, catarrh and influenza (Biswal *et al.*,1997). According to the reported data (Baruah *et al.,* 1978), steroids, terpenoids and 13 flavonoids were observed in this plant. This plant was so found that rich in flavonoids. There is no report concerning with investigation of flavonoid and biological activities in this plant so far in Myanmar. Therefore, in this study the phytochemical constituents, antitumor activity, antimicrobial activity, antioxidant activity, acute toxicity and identification of one isolated bioactive flavonoid compound from the leaves of *E.odoratum* were conducted.

Materials and Methods

Collection and Phytochemical Investigation of the Leaves of*E.odoratum*

The leaves of *E. odoratum*were collected from Nwe-kway-ywa, Htauk-kyant Township, Yangon Region, Myanmar. After cleaning, the leaves were air-dried at room temperature for three weeks and the dry sample was ground into powder by grinder. The dried powdered sample was stored separately in air-tight containers to prevent moisture changes and other contamination. These plants were identified at the Department of Botany, University of Yangon. The preliminary investigation of phytochemical constituents was carried out according to reported methods (M-Tin Wa, 1972; Harbone, 1984).

Determination of Nutritional Values and Elemental Analysis of the Leaves of *E. odoratum*

The nutritional values such as moisture content, ash content, fat content, protein content(micro Kjeldahl method), fiber content, total carbohydrate contents and the energy value were determined by AOAC method (AOAC,1990). In addition, some mineral elements such as Ca, Mg, Fe, Cd, Cu and Mn were analyzed on the sample by using AAS (Atomic

Absorption Spectrometry) technique at Universities' Research Center (URC), Yangon.

Isolation, Characterization and Identification of Phytoconstituent from the Leaves of *E. odoratum*

Thedried powdered sample (ca 300 g) was percolated in 1000 mL of pet-ether (60-80 $^{\circ}$C) with occasional shaking for one week and filtered. This procedure was repeated for three times. The combined filtrate was concentrated under vacuum rotatory evaporator to obtain pet-ether crude extract. The pet-ether crude extract was decolourized by charcoal to give decolourized pet-ether crude extract (Robison, 1983).

The decolourized pet-ether extract (3 g) was separated chromatographically on a silica gel column (4 cm diameter x 47 cm length) by gradient elution with different ratios of PE:EtOAc (18:1, 8:1, 3:1 v/v) solvent mixture and a total of 87 fractions (7 mL each) were collected. From the inspection of TLC chromatogram under UV lamp, the fractions which had similar appearance were combined. The combined fraction from fractions 35-79 provided a yellow colour solid after evaporation. It was recrystallized from PE:AcOEt to give a yellowish crystal in 0.12 %(0.36 g) of yield.

The above isolated compound was characterized by visualizing under UV-light, by determination of melting points and R_f values and by some colourtests. The melting point was examined on a Gallenkamp melting point apparatus. Thecolour tests were carried out by spraying with 5% $FeCl_3$ solution, $K_4Fe(CN)_6$ solution, aqueous NaOH solution, conc: H_2SO_4 and by exposure to NH_3vapour on precoated aluminium TLC chromatograms after developing in PE:EtOAc (8:1 v/v) and R_f value was determined. In addition, the chromatograms sprayed with HOAc followed by exposure to NH_3 vapor were examined under a long wavelength (365 nm) UV lamp. Furthermore, it was also treated with Mg/ conc. HCl.

The isolated compound was then identified by modern spectroscopic techniques such as UV-Visible, FT IR, ^{1}HNMR, ^{13}CNMR and MS spectroscopic techniques and also by comparing with the reported spectral data.The UV spectra of the isolated compound were recorded in methanol and also in the presence of some flavonoid shift reagents such as NaOH, $AlCl_3$ and $AlCl_3$/HCl, NaOAc and NaOAc/H_3BO_3 by using Shimadzu UV-240 UV-

Visible spectrophotometer at URC, Yangon. The infrared spectrum of isolated compound was recorded on a Perkin Elmer Spectrum GX FT IR spectrophotometer at URC, Yangon. The isolated compound was sampled as a 1% KBr pellet. ^{1}HNMR spectrum of the isolated compound was recorded in $CDCl_3$ (400 MHz) and ^{13}CNMR spectrum was recorded in $CDCl_3$(100 MHz) with TMS as internal standard at the Department of Chemistry, Kanazawa University, Japan. Electron impact mass spectrum (EI-MS) of the isolated compound was recorded on a JEOL SX-102, a mass spectrometer at the Department of Chemistry, Kanazawa University, Japan.

Screening of some Biological Activities of the Leaves of *E.odoratum*

Screening of antitumor activity of the leaves of *E.odoratum*

In the screening of antitumor activity, the tumor producing bacteria *Agrobacterium tumefaciens* was firstly isolated from gall tissues of leaves of *Sandoricum koetjape* Merr.(Thitto). The isolated bacteria was identified by its morphology, gram staining, spore staining, some biochemical tests and compared with the references. The morphology of isolated bacteria was examined under Microscope (Cruickshank, 1960). In gram staining method, ammonium oxalate crystal violet solution (Hucker's solution), gram's modification of Lugol's solution and counter stain solution were used. In biochemical assay: motility test, catalase test, starch hydrolysis test, gelatin test, nitrates reduction test, indole test and carbohydrate test were carried out. After that, 2 mL(5×10^9 cells/mL) of broth culture of *Agrobacterium tumefaciens* and 0.5 mL of methanol extract of the leaves sample were inoculated on each potato disc, spreading it over the disc surface. The plates were sealed with the tape to minimize moisture loss and incubated at room temperature for one week. After incubation, Lugol's solution (I_2&KI) was added and tumors were observed under the microscope and compared with control disc. The antitumor activity was detected with the result of tumor occurred or not (Ferrigni *et al*., 1982). This experiment was carried out at the Pharmaceutical Research Department, Ministry of Industry, Yangon.

Screening of antimicrobial activity of theleaves of *E. odoratum*

Agar well diffusion method (Balouiri, 2016) was employed for determining antimicrobial activity of the extracts such as PE, EtOH, MeOH,

EtOAc and watery extracts from the sample against six pathogenic microorganisms namely *Bacillus subtilis*, *Staphylococus aureus*, *Pesudomonas aeruginosa*, *Bacillus pumilus*, *Candida albicans* and *Escherichia coli*, conducted at the Pharmaceutical Research Department, Ministry of Industry, Yangon. The antimicrobial activity was determined by measuring the inhibition zone diameters appeared around the agar well indicated that the presence of antimicrobial activity (Cruickshank,1960).

Screening of antioxidant activity of the leaves of *E. odoratum*

Antioxidant activity of 95 % ethanol, watery extracts and the isolated compound was determined UV-visible spectroscopically by using DPPH (1,1-diphenyl, 2-picryl, hydrazyl) radical scavenging assay (Halliwell, 2012).

Firstly, a blank solution was prepared by mixing 1.5 mL of the test sample solution with 1.5 mL of 95 % ethanol and a control solution was prepared by mixing of 60 μM DPPH solution and 1.5 mL of 95 % ethanol using vortex mixer. The sample solution was prepared by mixing thoroughly 1.5 mL of 60 μM DPPH solution and 1.5 mL each of test sample in ethanol with different concentrations (3.125, 6.25, 12.5, 25, 50, 100, 200 and 400 μg/ mL). The solutions were allowed to stand at room temperature for 30 min. After 30 min, the absorbance of these solutions was measured at 517 nm by UV-visible spectrophotometer. Absorbance measurements were done in triplicate for each solution and the mean values so obtained were used to calculate the percent inhibition of oxidation by the following equation.

$$\% \text{ Oxidative Inhibition} = \frac{A_{control} - (A_{sample} - A_{blank})}{A_{control}} \times 100$$

$A_{control}$ = Absorbance of the DPPH solution

A_{sample} = Absorbance of the sample and DPPH solution

A_{blank} = Absorbance of the sample solution

Then, the antioxidant activity of the samples was expressed by theirIC_{50} (50 % oxidative inhibitory concentration) which were calculated by linear regressive excel program (Kahlonene, 1999).

Screening of acute toxicity of the leaves of *E. odoratum*

The acute toxicity of watery and 95 % ethanol extracts of the leaves sample was determined in *in vivo* by using albino mice model according to OECD guideline 425(OECD, 2000). This method is reproducible, used in very few animals and able to rank substances in a similar manner to the other acute toxicity testing methods (OECD, 2000).

In the present study, 24 albino rats were taken and divided into 8 groups (3 in each group) (Group I, II, III, IV, V, VI, VII, VIII). Then, Groups I, II, III and IV were orally treated with watery extract and Groups V, VI, VII and VIII treated with ethanol extract in different concentrations by using a stomach tube or a suitable intubation cannula. The dose levels administrated to each group were 175, 550, 1750 and 5000 mg/kg body weight/day and the sign of animals were observed daily up to 7 days and 14 days.

Results and Discussion

Phytochemical Constituents Present in the Leaves of *E.odoratum*

The leaves of locally grown *E. odoratum* were collected from New-kway-ywa, Htauk-kyant Township, Yangon, Myanmar in the middle of September. According to the preliminary phytochemical tests, it was found that glycosides, flavonoids, alkaloids, α-amino acid, carbohydrates, phenolic compounds, saponins, steroids, tannins and terpenoids are present in the *E. odoratum* leaves sample, whereas, cyanogenic glycosides, the harmful phytoconstituent, were not detected in the collected sample (Table 1).

In addition, from the analysis of nutritional value, the *E.odoratum* leaves were observed to contain 35.37 % of carbohydrate, 19.75 % of protein, 24.31 % of fiber, 3.52 % of fat, 7.51 % of ash and 9.54 % of moisture with 185 kcal/100 g of energy value, based on dry weight.

Furthermore, elemental analysis by using AAS method showed that the leaves of *E.odoratum* contained 122.18 ppm of Ca, 100.27 ppm of Mg and 34.34 ppm of Fe, and Cd, Cu and Mn were not found in the sample under experimental condition.

Table 1: Phytochemical Constituents Present in the Leaves of *E. odoratum*

Types of compounds	Extract	Test reagents	Observation	Remark
Alkaloids	1% HCl	Mayer's Dragendroff'sDragendroff's reagent Wagner's reagent	White ppt Orange ppt Brown ppt	+ + +
α-Amino acids	H_2O	Ninhydrin	Pink colour spot	+
Carbohydrates	H_2O	10 % α naphthol,conc. H_2SO_4	Red ring	+
Flavonoids	EtOH	Conc. HCland Mg ribbon	Pink colour	+
Glycosides	H_2O	10 % lead, acetate solution	White ppt	+
Phenolic compounds	EtOH	1% $K_3Fe(CN)_6$, 1 % $FeCl_3$	Blue/green colour	+
Steroids	PE	Acetic anhydride,conc:H_2SO_4	Greenish blue colour	+
Saponins	H_2O	Shaking	Frothing	+
Terpenoids	$CHCl_3$	Acetic anhydride and conc: H_2SO_4	Pink colour	+
Tannins	H_2O	1 % gelatin	White ppt	+
Cyanogenic glycosides	H_2O	Sodium picrate	No brick red colour	-

\+ = Presence - = Absence

Isolation and Identification of the Isolated Compound from the Leaves of *E. odoratum*

On silica gel coloum chromatographic separation by using PE:AcOEt (8:1 v/v) solvent system as eluent, a yellowish crystal was isolated from the decolourized pet-ether extract (3 g) of the leaves of *E. odoratum*in 0.36 g, 0.12 % of yield. Its R_f value was 0.45 in PE:AcOEt (8:1 v/v) solvent system and its melting point was observed to be 143-144º**C** (PE/AcOEt). This compound could be observed on TLC chromatogram under a long wavelength (365 nm) UV lamp, indicating the presence of conjugated double bonds.

The isolated compound was observed in brown colour on the precoated aluminium TLC chromatograms while spraying with 5 % $FeCl_3$ solution, in greenish blue colour while spraying with $K_4Fe(CN)_6$ solution, in

pale yellow colour while spraying with aqueous NaOH solution, in yellow colour while spraying with conc. $H_2SO_4$and in yellow colour by exposure to NH_3 vapour, indicating that it is a flavonoid compound containing phenolic group.

In addition, when the chromatogram was sprayed with HOAc, deep purple spot was observed to appear under a long wavelength (365 nm) UV lamp. The deep purple spot was found to change red under UV after exposure to NH_3 vapor. Furthermore, it did not give any colouration while treating with Mg/ conc. HCl. From these observation it may therefore, be assigned as a chalcone with a free 2- and 4-OH (Geissman, 1955).

According to UV-Visible spectra in MeOHas shown in Figure 1 (a), of the isolated chalcone, the major absorption band (Band I) occurred at 360 nm with a shoulder at 305 nm and a minor absorption band (Band II) at 230 nm. This information also pointed out that the isolated compound as a chalcone (Markhal, 1982).In the presence of NaOH, a 60 nm bathochromic shift of Band I with a decrease in the peak intensity occurred at 420 nm as a shoulder indicating that the chalcone cannot possess 4-OH group (Figure 1 (a)). According to 70 nm bathochromic shift of Band I (360 nm to 430 nm) in the presence of $AlCl_3$ as well as in $AlCl_3$/HCl (Figure 1 (b)), there may be a 2′ -OH group in the isolated chalcone. Band I of the compound was observed by 10 nm bathochromic shift in the presence of NaOAc as well as in NaOAc/H_3BO_3 (Figure 1 (c)). All of the observed UV-visible spectral data are listed in Table 2. On the basis of UV-Vis spectral data, the isolated compound might be assigned as a chalcone bearing a OH group at 2' position.

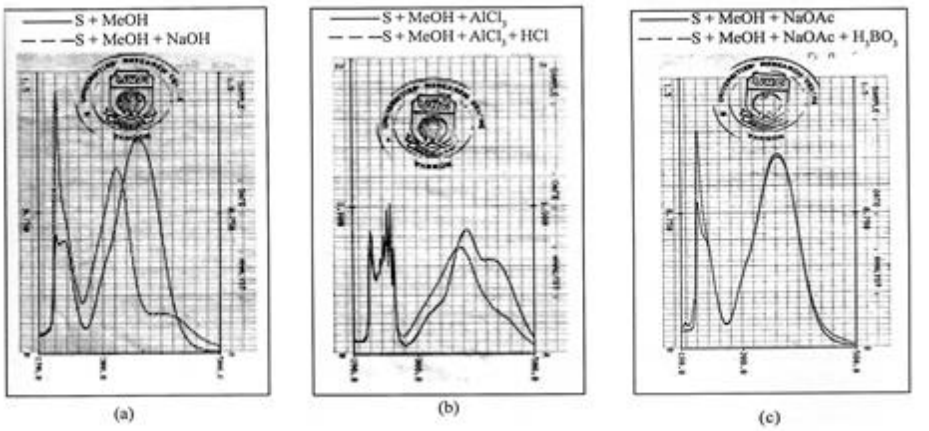

Figure 1: UV-Visible Spectra of the isolated compound from *E.odoratum* leaves

Table 2: UV-Visible Spectral Data of the Isolated Compound from the Leaves of *E. odoratum*

No.	Solvents and Shift reagents	λ_{max}(nm)
1	MeOH	230(II), 305(sh), 360(I)
2	MeOH + NaOH	225(II), 320(sh), 420(I)
3	MeOH + $AlCl_3$	230(II), 390(II), 430(I)
4	MeOH + $AlCl_3$ +HCl	228(II), 390(II), 430(I)
5	MeOH + NaOAc	230 (I), 270 (I), 370 (I)
6	MeOH + NaOAc + H_3BO_3	230(I), 270, 380(I)

The presence of OH group and α, β-unsaturated C=O group could also be confirmed with the peaks respectively appeared at 3450 cm^{-1} and 1625 cm^{-1} in FT IR spectrum (Figure 2 and Table 3) of the isolated compound. The characteristic bands at 2947, 2844, 1345, 1244 and 1020 cm^{-1} also showed the presence of aromatic O-CH_3 group. The bands appeared in the regions: 3010, 1602, 1174, 988, 874 and 836 cm^{-1} showed the presence of aromatic C=C and =C-H groups.

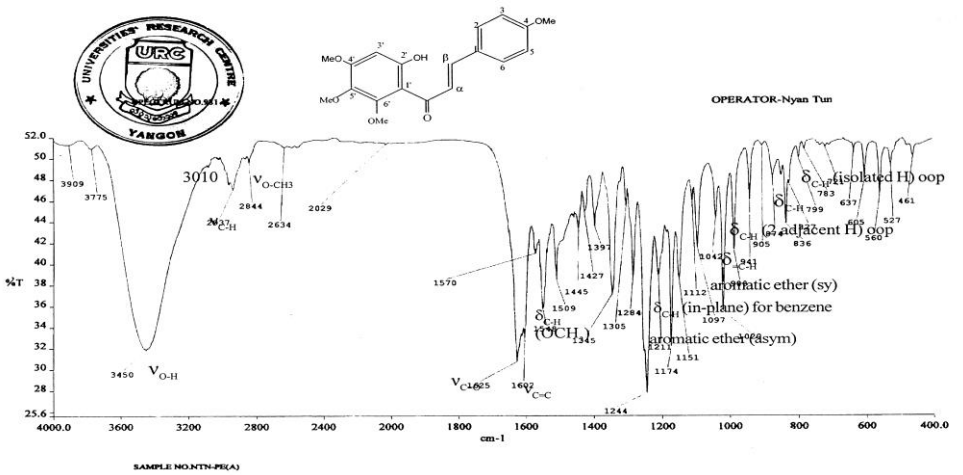

Figure 2: FT IR spectra of the isolated compound from the leaves of *E.odoratum*

Table 3: FT IR Spectral Data of the Isolated Compound from the Leaves of *E. odoratum*

Wave Number (cm^{-1})	Assignment
3450	ν_{O-H} of phenol
3010	$\nu_{=C-H}$ of aromatic ring
2947, 2844	Asymmetric and symmetric ν_{C-H} of CH_3 group
1625	$\nu_{C=O}$ of α, β -unsaturated carbonyl group
1602	$\nu_{C=C}$ of aromatic ring
1345	δ_{C-H} of CH_3 group
1244	Asymmetric ν_{C-O-C} of aromatic ether
1174	δ_{C-H} in plane bending of benzene
1020	Symmetric ν_{C-O-C} of aromatic ether
988	$\delta_{=CH}$ of aromatic ring
874	$\delta_{C-H(oop)}$ of two adjacent H in aromatic ring
836	$\delta_{C-H(oop)}$ of isolated H in aromatic ring

According to ^{1}H NMR ($CDCl_3$, 400 MHz) spectrum and spectral data (Figure 3 and Table 4), there were two *trans* olefinic protons (H-α and H-β) due to a singlet peak at 7.8 ppm. One phenolic protons appeared as a singlet at 13.75 ppm which indicated that the OH group is ortho to the CO group. The signals at 3.76 (s, 3H), 3.87 (s, 3H), 3.92 (s, 3H), 3.97 (s,3H) ppm were due to the protons of four methoxy groups. The H-2 and H-6 protons occurred at 7.73 ppm (2H, d, J= 8.78 Hz) as a doublet with coupling constant 8.78 Hz and H-3 and H-5 protons appeared at 7.03 ppm (2H, d, J=8.78 Hz) also as a doublet with same J value of 8.78 Hz. The H-3′ proton was occurred as a singlet at 6.33 ppm. The ^{1}HNMR spectral data of the isolated chalcone were found to be identical with the reported data (Table 4) for 2′-hydroxy-4,4′,5′,6′-tetramethoxychalcone (Mabry *et al.*, 1970). Therefore the structure of the isolated chalcone was assigned as follows.

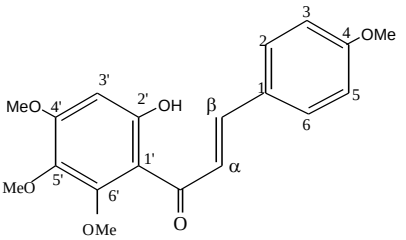

2′ -hydroxy-4,4′ ,5′ ,6′ -tetramethoxychalcone

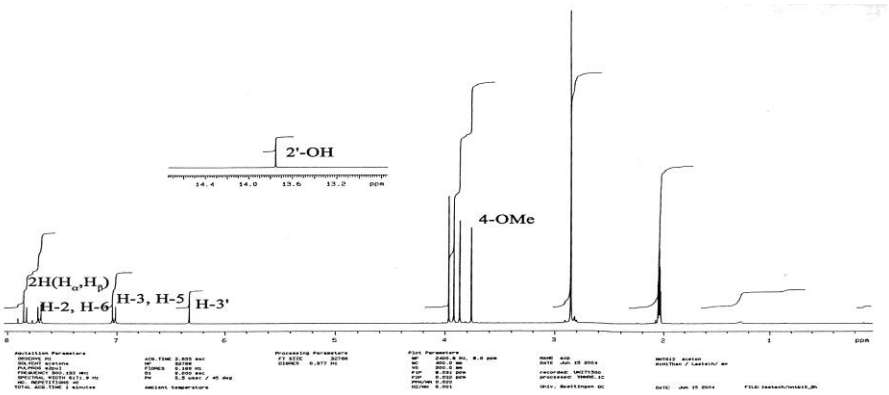

Figure 3: ^{1}HNMR spectrum ($CDCl_3$, 400 MHz) of the isolated compound from *E. odoratum* leaves

Table 4: ^{1}H NMR ($CDCl_3$, 400 MHz) Spectral Data of the Isolated Compound from *E. odoratum* Leaves and the Reported Data of 2□-hydroxy-4,4□,5□,6□-tetramethoxy chalcone

Chemical Shifts (□ /ppm)		Multiplicity	Remark
Observed	**Reported***		
3.76	3.82	s	3H (OMe)
3.87	3.85	s	3H (OMe)
3.92	3.90	s	3H (OMe)
3.97	3.92	s	3H (OMe)
6.33	6.27	s	1H (H–3′)
7.03	6.68	d (J=8.78 Hz)	2 H (H-3, H–5)
7.73	7.59	d (J=8.78 Hz)	2 H (H-2, H–6)
7.83	7.84	s	2 H (Hα , Hβ)
13.75	13.50	s	1 H (2′ –OH)

* Mabry*et al.*, 1970

^{13}CNMR spectrum and the spectral data interpreted are illustrated in Figure 4 and Table 5, respectively. From this spectrum, it was observed that four methoxy groups are appeared at 55.76, 56.48, 61.14 and 62.08 ppm. According to this spectrum, it was found that there were a total of 19 carbon atoms: 4 methyl carbons of 4 methoxy groups (55.76, 56.48, 61.14 and 62.08 ppm), one carbonyl carbon at 193.46 ppm and 14 double bond carbons (97.25, 109.11, 115.34, 124.68, 128.74, 131.11, 136.13, 144.01, 155.07, 161.28, 162.70 and 163.4 ppm) as summarized in Table 5. The numbers of carbon and types of carbons were observed to be that of 2′-hydroxy-4, 4′, 5′, 6′-tetramethoxychalcone.

In EI-MS spectrum (Figure 5), the molecular ion [M^+] peak appeared at m/z = 344 indicating that the molecular formula of the isolated chalcone is $C_{19}H_{20}O_6$. The fragmentation pattern of the compound could be expressed as in Figure 6 and that finally confirmed the isolated compound to be 2′-hydroxy-4, 4′, 5′, 6′-tetramethoxy chalcone

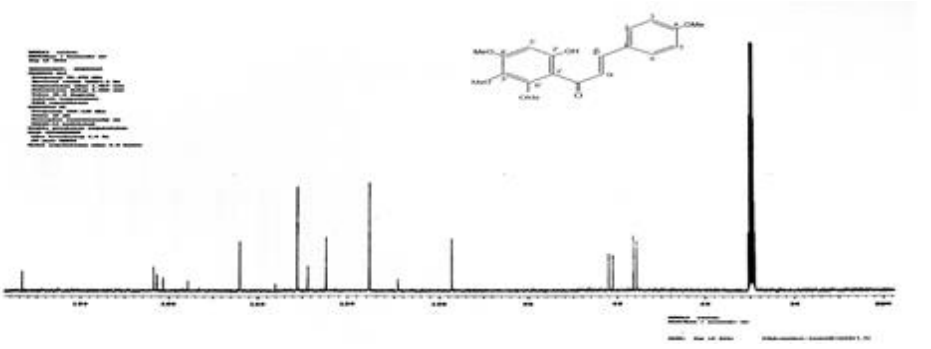

Figure 4: ^{13}CNMR spectrum ($CDCl_3$, 100 MHz) of isolated compound from *E.odoratum* leaves

Table 5: ^{13}CNMR ($CDCl_3$, 100 MHz) Spectral Data of the Isolated Compound from *E. odoratum* Leaves

δ_c (ppm)	Assignment
55.76 56.48 61.14 62.08	Methyl carbons of four methoxy group
97.25 109.11 115.34 124.68 128.74 131.11 136.13 144.01 155.70 161.28 162.70 163.47	Double bond carbons
193.46	Carbon of carbonyl group

Figure 5: EI -MS spectrum of the isolated compound from *E.odoratum* leaves

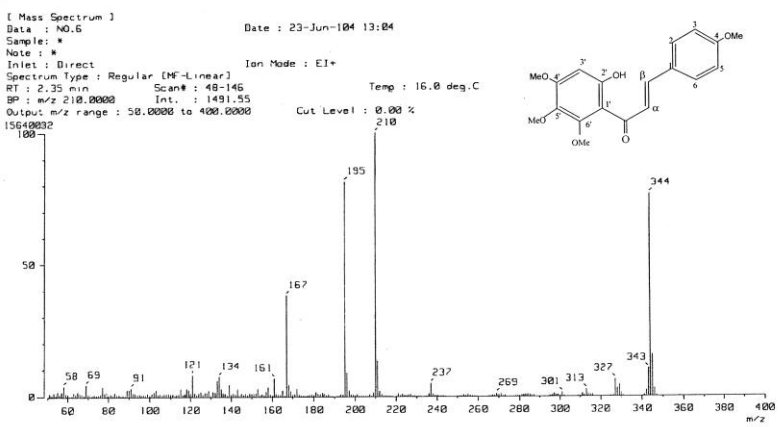

Figure 5:EI -MS spectrum of the isolated compound from *E.odoratum* leaves

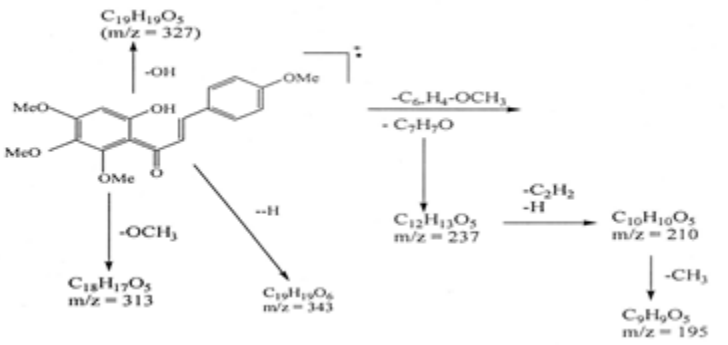

Figure 6: Fragmentation pattern of the isolated compound from *E. odoratum* leaves

Antitumor Activity of *E. odoratum*Leaves

The antitumor activity was determined on the methanol extract of *E. odoratum* leaves by using Potato Crown Gall test. *Agrobacterium tumefaciens* isolated from the leaves of *Sandoricum koetjape* Merr. (Thitto) was used for tumor formation on the potato disc. From this experiment, methanol extract was observed to inhibit the tumor formation with the dose of 25 μ g/disc.

Antimicrobial, Antioxidant and Acute Toxicity Activities of *Eupatorium odoratum* L.

The antimicrobial activity of MeOH extract (inhibition zone diameter35 mm) was exhibited the most potent antimicrobial activity against *Staphylococcus aureus*. The remaining extracts were showed antimicrobial activity against on six strains of microorganisms. The results of inhibition zone diameters are described in Figure 7 and Table 6.

The antioxidant activity was expressed as 50% oxidative inhibitory concentration (IC_{50}). The lower the IC_{50} values, the higher the antioxidant activity of the sample. By using DPPH free radical scavenging assay, the compound A was more potent antioxidant activity than 95 % ethanol and watery extracts. The results of antioxidant activity are shown in Table 7 and Figures 8 and 9.

In acute toxicity test, there is no lethality at the dose of 5000 mg/kg b.w of the extracts and hence LD_{50} was supposed to be higher than 5000 mg/ kg b.w. It can be concluded that the ethanol and watery extracts of *E.odoratum* were practically non-toxic.

Table 6: Inhibition Zone Diameters of Various Extract of *Eupatorium odoratum* L. against Six Microorganisms by Agar Well Diffusion Method

No.	Microorganisms	Inhibition Zone Diameter (mm)				
		PE	EtOH	MeOH	EtOAc	H_2O
1	*Bacillus subtilis*	20	23	18	22	14
2	*Staphylococcus aureus*	18	30	35	24	15
3	*Pseudomonas aeruginosa*	21	23	18	20	15
4	*Bacillus pumilus*	23	24	21	20	14
5	*Candida albicans*	23	20	24	20	16
6	*Escherichia coli*	21	24	18	18	15

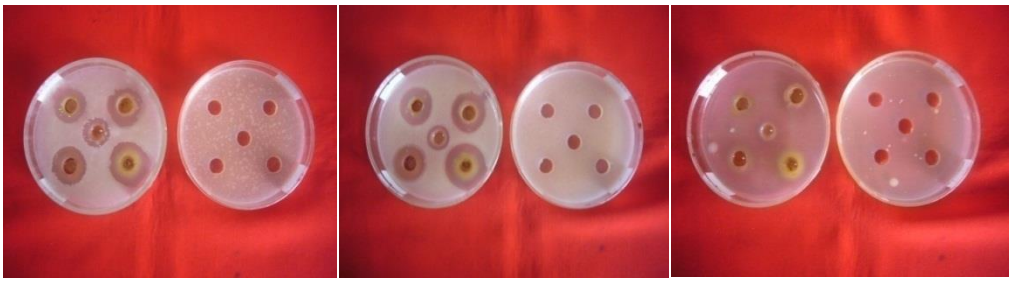

Bacillus subtilis, Staphylococcus aureus, Pseudomonas aeruginosa

Bacillus pumilus, Candida albicans, Escherichia coli

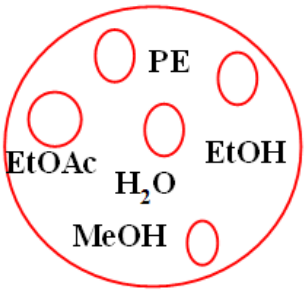

Figure 7: Inhibition zone diameter of crude extracts against six microorganisms

Table 7: Oxidative Percent Inhibitions and IC_{50} Values of Crude Extracts and the Isolated Compound A of *Eupatorium odoratum* L. and Standard BHT

Sample	% Inhibitions (Mean ± SD) in various Concentrations (μg/ml)								IC_{50}
	3.125	**6.25**	**12.5**	**25**	**50**	**100**	**200**	**400**	**(μg/ml)**
95 % EtOH	38.095 ± 3.863	36.395 ± 2.567	30.272 ± 7.167	27.347 ± 18.395	37.551 ± 4.081	54.762 ± 4.248	52.381 ± 5.802	59.372 ± 15.587	56.14
Watery	20.748 ± 0.601	35.034 ± 0.601	41.497 ± 1.202	64.966 ± 0.601	80.952 ± 0.601	94.217 ± 1.202	93.197 ± 0.601	93.06 ± 1.323	13.07
Compound A	20.748 ± 0.601	39.532 ± 0.601	52.262 ± 1.202	21.428 ± 0.601	25.17 ± 0.601	25.489 ± 0.601	24.499 ± 0.601	25.987 ± 0.531	9.69
Standard BHT	43.301 ± 1.40	53.582 ± 2.49	65.53 ± 1.132	74.82 ± 0.621	83.321 ± 0.782	87.412 ± 2.372	91.516 ± 1.113	94.702 ± 0.692	3.16

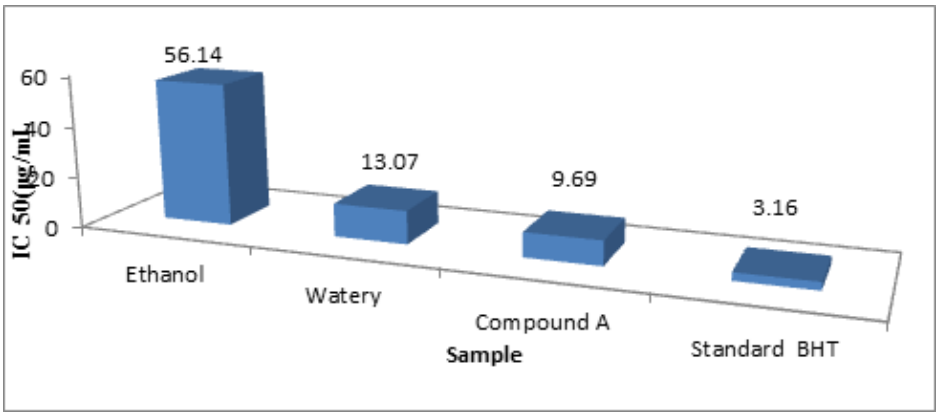

Figure 8: A bar graph of IC_{50} (µg/mL) values of different concentrations of watery, EtOH extracts and the isolated compound A from *E.odoratum*

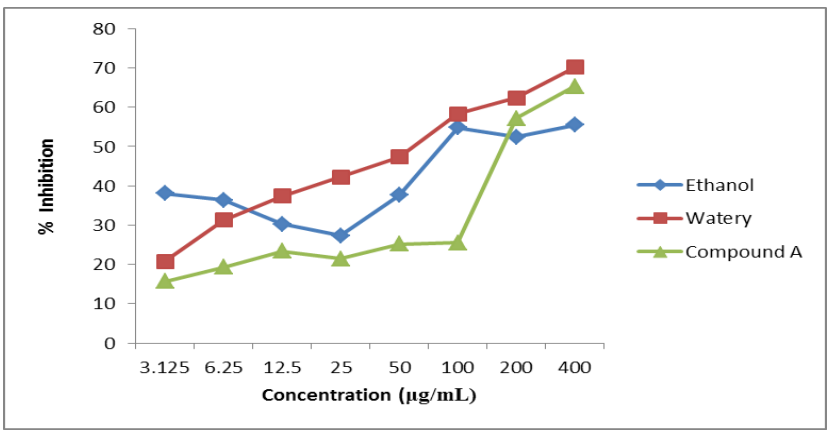

Figure 9: DPPH radical scavenging activity of different concentrations of watery, EtOH extracts and the isolated compound A from *E. odoratum*

Conclusion

The overall assessments of the research work, the preliminary phytochemical investigation indicated that alkaloids, α-amino acids, carbohydrates, glycosides, flavonoids, phenolic compounds, saponins, steroids, tannins and terpenoids were present and *the* cyanogenic glycosides were not detected in *E. odoratum.*The nutritional values as 35.37 % of carbohydrates, 19.75% of protein, 24.31 % of fiber, moisture 9.54 % and ash 7.51 % were observed in it. The energy value was observed to be 185 kcal/ 100g in collected sample.According to qualitative elemental analysis carried out by AAS spectrometry, Ca and Mg were occurred higher than Fe contents in*E.odoratum*.In order to find out the bioactive organic constituents from active decolourized pet-ether extract, silica gel column chromatographic separation using PE/ EtOAc solvent system with variousratio were carried out. One of the bioflavonoid compound: 2´- hydroxy - 4, 4´, 5´, 6´ - tetramethoxychalcone (0.12%, R_f = 0.45, mp = 143-144 °C) was successfully isolated from *E.odoratum* by column chromatographic separation. This compound was identified structurally by modern spectroscopy: UV, FTIR, ^{1}HNMR,^{13}CNMR and EI-MS.*E. odoratum* was observed to possess the prevention of tumor formation with the doses of 25 μg/disc of methanol extract by Potato Crown Gall Test. The MeOH extract of *E.odoratum* was found to show the highest antimicrobial activity (35 mm) against on *Staphylococcus aureus*. The remaining extracts also showed the antimicrobial activity against six microorganisms. The isolated chalcone compound (IC_{50} = 9.69μg/mL) was more potent than the watery extract (IC_{50} = 13.07 μg/mL) and 95% ethanol extract (IC_{50} = 56.14 μg/mL) in the antioxidant activity. There is no lethality up to the dose of 5000 mg/kg of the both watery and ethanol extracts. Consequently, it can be deduced that *E.odoratum* leaves may be useful for the treatment of the diseases related to bacterial infection and antitumor drug in the formulation of Myanmar Traditional medicine.

Acknowledgements

The authors would like to express sincere gratitude to Department of Higher Education, Ministry of Education, Myanmar, for guiding the good opportunities to do this research and for allowing to present this paper. Then, we specially wish to acknowledge to Rector Dr Tin Tun and Pro-rector Dr Mar Lar, Taungoo University, Professor and Head, Dr Mi Mi Kyaing and Professor Dr Nay Mar Soe, Department of Chemistry, Taungoo University for their valuable guidance and generous encouragements for successes of this research work.

References

AOAC. (1990). *Official Methods of Analysis*, Washington, DC: 5th Ed.

Ahmad, M., and M.N. Nabi, (1969).“Chemical Investigations on the Leaves of *Eupatorium odoratum*.” *Sci Res*, vol.6, pp 37-41.

Baruah R.N., R.P.Sharmac, G., Thayagarajan, and W.Herz, (1978). “Flavonoids of *Eupatorium odoratum* Linn.” *Phytochemistry* , vol. 7, pp1807:-8.

Biswal, P.R., K.K., Sardar, S.C., Parija, and P.R. Mishra, (1997). “Wound Healing Effect of *Eupatorium odoratum* Linn, and Himax in Rabbits”, *Indian Journal of Indigenous Medicines*, vol**.** 19 (1), pp 71-74.

Balouiri,M., M., Sadiki, and I., Koraichi, (2016), Methods for *in vitro* evaluating antimicrobial activity, *J of Pharmaceutical Analysi*, vol. 6, pp 71-79

Cruickshank, R. (1960). *Medical Microbiology*, London, 1st Ed., E.E. Livingstone Ltd, pp 81-95

Ferrigni, N.R, J.E. Putnan and B.Jacobsen. (1982). “Modification and Evaluation of the Potato Disc Assay and Antitumor Screening of Euphobiaceae Seeds”, *Journal of Natural Products*, vol. 45(6),pp 679-686

Geissman, T.A. (1955). *In Modern Methods of Plant Aalysis*, Springer Verlag, Heidel berg, vol. 3, pp 487.

Harborne, J.B. (1984), *Phytochemical Methods: A Guide to Modern Techniques of Plant Analysis*, Chapman and Hall, London ,pp 76-78

Halliwell, B. (2012). “Free Radicals and Antioxidants, Updating a Personal View”, Journal of Nutrition Reviews, vol.70(5), pp 65-257

Kahlonene, P. (1999). "Antioxidant Activity of Plant Extracts Containing Phenolic Compounds", *Journal of Agriculture., Food Chemistry*., vol. 47(3), pp 3954-3962

Mabry, T.J., K.R. Markham and M.B. Thomas (1970). *The Systematic Identification of Flavonoids*, New York: Springer – vela.

Markham, K.R., (1982). *Technique of Flavonoids Identification*, London Academic Press,

M-Tin Wa, (1972). "Phytochemical Screening Method and Procedures". *Phytochemical Bulletin of Botanical Society of America Inc.*Vol.5(3), pp 4-10

OECD, (2000)."Guidance Document on Acute Oral Toxicity”, Environmental Health and Safety Monograph Series on Testing and Assessment No 24.

Robison, T. (1983). *The Organic Constituents of Higher Plants*, North Amherst. 5th ed., Cordus Press, pp 7

CHEMICAL KINETIC PARAMETERS BY TLC VIDEO DENSITOMETRY IN THE SYNTHESIS OF 4-FLUOROACRIDIN-9(10*H*)-ONE UNDER SONOCHEMICAL ACTIVATION

Yar Zar Htun[1], T.N.Kudryavtseva[2]

Abstract

The present work highlights the synthesis of 4-fluoroacridone by intramolecular condensation of 2'-fluorodiphenylamine-2-carboxylic acidunder sonochemical activation. The kinetic parameters of reaction synthesis were determined by TLC video densitometry. In the synthesis, the effect of sonochemical activation on reaction rate and kinetic parameters such as time, temperatures, rate constants and activation energies were studied. The experimental results of traditional condition and sonochemical activation revealed the different kinetic parameters. The results indicated that activation energy of reaction decreased and the reaction rate greatly enhanced in sonochemical activation.

Keywords: Acridone, sonochemical activation, kinetic parameters, TLC video densitometry

Introduction

Derivatives of diphenylamine-2-carboxylic acid (2-(phenylamino) benzoic acid) and acridine-9(10*H*)-ones (acridones) possess important practical significance. Some of them having a broad spectrum of pharmaceutical activities are investigated as pharmaceuticals drug. Diphenylamine-2-carboxylic acids are basic intermediates products for synthesis of acridone derivatives. Based on these compounds, various dyes, indicators and biologically active compounds which possess as antitumor, anti-malarial, anti-viral and anti-bacterial action(Thorarense*etal*.,2007). In particular, acridone is commercially have been synthesized from diphenylamine-2-carboxylic acid and then from which 2-(9-oxoacridine-10(9H) -yl) (acridone acetic) is synthesized. Salts of this compounds are included in the list of life-saving drugs(Ершов *et al*., 1999). Therefore, improving the technology of synthesis of diphenylamine-2-carboxylic acids and acridones remains as an important task.

[1.] Assistant Lecturer, Department of Chemistry, Mohnyin Degree College
[2.] Dr, Professor, Department of Chemistry, Kursk State University (Russia)

At the current movement, much attention is given in the chemical research for the development of new energy-saving, cost-effective technologies and saving environmental hazardous processes. In this regard, great importance to search for new ways by activating chemical processes. During the last twenty years, most interesting process has been shown for chemical reactions which carried under ultrasonic radiation. Uses of this alternative sonochemical activation method in many cases have been shown significantly better results than that reaction performed under the traditional condition (Htun Yar Zar and Kudryavtseva 2013a, 2013b). However, in the scientific literature the practical experiment for the effect of sonochemical activation on the synthesis of diphenylamine-2-carboxylic acids has not been reported. Therefore, to study the effect of sonochemical activation and kinetic parameters on the synthesis of acrid one derivatives is an urgent task.

Materials and Methods

Preparation of TLC chromatogram to study the chemical kinetic

The quantity of samples were analyzed by TLC video densitometry. To calculate the content of substances in the analyzed samples, calibration was performed for each of the components of the mixture. For this purpose, standard solutions were prepared containing all possible components of the reaction mixture in known quantities in ethanol.

Firstly the pure micro samples of reactants and products were dissolved in ethanol or *N*, *N*-dimethylformamide, the concentration of each component being in the range of 0.001 to 0.050 M. The presence in the selected samples of phosphoric acid during dissolution with *N*, *N*-dimethyl for mamide does not affect the characteristics of chromatograms. Then the diluted samples were alternately placed with a microcapillaryonto a chromatographic plate. The spots of the samples were placed in order, depending on the reaction time (0, 10, 20, second or min).The volume of the applied sample on TLC plate was 1 ± 0.2 μL. Then the TLC plate was placed in a prepared chromatography chamber for elution. The special mobile or eluent carried out the spot of the analyzed samples. When eluent reached to the top of the TLC plate, the plate was dried in an oven at a temperature of 80 ± 5 °C for 5 min.

The chromatogram was processed on a video densitometer with UV ray at the wavelength of 254 nm.

Analytical methods used

The progress of the reaction was monitored by TLC (Sorbfil plates of PTSX-P-V-UV, Eluent: toluene, ethanol, acetone in various ratios). FT-IR spectra were recorded on IR-200 Nicolet and FSM 1201 "Monitoring" FT-IR spectrometers, in KBr tablets. Elemental analysis was performed by using a CHO 1109 analyzer (Carlo Erba), ^{1}H NMR spectra recorded on a Bruker AV-600 spectrometer and shifts measured relative to tetramethylsilane, solvent DMSO-d6. Mass spectra were recorded with the ACQUITY UPLC H-Class system with UV/mass-detectors ACQUITY SQD Waters (electrospray ionization), and a Chromatography-mass spectrometer Varian, detector Saturn-2000 (electron impact ionization). UV spectra were obtained on a spectrometer UV-1800 Shimadzu (solvent ethanol).

The melting point of compounds obtained was measured by using Electrothermal IA 9000 series instrument. The kinetic parameters of the reactions were studied by using a Denscan densitometer. To calculate the kinetic parameters, the programs "Sorbfil 1.8" and "Microsoft Office Excel" were used and the program "Sigma Plot 11.0" was used to create the kinetic diagrams. The influence of ultrasonic radiation on the course of processes was studied by using ultrasonic device IL100-6 /1laboratory apparatus.

Synthesis of 2'-fluorodiphenylamine-2-carboxylic acid ([2-((2-fluorophenyl) amino] benzoic acid)under sonochemical activation

12 mL of distilled water was introduced to a 250 mL round bottomed flask. 2.55 g (0.063mol) of sodium hydroxide was dissolved in it. After complete dissolution, 10 g (0.063mol) of 2-chlorobenzoic acid and 7.12 g (0.064mol) of 2-fluoroaniline were added. Sonotrode was immersed into the reactor. Then 0.5 g (0.005 mol) of copper(I) chloride was added to the reaction mixture and 6.37 g (0.076 mol) of sodium hydrogencarbonate was added by portion. The reaction mixture was heated for about 3 h by stirring at the temperature of 90 °C, the reaction progress was monitored by TLC. After 3 h the reaction mixture was poured into a beaker containing 100 mL of hot water and then sodium hydroxide solution and 5 g of activated charcoal were

added. The mixture solution was heated to boil and filtered. The resulting filtrate was acidified with concentrated hydrochloric acid. The precipitate was filtered and washed with hot water until neutral pH, then product was dried at 100 °C.

Yield = 46 %: T_{melt}= 185-186 °C. R_f = 0.22 (Sorbfil, toluene : acetone : ethanol = 10 : 3 : 2): UV-Visible (Ethanol) (λ nm): 304; FT-IR-spectrum (KBr),ῡ , cm^{-1}: O-H (3435): N-H (3321); =C-H (2800-3100); C=O (1651); C=C aromatic (1400-1600): Mass spectrum= $C_{13}H_{10}FNO_2$ m/z 231 $[M+H]^+$ (100%).

Acid-alkaline treatment of 2'-fluorodiphenylamine-2-carboxylic acid

10 % of diphenylamine-2-carboxylic acidsolution was prepared with water solvent and then 30% of sodium hydroxide solution was poured into the solution. 5 g of activated charcoal was added and boiled the solution. The hot solution was filtered by suction pump. The filtrate was acidified with 15% hydrochloric acid solution. The precipitate was filtered by suction, washed the residue with hot water. The product was dried at temperature 100 ºC in circulation oven. The yield percent of product was calculated.

Synthesis of 4-fluoroacridin-9(10*H*)-one

10 g (0.045 mol) of 2'-fluorodiphenylamine-2-carboxylic acid and 40 g of polyphosphoric acid (PPA)were mixed in the beaker. The mixture was stirred without heating to get homogeneous. Sonotrode was immersed into the reactor with the predetermined temperature and the reaction was carried out. After the reaction was completed, the reaction mixture was poured into beaker which contained 300 mL of boiled water. The residue was filtered by suction pump and then the residue was treated with sodium carbonate solution to remove trace amount of 2'-diphenylamine-2-carboxylic acid. After that the yellow colour precipitate was filtered and dried at 100°C. The yield % of 4-fluoroacridone was 97.82 %.

Yield = 97.82%: T_{melt} = 318°C. R_f = 0.76 (Sorbfil, toluene : acetone : ethanol = 10 : 3 : 2): UV-Visible (Methanol) (λ nm): 394, 376, 306, 294, 250,223,216. FT-IR-spectrum (KBr), ῡ , cm^{-1}: N-H (3437): C-H (2900-3300):

C=O (1641): C=C aromatic (1400-1600); C-F (Arylhalide) (1100-1250). Mass spectrum= $C_{13}H_8FNOm/z$: 213 $[M+H]^+$(100%).

^{1}HNMR (DMSO-d6) δ: 7.16 ppm (m,J=8.14Hz,^{1}H)7.29 ppm (m,J=11.1Hz,^{1}H), 7.22 ppm (t,J=7.96Hz, ^{1}H) 7.67 ppm (t,J=8.0Hz,^{1}H), 7.38 ppm (d,J=8.03Hz,^{1}H), 8.28 ppm (d,J=7.96Hz,^{1}H), 8.31 ppm (d,J=7.86Hz,^{1}H), 11.95 ppm (s,^{1}H).

Results and Discussion

Quantity of Substances in a Mixture of Samples Analyzed by Thin-Layer Chromatography with Video-densitometry

During the course of the study the quantitative analysis of samples of reaction mixtures was carried out by using video densitometry. The consumption of the initial components and the formation of the reaction products were monitored by taking the analyzed sample from reaction mixture at definite time intervals. The thin layer chromatography with video densitometry method was used to analyze the quantity of reactants and products from reaction mixtures and determined by comparing pure reactant 2'-fluorodiphenylamine-2-carboxylic acid and fluoroacridone samples products (Lundanes *et al*., 2013).

By analyzing the TLC chromatogram with video densitometry, a table of the relative areas of the peaks of the separated substances and the R_f values of each peak was obtained. To calculate the relative content of substances in the analyzed samples, a calibration was performed for each of the components of the mixture in accordance with the method of Маркович *et al*., (2008). According to the Table 1, the relative areas of the peaks of substances in standard solution and the known amount of each component in the standard solution, the ratio of the mass of the substance to its relative peak area K_i were determined by the equation (1).

$$K_i = \frac{m_i}{S_i} \quad (1)$$

where m_i is the mass of the each component in the standard mixture, S_i is the relative peak area of the each component. The average data for each component was calculated and that was used to convert the relative areas in the analyzed samples into mass fractions of W_i according to the equation(2).

$$W_i = K_i \frac{S_i}{\sum_{j=1}^{n} K_j S_j} \quad (2)$$

where n is the number of all components.

The actual amount of 2'-fluorodiphenylamine-2-carboxylic acid (FDPACA) in the first sample was taken as 100%, and the corresponding 4-fluoroacridone (4-FA) was 0%. Taking the amount of molecular masses of the substances and the mass fractions of all components were recalculated to the extent of accumulation or expenditure (in the case of FDPACA). Examples of processing experimental data are given in Tables 1 and 2.

Table 1: Ratios of the Mass of Substances in the Standard Solution Corresponding to the Area of Spots in the Mixture of 2'-Fluorodiphenylamine-2-carboxylic acid and 4-Fluorocridone

Components	**R_f**	**Relative peak area, S_i**	**Mass of component in solution m (g)**	**m/S_i**
FDPACA	0.28	4335	0.01	2.30×10^{-6}
4-FA	0.85	9488	0.01	1.05×10^{-6}

Table 2: The Degree of Accumulation of 4-Fluoroacridone and the Expenditure of 2'-Fluorodiphenylamine-2-carboxylic acid when it is Cyclized in PPA at 80 °□ under Sonochemical Activation

No.	**Time,s**	**Relative peak area, S_i**		**Mass fraction, W_i**		**Degree of expenditure**	**Degree of accumulation**
		FDPACA	**4-FA**	**FDPACA**	**4-FA**	**(FDPACA)**	**(4-FA)**
1	0	1	0	1	0	1	0
2	300	0.838	0.161	0.919	0.080	0.919	0.088
3	600	0.503	0.496	0.689	0.310	0.689	0.338
4	1200	0.456	0.543	0.648	0.351	0.648	0.384
5	1800	0.321	0.678	0.508	0.491	0.508	0.536
6	2400	0.238	0.761	0.360	0.679	0.370	0.708
7	3600	0.122	0.877	0.233	0.766	0.233	0.836
8	5400	0.072	0.927	0.146	0.853	0.146	0.932
9	7200	0.026	0.973	0.055	0.944	0.055	1.031

Kinetic Parameters of Cyclization Reaction of 2’-Fluorodiphenylamine-2-carboxylic acid under Sonochemical Activations

2’-fluorodiphenylamine-2-carboxylic acid was synthesized by condensation of 2-chlorobenzoic acid and 2-fluoroaniline in the presence of sodium hydrogencarbonate and copper(I) chloride. In polyphosphoric acid (PPA), 2-fluoroacridone was synthesized by intramolecular condensation of 2’-fluorodiphenylamine-2-carboxylic acid. The chemical equationis described in the following.

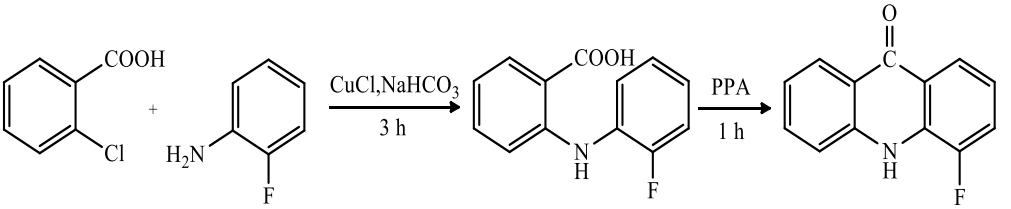

The kinetic parameters of intramolecular condensation of 2’-fluorodiphenylamine-2-carboxylic acid were determined by using numerical integration methods equation of reaction rate.

Determination of the kinetic parameters of cyclization of 2’-fluorodiphenylamine-2-carboxylic acid was carried out under conditions of sonochemical activation, but also under traditional conditions.

In the course of studies by using thin-layer chromatography with densitometry, kinetic curves for the consumption of 2’-diphenylamine-2-carboxylic acidvaries with temperature and time are illustrated in Figure 1.

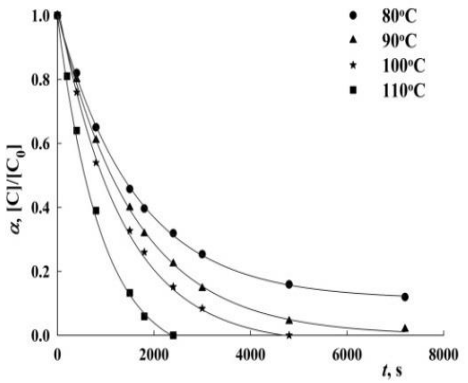

a

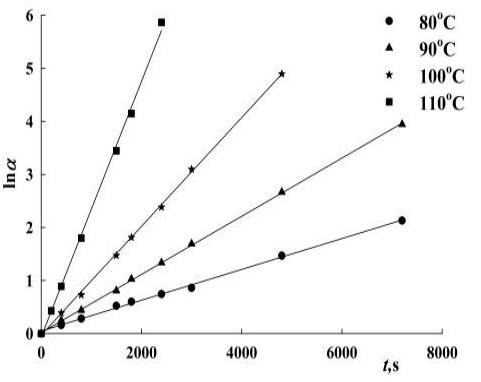

a'

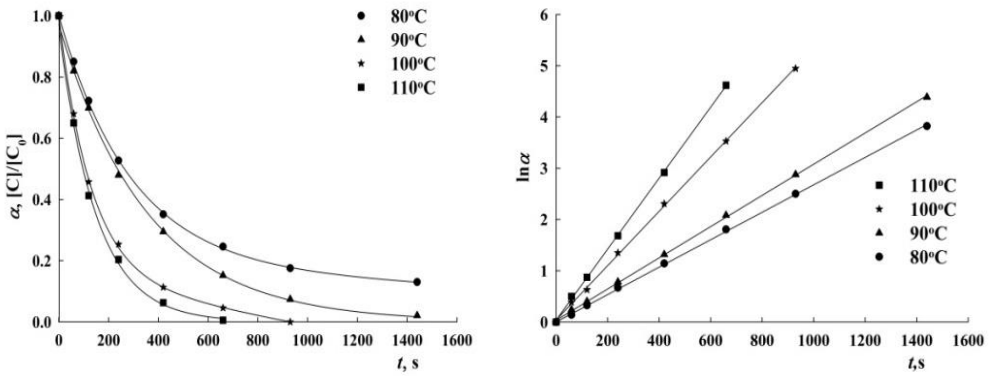

b b'

Figure 1: Kinetic curves for the consumption of 2'-diphenylamine-2-carboxylic acid in PPA under (a) thermal conditions and (b) sonochemical activations at different temperatures and their plots (a', b')

As can be seen from the curves shown in Figure 1 (b), under sonochemical activations, at the temperature of 80 °C the reaction time was 1 h and at 110 °C, only 15 min. In this case, under thermal conditions at a temperature of 80 °C, the reaction time was 4 h, and at 110 °C, 45 min. Thus, under sonochemical activations, the reaction time was greatly decreased. At the same time, it should be noted that the optimal reaction temperature can be considered at 100 °C to synthesis of acrid one derivatives. Since at lower temperatures the duration of the process was increased, and at 110 °C, according to chromatographic mass spectrometry data, traceamount of 2-fluorodiphenylamine was formed as by-product.

In kinetic equation, the order of the process of intramolecular condensation of 2'-fluorodiphenylamine-2-carboxylic acid in polyphosphoric acid under thermal and sonochemical activations was described by the first-order reactions, that was evidenced by the linear dependence of ln α -*t*.

Thus, for the cyclization of 2'-diphenylamine-2-carboxylic acid under thermal conditions, the rate constants of the reaction at the appropriate temperatures were: k_{80}= (29.92 ± 1.19) x 10^{-4} s^{-1}, k_{90} = (58.53 ± 2.34) x 10^{-4} s^{-1}, k_{100} = (106.43 ± 4.25) x 10^{-4} s^{-1}, k_{110} = (245.34 ± 9.81) x 10^{-4} s^{-1}. Under the

sonochemical activation, reaction rate constants was being as the following values: k_{80} = (21.69 ± 0.86) x 10^{-4} s^{-1}, k_{90} = (25.81 ± 1.03) x 10^{-4} s^{-1}, k_{100} = (52.89 ± 2.11) x 10^{-4} s^{-1}, k_{110} = (61.06 ± 2.46) x 10^{-4} s^{-1}.

To calculate the activation energy on the basis of the values of the rate constants of the reaction at different temperatures, the Arrhenius formula was used (Connors, 1990).

$$k = A \cdot e^{-\frac{E}{RT}} \quad (3)$$

$$\ln k = \ln A - \frac{E}{RT} \quad (4)$$

Figure 2 in the Arrhenius coordinates gives the dependence of the reaction rate constant on the temperature for the cyclization of 2'-fluorodiphenylamine-2-carboxylic acid.

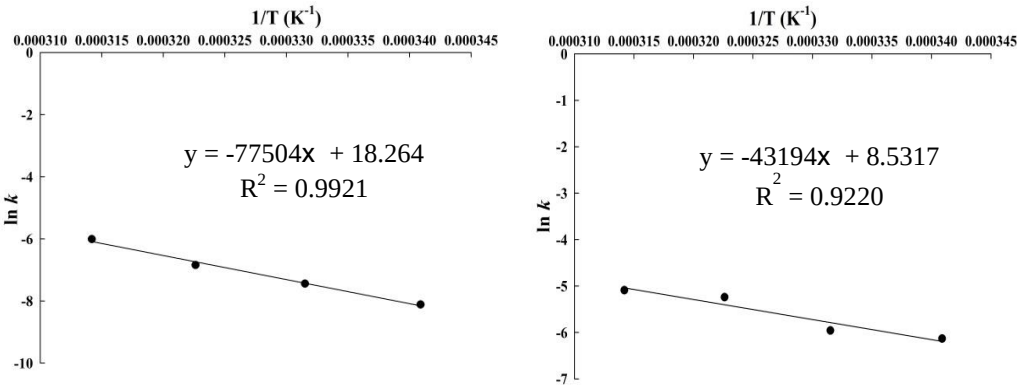

a b

Figure 2: Arrhenius plot for the processes of cyclization of 2'-fluorodiphenylamine-2-carboxylic acidin PAA under (a) thermal conditions and (b) sonochemical activation

The points fitted well to a straight line, from which the activation energy of was calculated. Under sonochemical activation the activation energy was 43.19 ± 4 kJ/mol and 77.50 ± 4 kJ/mol under thermal conditions. The obtained results show that under sonochemical activations the required activation energy was very low.

Conclusion

In this research, 2'-fluorodiphenylamine-2-carboxylic acid was synthesized by condensation of 2-chlorobenzoic acid and 2-fluoroaniline in the presence of copper(I) chloride. In polyphosphoric acid, 4-fluoroacridone compound was synthesized by intramolecular condensation of 2'-fluorodiphenylamine-2-carboxylic acidunder sonochemical activation. The synthesized compounds were identified by FT-IR Spectroscopy, Mass Spectrometry and ^{1}HNMR Spectroscopy methods. The effect of sonochemical activation on the synthesis of 4-fluoroacridone, the kinetic parameters: time, reaction rate constants, temperatures and activation energies were studied by TLC video-densitometry. According to the kinetic parameters, in the synthesis of 4-fluoroacridone under sonochemical activation, the reaction time was reduced, decreased activation energy and increased reaction rate, that was compared by relating the results of thermal conditions.

Acknowledgements

The authors thank Bogatyrev Kiril for technical assistance in the studies of chemical kinetic, Natalya Filatova for Mass spectra and Belousov Sergey (Head of Expert Research Department No 1 (CERD, RF) for FT-IR spectra. This study was supported by MOE (Ministry of Education, Myanmar). The authors also thank Dr Aye Aye Mon, Head and Professor, Department of Chemistry, Dr Daw San Myint, Associate Professor, Department of Chemistry, Mohnyin Degree College, for their wonderful supports.

References

Connors K. A. (1990).*Chemical Kinetics: The Study of Reaction Rates in Solution, Chemical kinetics*. New York: John Wiley & Sons, pp.187-191.

Ершов Ф.И., Романцов М.Г., Коваленко А.Л., Исаков В.А., Аспель В.Ю. (1999). "Циклоферон 12,5 % для инъекций: итоги и перспективы клинического применения: аннотированный сборник." Санкт-Петербург, pp 25.

Htun Yar Zar and Kudryavtseva T.N. (2013a). "The Kinetic Parameters of the Reaction of Intramolecular Condensation ofDiphenylamine-2-carboxylic acid underthe Sonochemical Activation." *Scientistsnotes Kursk GU*, Vol3(27).

HtunYarZar, and Kudryavtseva T.N. (2013b). "The Roleof Ultrasonic Radiationin the Synthesis of Diphenylamine-2-carboxylic acid and the Acridone." *Advances in Chemistry and Chemical Technology*, Vol27 (4), pp.89-92.

Lundanes E., Reubsaet L., Greibrokk T. (2013). "*Chromatography: Basic Principles, Sample Preparations and Related Methods*." 1st Ed,Wiley-VCH, pp 105-126.

Маркович Ю.Д., Пелевин Н.А., Кудрявцева Т.Н. and Лоторев Д.С. (2008). "Изучение Кинетики Реакций Циклизации Дифениамин-2-карбоновых кислот с Использованием Еонкослойной Хроматографии с Денситометрией."□□□□□□□□□□□ □□□□□□□□□□□. □□□□□□□□□□□□□□□□□□□□□, Vol 74 (4), pp.8-11.

Thorarensen A, Li J., Wakefield B.D., Romero D.L., Marotti K.R., Sweeney M.T., Zurenko G.E. and Sarver R.W. (2007)."Preparation of Novel Anthranilic Acids as Antibacterial Agents: Extensive Evaluation of Structural and Physical Properties on Antibacterial Activity and Human Serum Albumin Affinity."*Bioorg Medicinal Chemistry Letters*, Vol 17 (11), pp 3113-3116.

INVESTIGATION ON SOME PHYTOCONSTITUENTS AND BIOACTIVITY SCREENING OF LEAVES OF *Calotropis gigantea* R. Br. (Mayo)

Thandar Aung[1], Ye Myint Aung[2] , Theint Theint Phyo[3]

Abstract

In the present research, the leaf of *Calotropis gigantea* R.Br. (Mayo), Family- Apocynaceae, was chosen for investigation of some phytoconstituents and bioactivity studies such as acute toxicity, antitumor, and larvicidal activities. Acute toxicity of 95 % ethanol extract was studied with the dosage of 2000 mg/kg, 5000 mg/kg body weight in albino mice and no lethality was observed up to fourteen days after administration. The antitumor activities of PE, 95 % EtOH, EtOAc and H_2O extracts were screened on *Agrobacterium tumefaciens* by Potato Disc Assay method and all extracts exhibited antitumor activity after 5 days and 7 days observation. The larvicidal activities ($LC_{50\ and}\ LC_{90}$) of PE, 95 % EtOH, EtOAc and H_2O extracts were investigated in the range of 0.0125 to 0.2 g /100 mL by *Aedes* larvaemethod. The lowest knockdown of *Aedes* larvae was found at the concentration of 0.0125 g /100 mL of H_2O extract. The highest mortality rate (95.60 %) of *Aedes* larvae at the concentration of 0.2 g / 100 mL was found in the EtOAc extract. The lowest mortality rate (8.80 %) of H_2O extract was observed at concentration of 0.0125 g /100 mL. Among the tested four crude extracts, EtOAc extract showed the highest lethal activity (LC_{50} = 0.0235 g / 100mL and LC_{90} = 0.1224 g /100mL).

Keywords: acute toxicity, antitumor activities, *Calotropis gigantea* R.Br., larvicidal activities

Introduction

Calotropis gigantea R.Br. (Mayo), a member of the Apocynaceae family, is a well-known plant throughout the tropical world and they are native to the tropical and subtropical parts of Asia and Africa. Calotropis species are considered common weeds in some parts of the world. Flowers of these plants are fragrant and are often used in making floral tassels in some mainland Southeast Asian cultures. Fibers of these plants are called madar or mader (Bhagavathy and Jancy, 2015). In Myanmar, the plant is distributed in

1. Dr, Associate Professor, Department of Chemistry, Pathein University
2. Dr, Professor and Head, Department of Chemistry, Pathein University
3. MRes Candidate, Department of Chemistry, Pathein University

various regions and used as remedy for various medicinal purposes. Myint Myint Khine (2007) reported for her PhD dissertation that leaves of *C. procera* (Mayo) possessed antimicrobial activity. The importance of medicinal plants to the economy of low-income countries remains critical and strategic because medicines are keys to a health population that drives and sustain the economy. In this research work, the leaves of *C. gigantea* (Mayo) was chosen for determination of some phytochemical constituents, and screening of some bioactivities.

Botanical Aspect of *Calotropis gigantea* R.Br.

Family	: Apocynaceae
Sub-family	: Asclepiadaceae
Botanical name	: *Calotropis gigan*
Myanmar name	: Mayo
English name	: Swallow-Wort,]
Synonyms	: *Asclepias gigantea* L.
Part used	: Leaves

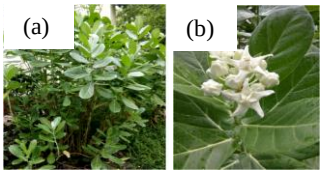

Image of *C.gigantea*
(a) plant (b) flower

Local Uses of *Calotropis gigantea* R.Br. (Mayo)

Traditional practice in Myanmar especially in Ayeyarwady Region, leave of *C.gigantea* is being used mainly by mixing leave with latex in the controlling of snake bite, treatment of paralysis, chronic sinusitis, swellings, and intermittent fevers, cold and asthma. Moreover, after boiling the whole parts of the plants, the obtained watery extract was used to relief arthritic. For low-income countries to attain any appreciable level of self-reliance regarding availability of safe and effective pharmaceuticals use for the management of endemic disease conditions, it was considered a priority because of the importance of self-reliance in the current and perhaps future economic. Today, traditional medical practice has been recognized by the world health organization (WHO) as a building block of primary healthcare. But, safety should be the overriding criterion in the selection of herbal remedies for use in healthcare (Patli and Saini, 2012).

Medicinal Uses of Various Parts of *Calotropis gigantea* R.Br. (Mayo)

The *C. gigantea* plant is used for skin diseases, boils and sores and as a tonic and purgative in small doses, and as an emetic in larger doses. The powdered root bark is used to cure dysentery, elephantiasis, and leprosy. The stem bark is diaphoretic and expectorant, and is used for dysentery, spleen complaints, convulsions, lumbago, scabies, ringworm, pneumatisms and tumors and also as an antiseptic, vermifuge, emetic and purgative, as well as for poisoning arrows. The powdered flowers are given for coughs, colds and asthma. The crushed and warmed leaves are applied on burns, headaches and rheumatic pains, and as a tincture for intermittent fever (Gaur *et al*., 2013). Milky white latex is sticky and the plant is popular amongst the common population because of this peculiarity. This is mildly poisonous and is considered as one of the plant toxins in Ayurveda. Though toxic, this latex can be purified and put to use as a very effective antidote as well as herbal medicine.

This paper focuses on the investigation of phytochemical constituents present in *C. gigantea* leaves and some of its biological activities such as acute toxicity, antitumor activity and larvicidal activity.

Materials and Methods

Sampling of Plant Material and Identification

The leaves of *C. gigantea* were collected from Ngawon Kyung Tha Street, Pathein Township, Ayeyarwady Region, Myanmar, during June to August, 2017. The collected leaves sample was identified as *Calotropis gigantea* R.Br. (Mayo) according to the authorized botanist from Department of Botany, Pathein University. The collected fresh leaves samples were washed and air dried at room temperature for two weeks and the dry leaves were ground into powder and then stored in air tight container.

Preliminary Phytochemical Investigation of the Leaves of *C. gigantea*

In order to classify the types of organic constituents present in samples, preliminary phytochemical tests on leaves samples were carried out according to the appropriate reported methods.

Preparation of Crude Extracts by Direct Extraction Method for Screening of Some Biological Activities

Each dried powdered sample (50 g) was extracted with 150 mL of pet-ether (60-80 °C) for 6 h by using Soxhlet extractor. The filtrate was concentrated by removal of the solvent under reduced pressure to give the respective PE crude extract. Ethyl acetate, 95 % ethanol, and watery extracts were also prepared by similar manner mentioned in above procedure. Each extract was dried at normal pressure on a water bath and stored under refrigerator for screening some bioactivities.

Screening of Some Bioactivities of the Crude Extracts of *C. gigantea*
(a)Determination of acute toxicity of the leaves of *C. gigantea*

To determine the consequent of the plant and to determine the nature and degree of toxicity produced by these extracts and to find out the medium lethal doses (LD_{50}) of the extracts, acute toxicity test was done. Usually the acute lethality of a compound is determined on the basis of deaths occurring in 24 h but the survivors should be observed for at least seven days in order to detect delayed effects. In this study, acute toxicity effect of ethanol extract of *C.gigantea* leaves (two doses) were determined on albino mice at Laboratory Animal Services Division, Department of Medical Research (DMR), Yangon.

Acute toxicity of different doses of ethanol extracts of *C.gigantea* (Mayo) leaves was evaluated by the methods of OECD Guidelines for the Testing of Chemicals 423 (OECD, 1998; OECD, 2000). According to the test description, total number of 18 adult female albino mice, weighing (25-30g) were selected and divided into three groups. Each group contained six animals. They were maintained in accordance with the recommendation of the Guide for the Care and Use of Laboratory Animals published by the US National Institutes of Health (NIH Publication N. 85-23, revised 1996) for studies involving experimental animals. They had free access to feed and clean drinking water during the three days acclimatization period and throughout the experimental period. They were fasted for 18 h before giving the extracts. Group (A) mice were orally administrated with 95 % EtOH extract of *C.gigantea* (Mayo) leaves 2000 mg/kg dose. Group (B) mice were given orally with 95 % EtOH extract of *C.gigantea* (Mayo) leaves 5000

mg/kg dose. Group (C) mice performed as a control group and they were treated with clean water and normal animal food. All groups of mice were kept in the three mouse cages in the separated room at the room temperature of 26 º C. After administration of extract, each group of animals was observed first 6 h continuously for mortality and behavior changes. Then the animals each was checked in 24 h for fourteen days (Table 1).

(b) Screening of antitumor behaviors of crude extracts by potato crown gall test or potato disc assay method

The antitumor activity screening of different crude extracts such as pet-ether, ethyl acetate, 95% ethanol, and watery extracts of leaves of *C. gigantea* was carried out against *Agrobacterium tumefacien* by Potato Crown Gall test or Potato Disc Assay method at the Pharmaceutical Research Department, Ministry of Industry, Yangon, Myanmar (Moh Moh Aye, 2009). Fresh, disease free potato tubers were obtained from local market and transferred within 48 h to the laboratory. Tubers of moderate sizes were surface-sterilized by immersion in 50 % sodium hypochlorite (Clorox) for 20 min. The ends were removed and soaked for 10 min more in Clorox. A core of the tissue was extracted from each tuber by using surface-sterilized (ethanol and flame) 1.5 cm wide cork borer. And, 2 cm pieces were removed from each end and discarded and the remainder of the cylinder is cut into 0.5 cm thick discs with a surface-sterilized cutter. The discs were then transferred to 1.5 % agar plates (1.5 g of Difco agar was dissolved in 100 mL of distilled water, autoclaved and 20 mL poured into each petri dish). Each plate contained three discs. The procedure was done in the clean bench in the sterile room. 50 mg, 100 mg and 150 mg of each extract was separately dissolved in 2 mL of dimethyl sulphoxide (DMSO); the solution was filtered through millipore filters (0.22 μm) into a sterile tube. 0.5 mL of this solution was added to 1.5 mL of sterile distilled water and 2 mL of broth culture of *A. tumefaciens* strain (48 h culture containing $3\text{-}5\times10^{9}$cells/mL) were added aseptically. Controls were made as mentioned above procedure.

Using a sterile disposable pipette, 1 drop (0.05 mL) from these tubes was used to inoculate each potato disc, spreading it over the disc surface. The process of cutting the potatoes and incubation must be conducted within

30 min. The plates were sealed with tape to minimize moisture loss and incubated at room temperature for 12 days. After incubation, Lugol's solution (I_2-KI) was added and the tumors were counted with a microscope and compared with control. The antitumor activity was examined by observation of tumor produced or not.

(c) Determination of larvicidal activity of the leaves of *C. gigantea* (Mayo)

Based on preliminary tests, dilutions of crude samples were prepared with same type of purified water. Different periods. Dead larvae were identified when the larvae failed to move after probing with a needle in the cervical region. Mortality rate was recorded after 24 h daily. The lethal concentrations of LC_{50} and LC_{90} values were calculated after 24 h using dose-effect probity.

Results and Discussion

The results of preliminary photochemical analysis of the leaves extract of *C. gigantea* showed that the leaves contain alkaloids, steroids, saponins, glycosides, tannins and α-amino acids. But reducing sugars, flavonoids, starch, phenolic compounds, carbohydrates, terpenoids and cyanogenic glycosides were found to be absent in the leaves of Mayo.

Acute Toxicity

Acute toxicity screening of 95% EtOH extract *C. gigantea* leaves, was done with the dosage of 2000 mg/kg and 5000 mg/kg body weight in each group of albino mice. The condition of mice groups were recorded after fourteen days administration (Table 1). The results show that no lethality of the mice was observed up to fourteen days administration. Each group of animals were also observed still alive and did not show any visible symptoms of toxicity like restlessness, respiratory disorders, convulsion, aggressive activities, coma and death.

Table 1: Acute Toxic Effect of Ethanol Extract of *C. gigantea* (Mayo) Leaves on Albino Mice Model after Two Weeks Administration

No.	Group	Extract Administration	Dosage (mg/kg)	No. of death	% of death after 14 days
1	Group A	95% EtOH	2000	Nil	0
2	Group B	95% EtOH	5000	Nil	0
3	Group C	No administration	Nil	Nil	0

Screening of Antitumor Behaviours of Some Crude Extracts from the Leaves of Mayo

The antitumor behaviours screening of different crude extracts **(**PE, EtOAC, EtOH and watery extracts) of the leaves of Mayo were carried out against *Agrobacterium tumefaciens* by Potato Crown Gall test or Potato Disc Assay method (Table 2 and Figures 2 and 3). All of the tested crude extracts of the leaves of Mayo were found to exhibit antitumor activity against *A. tumefaciens.*

Table 2: Comparsion among Antitumor Behavioues of Different Concentrations of Crude Extracts from the Leaves of Mayo

Extracts	Concentration (mg mL^{-1})	Antitumor Activity	
		Days-5	Days-7
PE	25	+	+
	50	+	+
	75	+	+
EtOAc	25	+	+
	50	+	+
	75	+	+
95% EtOH	25	+	+
	50	+	+
	75	+	+
H_2O	25	+	+
	50	+	+
	75	+	+

(+) = Exhibit antitumor activity (–) = No antitumor activity

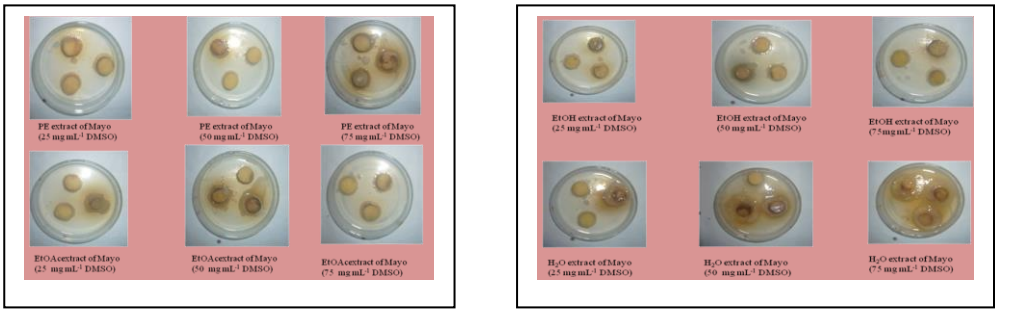

Figure 2: Antitumor behaviours of different concentrations of PE and EtOAc, EtOH and H_2O extracts of Mayo leaves on days 5

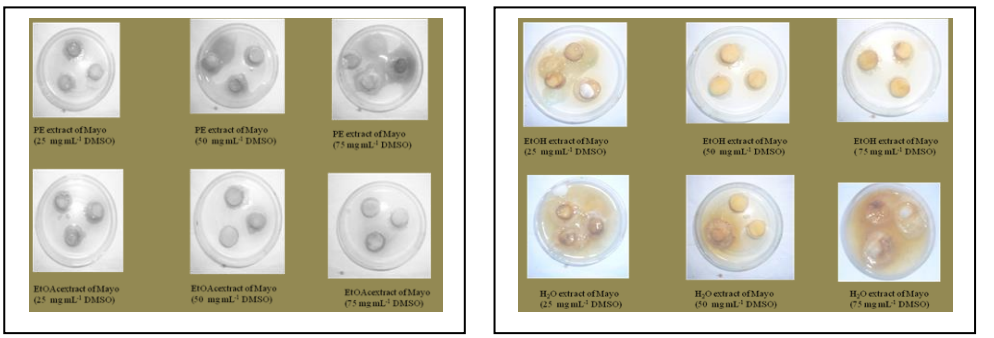

Figure 3: Antitumor behaviours of different concentrations of PE and EtOAc, EtOH and H_2O extracts of Mayo leaves on days 7

Larvicidal Activity of the Leaves of *C. gigantea* (Mayo)

According to the larvicidal activity study, the highest knockdown effect at the concentration of 0.2 g /100 mL was found to be 83.20 % in EtOH extract, followed by 82.80 % in EtOAc and 81.60% in PE extracts. The lowest effect was found as 67.20 % in H_2O extract was shown in Table 3. Moreover, the lowest knockdown of *Aedes* larvae was found at the concentration of 0.0125 g /100 mL of H_2O extract. The highest mortality rate of *Aedes* larvae at the concentration of 0.2 g /100 mL was found to be 95.60 % in EtOAc extract and followed by 94.00 % mortality in EtOH and PE extracts. In 0.1 g /100 mL concentrations of EtOH, EtOAc and PE extracts, mortalities were found as 86.80 %, 85.60 % and 80.40 % respectively as shown in Table 4.

Table 3: Knockdown Effect (within 60 min) of Different Dilutions of *C.gigantea* on the Instars *Aedes aegypti* Larvae

Concentration (g / 100mL)	Number of Knockdown and % Knockdown effect of different extracts			
	EtOH	PE	H_2O	EtOAc
0.20	208 (83.20)	204 (81.60)	168 (67.20)	207 (82.80)
0.10	172 (68.80)	168 (67.20)	146 (58.40)	172 (68.80)
0.05	137 (54.80)	119 (47.60)	76 (30.40)	187 (74.80)
0.025	103 (41.20)	67 (26.80)	48 (19.20)	118 (47.20)
0.0125	35 (14.00)	34 (13.60)	18 (7.20)	51 (20.40)
Control	0 (0)	0 (0)	0 (0)	0 (0)

Total Larvae-250

Table 4:Mortality Effect (within 24 h) of Different Dilutions of *C. gigantea* Leaves Extracts against 3rd and 4th Instars *Aedes aegypti* Larvae

Concentration (g/100mL)	Number of Mortality and % Mortality			
	95% EtOH	PE	H_2O	EtOAc
0.2	235 (94.00)	235 (94.00)	186 (74.40)	239 (95.60)
0.1	217 (86.80)	201 (80.40)	139 (55.60)	214 (85.60)
0.05	168 (67.20)	154 (61.60)	96 (38.40)	177 (70.80)
0.025	117 (46.80)	106 (42.40)	54 (21.60)	139 (55.60)
0.0125	83 (33.20)	86 (34.40)	22 (8.80)	75 (30.00)
Control	0 (0)	0 (0)	0 (0)	0 (0)

Total Larvae-250

Although mortality of H_2O extract was 55.60 %, the lowest mortality rates of all extracts were observed at the concentration of 0.0125 g /100mL. The doses of 50 % mortality (LC50) and 90 % mortality (LC90) values of all extracts against 3th and 4th instars *Aedes* larvae are shown in Table 5. The lowest dose for 50% mortality was found 0.0235g of EtOAc extract concentration followed by 0.0249 g / 100 mL and 0.0277 g / 100 mL of EtOH and PE extract respectively. H_2O extract found in highest amount of dose 0.0791g / 100 mL concentration was needed for 50% mortality of 3rd and 4th instars *Aedes* larvae. The lowest dose (highest efficiency) for 90% mortality was 0.1224 g / 100 mL of EtOAC extract concentration followed by 0.1386 g / 100 mL of 95% EtOH in the highest amount of dose and it was 0.4771 g/ 100 mL concentration for 90% mortality of 3rd and 4th instars *Aedes* larvae in 100 mL water.

Table 5: Lethal Concentration (LC) Values of *C. gigantea* Leaves Extracts against 3rd and 4th Instars *Aedes aegypti* Larvae

Lethal Concentration	*C.gigantea* Leaves Extracts (g / 100 mL)			
	95% EtOH	PE	H_2O	EtOAc
LC_{50}	0.0249	0.0277	0.0791	0.0235
LC_{90}	0.1386	0.1661	0.4771	0.1224
Chi Square X^2	3.5203	10.7585	0.5489	2.2458
Df	4	4	4	4
P value	0.05	0.05	0.05	0.05

Conclusion

The present study on the leaves of *C. gigantea* provides the following information. The preliminary phytochemical investigation revealed the presence of alkaloids, steroids, saponins, glycosides, tannins and α-amino acids in the leaves of *C. gigantea*. But, reducing sugars, flavonoids, starch, phenolic compounds, carbohydrates, terpenoids and cyanogenic glycosides were found to be absent in the leaves of *C. gigantea*. The constituents such as alkaloids and steroids present in the sample may contribute to possess bioactivities such as antimicrobial, antioxidant, anticancer, antitumor,

antipyretic, and antiulcer properties in Mayo. According to the screening of acute toxicity activity of the 95% EtOH extract of leaves of Mayo, the results showed that no lethality of the mice was observed up to fourteen days after administration. Each group of animals was also observed still alive and did not show any visible symptoms. And then, leaves extract of *C. gigantea* may have good larvicidal activity. Moreover, due to its antitumor activity, leaves of *C. gigantea* may be used to prevent the diseases related to tumor and cancer. From the acute toxicity test on leaves of Mayo, leaf extracts were found to be free from acute toxic. This study provides the health at affordable cost and *C.gigantea* leaves have valuable medicinal properties and may be used safely.

Acknowledgement

The authors would like to thank to the Myanmar Academy of Art and Science and its Editors, Ministry of Education in Myanmar, for giving us to present and press this research paper. We would like to thank to the Department of Higher Education, Ministry of Education in Myanmar, for giving us the opportunity to do this research. Our deepest gratitude is expressed to Dr Si Si Hla Bu, Rector, Pathein University, for her encouragement, kind guidance, and kind help to do this research. We wish to thank Dr Than Tun and Dr Nilar Myint, Pro-Rectors, Pathein University for their invaluable advices and encouragement. Thanks are also extended to Dr Than Than Oo (Professor), Department of Chemistry, Pathein University, for her helpful advice, precious suggestions and provision of research facilities at the Department of Chemistry, Pathein University, Myanmar.

References

Bhagavathy, S. and M. Jancy. (2015). "Antioxidant and Antidiabetic Potentials of *Calotropis gigantea* in RIN-5F Pancreatic Cell Lines". *International Journal of Pharmacy and Pharmaceutical Research.* vol 5 (1), pp 176-199

Gaur L.B.,. Bornare S.S., Chavan A.S., Mukh R., Singh S.P., Gaur S.C. and Sudhir K..(2013). "Biological Activities and Medicinal Properties of Madar (*Calotropis gigantea* R.Br)" *International Peer Reviewed Ayurved Journal* vol.1, pp-**(**1)

Moh Moh Aye. (2009). *Investigation of some Bioactive Organic Constituents from Roots of Sesgnia sesban* (L.) Merr.(*Ye-Thu-Gyi) and Morinda Tinctoria* Roxb.*(Tau-Ye-Yo) and Screening of some Biological Activities".* Ph.D. Dissertation, Chemistry Department, Yangon University, Myanmar, pp11-39

Myint Myint Khine. (2007).*Investigation of Organic Constituents and Antimicrobial Activities of Kaempferia Galanga* L. *(Kungsa-Ga-Mon) Rhizomes and Calotopis procera* R. Br. *(Ma-Yo) Leaves* Ph.D. Dissertation, Chemistry Department, Yangon University, Myanmar

OECD.(1998). Harmonized Integrated Hazard Classification System for Human Health and Environmental Effects of Chemical Substances as Endorsed by the 28th Joint Meeting of the Chemicals Committee and the Working Party on Chemicals, Part 2, pp.21

OECD.(2000). Guidance Document on Acute Oral Toxicity. Environmental Health and Safety Monograph Series on Testing and Assessment No. 24

Patli, S.M. and Saini, R. (2012). Antimicrobial Activity of Flower Extract of *Calotropis gigantea Int. J. Pharm. Phytopharmacological Research*,vol 1 (4), pp142-145

TREATMENT OF INDUSTRIAL WASTEWATER SAMPLES WITH SEQUENCING BATCH BIOFILM REACTOR

Thandar[1], Hnin Thanda Aung[2], Khaing Khaing Kyu[3]

Abstract

The aim of this research work is to prepare biofilm for the treatment of three industrial wastewater samples from dry cell battery factory, nickel plating factory and leather factory in industrial zones I and II, Mandalay Region, Myanmar by using sequencing batch biofilm reactor. Totally four bacterial strains were isolated from three wastewater samples and identified. Isolated bacterial strains were recultured on sponges that were used as biofilm in this study. Decolourization activity of sequencing batch biofilm reactor was studied and found to be 54.29% (after 72 h treatment), 74.13 % and 53.32 % (after 64 h treatment) for wastewater samples from dry cell battery, nickel plating and leather factories wastewater samples, respectively. The order of removal of metal ions from three industrial wastewater samples by using sequencing batch biofilm reactor was Cr^{3+}> Pb^{2+}> Cd^{2+}. Some physicochemical parameters such as pH, turbidity, total dissolved solids (TDS), dissolved oxygen (DO), chemical oxygen demand (COD) and biochemical oxygen demand (BOD) of industrial wastewater samples before and after treatment with sequencing batch biofilm reactor were also investigated.

Keywords: sequencing batch biofilm reactor, industrial wastewaters, bacterial strains,decolourization activity, heavy metals

Introduction

In the current era of globalization and rapid industrialization, the environmental issues are becoming more and more nuisance for human being. Heavy metals present in wastewater and industrial effluent is major concern of environmental pollution. Removal of heavy metals from the effluent are very important part of the research carried out in environmental field (Dhokpande and Kaware, 2013). The sequencing batch reactor (SBR) can be combined with biofilm growth on the surface of a support material, originating the sequencing batch biofilm reactor (SBBR) (Rajput and Khambete, 2015).

[1.] Dr, Lecturer, Department of Chemistry,Pathein University
[2.] Dr,Lecturer, Department of Chemistry,Kalay University
[3.] Dr, Professor, Department of Chemistry, University of Mandalay

Sequencing batch biofilm reactor (SBBR) systems, operated in a fill-and-draw mode, have been successful in the treatment of wastewater (Di Iaconi *et al*., 2004; Rodgers *et al*., 2004; Prendergast *et al*., 2005). Biofilm carriers are used for upgrading current wastewater treatment systems. In the SBBRs, the biomass grows as a biofilm on spongy carriers that move freely into the wastewater. In a biofilm process, dissolved organic materials and nutrients are directly absorbed from bulk phase to the biofilm by means of concentration gradient, where dissolved heavy metals are adsorbed onto and into biofilm as a result of interactions between metal ions and the negatively charged microbial surfaces, gradually reducing the aqueous metal concentration (Abu-Bakar *et al*., 2008;Rahman*et al*., 2013).

Microbial biomass can bind heavy metals either actively or passively or by a combination of both processes. Several studies have shown the effects of metal concentration on bacteria resistance to heavy metals and many of these research have proven that high resistance is related to high metal concentration. This means that there is a positive correlation between the metal concentration and bacterial tolerance to heavy metals and it can be effective to have access to a higher efficiency in biological purification of contaminated soils and wastewater samples (Nasrazadani *et al*., 2011).

This study was aimed to remove colour and heavy metals from industrial wastewaters using sequencing batch biofilm reactor.

Materials and Methods

Samples collection

Two selected wastewater samples from dry cell battery factory and nickelplating factory were collected from Industrial zone I in Pyigyitagun Township, Mandalay Region (Figure 1). Another wastewater sample from leather factory was collected from Industrial zone II in Amarapura Township, Mandalay Region (Figure 2). Location sites are shown in Figure 3.

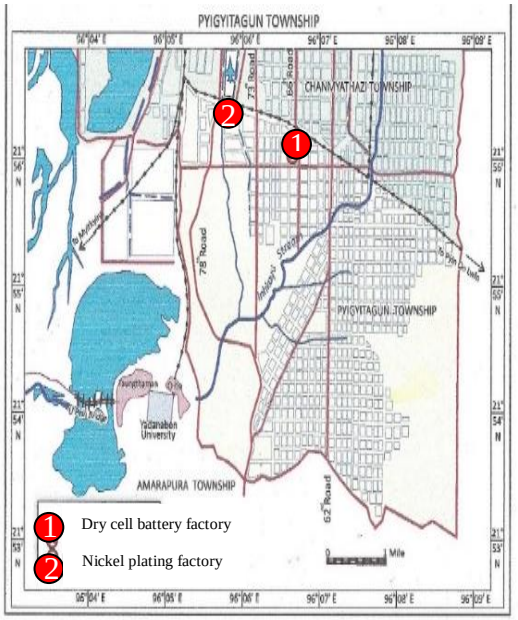

Figure 1: Location map of the study area (1)

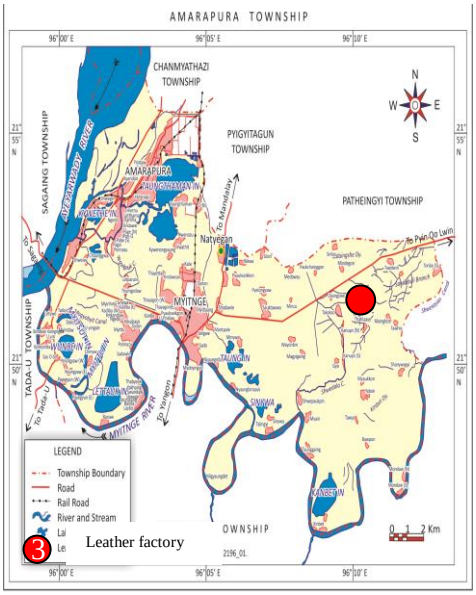

Figure 2: Location map of the study area (2)

(a) (b) (c)

Figure 3: (a) Dry cell battery factory, (b) Nickel plating factory and (c) Leather factory and their drainages

Wastewater Treatment by Using Sequencing Batch Biofilm Reactor

The sequencing batch biofilm reactor technology is a modification of the much popular activated sludge process (ASP) (Dutta and Sarkar, 2015). It was applied the wastewater treatment using with bacterial biofilm. For reducing the colour and toxic metal ions from wastewater effluent, sequencing batch biofilm reactor was used and detected by the activity of indigenous bacterial isolates and thus,is considered to be a suitable system for wastewater treatment in pilot scale. In this study, sequencing batch biofilm reactor was fabricated by steel with the dimension of 33 cm height, 26 cm diameter, total volume capacity of 17.7 L, and working volume of 14 L. The speed of impeller was adjusted at 220 rpm. There are three outlets (1, 2 and 3) in the reactor. Details of the reactor design are described in Table 1 and the reactor and its parts are shown in Figure 4.

Table 1 Reactor Configuration

Specification	Quantity
Diameter of reactor (cm)	26
Height of reactor (cm)	33
Total volume in reactor (L)	17.7
Working volume in reactor (L)	14
Type of support materials used in reactor	polyurethane sponges
Size of polyurethane sponges (cm ×cm × cm)	2.54 ×2.54 × 2.54
Number of polyurethane sponges	250
Total volume of polyurethane sponges (mL)	3769
Impeller speed (rpm)	220
Air flow rate	0.69 dmL/min

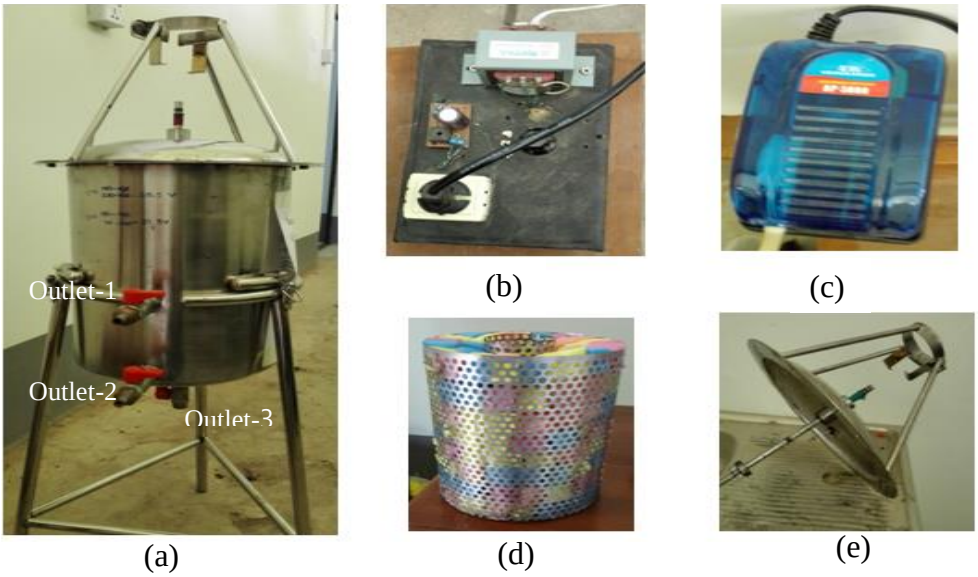

Figure 4: (a) Sequencing batch biofilm reactor and its parts used in this study (b) Impeller speed controller, (c) Air compressor, (d) Solid support container (e) Impeller

Isolation of Bacteria from the Wastewater Samples

To cultivate bacteria from wastewater samples, 1 mL of wastewater sample was directly cultured on nutrient agar in the sterile petri dish. It was incubated overnight at 37ºC. Numerous colonies with different morphologies appeared on the agar plate were obtained. The distinct clear colonies were collected and then, they were separately sub-cultured on nutrient medium to get the pure culture. Then, microscopic morphology of the bacterial isolates were determined using Gram's staining method.

Preparation of Media for Broth Culture

Firstly, 750 mL of distilled water was added in a 800 mL beaker containing 7.5 g of nutrient broth. The beaker was shaken with thermostatic control magnetic stirrer for 10 minto mix the ingredients thoroughly. The same solution was prepared to get 1500 mL nutrient broth. The flasks were plugged with cotton wool, sealed with aluminum foil and then sterilized in an autoclave at 121ºC for 15 min under 15 psi pressure. After cooling the broth

solution at room temperature, single colony of selective four bacterial strains were added. Before use, the bacterial strain from the plate was checked by Gram's staining method. Finally, the flasks were incubated at 37 ºC for 48 h. It was used as the mother culture.

Preparation of Stock Solution

$(NH_4)_2SO_4$ (0.75 g), glucose (15 g), yeast (30 g), molasses (750 mL) and distilled water (15 L) were mixed into the pot. Then, the solution was heated for boiling. After cooling the solution at room temperature, it was sterilized by autoclaving at 121ºC for 30 min.

Wastewater Treatment by Sequencing Batch Biofilm Reactor

At first, 250 numbers of polyurethane sponges (size: 2.54 cm × 2.54 cm × 2.54 cm) were filled into the steel solid support container. Then it was sterilized in an autoclave at 121 ºC for 30 min. The mother culture including four bacterial strains was then introduced into the reactor with the ratio of 1:10 culture broth and stock solution. After 3 days incubation for bacteria, the cultured broths in the reactor were drawn out from the sludge disposal. After that, the reactor was filled with the wastewater for the treatment. The treated samples were withdrawn at 4h intervals from the outlet 2. The decolourization activity was measured at 450 nm wavelength by UV spectrophotometer. Moreover, atomic absorption spectrophotometer was used for determination of metal ions (Cd^{2+}, Cr^{3+}, Pb^{2+}) from wastewater samples. The percent decolourization and the removal percentage of metal ions (Cd^{2+}, Cr^{3+}, Pb^{2+}) were computed.

Determination of some Physicochemical Parameters of Three Industrial Wastewater Samples

In this experiment, some physicochemical parameters such as pH, turbidity, total dissolved solids (TDS), dissolved oxygen (DO), chemical oxygen demand (COD) and biological oxygen demand (BOD) of industrial wastewater samples before and after treatment with sequencing batch biofilm reactor were analyzed according to standard analytical procedures (Government of India and Government of the Netherlands, 1999; PASCO,

2010) at Ministry of Agriculture, Livestock and Irrigation Department of Fisheries Aquaculture Division, Freshwater Aquaculture Research Water and Soil Examination Laboratory in Yangon.

Results and Discussion

Isolation and Identification of Bacteria from the Wastewater Sample

Totally four bacterial strains (two bacterial strains from wastewater sample of dry cell battery factory, P_1 and P_2, one bacterial strain from wastewater sample of nickel plating factory, $N_5$and one bacterial strain from wastewater sample of leather factory, L) were isolated. These isolated four bacterial strains were identified by Gram's staining reaction, colonial morphology and microscopic morphology. Colonial morphology and microscopic morphology of isolated strains are shown in Figure 5.

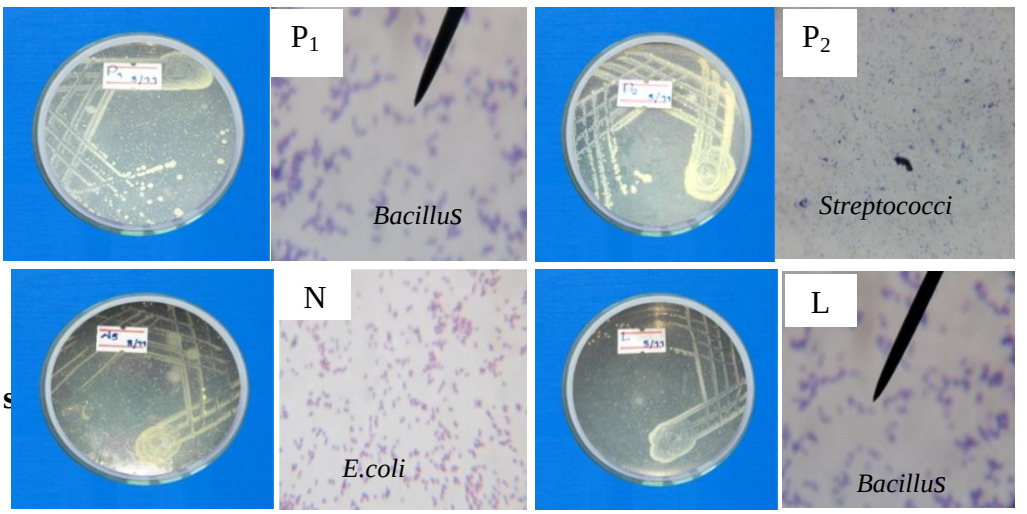

Figure 5: Colonial and microscopic morphology of the bacterial isolate P_1, P_2, $N_5$and L on nutrient media from three industrial wastewater

According to morphology study, two bacterial strains (P_1, P_2) from wastewater sample of dry cell battery factory and one bacterial strain (L) from wastewater sample of leather factory were gram positive (+). Another one bacterial strain (N_5) from wastewater sample of the nickel plating factory was

found to be gram negative (-). Among them, one gram positive (+) from wastewater samples of dry cell battery factory (P_1)and leather factory (L) were found to be *Bacillus*. Another gram positive (+) from wastewater sample of the dry cell factory (P_2) was found to be *Streptococci*. One gram negative (-) from wastewater sample of nickel plating factory (N_5) was *E.coli.*

Bacterial Biofilms

The biofilm of each bacterial isolate was prepared for wastewater treatment as shown in Figure 6.

(a) (b) (c)

Figure 6: Process of biofilm (a) Spongy in initial broth culture P_1, P_2, N_5, L (b) Broth culture after 2 days (c) Four biofilms

The sponge and the adsorption of each isolated bacterial strain on sponge under microscopic investigation are shown in Figures 7 and 8 respectively. The adsorption of isolated bacterial strains (P_1, P_2, N_5 and L) on sponge showed different morphologies under microscopic investigation.

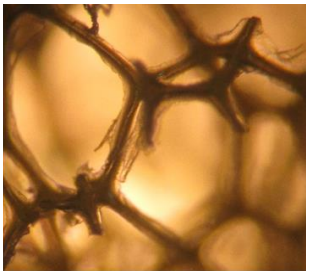

Figure 7: Sponge only under microscopic investigation

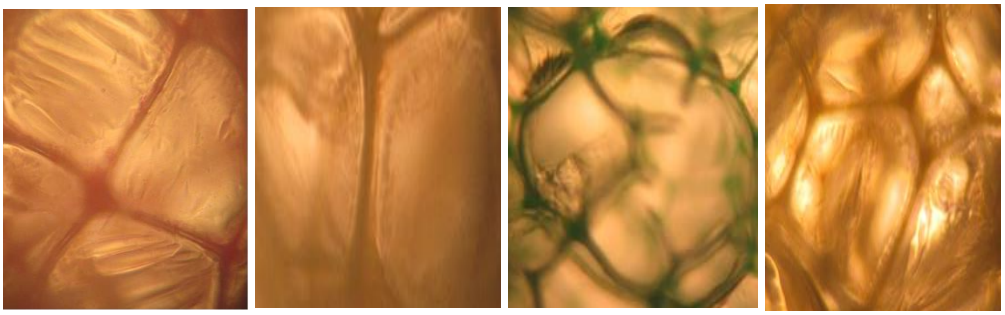

(a) (b) (c) (d)

Figure 8: Bacterial adsorption on sponge after 2 days incubation under microscopic investigation (a) *Bacillus* sp. (P_1) (b) *Streptococci* sp. (P_2) *(c) E.coli* (N_5) and (d) *Bacillus* sp. (L)

Wastewater Treatment by Using Sequencing Batch Biofilm Reactor

The decolourization activity and the removal percentage of metal ions after wastewater treatment by using sequencing batch biofilm reactor were investigated in this study. Firstly,the wavelengths of maximum absorption for industrial wastewater samples were determined.As shown in Table 2 and Figure 9, the wavelengths of maximum absorption for industrial wastewater samples from dry cell battery factory, nickel plating factory and leather factory were observed at 450 nm. Thus, the wavelength of 450 nm was chosen for the determination of decolourization activity.

Table 2: Relationship between Absorbance and Wavelength for Three Industrial Wastewater Samples from Factories

Wavelength (nm)	Absorbance of wastewater		
	Dry cell battery factory	Nickel plating factory	Leather factory
400	0.570	0.501	1.23
450	0.665	0.644	1.40
500	0.407	0.388	1.35
550	0.105	0.045	1.27
600	0.365	0.354	1.21
650	0.362	0.354	1.01

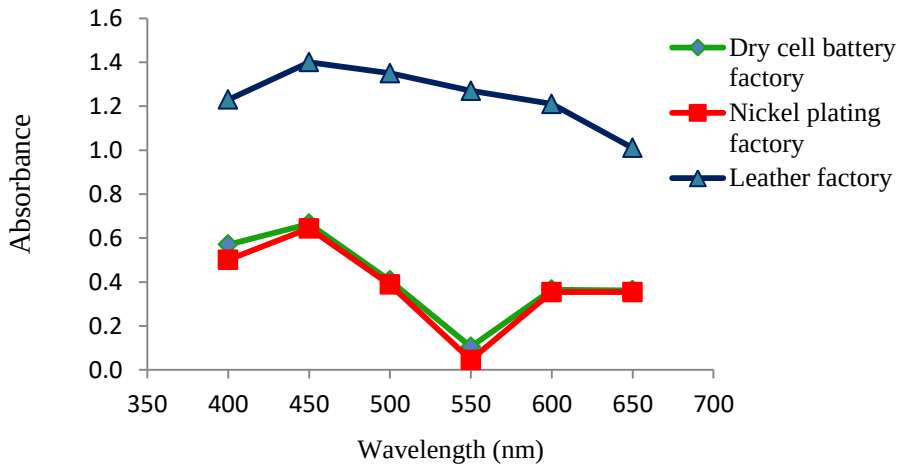

Figure 9: Plot of absorbance as a function of wavelength for three industrial wastewater samples

Decolourization of Wastewater Samples by Using Sequencing Batch Biofilm Reactor

Sequencing batch biofilm reactor was used for the decolourization of the wastewater samples from dry cell battery factory,nickel plating factory and leather factory.

As shown in Table 3 and Figure 10, sequencing batch biofilm reactor could decolourize54.29 % of the wastewater sample of dry cell battery factory after72 h treatment. Moreover, highest decolourization percent was achieved at 74.13% after 64 h treatment for wastewater sample of nickel plating factory as shown in Table 4. The wastewater from leather factory after treatment with sequencing batch biofilm reactor was decolourized53.32 % after 64 h treatment (Table 5).

Table 3: Percent Decolourization of Wastewater Sample of Dry Cell Battery Factory by Using Sequencing Batch Biofilm Reactor

No	Time (h)	Absorbance of treated sample	% Decolourization
1	16	0.408	38.64
2	20	0.208	53.68
3	24	0.424	36.24
4	40	0.314	52.78
5	44	0.458	31.13
6	48	0.350	46.77
7	64	0.107	53.83
8	68	0.320	51.87
9	72	0.104	54.29

Absorbance of control = 0.665

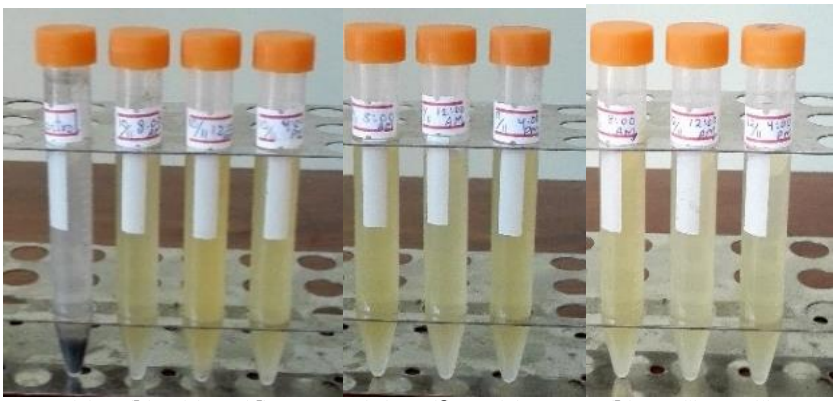

(a) (b) (c) (d) (e) (f) (g) (h) (i) (j)

Figure 10: Decolourization of wastewater sample from dry cell battery factory by using sequencing batch biofilm reactor
(a) Control (b) 16 h (c) 20 h (d) 24 h (e) 40 h (f) 44 h (g) 48 h (h) 64 h (i) 68 h and (j) 72h after treatment

Table 4: Percent Decolourization of Wastewater Sample of Nickel Plating Factory by Using Sequencing Batch Biofilm Reactor

No	Time (h)	Absorbance of treated sample	% Decolourization
1	16	0.191	44.76
2	20	0.142	58.72
3	24	0.122	64.53
4	40	0.096	72.09
5	44	0.095	72.38
6	48	0.094	72.67
7	64	0.089	74.13
8	68	0.093	72.96
9	72	0.191	72.67

Absorbance of control = 0.344

Table 5: Percent Decolourization of Wastewater Sample of Leather Factory by Using Sequencing Batch Biofilm Reactor

No	Time (h)	Absorbance of treated sample	% Decolourization
1	16	1.022	27.00
2	20	0.941	32.79
3	24	0.773	44.78
4	40	0.822	41.29
5	44	0.685	51.07
6	48	0.701	49.93
7	64	0.652	53.32
8	68	0.815	41.78
9	72	0.802	42.71

Absorbance of control = 1.40

Removal of Metal Ions from Wastewater Samples by Using Sequencing Batch Biofilm Reactor

As shown in Table 6 and Figure 11, sequencing batch biofilm reactor could remove metal ions, 21.48 % of Cd^{2+}, 47.72 % of Cr^{3+} and 45.60 % of Pb^{2+} from dry cell battery factory wastewater sample after 72 h treatment. Moreover,sequencing batch biofilm reactor **c**ould remove metal ions,35.76 % of Cd^{2+}, 51.97 % of Cr^{3+} and 42.96 % of Pb^{2+} from nickel plating factory

wastewater sample after 72 h treatment (Table 7 and Figure 12). The results from Table 8 and Figure 13 revealed that the bacterial biofilm could reduce 20.33 % of Cd^{2+}, 62.63 % of Cr^{3+} and 40.75 % of $Pb^{2+}$from leather factory wastewater sample after 72 h treatment.

Table 6: Removal Percentage of Cd^{2+}, Cr^{3+} and Pb^{2+} Ions from Wastewater Sample of Dry Cell Battery Factory by Using Sequencing Batch Biofilm Reactor

Metal ions	Untreated (mg/L)	Treated (mg/L)	Removal of metal ions (%)
Cd^{2+}	0.256	0.201	21.48
Cr^{3+}	0.352	0.184	47.72
Pb^{2+}	0.364	0.198	45.60

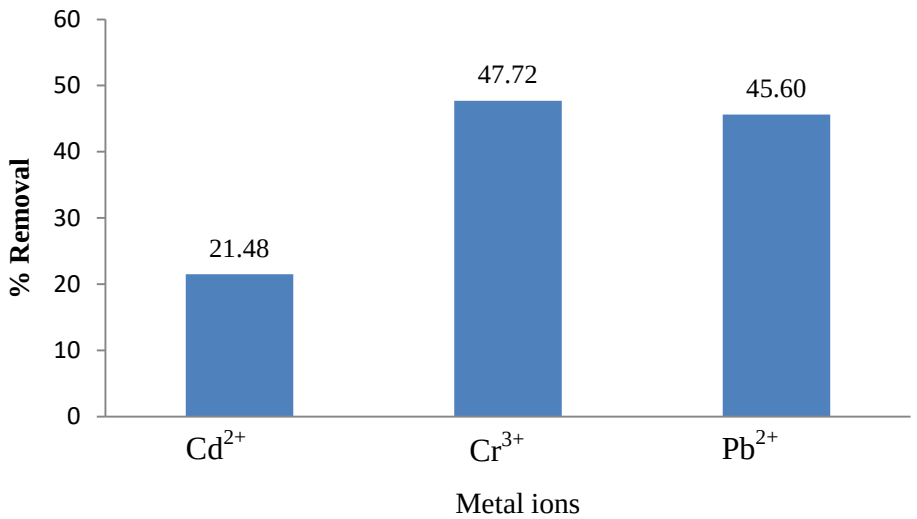

Figure 11: Removal percentage of Cd^{2+}, Cr^{3+} and Pb^{2+}ions from wastewater sample of dry cell battery factory by using sequencing batch biofilm reactor

Table 7: Removal Percentage of Cd^{2+}, Cr^{3+} and Pb^{2+} Ions from Wastewater Sample of Nickel Plating Factory by Using Sequencing Batch Biofilm Reactor

Metal ions	Untreated (mg/L)	Treated (mg/L)	Removal of metal ions (%)
Cd^{2+}	0.316	0.203	35.76
Cr^{3+}	0.356	0.171	51.97
Pb^{2+}	0.284	0.162	42.96

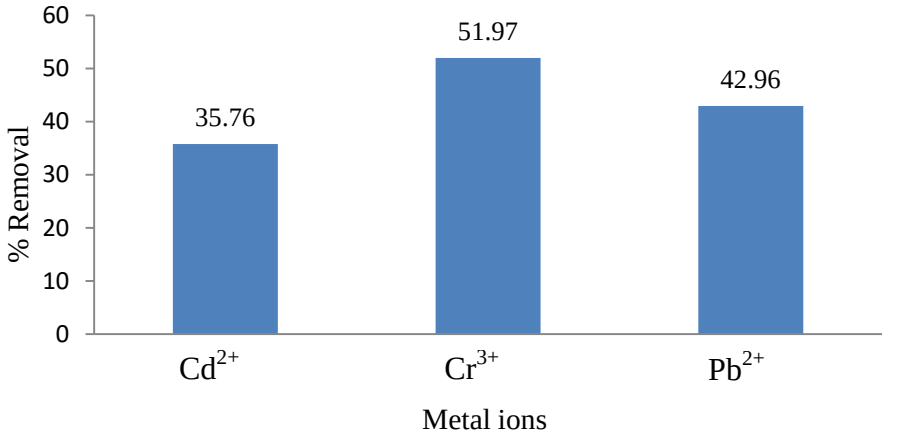

Figure 12: Removal percentage of Cd^{2+}, Cr^{3+} and Pb^{2+} ions from wastewater sample of nickel plating factory by using sequencing batch biofilm reactor

Table 8: Removal Percentage of Cd^{2+}, Cr^{3+} and Pb^{2+} Ions from Wastewater Sample of Leather Factory by Using Sequencing Batch Biofilm Reactor

Metal ions	**Untreated (mg/L)**	**Treated (mg/L)**	**Removal of metal ions (%)**
Cd^{2+}	0.246	0.196	20.33
Cr^{3+}	0.372	0.139	62.63
Pb^{2+}	0.265	0.157	40.75

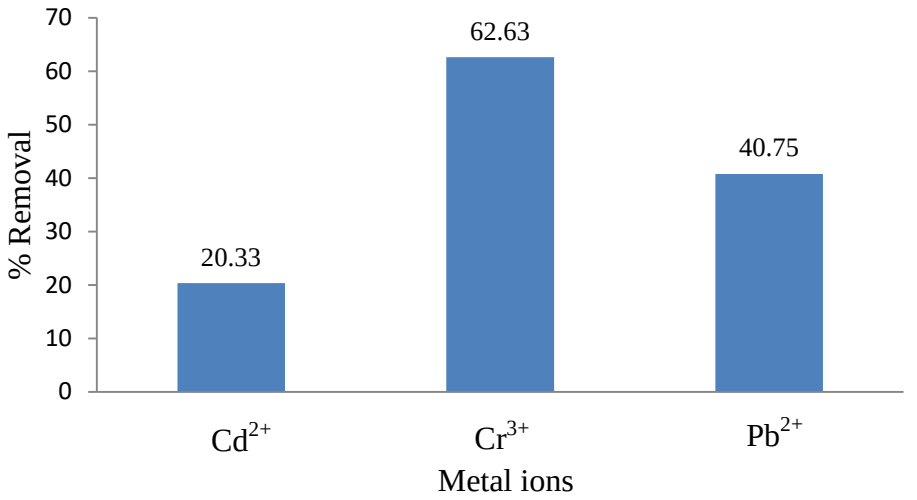

Figure 13: Removal percentage of Cd^{2+}, Cr^{3+} and Pb^{2+}ions from wastewater sample of leather factory by using sequencing batch biofilm reactor

Some Physicochemical Parameters of Three Industrial Wastewater Samples before and after Treatment by Using Sequencing Batch Biofilm Reactor

Some physicochemical parameters such as pH, turbidity, total dissolved solids (TDS), dissolved oxygen (DO), chemical oxygen demand (COD) and biological oxygen demand (BOD) of industrial wastewater samples before and after treatment by using sequencing batch biofilm reactorwere determined and the results are shown in Table 9.

The pH value of untreated wastewater samples from dry cell battery factory, nickel plating factory and leather factory were 8.0, 7.7 and 8.8 respectively. After treatment with sequencing batch biofilm reactor, the pH values of the wastewater samples were reduced to 7.6, 6.9 and 8.5 respectively.

The total dissolved solid (TDS) values of the untreated dry cell battery factory, nickel plating factory and leather factory were found to be 664 mg/L, 828 mg/L and 8588 mg/L respectively, however,after treatment with sequencing batch biofilm reactor TDS values were reduced to 330mg/L,

470 mg/L and 4152 mg/L. About half of the initial TDS values were reduced in wastewater from factories.

The turbidity of untreated wastewater samples from dry cell battery factory, nickel plating factory and leather factory were 101 NTU, 153 NTU and 883 NTU, respectively. After treatment with sequencing batch biofilm reactor the turbidity values of wastewater samples were reduced to greater than half of the initial values (52 NTU, 85 NTU and 313 NTU, respectively) of dry cell battery, nickel plating and leather factories).

Before treatment, the DO values of wastewater samples from dry cell battery factory, nickel plating factory and leather factory were respectively, found to be 1.48 mg/L, 1.47 mg/L and 0.95 mg/L. After treatment with sequencing batch biofilm reactor the DO values of treated wastewater samples from dry cell battery factory, nickel plating factory and leather factory were found to be 3.10mg/L, 2.89 mg/L and 2.20 mg/L, respectively. These DO values of three wastewater samples were found to increase after treatment.

Before treatment, COD values of wastewater samples from dry cell battery factory, nickel plating factory and leather factory were found to be 161 mg/L, 502 mg/L and 3538 mg/L, respectively. After treatment with sequencing batch biofilm reactor COD values of wastewater samples from dry cell battery factory, nickel plating factory and leather factory were found to decrease to 75 mg/L, 215 mg/L and 1230 mg/L, respectively.

In this study, the BOD values of untreated wastewater samples from dry cell battery factory, nickel plating factory and leather factory were 703 mg/L, 340 mg/L and 1875 mg/L, respectively. BOD values of the treated wastewater samples with sequencing batch biofilm reactor were found to reduce to 352 mg/L, 152 mg/L and 785 mg/L, respectively, for dry cell battery, nickel plating and leather factories.

Table 9: Some Physicochemical Parameters of Three Industrial Wastewater Samples before and after Treatment by Using Sequencing Batch Biofilm Reactor

Parameter	Unit	Dry cell battery		Nickel plating factory		Leather factory	
		Untreated	Treated	Untreated	Treated	Untreated	Treated
pH	-	8.0	7.6	7.7	6.9	8.8	8.5
TDS	mg/L	664	330	828	470	8588	4152
Turbidity	NTU	101	52	153	85	883	313
DO	mg/L	1.48	3.10	1.47	2.89	0.95	2.20
COD	mg/L	161	75	502	215	3538	1230
BOD	mg/L	703	352	340	152	1875	785

Conclusion

Four bacterial strains from wastewater samples were isolated and used as biofilm in the reactor in this study. Analysis for decolourization activity by spectrophotometer yielded that sequencing batch biofilm reactor could decolourize 54.29% of wastewater sample of dry cell battery factory after 72 h treatment, 74.13% of wastewater sample of nickel plating factory and 53.32% of wastewater sample of leather factory after 64 h treatment. After 72 h treatment, atomic absorption spectrophotometer analysis showed that sequencing batch biofilm reactor could reduce highest percentages of chromium ion (47.7 % to 62.63 %) followed by lead ion (40.75 % to 45.60 %) and cadminum ion (20.33 % to 35.76 %). According to the experimental data, the sequencing batch biofilm reactor could be applied in the wastewater treatment for removal of Cr^{3+} and Pb^{2+} ions. Moreover, some physicochemical parameters such as pH, turbidity, total dissolved solids (TDS), chemical oxygen demand (COD) and biochemical oxygen demand (BOD) of three industrial wastewater samples were found to decrease after treatment by using sequencing batch biofilm reactor. Thus,sequencing batch biofilm reactor could be effectively applied for the wastewater treatment.

Acknowledgements

The authors would like to thank the Myanmar Academy of Arts and Science for allowing to present this paper and Professor and Head Dr Ye Myint Aung, Department of Chemistry, Pathein University for his kind encouragement.

References

Abu-Bakar ,A., Abd-Rahman, R., Mohamad, A.B., Kadhum ,A.A.H., Abdullah ,S.R.S. (2008). Zinc Bioremoval from Wastewater of Rubber Glove Industry. *Journal of Sustainable Development,*vol.1(1), pp. 31-35

Dhokpande, S.R. and Kaware, J.P. (2013). "Biological Methods for Heavy Metal Removal, A Review". *International Journal of Engineering Science and Innovative Technology (IJESTI)*, vol. 2(5), pp. 304-309

Di Iaconi, C., Lopez, A., Ramadori, R., Di Pinto, A.C., Passino, R. (2004). "Combined Chemical and Biological Degradation of Tannery Wastewater by a Periodic Submerged Filter (SBBR)". *Wat Res*., vol. 36, pp. 2205-2214

Dutta, A. and Sarkar, S. (2015). *Sequencing Batch Reactor for Wastewater Treatment: Recent Advances*. India: Department of Civil Engineering, Institute of Technology

Government of India and Government of the Netherlands.(1999). *Standard Analytical Procedures for Water Analysis*. New Delhi: Hydrology Project, pp. 1-.80

Nasrazadani, A., Tahmourespour, A. and Hoodaji, M. (2011)."Determination of Bacteria Resistance Threshold to Lead, Zinc and Cadmium in Three Industrial Wastewater Samples". *Journal of* Environmental *studies*, vol. 36(56), pp. 25-27

PASCO. (2010).*Water Quality Field Guide*. Roseville CA: PASCO Scientific, United States, America, pp. 27-89

Prendergast, J., Rodgers, M. and Healy, M. G. (2005) "The Efficiency of A Sequencing Batch Reactor SBBR) in Organic Carbon and Phosphorus Removal". *Journal of Environmental Science and Health, Part A: Toxic/Hazardous Substances and Environmental Engineering*, vol. 40 (8), pp. 1619-1626

Rahman, R.A., Hasani, H., Kadhum, A.A.H., Wasmi, B.A., Amiery, A.A.A. and Mohamad, A.B. (2013)."Heavy Metal Biosorption Efficiencies of Expanded Bed Biofilm Reactor and Sequencing Batch Biofilm Reactor". *Asian Journal of Chemistry*, vol. 25 (13). pp. 7193-7198

Rajput, D.C. and Khambete, A. K. (2015)."Performance of Sequencing Batch Biofilm Reactor to Treat Sewage". *International Journal for Innovative Research in Science & Technology*, vol.1 (10), pp. 1-5

Rodgers, M., Zhan, X.-M., Burke, M.D. (2004)."Nutrient Removal in A Sequencing Batch Biofilm Reactor (SBBR) using A Vertically Moving Biofilm System". *Environ Tech*., vol. 25, pp. 211-218

STUDIES ON SOME PHYSICOMECHANICAL AND ANTIMICROBIAL PROPERTIES OF PREPARED CELLULOSE HYDROGEL FILMS

Thinzar Aye[1], Thinzar Nu[2], Cho Cho[3]

Abstract

In this research work, sugar cane bagasse waste (raw material) was used as a cellulose source which was chemically treated by sequential operation of sulphuric acid, sodium hydroxide and sodium hypochlorite. The yield percent of the purified cellulose fiber was 32.31 %. Fourier Transform Infrared (FT IR), Scanning Electron Microscope (SEM) and X-ray Diffraction (XRD) measurements were carried out to characterize the properties of raw material as well as cellulose fiber obtained from each sequential step. Cellulose fiber (1g) was dissolved in Dimethylacetamide /Lithium chloride (DMAc/LiCl) solution containing different lithium chloride concentration of 6, 8, 10 and 12 wt %. The different hydrogel films were obtained from above cellulose solutions of different solvent ratios leading to solid hydrogel in ethanol vapor by phase inverse method. The mechanical properties such as tensile strength, thickness, width, elongation, viscoelasticity and water content were measured to characterize the effect of LiCl concentrations on the resultant hydrogel films. Antimicrobial activities of cellulose solutions were tested for the purpose of using hydrogel films to biomedical applications.

Keywords: bagasse, cellulose hydrogel films, viscoelasticity, elongation, antimicrobial activities

Introduction

In recent years, there has been an increase in the level of research on the development of new biodegradable materials for use in packaging, agriculture, medicine and other areas. Generally, biodegradable polymer materials are increasingly important as environmental contamination and waste disposal problems associated with plastics and related products from synthetic polymers become more severe. Natural polymers have various advantages over synthetic polymers due to their low-cost, great availability and biodegradability (Zhou, *et al.,* 2008).

[1.] PhD Candidate, Assistant Lecturer, Department of Chemistry, Pyay University
[2.] Dr, Associate Professor, Department of Chemistry, University of Yangon
[3.] Dr, Professor and Head, Department of Chemistry, Yenangyaung Degree College

Cellulose hydrogel has become especially attractive to "tissuse engineering" as matrices for repairing and regenerating a wide variety of tissue and organs. Hydrogels consisted of hydrophilic polymer networks which can absorb from 10-20 % up to thousands of times of their dry weight in water. Various hydrogels from natural polymers were fabricated by using hyaluronate, chitosan and its derivatives, and cellulose in which there is a potential application in the biomaterials field. Among them, cellulose is the most abundant renewable resource on earth and may become a main chemical resource in the future. Therefore, this sustainable material in plants has numerous functional possibilities and can be expected with the demand for environmentally and biocompatible products (Svensson *et al.*, 2005).A wide range of lingocellulosic agricultural by-products has successfully been converted into cellulose hydrogel film including agave tequilana Weber bagasse (Karla *et al*., 2013), sugar cane bagasse (Kazuki and Kobayashi, 2016).

Sugarcane bagasse (SB), as the fibrous by-product remaining after sugar extraction from sugarcane, is one of the most important byproducts. About 54 million dry tons of SB are produced annually throughout the world (Ren*et al.*, 2006). Bagasses offer the advantages of being a cheap, plentiful and low polluting fuel (Mothe and Miranda, 2009). Commonly, all plant biomass consists of cellulose, hemicellulose, lignin, pectin and protein. Most of the plant biomass consists of about 33 % of cellulose as the major component of the rigid cell walls. Table 1 shows the percentage composition of sugarcane bagasse (Sun *et al.*, 2004)

Table 1: Percentage Composition of Sugar Cane Bagasse

Component	Composition (%)
Cellulose	44.6
Hemicellulose	33.5
Lignin	18.1
Ash	2.3
Wax	0.8
Other	0.7

Cellulose is a linear and high molecular weight polymer as well as natural, renewable and biodegradable material (Rachtanapun, 2009). Cellulose is aligned parallel to each other in fibrils, which are surrounded by a matrix of lignin and hemicellulose (Figure 1). In addition, cellulose has properties such as low density, good mechanical properties as well as biodegradability. Cellulose, the major chemical component of fiber wall and contributing 40-45 % of the dry weight. It is composed of linear chain of D-glucose linked by β -1,4-glycosidic bond with the degree of polymerization (DP) from 10,000 in native wood to 1,000 in bleached kraft pulps. Each D-anhydro glucopyranose unit possesses hydroxyl groups at C2, C3, and C6 positions, capable of undergoing the typical reactions known for primary and secondary alcohols. The molecular structure imparts cellulose with its characteristic properties: hydrophylicity, chirality, degradability, and broad chemical variability initiated by the high donor reactivity of hydroxyl groups.

Cellulose has a strong tendency to form intra - and inter-molecular hydrogen bonds by the hydroxyl groups on these linear cellulose chains, which stiffen the straight chain and promote aggregation into a crystalline structure and give cellulose a multitude of partially crystalline fiber structures and morphologies. Crystalline cellulose has very limited accessibility to water and chemicals (Edgar *et al.*, 2001).

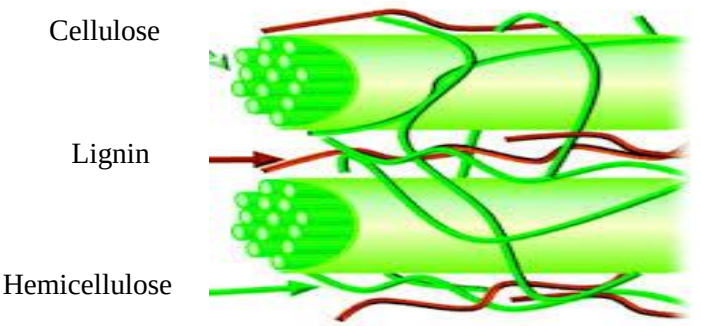

Figure 1: Components of primary cell wall

It is well known that native cellulose is very difficult to dissolve in common solvents. This is due to formation of strong hydrogen bond between abundant hydroxyl groups in the polymer chains. In addition, crystalline and

aggregated fibers of the cellulose also make it difficult in the solubilization. For this reason, studies on native cellulose hydrogel are fewer than cellulose derivatives. Therefore, solvents such as alkali-based aqueous system, N-methylmorpholine-N-oxide (NMMO), lithium chloride (LiCl)/ N, N-dimethylacetamide (DMAc) and ionic liquids (ILs) were developed for cellulose dissolutions. These solvent system provides great opportunities to prepare native cellulose hydrogel through physical cross-linking (Striegel, 1997).

For cellulose hydrogel films preparation has been reported by which a DMAc/LiCl system enables flexible cellulose hydrogel films using phase inversion processes. Hydrogels are networks of hydrophilic polymer chains in natural or synthetic polymers. They are highly water absorbent without being soluble in water. Here, the phase inversion process involves transformation from a liquid phase polymer solution to a solid state of the polymer (Kazuki and Kobayashi, 2016). In the present study, sugar cane bagasse was used to obtain cellulose hydrogel solution and the hydrogel film.

Materials and Methods

Collection of Sugar Cane Bagasse

Sugar cane bagasse was collected from Nawaday Sugar Mill, Pyay Township, Bago Region.

Bagasse Treatment

The bagasse was firstly washed with distilled water to remove remaining sugar components and then heated in oven at 50 ˚ C. For acid treatment, 10 g of bagasse was added into 300 mL of 4 vol % H_2SO_4 aqueous solution and stirred for 2 h at 90 ˚ C. Then, sample was washed with abundant distilled water five times to eliminate residues of the H_2SO_4 solution. And then 300 mL of 10 wt % NaOH solution was added and kept under stirring for 12 h at 90 ˚ C until a black liquor solution was obtained. The residues of fiber were washed with excess distilled water until neutral pH. After that the fiber was added into 300 mL of 10 vol % NaOCl solution and stirred for 3 h at 40 ˚ C. NaOCl was used as bleaching agent to obtain light coloured fiber for preparation of cellulose solution. Figure 2 shows sugarcane bagasse raw sample, acid treated sample, base treated sample and cellulose fiber. The

prepared cellulose fiber was used for the preparation of cellulose solution in DMAc/LiCl system.

(a) (b) (c) (d)

Figure 2: (a) Sugarcane bagasse raw sample (b) acid treated sample (c) base treated sample and (d) cellulose fiber

Preparation of Cellulose Hydrogel Solutions

The cellulose fiber (1 g) was stirred in 300 mL of distilled water at room temperature for 24 h to swell the fiber. After the swelling fiber was filtered by an adapter glass filter under vacuum, ethanol (300 mL) was added to the swelled fiber and the mixture was stirred for 24 h at room temperature. Ethanol was removed and the swelled fiber was added to 300 mL of DMAc. The mixture was then left overnight under stirring condition. Both dried LiCl and DMAc were added to the swelled bagasse fiber to dissolve the cellulose fiber and stirred at room temperature for 3 days. About 1 wt% cellulose in DMAc/LiCl containing different concentrations of LiCl (6, 8, 10 and 12 wt %) were obtained.

Preparation of Cellulose Hydrogel Films

Cellulose hydrogel films which containing different concentrations of LiCl (6, 8, 10 and 12 wt %) were prepared. 10 g of cellulose hydrogel solution was poured into a glass dish (9.1 cm diameter), and kept for 24 h in a plastic container filled with ethanol. In this step, cellulose was gradually progressed in the vapour at room temperature. Finally, the cellulose hydrogel films such as CHF-1, CHF-2, CHF-3 and CHF-4 were obtained by the phase inversion process from liquid to solid gel. The resultant transparent films as shown in Figure 3 were washed with excess distilled water and then placed in distilled water for 24 h to remove DMAc. The obtained hydrogel films were kept in plastic container filled with distilled water until further experiments.

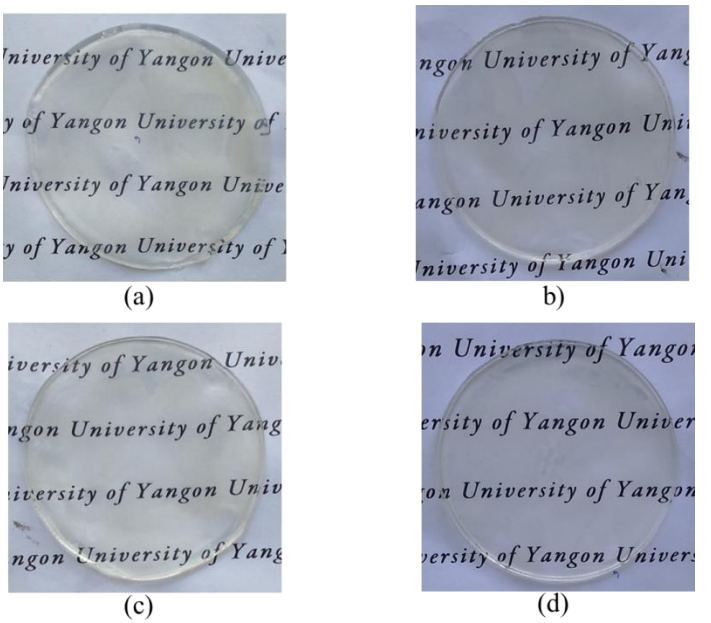

Figure 3: Prepared cellulose hydrogel films (a) CHF-1, (b) CHF-2, (c) CHF-3 and (d) CHF-4

Characterization of Raw Material and Treated Fibers

The formation of prepared cellulose fiber samples was monitored by FT IR, SEM and XRD. The structural changes of samples were analyzed by FT IR spectrometer (FT IR – 8400 SHIMADZU, Japan).FTIR analysis was in a range of wavenumber from 4000 to 400 cm^{-1}. Surface morphology of the samples was studied by SEM (JSM-5610 LV Scanning Microscope, JEOL, Japan). X-ray diffraction pattern of the sample was recorded on X-ray diffractometer (Rigaku, Tokyo, Japan), using CuK_{α} radiation (λ = 1.54 Å)at 40 kV and 40 mA. The diffraction angle ranged from 10˚ to 70˚ of 2θ .

Investigation of the Antimicrobial Activity of Cellulose Hydrogel Solutions

The cellulose hydrogel solutions such as 6 wt % cellulose hydrogel solution (CHS-1), 8 wt % cellulose hydrogel solution (CHS-2), 10 wt % cellulose hydrogel solution (CHS-3), 12 wt % cellulose hydrogel solution (CHS-4) and DMAc solvent were tested with *Bacillus subtilis*, *Staphylococcus aureus*, *Pseudomonas aeruginosa*, *Bacillus pumilus*, *Candida albicans* and

Escherichia coli species to investigate the nature of antimicrobial activity. After preparing the bacteriological media, about 0.1 mL of sample was introduced into the agar –disc and incubated at 37 ºC for 24 h. The inhibition zone (clear zone) which appeared around the agar-disc indicated the presence of antimicrobial activity. The results are shown in Table 3.

Determination of the Properties of Cellulose Hydrogel Films

Tensile strength and elongation of the hydrogel films were measured on a LTS -500N - S20 (Minebea, Japan) with universal testing machine equipped with a 2.5 kN cell. Strips with a length of 50 mm and a width of 10 mm were cut from cast film with a razor blade. Strain was recorded by means of Zwick Makrosense clip-on displacement sensors. One set of samples (five strips each) was measured and each set was repeated 3 times. Only samples which ruptured near mid-specimen length were considered for the calculation of tensile strength. The values of the tensile strength and elongation were calculated. The results are shown in Table 2.

Water content of the resultant hydrogel films were determined by weighing dry and wet samples according to the following procedure. Disk samples with 5 mm of diameter were cut from cast films and dried in vacuum oven for 24 h and weighed. Then, samples were emerged in distilled water for 36 h. After 36 h the specimens were removed from water and wrapped with filtered paper on the surface in order to remove excess of water, and then weighed. Finally, the water content was calculated with the weights of the wet (Ws) and dried (Wd) hydrogel films.

$$\text{Water content (\%)} = (Ws - Wd)/ Wd \times 100$$

The water content of cellulose hydrogel films are shown in Table 2.

Viscoelasticity of the hydrogel films with 2 cm in diameter and having 5 mm of thickness was determined by Anton Paar- Reoplus equipment (Anton Paar Japan, Tokyo) in wet conditions at 37 °C. The results are shown in Figure 7.

Results and Discussion

In Figure 2, sugar cane bagasse raw sample, acid treated sample, base treated sample and cellulose fiber are shown. In acid treatment, hemicellulose is removed because hemicellulose is hydrolyzed easily by a dilute acid or base. Alkali treatment results in a higher amount of swelling. Cellulose fiber by treatment with sodium hypochlorite gets white colour from brown colour.

Figure 4 shows FT IR spectra of the sugarcane bagasse, treated fibers and cellulose fibers at different treatment conditions. The FT IR spectra of all sample show the strong broad band around 3400 cm^{-1}which is due to the O-H stretching vibration. The strong band at around 2900 cm^{-1} which is due to C-H stretching vibration referred to CH_2 group. The absorption band at around 1730 cm^{-1} indicates the C=O stretching in carbonyl group of pyrone. Appearance of the band around 1600 cm^{-1} is a relative pure ring stretching mode strongly associated with the aromatic ring C=C in benzene as well as in pyrone ring. From the comparison of the FT IR spectra, the appeared peaks due to aromatic skeletal vibration of lignin around 1510 cm^{-1} showed the presence of lignin and lignocellulose in the initial raw sample. Moreover, the C-O-C stretching vibration of ester group of hemicellulose around 1200 cm^{-1} disappeared in treated fiber which is assigned the removal of hemicelluloses in cellulose fiber by bleaching. This clearly indicated that the amount of lignin from the sugar cane bagasse raw sample was successfully reduced by the chemical and temperature treatments.

SEM microphotographs of the treated samples indicated clearly the appearance surface morphologies of the samples. Figure 5(a) is SEM micrograph of sugar cane bagasse sample which shows the major constituents of natural fibers such as cellulose, hemicelluloses and lignin. The SEM images of treated samples in Figures 5(b) and (c) have been changed in their morphologies due to the removal of lignin and hemicelluloses. Finally Figure 5(d) can be seen that the main structural unit of cellulose in the plant wall consists of cellulose microfibrils bonded together in a polymeric matrix.

XRD measurement was carried out to evaluate the effect of treatment condition on the crystalline structure of bagasse, treated fibers and cellulose fibers. Figure 6 shows the XRD patterns of the bagasse and the purified fibers. The patterns of (a) – (d) exhibited typical crystalline lattice of cellulose with

peaks at 22.3° and 16.4° . The crystalinity indices of sugar cane bagasse raw sample, acid treated sample, base treated sample and cellulose fiber were 44.1%, 58.8%, 59.1% and 60.2% respectively. The increment of crystalinity in cellulose fiber was due to the removal of hemicelluloses and lignin by NaOH and NaOCl treatment.

The crystalinity index (CI) percent was calculated by using the following equation:

$$CI\ (\%) = (\ I_{002} - I_{am}\ ) / I_{002} \times 100$$

I_{002} = the maximum intensity of the peak (002) lattice diffraction

I_{am} = the intensity of diffraction attributed to amorphous cellulose

As shown in Table 2, the tensile strength and elongation values of 8 wt % LiCl cellulose hydrogel film (CHF-2) showed the highest value other than the other hydrogel films such as 6, 10 and 12 wt % LiCl cellulose hydrogel films (CHF-1, CHF-3 and CHF-4). However, the values of CHF-3 and CHF-4 were higher than CHF-1. Therefore, the effect could improve the resistance to the applied force in the higher LiCl case increasing the elongation value of the hydrogel films.

Table 2 lists the properties of hydrogel films. The values of water content decreased from 320 % to 156 % with the increment of the LiCl content from 6 to 12 wt % respectively. Therefore, water contents in the film became higher when the LiCl content was lower. It was noted that the hydrogel films had very soft and flexible shape even though there was no chemical crosslinking treatment.

Figure 7 shows relationship between *G'* and *G''* for the viscoelasticity of the hydrogel films. The strain was varied from 10^{-1} to 10^{2} % at 25 °C and constant frequency of 1 Hz. The crossover point of *G'* and *G''* meant fracture of material or inability to follow deformation, since rigid polymer network may not flow. So, crossover point at lager strain indicated flexible structure of the hydrogel film. In the case of 8 wt % LiCl, the *G'* and *G''* values were overlapped at 35.71 % strain. However, crossover points of 6, 10 and 12 wt % LiCl were lower which indicated less flexible structure of the hydrogel films comparing to 8 wt % LiCl.

Antimicrobial activity of 6 wt % cellulose hydrogel solution (CHS-1), 8 wt % cellulose hydrogel solution (CHS-2), 10 wt % cellulose

hydrogel solution (CHS-3), 12 wt % cellulose hydrogel solution (CHS-4) and DMAc solvent are shown in Table 3. The tested organisms were *Bacillus subtilis*, *Staphylococcus aureus*, *Pseudomonas aeruginosa*, *Bacillus pumilus*, *Candida albicans* and *Escherichia coli.* As seen in Figure 8, antimicrobial tests of CHS-1, CHS-2, CHS-3, CHS-4 and DMAc solvent were used in the agar medium cultivation. DMAc solvent was seen as inactive against *Bacillus subtilis*, *Staphylococcus aureus*, *Pseudomonas aeruginosa*, *Bacillus pumilus*, *Candida albicans* and *Escherichia coli*. CHS-1, CHS-2, CHS-3 and CHS-4 were observed to possess the antimicrobial activity against all six test organisms show the reaction. Among these, CHS-2 has the highest activity.

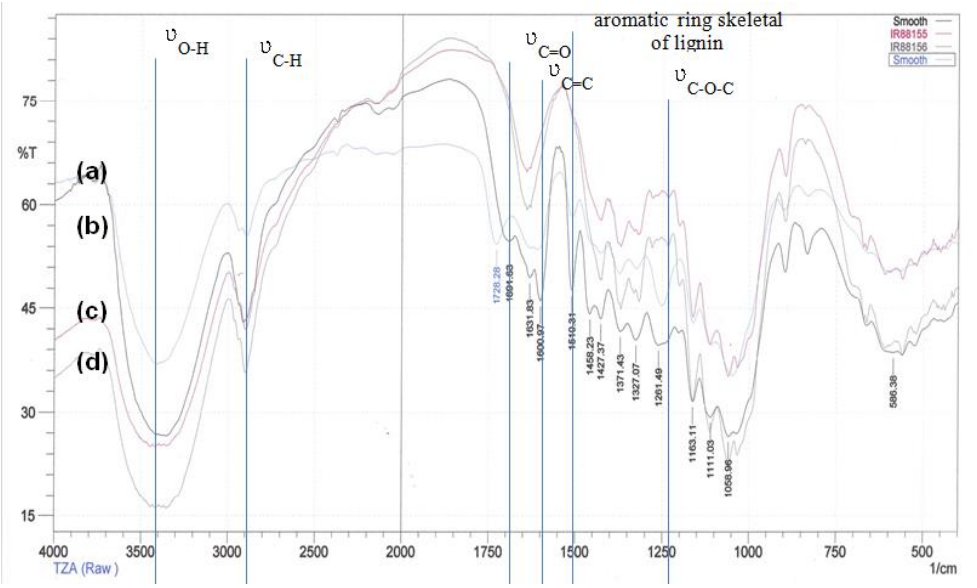

Figure 4: FT IR spectra of (a) sugar cane bagasse raw sample (b) acid treated sample (c) base treated sample and (d) cellulose fiber

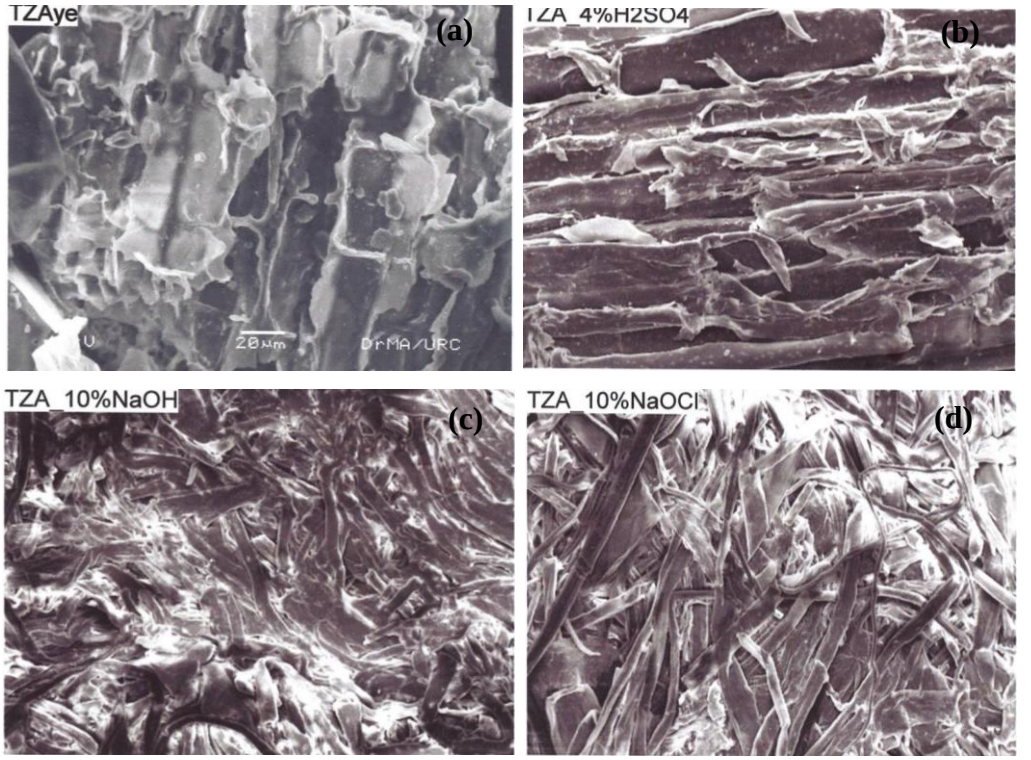

Figure 5: SEM photographs (20µ m magnification) of (a) sugar cane bagasse raw sample (b) acid treated sample (c) base treated sample and (d) cellulose fiber

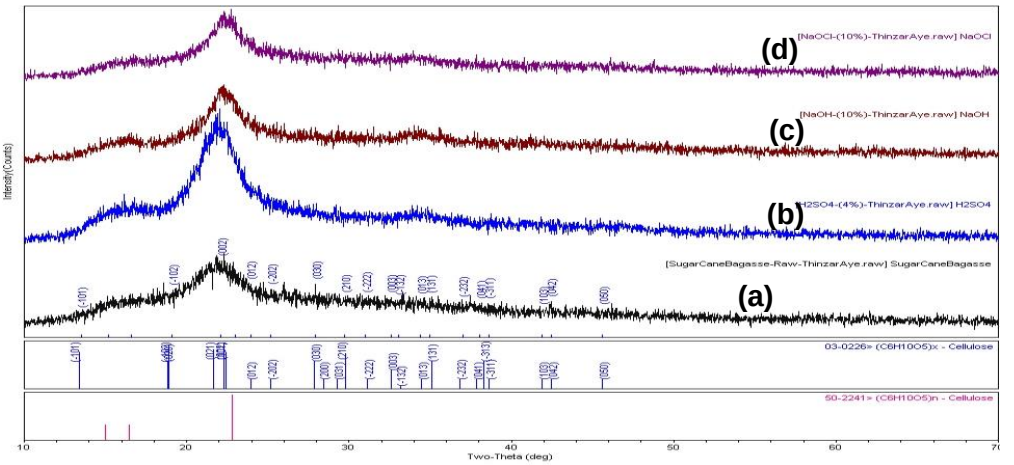

Figure 6: XRD patterns of (a) sugar cane bagasse raw sample (b) acid treated sample (c) base treated sample and (d) cellulose fiber

Table 2: Properties of Cellulose Hydrogel Films Prepared from Sugar Cane Bagasse

Type of Hydrogel Film	Width (mm)	Thickness (mm)	Tensile Strength (N/mm^2)	Elongation (%)	Water Content (%)
CHF-1	10.14	0.636	0.2499	22.58	320
CHF-2	9.96	0.592	0.3597	27.52	228
CHF-3	9.88	0.618	0.3113	24.82	186
CHF-4	10.02	0.612	0.3019	24.31	156

CHF-1 using 6 % LiCl in DMAc (w/w)
CHF-2 using 8 % LiCl in DMAc (w/w)
CHF-3 using 10 % LiCl in DMAc (w/w)
CHF-4 using 12 % LiCl in DMAc (w/w)

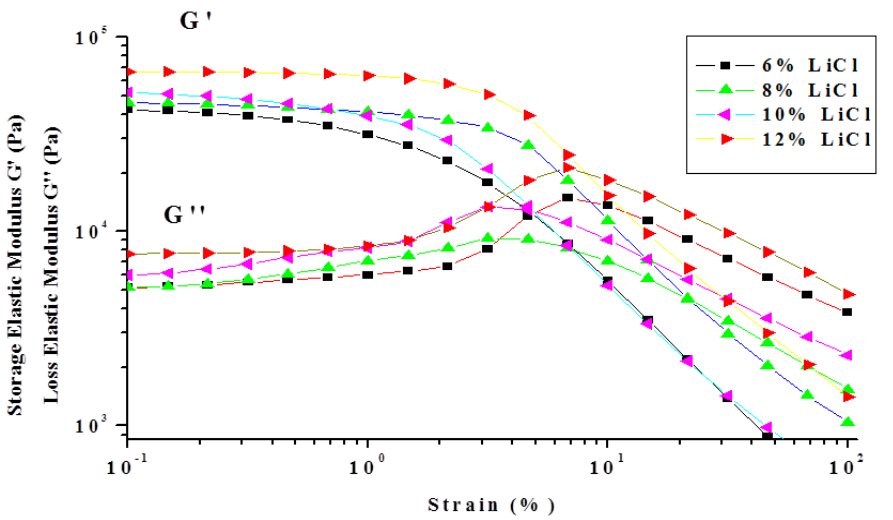

Figure 7: Viscoelasticity of cellulose hydrogels films of different LiCl contents for strain –G',-G" plots at 25 ˚ C

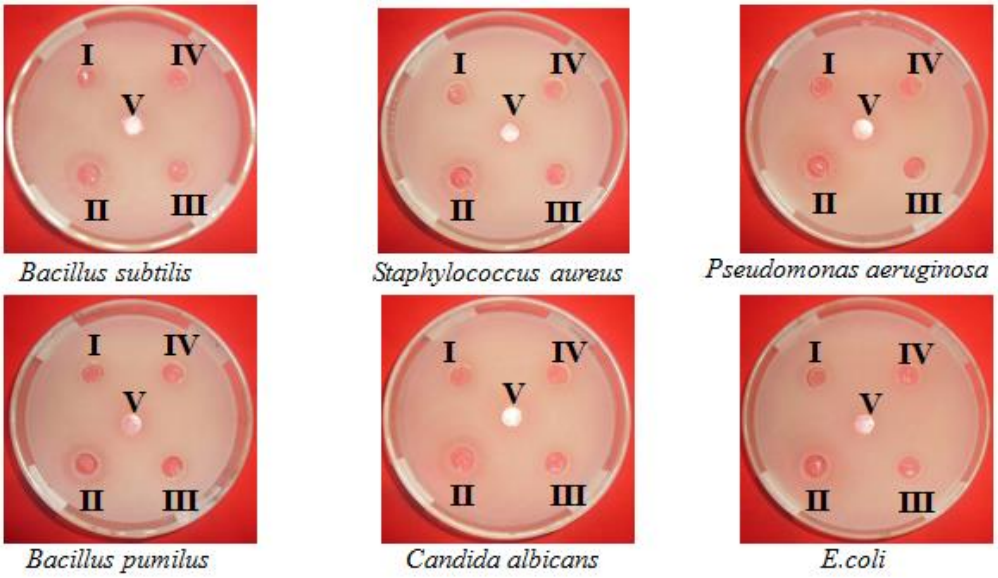

I = CHS-1, II = CHS-2, III = CHS-3, IV = CHS-4, V = DMAc

Figure 8: Antimicrobial activity of cellulose hydrogel solutions and DMAc solvent ondifferent bacterial strains

Table 3: Antimicrobial Activities of Cellulose Hydrogel Solutions

Type of Hydrogel Solutions	**Inhibition Zone Diameters of Different Cellulose Hydrogel Solutions Against Tested Organisms (mm)**				
	B. subtilis	***S.aureus***	***P. aeruginosa***	***B. pumilus***	***C. albicans***
CHS-1	11 (+)	11 (+)	11 (+)	11 (+)	11 (+)
CHS-2	16 (++)	17 (++)	16 (++)	18 (++)	17 (++)
CHS-3	11 (+)	12 (+)	11 (+)	11 (+)	11 (+)
CHS-4	11 (+)	12 (+)	11 (+)	11 (+)	11 (+)
DMAc solvent	10 (+)	10 (+)	10 (+)	10 (+)	10 (+)

Agar Well – 10 mm
10 mm ~ 14 mm (+)
15 mm ~ 19 mm (++)
20 mm above (+++)

Conclusion

Cellulose hydrogel films were successfully prepared from sugar cane bagasse by phase inversion of the DMAc solvent with LiCl. The sugar cane bagasse was used as starting material which was treated using sulphuric acid, sodium hydroxide and then bleached with sodium hypochlorite. The treated samples were characterized by FT IR, SEM and XRD. From the XRD data, percent crystalinity indices of sugar cane bagasse raw sample, acid treated sample, base treated sample and cellulose fiber were 44.1 %, 58.8 %, 59.1 % and 60.2 %, respectively. SEM and FT IR analyses clearly showed that the amount of liginin and hemicellulose from sugar cane bagasse sample was successfully reduced by chemical treatment and also proved that the final product was cellulose fiber. From the observation, obtained bagasse fiber was pure cellulose fiber which was used for preparation of cellulose hydrogel films. The different LiCl concentrations such as 6, 8, 10 and 12 wt % were used to prepare different hydrogel films. These films had good mechanical properties, although there were no chemical crosslinking. Depending on the LiCl concentrations, these hydrogel films exhibited varying nature in the deformation, tensile strength, elongation and water retainable property. Among these, the best mechanical properties, antimicrobial activities and suitable water retainable property were observed in hydrogel film (CHF-2) prepared at 8 wt % of LiCl. Showing the antimicrobial activities of cellulose solutions against six test organisms, the cellulose hydrogel films are possible to be utilized for biomedical applications.

Acknowledgements

The authors wish to thank to Professor Dr Hnin Hnin Aye, Head of the Department of Chemistry, University of Yangon for her encouragement. Warmest thanks are also extended to Professor Dr Ye Chan, Head of Department, Universities' Research Centre, University of Yangon for providing necessary research facilities.

References

Edgar, K.J., Buchanan, C.M., Debenham, J.S., Rundquist, P.A., Seiler, B.D., Shelton, M.C. and Tindall, D. (2001).“ Advanced in Celluloic Ester Performance and Application*”. Prog.Polym. Sci,* vol. 26**,** pp.1605

Karla, L.T., Satoshi, S.S., Tagaya, M. and Kobayashi, T. (2013).“ Fibroblast Compatibility on Scaffold Hydrogels Prepared from Agave Tequilana Weber Bagasse for Tissue Regeneration”. *J.Ind.Eng.Chem.Res*.,vol.52,pp.11607-11613

Kazuki, N. and Kobayashi, T. (2016).“ Effect of Pre-treatment of Sugar Cane Bagasse on the Cellulose Solution and Application for the Cellulose Hydrogel Films”. *J. Polym. Adv. Technol*., vol. 27, pp. 973-980

Mothe, C.G. and Miranda, I.C. (2009).“Characterization of Sugarcane and Coconut Fibers by Thermal Analysis and FTIR”. *Journal of Thermal Analysis and Calorimetry*, vol. 97 (2), pp. 661- 665

Rachtanapun, P. (2009). “Blended Films of Carboxymethyl Cellulose (CMCp) from Papaya Peel and Corn Starch”. *Kasetsart Journal (Natural Sciences)*, vol. 43(5), pp. 259-266

Ren,J., Kong, W. and Sun, R. (2006). “Bagasse-acrylic Absorbent”.*Journal of bioresources*, vol. 9 (2), pp. 3290-3303

Svensson, A., Nicklasson, E. Harrah, T., Panilaitis, B., Kaplan D, L., Brittberg, M. and Gatenholom, P. (2005). “Bacterial Cellulose as a Potential Scaffold for Tissue Engineering of Cartilage”. *Biomaterials* , vol. 26, pp. 419-423

Striegel, A., (1997). "Theory and Applications of DMAc/LiCl in the Analysis of Polysaccharides” *Carbohydr. Polym.*, vol. 34, pp. 267-274

Sun, J.X., Sun, X.F., Zhao, H. and Sun, R.C. (2004). “Isolation and Characterization of Cellulose from Sugarcane Bagasse”. *Polymer Degradation and Stability*, vol. 84, pp. 331-339

Zhou, R., Mo, Y., Li, Y., Zhao, Y., Zhang, G. and Hu, Y. (2008).“Quality and Internal Characteristics of Huanghua Pears (Pyruspyrifolia Nakai, cv. Huanghua) Treated with Different Kinds of Coating during Storage”. *Postharvest Biology and Technology*, vol. 49, pp. 171-179

PREPARATION AND CHARACTERIZATION OF POLYVINYL ALCOHOL-SILVER NANOPARTICLES COMPOSITE FILMS AND ITS ANTIMICROBIAL ACTIVITY

Aye Mya Nwe[1], Mya Kay Thi Aung[2], Khin Than Yee[3]

Abstract

In this research work, silver nanoparticles were synthesized by using green synthesis. In green synthesis, neem leaf extract was used as reducing agent. Silver nanoparticles (SNP) were prepared by mixing neem leaf extract and 0.01 M $AgNO_3$ solution in the different ratios of 1:4, 2:4 and 3:4 v/v and the resulting silver nanoparticles were designated as SNP-NL1, SNP-NL2 and SNP-NL3 respectively. The existence of SNP in colloidal solutions was confirmed by Tyndall effect and UV-visible spectroscopy. The UV-visible spectrum revealed the formation of silver nanoparticles by exhibiting the typical surface plasmon absorption maxima at 415-420 nm. The silver nanoparticles after centrifugation of colloidal solution were characterized by modern techniques XRD, FT IR, SEM and EDXRF analyses. In XRD analysis, it was found that average crystallite size of SNP powders are in the range of 4.80 nm to 8.46 nm. From XRD analyses, all of the prepared SNP powders had the crystalline nature. The high intensity peaks of the prepared samples confirmed the diffraction faces of silver. According to the XRD spectra of all of the prepared SNP-NL, there was impurity peaks in the SNP-NL1 and SNP-NL3 but no impurity peaks found in the SNP-NL2. The crystallite size of SNP-NL2 was 6.93 nm. From the FT IR spectra of all of the prepared SNP-NL, it was observed that the stretching and bending vibration of residual organic functional groups from the leaf extract are present. SEM micrographs of all of the prepared SNP-NL showed agglomeration and larger particle size distribution. From EDXRF analyses, the main constituent element in the SNP-NL2 is Ag (92.384 %). The different types of polyvinyl alcohol (PVA) film were prepared by using different concentrations (1 - 5 % w/v) of PVA in distilled water. The obtained PVA films were designated as PVA-1, PVA-2, PVA-3, PVA-4 and PVA-5. According to the physicomechanical properties, the optimum conditions of PVA-3 film has tensile strength (31.7 MPa), elongation at break (241 %) and tear strength (155.8 kNm^{-1}). The selected PVA-3 film was characterized by XRD, SEM, FT IR and TG-DTA analyses. The PVA-

1. Assistant Lecturer, Department of Chemistry, Pyay University
PhD Student, Department of Chemistry, University of Yangon
2. Dr, Lecturer, Department of Chemistry, University of Yangon
3. Dr, Lecturer, Department of Chemistry, University of Yangon

SNP composite films were prepared by varying the volume ratios of 3 % w/v PVA solution and colloidal SNP-NL2 solution. The antimicrobial activity of the prepared PVA-SNP composite films was investigated by using agar well diffusion method.

Keywords: Neem leaf extract, silver nanoparticles, green synthesis, PVA-SNP composite films, antimicrobial activity

Introduction

Nanoparticles are fundamental building blocks of nanotechnology. The most important and distinct property of nanoparticles is their larger surface area to volume ratio. Nanoparticles(NPs) are usually clusters of atoms in the size range of 1-100 nm (Lalitha, 2013). The properties of a metal NP are determined by its size, shape, composition, crystallinity, and structure. Silver nanoparticles(SNPs) have a number of application from electronics and catalysis to infection prevention and medical diognosis. SNPs has been known as excellent antimicrobial and anti-inflammatory agents and were used to improve wound healing. A number of physical and chemical strategies were employed for the synthesis of SNPs (Sivakumar, 2012).

An eco-friendly green mediated synthesis of inorganic nanoparticle is a fast growing research in the limb of nanotechnology. The biosynthesis method employing plant extract have drawn attention as a simple and viable alternative to chemical procedures an physical methods. Bioreduction of silver ions to yield metal nanoparticles using living plants, geranium leaf, neem leaf have been studied. *Azadirachtaindica* is one of the most versatile medicinal plant having a wide spectrum of biological activity. Every part of the tree has been used as a traditional medicine for household remedy againt various human ailment, from antiquity.

Azadirachtaindica leaf extract has been utilized for the synthesis of silver nanoparticles. The major advantage of using the neem leaves is that it is a commonly available medicinal plant and the antibacterial activity of the biosynthesized silver nanoparticle might have been enhanced as it was capped with the neem leaf extract (Lalitha, 2013). *Azadirachtaindica* leaf extract is used in the synthesis of various particles like gold, zinc oxide and silver etc. The phytochemicals present in neemleaf are namely terpenoids and flavonoids, which act as reducing agent as well as capping agent and helping

the stabilizing the nanoparticles. When silver salt is treated with neem leaf extract, the silver salt is reduced to SNPs (Verma, 2016).

Silver nanoparticles exhibit distinct optical activities that have found wide use in electronics, catalysis and in sensing based applications. Moreover, it displays antimicrobial activity against a broad spectrum of bacteria and fungi and thus finds use as a biocide and also in the preparation of bactericidal nanomaterials for wound dressings and surgical purposes. Silver nanoparticles are non-toxic to humans in low concentrations. The silver-nanoparticles can inactivate proteins, blocking respiration and electron transfer (Albrecht *et al*, 2006).

Polyvinyl alcohol (PVA) is a bio- friendly polymer as it is water soluble and has extremely low cytotoxicity. PVA belongs to the group of polymers which can be used in combination with silver nitrate. PVA is one of the synthetic, biodegradable, biocompatible polymer utilized in medical applications such as wound dressing, artificial skin, coatings, transdermal patches, cardiovascular devices and drug delivery systems (Sayed, 2014). In this research work, PVA-SNP composite films are investigated against strains of different bacteria.

Materials and Methods

Sample Collection

Neem leaves were collected from Pyay Township, Bago Region. The collected leaves were rinsed several times with running tap water and after that with distilled water. Then it was air- dried at room temperature.

Preparation of *Azadirachtaindica* A. Juss (Neem Leaf) Extract

Crudeneem leaf extract was prepared by taking 25 g of *Azadirachtaindica* leaves in a 500 mL Erlenmeyer flask with 200 mL of deionized water and then boiled the mixture for one hour on water bath. The sample solution was filtered and cooled at room temperature.

Green Synthesis of Silver Nanoparticles (SNPs)

Silver nanoparticles were prepared by mixing neem leaf extract and 0.01 M $AgNO_3$ solution in the ratios of 1:4, 2:4, 3:4 v/v in a 250 mL

Erlenmeyer flask. Dilute ammonium hydroxide (NH_4OH) solution was used to maintain the pH of the reaction mixture in the range of 8-9. The flask was kept for 2 h in magnetic stirrer at 80 rpm to achieve homogeneous reaction. Sonification was carried out to reduce size and purify the silver nanoparticles in the colloidal solution. The solution containing silver nanoparticles were centrifuged at 7000 rpm for 20 min. The purified particles were dried by using a hot air oven up to 70ºC for one and half hours. And then solid silver nanoparticles were obtained.

Confirmation for the Existence of Silver Nanoparticles in Solution by Tyndall Effect

The laser pointer was placed to the edge of the bottle containing SNP colloidal solution and the light was passed through the solution. The photograph of observation about the existence of silver nanoparticles in solution was presented in Figure 1.

Characterization of Silver Nanoparticles

UV-visible spectrophotometer model is SHIMADZU (UVmini-1240, JAPAN). UV spectra of the silver colloid in the range 330 nm - 460 nm were measured. UV absorption spectra have proved to be quite sensitive to the formation of silver colloids because silver nanoparticles exhibit an intense absorption peak due to the surface plasmon excitation. The absorption band in visible light region (350 nm- 550 nm) is typical for silver nanoparticles. The plasmon peak and the full-width at half-maximum (FWHM) depend on the extent of colloid aggregation.

The phase identification of the silver nanoparticles was carried out by X-ray diffraction method. The solid sample was grounded using a motar and pestle into powder.X-ray powder diffraction measurement was carried out by using (Rigaku,Miniflex-600) powder diffractometer with long fine focus Cu anode.

FT IR measurements were carried out to identify the biomolecules for capping and efficient stabilization of the metal nanoparticles synthesized. The samples were measured by using Perkin Elmer GX System, FT IR spectrophotometer.

Morphology ofthe silver nanoparticles were observed on JSM 5610 LV Scanning Electron Microscopy, JEOL-Ltd., Japan.

Elemental compositions in the prepared silver nanoparticles were determined by EDXRF using EDX-8000 spectrometer (Shimadzu Co.Ltd., Japan).

Preparation of Pure Polyvinyl Alcohol Films (PVA)

Polyvinyl alcohol (PVA) films were prepared by solution casting method. Different concentrations of PVA (molecular weight 14,000, degree of hydrolysis 98 %) (1, 2, 3, 4 and 5 % w/v) solution were prepared with distilled water by stirring and heating at 50 ºC. The PVA solutions were placed in an autoclave at 0.1 MPa and 121ºC for 20 min. Each polymer solution was casted on melamine plate and dried in air. The series of PVA films were obtained.

Preparation of Polyvinyl Alcohol- Silver Nanoparticles Composite Films (PVA-SNP)

Polyvinyl alcohol- silver nanoparticles composite films were prepared by mixing different volume ratios of 3 % (w/v) of PVA solution and the prepared SNP-NL2 solution (95:5, 90:10, 85:15, 80:20, 75:25, 70:30 v/v) to make up 100 mL. The mixed solutions were stirred by using a magnetic stirrer at 80 rpm for 20 min. Then polymer solutions were kept for sufficient time to remove any bubble formation. Each polymer solution was placed on melamine plate and dried in air. The melamine plates containing the composite solutions were left about 7 days to obtain PVA-SNP composite films. The composite films after drying were removed easily from the melamine plates.

Determination of the Antimicrobial Activity by Agar Well Diffusion Method

The PVA-SNP composite films were tested with (a) *Bacillus subtilis* (b) *Staphylococcus aureus* (c) *Pseudomonas aeruginosa* (d) *Bacillus pumilus* (e) *Candida albicans* (f) *Escherichia coli* species to investigate the nature of antimicrobial activity.

Results and Discussion

Biosynthesis of Silver Nanoparticles by Using Neem Leaf Extract as Reducing agent

Different volumes of neem leaf extract were mixed with 0.01 M $AgNO_3$ solution in three different ratios of 1:4, 2:4 and 3:4 v/v without varying the other conditions. Reduction of the silver ions to silver nanoparticles during exposure to the plant leaf extract was followed by colour change from pale yellow to reddish brown colour. This is due to the excitation of surface plasmon vibration in silver nanoparticles.

Tyndall Effect

Tyndall effect on silver nanoparticles (SNPs) is shown in Figure 1. It was found that the laser light passes through the solution due to the presence of nanoparticles.

Figure 1: Tyndall effect on the prepared SNPs by green synthesis

Characterization of Silver Nanoparticles

UV-visible Studies

The sample when treated with complete reaction conditions, change in colour of extracts suspension from pale yellow to brownish red was observed. This colour change preliminary showed the presence of silver nanoparticles or reduction of Ag^+ of $AgNO_3$ to Ag^0. After observing changes in colour of the extracts, the maximum absorbance was observed at 415 nm due to surface resonance of silver nanoparticles shown in the Figure 2.

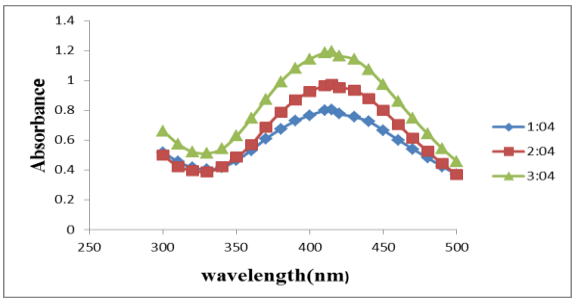

Figure 2:UV-visible spectra of prepared silver nanoparticles (SNP-NL)by green synthesis

X Ray Diffraction Studies

The XRD data were obtained in the 2θ range from 10º to 70º in step scan mode with 2θ step of 0.02º. The diffraction pattern indicated that the sample is the silver nanoparticles. The conversion of silver nitrate to silver nanoparticle was greater than ninty percent and smaller peaks contributed to neem extract impurity. The XRD pattern of SNPs is shown in the Figure 3 (a, b, c). From XRD analysis, all prepared silver nanoparticles give (111), (200) and (220) reflection planes between 2θ values 30º-70º and cubic crystal structure. However, SNP-NL2 samples show only single phase of Ag and no impurity peaks. Therefore, SNP-NL2 was chosen for the optimum sample. The crystallite sizes of all of the prepared SNP- powders were calculated by Debye-Scherrer equation in Table 1 (a, b, c). According to Table 2, the average crystallite size of the prepared SNP powders are SNP-NL1 (8.46 nm), SNP-NL2 (6.93 nm) and SNP-NL3 (4.8 nm).

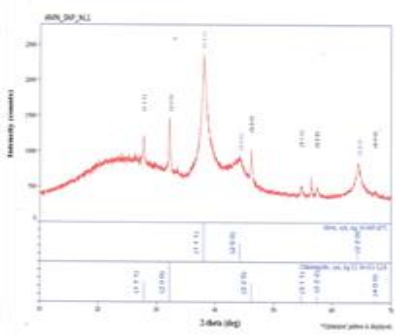

Figure 3:(a) XRD diffractogram of silver nanoparticles by green synthesis SNP-NL1

Table1(a)Crystallite Size of Silver Nanoparticles by XRD

2θ	FWHM	(hkl)	□ (Å)	Crystalline size (nm)
37.919	1.035	111	1.5406	8.48
44.050	1.910	200	1.5406	4.70
64.420	0.810	220	1.5406	12.20
		Average		**8.46**

(SNP-NL1)

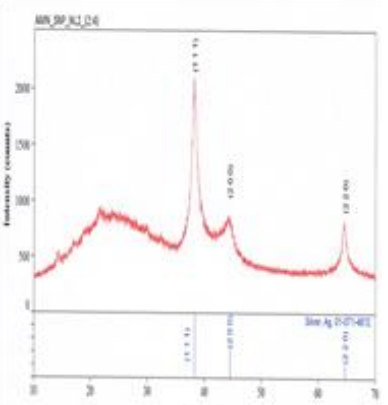

Figure3:(b) XRD diffractogram of silver nanoparticles by green synthesis SNP-NL 2

Table 1: (b) Crystallite Size of Silver Nanoparticles by XRD

2θ	FWHM	(hkl)	□ (Å)	Crystalline size (nm)
38.259	1.060	111	1.5406	8.28
44.210	2.070	200	1.5406	4.32
64.540	1.190	220	1.5406	8.20
Average				6.93

(SNP-NL2)

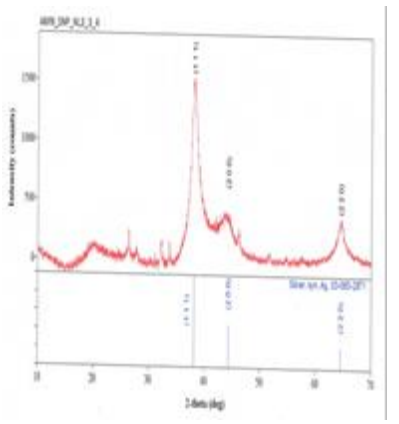

Figure3:(c) XRD diffractogram of silvernanoparticles by green synthesis SNP-NL 3

Table 1: (c) Crystallite Size of Silver Nanoparticles by XRD

2θ	FWHM	(hkl)	□ (Å)	Crystalline size (nm)
38.170	1.70	111	1.5406	5.15
44.080	3.13	200	1.5406	2.86
64.510	1.54	220	1.5406	6.39
Average				4.80

(SNP-NL3)

Table2: Average Crystallite Size of the Prepared SNP Powder Using Green Synthesis by XRD Analysis (0.01 M $AgNO_3$)

Samples	NL : $AgNO_3$(v/v)	Crystallite size (nm)	Crystal structure
SNP-NL1	1 : 4	8.46	Cubic
SNP-NL2	2 : 4	6.93	Cubic
SNP-NL3	3 : 4	4.80	Cubic

FT IR Analysis

Figure 4 shows theFT IR spectra of all of the prepared SNP-NL, the characteristic absorption bands at 3435, 2877, 1631, 1018 cm^{-1} were observed. These peaks correspond to groups present in the sample and are indicated to O-H stretching, C-H stretching, C=C stretching and C-O-C stretching which is the good correlation with that of literature. These bands were confirmed the presence of terpenoids and flavonoids in neem leaf. It was inferred that terpenoids present in neem leaf extract acts as stabilizing as well as capping agents. From FT IR spectrum of SNP-NL, it was observed that the carbonyl group from amino acid residues and proteins could possibly for the metal nanoparticles to prevent agglomeration and stabilize the medium. The biological molecules were performed dual functions of formation and stabilization of silver nanoparticles in the aqueous medium. Table 3 shows FT IR spectral peaks of SNP-NL1, SNP-NL2 and SNP-NL3.

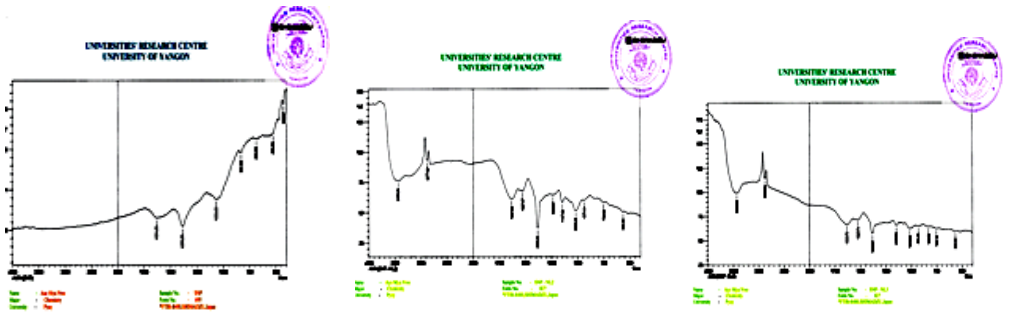

(a) (b) (c)

Figure 4: FT IR spectra of the prepared SNP-NL (a) SNP-NL1, (b) SNP-NL2 and (c) SNP-NL3

Table 3: FT IR Spectral Assignments of the Prepared Silver Nanoparticles

Experimental Frequency (cm^{-1})			***Literature Frequency (cm^{-1})**	**Band Assignments**
SNP-NL1	SNP-NL2	SNP-NL3		
-	3435	3435	3600-3000	-OH stretching vibration
-	2877	2875	2980-2800	C-H stretching vibration of sp^3 hydrocarbons
1631	1631	1633.7	1620-1580	C=C ring skeletal stretching vibration
1386	1383	1383.1	1380-1300	-OH bending vibration
1068	1018	1016.5	1100-1025	C-O-C stretching vibration
831,526, 428	565	833,567	830-500	C-H out of plane bending vibration

*Silverstein, (1998)

SEM Analysis

Futher characterization of silver nanoparticles was done by using scanning electron microscope (SEM). The scanning electron micrographs of the prepared silver nanoparticles are shown in Figure 5. It can be concluded that SNPs are initially monodispersed but drying process lead to agglomeration of many particles resulted into larger size particles.

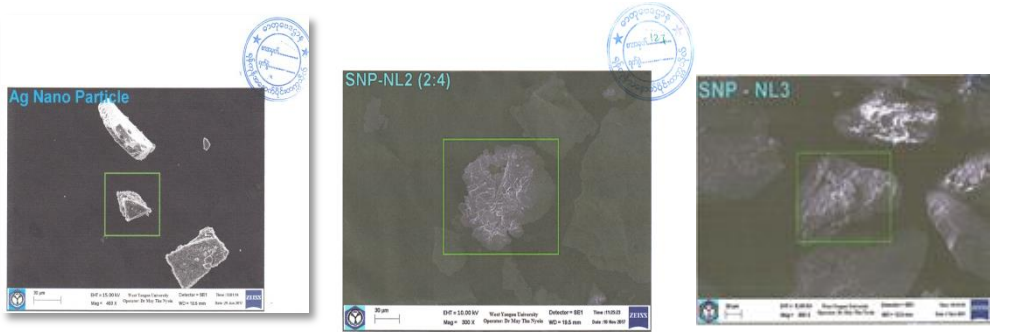

(a) (b) (c)

Figure 5: Scanning electron micrograph of silver nanoparticles by green synthesis(a) SNP-NL1, (b) SNP-NL2 and(c) SNP-NL3 a = 403 X magnification, b = 300 X magnification, c= 300 X magnification

EDXRF analysis

Figure 6 shows EDXRF spectra of SNP-NL2. According to the EDXRF spectra of the prepared SNP-NL2, silver were major constituent (92.384 %) and other were trace constituents. Table 4 shows the relative abundance of elements in the prepared SNP-NL2 by EDXRF.

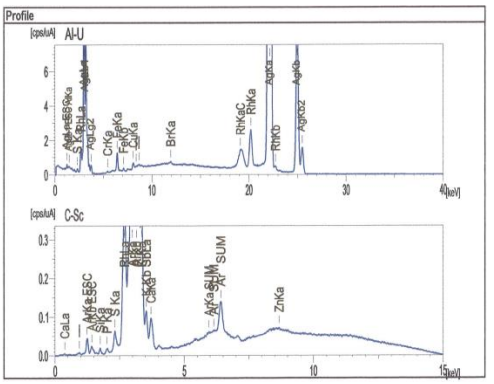

Figure 6 :EDXRF spectra of SNP-NL2

Table 4:Relative Abundance of Elements in Prepared SNP-NL2 by EDXRF

No.	Elements	Relative Abundance (%)
1	Silver	92.384
2	Aluminum	2.791
3	Potassium	1.503
4	Silicon	0.911
5	Calcium	0.808
6	Sulphur	0.532
7	Iron	0.532
8	Phosphorus	0.325
9	Copper	0.108
10	Chromium	0.075
11	Bromine	0.031

Table 5: Yield Percentage of Silver Nanoparticles

No	Sample	Weight of Silver in Silver nitrate (g)	Weight of Silver Particles (g)	Yield (%)
1	SNP-N 1	0.17	0.050	46.30
2	SNP-N 2	0.17	0.062	57.41
3	SNP-N 3	0.17	0.052	48.15

According to the Table 5, the yield percentage of silver nanoparticles was found to be SNP-NL1 (46.30 %), SNP-NL2 (57.41 %) and SNP-NL3 (48.15 %). Among them, SNP-NL2 gave more silver nanoparticles.

Aspect of the Preparation of Pure PVA Film

Pure PVA films were prepared using various percents of PVA (1 % to 5 % w/v) in distilled water by solution casting method. The prepared PVA films were designated as PVA-1, PVA-2, PVA-3, PVA-4 and PVA-5 according to the percent of PVA. The prepared pure PVA films appeared to be homogeneous, transparent and colourless. According to the physicomechanical properties (tensile strength, elongation at break and tear strength) of prepared PVA films, PVA-3 was chosen for the optimum films according to tensile strength, elongation at break and tear strength as shown in Figure 7 and Table 6.

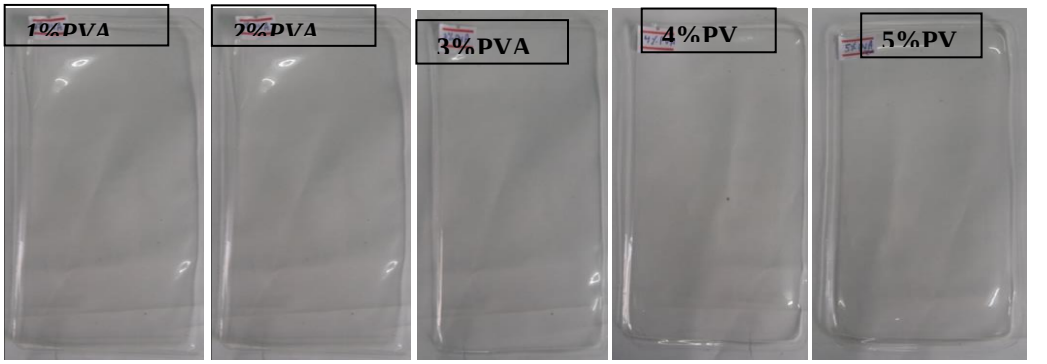

Figure 7: The photographs of (a) PVA-1 (b) PVA-2 (c) PVA-3 (d) PVA-4 (e) PVA-5 films

Table 6: Physicomechanical Properties of the Prepared Polyvinyl Alcohol Films

Prepared Films	PVA(%) w/v	Tensile Strength (MPa)	Elongation at Break(%)	Tear Strength (kNm^{-1})
PVA-1	1	26.0	128	96.3
PVA-2	2	29.7	202	114.0
PVA-3	3	31.7	241	155.8
PVA-4	4	27.1	216	87.9
PVA-5	5	33.0	282	101.0

Thickness = ~ 0.57 mm

Characterization of the Prepared PVA Film

The selected prepared PVA-3 film was characterized by modern techniques such as XRD, SEM, FT IR were shown in Figure 8. The XRD pattern of PVA film exhibits a broad diffraction peak due to the amorphous nature of the polymer. The SEM micrograph of the prepared PVA-3 membrane has smooth surface and homogeneous film. The FT IR spectrum of pure PVA film exhibits a major peaks associated with PVA. The major peaks were observed in the 3600 cm^{-1}, 2955 cm^{-1}, 1568 cm^{-1} and 1458 cm^{-1}. These major peaks showed the O-H stretching, C-H stretching, C=C stretching and O-H bending. As seen in Figure 9, the thermogram of PVA-3 film possesses three stages of distinct weight loss between 38 ºC to 600 ºC. The first stage ranged between 38 ºC and 120 ºC with 11.04 % of weight loss and this was due to the evaporation of loosely bound water. The second stage ranged between 120 ºC and 350 ºC was due to the scission of functional group of polymer chain. The third stage of weight loss indicated the degradation of polymer backbone and progressive rupture of chain, combustion and formation of residue.

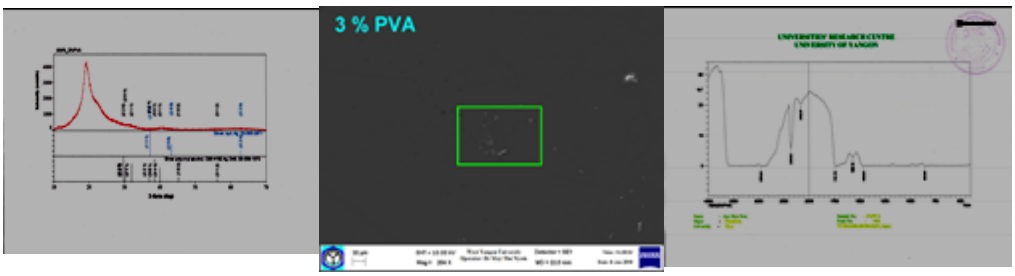

(a) (b) (c)

Figure 8: (a) XRD diffractogram, (b) SEMmicrograph and (c) FT IR spectrum of the prepared polyvinyl alcohol PVA-3 film

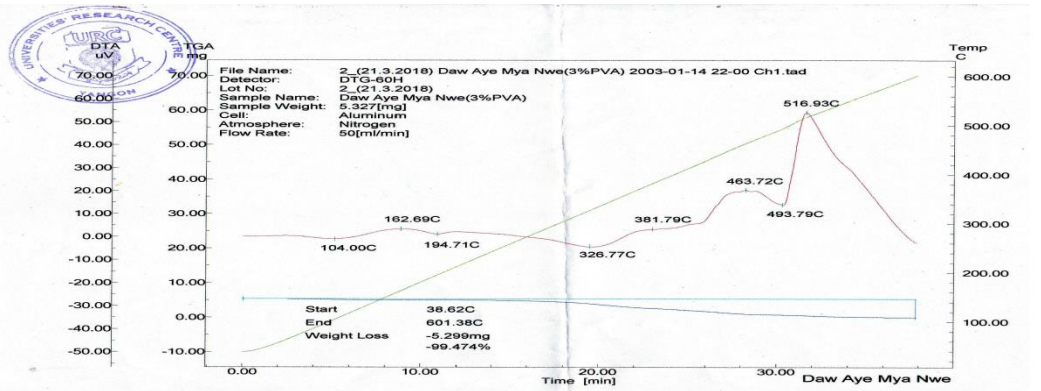

Figure 9: TG-DTA thermogram of the prepared polyvinyl alcohol PVA-3 film

Table 7: Thermal Analysis Data of the Prepared Polyvinyl Alcohol PVA-3 Film

TG Thermogram			Nature of Peak DTA	Remark
Temperature Range (°C)	**Total Weight Loss (%)**	**Break in Temperature (°C)**		
38-120	11.04	104	endothermic	-due to the evaporation of loosely bound water
120-350	33.13	326	endothermic	due to the scission of functional group of polymer chain
350-600	55.30	463 516	Exothermic	Due to the degradation of polymer backbone and progressive rupture of the chain, combustion and formation of residue

Aspect of Preparation of PVA-SNP Films

The PVA-SNP composite films were prepared by solution casting method from solutions of PVA-3 and SNP–NL2 in deionized water at various compositional ratios. The basic method for the synthesis of NPs in PVA is to disperse metal ion solution in the polymer and reduce to zero valent states. The PVA-SNP composite films were prepared by using different volume ratios of PVA-3 solution and SNP-NL2 colloidal solutions (95:5, 90:10, 85:15, 80:20, 75:25 and 70:30). The obtained composite films were designated as PVA-SNP-1, PVA-SNP-2, PVA-SNP-3, PVA-SNP-4, PVA-SNP-5 and PVA-SNP-6 respectively. The effect of composite films composition on mechanical properties and antimicrobial activity were studied. Solutions of PVA-SNP appeared to be homogeneous and transparent. The colour of the solution varied from colourless of pure PVA solution to dark brown colour with increasing SNP content. The distinctive colours of nanosilver are due to the phenomenon known as plasmon absorbance. Incident light creates oscillations in conduction electrons on the surface of the NPs and electromagnetic radiation is absorbed. This indicates the formation of AgNPs. With an increase in reaction time, particle size and aggregation of silver nanocrystal gradually increased together. After evaporation of the solvent, the prepared films of PVA-SNP composite films were found to be transparent. Figure 10.

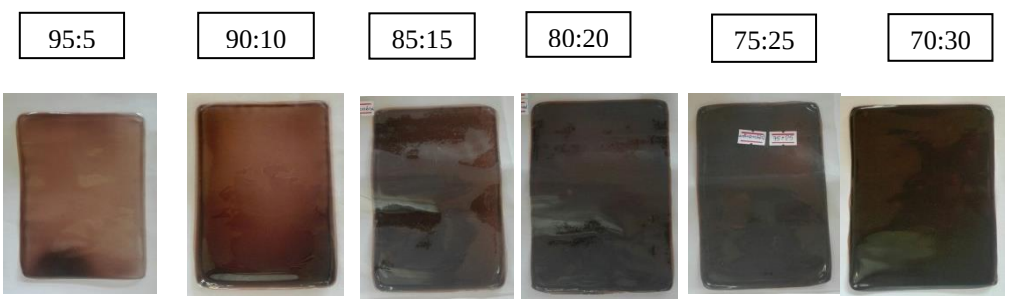

(a) PVA-SNP-1 (b)PVA-SNP-2 (c)PVA-SNP-3 (d) PVA-SNP-4 (e) PVA-SNP-5 (f) PVA-SNP-6

Figure 10: The photographs of PVA-SNP composite films with various volume ratios of PVA-3 solution and colloidal SNP solution

Aspect of Physicomechanical Properties of Polyvinyl Alcohol- Silver Nanoparticles Composite Films

The physicomechanical properties of polyvinyl alcohol-silver nanoparticles composite films were shown in Table 8. From the resulting data, PVA-SNP- 3 composite film was found that tensile strength of 30.8 MPa, elongation at break of 231 % and tear strength of 117 kNm^{-1}. Therefore, PVA-SNP-3 was chosen for optimum film due to its highest elongation at break.

Table 8: Physicomechanical Properties of Polyvinyl Alcohol- Silver Nanoparticles composite Films

No.	Parameters	PVA-SNP Composite Films					
		PVA-SNP-1	**PVA-SNP-2**	**PVA-SNP-3**	**PVA-SNP-4**	**PVA-SNP-5**	**PVA-SNP-6**
1	Tensile strength (MPa)	3.0	26.1	30.8	29.2	29.7	33.3
2	Elongation at Break (%)	133	147	231	168	89	221
3	Tear Strength(kNm^{-1})	16.7	152.7	117.0	128.7	56.0	123.0

Thickness = ~ 0.43 mm

Antimicrobial Activity of PVA-SNP Composite Films

Silver is known for its antimicrobial properties and has been used for many years in the medical field for antimicrobial applications. Additionally, silver has been used in water and air filtration to eliminate microorganisms. Inhibition zone values were obtained from the synthesized PVA, PVA-SNP composites tested against six microorganisms: (a) *Bacillus subtilis* (b) *Staphylococcus aureus* (c) *Pseudomonas aeruginosa* (d) *Bacillus pumilus* (e) *Candida albicans* (f) *Escherichia coli*. Antimicrobial activity of PVA-SNP composite films has been investigated by agar well diffusion method as shown in Figure 11 and Table 9. It was observed that the prepared PVA-3 film did not show antimicrobial activity, however PVA-SNP composite films showed the antimicrobial activity.

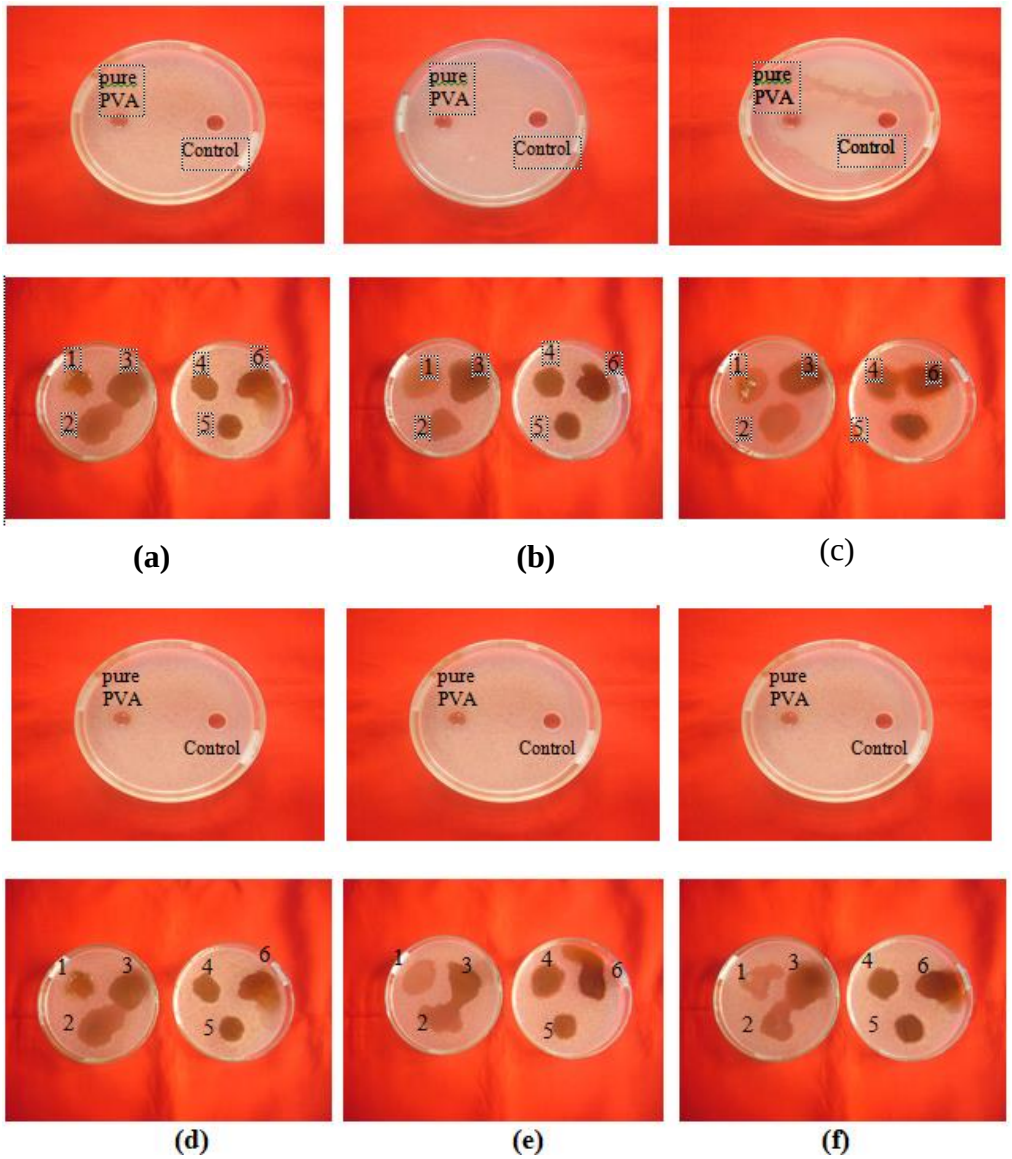

Figure 11: Antimicrobial activity of the prepared (1) PVA-SNP-1, (2) PVA-SNP-2, (3) PVA-SNP-3, (4) PVA-SNP-4, (5) PVA-SNP-5 and (6) PVA-SNP-6 composite films(a) *Bacillus subtilis*(b) *Staphylococcus aureus*(c) *Pseudomonas aeruginosa*(d) *Bacillus pumilus* (e) *Candida albicans*(f) *Escherichia coli*

Table 9: Antimicrobial Activity of the Prepared Polyvinyl Alcohol-Silver Nanoparticles Composite Films by Agar Well Diffusion Method

Sample Films	Inhibition zone diameters of the samples against six microorganisms (mm)					
	(a) *Bacillus subtilis*	(b) *Staphylococus aureus*	(c) *Pseud-omonasaerug inosa*	(d) *Bacillus pumilus*	(e) *Candida albicans*	(f) *Escher-ichia Coli*
Pure PVA	-	-	-	-	-	-
PVA-SNP-1	15 mm	19 mm	17 mm	15 mm	16 mm	16 mm
PVA-SNP-2	19 mm	18 mm	18 mm	18 mm	17 mm	17 mm
PVA-SNP-3	18 mm	19 mm	19 mm	19 mm	17 mm	19 mm
PVA-SNP-4	17 mm	17 mm	16 mm	16 mm	17 mm	15 mm
PVA-SNP-5	15 mm	15 mm	15 mm	15 mm	15 mm	15 mm
PVA-SNP-6	17 mm	17 mm	16 mm	16 mm	16 mm	16 mm

Agar Well 10 mm (-), 10 mm ~14 mm (+), 15 mm ~19 mm (++), 20 mm ~above (+++)

Conclusion

In this research work, the silver nanoparticles were synthesized from neem leaf extract by green synthesis. The synthesized silver nanoparticles were characterized by UV-visible spectroscopy, FT IR, SEM, EDXRF and XRD analysis. By the determination of UV-visible spectra, the maximum absorption peak of colloidal silver nanoparticles were appeared at 415 nm. FT IR spectrum of SNP-NL indicated the absorption bands at 3435, 2877, 1631 and 1018 cm^{-1}. The absorption band at 3435 cm^{-1} is corresponding to O-H stretching, 2877 cm^{-1} is due to C-H stretching, 1631 cm^{-1} is due to C=C stretching and 1018 cm^{-1} is due to C-O-C stretching . The band at 565 cm^{-1} is corresponding to C-H out of plane bending that is responsible for reducing the Ag^{+} to Ag^{0}. From XRD analysis, the average crystallite sizes of all of the prepared SNP-NL were 8.46 nm (SNP-NL1), 6.93 nm (SNP-NL2) and 4.80 nm (SNP-NL3). According to XRD specrta of all of the prepared SNP-NL, there was no impurity peaks in the SNP-NL2. From SEM analysis, all of the prepared SNP-NL were initially monodispersed but drying process caused agglomeration of many particles resulted into larger size particles. According to EDXRF spectra of the prepared SNP-NL2, silver were major constituent (92.384 %) and other were trace constituents. The yield percentage of all of the prepared SNP powders were 46.30 % (SNP-NL1), 57.41 % (SNP-NL2)

and 48.15 % (SNP-NL3). Among them, SNP-NL2 gave more silver nanoparticles. The pure PVA films were prepared by varying different weight percents of 1-5 % w/v PVA solution by using solvent evaporating method. According to the mechanical properties of PVA films, PVA-3 film was chosen for the preparation of PVA-SNP composite film. The characterization by modern techniques such as XRD, SEM, FT IR and TG-DTA were able to reveal the surface morphological texture, pronounced functional groups as well as thermal stabilities of the prepared films. According to the TG-DTA thermogram of the prepared PVA-3 film, three stages of weight loss were observed. These weight loss were due to the evaporation of loosely bound water, the scission of functional group of polymer chain and the degradation of polymer backbone and progressive rupture of the chain, combustion and formation of residue. According to the physicomechanical properties of the prepared PVA-SNP composite film, PVA-SNP-3 has optimum tensile strength (30.8 MPa), elongation at break (231 %) and tear strength (117 kNm^{-1}). Although the prepared PVA-3 film did not show the antimicrobial activity, PVA-SNP composite films were observed to exhibit the antimicrobial activity against all of the tested microorganisms.

Acknowledgements

The authors would like to thank Professor and Head Dr Myint Myint Than, Department of Chemistry, Pyay University and Professor and Head Dr Ni Ni Than, Department of Chemistry, University of Yangon for their kind encouragement.

References

Albrecht, M.A., Evans, C. and Raston, C. (2006).“Green Chemistry and the Health Implications of Nanoparticles’’. *Journal of Green Chem*, vol.,8,pp, 415- 417

Lalitha, A., Subbaiya, R. and Ponmurugan, P. (2013).“Green Synthesis of Silver Nanoparticles from Leaf Extract Azadirachtaindica and To Study its Anti-bacterial and Antioxidant Property’’. *International Journal of Current Microbiology and Applied Science*, vol.,2(6), pp, 228-235

Sayed, M. (2014).“Green Synthesis and Characterisations of Antibacterial Silver- Polyvinyl Alcohol Nanocomposite Films for Wound Dressing”. *Journal of Applied Polymer Science*, vol., 3, pp, 229-234

Silverstein, R. M. and Webster, F. X. (1998). *Spectrometric Identification of Organic Compounds*. New York : 2nd ed., John Wiley and Sons, Inc., USA, 81-109

Sivakumar, T. (2012).“Isolation and Characterization of Silver Nanoparticles from *Fusariumoxysporum*”. *International Journal of Current Microbiology and Applied Sciences*, vol., 1, pp, 56-62

Verma, A., Mohan, S. (2016). “Controllable Synthesis of Silver Nanoparticles using Neem leaves and their Antimicrobial Activity”. *Journal of Radiation Research and Applied Science*, vol.,9, pp, 109-115

ISOLATION OF METHYL PIPERATE FROM THE FRUIT OF *Piper longum* L. (PEIK-CHIN) AND ANTIBACTERIAL SCREENING OF THE CRUDE EXTRACTS AND METHYL PIPERATE

Ei Ei Khaing*

Abstract

The fruit of *Piper longum* L. (Peik-chin) used in the treatment of diarrhoea and dysentery in traditional Myanmar medicinal system was chosen for present study. The aim of the study is to isolate methyl piperate from the fruit of *Piper longum* L. (Peik-chin) and to screen the antibacterial activity of its crude extracts and methyl piperate. At first, four crude extracts of the sample were prepared by using various solvents; petroleum ether, ethyl acetate, 96 % ethanol and 50 % ethanol. *In vitro* antibacterial activity of four crude extracts was investigated against 19 bacterial strains by using agar disc diffusion method. Among the four crude extracts, the most active ethyl acetate extract was selected for isolation of active compound by column chromatographic method by using the solvent systems (v/v) PE : EtOAc (19:1, 9:1, 4:1, 1:1) consecutively. The isolated compound, methyl piperate (0.084 %) was identified by TLC and spectroscopic methods; Ultraviolet, Fourier transform infrared, Proton nuclear magnetic resonance spectroscopy, Electron impact mass spectrometry and then tested on 11 bacteria; *Klebsiella* species, *Salmonella paratyphi* A, *Citrobacter* species, *Escherichia coli* ATCC, *Pseudomonas aeruginosa*, *Salmonella typhi*, *Escherichia coli* YCH 149, *Shigellaflexneri*, *Proteus* species, *Staphylococcus aureu s*and *Vibrio cholerae* O1 by agar disc diffusion method. In addition, minimum inhibitory concentration (MIC) of methyl piperate determined by microtitre plate dilution method was 0.03 mg/mL on six tested bacteria; *E. coli* LT, *S. epidermidis* (MKL-50), *S. epidermidis* (MKL-68), *E. coli* EHEC, *S. aureus* and *B. subtilis*.

Keywords: *Piper longum*, Peik-chin, methyl piperate, antibacterial activity, MIC

Introduction

Diarrhoea and dysentery are important health problems in worldwide especially developing countries. So the Government of Myanmar has initiated a national programme for the development of Traditional Medicine System in

* Dr, Associate Professor, Department of Chemistry, Hinthada University

combating six major types of diseases: namely; malaria, tuberculosis, diarrhoea, dysentery, diabetes and hypertension.

Diarrhoea is the host response to infection of the gastrointestinal tract by a variety of viruses, bacteria and parasites. There are three types of diarrhoea, namely acute diarrhoea, persistent diarrhoea and chronic diarrhoea. Acute diarrhoea is usually defined as the passage of 3 (or) more liquid motions within 7 days. Persistent diarrhoea have a usually long duration, more than 2 weeks, but usually less than 2 weeks duration. Chronic diarrhoea lasts for more than three weeks (Khan, 2001).

Dysentery is an inflammatory disorder of the lower intestinal tract, usually caused by bacteria, parasite, or protozoa infection and resulting in pain, fever, and severe diarrhoea, often accompanied by the passage of blood and mucous. Dysentery is caused by an *Amoeba* or *Bacillus* that infects the colon (Boyd and Marr, 1980).

In this study, Myanmar medicinal plant, *Piper longum* L. (Peik-chin) (Figure 1) was selected to find out of active principle for the treatment of dysentery and diarrhoea. *P. longum*plants are found in the north temperate regions and South East Asia (Fluck, 1976). It is cultivated in India, Indonesia, Malaysia, Sri Lanka, Pakistan, Singapore and Bangladesh. *P. longum* is indigenous and grows wild in Myanmar especially in Mon and Kayin States and hilly regions of Northern Myanmar. The pale yellow crystal, methyl piperate is one of the constituents responsible for medicinal properties of *P. longum* (Jalalpure*et al*.,2003). In Myanmar, *P. longum* is used in treating diarrhoea, dysentery, fever, cough, indigestion, stomachaches and asthma (Mar MarNyein*et al*., 2006).

P.longum contains methyl piperate that shows antioxidant, antibacterial activity as well as antimicrobial activity. The fruit of *P. longum* has been also used in the treatment of gastrointestinal (GI) problems, pneumonia, tumor, flatulence and then used as spice in food industry like a Nga-yoke-kaung (Krool, 2001; Kumar *et al.*, 2011). Therefore, antibacterial activity investigation on four crude extracts (PE, EtOAc, 96 % EtOH, 50 % EtOH) and some isolated phytoconstituents from the fruit of *P. longum*were carried out by using agar disc diffusion method. In this study, Minimum inhibitory concentration (MIC) of active constituent was also determined by microtitre plate dilution method.

Botanical Aspects of *Piper longum* L.

Name : Peik-chin (in Myanmar),
Long pepper (in English)
Botanical Name : *Piper longum*L.
Family : Piperaceae
Genus : *Piper*
Fruit : Fleshy spikes 2.5 - 3.5 blunt, blackish green from small shrub (Kress *et al*., 2003)

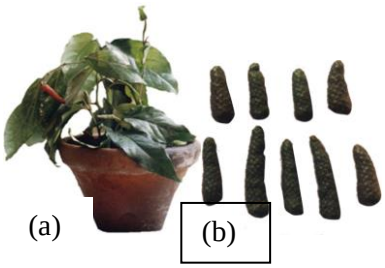

Figure 1: (a) Plant of *P. longum* L.
(b) Fruit of *P. longum* L.

Distribution

P. longum (Peik-chin) is widely distributed in shady places and hilly regions of Myanmar and often planted for its medicinal properties.

Chemical Constituents

The fruit of *P. longum* (Peik-chin) contained a large number of alkaloids and related compounds, the most abundant of which is piperine, followedby methyl piperate, pipernonaline, piperettine, tetrahydropiperlongumine, piperidine, volatile oil, palmitic acid, tetrahydropiperic acid and vitamins A and E (Kumar *et al.*, 2011).

Materials and Methods

Plant Materials

The fruit of *P. longum* L. (Peik-chin) was collected from Mawlamyine, Mon State. The plant was identified at Department of Botany, Yangon University. The fruit of *P. longum* was washed, cleaned and dried at room temperature for three weeks. Then the dried sample was powdered and stored in air- tight container.

Instruments: Shimadzu UV-240 (MeOH), Shimadzu FT IR- 8400 (KBr) (at URC), ^{1}H (300 MHz) NMR, EI MS (at University of Goettingen, Germany).

Chemicals : CC; Merck Silica gel 60 (70-230) mesh, eluents; Petroleum ether (PE), ethyl acetate (EtOAc), TLC; precoated silica gel 60 (F_{254}, Merck)

Extraction and Isolation of Methyl Piperate from Fruit of *Piper longum* L.
Preparation of extracts from fruit of *Piper longum* L.

The air-dried powder (1 kg) was individually cold extracted with (2500 mL) of solvents; petroleum ether (60-80 °C), ethyl acetate, 96 % ethanol and 50 % ethanol, respectively for 7 days and then filtered. The filtrate was evaporated to dryness at normal pressure on a water bath and desiccated. The yield % of petroleum ether extract, ethyl acetate extract, 96 % ethanol extract and 50 % ethanol extract were determined.

Isolation of phytoconstituents from EtOAc extract of fruit of *Piper longum* L.

The EtOAc extract was subjected to isolate the active phytoconstituents from Peik-chin fruit by column chromatography. The column was packed with silica gel (400 g) by the wet method using petroleum ether. The column was eluted consecutively with the solvent systems of PE :EtOAc in the ratio of 19:1, 9:1, 4:1, 1:1 v/v according to their increasing polarity. Five fractions were monitored by thin layer chromatography (TLC). The fractions that gave similar spots on thin layer chromatography (TLC) plates were combined together and the solvent was evaporated. Finally, pure compound obtained from fraction IV, pale yellow crystal (0.12 g, 0.084 %) was characterized as methyl piperate by UV, FT IR, ^{1}HNMR and EI MS spectroscopic methods.

***In vitro* Studies on the Antibacterial Activity of Fruit of *Piper longum* L. by Agar Disc Diffusion Method**
Screening of antibacterial activity of crude extracts against 19 tested bacterial strains

Agar disc diffusion method was used for the detection of antibacterial activity for four crude extracts from *P. longum* fruit. The test procedure was as follows: the extracts (1 g each) were dissolved in 1 mL of their respective solvents; petroleum ether, ethyl acetate, 96 % ethanol and 50 % ethanol, and introduced into sterile petridishes for testing 19 cultural bacterial strains. The discs having 6 mm diameter each with 20 µg extract/disc were allowed to dry at 42 $^{\circ}$C in incubator.

The bacterial suspension from trypticase soy broth was streaked evenly into three places on the surface of the trypticase soy agar plates with sterile cotton swab (Puritan, USA). After the inoculums had dried for 5 min, the dried disc impregnated with extracts were placed on the agar with flamed forceps and gently pressed down to ensure proper contact. A disc impregnated with solvent only was used as control and antibiotics tetracycline was also used as standard for this study.

After overnight incubation at 37 °C, the zones of inhibition diameter including 6 mm discs were measured. Out of four crude extracts, the most active extract (EtOAc) was selected for isolation of active compound and MIC determination.

Screening of antibacterial activity of EtOAc extract and the isolated methyl piperate from active EtOAc extract of fruit (*Piper longum* L.) against 11 tested bacterial strains

The selected most active EtOAc extract and isolated compound methyl piperate (0.12 g, 0.084 %) were subjected to study antibacterial activity against 19 tested bacteria from clinical sources, National Health Laboratory (NHL), Yangon; related to acute diarrhoea (cholera), dysentery, abscess, pneumonia and typhoid.

Determination of Minimum Inhibitory Concentration (MIC) by Microtitre Plate Dilution Method

The MIC value of isolated compound, methyl piperate from *P. longum* was tested with 6 strains; *E. coli* LT, *S. epidermidis* (MKL-50), *S. epidermidis* (MKL-68), *E. coli* EHEC, *S. aureus* and *B. subtilis* by microtitre plate dilution method.

Microtitre plate dilution method was done by using trypticase soy broth by dissolving with appropriate soluble compound, methyl piperate in 2-fold dilutions. First, an inoculum of pure culture of respective bacteria was seeded in 5 mL of trypticase soy broth (TSB) and incubated at 37 °C for 3-4 h to obtain a turbidity of 0.05 by MacFarland nephelometer which corresponded to a bacterial suspension of 10^6 organisms per mL. Prior to the experiment, 50 L of TSB was introduced into all wells of 96-well microtitre plate. The compound (methyl piperate) was dissolved in ethyl acetate and diluted with

trypticase soy broth to obtain the following concentration: 0.12 mg/mL, 0.06 mg/mL, 0.03 mg/mL, 0.015 mg/mL, 0.008 mg/mL, 0.004 mg/mL, 0.002 mg/mL, 0.001 mg/mL, 0.0005 mg/mL, 0.00025 mg/mL, 0.000125 mg/mL and 0.0000625 mg/mL, in 96 - well microtitre plates.

Then 0.02 µL of the prepared inoculum was introduced to its respective wells and the microtitre plates were incubated at 37 °C for 18 h. The contents of all wells were thoroughly mixed with a multi-channel pipetter to resuspend clamped cells at the bottom of the wells in a solution. Growth of the bacteria was determined by automated microplate reader (Bio Rad) at a wavelength of 450 nm as well as confirmed by the growth of culturing onto trypticase soy agar to incubate at 37 °C for overnight. The concentration of the compound in the last well with no growth of bacteria was taken to represent the minimum inhibitory concentration (MIC)of the compound.

Results and Discussion

Isolation and Characterization of Methyl Piperate from Ethyl Acetate Extract of *Piper longum* L. Fruit

The dried fruit powder collected from Mawlamyine, Mon State was extracted with various solvents and the yield % of petroleum ether extract (1.5%), ethyl acetate extract (3.5 %), 96 % ethanol extract (4.5 %) and 50 % ethanol extract (6.2 %) were obtained respectively. Methyl piperate (0.084 %) was isolated from ethyl acetate extract of *P. longum*by column chromatographic separation method using petroleum ether: ethyl acetate solvent system. The isolated compound as methyl piperate was then identified by melting point, TLC determination, UV (Figure 2), FT IR (Figure 3), and ^{1}HNMR (Figure 4) and EI MS (Figure 5) spectrometry. Melting point of the isolated compound was found to be 140-14 °C which was identical with reported value of methyl piperate (Mohring and Necker, 1979). Isolated compound gave R_f value 0.63 with petroleum ether - ethyl acetate (4:1) system and was observed blue colour with anisaldehyde-conc. H_2SO_4 in TLC chromatogram.

Methyl piperate: Pale yellow crystal (0.12 g, 0.084 % yield); λ_{max}^{MeOH} 310, 340 (nm); FT IR ν cm^{-1} 2926, 2854 (ν CHasym & sym of methyl) , 1707 ($\nu_{C=O}$ of ester), 1618, 1607 ($\nu_{C=C}$ asym & sym diene), 1496 ($\nu_{C=C}$ -aro), 1452 (δ_{CH_2}), 1373 (δ_{CH_3}), 1265, 1244 ($\nu_{asym\ C\text{-}O\text{-}C}$), 1142 ($\nu_{sym\ C\text{-}O\text{-}C}$), 948, 928 ($\delta_{CH}$ of trans CH=CH group), 865, 839, 814 (δ_{CH} out of plane bending); ^{1}HNMR (300 MHz,$CDCl_3$) / δ_H (ppm), ~3.78 (3H, s, OC**H$_3$**), ~5.85 (1H, d, -CH=C**H**-CO-), ~6.0 (2H, s, -O-C**H$_2$**-O-), ~6.62 (1H, d, aromatic H), ~6.67 (1H, d, -C**H**=CH-), ~6.70 (1H, d, aromatic H), ~6.80 (1H, d, aromatic H), ~6.85 (1H, t, -CH=C**H**-CH=), ~7.42 (1H, dd, -C**H**=CH-CO-); EI MS, m/z 232.9 [$M^{+\circ}$], 233.9 [$M+H^+$] 201.2 [$M - OCH_3^+$] [$C_{13}H_{12}O_4$] (Figures 2,3,4 and 5) (Silverstein *et al*., 1991)

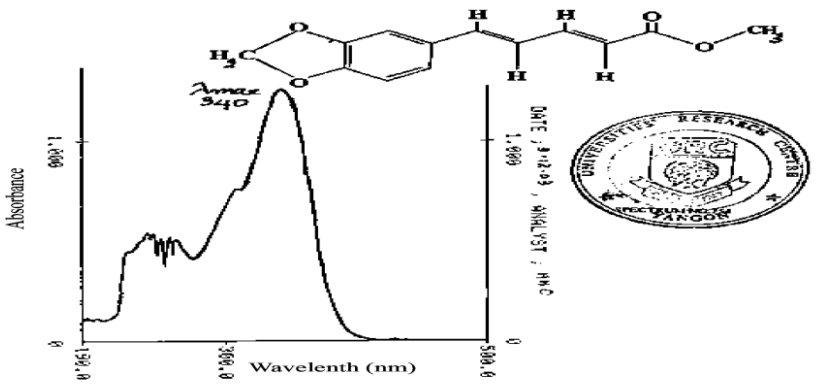

Figure 2 : Ultraviolet spectrum of isolated compound from fruit of *P. longum* (MeOH)

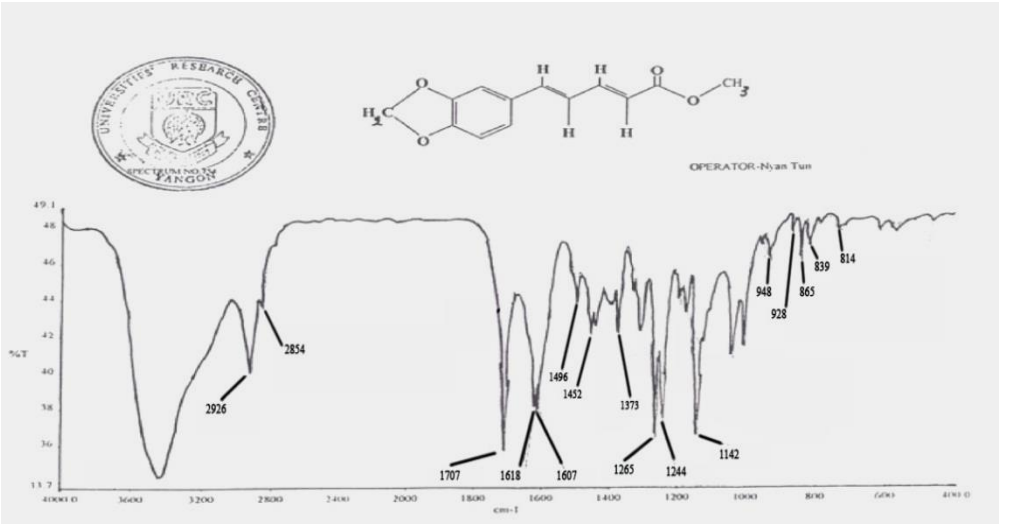

Figure 3: FT IR spectrum of isolated compound from fruit of *P. longum* (KBr)

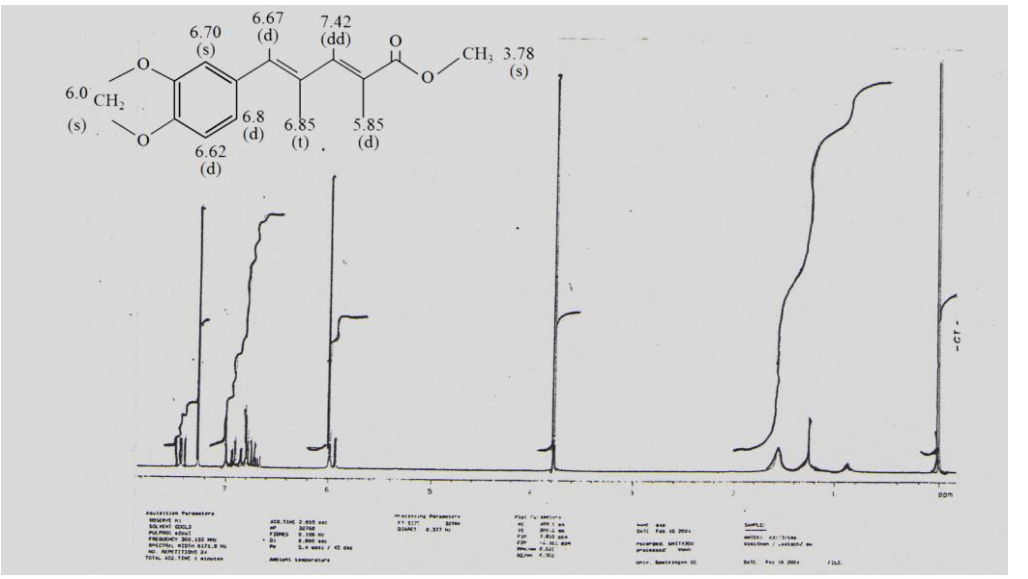

Figure 4: ^{1}HNMR (300 MHz, $CDCl_3$) spectrum of the isolated compound from fruit of *P. longum*

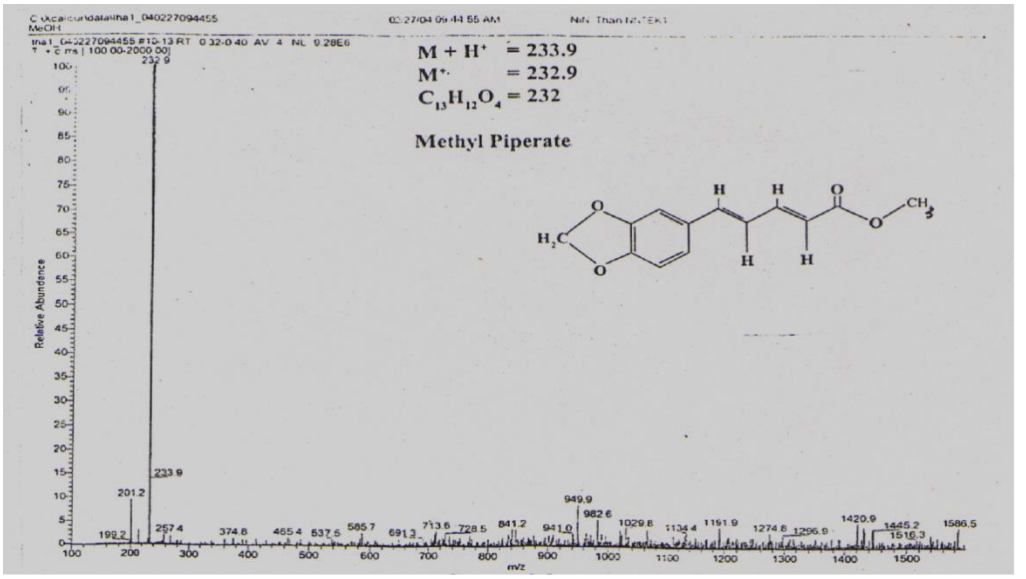

Figure 5: EI MS spectrum of the isolated compound from fruit of *P.longum*

Screening of Antibacterial Activity of Crude Extracts and Isolated Methyl Piperate

Screening of antibacterial activity of 4 crude extracts has been done by agar disc diffusion method. The inhibition zone diameters of extracts tested with 19 strains of bacteria from clinical sources are shown in Table 1. The most active ethyl acetate extract with the range of inhibition zone diameter (12-20) mm against 19 strains; *Salmonella derby*, *Escherichia coli* LT, *Escherichia coli* O128, *Escherichia coli* EHEC, *Staphylococcus aureus*ATCC, *Salmonella paratyphi*, *Salmonella stanley*, *Shigella boydii*, *Salmonella pollorum*, *Shigella dysenteriae*, *Vibrio chlolerae* Inaba, *Escherichia coli* ATCC, *Pseudomonas pyocyanea*, *Vibrio cholerae* O1, *Salmonella typhi*, *Vibrio cholerae* O139, *Shigella flexneri Bacillus subtilis* and *Staphylococcus aureus*was selected for isolation of active compound. But petroleum ether extract only showed activity (12 mm) against *Pseudomonas pyocyanea.* And then antibacterial activity of ethyl acetate extract and isolated methyl piperate were being compared on 11 tested bacteria from clinical sources shown in Table 2 and Figure 6. In Table 2 it was found that the isolated methyl piperate showed more potent activity with inhibition zone diameters (16-42) mm of all

strains but ethyl acetate extract exhibited less potent to 11 strains with inhibition zone diameter (13-24) mm. According to these zone diameters, theantibacterial activity of methyl piperate against *Klebsiella* species, *Citrobacter* species, *Pseudomonas aeruginosa,Salmonella typhi*, *Escherichia coli* YCH 149,*Shigellaflexneri*, *Proteus species, Staphylococcus aureus* and *Vibrio cholerae* O1 are more potent than tetracycline (standard) except *Salmonella paratyphi* A and *Escherichia coli* ATCC. From the screening results, it can be generally deduced as follows. The EtOAc extract and isolated methyl piperate from *P. longum* were found to inhibit the tested bacteria with regard to acute diarrhoea (cholera), dysentery, pneumonia, typhoid, urinary tract infection, sepsis and abscess. In addition, methyl piperate yielded (0.084 %) from *P. longum*was employed by microtitre plate dilution method for minimum inhibitory concentration (MIC) determined with 2 strains of *Escherichia coli*, 2 strains of *S. epidermidis*, each strain of *Staphylococcus aureus* and *B. subtilis* obtained from clinical sources at Bacteriology Research Division, DMR (LM) (Table 3). The microtitre plate dilution method also elaborates the specificity, sensitivity and the least amount required for media, reagents and glassware. It also saves time and working space in conducting the experiments. The minimum inhibitory concentration (MIC), 0.03 mg/mL of methyl piperate with all tested bacteriashowed that the plant possess potent bactericidal activity on them. From the MIC elucidation, methyl piperate isolated from the fruit of Peik-chin would be more effective for the treatment in diarrhoea, urinary tract infection, food poisoning and abscess. It has antibacterial action against *E. coli* responsible for diarrhoea, *S. epidermidis* responsible for urinary tract infection, *B. subtilis* responsible for food poisoning and *Staphylococcus aureus* responsible for abscess occurred in skin, mouth and nose.

Table 1:Results of Antibacterial Activity of Four Extracts of *P. longum* on 19 Species of Bacteria

No.	Type of bacteria	Inhibition zone diameter (mm)			
		EtOAc extract	**96%EtOH extract**	**50%EtOH extract**	**PE extract**
1	*Salmonella derby*	14	-	14	-
2	*Escherichia coli* LT	16	16	20	-
3	*Escherichia coli* O128	14	7	-	-
4	*Escherichia coli* EHEC	18	8	12	-
5	*Staphylococcus aureus*ATCC	13	20	17	-
6	*Salmonella paratyphi*	12	12	-	-
7	*Salmonella stanley*	12	11	16	-
8	*Shigella boydii*	17	8	-	-
9	*Salmonella pollorum*	16	-	12	-
10	*Shigella dysenteriae*	18	12	-	-
11	*Vibrio cholerae* Inaba	12	13	13	-
12	*Escherichia coli* ATCC	15	-	-	-
13	*Pseudomonas pyocyanea*	20	20	12	12
14	*Vibrio cholerae* O1	20	22	-	-
15	*Salmonella typhi*	14	-	-	-
16	*Vibrio cholerae* O139	12	-	20	-
17	*Shigella flexneri*	15	12	-	-
18	*Bacillus subtilis*	12	10	11	-
19	*Staphylococcus aureus*	20	20	20	-

(-) = no activity
Disc diameter = 6 mm

Table 2: Antibacterial Activity of EtOAc Crude Extract and Methyl Piperate, Isolated from Fruit of *P. longum*

Sample	Inhibition zone diameter (mm)										
	1	**2**	**3**	**4**	**5**	**6**	**7**	**8**	**9**	**10**	**11**
EtOAc Crude Extract	14	20	19	21	21	18	23	18	13	2031	24
Methyl piperate	38	24	31	16	42	42	37	30	19	-	32
Blank	-	-	-	-	-	-	-	-	-	-	-
EtOAc solvent (control)	-	-	-	-	-	-	-	-	-	29	-
Tetracycline (standard)	13	25	25	25	15	10	25	12	-		29

Tested Bacteria (From Clinical Sources*)

1 = *Klebsiella* species
2 = *Salmonella paratyphi* A
3 = *Citrobacter* species
4 = *Escherichia coli* ATCC
5 = *Pseudomonas aeruginosa*
6 = *Salmonella typhi*
7 = *Escherichia coli* YCH 149
8 = *Shigellaflexneri*
9 = *Proteus* species
10 = *Staphylococcus aureus*
11 = *Vibrio cholerae* O1

Disc diameter = 6 mm

- = no activity

***** National Health Laboratory (NHL), Yangon

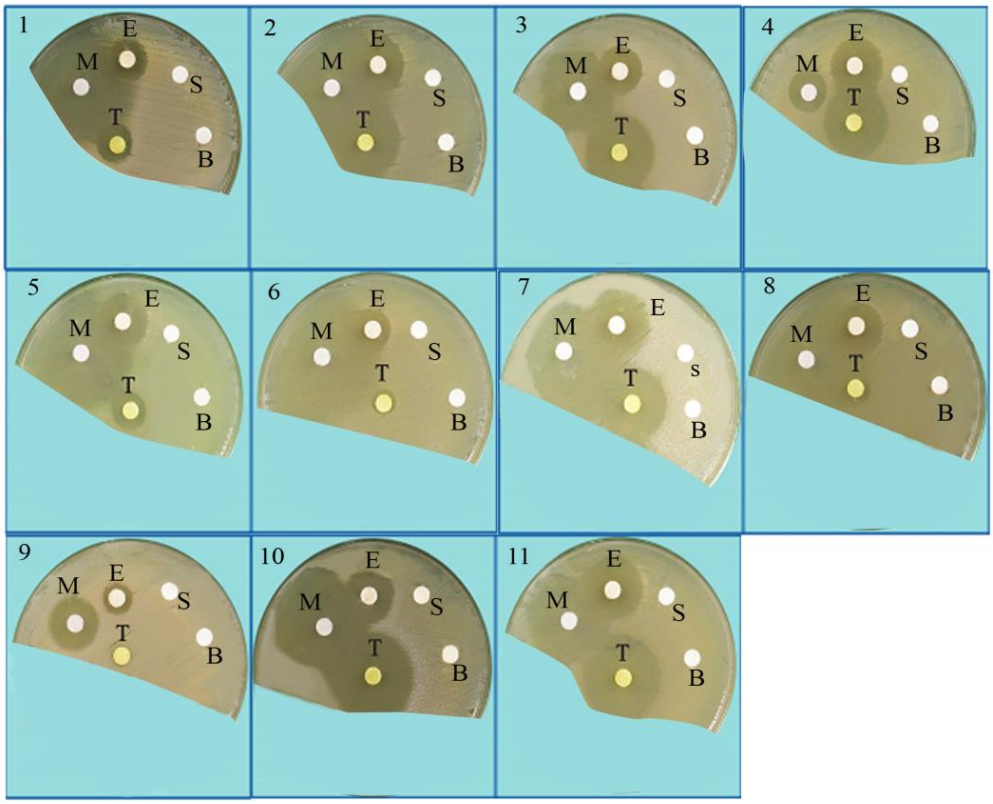

1 = *Klebsiella* species
2 = *Salmonella paratyphi* A
3 = *Citrobacter* species
4 = *Escherichia coli* ATCC
5 = *Pseudomonas aeruginosa*
6 = *Salmonella typhi*
7 = *Escherichia coli* YCH 149
8 = *Shigellaflexneri*
9 = *Proteus* species
10 = *Staphylococcus aureus*
11 = *Vibrio cholerae* O1

E = EtOAc crude extract (Peik-chin)
M= Methyl piperate
S = EtOAc solvent (control)
B = Blank
T = Tetracycline (standard)

Figure 6: Antibacterial activity of EtOAc crude extract and methyl piperate, isolated from *P. longum* (Peik-chin)

Table 3: Minimum Inhibitory Concentration (MIC) of Active Isolated Compound Methyl Piperate (mg/mL) of *P. longum*

No.	Bacteria	MIC(mg/mL)
1	*Escherichia coli* LT	0.03
2	*Staphylococcus epidermidis* (MKL-50)	0.03
3	*Staphylococcus epidermidis* (MKL-68)	0.03
4	*Escherichia coli* EHEC	0.03
5	*Staphylococcus aureus* (WS)	0.03
6	*Bacillus subtilis* T-34	0.03

Conclusion

From the fruit of *P. longum* L., four crude extracts: PE extract (1.5 %), EtOAc extract (3.5 %), 96 % EtOH extract (4.5 %) and 50 % EtOH extract (6.2 %) were obtained and screened the antibacterial activity against 19 tested bacteria by agar disc diffusion method. Among the four crude extracts of Peik-chin, only EtOAc extract showed the most potent antibacterial activity with the related larger zone diameter (12-20) mm on 19 bacterial strains; *Salmonella derby*, *Escherichia coli* LT, *Escherichia coli* O128, *Escherichia coli* EHEC, *Staphylococcus aureus*ATCC, *Salmonella paratyphi*, *Salmonella stanley*, *Shigella boydii*, *Salmonella pollorum*, *Shigella dysenteriae*, *Vibrio chlolerae* Inaba, *Escherichia coli* ATCC, *Pseudomonas pyocyanea*, *Vibrio cholerae* O1, *Salmonella typhi*, *Vibrio cholerae* O139, *Shigella flexneri*, *Bacillus subtilis* and *Staphylococcus aureus*. Using column chromatographic separation, pale yellow crystal (0.084 %) was isolated from the most active EtOAc extract of *P. longum* (Peik-chin) and identified as methyl piperate by UV, FT IR, ^{1}HNMR and EI MS spectrometry.

In vitro antibacterial activity of ethyl acetate crude extract and methyl piperate was also investigated. It was found that methyl piperate showed the range of inhibition zone diameter between (16-42) mm whereas inhibition zone diameter of EtOAc extract ranged between (13-24) mm. It may be concluded that the antibacterial activity of methyl piperate, pure compound was more potent than that of the crude EtOAc extract against 11 tested

bacteria; *Klebsiella* species, *Salmonella paratyphi* A, *Citrobacter* species, *Escherichia coli* ATCC, *Pseudomonas aeruginosa*, *Salmonella typhi*, *Escherichia coli* YCH 149, *Shigellaflexneri, Proteus* species, *Staphylococcus aureus* and *Vibrio cholerae* O1. They are effective for the treatment of dysentery, urinary tract infection, food poisoning, abscess and diarrhoea.

Minimum inhibitory concentration (MIC) values of methyl piperate against six tested bacteria were determined by using microtitre plate dilution method. Then MIC value of methyl piperate was found to be the same 0.03 mg/mL against all six bacteria; *E.coli* LT, *S. epidermidis* (MKL-50), *S. epidermidis* (MKL-68), *E.coli* EHCC, *S. aureus* (WS) and *B. subtilis* T-34. From these observations, it may be recommended that the ethyl acetate extract of fruit of *P. longum*(Peik-chin) and isolated methyl piperate may be used as main materials for the traditional medicine formulation in the treatment against dysentery, urinary tract infection, food poisoning, abscess and diarrhoea.

Acknowledgements

I would like to express my thanks to Dr Tin Htwe, Rector and Dr. Marlar, Pro-Rector, Hinthada University, for giving the permission to report this research work. I would also like to extend my gratitude to Dr Cho Cho Than, Professor (Head), Department of Chemistry, Hinthada University, for her enthusiastic participation in this research work. I am also grateful to Dr Than Soe, Rector (Retired), Myitkyina University and Dr Mar Mar Nyein, Director (Retired), Bacteriology Research Division, Department of Medical Research (Lower Myanmar) for their valuable suggestions and guidance.

References

Boyd, R.F. and Marr, J. J. (1980). *Medical Microbiology.* Boston: 1st Ed., Little Brown and Company, p. 597

Fluck, H. (1976). *Medicinal Plants and their Uses*. London: 2nd Ed., W. Foulsham & Co. Ltd., pp. 101-110

Jalalpure, S. S., Patil, M. B., Sprakash, N., Hemalata, K. and Manvi, F.V. (2003). "Hepatoprotective Activity of the Fruits of *Piper longum* Linn.".*Indian J. Pharm. Sci.*, vol. 65 (4), pp. 363-366

Khan, M.R. (2001)."Antibacterial Activity of Some Tanzanian Medical Plants".*Pharmaceutical Biology*, vol. 39 (3), pp. 206-212

Kress, W.J., Defilipps, R.A., Farr, E. and Daw Yin Yin Kyi.(2003). *A Checklist of the Trees, Shrubs, Herbs and Climbers of Myanmar.* Washington, DC, USA: 1st Ed., Department of Systematic Biology-Botany, National Museum of Natural History, p. 37

Krool, D. J. (2001). "Natural Compounds in Cancer Therapy: Promising Nontoxic Antitumor Agents from Plants and other Natural Sources," *J. of Natural Products*, vol.64, pp. 1605-1606

Kumar, S., Kamboj, J. and Sharma, S. (2011). "Overview of Various Aspects of the Health Benefits of *Piper longum* L.".*J. of Acupuncture and Meridian Studies*, vol. 4, pp. 134-140

Mar Mar Nyein, Mi Mi Htwe, Ba Han and Ei Ei Khine.(2006). "Antibacterial Activity of Some Plants and Formulations and Determination of Minimum Inhibitory Concentration (MIC) by Microtitre Plate Dilution Method". *The Myanmar Health Sciences Research Journal*, vol. 18 (1), pp. 26-30

Mohring, J. R. and Necker, D. C. (1979).*Laboratory Experiments in Organic Chemistry*. New York: 3rd Ed., D. Van Nostrand Co. Ltd., p. 531

Silverstein, R.M., Bassler, G.C. and Terence, C.M. (1991).*Spectrometric Identification of Organic Compounds*, Singapore: 5th Ed., John Wiley and Sons, Inc., pp. 289-315

PREPARATION, CHARACTERIZATION AND APPLICATION OF MICRO-FIBRILLATED CELLULOSE FROM SAWDUST

Hnaung Hnaung Win[1], Lu Lu Toung Mai[2]

Abstract

In this research, micro-fibrillated cellulose (MFC) was prepared from sawdust of geland wood by three steps such as alkali treatment, bleaching and acid hydrolysis. The acid hydrolysis has been performed by two different H_2SO_4 concentrations (3N and 5N) whereas other conditions are remained unchanged. The physicochemical properties such as moisture content, ash content, particle density, porosity and water absorption capacity of sawdust and prepared MFC were determined by conventional methods. The bleached pulp and prepared MFC were characterized by EDXRF, FT-IR, TG-DTA, XRD and SEM spectroscopic methods. The relative abundance of elements present in MFC was obtained from the results of EDXRF. The oxidation reaction takes place during the preparation of MFC by using high concentrations of H_2SO_4 which has been detected by FTIR spectroscopy. The thermal behavior of bleached pulp and MFC were observed by TG-DTA. From the XRD results, the crystallinity of bleached pulp and prepared MFC was found to be 63.63% and 66.67% respectively. The films of polyvinyl alcohol (PVA) and PVA/MFC composites at different mass ratios of PVA:MFC (1:0.1, 1:0.2, 1:0.3, 1:0.4 and 1:0.5) were made by using the prepared MFC as reinforcement. The surface morphology of prepared films was revealed by SEM. The physical and mechanical properties such as thickness, tensile strength, elongation at break, tear strength and water vapour transmission rate of prepared films have been evaluated.

Keywords: Micro-fibrillated cellulose, sawdust, composite films, reinforcement

Introduction

The use of renewable materials for industrial applications is becoming impellent due to the increasing demand of alternatives to scarce and unrenewable petroleum supplies. Plant based fiber is sustainable in its supply and it is biodegradable and renewable. In particular, cellulose is the most abundant renewable polymer resource available today, and it is considered an almost inexhaustible source of

[1]. Dr, Associate Professor, Department of Chemistry, Myitkyina University
[2]. Demonstrator, Department of Chemistry, Myitkyina University

raw material for the increasing demand for environmentally friendly and biocompatible products.

Substances used as raw materials should come from plants with a low economic and have no adverse effect on the environment. Among the natural plant wastes, sawdust is used as a raw material for the production of micro-fibrillated cellulose.

Sawdust refers to the tiny-sized and powdery wood waste produced by the sawing of wood. Sawdust is composed of three important constituents such as cellulose, lignin and extractives. The benefits of using sawdust as a woody biomass in compost manufacture are its favorable physical properties such as low apparent specific gravity (density), high porosity, high water retention, high bacteria tolerance and biodegradability at an acceptable rate (Nanci, et.al, 2016).

In this regard, micro-fibrillated cellulose (MFC), the most abundant biopolymer, is one of the most promising materials. Micro-fibrillated cellulose is a man-made substance which is obtained from the naturally occurring compound i.e., cellulose. On account of its small size, very high surface area and high aspect ratio, MFC is a potential reinforcing material with the advantages of being derived from renewable resources (Priya, et.al, 2015). MFC is really potential especially when it comes to replacing synthetic raw materials. Thus it is one of the most sustainable alternatives on the market (Ghani, et.al, 2014). Products which are produced from natural raw materials may be safe, hygiene and economic for customers. These are very important facts for the production of micro-fibrillated cellulose from sawdust.

Polyvinyl alcohol (PVA) has been widely used for the preparation of many blends and composites with several natural, renewable polymers and applied them in the development of green composite technology to achieve ecological sustainability. Composite films which consist of PVA with natural fibers are improved the biodegradability and physical properties of PVA. The interaction between fibers and PVA results a good composite property and satisfactory performance (Abas, 2016).

The aim of this research is to prepare and characterize the micro-fibrillated cellulose (MFC) from sawdust and to apply the prepared MFC as reinforcement for the preparation of composite films by using various mass ratios of PVA to MFC. The prepared films have been assessed according to their physicomechanical properties.

Materials and Methods

All chemicals used in this research were obtained from British Drug House (BDH), England. The experimental works were conducted at the Department of Chemistry, Myitkyina University. Sawdust sample from the geland wood used as a raw material for the preparation of MFC was collected from Hpokalar Sawmill, Tutgone Quarter, Myitkyina Township in Kachin State.

Preparation of Micro-fibrillated Cellulose from Sawdust

(a) Preparation of alkali treated fibers

The sawdust sample collected from sawmill was clarified by using several physical methods such as sieving and washing to remove large particles like as stone, concrete, bark etc.. The dry sawdust was immersed in 17% (w/v) sodium hydroxide solution at room temperature for 3 hours with occasional stirring by glass rod and the solid-liquor ratio was maintained at 1:50 (w/v). The alkali treated sawdust was washed several times thoroughly by distilled water and neutralized with very dilute acetic acid. The alkali treated sawdust fiber was dried in air and followed by an electric oven at 100 ± 5°C for 6 hours and stored in airtight plastic bag.

(b) Treatment of bleached pulp

The alkali treated fibers were bleached with 1% (w/v) sodium chlorite ($NaClO_2$) solution for 90 minutes at 85-95°C. The fiber-liquor ratio was maintained at 1:50 (w/v). In this process the pH was controlled at 4. A buffer mixture of pH 4 (acetic acid-sodium acetate) was added to the chlorite solution in the proportion of 1 mL of buffer solution for every 10mL of sodium chlorite solution. After the treatment, the resulting bleached pulp was filtered over a sintered funnel and washed thoroughly with distilled water. The pulp was then treated with 0.2% (w/v) sodium meta-bisulphite solution for 20

minutes with fiber-liquor ratio 1:20 (w/v). The pulps were filtered and washed thoroughly with distilled water and dried in an electric oven at 100 ± 5°C.

(c) Preparation of micro-fibrillated cellulose by acid hydrolysis

10g of each bleached pulps were added into the solutions of 3N and 5N sulphuric acid. The fiber-liquor ratio was maintained at 1:50 (w/v). The pulp suspensions were then placed on a magnetic stirrer and continued stirring up to 6 hours by a magnetic bar. After 6 hours acid hydrolysis, the white powder like MFC was formed and then it was filtered and washed thoroughly with distilled water. The prepared MFC's were kept in acetone and sonication was performed for 12 hours in an ultrasonic bath (Priya, et.al, 2015).

Preparation of Polyvinyl Alcohol (PVA) Film and PVA/MFC Composite Films

(a) Preparation of PVA film

Polyvinyl alcohol (PVA) was added to deionized water at a weight ratio of 1:9 to form a PVA solution. After that the solution was kept in a water bath at 90°C and stirred for 1.5 hours. The solution was cast on a glass plate and dried at 40°C to obtain a PVA film.

(b) Preparation of PVA/MFC composite films

PVA solution was added to the MFC dispersion at different mass ratios PVA : MFC (1:0.1, 1:0.2, 1:0.3, 1:0.4 and 1:0.5). These mixtures were stirred at 90°C for 1.5 hours and then cast on each of the glass plates. The corresponding PVA/MFC composite films were obtained by drying at 40°C.

Determination of the Physicochemical Properties of Sawdust and MFC
Determination of moisture content

Moisture present in sawdust and MFC were determined by oven-drying method at (100 ± 5ºC), according to AOAC., (2000). The results are shown in Table 1.

Determination of ash content

The ash contents of sawdust and MFC were determined by procedure according to AOAC., (2000). The results are shown in Table 1.

Determination of particle density

Each samples, sawdust and MFC, were placed into graduated volumetric cylinders to reach the marked 100 cm^3 volume (V_o), and its weight (gram) could then be known by subtracting the combined weight of sample and volumetric cylinder (W_b) with the weight of empty volumetric cylinder (W_a) alone. The particle density of sample could then be calculated using the formula presented in following formula. The results are shown in Table 1.

$$\text{Particle density (g cm}^{-3}) = (W_b - W_a) / V_o$$

Determination of porosity

Each of samples (sawdust and MFC) with apparent volume of 100 cm^3 and known weight (W_s in grams) was placed in a volumetric cylinder. Tap water was then poured gently into it until the surface of water reached a marked line at the 100 cm^3 level. Porosity of each sample was calculated as the formula represented in the following. The results are shown in Table 1.

$$\text{Porosity (\%)} = (V_a / V_o) \times 100\%$$

$$[V_a\ (cm^3) = W_{comb} - W_s - W_{vs}]$$

V_a = the volume of poured water (cm^3) together with the water in the sample

V_o = the volume of sample (100 cm^3)

W_{comb} = the combined weight of volumetric cylinder, sample particles and poured water (g)

W_s = the weight of sample particles (g) (oven-dry weight equivalent)

W_{vs} = the weight of volumetric cylinder (g)

Determination of water absorption test

The samples (sawdust and MFC) were first dried at 100 ± 5°C for 24 hours. 1 g of each sample was put in to a centrifuge tube and then tap water was poured into the each tube. The samples were centrifuged after soaking in water for a separated time period of 30 minutes and then decanted. After that the centrifuge tube was weighed.

The percentage of water absorption (%) for each sample was then calculated according to the following formula. The results are shown in Table 2 and Figure 4.

$$\text{Water absorption (\%)} = \frac{\text{weight of absorbed water}}{\text{weight of sample}} \text{ x } 100\%$$

Characterization of Prepared Pulp, MFC and Films

The prepared bleached pulp and MFC were characterized by modern techniques such as EDXRF, FTIR, TG-DTA, XRD and SEM.

Elemental analysis by EDXRF

The elements present in the sample, MFC, was measured by means of an EDX-8000 Shimadzu, Japan at Department of Chemistry, West Yangon University. The resultant data and EDXRF spectrum of MFC are present in Figure 5.

Fourier transform infrared spectroscopy (FTIR)

The procedure was in accordance with the catalogue instruction as reported in FTIR spectrophotometer, (IR Tracer-100, Shimadzu, Japan). The FTIR spectra of samples are shown in Figure 6 (a), (b) and (c), respectively.

Thermogravimetric and differential thermal analysis (TG-DTA)

The procedure was in accordance with the recommended standard procedure as reported in DTG-60H Thermal Analyzer (Shimadzu) instrument. The TG-DTA spectra of samples are shown in Figure 7 (a) and (b).

Degree of crystallinity determination by XRD

The procedure was in accordance with the recommended standard procedure as reported in XRD instrument. The XRD spectra of samples are shown in Figure 8 (a) and (b).

Scanning electron microscope analysis (SEM)

Prepared samples were examined by Scanning Electron Microscope (ZEISS, Germany), for a visual inspection of external

porosity and topological textures. The SEM micrographs of samples are shown in Figure 9 (a), (b), (c) and (d).

Determination of Physicomechanical Properties of PVA and PVA/MFC Composite Films

The evaluations of the physical and mechanical properties such as thickness, tensile strength, elongation at break and tear strength of PVA and PVA/MFC composite films were performed at the Department of Rubber Technology, Yangon.

(a) Determination of the tensile strength and elongation at break

The prepared films were cut off according to JISK 7127 and the dimensions of test pieces were described. Both ends of the test pieces were firmly clamped in the jaw of tensile strength machine. One jaw was fixed and other was movable. The movable jaw moved at the rate of 10 mm/min. The resultant data were shown in the recorder. This procedure was repeated three times for each test. The tensile strength and elongation at break were calculated as the following equations. The results are represented in Table 5 and Figure 10 (a) and (b).

$$T_s = \frac{F}{W \times t}$$

where, T_s = tensile strength in Mega Pascal (MPa)

F = the maximum force record in Newton (N), T = thickness of the test length (mm)

$$E_b = \frac{L - L_0}{L_0} \times 100$$

where, E_b = elongation at break in percentage

L_0 = initial length in mm, L = test length at break in mm

(b) Determination of the tear strength

The specimen to be tested was cut out by the die from the above films. Specimen was cut with a single nick (0.05 mm) at the entire of the inner concave edge by a special cutting device using a razor blade. The clamping of the specimen in the jaw of test machine

is aligned with travel direction of the grip at the rate of 100 mm/min. The recorder of the machine showed the highest force to tear from a specimen nicked. This procedure was repeated three times for each test. The tear strength was calculated as the following equations. The results are represented in Table 5 and Figure 10 (c).

$$T_s = L \times \frac{t_1}{t_2}$$

(c) Determination of water vapour transmission rate of films

The water vapour transmission rate (WVTR) was determined gravimetrically at room temperature. Beakers containing 3 g of anhydrous calcium chloride were prepared. The test films were placed inside the beakers and the assembly was weighed. The beakers were then placed in a desiccator containing saturated sodium chloride solution at room temperature. After that the assembly was weighed at a given time intervals and put in the desiccator again. Weight differences of the beakers were measured at 1 hour intervals for 1 day which were used to calculate the water transferred through the films, which were absorbed by the anhydrous calcium chloride. The results are represented in Table 6.

$$\text{Water vapour transmission rate} = \frac{\Delta W}{\Delta t \times A}$$

ΔW = weight difference at different interval time (g)

Δt = time interval (hour), A = area of film (m^2)

Figure 1: Photograph of the experiment for water vapour transmission of films

Results and Discussion

Preparation of Micro-fibrillated Cellulose (MFC)

Pure and quality product, micro-fibrillated cellulose (MFC), was prepared from sawdust of geland wood by performing three steps such as alkali treatment, followed by $NaClO_2$ bleaching and acid hydrolysis as represented in the experimental work. The following photographs are the results from each step of the preparation of MFC from sawdust of geland wood.

(a) (b) (c)

(d) (e) (f)

Figure 2: Photographs of (a) sawdust (b) alkali treated fiber (c) bleached pulp (d) dried pulp (e) acid hydrolysis of bleached pulp and (f) dried MFC

MFC serves as a prom ising material to various applications, such as bio-composites and packaging materials, due to its abundance, high strength, low weight and biodegradability. Polyvinyl alcohol (PVA) is an environmentally-friendly, biodegradable and renewable polymer (Siró and Plackett, 2010).

This research is focused on the use of MFC as reinforcement of coating for packaging. So, the films of polymer based composites with various mass ratios of (PVA/MFC) were made by using prepared MFC. A finding of relatively small improvement in barrier properties would make MFC suitable for various industrial applications. Figure 3(a) is represented for PVA film and Figure 3 (b), (c), (d), (e) and (f) are represented for the prepared PVA/MFC films.

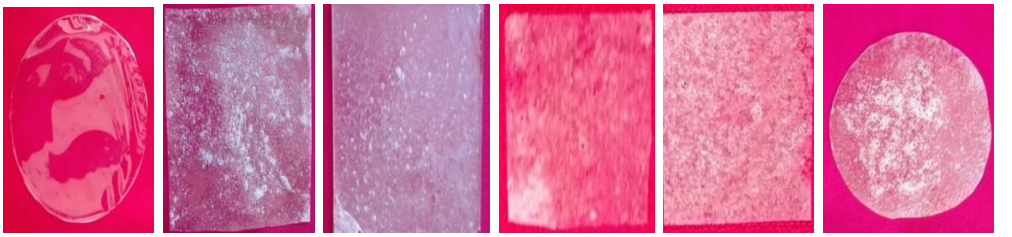

(a) (b) (c) (d) (e) (f)

Figure 3: Photographs of prepared films (a) PVA (b) Composite-1 (c) Composite-2 (d) Composite-3 (e) Composite-4 and (f) Composite-5

Plastic materials are indispensable in our lives but they pose of environmental pollution. In order to reduce the environmental load generated from the disposal of used plastic materials, a growing interest has been focused on biodegradable polymers based materials. The composites materials should be able to recycle, reuse, reprocesses or biodegradable, to minimize its impact to ecosystem.

Determination of the Physicochemical Properties of Sawdust and MFC

Regarding the utilization of woody biomass into compost, it is important to pay attention to its physicochemical properties. This study was carried out to determine such appropriate physicochemical properties including moisture content, ash content, particle density, porosity and water absorption capacity for sawdust particle and MFC.The resultant data are presented in Table 1 and 2.The contents of moisture, ash and particle density decrease in MFC than that in sawdust. Porosity of samplecan be defined as a measure of voidsvolume of sample grains, composed principally of inter-spaces among and intra-spaces within the particles or the percentage of samplevolume occupied by air and water that filled voids. The

porosity (%) of MFC is more present than that of sawdust due to the consisting of large voids that occupied by water. From the experimental results, water absorption capacity of MFC is also greater than that of sawdust for each of separated times. That is why the quality material MFC produced from sawdust is preferable use for a reinforcement of polymer composite films in the manufacture of packaging materials.

Table 1: Physicochemical Properties of Sawdust and Micro-fibrillated Cellulose (MFC)

Sr. No	Test Parameter	Result	
		Sawdust	MFC
1	Moisture (%)	11.10	8.96
2	Ash (%)	15.27	5.31
3	Particle density (gmL^{-1})	0.46	0.23
4	Porosity (%)	71.24	86.52

Table 2:Water Absorption Capacities of Sawdust and Micro-fibrillated Cellulose (MFC)

Time (min)	Water absorption capacity (%)	
	Sawdust	MFC
30	12.35	16.71
60	29.57	37.43
90	40.63	58.01
120	71.86	84.12
150	72.05	84.25
180	72.42	84.58

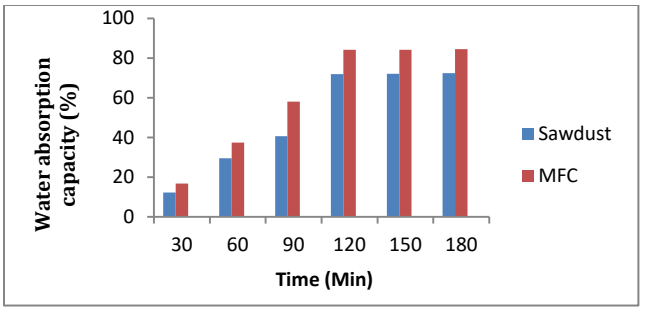

Figure 4: Water absorption capacities (%) of sawdust and micro-fibrillated cellulose

Characterization of Sawdust, Bleached Pulp and Micro-fibrillated Cellulose (MFC)

The elemental analysis, thermal property, degree of crystallinity and morphology of MFC and reference bleached pulp prepared from sawdust were characterized by energy dispersive X-ray fluorescence (EDXRF), fourier transform infrared spectroscopy (FTIR), thermogravimeteric and differential thermal analysis (TG-DTA), X-ray diffractogram (XRD) and scanning electron microscopy (SEM).

Elemental analysis by EDXRF

Figure 5 shows the EDXRF spectrum of MFC. The relative abundance of elements present in MFC is observed from the resultant data. According to the results, there is no element that causes harm for the people. Thus, MFC is suitable for a coating material in polymer composite films used for food packaging.

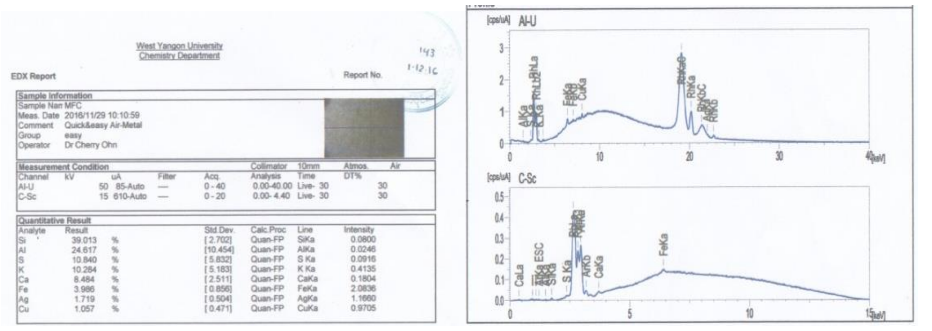

Figure 5: EDXRF spectrum of MFC

Functional Groups Determination by FT IR Spectra

T The FTIR spectra of bleached pulp and MFC's are shown in the Figure 6 (a), (b) and (c). The hydrophilic tendency of the cellulose and micro-cellulose samples is reflected in the broad absorption band in the 3700-3100 cm^{-1} region, which is related to the -OH groups present in their main components. In the 1600- 900 cm^{-1} region, it is possible to appreciate in fibers vibrations of chemical components of the lignin, at frequencies of between 1597 cm^{-1} and 1508 cm^{-1} for O-H bending of guaiacyl and 1427 cm^{-1}, 1369 cm^{-1} and 1317 cm^{-1} associated with syringyl. These absorptions are consistent with those of the typical cellulose backbone (Silverstein, 1963). Furthermore, almost the same absorption peaks as shown in the cellulose fibers are observed in the spectrum of the MFC. This indicates that the structure of cellulose has not been damaged after the treatments.

On the other hand, the peak centered at 1643 cm^{-1} in the FTIR spectrum of cellulose and MFC may be due to the C=O bond of hemicellulose. The intensity of the peak decreases from cellulose to MFC as the hemicellulose is removed gradually by acid hydrolysis.

(a) (b) (c)

Figure 6: FTIR spectra of (a) bleached pulp (b) MFC (hydrolysis by 3 N H_2SO_4) and(c) MFC (hydrolysis by 5 N H_2SO_4)

Thermogravimetric and differential thermal analysis (TG-DTA)

The thermal behavior of bleached pulp and MFC are presented in Figure 7 (a) and 7 (b). The summary of weight loss in different temperature ranges is also depicted by Table 3. For convincing

explanation, three different temperature ranges (39-280°C, 281-440°C and 441-601°C) were considered on the basis of the degradation of the constituent of fibers. The first weight loss at the range 39-280°C is found due to removal of moisture and hemicellulose. The further degradation occurs at the range of 281-440°C for removal of cellulose and then final weight loss happens for degradation of residual cellulose and lignin together at the range of 441-601°C. According to the results, it is observed that the amount of moisture content in bleached pulp is more present than that in MFC.

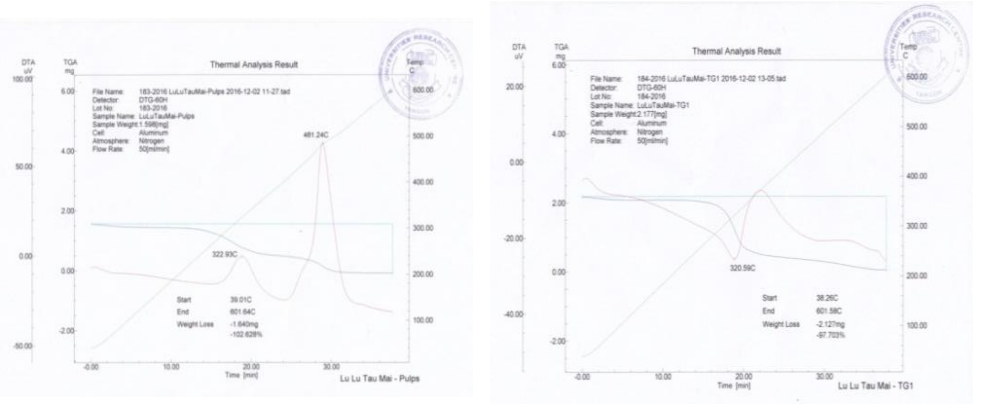

(a) (b)

Figure 7: TG-DTA thermograms of (a) bleached pulp and (b) MFC

Table 3: Weight Loss of Bleached Pulp and Micro-fibrillated Cellulose (MFC) at Various Temperature Ranges

Samples	Weight loss (%) at 39-280 ºC	Weight loss (%) at 281-440 ºC	Weight loss (%) at 441-601 ºC
Bleached pulp	24.90	74.97	87.48
MFC	8.13	67.03	76.22

Degree of crystallinity determination by XRD

The degree of crystallinity in the cellulosic materials may be measured in several ways by an X-ray diffractogram. This review compiles peak height method to evaluate the degree of crystallinity reported in the literature (Priya, et al., 2015). In this approach, the X-ray apparent crystallinity (%) of cellulose is calculated from the height ratio between the intensity of the crystalline peak and the total intensity after the subtraction of the background signal (non-crystalline) measured without cellulose according to the following equation:

$$C\ (\%) = \frac{I_{crystalline} - I_{noncrystalline}}{I_{crystalline}} \times 100$$

where C expresses the apparent crystallinity (%). $I_{crystalline}$ and $I_{noncrystalline}$ represent the intensities of diffraction of the crystalline and non-crystalline materials.

According to Figure 8 (a) and 8 (b), it is observed that all the cellulose peaks consist near 2θ =22.4 degree. Comparison between the crystallinity of bleached pulp and MFC are found to be 63.63% and 66.67% respectively. The increase in diffraction intensity indicates that the acid hydrolysis induces the crystallinity (%) due to the removal of amorphous materials like hemicellulose, lignin, and some other non-cellulosic materials, which is revealed by the resultant data in Table 4.

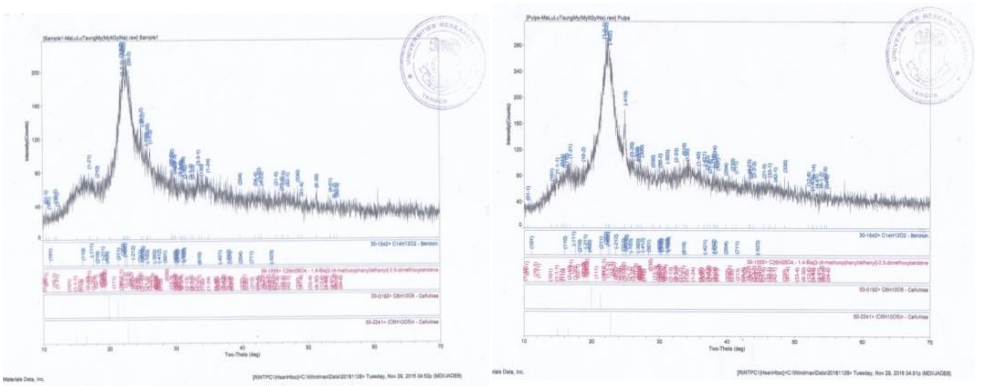

(a) (b)

Figure 8:X- ray diffractograms of (a) bleached pulp and (b) MFC

Table 4: Crystallinity (%) of Bleached Pulp and Micro-fibrillated Cellulose (MFC)

Samples	Intensity of crystalline peak (2□=22.4°)	Intensity of non-crystalline peak (2□ =16.2°)	Crystallinity (%)
Bleached pulp	220	80	63.63
MFC	180	60	66.67

Scanning electron microscope analysis (SEM)

Figure 9 (a), (b), (c) and (d) show the images of SEM for the cross-sectional surface of bleached pulp, MFC, PVA film and PVA/MFC composite-4 film. From the Figure 9 (a) and 9 (b), it is found that microporous materials consist of a regular organic or inorganic framework supporting a porous structure. The SEM image of Figure 9 (c) shows the homogeneous smooth surface texture of PVA. The SEM image of Figure 9 (d) shows that MFC is uniformly distributed in PVA and the rough surface in PVA/MFC film which is composed of aggregate particles.

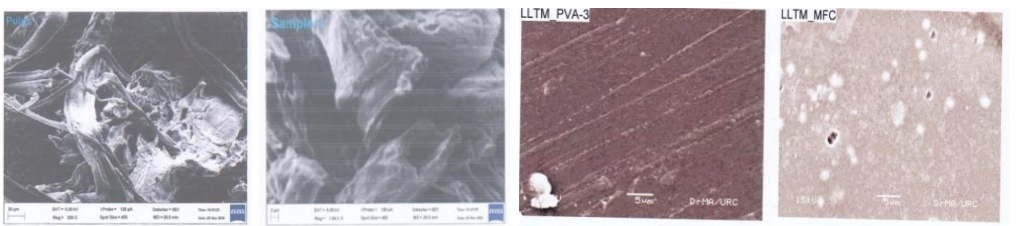

(a) (b) (c) (d)

Figure 9: SEM images of (a) bleached pulp (b) MFC (c) PVA film and (d) PVA/MFC composite film

Physicomechanical Properties of PVA and Composite Films

The physical and mechanical properties in terms of thickness, tensile strength, elongation at break and tear strength are important parameters for the evaluation of the prepared composite films. The results of the physicomechanical properties of PVA and PVA/MFC composite films are represented in Table 5 and Figure 10 (a), (b) and (c).

The tensile properties of natural fiber reinforce polymers are mainly influenced by the interfacial adhesion between the matrix and the fibers. Tensile properties are frequently included in material specifications to ensure quality. Tensile properties are often measured during development of new materials and processes, so that different materials and processes can be compared...

Table 5: Physical and Mechanical Properties of PVA and Composite Films

No	Test	PVA	Composite-1	Composite-2	Composite-3	Composite-4	Composite-5
1	Thickness (mm)	0.15	0.16	0.18	0.20	0.30	0.35
2	Tensile Strength (MPa)	6.7	9.9	10.8	11.2	11.4	11.3
3	Elongation at break (%)	98	68	59	41	39	36
4	Tear Strength (kN/m)	66.5	78.3	80.5	87.2	87.7	86.4

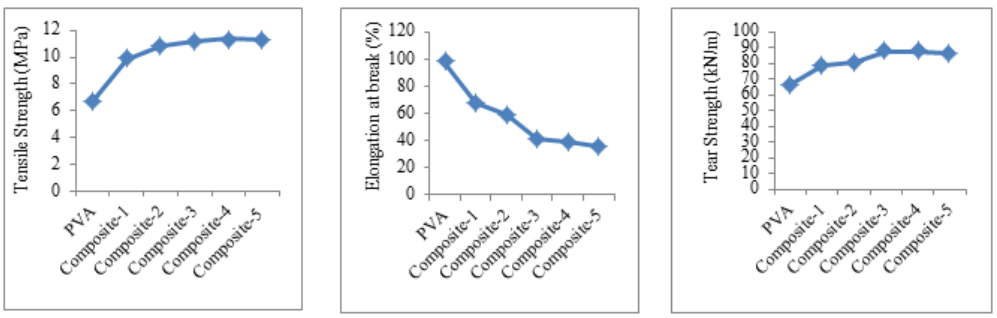

Figure 10: Physical and mechanical properties of PVA and composite films

The addition of MFC increases the tensile strength and tear strength of the composite films. This indicates a reinforcement of the relatively compliant PVA matrix by the stiffer and stronger cellulose microfibrils. For the present samples, when the addition of MFC is greater than mass ratio (1: 0.4) PVA/MFC, no further increases in the tensile strength and tear strength of the composites are observed. This may be due to the formation of fibril aggregates, which reduces the effective aspect ratio.

According to the resultant data, it is observed that the composite-3 mass ratio (1: 0.3) of PVA/MFC (thickness = 0.2 mm, tensile strength = 11.2 MPa, elongation at break = 41% and tear strength = 87.2 kN/m) and composite-4, mass ratio (1: 0.4) of PVA/MFC (thickness = 0.3 mm, tensile strength = 11.4 MPa, elongation at break = 39% and tear strength = 87.7 kN/m) are more suitable films for packaging compare to those of composite-1, composite-2 and composite-5.

Determination of the water vapour transmission rate of films

The barrier performance of a film is measured by the water vapor transmission rate (WVTR). WVTR measures the rate at which water vapor permeates through the film at a specified temperature and relative humidity. The barrier properties of MFC films are determined largely by the crystallinity and the network structure formed by fibers in a dry film. It is difficult for other molecules to penetrate the crystalline parts or the very dense network (Kumar et al., 2014). The results from determination of the water vapour transmission rate of films are represented in Table 6. According to the experimental results, it is found that the composite films can prevent the transmission of water vapour. The greater the mass content of MFC present in the film, the less transmission rate of water vapour. So, the PVA/MFC composite films are more suitable for packaging materials than the film of neat PVA.

Table 6:Determination of the Water Vapour Transmission Rate of Films

No	Type of film	WVTR(g/h m^2)
1	PVA	3.26
2	Composite-1	2.45
3	Composite-2	2.31
4	Composite-3	1.97
5	Composite-4	1.78
6	Composite-5	1.71

Conclusion

In this research, highly purified MFC was prepared from clarified sawdust by hydrolysis with different concentrations of H_2SO_4 solutions. The composite films with various mass ratios of PVA/MFC were made by using the MFC as reinforcement.

The prepared MFC were confirmed by modern techniques such as XRD, SEM, EDXRF, FT-IR and TG-DTA. The relative abundant of elements present in MFC were obtained from the EDXRF spectrum. According to the resultant data, there is no element that causes harm for people in an unacceptable limit. According to the FTIR analysis, it was observed that fibers contain the typical vibration bands of the component mainly corresponding to cellulose, hemicellulose and lignin. From the results of XRD, the crystallinity of prepared bleached pulp and MFC can be estimated to be 63.63% and 66.67% respectively. According to SEM spectrum, it is found that micro-porous materials consist of a regular organic or inorganic framework supporting with porous texture. As the TGDTA spectra, the weight losses of the bleached pulp and MFC were determined for three different temperature ranges. The first weight loss at the range 39-280 ºC is found due to removal of moisture and hemi-cellulose. The weight loss at the range of 281-440 ºC happens for degradation of cellulose and that of above 440 ºC is due to the degradation of residual cellulose and lignin together.

The evaluation of the composite films were made by the determination of their physical and mechanical properties such as thickness, tensile strength, elongation at break, tear strength and water vapour transmission rate.

According to the physical and mechanical properties of prepared films, the composite-3 (1:0.3) and composite-4 (1:0.4) of PVA/MFC films have the suitable results for coating of packaging materials in tensile strength (11.2 MPa and 11.4 MPa) and tear strength (87.5 kN/m and 87.7 kN/m) respectively.

Water vapour transmission rate of prepared films were determined to evaluate their barrier properties. As the experimental results, it is observed that the PVA/MFC composite films are more suitable for packaging materials than neat PVA film.

From the assessments of the prepared films, it is observed that the composite-3 and composite-4 PVA/MFC films may be substituted in packaging of plastic polymers. The enhancement in mechanical properties of composites by addition of MFC represents a strong opportunity for industrial sector.

Acknowledgements

The authors wish to thank the Department of Higher Education, Ministry of Education, Myanmar, for the financial support of this research programme. We are also greatly indebted to Dr Ni Ni Aung, Professor and Head of the Department of Chemistry, Myitkyina University for her kind provision of the research facilities.

References

Abas, F. O., (2016), "Improvement of Mechanical Properties of Polyvinyl Alcohol by Addition of Biomaterials for Production of Environmental Friendly Product", *J. Mesop-environ*, **2**(4), 1-8

AOAC., (2000), "Official Methods of Analysis, Association of Official Analytical Chemist", Washington D.C: 17th Ed.

Ghani, W.A., G. Silva, A.B. Alias, (2014), "Physico-Chemical Characterizations of Sawdust-derived Biochar as Potential Solid Fuels", *The Malaysian Journal of Analytical Sciences*, **18**(3), 724-729

Kumar, V., R. Bollström, A. Yang, Q. Chen, G. Chen, P.Salminen, D. Bousfield, and M. Toivakka, (2014)"Comparison of Nano- and Microfibrillated Cellulose Films", *Cellulose*, **21**(5), 3443–3456

Nanci, V., Ehman, Q.Tarres, and E. Maria, (2016), "From Pine Sawdustto CelluloseNanofibers", *J. Cellulose Chem. Technol.*, **50** (3), 361-367

Priya, S.Y., G. M.Arifuzzaman, M. H. Uddin and M.Haque, (2015), "Characterization of Micro-fibrillated Cellulose Produced from Sawmill Wastage: Crystallinity and Thermal Properties", *J. American Chemical Science*, **9**(1), 1-8

Silverstein, M.R., (1963), "Spectrometric Identification of Organic Compounds", John Wiley & Sons, New York

Siró, I., and D.Plackett, (2010) "Micro-fibrillated Cellulose and New Nanocomposite Materials: a Review", *J. Cellulose*,**17**(3), 459–494

PREPARATION AND CHARACTERIZATION OF BROMINATED POLYPHENYLENE OXIDE MEMBRANES

Myint Myint Khaing[1], Aye Thidar Kyaing[2], Thida Kyaw[3]

Abstract

In present research work, three different ratios of brominated polyphenylene oxide (BPPO) membranes were prepared by mixing with dimethyl form amide (DMF) as a solvent with the help of magnetic stirrer. The possible structure of membrane was determined by using Fourier-Transform Infrared spectroscopy (FT IR). In addition, the ion exchange capacity of each membrane was investigated by Mohr titration method. The resistance of the membrane was determined by Multimeter at the Department of Physics, Mandalay University. The morphology of the membranes was studied by Scanning Electron Microscopy (SEM). The solubility of each membrane was determined by dipping the membrane in various solvents such as water, ethanol, chloroform, distilled water and sodium hydroxide. The characteristic peak C-Br of membranes appeared at 1018.15 cm^{-1} was determined by FT IR spectroscopy. In addition, the ion exchange capacity measurement informs that 45 % BPPO membrane gives 1.48 mmol/g which is in agreement with the anion exchange membrane (AEM) membrane that can be used for fuel cell. The resistance of the membrane was determined by Multimeter and 45 % brominated (BPPO) membrane showed the suitable resistance value of 6 MΩ before immersing in 1 M NaOH solution as well as it shows 4.5 MΩ after immersing in 1 M NaOH solution. Furthermore, the swelling ratio of 45 % BPPO membrane indicates that informs the more ion exchange group corresponds to greater swelling ratio and high solubility.

Keywords: membrane; morphology; poly phenylene oxide; resistance; characterization

Introduction

Poly (p-phenylene oxide) or poly (p-phenylene ether) (PPE) is a high-temperature themoplastic. It is rarely used in its pure form due to difficulties in processing. It is mainly used as blend with polystyrene, high impact styrene –butadiene copolymer or polyamide. PPO is a registered trademark of SABIC innovative Plastics IP B.V. under which various polyphenylene ether resin are

[1]. Dr, Lecturer, Department of Chemistry, University of Mandalay
[2]. MRes candidate, Department of Chemistry, University of Mandalay
[3]. Dr, Associate Professor, Department of Chemistry, Yadanabon University

sold. Polyphenylene ether was discovered in 1956 by Allan Hay, and was commercialized by General Electric in 1960. While it was one of the cheapest high-temperature resistant plastics, processing was difficult and the impact and heat resistance decreased with time. Mixing it with polystyrene in any ratio could compensate for the disadvantages. In the 1960s, modified PPE came into the market under the trademark.

PPE is an amorphous high-performance plastic. The glass transition temperature is 215 °C, but it can be varied by mixing with polystyrene. Through modification and incorporation of fillers such as glass fibers, the properties can be extremely modified. PPE blends are used for structural parts, electronics, household and automotive items that depend on high heat resistance, dimensional stability and accuracy. They are also used in medicine for sterilizable instruments made of plastic.

Alkaline fuel cells (AFCs, hydrogen fuel cells with an alkaline liquid electrolyte such as KOH(aq)) are the best performing of all known conventional hydrogen-oxygen fuel cells operable at temperatures below 200 ºC. This is due to the facile kinetics at the cathode and at the anode; cheaper non-noble metal catalysts can be used (such as nickel and silver), reducing cost. McLean *et al*. gave comprehensive review of alkaline fuel cell technology. The associated fuel cell reactions both for a traditional AFC and also for an AMFC are:

Anode :$2H_2 + 4OH^- \rightarrow 4H_2O + 4e^-$

Cathode: $O_2 + 2H_2O + 4e^- \rightarrow 4OH^-$

Overall: $2H_2O + O_2 \rightarrow 2H_2O$

Rovert C.T Slade and Jamine P.Kizewski (2017)

Aim and Objectives

Aim

The aim of this research is study the conductivity performance and the alkaline stability of polyphenylene oxide modified anion exchange membrane (AEM) membrane for fuel cell technology.

Objectives

- To combine the brominated polyphenylene oxide (BPPO) and dimethyl formamide (DMF) in different molecular weights
- To measure the resistance of BPPO membranes
- To determine the conductivity
- To study the swelling ratio
- To investigate the morphology
- To study the water uptake and to measure the tear strength

Materials and Methods

Materials

1. Poly(2,6-dimethyl-1,4-phenylene oxide)(PPO)
2. Dimethyl Formamide (DMF)
3. 45% brominated polyphenylene oxide (BPPO)
4. 35% brominated polyphenylene oxide (BPPO)
5. 30% brominated polyphenylene oxide (BPPO)
6. Sodium Hydroxide
7. Hydrochloric Acid
8. Deionized Water

Methods

1. Fourier Transform Infrared Spectroscopy (FT IR)
2. Water Uptake and Swelling Ratio Measurement by comparing the wet and dry weights of the membranes
3. Ion Exchange Capacity (IEC) by Mohr titration method
4. Resistance Measurement by Multimeter
5. Scanning Electron Microscopy (SEM)

Determination of Resistance of Brominated Polyphenylene Oxide Membrane

Resistance of brominated polyphenylene oxide membranes were determined by Multimeter (Figure 1) at the Department of Physics, University of Mandalay.

Figure 1: Multimeter

Determination of Thickness of Membrane

The thickness of brominated polyphenylene oxide membranes were determined by Micrometer (Figure 2) at the Department of Physics, University of Mandalay.

Figure 2: Micrometer

Determination of Solubility of Membrane

The solubility of each membrane was measured by immersing the membranes in 1 M sodium hydroxide solution, chloroform, ethanol, distilled water and water for 24 hours (Figure 3).

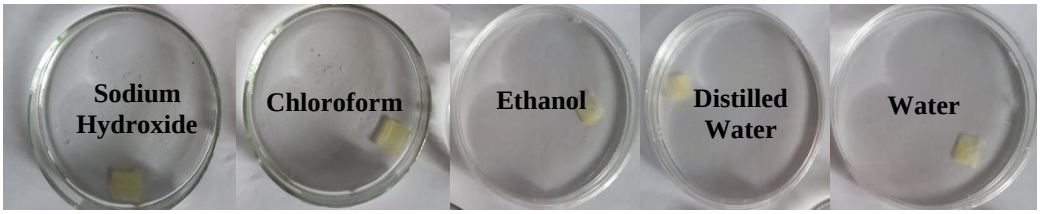

Figure 3: Solubility test of membrane in 1 M NaOH, $CHCl_3$, EtOH, distilled water and water

Identification of Brominated Polyphenylene Oxide Membrane by Fourier Transform Infrared Spectroscopy

Brominated polyphenylene oxide membranes were identified by Fourier Transform Infrared Spectroscopy at Department of Chemistry, Monywa University.

Determination of Water Uptake (WU) and Swelling Ratio

The water uptake of brominated polyphenylene oxide membrane were measured by weight differences between the wet and dry weight of membrane. The membranes were soaked in water for 24 hours (Figure 4).

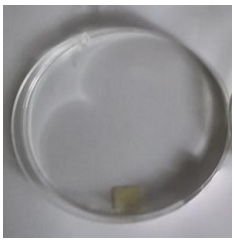

45 % brominated membrane

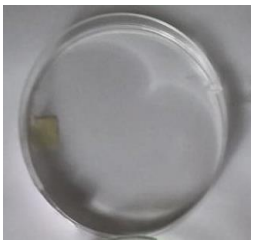

35 % brominated membrane

30 % brominated membrane

Measurement of Ion Exchange Capacity (IEC)

Ion exchange capacity (IEC) was determined by a back titration method derived from Slade and Varcoe (2013). The membranes were soaked in 1.0 M sodium hydroxide solution to exchange the bromide ion for hydroxide. And then the membranes were washed with deionized water and again dipped into this sodium hydroxide solution. After rinsing the membranes until neutral, they were dried in vacuum and immersed into 10 mL of 0.01 M hydrochloric acid. After soaking a day, the acid was titrated with 0.01 M sodium hydroxide. The ion exchange capacity of each membrane was calculated by the following equation:

$$IEC = \frac{C_{HCl}V_{HCl} - C_{NaOH}V_{Na}}{m_{dry}}$$

where C is the concentration of acid or base, V is the volume of the acid or base, and m_{dry} is the dry weight of the membrane after ion exchange.

Procedure for 45 %, 35 % and 30 % Brominated Polyphenylene Oxide Membranes

Firstly, 0.25 g of 45 % brominated sample was placed in round-bottomed flask and 15 mL of dimethyl formamide (DMF) was added. The mixture was stirred with the help of magnetic stirrer at 80°C for 24 hours. After the mixture was dissolved in DMF, it was poured into petridished and dried in oven for 24 hours. Finally, 45 % brominated polyphenylene oxide membrane was obtained. Similarly, the same procedure was done for 35 % and 30 % brominated poly phenylene oxide membranes.

Figure 4: 45 % brominated polyphenylene oxide memembrane

Results and Discussion

Determination of Resistivity Value of 45 % Brominated Membranes

Table 1: The Resistivity Value of 45 % Brominated Membrane Before and After Immersing in Various Solvents

Solvents	Resistivity values before immersing in solvents M□	Resistivity values after immersing in solvents M□
Sodium Hydroxide	6	4.5
Ethanol	6	-
Chloroform	6	-
Distilled Water	6	-
Water	6	-

According to the experimental result, the resistivity value of 45 % brominated membrane immersing in sodium hydroxide responds the excellent value of 4.5 MΩ that is suitable for conductor. In other solvents such as ethanol, chloroform, distilled water and water, it was found that the resistivity values of 45 % brominated membrane couldn't be detectable.

Determination of Resistivity Value of 35 % Brominated Membranes

Table 2: The Resistivity Values of 35 % Brominated Membrane Before and After Immersing in Various Solvents

Solvents	**Resistivity values before immersing in solvents** MΩ	**Resistivity values after immersing in solvents** MΩ
Sodium Hydroxide	9	8
Ethanol	9	-
Chloroform	9	-
Distilled Water	9	-
Water	9	-

Similarity, the resistivity value of 35% brominated membrane immersing in sodium hydroxide responds the excellent value of 8 MΩ that is suitable for conductor. In other solvents such as ethanol, chloroform, distilled water and water, it was found that the resistivity values of 35 % brominated membrane couldn't be detectable.

Determination of Resistivity Value of 30 % Brominated Membranes

Table 3: The Resistivity Values of 30 % Brominated Membrane Before and After Immersing in Various Solvents

Solvents	**Resistivity values before immersing in solvents** MΩ	**Resistivity values after immersing in solvents** MΩ
Sodium Hydroxide	9.6	10
Ethanol	9.6	-
Cholroform	9.6	12
Distilled Water	9 .6	64
Water	9.6	60

The resistivity value of 30% brominated membrane immersing in sodium hydroxide responds the resistivity value of 8MΩ , 12 MΩ in chloroform, 64 MΩ in distilled water and 60 MΩ in water that point out the resistivity values of 30 % brominated membrane are lower than their original value ie., before immersing in the solvents.

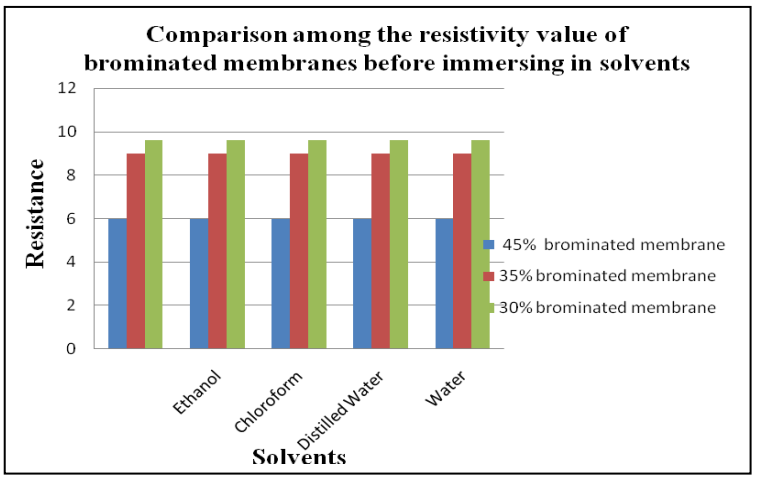

Figure 5: Resistivity values of brominated membranes before immersing in solvents

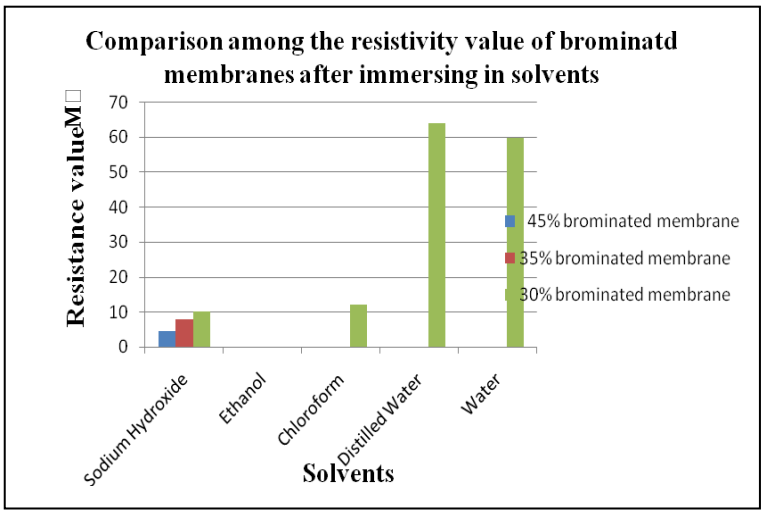

Figure 6: Resistivity values of brominated membrnaes after immersing in solvents

Determination of Thickness and Swelling Ratio of 45% Brominated Membrane

Table 4: The Thickness and Swelling Ratio of 45 % Brominated Membrane Before and After Immersing in Various Solvents

Solvents	Membrane thickness before immersing in solvents □m	Membrane thickness after immersing in solvents □m	Swelling Ratio %
Sodium Hydroxide	10	40	67
Ethanol	10	-	Undefined
Chloroform	10	60	34
Distilled Water	10	55	33
Water	10	60	20

From the result of the table, it was found that 45 % brominated membrane immersing in distilled water shows the highest swelling ratio.

Determination of Thickness and Swelling Ratio of 35% Brominated Membrane

Table 5: The Thickness and Swelling Ratio of 35 % Brominated Membrane Before and After Immersing in Various Solvents

Solvents	Membrane thickness before immersing in solvents □m	Membrane thickness after immersing in solvents □m	Swelling Ratio %
Sodium Hydroxide	50	75	50
Ethanol	50	50	0
Chloroform	50	30	0
Distilled Water	50	45	33
Water	50	80	22

From the result of the table, it was found that 35 % brominated membrane immersing in distilled water shows the highest swelling ratio.

Determination of Thickness and Swelling Ratio of 30% Brominated Membrane

Table 6: The Thickness and Swelling Ratio of 30 % Brominated Membrane Before and After Immersing in Various Solvents

Solvents	Membrane thickness before immersing in solvents □m	Membrane thickness after immersing in solvents □m	Swelling Ratio %
Sodium Hydroxide	50	76	64
Ethanol	50	45	0
Chloroform	50	60	33
Distilled Water	50	60	33
Water	50	55	22

From the result of the table, it was found that 30 % brominated membrane immersing in distilled water shows the highest swelling ratio.

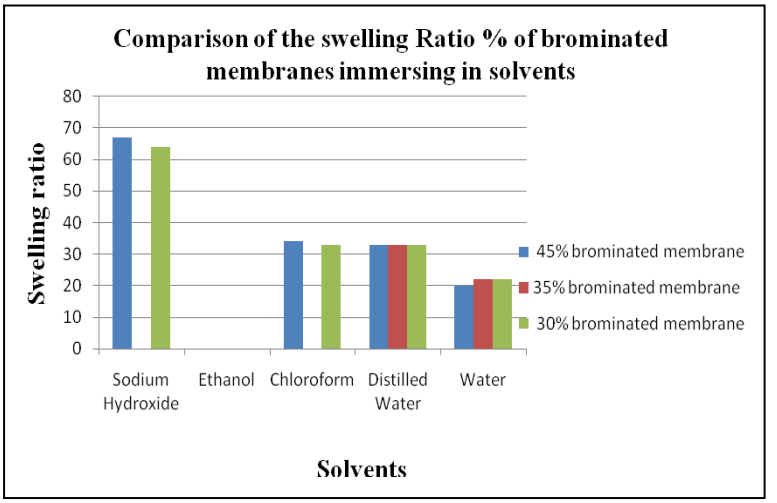

Figure 7: Swelling ratio % of brominated membranes immersing in solvents

Determination of Ion Exchange Capacity

Table 7: The Ion Exchange Capacity Value of Membrane

Membrane	IEC (mmol/g^{-1})
45 % brominated membrane	1.48
35 % brominated membrane	1.22
30 % brominated membrane	1.05

The ion exchange capacity (IEC) value, water uptake, degree of swelling, and mechanical properties of the membranes are shown in table. The IEC represents the ion exchange capacity group in the membranes, and the IEC values can strongly interrlate to the water uptake, swelling ratio and hydroxide conductivity of the AEMs. Among the three membranes, 45 % brominated membrane has the highest IEC value of 1.48 mmol/g^{-1}.

The water uptake (Wu) value was found to be a reasonable amount associated with the IEC values. 35 % brominated membrane has the less amount of water content (50 %). Wu values of 45 % brominated membrane and 30 % brominated membrane were found to be (67 %) and (64 %), respectively. It was found that the modified membrane has a great thermal stability under boiling water. The water uptake and swelling ratio of three membranes were summarized in above tables. The influence of water uptake and swelling ratio of the membranes correspond to the hydroxide conductivity of the membrane. Wu value is measured by the weight difference between the wet and dry form of the membrane. These values indicate that the BPPO membrane has a good performance in the application of the membranes. The ionic exchange capacity (IEC) value is reliable to the capacity of membrane which may influence the power of AEMs in fuel cell application. The higher value of the water uptake and swelling ratio provide the greater power of hydroxide conductivity. But the thermal stability of the membrane can be decreased due to the higher value of water uptake. It was found that BPPO membranes have moderate amount of water content and swelling ratio. These attachments are the great performances of AEM membranes that are required for the satisfaction of ion exchange capacity.

Identification of Brominated Polyphenylene Oxide Membrane by Fourier Transform Infrared Spectroscopy

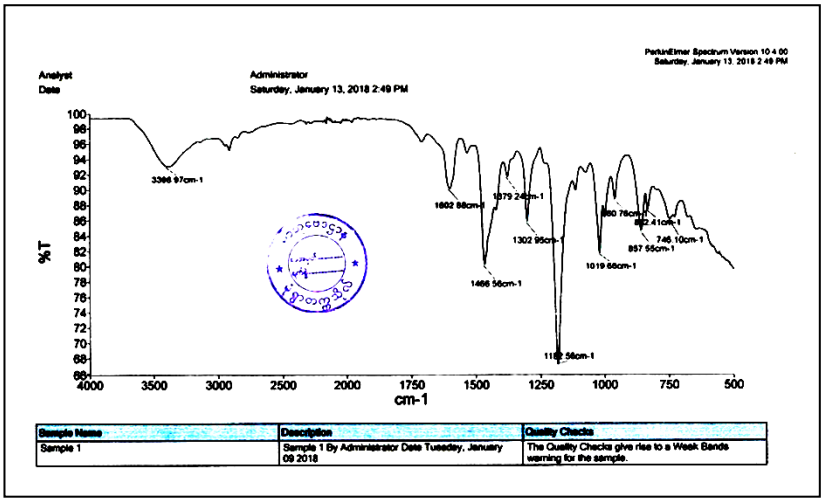

Figure 8: FT-IR spectrum of brominated polyphenylene oxide

Identification of Brominated Polyphenylene Oxide Membrane by Fourier Transform Infrared Spectroscopy

Table 8: FT-IR Assignments of 45 % Brominated Polyphenylene Oxide (BPPO) Membrane

No.	Wave Number	Stretching Frequency
1.	3398.97 cm^{-1}	N-H stretching vibration
2.	3005.10 cm^{-1}	C-H stretching vibration of unsaturated hydrocarbon
3.	2902.50 cm^{-1}, 2842. cm^{-1}	C-H stretching vibration of saturated hydrocarbon
4.	1602.88 cm^{-1}	C=C Stretching Vibration of ring skeleton
5.	1466.56 cm^{-1}, 1379.24 cm^{-1}, 1302. cm^{-1}	C-H bending vibration of methyl group
6.	1182.56 cm^{-1}	C-O stretching vibration of ether
7.	1019.66 cm^{-1}	C-Br stretching vibration
8.	960. cm^{-1}	C-H bending Vibration
9.	857.55 cm^{-1}	C-H out of plane Bending Vibration

Conclusion

In this research work, the three different ratios of brominated polyphenylene oxide (BPPO) membranes were firstly prepared by mixing with DMF solvent and stride using of magnetic stirrer. The characteristic properties of membranes were determined by FT-IR and SEM spectroscopy. In addition, the ion exchange capacity measurement indicates that 45 % BPPO membrane gives 1.48 $mmolg^{-1}$ which is in agreement with the AEM membrane that can be used for fuel cell. The resistance of the membranes was determined by Multimeter at the Department of Physics, Mandalay University where as 45 % brominated (BPPO) membrane shows the suitable conductivity value of 6 MΩ before immersing in 1 M NaOH solution as well as it shows 4.5 MΩ after immersing in 1 M NaOH solution. Furthermore, the swelling ratio of 45 % BPPO membrane indicated unexpected mechanical properties that informs the more ion exchange group corresponds to greater swelling ratio and high solubility.

Acknowledgements

We are greatly thanks to MAAS Committee and Dr Yi Yi Myint (Professor and Head of Department of Chemistry) for her strong encouragements to promote research level.

References

J. Mater. Chem.A, 2016,4,11924. Journal of Materials Chemistry A .

Mong Lian, Yong-Jhao Jhuang, Chun-Fu Zhang, Wei-Jhuan Tsai, Hui_Chuan Feng, Department of Applied Chemistry, National Chia-Yi University, Chia-Yi 600, Taiwan. European Polymer Journal.

Polyphenylene Ethers and their Alloys, Authors R. Ingrid Warren, First published: June 1985 Full publication history. DOI:10.1002/pen.760250809 View/save citation .Cited by(CrossRef): 8 articles .

Rovert C.T Slade and Jamine P.kizewski ,Simon D.Poynton, Rong Zeng, and John R.Varcoe Department of Chemistry, University of Surrey, Guildford GU2 7 XH, UK e-mail: R.Slade@surrey.ac.uk. Springer Science+ Business Media New York 2013.

Z.Sun, Prof. F. Yan, Department of Polymer Science and Engineering College of Chemistry, Chemical Cngineering and Materials Science Soochow University, Suzhou, 215123(P.R. China). Dr.B Lin School of Materials Science and Engineerign Jiangsu Collaborative Innovation Center of Photovoltaic Science and Technology, Changzhou University Changzhiy 213164, Jiangsu(P .R. China)." Anion-Exchange Membranes for Alkaline Fuel-Cell Applications : The Effects of Cations".

Online Materials

https://enwikipedia.org/wiki/Poly(P-phenylene-oxide)

http://en.wikipedia.org/wiki/Polyphenyl_ether

http://www.machinekesign.com/basics-design/polyphenylene -ether

https://www.rtpcompany.com/products/product-guide/modified-polyphenylene-oxide-ppo/

https://www.azom.com/article.aspx?ArticleID=1999

http://www.makeitfrom .com/material-propertsies/Polyphenylene-Odide-PPO

http://www.machinedesign.com/basics-design/polyphenylene -ether

http://www.bpf.co.uk/plastipedia /polymers/PPo.aspx

http://www.sdplastic.com/moryl.html

http://plastics.ulprospector.com/generics/40/polyphenylene-ether-ppe

http://en.wikipedia .org/wiki/Polyphenyl_ether

En.wikipedia.org/wiki/tensile strength

http://en.wikipedia.org/wiki/fuel-cell#Applications

http://www.Fuelcelltoday.com/technologoes

ANTIMICROBIAL ACTIVITY OF ISOLATED PORPHYRIN DERIVATIVE COMPOUNDAND STUDY ON THE CYTOTOXICITY, ANTIOXIDANT ACTIVITY OF CRUDE EXTRACTS OF THE WHOLE PLANT OF *Corallodiscus lanuginosus* (Wall. ex R.Br.)Burtt

Thinn Myat Nwe*

Abstract

In this research paper, *Corallodiscus lanuginosus* (Wall. ex R.Br.)Burttwhich is one of the Myanmar indigenous medicinal plants known as Pan ma o` was selected for the study on the cytotoxicity and antioxidant activity. The cytotoxicity of the ethanol extract of the selected sample was more toxic to brine shrimp than the water extract. The LD_{50} values of ethanol and water extracts were 380μg/mL and 423μg/mL, respectively. On the other hand, the EtOH and water extracts were cytotoxic to brine shrimp up to maximum dose of 1000 μg/mL. The LD_{50} values of standard $K_2Cr_2O_7$ and caffeine are 265 μg/mL and >1000 μg/mL, respectively. In addition, the larger radical scavenging activity to scavenge DPPH radical was observed in ethanol extract, which inhibited 50% of free radicals at the concentration (IC_{50}) of 7.10 μg/mL than the water extract which inhibited 50% of free radicals at the concentration (IC_{50}) of 11.13 μg/mL. Moreover, antimicrobial activities of the isolated porphyrin derivative compound were examined by using agar well diffusion method. The ethyl acetate extract of this porphyrin derivative compound responds high activities on *Bacillus subtilis, Pseudomonas aeruginosa, Bacillus pumilus, Candida albicans and Escherichia coli.*

Keywords: Pan ma o`, porphyrin, cytotoxicity, antioxidant activity, antimicrobial activity

Introduction

The knowledge, skills and practices based on the theories, beliefs and experiences indigenous to different cultures are used by traditional medicine in the maintenance of health and in the prevention, diagnosis, improvement or treatment of physical and mental illness" (WHO, 2010).There are many different systems of traditional medicine, and the philosophy and practices of each are influenced by the prevailing conditions, environment, and geographic

* Dr, Associate Professor, Department of Chemistry, Mandalay University of Distance Education.

area within which it first evolved (WHO, 2005), however, a common philosophy is a holistic approach to life, equilibrium of the mind, body, and the environment, and an emphasis on health rather than on disease. Generally, the focus is on the overall condition of the individual, rather than on the particular ailment or disease from which the patient is suffering, and the use of herbs is a core part of all systems of traditional medicine (Engebretson, 2002; Conboy *et al.*, 2007; Rishton 2008; Schmidt *et al.*, 2008).Over the past 100 years, the development and mass production of chemically synthesized drugs have revolutionized health care in most parts of the word. However, large sections of the population in developing countries still rely on traditional practitioners and herbal medicines for their primary care. In Africa up to 90% and in India 70% of the population depend on traditional medicine to help meet their health care needs. In China, traditional medicine accounts for around 40% of all health care delivered and more than 90% of general hospitals in China have units for traditional medicine (WHO, 2005). However, use of traditional medicine is not limited to developing countries, and during the past two decades public interest in natural therapies has increased greatly in industrialized countries, with expanding use of ethnobotanicals. In the United States, in 2007, about 38% of adults and 12% of children were using some form of traditional medicine (Ernst *et al*., 2005; Barnes *et al.*, 2008).

Materials and Methods

Determination of Cytotoxicity of Crude Extracts by Brine Shrimp Lethality Bioassay

Cytotoxicity of crude extracts of selected sample was investigated by brine shrimp lethality bioassay according to the procedure described by Dockery and Tomkins (2000).

Preparation of solutions

(a) Preparation of sample solutions

Each crude extract (5 mg) was dissolved in 5 mL of distilled water to obtain stock solution (1000 μg/mL). Desired concentrations (1000, 500, 250, 125, 62.5, 31.25 and 15.125 μg/mL) of each crude extract were prepared from this stock solution by two fold serial dilution with distilled water.

(b) Preparation of standard solutions (Potassium dichromate and caffeine)

Each of potassium dichromate (5 mg) and caffeine (5 mg) was dissolved in 5 mL of distilled water. These stock solutions were two fold serially diluted with distilled water to get the standard solutions with the concentrations of 1000, 500, 250, 125, 62.5, 31.25 and 15.125 µg/mL.

(c) Preparation of artificial sea water

Artificial sea water [3.8% (w/v) NaCl] was prepared by dissolving (38 g) of sodium chloride in 1 L of distilled water.

Hatching of brine shrimp

The brine shrimp (*Artemiasalina*) was used in this study for cytotoxicity bioassay (Ali *et al*., 2013). Brine shrimp cysts were purchased from pet shop, Baho Road, Hlaing Township, Yangon Region.

Brine shrimp cysts (0.5 g) were added to the 1.5 L of artificial sea water bottle. The suspension was aerated by bubbling air into the funnel and kept for 24 h at room temperature.

Procedure

After aeration had been removed, the suspension was kept for 1 h undisturbed, whereby the remaining unhatched eggs dropped. In order to get a higher density of larvae, one side of the separating funnel was covered with aluminium foil and the other illuminated with a lamp, whereby the phototropic larvae were gathering at the illuminated side and could be collected by pipette. The shrimp larvae were transferred to an agar well filled with 9 mL of salt water and the dead larvae counted (number N). A solution of crude extract (31.25 - 1000 ppm) (1 mL reach) was added and the plate kept at room temperature in the dark. After 24 h, the dead larvae were counted in each well under the microscope (number A). The still living larvae were killed by addition of ca. 0.5 mL methanol so that subsequently the total number of the animals could be determined (number G). The mortality rate M was calculated in percent. Each test row was accompanied by a brine solution (number B). The mortality rate M was calculated by using the following formula:

$$M = \left[\frac{(A - B - N)}{(G - N)} \right] \times 100$$

M = percent of the dead larvae after 24 h

A = number of the dead larvae after 24 h
B = average number of the dead larvae in the brine solution after 24 h
N = number of the dead larvae before starting of the test
G = total number of brine shrimps

The control solution was prepared as the above procedure by using distilled water instead of sample solution. The results are summarized in Table1.

Determination of Antioxidant Activity of Crude Extracts by DPPH Free Radical Scavenging Assay

The free radical scavenging activity of crude extracts (ethanol and water extracts) of Pan ma o` was measured by using DPPH free radical scavenging assay (Marinova and Batchvarov, 2011).

Preparation of solutions

(a) Preparation of 0.002% (w/v) DPPH solution

0.002% DPPH solution was prepared in the brown coloured bottle by dissolving 2 mg of DPPH powder in 100 mL of ethanol. It must be stored in the refrigerator for no longer than 24 h.

(b) Preparation of standard solutions (Gallic acid)

The stock solution (200 μg/mL) of standard gallic acid was prepared by dissolving (2 mg) of each compound in 10 mL of ethanol. The stock solutions were two fold serially diluted with ethanol to get the standard solutions with the concentrations of 200, 100, 50, 25, 12.5, 6.25 and 3.125 μg/mL.

(c) Preparation of test sample solutions

The stock solution (200 μg/mL) of the crude extract was prepared by dissolving (2 mg) of respective crude extract in 10 mL of ethanol. The stock

solutions were two fold serially diluted with ethanol to get the sample solution with the concentrations of 200, 100, 50, 25, 12.5, 6.25 and 3.125 µg/mL.

(d) Preparation of blank solution

Blank solution was prepared by mixing 1.5 mL of sample solution with 1.5 mL of ethanol.

Procedure

DPPH radical scavenging activity was determined by UV-visible spectrophotometer (Marinova and Batchvarov, 2011).

The control solution was prepared by mixing 1.5 mL of 0.002% DPPH solution and 1.5 mL of ethanol in the brown bottle. The sample solution was also prepared by mixing 1.5 mL of 0.002% DPPH solution and 1.5 mL of test sample solution. These bottles incubated at room temperature were shaken on shaker for 30 min. After 30 min, the absorbance values of these solutions were measured at 517 nm and the percentage of radical scavenging activity (% RSA) was calculated by the following equation.

$$\% \text{ RSA} = [\{(A_{DPPH} - A_{Sample}) - A_{Blank}\}/ A_{DPPH}] \times 100$$

where, % RSA = % radical scavenging activity of test sample

A_{DPPH} = absorbance of DPPH in ethanol solution

A_{Sample} = absorbance of sample + DPPH solution

A_{Blank} = absorbance of sample + EtOH solution

The antioxidant activity (IC_{50}) is expressed as the test substance concentration (µg/mL) that results in a 50% reduction of initial absorbance of DPPH solution. IC_{50}(50% inhibition concentration) values were calculated by linear regressive excel program. The standard deviation was also calculated by the following equation.

$$\text{Standard Deviation (SD)} = \sqrt{\frac{(\bar{x} - x_1)^2 + (\bar{x} - x_2)^2 + \ldots (\bar{x} - x_n)^2}{(n-1)}}$$

Results and Discussion

Cytotoxicity of Crude Extracts

The cytotoxicity of water and ethanol extracts ofselected sample were evaluated by brine shrimp cytotoxicity bioassay. This bioassay is general toxicity screening for bioactive plants and their derivatives. A model animal that has been used for this purpose is the brine shrimp, *Artemiasalina* (Tawaha, 2006).

The cytotoxicity of crude extracts were expressed in term of mean ± SEM (standard error mean) and LD_{50} (50 % Lethality Dose) and the results are shown in Table 1 and Figure 1. In this experiment, standard potassium dichromate ($K_2Cr_2O_7$) and caffeine were chosen because $K_2Cr_2O_7$was well-known for its toxicity in this assay (Salinas andFernandez, 2006) and caffeine is a natural product.

As shown in Table 1, the cytotoxicity of the ethanol extract of the selected sample was more toxic to brine shrimp than the water extract. The LD_{50} values of water and ethanol extracts were 423μg/mL and 380 μg/mL respectively. The water and ethanol extracts were cytotoxic to brine shrimp up to maximum dose of 1000 μg/mL. The LD_{50} values of standard $K_2Cr_2O_7$ and caffeine are 265μg/mL and >1000 μg/mL, respectively.

Table 1: Cytotoxicity of Ethanol and Water Crude Extracts

Samples	**Percent (%) of the dead larvae at different concentrations of the samples after 24 h**							**LD_{50} (□g/mL)**
	15.625	**31.25**	**62.5**	**125**	**250**	**500**	**1000**	
Water Extract	5.56	13.79	20.00	27.27	40.00	54.55	58.06	423
EtOH Extract	12.75	17.65	39.29	34.48	35.29	63.89	70.00	380
*$K_2Cr_2O_7$	17.50	23.53	35.48	42.31	49.02	69.23	74.47	265
*Caffeine	3.19	10.81	11.43	23.53	29.03	30.43	37.14	>1000

*****standard

These results revealed that the plant extracts possess cytotoxic activity and can be the sources of cytotoxic compounds. The selected plant sample can

be used in traditional medicine to treat many kinds of diseases. The reported cytotoxic plants in this study are worth of further pharmacological and phytochemical studies in order to define what kind of bioactivity they have and to isolate the natural active constituent, which are responsible for the activity.

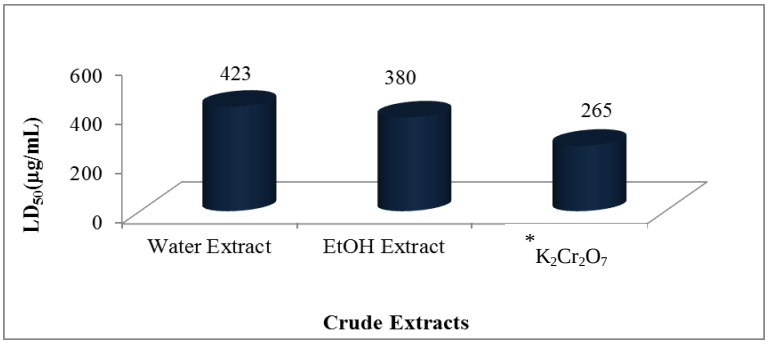

Figure 1: A bar graph representing LD_{50} values of watery and ethanol extracts of the selected sample and standard $K_2Cr_2O_7$

Antioxidant Activity of Crude Extracts by DPPH Free Radical Scavenging Assay

Most of the medicinal plants possess phytochemicals and antioxidant activity. Flavonoids and tannins are phenolics which are a major group of compound in plants. These compounds act as primary antioxidant or free radical scavengers (Ayoola *et al*., 2008). The antioxidant activity of water and ethanol extracts of selected sample were studied by DPPH free radical scavenging assay (Marinova and Batchvarov, 2011). Gallic acid was used as standard.

The DPPH (2, 2-diphenyl-1-picrylhydrazyl) assay is widely used to investigate the scavenging activities of several natural compounds such as crude extracts of plants. DPPH radical is scavenged by antioxidant through the donation of electron forming the reduced DPPH. Sample's colouris changed from purple to pale yellow which can be quantified by its decrease in absorbance at wavelength 517 nm (Maw *et al*., 2011). The radical scavenging activity of crude extracts was expressed in terms of % RSA (Table 2 and Figure 2) and IC_{50}(50 % inhibition concentration) (Table 3 and Figure 3).

From these observations, the larger radical scavenging activity to scavenge DPPH radical was observed in ethanol extract, which inhibited 50% of free radicals at the concentration (IC_{50}) of 7.10µg/mL than the water extract which inhibited 50% of free radicals at the concentration (IC_{50}) of 11.13µg/mL. These results were found to be slightly higher than standard gallic acid (IC_{50}= 3.79µg/mL).

It can be concluded that the antioxidant potency of the ethanol extract was found to be stronger than that of the water extract, but weaker than the standard gallic acid.

Table 2: Radical Scavenging Activity of Crude Extracts

Samples	% RSA ± SD at Different Concentrations (µg/mL)						
	3.125	**6.25**	**12.5**	**25**	**50**	**100**	**200**
Ethanol extract	36.58	48.96	56.69	71.38	79.27	84.15	91.49
Water extract	16.47	18.02	59.78	75.64	87.32	89.48	94.20
Gallic acid	47.95	57.64	62.40	67.00	77.83	92.61	96.06

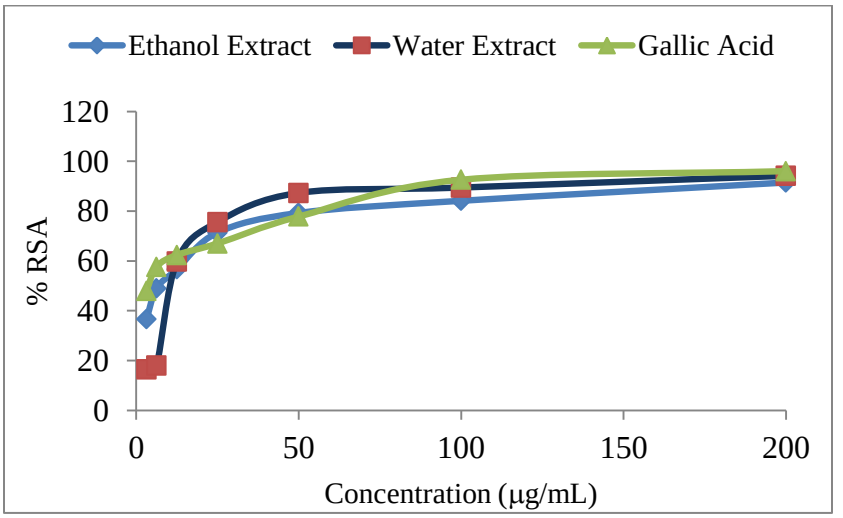

Figure 2: % RSA of crude extracts comparison with standard gallic acid

Table 3: IC_{50} of Crude Extracts and Gallic Acid

No.	Sample	IC_{50} (µg/mL)
1	EtOH extract	7.10
1	EtOH extract	7.10
1	EtOH extract	7.10

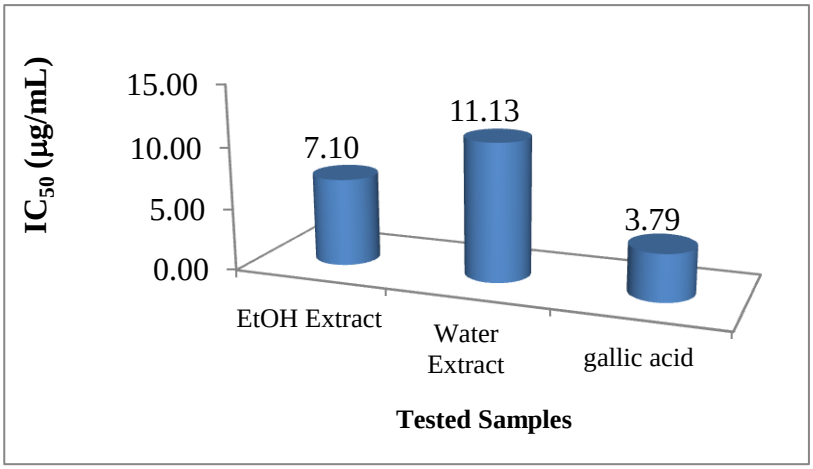

Figure 3: IC_{50} values of crude extracts and gallic acid

Antimicrobial Activities of the Porphyrin Derivative Compound

Porphyrin derivative compound could be isolated from the whole plant of Pan ma o` in January 2017 at Department of Chemistry, Mandalay University (Thinn Myat New *et al.*, 2017). It had been reported in Myanmar Academy of Arts and Science, 2017 (Thinn Myat Nwe and Myo Myo, 2017). Antimicrobial activities of isolated compound were checked by using agar well diffusion method on six selected organisms. The results are described in Table 4 and Figure 4.

Table 4: Results of Antimicrobial Activities of Porphyrin Derivative Compound

Sample	Solvent	Organisms and Inhibition Zone					
		I	**II**	**III**	**IV**	**V**	**VI**
Pure compound	EtOAc	+++ 29.11	–	+++ 27.45	+++ 28.03	+++ 27.13	+++ 29.85
Control	EtOAc	–	–	–	–	–	–

agar well ~ 10mm
10 mm ~ 14 mm (+)
15 mm ~ 19 mm (++)
20 mm above (+++)

Organisms
I *Bacillussubtilis*
II *Staphylococcus aureus*
III *Pseudomonousaeruginosa*
IV *Bacillus pumilus*
V *Candida albicans*
VI *E. coli*

According to this table, the ethyl acetate extract of isolated compound gives rise to high activities on all selected organisms except *Staphylococcus aureus*.

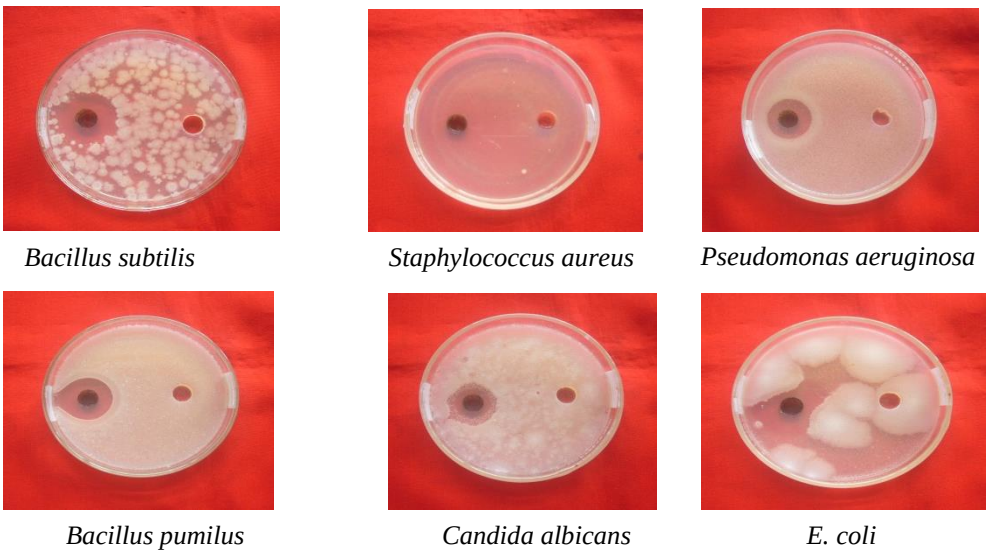

Figure 4: Antimicrobial activities of porphyrin derivative compound

Conclusion

In this research work, one of Myanmar indigenous medicinal plants, locally known as Pan ma o` was selected for the examination of cytotoxicity, antioxidant activity andthe determination of antimicrobial activities of isolated porphyrin derivative compound.

The antimicrobial activities of isolated porphyrin derivative compound give rise to high activities on all selected organisms except *Staphylococcus aureus*. The cytotoxicity of the ethanol extract of the sample was more toxic to brine shrimp than the water extract. The LD_{50} values of ethanol and water extracts were 380μg/mL and 423 μg/mL, respectively. In cytotoxicity, both extracts were lower than $K_2Cr_2O_7$ (LD_{50} = 265 μg/mL), higher than caffeine (LD_{50}>1000 μg/mL). In addition, the larger radical scavenging activity to scavenge DPPH radical was observed in ethanol extract, which inhibited 50% of free radicals at the concentration (IC_{50}) of 7.10 μg/mL than the water extract which inhibited 50% of free radicals at the concentration (IC_{50}) of 11.13 μg/mL.

Acknowledgements

The authors would like to thank the MyanmarAcademy of Arts & Science for allowing to present this paper, Professor and Head, Dr Daw Khin Aye Tint Nwe and Professor Dr Khin Mar Yee, Department of Chemistry, Mandalay University of Distance Education, Myanmar, for their valuable advice and permission. The author is also thankful to Dr Khine Zar Wynn Lae, Lecturer, Department of Chemistry, YangonUniversity for her providing to complete this research work.

References

Ali, N., Allen, U., Shah, S. W. A., Shah, I., Junaid, M., Ahmed, G., Ali, W. and Ghias, M. (2013).“Acute Toxicity, Brine Shrimp Cytotoxicity, Anthelmintic and Relaxant Potentials of Fruits of *Rubusfruiticosis*Agg.”*BMC Complement.Altern. Med.*, vol. 13, pp. 138–143

Ayoola, G. A., Coker, H. A. B., Adesegun, S. A., Bello, A. A. A., Obaweya, K., Ezennia, E. C. and Atangbayila, T. O. (2008). “Phytochemical Screening and Antioxidant Activities of Some Selected Medicinal Plants Used for Malaria Therapy in Southwestern Nigeria.”*Tropical Journal of Pharmaceutical Research*, vol. **7**, pp. 1019–1024

Barnes, P. M., Bloom, B. and Nahin, R. L.(2008). "Complementary and Alternative Medicine Use AmongAdults and Children: United States, 2007." *National Health Statistics Report*, vol.10(12), pp. 1-23

Conboy, L., Kaptchuk, T. J., Eisenberg, D. M., Gottlieb, B. and Acevedo-Garcia, D. (2007)."The Relationship between Social Factors and Attitudes toward Conventional and CAM practitioners."*Complement Ther Clin Pract*, vol. 13, pp. 146–157

Dockery, M. and Tomkins, S. (2000). *Brine Shrimp Ecology*.London: 1st ed., TheBritish Ecology Society, pp. 92–93

Engebretson, J. (2002). "Culture and complementary therapies."*Complement TherNurs Midwifery*, vol. 8 (4), pp. 177–184

Ernst, E., Schmidt, K. and Wider, B. (2005). "CAM Research in Britain: The last 10 years."*Complement TherClinPract*., vol. 11 (1), pp. 17–20

Marinova, G. and Batchvarov, V. (2011)."Evaluation of the Methods for Determination of the Free Radical Scavenging Activity by DPPH."*Bulgarian Journal of Agricultural Science*, vol. 17, pp. 11–24

Maw, S. S., Mon, M. M. and Oo, Z. K. (2011). "Study on Antioxidant Activities of Some Herbal Extracts." *WorldAcademy of Science, Engineering and Technology*, vol. 51, pp. 450–452

Rishton, G. M. (2008)"Natural Products as a Robust Source of New Drugs and Drug leads: Past Successes and Present Day Issues." *Am J Cardiol*. vol. 101, pp. 43D–49D

Salinas, M. M. G. and Fernandez, S. S. (2006). "A Modified Microplate Cytotoxicity Assay with Brine Shrimp Larvae(*Artemiasalina*)."*Pharmacology*, vol. 3, pp. 633–638

Sahgal, G., Ramanathan, S., Sasidharan, S., Mordi, M. S., Ismail, S. and Mansor, S. M., (2010). "Brine Shrimp Lethality and Acute Oral Toxicity Studies on *Swieteniamahagoni*(Linn.)Jacq. Seed Methanolic Extract", *Pharmacognosy Res*., vol. 2, pp. 215–220

Schmidt, B., Ribnicky, D. M., Poulev, A., Logendra, S., Cefalu, W. T. andRaskin,I. (2008)."A natural history of botanical therapeutics."*Metabolism*. vol. 57 (7 suppl. 1), pp. S3–9

Tawaha, K. A. (2006). "Cytotoxicity Evaluation of Jordanian Wild Plants Using Brine Shrimp Lethality Test." *J. J. Appl. Sci*., vol. 8, pp. 12–17

Thinn Myat Nwe and Myo Myo. (2017). "Molecular Formula Determination and Structure Elucidation of Bioactive Porphyrin Derivative Compound Isolated from the Whole Plant of *Corallodiscuslanuginosus* (Wall. ex R.Br.)Burtt.", vol. XVI. No. 1A, pp. 109-128

World Health Organization (WHO). (2010). "*Traditional Medicine*." http://www .who.int/topics/traditional_medicine/en/ (accessed July 21,2010)

World Health Organization (WHO).(2005). "National Policy on Traditional Medicine and Regulation of Herbal Medicines." Geneva, Report of WHO global Survey.

SYNTHESIS AND CHARACTERIZATION OF GOAT BONE-DERIVED HYDROXYAPATITE - ZINC OXIDE NANOCOMPOSITES FOR BIOMEDICAL APPLICATION

Lin Lin Naing[1], Ni Ni Sein[2], Thida Win[3]

Abstract

Hydroxyapatite (HAp) obtained from the chemical treatment (HCl and NaOH) and calcination at 900 ºC of fresh goat bone were incorporated with different amounts of zinc oxide (ZnO) nanoparticles (5 % and 10 %) to give HAp-ZnO nanocomposites (20:1 and 20:2). These nanocomposites were indexed as hexagonal structure with equal length of a and b but shorter c. FT IR spectral data revealed the characteristic absorption peaks of PO_4^{3-}, OH^- and ZnO in HAp-ZnO nanocomposites. SEM images of HAp-ZnO nanocomposites were elongated crystalline structures with agglomeration of ZnO on the surface of HAp. The bulk density of the nanocomposites slightly increased and the porosity percentage decreased as the temperature and amount of zinc oxide increased. HAp and HAp-ZnO nanocomposites (20:1 and 20:2) prepared at 1000 ^oC showed no cytotoxic effect tested by brine shrimp assay. Orthopedic applications of HAp and HAp-ZnO nanocomposites were conducted by using Wistar rats. By X-ray diagnosis HAp-ZnO composites exhibited as a promising filler of bone defect. Histological findings showed that HAp-ZnO composites with ratio of 20:2 at 1000 °C group was found to be the best with the good scoring within 30 days after application.

Keywords: Goat bone, hydroxyapatite, zinc oxide, nanocomposites, brine shrimp assay, orthopedic applications

Introduction

Bone is a highly specialized supporting frame-work of the body (Kini and Nandeesh, 2012). It comprises of organic and inorganic fractions being in continuous interchange with each other for bone-forming and resorbing. The main part of the hard inorganic structure of the bone is hydroxyapatite [$Ca_{10}(PO_4)_6(OH)_2$]. Hydroxyapatite (HAp) is chemically identical to the inorganic matrix of living bones (Ylinen, 2006). HAp exhibits excellent

[1.] Dr, Assistant Lecturer, Department of Chemistry, Mandalar Degree College
[2.] Dr, Professor (Retired), Department of Chemistry, University of Yangon
[3.] Dr, Rector, University of Mandalay

biocompatibility both with hard tissue and with soft tissue (Okada and Matsumoto, 2015; Zhou and Lee, 2011).

Currently, metals are widely used in orthopedics to increase the bioactivity of hydroxyapatite. Among these metals, zinc is an essential trace element present in human bones and teeth. It plays important roles in increasing osteoblast adhesion and alkaline phosphatase activity of bone cells (Deepa *et al*., 2013). Zinc oxide (ZnO) creates much attention as a future material because it can be used as a versatile material for immense applications (Zak *et al*., 2013). Zinc oxide is a white inorganic compound and insoluble in water. ZnO is a key technological material (Singh *et al*, 2012). It is a bio-safe and biocompatible material and can be directly used for biomedical applications without coating (Anita *et al*, 2010).

Hydroxyapatite with various additives like ZnO and MgO were mainly prepared to obtain superior quality materials suitable for use in artificial bone substitution. Properties of HAp such as morphology, crystallinity and crystal size distribution have great influence in the production of materials for biomedical applications. Therefore, it is essential to optimize how these properties of HAp are affected by different additives (Deepa *et al*, 2013).

The aim of the present study is to synthesize and characterize goat bone-derived hydroxyapatite and zinc oxide nanocomposites and to study the biomedical application of the prepared nanocomposites.

Materials and Methods

Sample Collection

The raw goat bone samples were directly collected from retail market in Mandalay Region.

Preparation of Hydroxyapatite from Waste Goat Bone

The goat bones were firstly cleaned with water to remove dirty substances and then boiled in a pot at 100 ˚ C for several hours to get rid of any remaining unwanted materials. The bones (500 g) were initially deproteinized through external washing with 1 L of 1 M hydrochloric acid solution for 24 h at room temperature. Next, the deproteinized goat bones

were thoroughly washed several times with distilled water. After that, the bones were treated with 1 L of 1 M sodium hydroxide solution for 24 h to remove the remaining proteins of goat bones. After filtration, the goat bones were thoroughly washed with distilled water again and again and then dried at 60 ° C in hot air oven for several hours. The dried bones were crushed into small chips and transformed to fine powder using a mortar and pestle. Finally, a yellowish white hydroxyapatite powder was obtained. Then it was calcined at 900 ^{o}C in a muffle furnace (DFM-05, Korea) for 3 h. The calcined powder samples were cooled and then stored in a desiccator for further studies.

Preparation of Zinc Oxide Nanoparticles

ZnO nanoparticles were prepared by wet chemical method (Nawaz *et al*., 2011). The precursors used in the preparation of ZnO were zinc nitrate hexahydrate and sodium hydroxide. Soluble starch as stabilizer was also used in the preparation of zinc oxide sample (Yadav *et al*., 2006). Initially, 100 mL of 0.1 % starch solution was prepared in distilled water. Then, 0.4 mol of zinc nitrate was added to 0.1 % starch solution. To achieve complete dissolution of zinc nitrate, the solution obtained was mixed using a magnetic stirrer under constant stirring. After that, 0.8 mol of sodium hydroxide solution was poured drop-wise along the side walls of the above mixture solution vessel under continuous stirring. After complete addition of sodium hydroxide, the mixture was continued to stir for 2 h. When the reaction was complete, the solution was kept overnight. The supernatant liquid was carefully decanted and the remaining solution was centrifuged at 4500 rpm for 10 min. Moreover, to remove the by-products and any starch bound to the sample, the resulting sample was washed 2-3 times with ethanol-water using centrifugal apparatus. The final step was to dry the sample in an oven at 80 °C for 3 h and to anneal in a muffle furnace at 400 °C for 3 h for conversion of $Zn(OH)_2$ to ZnO.

Preparation of HAp-ZnO Nanocomposites

The solution of ZnO (25 % w/v in distilled water) was prepared with the aid of a magnetic stirrer for 1 h. The HAp solution was also prepared using the ratio of 1:1 for powder (g) and water (mL) by means of magnetic stirring

for 1 h to get homogeneity of the dispersion. In order to prepare HAp-ZnO nanocomposites, the weight percentages (wt %) of ZnO were chosen as 5 and 10. The prepared ZnO solution was poured into the HAp solution and then thoroughly mixed using stirrer at 80-90 °C for 1 h. The obtained suspension was cooled to room temperature for 12 h. In addition, it was filtered using a funnel through filter paper. The residues were washed 2 to 3 times with distilled water. Then, it was transferred into porcelain basin and placed in an oven at 120 °C for 4 h to obtain dried sample. Moreover, the resulting products were calcined at 600 °C, 800 °C and 1000 °C for 2 h.

Characterization Techniques

The phase purity was examined by using Rigaku X-ray diffractometer (Rigaku Co., Japan) with Cu Kα (λ =1.54056 Å) radiation over a range of 2θ angles from 10° to 70°. Various functional groups present in the prepared HAp-ZnO composites calcined at different temperatures were identified by FT IR (Perkin Elmer). The scanning electron microscope (SEM, JEOL-JSM-5610 LV, Japan) was used for the morphological study of HAp-ZnO composites. Relative abundances of elements in HAp-ZnO composites were qualitatively determined by EDXRF analysis using EDX-702 spectrometer (Shimadzu Co. Ltd., Japan) at Universities' Research Center, Yangon.

Physical Properties of HAp and HAp-ZnO Nanocomposites

pH was determined by pH meter, and bulk density and porosity of the samples were determined by tapping method and liquid displacement method respectively.

Cytotoxicity Assay

The brine shrimp *(Artemia salina*) was used in this study for cytotoxicity bioassay. Brine shrimp cysts (0.5 g) were added to the 1.5 L of artificial sea water bottle. Artificial sea water was prepared by dissolving 26.518 g of sodium chloride, 2.447 g of magnesium chloride, 3.305 g of magnesium sulphate, 1.141 g of calcium chloride, 0.725 g of potassium chloride, 0.202 g of sodium hydrogen carbonate and 0.083 g of sodium bromide in distilled water in a 1 L volumetric flask and the volume made up

to the mark with distilled water (Sverdrup *et al*., 1942). The bottle containing the brine shrimp was placed near a lamp. Light is essential for the cysts to hatch. Brine shrimp cysts required to hatch constant supply of oxygen for 24 h incubation at room temperature.

Artificial sea water (9 mL) and 1 mL of each of HAp, different concentrations of HAp-ZnO composites with the weight ratios of 20:1 and 20:2 (0.1, 1, 10, 100 and 1000 µg/mL) and standard potassium dichromate solutions were added to each chamber. Alive brine shrimp (10 nauplii) were then taken with pasture pipette and placed into each chamber. After incubation at room temperature for about 24 h, the number of dead brine shrimps was counted and 50 % lethality dose (LD_{50}) was calculated. The control solution was prepared as the above procedure by using distilled water instead of sample solution.

Biomedical Application of Hydroxyapatite-Zinc Oxide Nanocomposites by Animal Experiment (*in vivo* Test)

Eight healthy Wistar rats (male with 250-300 g body weight) were chosen for this experiment. Rats were provided by Laboratory Animal Service Division, Department of Medical Research, Yangon. Animals were kept individually in standard rat cages with an ambient temperature of 24 ºC and 12/12 light/dark cycle. The animals had free access to drinking water and standard laboratory pellets.

Animals were divided into four individual groups in this experiment. For Group I, skull defect was filled with HAp calcined at 900 ^{o}C after surgery procedure. For Group II, the skull defect was filled with HAp-ZnO (20:1) calcined at 1000 ^{o}C and for Group III it was filled with HAp-ZnO (20:2) calcined at 1000 ^{o}C. However, skull defect was not filled any composites materials for Group IV.

All animals used for surgical performance in this study received general anesthesia via an intramuscular injection with 0.5 mL Ketamine associated with 0.1 mL Xylazine. The hair of each rat skull was firstly shaved and the area was cleaned before operation. After shaving the area, a linear skin incision was made in the dorsal portion of skull bone of each rat with surgical knife. Then, the skull bone area was created the identical bony defect

well of such animal using stainless hand drill under anaesthetized condition. The nanocomposite powder was taken in a watch glass and distilled water added dropwise till the powder got fully wet and then stirred to become paste. The paste was molded in the skull bone cavity before suturing. Defects were gently packed with HAp at 900 °C paste for Group (I) animal, HAp-ZnO nanocomposite (20:1) at 1000 °C paste for Group (II) animal, HAp-ZnO nanocomposite (20:2) at 1000 °C for Group (III) and other defect was left unfilled, i.e., control for Group (IV) animal.

After obtaining adequate hemostasis, the flap (skin layer) was closed with suturing cat gut continuously after the operation procedures and dressed with betadine solution for the superfacial wound healing. After surgery, animals were kept in separate cages and were fed with pellet food made in DMR and clean water *ad libitum*. All animals showed good general health condition throughout the study as assessed by their weight gain.

Radiologic examination of skull bone defects progression was carried out at 14 days and 30 days after surgery at Crown Veterinary Resources. For histological analysis the samples were fixed in a 10 % phosphate-buffer formaldehyde solution for at least 3 days. The stained sections of each test sample were examined using light microscopy for tissue inflammatory reaction and the presence of the characteristic features of bone formation and cellular reaction to the implanted materials.

Results and Discussion

X-Ray Diffraction (XRD) Analysis of Prepared HAp, ZnO and HAp-ZnO Nanocomposites

Sharp and narrow peaks of HAp with high intensity of crystalline patterns were observed in the XRD spectrum of HAp calcined at 900 ^{o}C (Figure 1a). The well-defined peaks of ZnO observed in XRD spectrum of ZnO calcined at 400 ^{o}C (Figure 1b) are in agreement with the library data of ZnO. In comparison with the standard ZnO, no other diffraction peaks were detected which proved that the prepared ZnO is pure.

Figure 2 shows XRD patterns of HAp-ZnO nanocomposites with weight ratios of 20:1 and 20:2 at three different temperatures of 600 ^{o}C,

800 ^{o}C and 1000 ^{o}C. Well-defined peaks of HAp and ZnO were clearly seen. Diffraction peaks of HAp-ZnO nanocomposites revealed that the principal components of HAp and ZnO were well developed in all of these samples. The same observation was reported by Moldovan *et al.* (2015). The principal peaks of HAp appeared at Miller indices of (211), (112), (300), (130), (222) and those of ZnO at (100), (002), (101), (110) and (103).

Table 1 shows the changes in size and crystallinity percentages of HAp-ZnO nanocomposites obtained by two different ratios of 20:1 and 20:2 at 600 ^{o}C, 800 ^{o}C and 1000 ^{o}C. Crystallite sizes of HAp-ZnO (20:1) were 40.28 nm, 41.00 nm and 44.63 nm and those of HAp-ZnO (20:2) were 40.25 nm, 42.01 nm and 49.10 nm for the samples calcined at 600 ^{o}C, 800 ^{o}C and 1000 ^{o}C, respectively. All the crystallite sizes were within the nano range. Crystallite size increased with increase in temperature. Similar changing patterns of crystallinity percentages were observed for HAp-ZnO nanocomposites. Crystallinity percentages were in the range of 61.29 to 67.56 % and 65.79 to 75.20 % for HAp-ZnO nanocomposites (20:1) and (20:2), respectively. Furthermore, changes of lattice constants of HAp derived from goat bone and HAp-ZnO nanocomposites are shown in Table 2. It was observed that lattice constants a, b and c of HAp derived from goat bone changed after incorporation of ZnO.

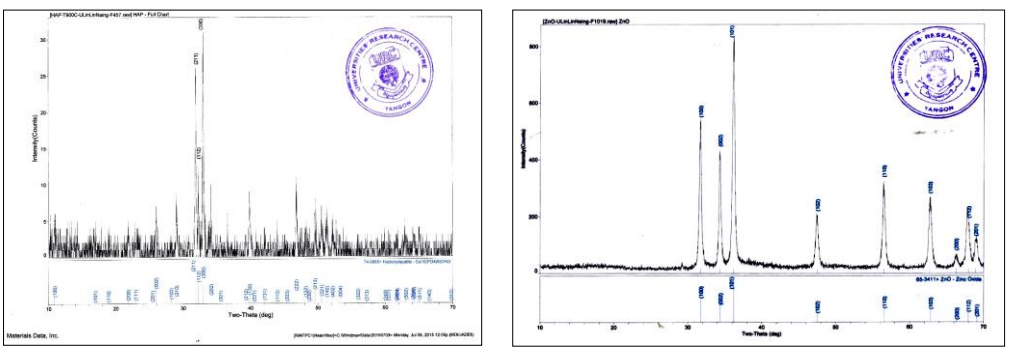

(a) (b)

Figure 1: XRD diffractograms of (a) HAp calcined at 900 °C and (b) ZnO calcined at 400 °C

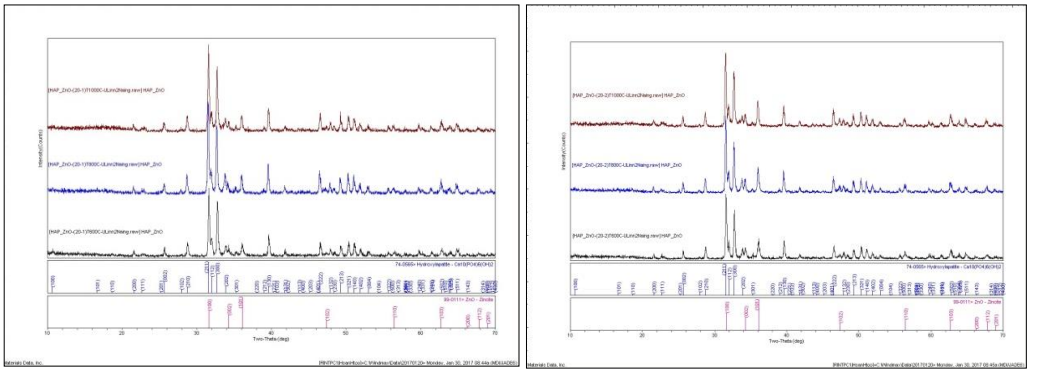

(a) (b)

Figure 2 : Comparison of XRD diffractograms of (a) HAp-ZnO (20:1) at 600 °C, 800 °C and 1000 °C (b) HAp-ZnO (20:2) at 600 ºC, 800 ºC and 1000 ºC

Table 1: Comparison of Average Crystallite Sizes and Percent Crystallinity of HAp, ZnO Nanoparticles and HAp-ZnO Nanocomposites

No	Samples	Average crystallite size (nm)	Percent crystallinity (%)
1	Hydroxyapatite at 900 ºC	81.13	59.35
2	HAp-ZnO (20:1) at 600 ºC	40.28	61.29
3	HAp-ZnO (20:1) at 800 ºC	41.00	65.63
4	HAp-ZnO (20:1) at 1000 ºC	44.63	67.56
5	HAp-ZnO (20:2) at 600 ºC	40.25	65.79
6	HAp-ZnO (20:2) at 800 ºC	42.01	69.82
7	HAp-ZnO (20:2) at 1000 ºC	49.10	75.20
8	ZnO	24.12	

Table 2: Comparison of Lattice Constants of HAp, ZnO Nanoparticles and HAp-ZnO Nanocomposites

Samples	Lattice Constants (Å)			Crystal structure
	a	b	c	
Hydroxyapatite at 900 ºC	9.3893	9.3893	6.8688	Hexagonal
HAp-ZnO (20:1) at 600 ºC	9.4834	9.4834	6.8913	Hexagonal
HAp-ZnO (20:1) at 800 ºC	9.5053	9.5053	6.9494	Hexagonal
HAp-ZnO (20:1) at 1000 ºC	9.4930	9.4930	6.8575	Hexagonal
HAp-ZnO (20:2) at 600 ºC	9.4914	9.4914	6.9104	Hexagonal
HAp-ZnO (20:2) at 800 ºC	9.5146	9.5146	6.9200	Hexagonal
HAp-ZnO (20:2) at 1000 ºC	9.5187	9.5187	6.8548	Hexagonal
Zinc Oxide	3.2580	3.2580	5.2126	Hexagonal

Fourier Transform Infrared (FT IR) Analysis of HAp-ZnO nanocomposites

The FT IR spectra of HAp-ZnO nanocomposites with two different ratios calcined at 600 ^{o}C, 800 ^{o}C and 1000 ^{o}C are illustrated in Figures 3. The main chemical groups that characterize HAp and ZnO structures such as PO_4^{3-}, OH^-, CO_3^{2-} and ZnO were found in the FT IR spectra. From the spectral data, the characteristic absorption bands of zinc oxide were observed in the range of 400-500 cm^{-1} due to stretching mode of Zn-O (Vanaja and Rao, 2016). Absorption peak of ZnO (418 cm^{-1}) shifted to higher wavenumbers in the range of 437 to 474 cm^{-1} in HAp-ZnO nanocomposites. The peaks around 1091 cm^{-1} and 1045 cm^{-1} correspond to the stretching of P-O in phosphate group. The bands observed around 1460 cm^{-1} and 1413 cm^{-1} are attributed to carbonate group (Figueiredo *et al*., 2010). Moreover, O-H stretching vibration of hydroxyl group was observed at 3400-3500 cm^{-1}. There is no apparent change in band positions in HAp-ZnO nanocomposites with different temperatures and various ratios of zinc oxide. However, the band positions of P-O stretching and bending vibrations and O-H stretching vibrations of HAp slightly shifted from their original positions after incorporation of ZnO.

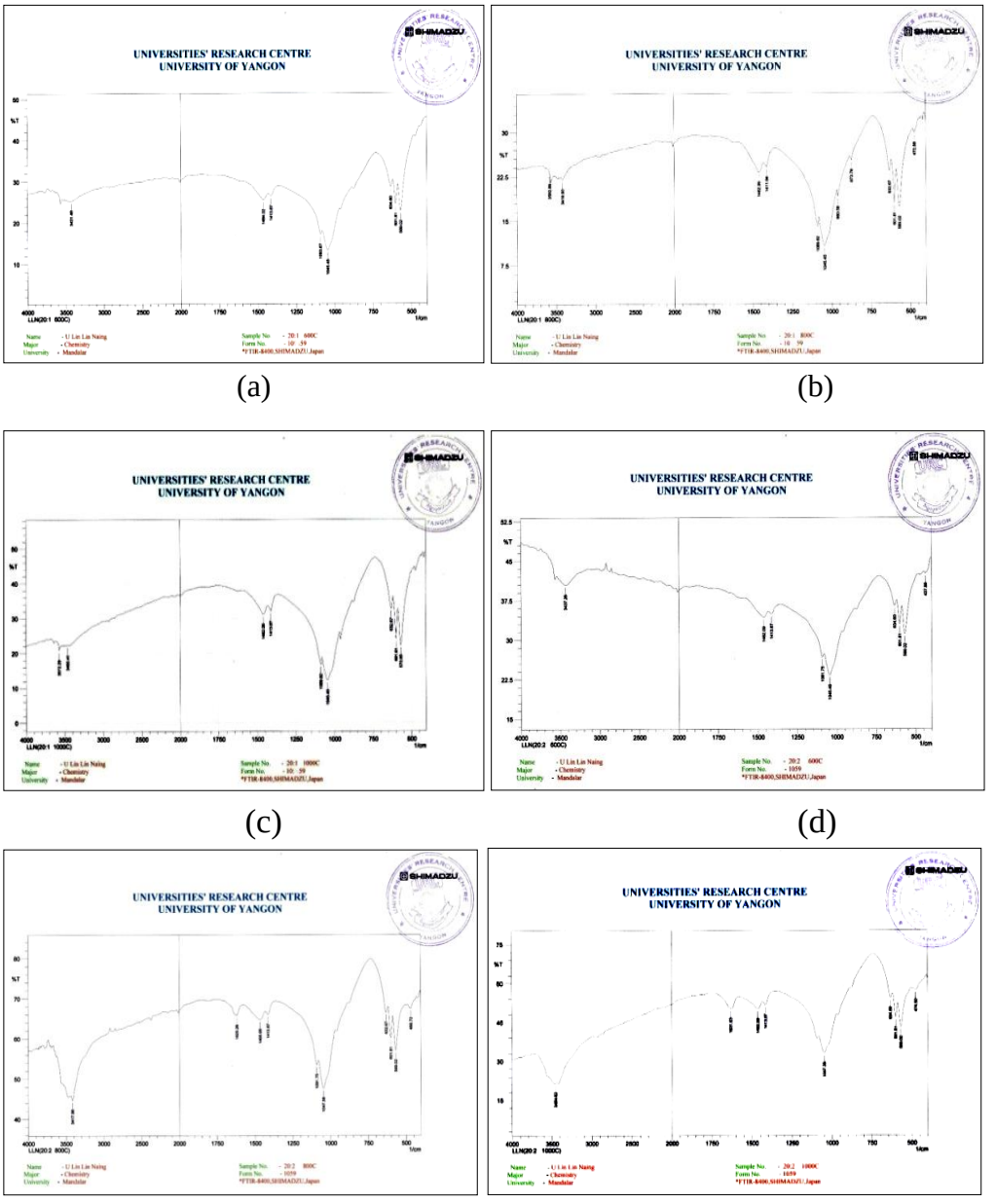

Figure 3: FT IR spectra of HAp-ZnO (20:1) calcined at (a) 600 ºC (b) 800 ºC (c) 1000 ºC and HAp-ZnO (20:2) calcined at (d) 600 ºC (e) 800 ºC and (f) 1000 ºC

Scanning Electron Microscopy (SEM) Analysis of Prepared HAp and HAp-ZnO Nanocomposites

SEM images of HAp-ZnO nanocomposites are depicted in Figure 4. Discrete particles of HAp particles were observed in HAp derived from goat bone calcined at 900 ^{o}C. After incorporation of ZnO to HAp the elongated crystalline forms were observed in all HAp-ZnO nanocomposites. Furthermore, agglomeration of ZnO nanoparticles on the surface of HAp were noted.

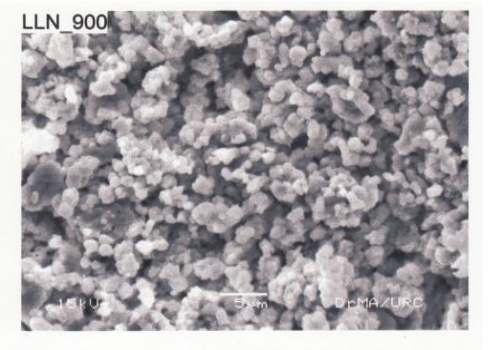

(a)

(b)

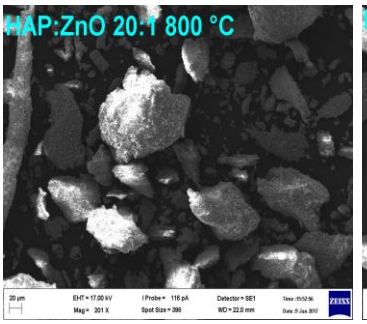

(c)

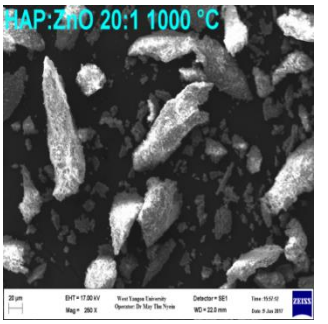

(d)

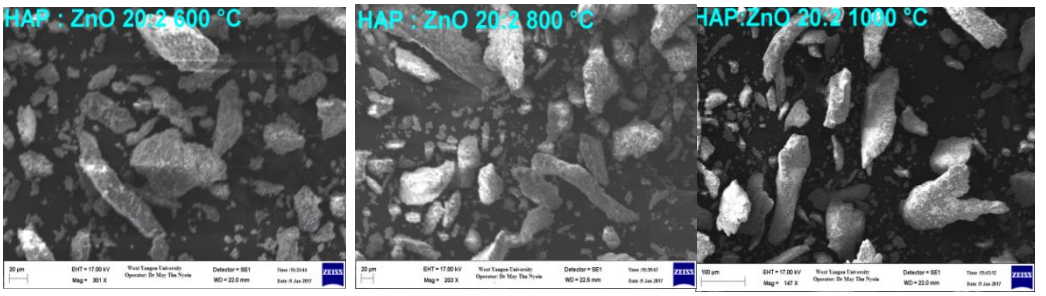

(e) (f) (g)

Figure 4 : SEM images of (a) HAp (900 ^{o}C) (1000X magnification)
(b) HAp-ZnO 20:1 (600 ^{o}C) (242X magnification)
(c) HAp-ZnO 20:1 (800 ^{o}C) (201X magnification)
(d) HAp-ZnO 20:1 (1000 ^{o}C) (260X magnification)
(e) HAp-ZnO 20:2 (600 ^{o}C) (301X magnification)
(f) HAp-ZnO 20:2 (800 ^{o}C) (203X magnification)
(g) HAp-ZnO 20:2 (1000 ^{o}C) (147X magnification)

Energy Dispersive X-Ray Fluorescence (EDXRF) Analysis of HAp-ZnO Nanocomposites

Relative abundances of elemental oxides in HAp-ZnO nanocomposites are shown in Figure 5 and the corresponding data are presented in Table 3. It was observed that the concentrations of CaO, P_2O_5 and ZnO were the highest percentages (in order of decreasing content) in each composites. Other metal oxides were also found in minute amounts in all prepared composites. The amount of ZnO increased in the composites with increase in amount of ZnO nanoparticles added in HAp-ZnO nanocomposites.

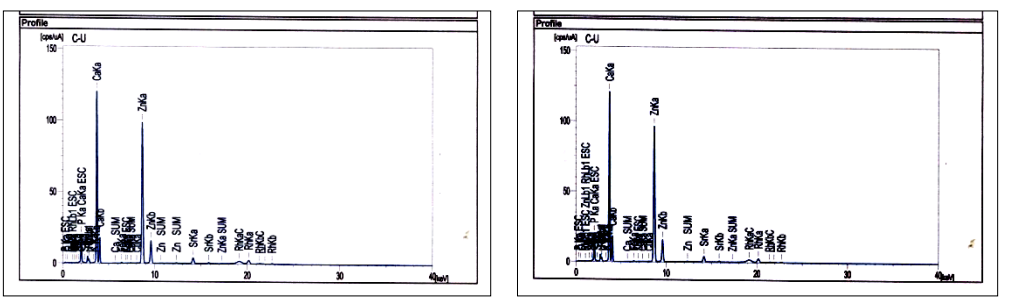

(a) (b)

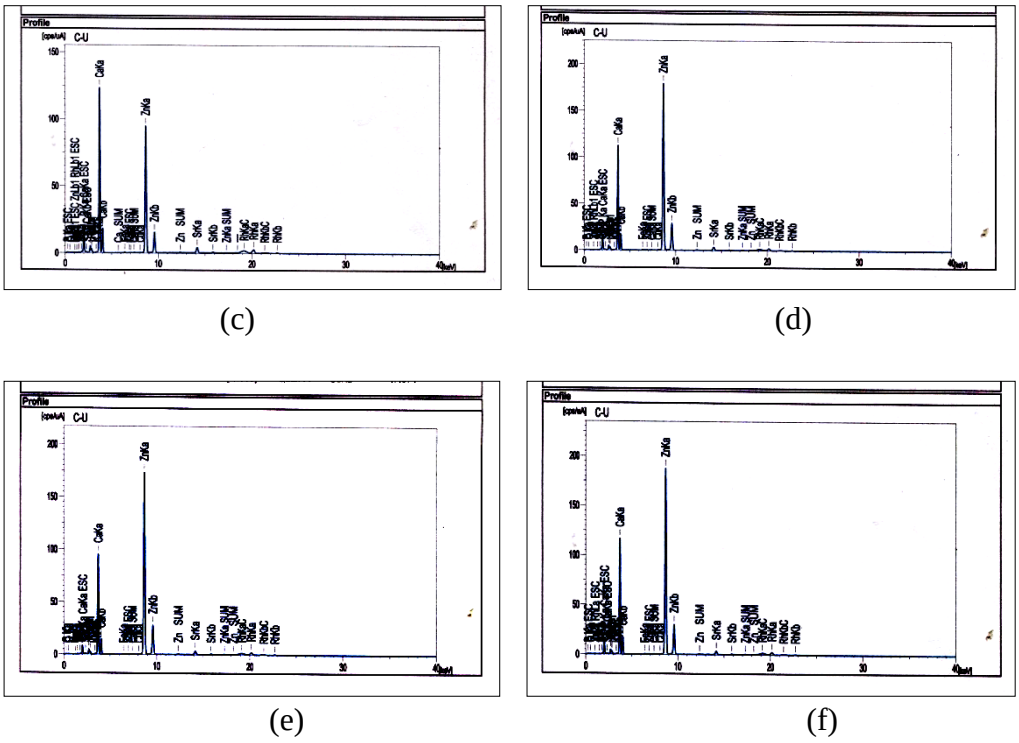

Figure 5: EDXRF spectra of HAp-ZnO (20:1) calcined at (a) 600ºC (b) 800 ºC (c) 1000 ºC and HAp-ZnO (20:2) calcined at (d) 600 ºC (e) 800 ºC and (f) 1000 ºC

Table 3: Relative Abundances of Elemental Oxide in HAp-ZnO Composites

Sample	Elemental oxide (%)										
	CaO	**P_2O_5**	**ZnO**	**MgO**	**SiO_2**	**Al_2O_3**	**SO_3**	**K_2O**	**SrO**	**Fe_2O_3**	**CuO**
1	50.370	34.473	5.884	2.985	2.593	2.505	0.660	0.294	0.151	0.077	0.009
2	51.882	35.166	5.977	-	2.565	3.071	0.798	0.299	0.155	0.077	0.010
3	50.337	34.510	5.500	2.782	2.741	3.091	0.534	0.276	0.147	0.073	0.009
4	49.555	32.343	11.622	-	2.280	2.936	0.730	0.297	0.157	0.066	0.014
5	53.949	31.766	13.634	-	-	-	-	0.376	0.185	0.073	0.018
6	50.865	31.107	12.246	-	2.354	2.486	0.401	0.298	0.168	0.060	0.015

1 = HAp - ZnO (20:1) at 600 ºC
2 = HAp - ZnO (20:1) at 800 ºC
3 = HAp - ZnO (20:1) at 1000 ºC
4 = HAp - ZnO (20:2) at 600 ºC
5 = HAp - ZnO (20:2) at 800 ºC
6 = HAp - ZnO (20:2) at 1000 ºC

Physical Properties of HAp, ZnO and HAp-ZnO Nanocomposites

pH of the HAp calcined at 900 ^{o}C was found to have 9.8. After incorporation of ZnO nanoparticles the pH values slightly decreased in the range of 9.3 to 9.6. However, addition of increase amount of ZnO did not appreciably change the pH value (Table 4).

Bulk density of HAp sample was 1.56 g mL^{-1}. The bulk density also slightly increased in HAp-ZnO nanocomposites compared to HAp sample. The bulk densities of the HAp-ZnO nanocomposites were in the range of 1.61 to 1.79 g mL^{-1}. It was found that among the nanocomposite samples, the porosity percent slightly decreased with increasing both temperature and amount of ZnO.

Table 4: Physical Properties of the Prepared Hydroxyapatite and Hydroxyapatite- Zinc Oxide Nanocomposites Calcined at Different Temperatures

No		Samples						
		HAp	HAp-ZnO (20:1)			HAp-ZnO (20:2)		
		900 ^{o}C	600 ^{o}C	800 ^{o}C	1000 ^{o}C	600 ^{o}C	800 ^{o}C	1000 ^{o}C
1	pH	9.8	9.5	9.3	9.6	9.4	9.3	9.5
2	Bulk density (g/mL)	1.56	1.59	1.61	1.61	1.61	1.70	1.72
3	Porosity (%)	18.32	9.60	9.30	6.94	7.53	5.85	5.56

Cytotoxicity Test of Prepared HAp and HAp-ZnO Nanocomposites

The cytotoxicity of HAp and HAp–ZnO nanocomposites were evaluated by brine shrimp cytotoxicity bioassay. The cytotoxicity of HAp and HAp-ZnO composites was expressed in terms of mean ± SEM (standard error mean) and LD_{50} (50 % Lethality Dose) and the results are shown in Table 5. In this experiment, standard potassium dichromate ($K_2Cr_2O_7$) was chosen because $K_2Cr_2O_7$ has well-known toxicity in this assay. The LD_{50} values of HAp sample, HAp-ZnO composites with two different ratios of 20:1 and

20:2 calcined at 1000 ^{o}C were found to be >1000 µg/mL. The LD_{50} values of standard $K_2Cr_2O_7$ was found to be 13.79 µg/mL.

According to Meyer's toxicity index, the sample with LD_{50} < 1000 µg/mL are considered as toxic, while the sample with LD_{50} > 1000 µg/mL are considered as non-toxic (Meyer *et al*., 1982). So HAp and HAp-ZnO composites prepared in this work showed no cytotoxic effect.

Table 5: Cytotoxicity of HAp Sample, HAp-ZnO Composites with Two Different Ratios of 20:1 and 20:2 Calcined at 1000 ^{o}C against *Artemia salina* (Brine Shrimp)

Samples	Percentages of Dead Brine Shrimp (Mean ± SEM) in Various Concentrations (µg/mL) of Samples					LD_{50} (µg/mL)
	0.1	1	10	100	1000	
HAp	0	0	0	0	3.33±5.77	> 1000
HAp-ZnO (20:1)	0	0	0	3.33±5.77	3.33±5.57	> 1000
HAp-ZnO (20:2)	0	0	0	3.33±5.77	3.333±5.57	> 1000
$K_2Cr_2O_7$*	3.33± 5.57	6.67 ± 5.77	20.00± 0.00	100.00 ± 0.00	100.00 ± 0.00	13.79

* Used as Cytotoxic Standard

Radiological Results of Skull Bone Defects Filled with HAp and HAp-ZnO Nanocomposites

After 14 days of operation incomplete skull bone defects were observed in the Wistar rat filled with HAp and control. On the other hand, bony defect was still observed in Wistar rat filled with HAp-ZnO (20:1) nanocomposites calcined at 1000 ^{o}C. However, a tiny bone defect remained in Wistar rat filled with HAp-ZnO (20:2) nanocomposites (Figure 6). After 30 days of operation, bony defect remained in the control whereas a tiny hole bone defect was observed in Wistar rat filled with HAp (Figure 7). Furthermore, in Wistar rat filled with HAp-ZnO nanocomposites (20:1) there was very little pointed bony defect remained. Complete bone healing was

observed by using HAp-ZnO (20:2). The composites bridge the defect and new bone was formed.

According to X-ray visions, it has some differences among different composite applications. HAp-ZnO composite defect bone applications showed better than other two X-ray visions.

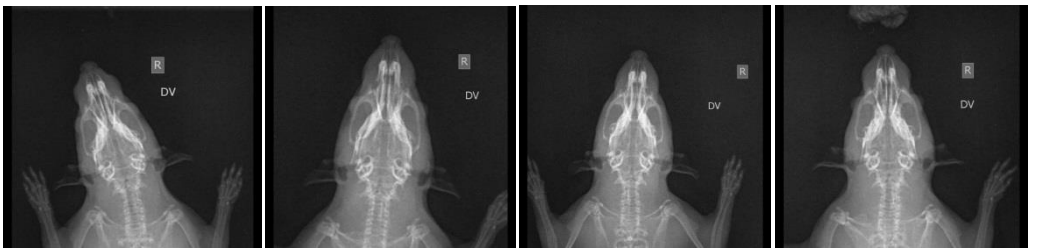

(a) (b) (c) (d)

Figure 6: 14 days Progressiveness of Bone Defect Healing in X-ray Diagnosis (a) Control (b) HAp at 900 ^{o}C (c) HAp-ZnO (20:1) calcined at 1000 °C

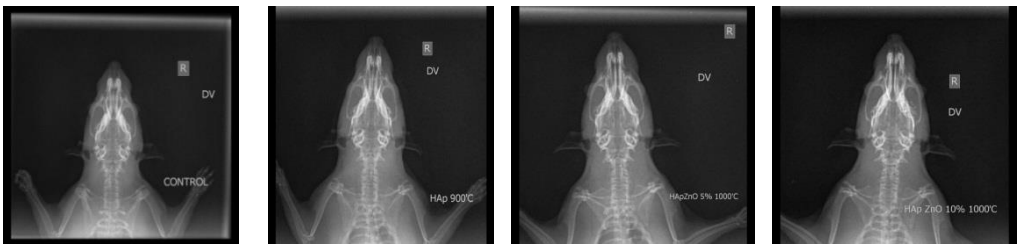

(a) (b) (c) (d)

Figure 7: 30 days Progressiveness of Bone Defect Healing in X-ray Diagnosis (a) Control (b) HAp at 900 ^{o}C (c) HAp-ZnO (20:1) calcined at 1000 °C (d) HAp-ZnO (20:2) calcined at 1000 °C

Histological Results of Skull Bone Defects Filled with HAp and HAp-ZnO Nanocomposites

At 14 days after the surgery, histology of fracture skull bone revealed that connective tissue was occupied especially fibroblast and admixed with net work of delicate bone trabeculae lined with osteoblast and formed from inner surface of wall of skull bone. Blood clot remnants were observed. Non-union

of skull bone was resulted (Figure 8a). Fracture site was filled with fibroblast and blood clots. Net work of delicate bone trabeculae lined with osteoblast and formed from inner surface of wall of skull bone. Incomplete cartilage union was found (Figure 8b). Coagulum (blood clot) was reduced in size and observed woven bone formation composed of few osteoblast and increased amount of chondrocytes. Complete with cartilage union was observed (Figure 8c). A few coagulum was found and mixed with few fibroblast. Woven formation was noted and accompanied with increased osteoblast and chondrocytes. A fracture site was replaced by few amount of trabecular bone. Predominantly cartilage with some trabecular bone was detected (Figure 8d).

The histological findings at 30 days showed that new trabecular bone formation was started from fracture site and composed of osteoblast and increased amount of chondrocytes. Predominantly cartilage with some trabecular bone was seen (Figure 9a). Trabecular bone formation was well organized and absence of blood clots and fibroblast was observed. Osteoblast was seen in inner layer of fracture bone. Chondrocytes are filled in some trabecular bone areas. Incomplete bony union with intermediate ossification was observed. Equal amounts of cartilage and trabecular bone was detected (Figure 9b). There was increased amount of osteocytes in centre area of bony fracture site. Chondrocytes were filled in some trabecular bone areas. Incomplete bony union with late ossification was detected. Predominantly trabecular bone with some cartilage was observed (Figure 9c). There was complete new formation of trabecular bone in fracture site. Complete union of fracture area was observed in entire bony fracture site. Complete union of fracture bone was resulted (Figure 9d).

Due to histological findings, HAp-ZnO composite with ratio of 20:2 at 1000 °C group was the best with good scoring within 30 days after application.

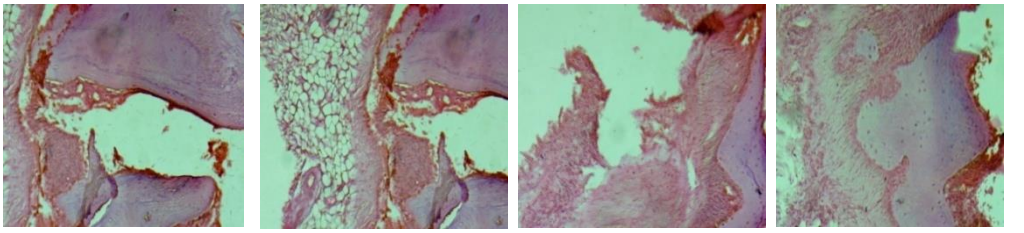

(a) (b) (c) (d)

Figure 8: Photomicrographs of histopathology of 14 days bony healing with (a) Control (b) HAp calcined at 900 ºC (c) HAp : ZnO (20 : 1) calcined at 1000 ºC (d) HAp : ZnO (20 : 2) at 1000 ºC

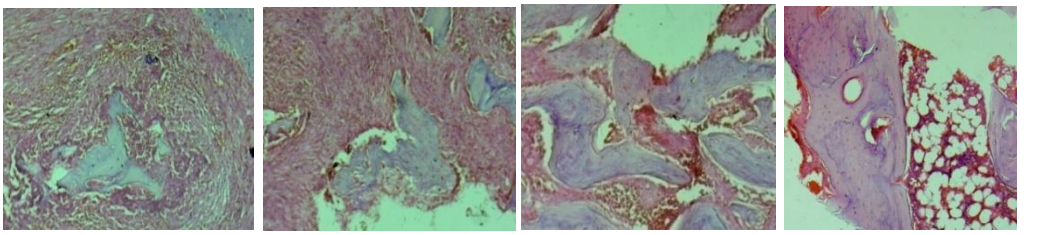

(a) (b) (c) (d)

Figure 9: Photomicrographs of histopathology of 30 days bony healing with (a) Control (b) HAp calcined at 900 ºC (c) HAp : ZnO (20 : 1) calcined at 1000 ºC (d) HAp : ZnO (20 : 2) at 1000 ºC

Conclusion

HAp-ZnO nanocomposites were successfully prepared by incorporation of ZnO nanoparticles to HAp derived from waste goat bone calcined at 900^{o}C with the ratio of 20:1 and 20:2. After incorporation of ZnO to HAp with the ratios of 20:1 and 20:2, the characteristic peaks of both HAp and ZnO were found in the X-ray diffractograms of HAp-ZnO nanocomposites. The crystallite sizes were in the range of 40.28 nm to 49.10 nm and found to increase with increase in temperature and with increase in amount of ZnO. The shifts in peak positions and the change of lattice constant of HAp after incorporation of ZnO nanoparticles indicated the substitution of Zn ion in Ca ion. FT IR spectral data revealed the characteristic

absorption peaks of PO_4^{3-}, OH^- and ZnO. The absorption peaks of ZnO shifted from 418 cm^{-1} to higher wavenumbers (437 to 474 cm^{-1}) in HAp-ZnO nanocomposites. HAp-ZnO nanocomposites showed elongated crystalline structures in SEM analysis. EDXRF spectra showed the highest content of CaO,P_2O_5 and ZnO in these nanocomposites.

Brine shrimp cytotoxicity bioassay indicated that HAp and HAp-ZnO nanocomposites were not cytotoxic. Orthopedic application of HAp and HAp-ZnO nanocomposites as filling material were conducted on Wistar rats. After 30 days implantation, the newly formed bone tissue appeared within the bone defect in the Wistar rat. X-ray diagnosis and histological findings confirmed the successful filling of the prepared samples. Thus, HAp-ZnO nanocomposites have the potential to improve numerous orthopedic and dental applications.

Acknowledgements

The authors would like to thank the Myanmar Academy of Art and Science for allowing to present this paper and Professor and Head Dr Tin Tin Mya, Department of Chemistry, Mandalar Degree College for her kind encouragement.

References

Anita, S., Ramachandran, T., Koushik, C.V., Rajendran, R. and Mahalakshmi, M. (2010). "Preparation and Characterization of Zinc Oxide Nanoparticles and A Study of the Anti-microbial Property of Cotton Fabric Treated with the Particles". *JIATM*, vol.6 (4), pp.1-6.

Deepa, C., Begum, A. N. and Aravindan, S. (2013). "Preparation and Antimicrobial Observations of Zinc Doped Nanohydoxyapatite". *Nanosystems: Physics, Chemistry, Mathematics,*vol.4 (3), pp. 370-377.

Figueiredo,M., Fernando, A., Martins, G., Freitas, J., Judas, F. and Figueiredo, H. (2010). "Effect of Calcination Temperature on the Composition and Microstructure of Hydroxyapatite Derived from Human and Animal Bones". *Ceramics International*,vol.36, pp. 2383-2393.

Kini, U. and Nandeesh, B. N. (2012). Physiology of Bone Formation, Remodeling and Metabolism. In *Radionuclide and Hybrid Bone Imaging*. (Eds.) Foggelman, I., Gnanasegaran, G. and Wall , H. Berlin: Springer, pp. 29-57.

Meyer, B.N., Ferrigni, N.R., Putnam, J.E., Jacobsen, L.B., Nichols, D.E. and McLaughlin, J.L. (1982). "Brine Shrimp: A Convenient General Bioassay for Active Plant Constituents". *Planta Medica*, vol.45**,** pp. 31-34

Moldovan, M., Prodan, D., Popescu, V., Prejmerean, C., Sarosi, C., Saplonț ai, M., Tă lu, S. and Vasile,E. (2015). "Structural and Morphological Properties of HA-ZnO Powders Prepared for Biomaterial". *Open Chem.,* vol.13, pp. 725–733.

Nawaz, H. R., Solangi, B.A., Zehra, B. and Nadeem, U. (2011). "Preparation of Nano Zinc Oxide and its Application in Leather as Retaining and Antibacterial Agent". *Canadian Journal on Scientific and Industrial Research*,vol.2(4), pp. 165-170

Okada, M. and Matsumoto, T. (2015). "Synthesis and Modification of Apatite Nanoparticles for Use in Dental and Medical Applications". *Japanese Dental Science Review*, vol.51, pp.85-95

Singh, A., Kumar, R., Malhotra, N. and Suman. (2012). "Preparation of ZnO Nanoparticles by Solvothermal Process". *International Journal for Science and Emerging Technologies with Latest Trends*,vol.4(1), pp.49-53

Sverdrup, H.U., Johnson, M.W. and Fleming, R.H. (1942). "*The Oceans Their Physics, Chemistry and General Biology*". New York: Prentice-Hall, Inc., p. 186

Vanaja, A. and Rao, K. S.. (2016). "Precursors and Medium Effect on Zinc Oxide Nanoparticles Synthesized by Sol-Gel Process". *International Journal of Applied and Natural Sciences,* vol. 5(1), pp. 53-62

Yadav, A., Prasad, V., Kathe, A. A., Raj, S., Yadav, D., Sundaramoorthy, C. and Vignesharan, N. (2006). "Functional Finishing in Cotton Fabric using Zinc Oxide Nanoparticles". *Bull Matter Sci*, vol.29(6), pp. 641-645

Ylinen, P. (2006). *Applications of Coralline Hydroxyapatite with Bioabsorbable Containment and Reinforcement as Bone Graft Substitute*. Helsinki: Academic Dissertation, University of Helsinki

Zak, A. K., Majid, W.H.A., Mahmoudian, M. R., Darroudiand, M. and Yousefi, R. (2013). "Starch-stabilized Synthesis of ZnO Nanopowders at Low Temperature and Optical Properties Study". *Advanced Powder Technology,* vol.24, pp.618-624

Zhou, H. and Lee, J. (2011). "Nanoscale Hydroxyapatite Particles for Bone Tissue Engineering". *Acta Biomater***,** vol.7(7), pp.2769- 2781

ISOLATION, STRUCTURE ELUCIDATION AND SCREENING OF THE ANTIOXIDANT AND CYTOTOXIC ACTIVITIES OF SECONDARY METABOLITES FROM THE STEM BARK OF *Aegle marmelos* (L.) Corrêa. (Ohshit)

Thu Zar[1], Hnin Thanda Aung[2], Myint Myint Sein[3]

Abstract

Three coumarin compounds (**1**), **(2)**, **(3)** and two alkaloid compounds **(4)** and **(5)** were isolated from the stem bark of *Aegle marmelos*, collected from Sagaing Region, Myanmar. The structures of these compounds were elucidated mainly by extensive spectroscopic analysis (1D and 2D NMR). The isolated compounds were screened for free radical scavenging activity using DPPH radical-scavenging assay. In addition, compounds (**1-5)** were evaluated in vitro for their cytotoxic activity against Hela cells. It was observed that pure compounds (**1**), **(2)**, **(3)**(EC_{50}>100 μM) exhibited lowerantioxidant activity than ascrobic acid(EC_{50} 27.5 μM). The compound **(4)** (IC_{50} 55 μM) exhibited low cytotoxic activity against Hela cell lines while compounds **(1)** and **(5)** displayed very weak cytotoxic activity with IC_{50} value > 100 μM.

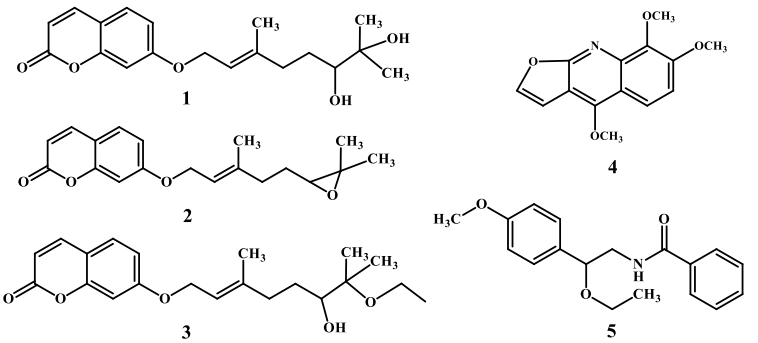

1 **2** **3** **4** **5**

Keywords: *Aegle marmelos*, coumarin, alkaloid, Hela cells

Introduction

Aegle marmelos (L.)Corrêa. is locally known as Ohshit belonging to the family Rutaceae. It is medium sized tree growing throughout the forest of

1. Dr, Lecturer, Department of Chemistry, University for the Development of the National Races of the Union, Sagaing
2. Dr, Lecturer, Department of Chemistry, Kalay University
3. Dr, Professor and Head (Retired), Department of Chemistry, University of Mandalay

India of altitude 1200 meter. It is found all over India, from sub-Himalayan forest, Bengal, central and south India. It is also found in Bangladesh, Egypt, Malaysia, Myanmar, Pakistan, Sri Lanka and Thailand (Lambole *et al.*, 2010).In all natural habitats, plants are surrounded by an enormous number of potential enemies (biotic) and various kinds of abiotic environmental stress. Nearly all ecosystems contain a wide variety of bacteria, viruses, fungi, nematodes, mites, insects, mammals and other herbivorous animals, greatly responsible for heavy reduction in crop productivity. By their nature, plants protect themselves by producing some compounds called as secondary metabolites. Secondary metabolites, including terpenes, phenolics and nitrogen (N) and sulphur (S) containing compounds, defend plants against a variety of herbivores and pathogenic microorganisms as well as various kinds of abiotic stresses (Mazid *et al.*, 2011).The different parts of *Aeglemarmelos* plant contain number of coumarins, alkaloids, sterols and essential oils(Lambole *et al.*, 2010).According to Khare (2007) a number of coumarins (including xanthotoxol and alloimperatorin methyl ether), flavonoids (including rutin and marmesin), alkaloids (including alpha-fagarine), sterols and essential oils have been isolated from plant parts. According toKumar *et al.*, *Aeglemarmelos* is used to treat fevers, abdomen pain, palpitation of the heart, urinary troubles, melancholia, anorexia, dyspepsia, diabetes and diarrhea in Indian traditional systems of medicine (Kumar *et al.*, 2013).Plant parts like root, stem bark and fruit have been reported for various medicinal properties such as antidiabetic, anticancer, antibacterial, antifungal, antipyretic, analgesic, antioxidant, cardio protective, radioprotective, antidiarrheal, antidysentery, antiulcer, wound healing and many more (Verma *et al.*, 2013). The main aim of the present research work is to perform the isolation and structural elucidation of secondary metabolites from the stem bark of one Myanmar indigenous medicinal plant, *Aeglemarmelos* (L.) Corrêa., Ohshit and screening of the antioxidant and cytotoxic activities of the isolated compounds.

Materials and Methods

General Procedure

FTIR spectra were recorded on FT IR-410 spectrophotometer. NMR spectra were recorded in methanol-d_4 using a Bruker Avance III HD600 spectrophotometer equipped with Prodigy liq. Nitrogen cryoprobe. Chemical shifts for ^{1}H and ^{13}C NMR are given in parts per million (δ) relative to solvent signal (MeOH-d_4: δ_H 3.30 and δ_C49.0; $CDCl_3$: δ_H7.26 and δ_C77.0) as internal standard. Positive mode FAB mass was obtained by using a JEOL JMS HX-110 mass spectrophotometer with m-nitrobenzyl alcohol as matrix. Optical rotations were recorded on a JASCO P-1020 polarimeter (cell length 100 mm). HPLC reversed phase column (C-8-UG-5) was used for purification of compounds. The specific optical rotations were measured on a JASCO P-2200 Polarimeter.The melting point of the pure compounds in crystal form was measured by Stuart SMP 30 melting point apparatus. For cytotoxic assay, cell densities were measured at 450 nm by using Bio-RAD Model 550 Microplate Reader.

Plant Material

Thestembark of *Aeglemarmelos*(L.) Corrêa., Ohshitwas collected from Ywa-thit-kyi village, Sagaing Township, Sagaing Region in October 2014. The plant materials were authenticated by the authorized botanist from Botany Department, University of Mandalay.

Extraction and Isolation

The air dried sample of the stem bark of *A.marmelos* (1 kg) was extracted with95% ethanol (3.0 L) at room temperature for one month to obtain the ethanolic extract. The ethanolic extract was concentrated by evaporator, and dried extract (96.6 g) was obtained. The ethanolic extract was then extracted with ethyl acetate to give 26.44 g of ethyl acetate extract. Then, 2 g of ethyl acetate extract was separated on silica gel eluting with the solvent systems with various ratios:such as n-hexane only, n-hexane : EtOAc (19:1 to 1:4) and EtOAc only. Totally 500 fractions were obtained. Each fraction was checked by TLC, iodine vapour and UV lamp. Then, the fractions of the same R_f value were combined and 26 combined fractions were obtained. The

combined fraction 7 (178 mg) was purified by HPLC reversed phase column (C-8-UG-5) using a gradient system of (A) methanol-water (2:98) and (B) MeOH with A: B (50:50 to 0:100) as a mobile phase to yieldcompounds **(1)** (5.1 mg), **(2)** (4.1 mg), **(3)** (5.2 mg) and **(5)** (11.7 mg) as colourless oil forms and compound **(4)** (0.8 mg) as a white crystal (m.p. 177-179°C).The yield percentages of compounds (**1-5)** were found to be 0.26%, 0.21%, 0.26%, 0.04% and 0.59 % based on ethyl acetate extract respectively.

Antioxidant Activity Screening of the Isolated Compounds (1-5)

The antioxidant activities of the isolated pure compounds were determined by using 2, 2-diphenyl-1- picrylhydrazyl radical scavenging activity assay (Yamaguchi *et al*., 1998).Its reaction principle was based on mechanism of free radicals inhibition by hydrogen transfer.The antioxidant activity of sample was expressed in EC_{50} (50% effective concentration). 500 μL of test solutions in various concentrations (100 μg/mL, 50μg/mL and 10 μg/mL) and 500 μLof 0.2 M acetate buffer(pH 5.5)solution were mixed in a test tube. 250 μL of $5x10^{-4}$ M DPPH solution was added to the mixture in dark. The mixture was homogenized by using a vortex mixer in a dark room (resistant to UV light) and stands for 30 min at room temperature. After that, absorbance of the mixture was measured at λ_{max} 517 nm by a UV-Vis spectrophotometer. Vitamin C was used as a reference compound in the same concentration range as the test compounds. A control solution was prepared by mixing 500 μL of buffer (pH 5.5) solution, 500 μL of ethanol and 250 μL of 5×10^{-4} M DPPH solution in the test tube. Blank solution was prepared by mixing 500 μL of buffer (pH 5.5) solution with 750 μL of ethanol in the test tube. The mean values were obtained from triplicate experiments. The capability of scavenging DPPH radicals as a percentage of DPPH remaining in the resulting solution was determined using the following equation:

$$\text{DPPH}\ (\%) = \frac{\text{Abs}_{\text{control}} - \text{Abs}_{\text{sample}}}{\text{Abs}_{\text{control}}} \times 100\ \%$$

where $Abs_{control}$ is absorbance of control and Abs_{sample} is absorbance of sample. The antioxidant power (EC_{50}) is expressed as the concentration of test substance (μg/mL) that result in a 50% reduction of initial absorbance of DPPH solution and that allows to determine the concentration. EC_{50} (50%

effective concentration) values were calculated by linear regressive excel program (Yamaguchi *et al*., 1998).

Cytotoxicity Test of the Isolated Compounds (1-5)

In vitro cytotoxic effects of the isolated compounds (1-5) were measured on a Hela(cervix adenocarcinoma) cell line by the colorimetric method using a Cell Counting kit-8 that was based on the tetrazolium salt/formazan system (Ishiyama *et al*., 1993). HeLa cell (JCRB9004) was obtained from Japanese Collection of Research Bioresources (JCRB) cell bank. Cells were cultured in minimum essential media (MEM) supplemented with 10 % fetal bovine serum. For the cytotoxic assay, cells were seeded at a density of 5×10^3 cells/well in 0.2 mL of medium in 96-multiwell plates and adhered. Samples were dissolved in saline containing 10% DMSO and sterilized by filtration. Series of the diluted samples (0.2 mL) were then added to the cells. The plate was incubated at 37°C under 5% CO_2 atmosphere for 48 h. Twenty microliters of cell counting kit-8 (based on the tetrazolium salt/formazan system) was added to each well, and the microplate was incubated for 1 h, after which cell densities were measured at 450 nm using Bio-RAD Model 550 Microplate Reader.

Results and Discussion

The crude ethyl acetate extract of the stem bark of *Aegle marmelos*was separated by silica gel column chromatography and purified by HPLC reversed phase column to furnish three coumarin compounds (**1**), **(2)**, **(3)** and two alkaloid compounds **(4)** and **(5)**. The structures were elucidated by FT IR and detailed NMR investigations including ^{1}H and ^{13}CNMR, COSY, HSQC and HMBC spectra (Silverstein *et al*., 2005).

Compound (1): colourless oil; $[\alpha]_D$+ 25.45 (c 0.022, $CHCl_3$),FTIR (KBr) ν_{max} cm^{-1}: 3423, 3080, 2972, 2862, 1730,1613, 1507, 1464, 1402, 1350, 1278, 1231, 1199, 1128,1078, 999, 893. FAB-MS *m/z*: 333 $[M+H]^+$ (calc. 332 for $C_{19}H_{24}O_5$), ^{13}Cand ^{1}HNMR: (Table 1).

Compound (2): colourless oil; $[\alpha]_D$: + 16 (c 0.022, $CHCl_3$). FT IR (KBr) ν_{max} cm^{-1}: 3078, 2927, 2852, 1732,1612, 1507, 1456, 1402, 1349,1277, 1230,

1197, 1124, 891. FAB-MS *m/z*: 315 $[M+H]^+$ calc. 314 for $C_{19}H_{22}O_4$), ^{13}Cand ^{1}HNMR: (Table 1).

Compound (3): colourless oil; $[\alpha]_D$+ 32 (c 0.03, $CHCl_3$).FTIR (KBr) ν_{max} cm^{-1}: 3471, 3082, 2974, 2876, 1733, 1613, 1507, 1463, 1402, 1350, 1278, 1231, 1197, 1125, 1071, 1000, 891. FAB-MS *m/z*: 361 $[M+H]^+$ (calc. 360 for $C_{21}H_{28}O_5$),^{13}Cand ^{1}HNMR: (Table 1).

Compound (4): white crystals; m.p. 177 – 179°C**.**FT IR(KBr) ν_{max} cm^{-1}: 3042, 2940, 2842, 1614, 1577, 1507, 1456, 1394, 1270, 1239. Mass spectrum *m/z* (% intensity): 259 (M+, 59), 244 (29), 216 (10), 162 (100), 153 (57), 134 (41). ^{13}Cand ^{1}HNMR: (Table 2).

Compound (5): colourless oil; $[\alpha]_D$+ 10.2 (c 0.02, $CHCl_3$). FT IR (KBr) $\nu_{max}$$cm^{-1}$:3316,3063, 2968, 2937, 1652, 1611, 1509, 1462, 1294, 1246, 1095, 831, 711.FAB-MS *m/z*: 322 $[M+Na]^+$ (calc. 299 for $C_{18}H_{21}NO_3$), ^{13}Cand ^{1}HNMR: (Table 3).

Structural Elucidation of Coumarin Compound (1)

Compound **(1)** was isolated as a colourless oil with a molecular formula of $C_{19}H_{24}O_5$ determined by FAB-MS with *m/z*333 $[M + H]^+$which indicated the molecular mass (*m/z*332).The unsaturated degree of 8 was calculated from the molecular formula. FT IR spectrum showed the presence of broad peak at 3423cm^{-1} exhibited OH group.Peak at 3080 cm^{-1} revealed the aromatic C-H, whereas peaks at 2972 and 2862 cm^{-1} were due to aliphatic C-H stretching vibration. The band at 1730 cm^{-1} indicated the presence of δ- lactone group. Intense bands at 1613, 1507 and 1464 cm^{-1} were the characteristics of conjugated C=Cbonds. The absorption bands at 1350 and1278-1078 cm^{-1} confirmed the presence of gem dimethyl group and ether groups respectively. The DEPT spectrum indicated the presence of three methyl carbons, three methylene carbons, seven methine carbons, five quaternary C-atoms and one carbonyl carbon. The ^{1}HNMR spectrum (Table 1) exhibited three aliphatic methyl signals [δ_H 1.78 (3H, s); 1.17 (3H, s); 1.21 (3H, s)], an olefinic signal [δ_H 5.53, (1H, t, 6.5 Hz)] and three methylene signals [δ_H 4.62 (2H, d, 6.5 Hz); 2.37, 2.17, (2H, m); 1.65, 1.46 (2H, m)]. In addition, there were five sp^2 signals, including double doublet signal of δ_H 6.85 with 7.36 [an *o*-coupling (J = 8.6 Hz)] and that of δ_H 6.85 with 6.82

[a*m*-coupling (*J* = 2. 3 Hz)], as well as two doublet signals at δ_H 6.24 and 7.63, with an *o*-coupling (*J* = 9.4 Hz), each with one integrated proton. A pair of doublets, each with coupling constant 9.4 Hz at δ_H6.24 and 7.63 in the ^{1}HNMR spectrum was typical of H-3 and H-4 of the coumarinnucleus and another pair of doublets, each with coupling constant 8.6 Hz at δ_H7.36 and 6.85 was assigned to H-5 and H-6, respectively. The ^{1}H, ^{1}H-COSY analysis of **(1)** led to the four substructures indicated by boldfaced lines in (Figure1) which were supported by HMBCs (Figure1). The COSY correlations (Figure 1) between H-3 (δ_H6.24)/ H-4 (δ_H 7.63), H-6 (δ_H6.85)/H-5 (δ_H7.36) and H-6 (δ_H6.85)/H-8 (δ_H 6.82) and HMBC correlations (Figure1)observed from H-5 to C-7 (δ_C162.07) and C-8a (δ_C155.87), from H-6 to C-8 (δ_C101.59) and C-4a (δ_C 112.48), from H-8 to C-2, C-6, C-7, C-8a and C-4a, from H-4 to C-3 (δ_C113.02), C-2 (δ_C161.24) and C-8a (δ_C155.87)proved the presence of coumarin nucleus (chromen-2-one moiety). The COSY correlations (Figure1)between H-5′ ($\delta_H\delta$ 1.46, δ_H1.65)/H-4′ (δ_H2.17, δ_H2.37) and H-1′ (δ_H4.62)/H-2′ (δ_H5.53) and HMBC correlations (Figure 1) of H-7' -Me (δ_H 1.21 and δ_H1.17) with C-6′ (δ_C77.98) and C-7′ (δ_C73.05), H-3' -Me (δ_H 1.78) with C-2′ , C-3′ and C-4′ , H-2′ with C-3' -Me (δ_C16.75) and C-3′ (δ_C142.14), H-1′ (δ_H4.62) with C-2′ , C-3′ and H-5′ with C-3′ and C-4′ suggested the presence of dimethyl oct-2-ene moiety. The two moieties could be logically connected by an oxygen atom because of the presence of HMBC correlation (Figure1)between the H-1′ (δ_H4.62) and C-7 (δ_C162.07) that occurred in the lower magnetic field. From this it was presumed that this carbon was attached to oxygen and the proposed molecular formula ($C_{19}H_{22}O_3$) required two hydroxyl groups. Therefore, these two hydroxyl groups could be connected to the downfield chemical shift carbons at C-6′ (δ_C77.98) and C-7′ (δ_C 73.05). Hence, compound **(1)** was identified as (*E*)-7-((6, 7-dihydroxy-3, 7-dimethyl oct-2-en-1-yl) oxy)-*2H*- chromen-2-one (Figure2).

Structural Elucidation of Coumarin Compound (2)

Compound **(2)** was also isolated as colourless oil, and assigned as the molecular formula of $C_{19}H_{22}O_4$ on the basis of FAB-MS spectral data

$[M+H]^+$, *m/z* at 315 which indicated the molecular mass (*m/z* 314).The FT IR absorption bands at 3078, 1732, 1456, 1349,1277 and 1124 cm^{-1} confirmed the presence of the aromatic C-H, an ester carbonyl group, a conjugated double bond (C=C), gem dimethyl group and ether group, respectively. The unsaturated degree of 9 was calculated from the molecular formula, $C_{19}H_{22}O_4$. The ^{1}HNMR and ^{13}CNMR spectral data of compound **(2)**(Table 1) were very similar to those of compound **(1)**, except for the appearance of an epoxide ring instead of two hydroxyl groups of compound **(1).** The ^{1}HNMR and ^{13}CNMR data for the coumarin nucleus of compound **(2)**were almost identical with those of compound **(1).**In the side chain, two hydroxyl groups in compound **(1)** were replaced by an oxymethine at δ_H2.75 (1H, t, 6.2, 12.5 Hz), typical of an epoxide. The C-6' methine signal was also shifted to higher field at δ_H2.75 indicating the characteristics of an epoxide ring. Selective C-H long range correlations provided the carbon framework of **(2)** as shown in (Figure 1).The^{1}HNMR spectrum (Table 1) exhibited three aliphatic methyl signals [δ_H 1.77 (3H, s); 1.26 (3H, s); 1.26 (3H, s)], an olefinic signal [δ_H 5.53 (1H, t, 6.5 Hz)], three methylene signals [δ_H 4.68 (2H, d, 6.5 Hz); 2.23, 2.24 (2H, m), 1.68, 1.69 (2H, m)]. In addition, there were five sp^2 signals, including double doublet signal of δ_H 6.92 with 7.52 [an *o*-coupling (*J* = 8.7 Hz)] and that ofδ_H 6.92 with 6.89 [a*m*-coupling(*J* = 2.3 Hz)], as well as two doublet signals at δ_H 6.23 and 7.87 with an *o*-coupling (*J* = 9.5 Hz), each with one integrated proton. ^{13}CNMR spectrum (Table 1) showed 19 carbon signals, including one ester carbonyl (δ_C163.40), five quaternary carbons, seven methine carbons, three methylene carbons and three methyl carbons. The ^{1}HNMR and ^{13}CNMR assignments of **(2)** were confirmed by analysis of the 2D NMR spectra (COSY, HSQC and HMBC). The ^{1}H, ^{1}H-COSY analysis of **(2)** led to the four substructures indicated by boldfaced lines in (Figure1).The COSY spectrum of **(2)** showed the connection of H-3↔H-4, H-5↔H-6↔H-8, H-4'↔H-5'↔H-6' and H-1'↔H-2' (Figure1)**.** The HMBC spectrum revealed that H-3 correlated with C-2; H-4 with C-2, C-3and C-8a; H-5 with C-7 and C-8a, H-6 with C-4a and C-8; H-8 with C-2, C-6 and C-4a; H-1' with C-7; H-5' with C-3' and C-7'; H-7' -Me with C-5', C-6' and C-7'; H-3' -Me with C-2' and C-3' ; H-2' with C-3' , C-4' which supported the structure of **(2)** (Figure1) and identified as (*E*)-7-((5-(3, 3-dimethyloxiran -2-yl) - 3-methylpent-2-en-1-yl) oxy)-*2H*-chromen- 2-one (Figure 2).

Structural Elucidation of Coumarin Compound (3)

Compound **(3),** colourless oil,$C_{21}H_{28}O_5$was identified as (*E*)-7-((7-ethoxy-6-hydroxy-3,7-dimethyloct-2-en-1-yl)oxy)-*2H*-chromen-2-one (Figure2) by the following spectroscopic data. The result of FAB-MS spectrum gave a molecular formula of $C_{21}H_{28}O_5[M+H]^+$, *m/z* at 361 which indicated the molecular mass (*m/z* 360).The unsaturated degree of 8 was calculated from the molecular formula. The FT IR absorption bands at 3471, 3082, 1733, 1613, 1507, 1463, 1350, 1278 and 1071 cm^{-1} confirmed the presence of a hydroxyl group, aromatic C-H, an ester carbonyl group, conjugated double bonds (C=C), gem dimethyl group and ether groups respectively. The IR spectrum was informative with the presence of δ lactone carbonyl functionality at 1733 cm^{-1}.The ^{1}HNMR spectrum of compound **(3)**(Table 1) was very similar to those of compound **(1)**, except that a hydroxyl group at C-7 was replaced by an ethoxy group. The ^{1}HNMR spectrum (Table 1) exhibited four aliphatic methyl signals [$\square_H$1.78 (3H, s); 1.09 (3H, s); 1.12 (3H, s); 1.15 (3H, t)], an olefinic signal [$\square_H$ 5.52 (1H, t, 6.5 Hz)], three methylene signals[$\square_H$ 4.62 (2H, d, 6.5 Hz);2.41, 2.16 (2H, m),1.55, 1.47 (2H, m)]. In addition, there were five sp^2 signals, including double doublet signal of $\square_H$ 6.85 with 7.36 [an *o*-coupling (*J* = 8.5 Hz)] and that of $\square_H$ 6.85 with 6.82 [a*m*-coupling (*J* = 2.4 Hz)], as well as two doublet signals at$\square_H$ 6.24 and 7.63, with an *o*-coupling (*J* = 9.4 Hz), each with one integrated proton.^{13}CNMR spectrum of compound **(3)**(Table 1) shows 21 carbon signals, including one ester carbonyl ($\square_C$161.24), five quaternary carbons, seven methine carbons, four methylene carbons and four methyl carbons.The ^{1}H, ^{1}H-COSY analysis of **(3)** led to the five substructures indicated by boldfaced lines in (Figure 1).The COSY correlations (Figure 1)between H-3 ($\square_H$6.24)/H-4 ($\square_H$7.63), H-6 ($\square_H$ 6.85)/H-5 ($\square_H$ 7.36) and H-6 ($\square_H$ 6.85)/H-8 ($\square_H$ 6.82) and HMBC correlations (Figure 1)observed from H-5 to C-7 ($\square_C$ 162.16) and C-8a ($\square_C$155.89), from H-6 to C-8 ($\square_C$101.61) and C-4a ($\square_C$112.44), from H-8 to C-2, C-6, C-7, C-8a and C-4a, from H-4 to C-3 ($\square_C$112.99), C-2 ($\square_C$161.24) and C-8a proved the presence of coumarinnucleus (chromen-2-one moiety). The COSY correlations (Figure 1)between H-5′ ($\square_H$1.55, δ 1.47)/H-4′ ($\square_H$2.41,$\square_H$2.16) and H-1′ ($\square_H$4.62)/H-2′ ($\square_H$ 5.52) and HMBC

correlations between H-7' -Me ($\square_H$1.09 and $\square_H$1.12)/C-6′ ($\square_C$76.40)/C-7′ ($\square_C$78.0), H-3' -Me ($\square_C$1.78)/C-2′ /C-3′ and C-4′ , H-2′ /C-3' -Me ($\square_C$16.86)/C-3′ , H-1′ ($\square_H$ 4.62)/C-2′ /C-3′ and H-5′ /C-3′ /C-4′ suggested the presence of dimethyl oct-2-ene moiety. The two moieties could be logically connected by an oxygen atom because of the presence of HMBC correlation between the H-1′ ($\square_H$ 4.62)/C-7 ($\square_C$162.16) that occurred in the lower magnetic field. Based on HMBC data (Figure 1),there were two methyl proton signals that were substituted on the quaternary carbon (C-7') and showed HMBC correlations to C-6' and C-7' . Moreover, the COSY correlation between CH_2 (7' -OEt) ($\square_H$3.42)/CH_3(7' -OEt) ($\square_H$1.15) gave an ethyl group which could be connected to C 7' by an oxygen atom due to the presence of down field chemical shift carbon atoms CH_2 (7' -OEt) (δ_C 56.43) and C 7' (δ_C 78). It was proven by HMBC correlation (Figure 1) of sp^3 methylene protons at [δ_H3.42, CH_2 (7' -OEt)] with C-7' (δ_C 78).

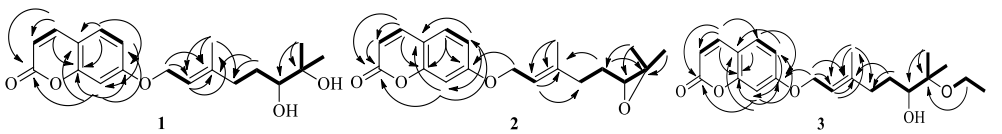

Figure 1 Key (—) COSY and ( ) HMBC correlation of (1-3)

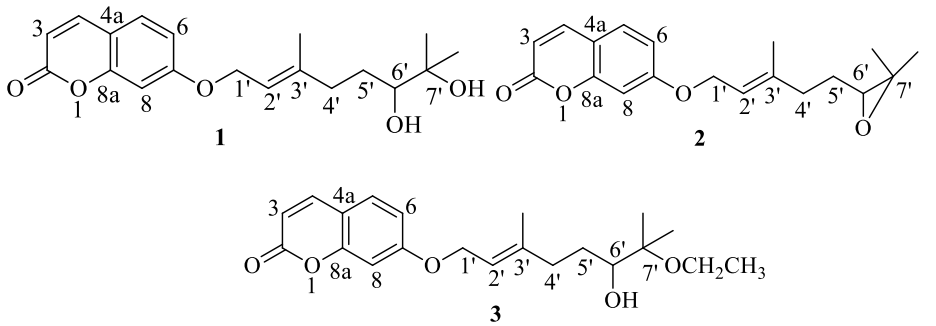

Figure 2: Structures of compounds (1-3)

Table 1: ^{1}H NMR (600 Hz) and ^{13}C-NMR (150 MHz) Data for Compounds (1), (2) and (3)

No.	(1) (chloroform-d)		(2) (chloroform-d)		(3) (chloroform-d)	
	^{13}CNMR δ_C, (ppm)	^{1}HNMR δ_H, (ppm)	^{13}CNMR δ_C, (ppm)	^{1}HNMR δ_H, (ppm)	^{13}CNMR δ_C, (ppm)	^{1}HNMR δ_H, (ppm)
2	161.24	-	163.40	-	161.24	-
3	113.02	6.24, d, 9.4 Hz	113.27	6.23, d, 9.5 Hz	112.99	6.24, d, 9.4 Hz
4	143.4	7.63, d, 9.4 Hz	145.78	7.87, d, 9.5 Hz	143.39	7.63, d, 9.4 Hz
4a	112.48	-	113.97	-	112.44	-
5	128.68	7.36, d, 8.6 Hz	130.39	7.52, d, 8.7 Hz	128.66	7.36, d, 8.5 Hz
6	113.26	6.85, d, 2.3, 8.6 Hz	114.48	6.92, d, 2.3,8.7 Hz	113.22	6.85, d, 2.4, 8.5 Hz
7	162.07	-	163.81	-	162.16	-
8	101.59	6.82, d, 2.3 Hz	102.51	6.89, d, 2.3 Hz	101.61	6.82, d, 2.4 Hz
8a	155.87	-	157.11	-	155.89	-
1'	65.40	4.62, d, 6.5 Hz	66.46	4.68, d, 6.5 Hz	65.49	4.62, d, 6.5 Hz
2'	118.94	5.53, t, 6.5 Hz	120.99	5.53, t, 6.5Hz	118.66	5.52,t, 6.5Hz
3'	142.14	-	141.52	-	142.48	-
4'	36.53	2.37, m 2.17, m	37.13	2.23, 2.24, m	36.64	2.41, m 2.16, m
5'	29.43	1.65, m 1.46, m	28.05	1.68, 1.69, m	29.20	1.55, m 1.47, m
6'	77.98	3.35, dd, 2.0,10.4 Hz	65.55	2.75, t, 6.2, 12.5Hz	76.40	3.40, dd, 2.0, 10.4 Hz
7'	73.05	-	60.25	-	78.0	-
3' -Me	16.75	1.78, s	16.66	1.77, s	16.86	1.78, s
7' -Me	23.28	1.17, s	18.86	1.26, s	19.34	1.09, s
7' -Me	26.53	1.21, s	24.95	1.26, s	21.47	1.12, s
CH_2 (7' -OEt)	-	-	-	-	56.43	3.42, t
CH_3 (7' -OEt)	-	-	-	-	16.10	1.15, t, 7.0, 14 Hz

C=C

Structural Elucidation of Alkaloid Compound (4)

Compound (4): Skimmianine appeared as white crystals withm.p. 177-179°C**.**The EI MS spectrum shows molecular ion at odd number *m/z* 259, corresponds to molecular formula $C_{14}H_{13}NO_4$.FT IR spectrum exhibited the presence of the C-H aromatic and C-H aliphatic at 3042 and 2940 cm^{-1}. Peaks at 1614, 1577, 1507, 1489 and 1456 cm^{-1} appeared due to C=C and C=N ring skeletal stretching vibrations, while C-O-C bond was represented by peaks at 1270 and 1239 cm^{-1}. The strong singlet ^{1}H NMR signals (Table 2) at δ_H4.49, 4.02 and 3.97 were typical of methoxy groups. The rest of the signals occurred in the aromatic region. A pair of doublet at δ_H8.06 and δ_H7.37 with coupling constant (*J*=9.4 Hz) was assigned to ortho coupling protons at C-5 and C-6. Another pair of doublet at δ_H7.76 and δ_H7.33 (*J*=2.82 Hz) was typical of adjacent of furan protons (H-2' and H-3'). ^{13}C NMR spectrum showed the presence of fourteen carbons in which three of them were methyl carbons resonated at δ_C60.08, 57.25and 61.72 ppm. Other signals included four methine and seven quaternary carbon absorptions. The assignment of ^{1}H and ^{13}CNMR data was further substantiated by HSQC, COSY and HMBC spectral data (Table 2). The ^{1}H, ^{1}H-COSY analysis of **(4)** gave rise to the two substructures indicated by boldfaced lines in (Figure 3) which were supported by HMBCs (Table 2 and Figure 3).The complete assignment and correlations are summarized in (Table 2). Based on these data, the structure of the compound (4) was identified as 4,7,8-trimethoxyfuro [2,3-b] quinoline or skimmianine (Figure 4).

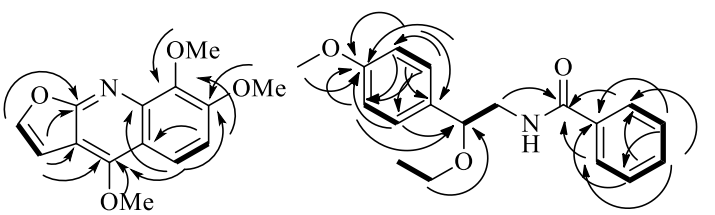

Figure 3. Key (—) COSY and (↷) HMBC correlation of (4) and (5)

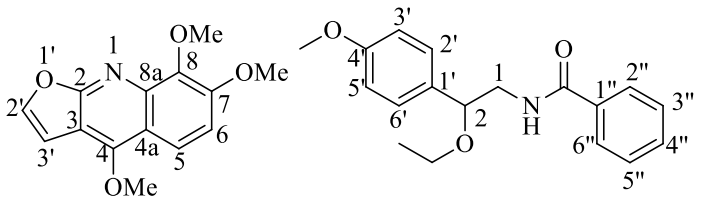

Figure 4: Structures of compounds (4) and (5)

Table 2: ^{1}H NMR (600 Hz) and ^{13}C NMR (150 MHz) Data for the Isolated Compound (4)

C position	^{13}CNMR δ_C, (ppm)	^{1}HNMR δ_H, (ppm)	COSY correlation	HSQC correlation	HMBC correlation
2	166.09	-	-	-	H-2' , H-3'
3	103.40	-	-	-	H-3'
4	159.29	-	-	-	H-3' ,4-Me, H-5
4a	115.93	-	-	-	H-6
5	119.65	8.06,d 9.4 Hz	H-6	H-5	-
6	113.55	7.37,d,9.4 Hz	H-5	H-6	-
7	153.90	-	-	-	H-5,7-OMe
8	142.70	-	-	-	H-6,8-OMe
8a	142.07	-	-	-	H-5
2'	144.47	7.76,d,2.82 Hz	H-3'	H-2'	-
3'	106.30	7.33, d, 2.82 Hz	H-2'	H-3'	-
4-OMe	60.08	4.49, s	-	H-4-OMe	-
7-OMe	57.25	4.02, s	-	H-7-OMe	-
8-OMe	61.72	3.97, s	-	H-8-OMe	-

Structural Elucidation of Alkaloid Compound (5)

Compound (**5)** appeared as colourless oily form, had molecular formula $C_{18}H_{21}NO_3$ by FAB-MS because of the $[M+Na]^+$, *m/z* at 322 which indicated the molecular mass (*m/z* 299). FT IR spectrum showed the presence of N-H as sharp peak around 3316 cm^{-1}. Peak at 3063cm^{-1} revealed the aromatic C-H, whereas peaks at 2968 and 2937 cm^{-1} were due to aliphatic C-H stretching vibrations. The existence of carbonyl group conjugated to a double bond was represented by the strong peak at 1652 cm^{-1}. In addition, peaks at 1611 and 1509cm^{-1} were attributed of C=C and aromatic ring system.

Weaker band at 1294 cm^{-1}resulted from interaction between N-H bending and C-N stretching. The presence of ether group was shown by peaks at 1246 and 1095 cm^{-1}. The band appeared at 711 cm^{-1} was due to the absorption of N-H wagging. ^{1}HNMR spectrum exhibited that a singlet atδ_H 3.78, integrated for three protons was attributed a methoxy group (H-4' -OMe). Mono-substituted aromatic protons were represented by H-2'' and H-6'' which appear as doublet of doublet at δ_H7.75 (*J*=7.4,*J*=1.3 Hz), while H-3'' and H-5'' resonate as triplet at δ_H7.44 (*J*=7.4, *J*=1.44 Hz) and H-4'' exhibits a doublet of doublet at δ_H7.52(*J* = 7.4,*J* = 1.44 Hz). Another pair of doublet (*J*=8.64Hz) were given by H-3' and H-5' (δ_H 6.92) which ortho-coupled to H-2' and H-6' (δ_H 7.29). The inequivalent methylene protons at C-1 appeared as two doublet of doublet at δ_H3.52 (*dd, J*=13.59, *J*=7.95 Hz) and δ_H 3.54(*dd, J*=13.59,*J*=7.95 Hz). The neighbouring methine proton at C-2 which is coupled to protons (H-1) resonates to give another doublet of doublet atδ_H 4.51 (*dd, J*= 8.28, *J*=3.0 Hz). Another inequivalent methylene protons at CH_2 (2-OEt) appeared as multiplets at δ_H 3.42 and δ_H 3.36. The neighbouring methyl protons at CH_3 (2-OEt) are coupled to inequivalent methylene protons CH_2 (2-OEt) to give another doublet of doublet at δ_H1.16 (*dd, J*= 7.02, *J*=14.04 Hz). All of the coupling interactions between protons were confirmed by COSY spectrum such as the cross peaks which were due to the interaction between H-1 and H-2, between inequivalent methylene protons at CH_2 (2-OEt) and neighbouring methyl protons at CH_3 (2-OEt) and between appropriate aromatic protons (Table 3 and Figure 3). The ^{1}H, ^{1}H-COSY analysis of **(5)** produced the five substructures indicated by boldfaced lines in (Figure 3) which were supported by HMBCs (Table 3 and Figure 3).^{13}C NMR spectrum gave absorption peaks representing mostly aromatic and sp^3 carbons. The presence of carbonyl group was shown by peak at δ_C 170.33. The assignment of ^{1}H and ^{13}C NMR data was further substantiated by HSQC and HMBC spectrum, which the complete assignment and correlations are summarized in (Table 3). Based on these spectral data the compound **(5)** was identified as *N*-(2-ethoxy-2-(4-methoxyphenyl) ethyl) benzamide(Figure 4).

Table 3:^{1}H NMR (600 Hz) and ^{13}C-NMR (150 MHz) Data of the Isolated compound (5)

C position	^{13}CNMR δ_C, (ppm)	^{1}HNMR δ_H, (ppm)	COSY correlation	HSQC correlation	HMBC correlation
1	47.46	3.54, 3.52, dd, 13.59, 7.95 Hz	H 2	H 1	-
2	81.05	4.51,dd, 8.28, 3.0 Hz	H 1	H 2	H 5' , H 6' ,CH_2 (2-OEt)
1'	133.50	-	-	-	H 3'
2' , 6'	129.07	7.29, d, 8.64 Hz	H 3' , H 5'	H 2' , H 6'	H 2' , H 6'
3' , 5'	114.94	6.92, d, 8.64 Hz	H 2' , H 6'	H 3' , H 5'	H 2' ,H 3' , H 5'
4'	161.03	-	-	-	H 2' , H 6' , H 3' , H 5' , H 4' -OMe
1' '	135.80	-	-	-	H 3' ' , H 5' '
2 ' ' , 6' '	128.23	7.75, dd, 7.4, 1.3 Hz	H 3' ' , H 5' ' H 4' '	H 2 ' ' , H 6' '	H 4' ' H 2 ' ' , H 6' '
3' ' , 5' '	129.53	7.44, t, 7.4, 1.3 Hz	H 2 ' ' , H 6' ' H 4' '	H 3' ' , H 5' '	H 3' ' , H 5' ' H 4' '
4' '	132.61	7.52, dd, 7.4, 1.44 Hz	H 3' ' , H 5' ' H 2' ' , H 6' '	H 4' '	-
4' -OMe	55.71	3.78, s	-	H 4' -OMe	-
-CONH	170.33	-	-	-	H 1, H 2 ' ' , H 6' '
CH_2(2-OEt)	65.09	3.42, 3.36, m	CH_3(2-OEt)	CH_2(2-OEt)	-
CH_3(2-OEt)	15.59	1.16, dd, 7.02,14.04Hz	CH_2(2-OEt)	CH_3(2-OEt)	-

The Antioxidant Activity and Cytotoxic Activity of the Isolated Compounds (1-5)

The antioxidant activity and cytotoxic activity of the isolated compounds are shown in Tables 4 and 5. Compounds (**1) – (5)** were tested for antioxidant activity by using DPPH assay. According to these data, DPPH radical scavenging activities of isolated pure compounds**(1), (2), (3)** (EC_{50}>100 μM) exhibited lower activity than ascrobic acid(EC_{50} 27.5 μM). However, the pure compounds **(4)** and **(5)** did not show any DPPH radical scavenging activity. In addition, compounds (**1) – (5)**were further evaluated for their *in vitro* cytotoxic activities against Hela cell lines by using cell counting kit 8. In accordance with these data, compound (**4)**displayed low cytotoxicactivity against Hela cell lines with IC_{50} values of (55 μM) while compounds (**1)** and (**5)** displayed very weak cytotoxic activity with IC_{50} value > 100 μM.

Table 4: Antioxidant Activity (EC_{50}) of Ascorbic acid and Compounds (1-5) Isolated from *Aeglemarmelos*

Compounds	EC_{50}(μM)
Ascorbic acid	27.5
1	>100
2	>100
3	>100
4	ND
5	ND

ND = Not detected

Table 5:The Cytotoxic Activity of Isolated Compounds (1-5) from *Aeglemarmelos*

Compounds	Cytotoxic Activity IC_{50} (μM)
1	> 100
2	-
3	-
4	55
5	> 100

Conclusion

In this research work, one of Myanmar medicinal plants, stem bark of *Aegle marmelos* was used for isolation and structural elucidation of secondary metabolites and screening of the antioxidant and cytotoxic activities. The structures of three coumarin compounds (**1**), **(2)**, **(3)** and two alkaloid compounds **(4)** and **(5)** could be assigned by advanced spectroscopic techniques.Moreover, evaluation of antioxidant activities and cytotoxic activities of the pure compounds were also performed. According to these data, it was found that DPPH radical scavenging activities of isolated pure compounds(**1**), **(2)**, **(3)**(EC_{50}>100 μM) exhibited lower activity than ascrobic acid(EC_{50} 27.5 μM). The compound **(4)**(IC_{50} 55 μM) showed low cytotoxic activity against Hela cell lines while compounds **(1)** and **(5)** indicated very weak cytotoxic activity with IC_{50} value > 100 μM.

Acknowledgements

We would like to express our thanks to Rector and Pro-rectors of University for the Development of the National Races of the Union, Sagaingfor their kind permission to submit this paper. We are greatly thankful to the Myanmar Academy of Arts and Science for allowing to present this paper.

References

Ishiyama, M., Shiga, M., Sasamoto, K., Mizoguchi, M. and He, P. (1993).“A New Sulfonated Tetrazolium Salt that Produces a Highly Water-soluble Formazan Dye.”*Chem. Pharm. Bull*. vol. 41, pp. 1118-1122.

Khare, C.P. (Ed.). (2007). *Indian Medicinal Plants: An Illustrated Dictionary*. New Delhi: Springer, LLC.p. 21.

Kumar, V., Ahmed, D., Verma, A., Anwar, F., Ali, M. and Mujeeb, M. (2013).“Umbelliferone β-D-galactopyranoside from *Aeglemarmelos* (L.)Corr.An Ethnomedicinal Plant with Antidiabetic, Antihyperlipidemic and Antioxidative activity.”*BMC Complementary and Alternative Medicine*, vol. 13, p. 273

Lambole, V. B., Murti, K., Kumar, U., Sandipkumar, P. B. and Gajera, V. (2010).“Phytopharmacological Properties of *Aegle Marmelos* as a Potential Medicinal Tree.”*International Journal of Pharmaceutical Sciences Review*, vol. 5 (2), p. 67.

Mazid, M., Khan, T. A. and Mohammad, F. (2011).“Role of Secondary Metabolites in Defense Mechanisms of Plants.”*Biology and Medicine*, vol.3 (2), pp. 232-249.

Silverstein, R. M.,Webster, F. X. and Kiemle, D. J. (2005). *Spectrometric Identification of Organic Compound*. New York:7th ed. John Wiley & Sons, Inc. U.S.A.

Verma, S. C., Rani, R., Vashishth, E., Basu, K., Pant, P. and Padhi, M. M. (2013).**“**Simple, Rapid and Precise Method for Quality Assessment of Different Parts of *Aeglemarmelos* L. Used in Indian System of Medicine.”*Research J. Pharmacology and Phytochemistry*, vol. 5(5), pp. 236-243**.**

Yamaguchi, T., Takamura, H., Matoba, T. and Terao, J. (1998).“HPLC Method for Evaluation of the Free Radical-scavenging Activity of Foods by Using 1, 1-Diphenyl-2-Picrylhydrazyl.” *Biosci., Biotechnol., Biochem*., vol. 62, pp. 1201-1204.

PURIFICATION, IMMOBILIZATION AND APPLICATION OF UREASE ENZYME FROM PIGEONPEA SEEDS (*Cajanus cajan* L.)

Hnin Yi San*

Abstract

Urease (E.C 3.5.1.5) was isolated and purified from dehusked pigeonpea seeds (*Cajanus cajan* L.). The purification method involved ammonium sulphate precipitation, Sephacryl S-200 gel filtration and DEAE Sepharose ion-exchange chromatography. The specific activity, the relative purity of the enzyme urease was increased by 398 fold over that of crude extract. The purified urease enzyme was found to have the specific activity of 306.67 μmol $min^{-1}mg^{-1}$ of protein. The purity of the enzyme was confirmed by non SDS-PAGE as single band. The molecular weight for purified urease was found to be 478 kDa (kilodalton). The immobilization of the purified urease was carried out by gel entrapment technique using sodium alginate. Determination of urea content in dried skate fish before and after removal by pigeonpea urease was carried out by using immobilized urease. After 66 h, 75.94 % of urea was removed from dried skate fish.

Keywords: Urease, Pigeonpea, non SDS-PAGE, immobilization, sodium alginate, gel entrapment technique

Introduction

Urease (urea amidohydrolase, EC 3.5.1.5) is a nickel-containing enzyme that catalyzes the hydrolysis of urea to yield ammonia and carbamate, the latter compound decomposes spontaneously to generate a second molecule of ammonia and carbon dioxide (Andrew *et al.*, 1986; Hausinger, 1993; Mobely*et al.,* 1995; Park and Hausinger, 1995).

$$H_2N–CO–NH_2 + H_2O \xrightarrow{\text{Urease}} NH_3 + NH_2–COOH \xrightarrow{\text{Spontaneous}} 2NH_3 + CO_2$$

Urease has many industrial applications, e.g., in diagnostic kits for measuring urea, in alcoholic beverages as a urea reducing agent (Fujinawa and Dela, 1990; Fumuyiwa and Ouch, 1991), and in biosensors of haemodialysis systems for determining blood urea (Smith *et al.,* 1993). Urease is also

* Dr, Lecturer, Department of Chemistry, Banmaw University

important in medical field because it may help human pathogens survive in the stomach lining and cause peptic ulcers.

Pigeonpea(Figure 1) is widely cultivated in Upper Myanmar. Thus, urease can be obtained from a rather inexpensive and readily available source like Pigeonpea. In this research work, urease was isolated and purified from Pigeonpea seeds collected from Natogyi Township, Mandalay Region.

Botanical description of Pigeonpea as follows.

Family	-	Fabaceae
Genus	-	*Cajanus*
Species	-	*cajan*
Scientific Name	-	*Cajanuscajan* L.
English Name	-	Pigeonpea
Myanmar Name	-	Pe-sin-ngone

(a) (b) (c)

Figure 1: (a) Flower, (b) pods and (c) seeds of Pigeonpea

Materials and Methods

Common laboratory tools were used throughout the experiment at the Biochemistry Research Division, Department of Medical Research (Lower Myanmar). The advanced instruments which are used in the characterization of samples and purification of pure compound are shown below.

1. Dialysis bag, digital balance (A-200S, Sartorius Service Hot Lines, Japan)
2. Lyophilizer (Freeze-dryer machine) (J.T/C, 4451F, LABCONCO,–150ºC)

3. Refrigerated centrifuge (Model CD-70 SR, maximum speed 5,000 rpm, Tomy Seiko Co., Ltd, Tokyo, Japan)
4. UV visible spectrophotometer (Bausch and Lomb Spectronic – 21)
5. Perista mini-pump (SJ-1220)
6. Biomini UV-monitor (AC-5200 L), mini-recorder (SJ-3462)
7. Mini-collector (SJ-1400NC) (Atto Corporation, Tokyo, Japan)
8. Fraction collector (SF-200A, Toyo Co., Ltd., Japan)

Sample Collection

Pigeonpea seeds were collected from Natogyi Township, Mandalay Region.

Dehusked pigeonpea seeds were ground into fine powder by a blender. Then the raw materials were stored under 4ºC in the well-stoppered glass bottle and used throughout the experiment.

Extraction of Urease from Dehusked Pigeonpea Seeds

Dehusked pigeonpea seeds were ground into fine powder by a blender. Pigeonpea seed powders (227 g) were thoroughly mixed with 800mL of phosphate buffer of pH 7.0 containing 1mM EDTA and 1mM β-mercaptoethanol and left for overnight at 4ºC. The mixture was filtered through two layers of muslin and the filtrate was collected.

Solid ammonium sulphate (50.00 g) was added slowly to the resulting filtrate to make 20% saturation, stirred slowly for 20 min and centrifuged at 3200 rpm for 30 min. The pellet (0-20 portion) was discarded and the supernatant fraction brought to 60% saturation by slow addition of 101.40 g of solid ammonium sulphate. Precipitated protein urease was sedimented as above. The protein suspension was transferred to a dialysis tubing and dialyzed against in a 10-fold excess of the same buffer with three changes after allowing 2h for equilibration.

After removal of ammonium sulphate by dialysis, the dialyzed sample was concentrated with acetone and then the concentrated sample was kept in a lyophilizer for 20 min. Then it was centrifuged at 3500 rpm for 10 min. After that, the enzyme precipitate was collected yield %. Urease activity was

determined by Nessler's method at 480 nm and protein content was determined using Bovine Serum Albumin from Sigma at 550 nm.

Purification of Urease Enzyme by gel filtration Chromatography

Gel filtration was carried out in a column (2 x 39 cm) packed with pre-swollen Sephacryl S-200 using 0.1M phosphate buffer (pH 7.0) and equilibrated with the same buffer (500 mL).

Crude urease (1.0 g) was dissolved in 2 mL of pH 7.0 phosphate buffer. This solution was applied to a Sephacryl S-200 gel filtration column (2 x 39 cm) previously equilibrated with the same buffer. The flow rate was adjusted to 12 mL hr^{-1} by a mini-pump and 1.5 mL fractions were collected per tube using a fraction collector. After collection, the protein content of each tube was checked by measuring the absorbance at 280 nm wavelength using a UV-visible spectrophotometer.Each tube was also measured for urease activity in the same manner.The fractions with highest urease activities were pooled and concentrated with acetone (1:9 ratio).

Purification by Ion Exchange Chromatography

The ion exchange chromatography was packed in a column (1 × 25 cm) with DEAE Sepharose using 0.1M sodium phosphate buffer (pH 7.0) and equilibrated with the same buffer.

The concentrated urease fraction obtained by Sephacryl S-200 gel filtration column was applied to a DEAE Sepharose. The flow rate was adjusted to 12 mL/h using a mini-pump and 1.5mL fraction was collected per tube using a mini-collector. During collection, the protein content of each tube was continuously monitored at 280 nm wavelength by a bio-mini UV-monitor. After collection, the protein content of each tube was confirmed by measuring at 280 nm wavelength using a UV-visible spectrophotometer.

The active protein fractions of fraction numbers 10 to 16 and 31 to42 were pooled. The pooled fraction of highest urease activity was concentrated with acetone (1:9 ratio) and kept in a lyophilzer for 10 min. Then it was centrifuged at 5000 rpm for 5 min, and the enzyme precipitate was taken out.

Electrophoresis and molecular weight determination

Electrophoresis was begun when the polymerized gel slab was placed in the electrophoresis apparatus containing electrophoresis buffer (pH 8.3). The 20 µL sample contained 100 µg of protein. Both sample (20 µL) containing 100 µg of protein and standard molecular weight marker proteins (20 µL) containing Urease-tetramer, Urease dimer, Albumin, bovine dimer and Albumin, chicken egg were loaded in the sample well and standard well respectively.

Initially, the current was maintained at 15 mA (100 V) for 15 min until the samples had travelled through the stacking gel. Then the current was increased to 30 mA (200 V) until the bromophenol blue dye had reached near the bottom of the gel slab. It was required for 1.5 h.

At the end of running, the gel was washed with distilled water for five times, and fixed with fixing solution. Then the gel was placed in Petri dish with staining solution for 2 h, and subsequently destained with destaining solution until a clear gel was obtained.

Immobilization of Urease Enzyme by Gel Entrapment

Sodium alginate powder (3.0 g) was added to the distilled water (100 mL) in a 500 mL beaker and stirred for 30 min. After sodium alginate was completely dissolved, the solution was left undisturbed for 30 min to eliminate air bubbles that could later be entrapped and cause the beads to float. It was boiled until sodium alginate had hydrated and left to cool. Next, 1 mL urease enzyme solution was mixed with 10 mL of 3% sodium alginate solution. The enzyme alginate mixture was obtained.

With a 5 mL disposable syringe, enzyme alginate mixture was dipped into 1% calcium chloride solution from a height of approximately 10 cm. The beads formed were hardened in calcium chloride solution for 30 min and then washed with distilled water before use. The alginate beads were stored at 4°C in 0.1 M phosphate buffer (pH 7.0)

Comparison of the Activities of Soluble Urease and Immobilized Urease

The procedure for urease activity determination was the same as mentioned above except that the final purified free enzyme solution (0.1 mL) and 13 immobilized enzyme beads (0.1 mL) were used in each test tube.

For comparative study of urease activities between soluble and immobilized urease enzyme, the absorbance of the orange brown colour of each reaction mixture was measured at 480 nm.

Determination of Optimum pH for Soluble and Immobilized Urease Catalyzed Reaction of Urea

For soluble urease, an aliquot (0.1 mL) of phosphate buffer (pH 7) and 0.1 mL of 0.5 M urea solution were brought to incubate at 37°C for 5 min. The reaction was started by adding 0.1 mL of final purified enzyme solution. After 5 min, 0.1 mL of 0.5 M hydrochloric acid was added to terminate the reaction. After that, 4 ml of distilled water and 0.1 mL of Nessler's reagent were added. The amount of ammonia liberated was measured at 480 nm in a UV-visible spectrophotometer against the reagent blank.

For immobilized urease, the whole of the above procedure was carried out using 13 beads (0.1 mL) of immobilized urease in place of 0.1 mL of enzyme solution.For blank solution, 0.1 mL of distilled water was used in place of 0.1 mL of enzyme solution.Similarly phosphate buffer solution of different pH values (5.0, 5.5, 6.0, 6.5, 7.5 and 8.0) were employed in the above experiment instead of phosphate buffer (pH 7.0) for each experimental run. The absorbance values were measured at 480 nm and the optimum pH was found from the enzyme activity *vs* pH plot.

Application of Immobilized Urease for Determination of Urea in Dried Skate Fish

Immobilized urease was used for determination of urea in dried skate fish (Figure 2 a). Dried skate flesh (Figure 2 b) (without bone) (20 g) was ground using 20 mL of distilled water and the liquid was squeezed and this process was repeated for another 2 times. Then residual precipitate was

ground with 10 mL of distilled water and the liquid was squeezed and process was repeated for another 3 times. The total liquid was centrifuged at 3200 rpm for 30 min and the clear supernatant fluid was made up to 100 mL with distilled water in a volumetric flask to obtain the sample solution.

(a) (b)

Figure 2: (a) Skate fish and (b) Skate flesh

Sample solution (0.1 mL) was added to a test tube and 0.1 mL of phosphate buffer (pH 7.0) were also added. After that, this mixture was incubated at 37°C for 5 min. The reaction was started by adding 13 beads of immobilized enzyme (0.1 mL of enzyme solution). After that, this mixture was incubated at 37°C for 5 min. A0.1 mL of 0.5 M HCl was added to the reaction mixture in order to terminate the reaction. After that, 4 mL of distilled water and 0.1 mL of Nessler's reagent were added. The absorbance of the orange brown colour of the reaction mixture was measured at 480 nm.

Urea content in dried skate flesh was removed by prepared urease and the remaining urea content in dried skate flesh was determined by prepared immobilized urease. Dried skate flesh (200 g) was thoroughly mixed with 10 mL of 1% of urease enzyme solution and dried in sunlight.

After 12 h, 20 g of dried skate flesh was taken out and ground using 20 mL of distilled water and urea content was determined using immobilized urease. Determinations of urea content were also carried after 18 h, 36 h, 42 h and 66 h after mixing with prepared urease and dried in sunlight.

Results and Discussion

Urease was isolated from dehusked pigeonpea seed powder by ammonium sulphate precipitation method. Ammonium sulphate precipitation method was chosen for salt fractionation because of its high solubility in water, lack of toxicity, cheapness and lack of harmful effects on enzyme activity.

Urease Purification

Urease was purified by gel filtration chromatography employing Sephacryl S-200 followed by anion exchange chromatography using DEAE-Sepharose (Figure 3).

Purification of pigeonpea urease is summarized in Table1. The enzyme was enriched 398 fold compared to its crude extract. The purified enzyme displayed a specific activity of 306.67 µmol min^{-1} mg^{-1} protein.

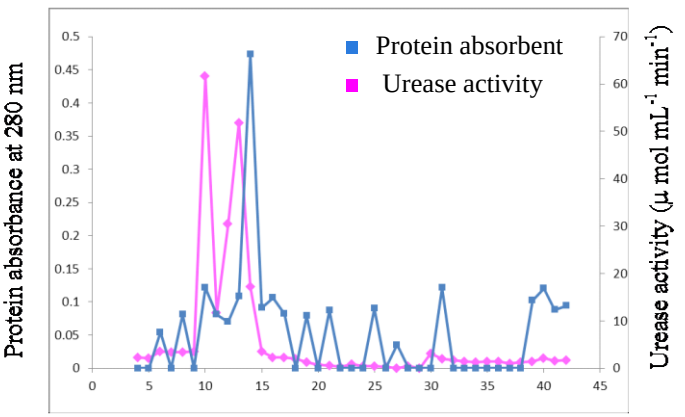

Figure 3: Chromatogram of urease activity on DEAE sepharose after sephacryl S-200 gel filtration chromatography

Table 1: Purification of Pigeonpea Urease

Purification step	Total Activity (µmol min^{-1})	Total protein (mg)	Specific activity (µmol min^{-1} mg^{-1})	Purification (fold)
Crude extract	51962.65	67195.00	0.77	1.00
20%$(NH_4)_2SO_4$ Precipitation	49504.66	5926.25	8.35	10.84
Dialyzed sample after 60 % $(NH_4)_2$ SO_4 precipitation	812.30	38.80	20.93	27.18
Sephacryl S-200	653.64	23.28	28.10	36.49
DEAE-Sepharose	263.74	0.86	306.67	398.00

Molecular Weight Determination by Non SDS-PAGE

In this study, proteins from the Pharmacia high molecular weight (HMW) calibration kit: urease tetramer (480,000), urease dimer (240,000), albumin, bovine dimer (132,000) and albumin, chicken egg (45,000) were used for molecular weight determination by non SDS-PAGE. Proteins migrated in polyacrylamide gels of the correct porosity according to protein size. Figure 4 depicts the electrophoretic examination of the urease from final purification step.

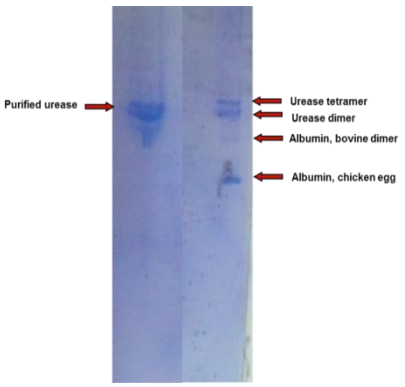

(a) (b)

Figure 4: Photograph of sodium dodecylsulphate polyacrylamide gel electrophoresis
Lane (a)Purifiedurease
Lane(b)Standardhigh molecular weight marker proteins

The purified urease enzyme showed a single band on non SDS-PAGE.

The distance migrated by each protein was used to construct a standard curve from which the molecular mass of urease can be calculated based on the mobility under the same electrophoretic condition (Table 2).

Table 2: Relationship between molecular weight of standard high protein markers (HMW) and relative mobility (R_f) values obtained from non SDS-PAGE

No.	HMW marker protein	Molecular weight (Dalton)	Log molecular weight	R_f
1.	Urease tetramer	480,000	5.681	0.486
2.	Urease dimer	240,000	5.380	0.527
3.	Albumin, bovine dimer	132,000	5.121	0.625
4.	Albumin, chicken egg	45,000	4.653	0.777

The R_f value of purified urease was found to be 0.49. From Figure 5 the standard curve of log of known HMW marker proteins *vs*R_f values, the molecular weight of urease from dehusked Pigeonpea seedswas determinedas 478 kDa.

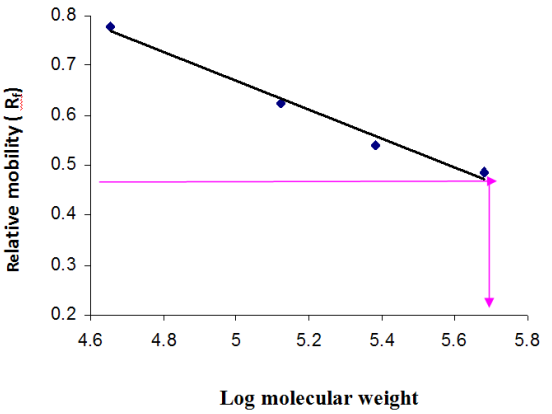

Figure 5: Log molecular weight of standard protein markers as afunction of $R_f$values

Immobilization of Urease by Entrapment in Calcium Alginate Beads

Figure 6 shows the immobilized urease enzyme beads by gel entrapment method. The total amount of urease immobilized within calcium alginate bead was 7.4 µLprotein per bead.

Figure 6 : Photograph of immobilized urease in calcium alginate beads

Comparison of the Activities of Soluble Urease and Immobilized Urease

The activities of both soluble urease and immobilized urease were examined in 0.1 M phosphate buffer (pH 7) at 37°C. The enhancement in the activity of the entrapped enzyme in comparison to that in the usual aqueous medium was noted. The data recorded in Table 3 showing about 1.6 fold increase in the activity.

Table 3: Comparison of the Activities of Soluble Urease and Immobilized Urease

No.	Urease Activity (µmol min^{-1} ml^{-1} of ammonia)		Ratio = $\frac{B}{A}$
	In aqueous medium(A)	Entrapped medium (B)	
1	309.74	493.72	1.59
2	291.65	482.45	1.65
3	282.73	474.61	1.67

Effect of pH on the Activities of Soluble and Immobilized Urease

The pH at which a certain enzyme will cause a reaction to progress most rapidly is called the optimum pH. At optimum pH, enzyme activity is maximum and above and below this pH, the activity is low (Lehningher, 1975).

In the present work the activities of soluble urease and immobilized urease were investigated at different pH values (5.0, 5.5, 6.0, 6.5, 7.0, 7.5 and 8.0) with urea substrate. Effect of varying pH of the assay buffer (0.1M phosphate) is shown in Table 4 and Figure 7.

The results indicated that soluble urease had an optimum at pH.7 for urea and that enzyme activity decreased rapidly on either side of this value particularly towards more acidic pH values. The decrease in activity was due to the ionic states of the amino acid residues of the urease enzyme and substrate urea molecules, causing varying efficiency in the binding of substrate.

Table 4: Effect of pH on the Activities of Soluble and Immobilized Urease Catalyzed Reactions

pH	Soluble urease ($\mu mol\ ml^{-1}min^{-1}$)	Immobilized urease ($\mu mol\ ml^{-1}min^{-1}$)
5.0	112.03	223.90
5.5	117.58	229.28
6.0	162.95	284.00
6.5	227.76	315.70
7.0	287.95	495.64
7.5	162.95	612.09
8.0	129.61	199.27

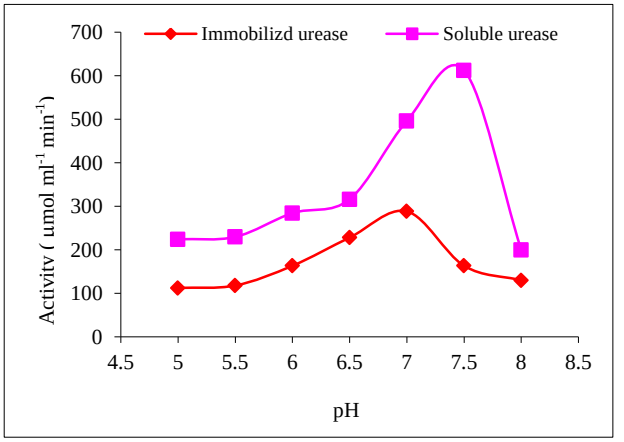

Figure 7: Plot of soluble and immobilized urease activities as a functionof pH

Application of Immobilized Urease for the Determination of Urea

Skate, fish of the family Rajidae contains urea and trimethylamine in large amounts making it unpopular as daily dishes due to its ammonicalodour. In this investigation, urea content in dried skate (*Raja hollandi*) flesh was determined by urease immobilized in calcium alginate beads. It was observed that urea content in dried skate flesh was 4.53 %. In the present work urea content in dried skate fish was removed by urease and the residual urea content was determined by prepared immobilized urease. Table 5 and Figure 8 show that the urea content decreased gradually with increased in time. After 66 h, 75.94 % of urea was removed.

Table 5: Removal of Urea Content as a Function of Time

Time (h)	Urea (%)	Removal percent (%)
0	4.53	-
12	3.32	26.71
18	2.89	36.20
36	2.25	50.33
42	1.85	59.16
66	1.09	75.94

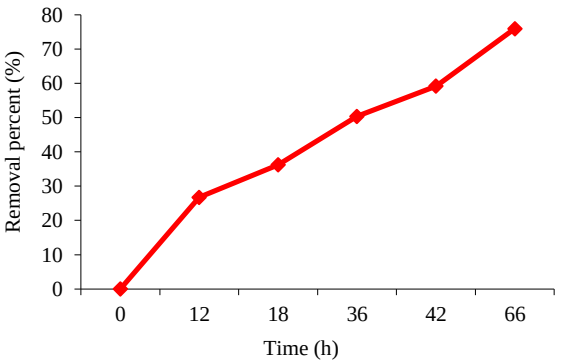

Figure 8: Plot of removal of urea content as a function of time

Conclusion

Urease was isolated and purified from Pigeonpea seeds collected from Natogyi Township, Mandalay Region. Ammonium sulphate precipitation method, gel filtration chromatographic method (SephacrylS-200) and ion-exchange chromatographic method (DEAE Sepharose) were used successively to get better purity. The purity of urease enzyme was confirmed by non SDS-PAGE technique as single band and the molecular weight of purified urease was determined to be 478 kDa. The immobilization of the purified urease was carried out by using gel entrapment technique using sodium alginate. Comparative studies of optimum pH between soluble and immobilized enzymes were carried out.

Immobilized urease showed a shift in optimum pH from 7 (soluble enzyme) to 7.5 in phosphate buffer. Immobilized urease was used for the determination of urea content in dried skate fish sample. Urea contents were found to be 4.53% in these samples. Moreover, removal of urea in dried skate fish was carried out by mixing the flesh of dried skate fish with purified urease. The residual urea was determined by Nessler method employing immobilized urease. After 66h, 75.94 % of urea was removed from dried skate fish due to the loss of ammonia the dried skate fish were more palatable to the consumers.

Acknowledgements

The author would like to thank Professor and Head, Dr New New Oo (Deputy Director/Head, Retired) and Dr Thet Thet Mar (Research Officer), Department of Medical Research (Lower Myanmar), for their valuable advice and permission.

References

Andrews, R.K., A. Dexter, R.L.Blakeley, and B.Zener. (1986). "Jack Bean Urease (EC 3.5.1.5), on the Inhibition of Urease by Amides and Esters of Phosphoric Acid ", *J.Am. Chem*. Soc., vol. **108**: pp. 7124-7125

Fujinawa, S.B.G. and T.P.Dela.(1990). "Application of Acid Urease to Reduction of Urea in Commercial Wines", *Am. J. Enol. Viticul*,vol. **42**: pp. 350-354

Fumuyiwa, O.O. and C.S. Ouch.(1991). "Modification of Acid Urease Activity by Fluoride Ions and Malic Acid in Wines", *Am.J. Enol.Viticul*, vol. **91**: pp. 350-359

Hausinger, R.P. (1993)."Biochemistry of Nickel", Plenium Publishing Corp.New York, USA

Lehningher, A.L., (1975). "Biochemistry", The John Hopkin's University Worth Pub, Inc, New York, pp. 183-190

Mobely, H.L.T., M.D.Island and R.P.Hausinger.(1995). "Molecular Biology of Microbial Urease", *Microbial. Rev.*, vol. **59**: pp. 451-479

Park, L.S. and R.P.Hausinger.(1995). "Evidence for the Presence Urease Apoprotein Complexes Containing UreD, UreF, and UreG in Cells that are Competent for *in vivo* Enzyme Activation*", J. Bacteriol*, vol. **177**: pp. 1947-1951

Smith, P.T., A.K.J.Douglas and N.Goodman.(1993). "Isolation and Characterization of Urease from *Aspergillusniger", J. Gen. Microbiol.,* vol. **139**: pp. 957-962.

PRE- AND POST- MONSOON VARIATION IN PHYSICOCHEMICAL CHARACTERISTICS OF WATER QUALITY OF SITTAUNG RIVER IN TAUNGOO AREA

Myat Sandar Hla*

Abstract

This paper is concerned with investigation of the water quality of Sittaung River in Taungoo area during 2011 to 2015.Water samples were collected at the periods of post-monsoon and pre-monsoon. Higher total alkalinity values of 130 ±15 ppm was observed in pre-monsoon periods compared to post-monsoon periods(100± 10)ppm. No significant difference of total hardness was observed between two collection periods. Total dissolved solids values in pre-monsoon periods were higher than the post monsoon periods. Positive correlation between total dissolved solids and temperature (r = 0.608) and also total suspended solids and temperature (r =0.766) were regarded as strong. Electrical conductivity values were less than 250 µS/ cm and it was classified as excellent for irrigation purpose. Higher dissolved oxygen values (4.8±1.0 ppm) were found in post-monsoon periods compared to those in pre-monsoon periods (3.4±0.9ppm).Both biochemical oxygen demand and chemical oxygen demand were far below the permissible limit. Nitrite nitrogen, nitrate nitrogen and ammonia nitrogen in river water for both collection periods were below the permissible limit. However, phosphate contents were slightly higher than the permissible level of 0.01 ppm. Lower sodium hazard of Sittaung river water was found so that river water did not pose problem on plant cultivation. Most of the chemical properties of the Sittaung River water in post-monsoon periods and pre-monsoon periods were different significantly. Data analysis were performed using Statistical Package for Social Science (SPSS) version 22.0.Correlation analysis among variables was performed by using Pearson correlation coefficient to measure the strength of the relationship between some variables.

Keywords: Sittaung River, water quality, sodium hazard, SPSS,correlation analysis

Introduction

The Sittaung River is a river in south central Myanmar in Bago Region. The river originates at the edge of the Shan Plateau and South East of

1. Dr, Associate Professor, Department of Chemistry, Sagaing University

Mandalay and flows south-ward to the Gulf of Mottama. River flows connect different habitats for water- dependent animals and plants. The alluvial plain occupies the central part of Sittaung River basin. The area of that basin is about 31944.4 sq-km. Sittaung River basin connect wetlands, floodplains, upstream and downstream habitats. Its length is of 420 km.The width of the river in monsoon period is (30.8-45.72) meters at upper Paunglong, about 91.44 meters near Pyinmana, 106.88 meters in the area of Taungoo, and (152.4-182.88 meters) in the area of mouth (TunKo, 2005). River regulation has reduced the size and frequency of the river flows that connect river with floodplains and sea. There are small scale farmlands along Sittaung river bank in Taungoo area. These are irrigated by Sittaung River during dry season (from November to May). In Monsoon, these are also used as rain-fed. Rivers are complex systems of flowing waters drawing specific land surfaces which are defined as river basins or watersheds. The characteristics of the river or rivers within the total basin system are related to a number of features. These features include the size, form and geological characteristics of basin and climatic conditions which determine the quantities of water to be drained by the river network (Chapman,1996). Water quality variability depends on the hydrological regime of the river. Agricultural water quality monitoring is particularly interested in five categories of water contaminants: sediments, nutrients, bacteria, pesticides and dissolved solids that rapidly deplete oxygen from stream. The impact of river maintains on drainage and agriculture performance can deliver standard of drainage and provides service to agriculture land use (Dunderdale and Morris, 1997).

The main aim of this research is to investigate the quality of Sittaung River Water during pre- and post- monsoon periods for domestic and irrigation purposes.

Materials and Methods

Sample Collection

Sittaung River water samples from six sampling sites were collected at the pre-monsoon periods (late May) of years 2012, 2013, 2014 and 2015 and post-monsoon periods (early November) of years 2011, 2012, 2013 and 2014.Locations of sampling sites for river water are shown in Table 1 and

Figure 1. Exact coordinate of sampling locations were recorded by using a Global Positioning System (GPS) device.

Table 1: Sampling Sites of Irrigated River Water Samples

No	Sampling site	Position	
		Longitude	Latitude
1	W_1 Near Myogyiharbour	96°28' 22.83" E	18°55' 3.69" N
2	W_2 East part of Do Thaung	96°27' 54.02" E	18°55' 27.34" N
3	W_3 Middle part of Do Thaung	96°27' 39.12" E	18°55' 44.89" N
4	W_4 West part of Do Thaung	96°27' 39.76" E	18°55' 13.40" N
5	W_5 Edge of ThaPhanpin	96°27' 14.61" E	18°55' 13.67" N
6	W_6 East part of ThaPhanpin	96°26' 50.70" E	18°55' 32.13" N

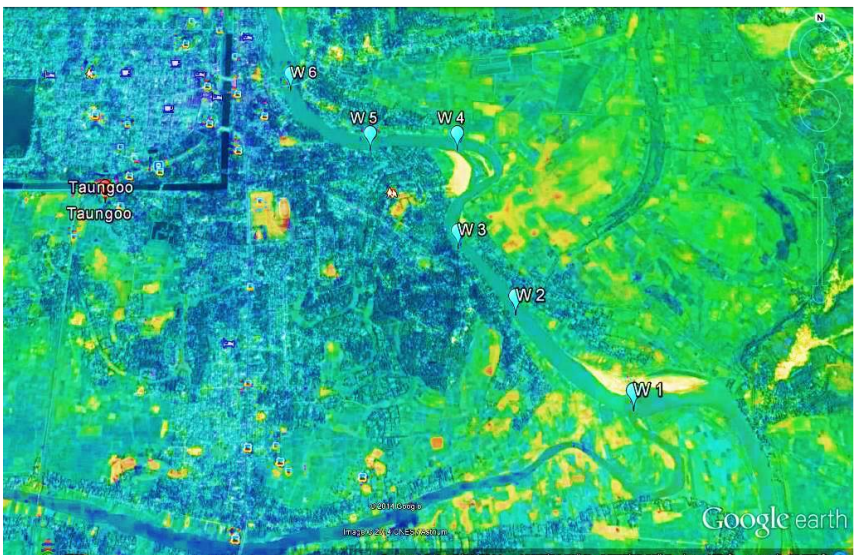

Figure 1: Google earth map of locations of river water sampling sites

Determination of Some Physicochemical Properties of the Sittaung River Water

pH and temperature were determined by pH meter (Model EIL-7020, ABB England) and total alkalinity, total hardness and chemical oxygen demand by titration methods, biochemical oxygen demand by incubation method, electrical conductivity by electrical conductivity meter(Model 1152, US), nitrite nitrogen, ammonia nitrogen, nitrate nitrogen, phosphate values by spectrophotometric method using spectrophotometer (PD-303, APEL, Japan) were determined. Sodium adsorption ratios of river water samples were calculated.

Results and Discussion

Sittaung River water samples from six selected irrigated sources were collected and then properties of River water were determined during the study period.

pH

pH values of river water samples in post- and pre-monsoon periods are shown in Figure 2. It was found that the pH values were found to be nearly neutral in post-monsoon period and the mean was 6.6 ± 0.1. In pre- monsoon periods, the pH values were found to be neutral as well as slightly alkaline and the mean value was 7.3 ± 0.2. pH values in post-monsoon periods and pre-monsoon periods were found to be significantly different ($p < 0.01$). Sittaung River water was found to possess no threat of drinking and irrigation because pH values obtained were within the permissible limit (6.5-8.5) (FAO/WHO, 1994).

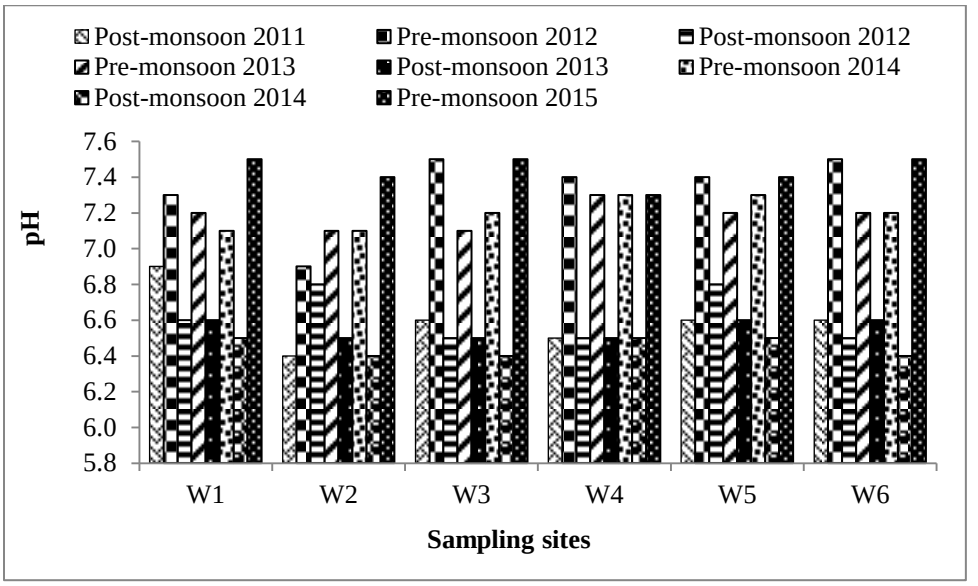

Figure 2: pH values of Sittaung river water samples at different sampling sites in post-monsoon and pre-monsoon periods

Temperature and Total alkalinity

During the study periods the mean temperature in post-monsoon periods was 25.4 ± 2.2˚ C and the mean value in pre-monsoon period was 30.7 ± 2.0°C. Significant differences in temperature were observed between post-monsoon periods and pre-monsoon periods ($p < 0.01$).Total alkalinity values of river water sample were found with the mean value of 100 ± 14 ppm in post-monsoon periods (Figure 3). In pre-monsoon periods, the total alkalinity values were higher than those in pre-monsoon periods with mean value of 130 ± 15 ppm. The higher values of total alkalinity during pre-monsoon periods ($p < 0.05$) may be due to the fact that the river water becomes concentrated during the period having high temperature. All of the total alkalinity values in this study were below the permissible limit of 200-600 ppm recommended by (USEPA, 1997).In this study a positive correlation was observed between total alkalinity and temperature ($r = 0.656$).

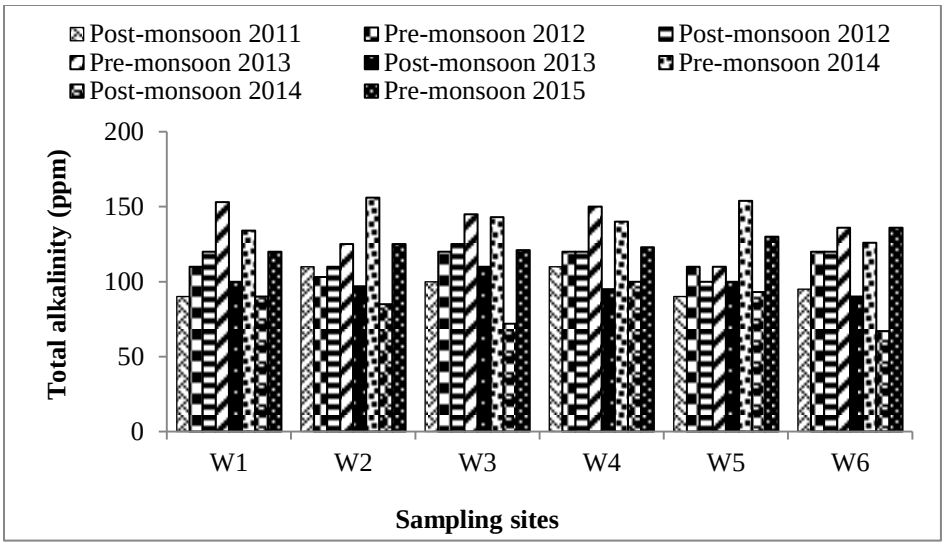

Figure 3: Total alkalinity values of Sittaung river water samples at different sampling sites in post-monsoon and pre-monsoon periods

Total Hardness

Total hardness values of river water samples in both periods are shown in Figure 4. Total hardness values ranged between 110 to 150 ppm in post-monsoon periods with the mean value of 126 ± 11 ppm and in pre-monsoon periods ranged between 100 to 146 ppm with the mean value of 127 ± 11 ppm. No significant difference in total hardness was observed between the two periods ($p > 0.05$).Water that has a hardness less than 61 mg/L is considered soft; 61-120 mg/L, moderately hard; 121-180 mg/L, hard; and more than 180 mg/L, very hard (Heath, 1983). Thus, total hardness values of river water were found to be soft and these values were within the permissible range of 110-150 ppm (USEPA, 1997).

Total Dissolved Solid

In post-monsoon periods, mean value of total dissolved solid was 158 ± 25 ppm and in pre-monsoon it was 188 ± 23 ppm (Figure 5).Total dissolved solids values of river water of the most sampling sites in pre-monsoon periods were higher than those in post-monsoon periods ($p < 0.05$).This is due to higher temperature in pre-monsoon period which cause the evaporation of

water. In this study total dissolved solid and temperature were positively correlated (r = 0.608).It was noted that total dissolved solid values in both seasons were far below the permissible limit for 500 ppm (USEPA, 1997; WHO,2006).

Total Suspended Solids

Total suspended solids values of river water samples are shown in Figure 6.In post-monsoon periods total suspended solids were in the range of 75 to 140 ppm with the mean value of 105 ± 18 ppm and in the pre-monsoon periods the values were in the range of 110 to 170 ppm with the mean value of 144 ± 17 ppm. The differences in total suspended solid in post-monsoon periods and pre-monsoon periods were not significant ($p>0.05$) in the study period. Strong positive correlation was observed between total suspended solids and temperature (r =0.766).However, total suspended solid values of Sittaung river water were lower than the permissible level of irrigation purpose of 200 ppm (ISI, 1985).

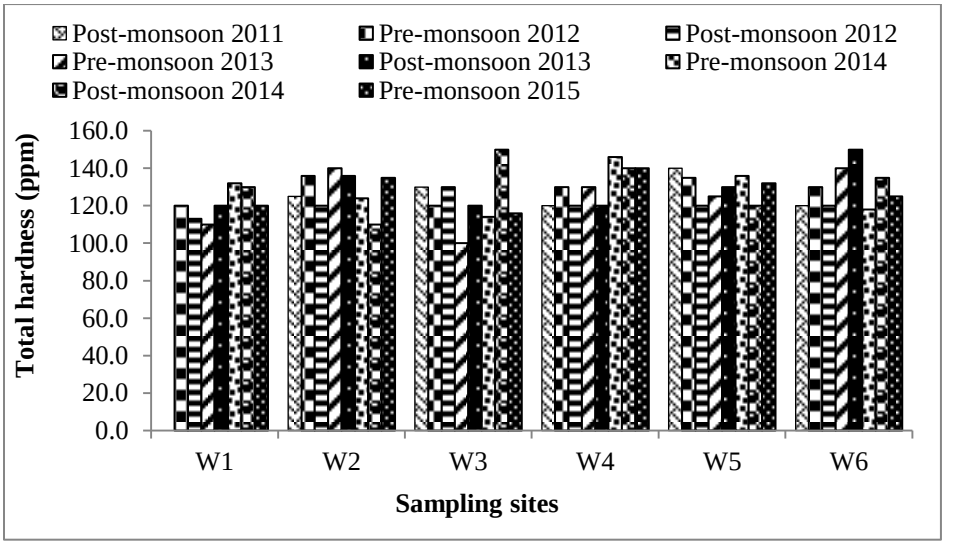

Figure 4: Total hardness values of Sittaung river water samples at different sampling sites in post-monsoon and pre-monsoon periods

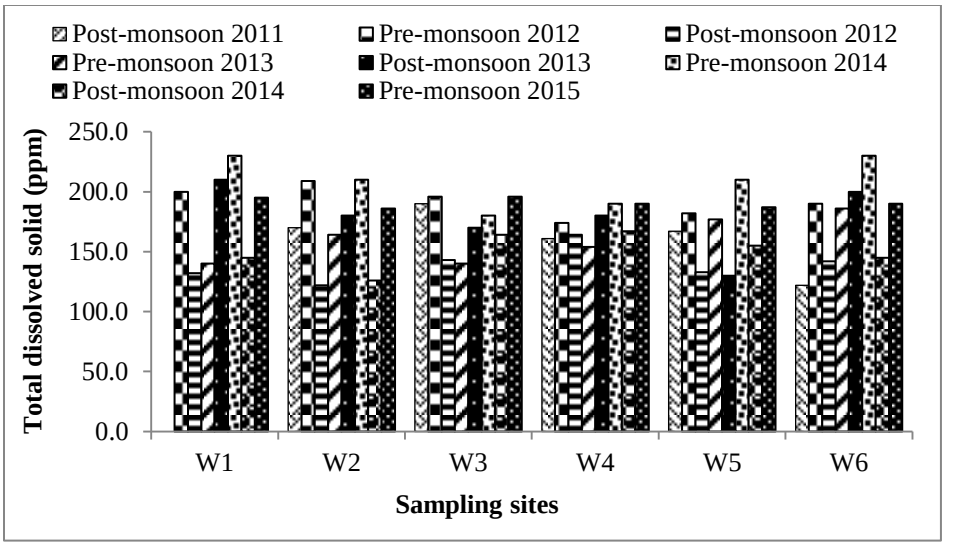

Figure 5: Total dissolved solid values of Sittaung river water samples at different sampling sites in post-monsoon and pre-monsoon periods

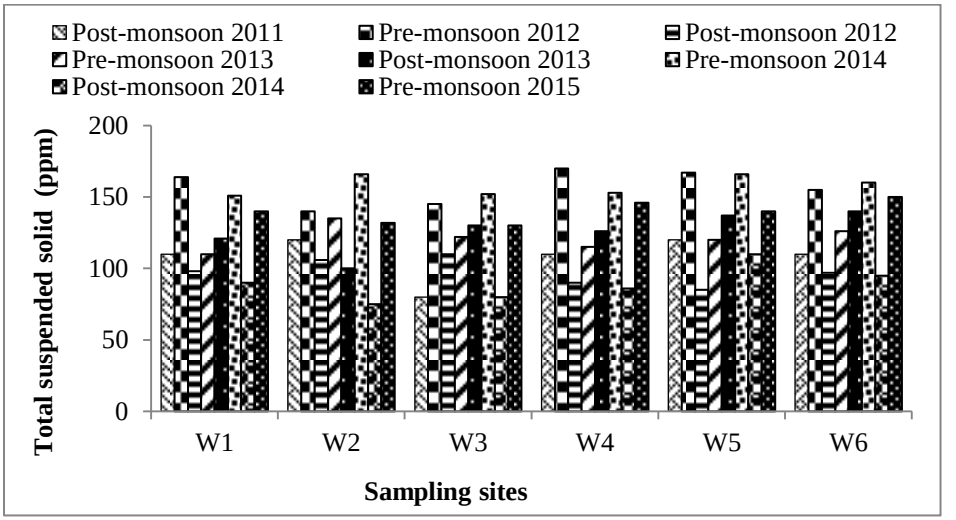

Figure 6: Total suspended solid values of Sittaung river water samples at different sampling sites in post-monsoon and pre-monsoon periods

Electrical Conductivity

Electrical conductivity values of river water samples in pre- and post-monsoon periods are shown in Figure 7. It was found that the electrical conductivity values were in the range of 80.7 to 167.4 µS/cm with mean value of 119.3 ± 22.2 µS/cm in post-monsoon periods and in the range of 80.7 to 167.4 µS/cm with the mean value of 144.0 ± 29.0 µS/cm in pre- monsoon periods. Electrical conductivity values in post-monsoon periods were lower than those in pre-monsoon periods ($p>0.05$).A positive and strong significant relationship ($r = 0.608$) between electrical conductivity and total dissolved solids was observed because conductance of electric current depends upon the dissolved ionic species. Hence high electrical conductivity values corresponds to high total dissolved solids (Siosemarde *et al*., 2010). Since the electrical conductivity values were < 250 µS/cm the Sittaung river water was regarded as excellent one for irrigation purpose (Ayers and Wescot 1997) .

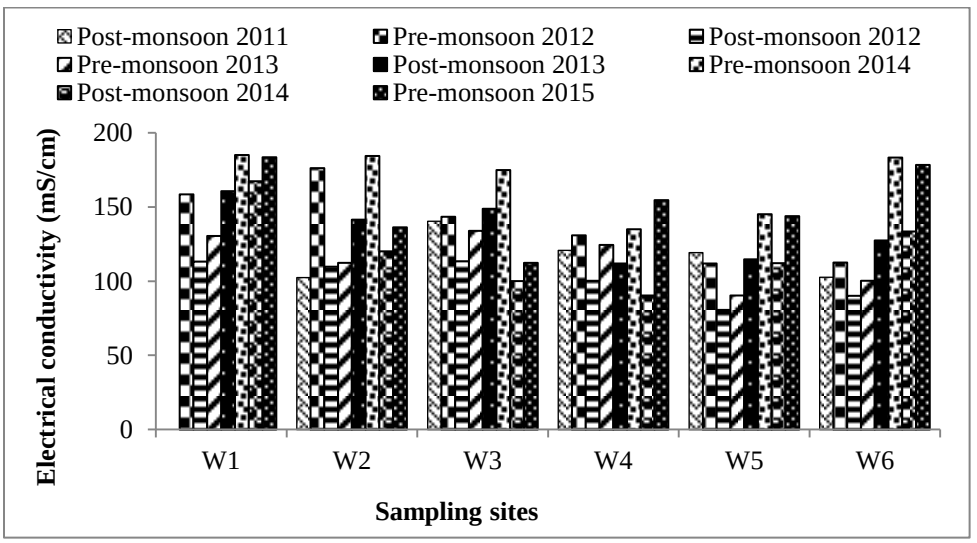

Figure 7: Electrical conductivity values of Sittaung river water samples at different sampling sites in post-monsoon and pre-monsoon periods

Dissolved Oxygen

Table 2 shows dissolved oxygen values of river water samples. In this study dissolved oxygen values were in the range of 2.9 to 6.8 ppm with the mean value of 4.8±1.0 ppm in post-monsoon periods and those in pre-monsoon periods were in the range of 2.2 to 4.8 ppm with the mean value of 3.4±0.9 ppm. In the course of study period, dissolved oxygen values of river water in post-monsoon periods were higher than those of water in pre-monsoon periods ($p < 0.01$). This is because high temperature favours the growth of microbes and algae which are main source of oxygen consumption (Naseema *et al*., 2013).In this study a weak negative correlation ($r = - 0.1840$) was observed between temperature and dissolved oxygen. Dissolved oxygen values of almost every sampling sites falls within the permissible limit of 4 to 6 ppm (BSI, 2012) which ensure better aquatic life in water body (Gupta *et al*., 2017).

Table 2: Dissolved Oxygen Values of Sittaung River Water Samples at Different Sampling Sites in Post-monsoon and Pre-monsoon Periods

Sample	Dissolved oxygen (ppm)							
	Post-monsoon 2011	Pre-monsoon 2012	Post-monsoon 2012	Pre-monsoon 2013	Post-monsoon 2013	Pre-monsoon 2014	Post-monsoon 2014	Pre-monsoon 2015
W_1	5.4	4.5	3.9	2.2	6.4	4.6	4.2	3.5
W_2	3.8	2.4	4.1	3.4	5.8	4.0	3.9	2.2
W_3	4.2	3.8	3.2	2.8	6.3	4.6	4.5	3.9
W_4	4.8	3.3	2.9	2.5	5.6	3.5	3.2	2.2
W_5	5.8	4.8	5.1	4.8	5.8	3.6	4.2	3.1
W_6	4.8	2.2	4.9	3.4	6.8	4.7	4.8	2.8
(Mean ±SD)	Post-monsoon(4.8 ± 1.0 ppm)				Pre-monsoon (3.4 ± 0.9 ppm)			
Permissible limit	(2.0-6.0) ppm (BSI, 2012)							

Biochemical Oxygen Demand

Biochemical oxygen demand is a measure of how much dissolved oxygen is being consumed as microbe break down organic matter.The biodegradation of the organic materials exerts oxygen tension in the water and increases the biochemical oxygen demand (Abida and Harikrishna, 2008).Biochemical oxygen demand of river water samples are shown in Table 3. It was found that the mean values of biochemical oxygen demand in the post-monsoon periodswas3.0±0.7 ppm and that in pre-monsoon periods was 4.9±1.5 ppm. No significant difference in biochemical oxygen demand values of river water in post-monsoon periods and in pre- monsoon period was observed ($p>0.05$). All of the values in both periods were far below the permissible values for irrigation, 100 ppm (ISI, 1985). In this study a negative correlation ($r = - 0.541$) was observed between biochemical oxygen demand and dissolved oxygen.This is because the oxygen available in the water is being consumed by the bacteria (Sawyer *et al*., 2003).

Table 3: Biochemical Oxygen Demand Values of Sittaung River Water Samples at Different Sampling Sites in Post-monsoon and Pre-monsoon Periods

Sample	Biochemical oxygen demand (ppm)							
	Post-monsoon 2011	Pre-monsoon 2012	Post-monsoon 2012	Pre-monsoon 2013	Post-monsoon 2013	Pre-monsoon 2014	Post-monsoon 2014	Pre-monsoon 2015
W_1	1.8	4.8	4.3	5.8	2.0	2.9	2.7	2.1
W_2	2.5	3.7	3.6	4.3	2.0	2.9	2.4	5.6
W_3	2.7	6.2	4.3	6.7	3.0	3.5	2.8	5.3
W_4	1.9	4.6	3.9	8.3	3.3	3.8	3.1	5.7
W_5	3.5	3.4	3.2	7.3	2.5	3.2	4.3	6.8
W_6	2.8	3.1	3.7	4.9	3.1	4.2	3.1	4.4
(Mean ±SD)	Post-monsoon(3.0±0.7 ppm)			Pre-monsoon (4.9 ± 1.5 ppm)				
Permissible limit	100 ppm (ISI, 1985)							

Chemical Oxygen Demand

Chemical oxygen demand indicates the presence of all forms of organic matters, both biodegradable and non-biodegradable and hence the degree of pollution in water.Table 4 shows the chemical oxygen demand values of river water samples in post-monsoon and pre- monsoon periods were 4.7±1.4 ppm and 9.5± 1.8 ppm respectively. Chemical oxygen demand values between two seasons were significantly different ($p< 0.05$). Chemical oxygen demand values of pre- monsoon periods were higher than those of samples in post-monsoon periods. This is due to more farming activities throughout the dry seasons. All of the values in both periods were far below the permissible values of 200 ppm for irrigation purpose (ISI, 1985).

Table 4: Chemical Oxygen Demand Values of Sittaung River Water Samples at Different Sampling Sitesin Post- monsoon and Pre-monsoon Periods

Sample	Chemical oxygen demand (ppm)							
	Post-monsoon 2011	Pre-monsoon 2012	Post-monsoon 2012	Pre-monsoon 2013	Post-monsoon 2013	Pre-monsoon 2014	Post-monsoon 2014	Pre-monsoon 2015
W_1	3.7	8.5	4.3	8.6	4.7	9.2	3.9	11.7
W_2	3.9	9.5	6.3	7.8	2.6	12.8	4.7	9.8
W_3	6.8	11.2	5.8	9.4	3.3	7.3	5.9	8.5
W_4	5.9	13.5	4.7	6.5	2.5	11.0	6.8	9.4
W_5	6.4	9.4	3.8	8.6	3.1	8.1	5.2	7.9
W_6	4.8	7.6	2.9	10.4	4.1	12.8	7.5	10.5
(Mean ±SD)		Post-monsoon(4.7 ±1.4ppm)			Pre-monsoon (9.5± 1.8 ppm)			
Permissible limit 200 ppm (ISI, 1985)								

Nitrite Nitrogen, Nitrate Nitrogen and Ammonia Nitrogen

Inorganic nitrogen exists in free state or nitrite, nitrate and ammonia forms.Nitrite nitrogen values of river water samples were found to be 0.010 to 0.060 ppm with the mean values of (0.030±0.015ppm) in post-monsoon and 0.001 to 0.004 ppm with the mean values of (0.002 ± 0.001 ppm) in pre-monsoon periods respectively(Table 5). Nitrite nitrogen values between the two periods were significantly different ($p< 0.01$). The major source of nitrate and nitrite concentration in some rivers come from urban wastewater and some industrial wastewater.Therefore , nitrite values of some sampling sites were slightly higher than permissible limit of 0.01 ppm (ISI,1985).

Table 5: Nitrite Nitrogen Values of Sittaung River Water Samples at Different Sampling Sites in Post-monsoon and Pre-monsoon Periods

Sample	Nitrite nitrogen (ppm)							
	Post-monsoon 2011	Pre-monsoon 2012	Post-monsoon 2012	Pre-monsoon 2013	Post-monsoon 2013	Pre-monsoon 2014	Post-monsoon 2014	Pre-monsoon 2015
W_1	0.010	0.001	0.050	0.001	0.010	0.001	0.020	0.002
W_2	0.020	0.002	0.060	0.001	0.020	0.001	0.020	0.003
W_3	0.030	0.001	0.040	0.002	0.010	0.002	0.010	0.004
W_4	0.040	0.001	0.020	0.001	0.020	0.003	0.020	0.003
W_5	0.050	0.001	0.030	0.003	0.010	0.003	0.020	0.003
W_6	0.040	0.001	0.010	0.004	0.010	0.004	0.020	0.004
(Mean ±SD) Post-monsoon(0.030±0.015 ppm) Pre-monsoon (0.002 ± 0.001 ppm)								
Permissible limit 0.01 ppm (USEPA, 1997)								

Table 6 shows the nitrate nitrogen values of Sittaung River Water during pre-monsoon and post-monsoon periods.Nitrate nitrogen values were in the range of 0.01 to 0.02 ppm in the years of 2012,2013 and 2014 but found to be below detectable limit in 2011 indicating inhibition of nitrification by microorganism.The mean values of nitrate nitrogen was 0.01±0.01 ppm in pre- monsoon periods. These were below the permissible limit of 50 ppm (FAO/WHO, 1994).Lower nitrates were due to decrease in degradation of organic matter by microbial activities.

Table 6: Nitrate Nitrogen Values of Sittaung River Water Samples at Different Sampling Sites in Post-monsoon and Pre-monsoon Periods

Sample	Nitrate nitrogen (ppm)							
	Post-monsoon 2011	Pre-monsoon 2012	Post-monsoon 2012	Pre-monsoon 2013	Post-monsoon 2013	Pre-monsoon 2014	Post-monsoon 2014	Pre-monsoon 2015
W_1	ND	0.02	0.01	0.03	0.01	0.05	0.02	0.01
W_2	ND	0.03	0.01	0.06	0.02	0.03	0.01	0.03
W_3	ND	0.01	0.02	0.05	0.01	0.01	0.01	0.01
W_4	ND	0.02	0.01	0.06	0.01	0.02	0.01	0.01
W_5	ND	0.01	0.01	0.04	0.01	0.01	0.02	0.02
W_6	ND	0.03	0.01	0.02	0.01	0.03	0.02	0.02
(Mean ±SD)					Pre-monsoon (0.01 ± 0.01 ppm)			
Permissible limit 50 ppm (FAO/WHO, 1994)								
ND= not detected								

Table 7 shows the ammonia nitrogen contents in Sittaung River water during pre-monsoon and post-monsoon periods. In post-monsoon periods of of the years 2012, 2013 and 2014 the ammonia nitrogen contents were in the range of 0.01 to 0.02 ppm. However, in 2011 ammnonia nitrogen contents were not detected. In pre- monsoon periods ammnonia nitrogen contents were in the range of 0.01 to 0.06 ppm with the mean value of 0.03±0.01 ppm. Water samples of all sampling sites were found to have lower values than the permissible upper limit of 0.1 ppm (FAO/WHO, 1994).

Table 7: Ammonia Nitrogen Values of River Water Samples at Different Sampling Sites in Post-monsoon and Pre-monsoon Periods

Sample	Ammonia nitrogen (ppm)							
	Post-monsoon 2011	Pre-monsoon 2012	Post-monsoon 2012	Pre-monsoon 2013	Post-monsoon 2013	Pre-monsoon 2014	Post-monsoon 2014	Pre-monsoon 2015
W_1	ND	0.02	0.01	0.03	0.01	0.05	0.02	0.01
W_2	ND	0.03	0.01	0.06	0.02	0.03	0.01	0.03
W_3	ND	0.01	0.02	0.05	0.01	0.01	0.01	0.01
W_4	ND	0.02	0.01	0.06	0.01	0.02	0.01	0.01
W_5	ND	0.01	0.01	0.04	0.01	0.01	0.02	0.02
W_6	ND	0.03	0.01	0.02	0.01	0.03	0.02	0.02
(Mean ±SD)					Pre-monsoon (0.03 ± 0.01 ppm)			
Permissible limit 0.015-0.100 ppm (FAO/WHO, 1994)								

Phosphate

Table 8 shows the phosphate contents of Sittaung River water during the study periods.The mean values of phosphate in post-monsoon and pre-monsoon periods were found to be 0.020±0.008 ppm and 0.011±0.007 ppm, respectively. Higher phosphates values were observed in post-monsoon periods than in pre-monsoon periods indicating more anthropogenic activities. Phosphate values of the water samples were slightly higher than the permissible value of 0.01 ppm (USEPA, 1997)due to perennial trees along the river sides and high rate of biodegradation of biomass in windy weather.

Sodium Adsorption Ratio

Sodium adsorption ratio (SAR) is the ratio of sodium concentration to the concentration of square root of the average concentration of calcium and magnesium in water or the soil solution (Miller and Gardiner, 2007).SAR of Sittaung River water during post- and pre- monsoon periods are shown in Table 9.In post- monsoon periods the mean SAR value was 0.70±0.23 and that in pre-monsoon periods was 0.51± 0.12 .According to the classification of sodium hazard of water based on SAR values, SAR values of 1-2 cause low

sodium hazard of water (Mass, 1990). Thus, the Sittaung River water does not pose any problem on growth of plants.

Table 8: Phosphate Values of Sittaung River Water Samples at Different Sampling Sites in Post-monsoon and Pre-monsoon Periods

Sample	Phosphate (ppm)							
	Post-monsoon 2011	Pre-monsoon 2012	Post-monsoon 2012	Pre-monsoon 2013	Post-monsoon 2013	Pre-monsoon 2014	Post-monsoon 2014	Pre-monsoon 2015
W_1	0.021	0.011	0.031	0.030	0.012	0.010	0.025	0.010
W_2	0.032	0.012	0.022	0.020	0.011	0.010	0.015	0.010
W_3	0.032	0.012	0.025	0.020	0.012	0.011	0.016	0.020
W_4	0.031	0.014	0.034	0.010	0.012	0.011	0.014	0.010
W_5	0.023	0.013	0.023	0.010	0.013	0.011	0.015	0.010
W_6	0.021	0.011	0.035	0.020	0.012	0.010	0.014	0.010
(Mean±SD)	Post-monsoon (0.020 ± 0.008 ppm)				Pre-monsoon (0.011 ± 0.007 ppm)			
Permissible limit 0.01 ppm (USEPA, 1997)								

Table 9: Sodium Adsorption Ratios of River Water Samples from Different Sampling Sites

Sample	Sodium adsorption ratios(SAR)							
	Post-monsoon 2011	Pre-monsoon 2012	Post-monsoon 2012	Pre-monsoon 2013	Post-monsoon 2013	Pre-monsoon 2014	Post-monsoon 2014	Pre-monsoon 2015
W_1	0.83	0.69	1.05	0.66	0.85	0.54	0.34	0.45
W_2	0.79	0.78	1.02	0.52	0.90	0.46	0.49	0.41
W_3	0.63	0.50	0.83	0.38	0.71	0.37	0.37	0.63
W_4	0.57	0.43	0.98	0.59	0.86	0.35	0.32	0.38
W_5	0.48	0.49	0.96	0.47	0.80	0.54	0.37	0.47
W_6	0.49	0.60	0.90	0.51	0.84	0.56	0.39	0.45
(Mean ±SD)	Post-monsoon(0.70±0.23)				Pre-monsoon (0.51± 0.12)			

Conclusion

The physicochemical parameters of surface water samples collected from Sittaung River were investigated in this study. Most of the chemical properties were found to have higher values in pre-monsoon periods compared to post-monsoon and below the permissible limit. Dissolved oxygen values in some sampling sites in post-monsoon periods were slightly higher than the permissible limit.Nitrite contents of some sampling sites and phosphate contents of most sampling sites were higher than the permissible limit.Excessive presence of nitrogen and phosphorus will made the river prone to eutrophication, which ultimately results into degradation of water quality as well as the aquatic environment. Nutrients from induced fertilizers, human activities and other animal wastes are the main causes of this problem. It is vital to monitor nutrient level- especially phosphorus –nitrates in rivers that exhibit an over abundance or lack of algae. Practicing the climate smart agriculture and green agriculture may facilitate the healthy riverine system. The results reveal that Sittaung River is not polluted and can be used for domestic and irrigation purposes in Taungoo area.

Acknowledgement

The author would like to thank the Department of Higher Education (Yangon Office), Ministry of Education, Yangon, Myanmar, for provision of opportunity to do this research and Myanmar Academy of Arts and Science for allowing to present this paper.

References

Abida, B. and Harikrishna, M. (2008).“ Study on the Quality of Water in Some Streams of Cauvery River”. *E-J.Chem*., vol. 5 (2),pp.377-384

Ayers,R.S. and Wescot, D.W.(1997).“Water Quality for Irrigation”. *Journal of Irrigation and Drainage*,vol.103(IR2),p.140

BSI. (2012).*Specification for Drinking Water*. New Delhi: Bureau of Indian Standards, Indian Standards Institution,pp.1-5

Chapman, D. (1996).*Water Quality Assessment: A Guide to Use of Biota, Sediment and Water in Environmental Monitoring.*UK:2nd edn., Chapman and Hall, 420-45

Dunderdale, J.A.L. and Morris, J.(1997). “Agricultural Impacts of River Maintenance Activities: A Method of Assessment”. *J.Agric. Engg. Res.*,vol.68(4), pp.317-332

FAO/WHO. (1994).*Food Additive and Contaminants.* Rome: Joint Food and Agriculture Organization of the United Nations and World Health Organization Food Standard Programme, Codex Alimentarius Commission

Gupta,N.,Pandey, P. and Hussain,J.(2017). “Effect of Physicochemical and Biological Parameters on the Quality of River Water of Narmada, Madhya Pradesh, India ”. *Water Science*,vol. 31,pp. 11-23

Heath, R.C. (1983). Basic Ground-Water Hydrology. Virginia, USA : U.S Geological Survey Water-Supply paper 2220

ISI. (1985).*Indian Standard Specifications of Different Fertilizer*.New Delhi: pp. 4-6

Mass, E.V. (1990). *Crop Salt Tolerance.*In *Agricultural Assessment and Management Manual.* Tanji. K.K. (ed). New York: ASCE, pp. 260-304

Miller, R.T. and Gardiner, D.T. (2007).*Soils in Our Environment*. New Jersey: 9thedn., Prentice Hall Inc.,pp.452-461

Nassema, K., Masihur R., and Husain, K.A. (2013)."Study of Seasonal Variation in the Water Quality among Different Ghats of River Ganga Kanpur, Indian".*J. Environ. Res. Develop.*,vol.8(1),pp.1-9

Sawyer, C.N.,Mc Carty, P.L.andParkin, G.F.(2003). *Chemistry for Environmental Engineering and Science*. New York : 5th edition, McGraw-Hill

Siosemarde, M., Kave, F., Pazira, E., Sedghi, H. and Ghaderi, S.J. (2010). “Determination of Constant Coefficients to Relate Total Dissolved Solids to Electrical Conductivity”. *World Academy of Science Engineering and Technology*, vol. 46, pp. 258–260

TunKo.(2005). *The Variation in the Drainage Basin Morphometry within Sittaung Valley*. PhD Dissertation, Department of Geography, University of Yangon, Myanmar

USEPA.(1997). *Exposure Factors Handbook(Final Report)*. Washington DC: Environmental Protection Agency (EPA Publication 600/P/95)

WHO.(1993).*Guidelines for Drinking Water Quality.* Geneva: 2nd edition., vol.1**,**World Health Organization

WHO. (2006).*Guidelines for Drinking Water Quality.* Geneva: 3rd edition., vol.1**,**World Health Organization,pp. 491- 493

INVESTIGATION OF PLASTICIZERS AND NON-INTENTIONALLY ADDED SUBSTANCES (NIAS) FROM THE YOGHURT BOTTLES AND DISPOSABLE PLASTIC CUPS

Ei Ei Htway[1], Aye Aye Phyu[2], Myint Myint Khaing[3], and Hla Myoe Min[4]

Abstract

The aim of this research work is to investigate the presence and comparative amount of plasticizers and non-intentionally added substances (NIAS)from the yoghurt bottles and disposable plastic cups. The types of polymer were identified by Fourier Transform Infrared (FT IR) spectrophotometer and plasticizers and NIAS were identified by Gas Chromatography-Mass Spectrometry (GC-MS).The type of polymer of the yoghurt bottle samples was high density polyethylene (HDPE) and that of disposable plastic cups was polypropylene (PP). The plasticizers and NIAS mostly found in both types of polymers were Fatty Acid Methyl Ester (FAME) compounds and long chain hydrocarbon compounds. The other compounds found from these types of food containers were aromatic hydrocarbon compounds, ether compound, ketone, bicyclic compounds, epoxy compound and sulphur containing compounds. Overall migration percents were evaluated by using three solvents, chloroform, water and olive oil. The migration percents of HDPE polymer were found to be 0.11 %, 0.81 % and 0.06 % and those of PP polymer were found to be 0.34%, 1.35 % and 0.07% in water, chloroform and oil, respectively.Elemental analysis of the samples by Wavelength Dispersive X-ray Fluorescence (WDXRF) showed that the common elements found in both types of polymer samples were Ti, Zn, Ca, Fe, Cl, Si, K and Al.

Keywords: plasticizers, NIAS, high density polyethylene, polypropylene, migration percents

1. Dr, Research Scientist,Pharmacology Research Division, Department of Medical Research (Pyin Oo Lwin Branch)
2. Research Assistant-2,Pharmacology Research Division, Department of Medical Research (Pyin Oo Lwin Branch)
3. Dr, Lecturer, Department of Chemistry,University of Mandalay
4. Dr, Associate Professor,Department of Chemistry,University of Mandalay

Introduction

Food packaging and disposable plastic wares are an important part of the food industry for preservation of food as well as mechanical support and protection in transit. A range of different polymers are used in food packaging with their compatible plasticizer and other additives such as fungicides, flame retardants, stabilizers and antioxidants that applied on the specific characteristics of the food products, the storage conditions, and the shelf life. Among various types of food packaging polymers, the polymer used in yoghurt bottles and disposable plastic cups are most interesting areas by consumers due to their wide range of applications. Even the plastic additives are inert and non-toxic; they can interact with food and become harmful in large doses (Kerry *et al.*, 2006). A number of factors can influence the migration of plasticizers, other additives and degradation products of polymer to food, including the chemical properties of the compound, the contact surface and the type of plastic material, the character of food, the packaging temperatures, the heat or sterilization treatment, and the storage time of the product. The presence of plastic additive or plasticizer at high concentration may trigger health problems.

Besides the plastic additives some non-intentionally added substances (NIAS) may be present in polymer products and they can also migrate into food and drinks. The presence of NIAS has been suggested as the source of toxicological effects (Leivadara *et al*., 2008). Due to their leaching potential and widespread use, independent research, such as recording current materials used in common supermarket products, was conducted to obtain a better understanding of what polymers are currently used in food packaging. And then, it was then important to understand the impact on both society and the consumer by researching possible hazards in the use of plastics food containers to assess whether there are any public health and safety risks by determining a range of chemicals having potential to migrate from food packaging into foods.

The aim of this research work is to investigate the presence of plasticizers and NIAS and relative amount of those plasticizers and NIAS from the yoghurt bottles and disposable plastic cups and relative abundance of elements.

Materials and Methods

Sample Collection

The Yoghurt bottle (150 mL, imported brand) and disposable plastic cup (150 mL, 7 cm (diameter) x 8.5 cm (height) new container) were collected from the market of Pyin Oo Lwin Township, Mandalay Region. The samples were cleaned by distilled water and cut into small pieces and stored for further analysis.

Identification of Types of Polymer

The types of polymer of the selected samples were identified by FT IR by using modified KBr method. In this method, the samples were cut into disc and inserted in the KBr holder and pressed by hydraulic press. The prepared discs were analyzed in the mid-IR region. The spectra obtained were compared with the library spectra of specialized data-base software. These measurements were done at the Pharmacology Research Division, Department of Medical Research (Pyin Oo Lwin Branch).

Extraction of Polymer Components from the Polymer Samples

In this experiment, three selected solvents were used to extract the polymer components from both samples. The three solvents were chloroform, distilled water and olive oil. The exact weight (1.0 g) of each sample was refluxed with 30 mL of solvents, chloroform and distilled water at refluxing temperature for 3 h and the olive oil at 95- 110 ℃ for half hour. Then,each extract was filtered through the filter paper and the weights of residual extracts were also recorded. The filtrates were analyzed by GC-MS (GCMS-QP 2010).

Identification of Polymer Components from the Extracts

Each extract was subjected to measure the GC-MS in order to identify all the components present in the extract. The chloroform extract and distilled water extract were measured directly without measuring the solvents by setting as blank. But in the case of olive oil extract, olive oil was first measured for GC-MS to set it as blank. Then, all extracts were measured under specified conditions. GC was equipped with the normal septum. The GC conditions were as follows: GCMS-QP 2020 (Shimadzu, Kyoto, Japan)

equipped with a methyl silicone coated fused-silica capillary DB-5MS (0.25 mm i.d. x 30 m, 0.25 µm film thickness) column were used.The oven temperature was maintained at 50 ^{o}C for the first 1 min and then ramped up at 10 ^{o}C min^{-1} to 270 ^{o}C where it was held for 22 min. The injection port and interface were kept at 260 ^{o}C. Helium (100.0 kPa) served as the carrier gas. The injection mode was splitless, the sampling time was 3 min, and the injection volume was 1 µL. An auto-injector and auto-sampler AOC-20 i+s(Shimadzu,Japan) were used. The MS conditions were as follows: ionization mode, electron impact and detection voltage at 1.3 kV. The analysis was carried out at the Pharmacology Research Division, Department of Medical Research (Pyin Oo Lwin Branch).

Elemental Analysis of Polymer Samples by WDXRF

Relative abundance of elements of the polymer samples were determined by WDXRF (Wavelength Dispersive X-ray Fluorescence)at Department of Research and Innovation on Science, Yangon. In this analysis the sample powders were used.

Results and Discussion

Identification of Types of Polymer Samples by FT IR

In this FT IR analysis, Raman of Basic Monomers and Polymers data-base library software was applied for polymer identification.

The FT IR spectrum of Yoghurt bottle sample is shown in Figure 1 and the compared FT IR spectrum of Yoghurt bottle sample with library software are shown in Figure 2. According to the FT IR spectra, the Yoghurt sample was confirmed as a type of polyethylene polymer. All of the absorption maxima of the individual peaks in the sample are consistent with those of library spectrum of polyethylene polymer. It was found that asymmetric and symmetric stretching vibrations of C- H appeared at 2920 cm^{-1} and 2850 cm^{-1} respectively. Moreover, CH_2 bending at 1470 cm^{-1} and CH_2rocking at 730 cm^{-1} (Jung *et al*., 2018) were also observed in FT IR spectrum of Yoghurt bottle sample.

The FT IR spectrum of the disposable cup sample is shown in Figure 3 and the compared FT IR spectrum of the disposable cup sample with library software is shown in Figure 4.Based on the observed absorption maxima of the sample and those of library spectrum, the major peaks are found relatively in the same position and the library software also showed that the disposable cup sample was polypropylene sample. Asymmetric and symmetric stretching vibrations of C-H appeared at 2950 $cm^{-1}$and 2830 cm^{-1}, respectively. The peaks at 1450 $cm^{-1}$and 1370 cm^{-1} are due to CH_2 bending and CH_3 bending respectively. The peaks due to CH_3 rocking appeared at 1150 cm^{-1},1000 cm^{-1} and 970 cm^{-1} and CH_2 rocking appeared at 830 cm^{-1} and 811 cm^{-1} (Jung *et al*., 2018).

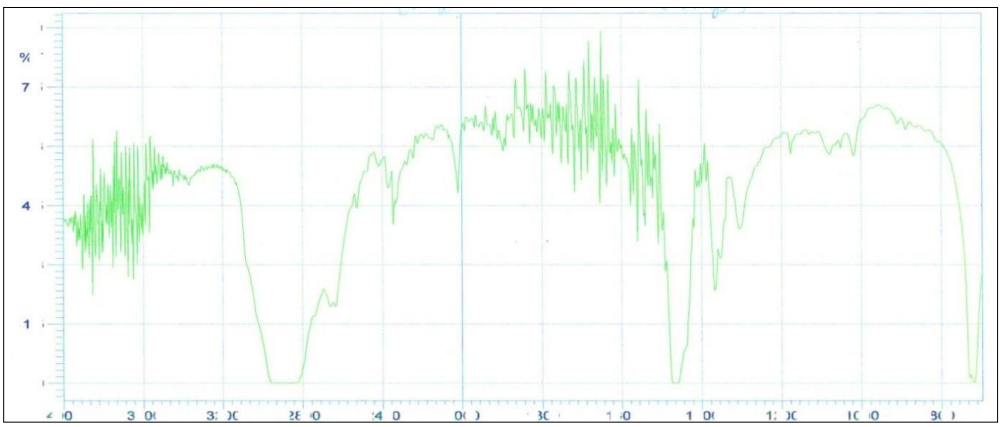

Figure 1: FT IR spectrum of Yoghurt bottle sample

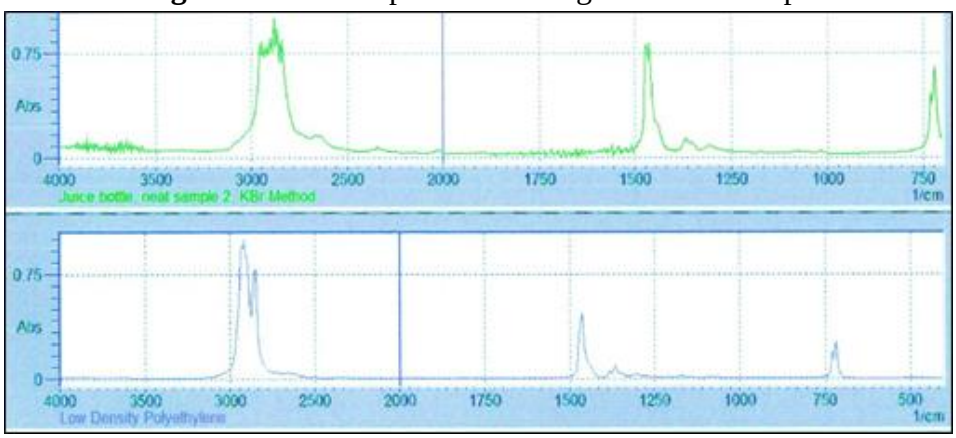

Figure 2: Comparison of FT IR spectra of Yoghurt bottle sample and library spectral data

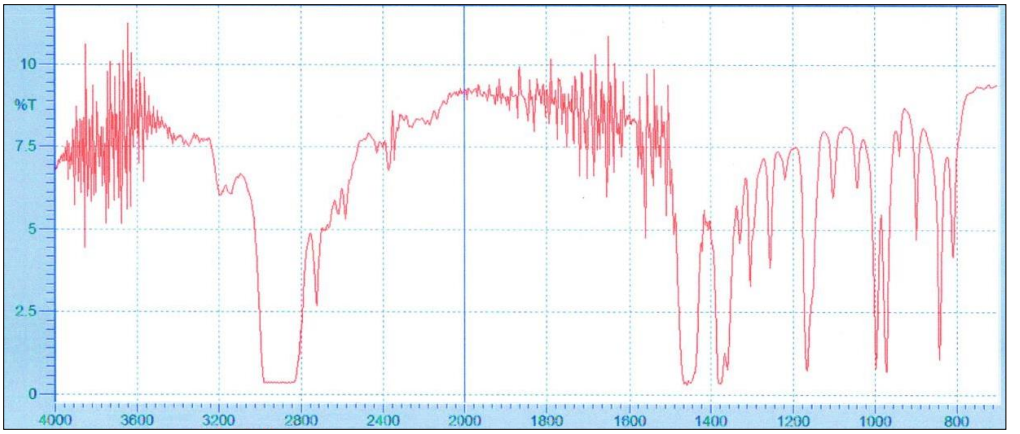

Figure 3: FT IR spectrum of disposable plastic cup sample

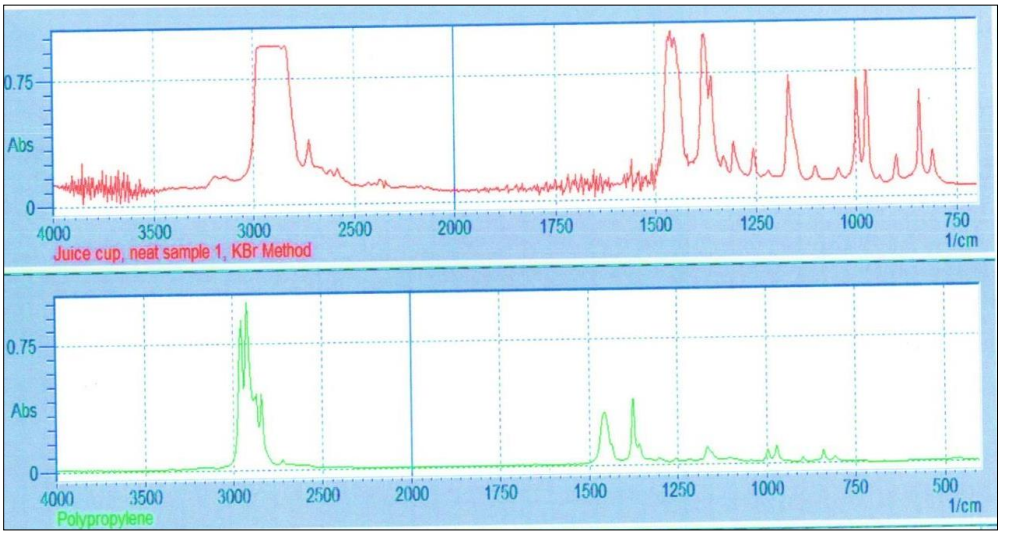

Figure 4: Comparison of FT IR spectra of disposable plastic cup sample and library spectral data

Migration Percents of High Density Polyethylene (HDPE) and Polypropylene (PP) Polymers

In the extraction of polymer components from the confirmed type of polymer samples, the migration percent of polymer constituents were directly calculated based upon the water extract and chloroform extract. But the migration percent into the oil was calculated by using 95 % ethanol

(Cromptom, 2007) due to the fact that both of the polymer samples were partially dissolved into the oil during extraction. The migration percents of HDPE polymer into water, chloroform and oil were found as 0.11 %, 0.81 % and 0.06 % while those of PP polymer into water, chloroform and oil were 0.34% ,1.35% and 0.07 %, respectively (Table 1).

Table 1: Migration Percents of HDPE and PP Polymers

No.	Type of Polymer	Migration percent (%)		
		Water	Chloroform	Olive Oil
1.	HDPE	0.11	0.81	0.06
2.	PP	0.34	1.35	0.07

Identification of Polymer Components by GC-MS

GC/MS-QP 2020 was applied for identification of plasticizers, NIAS and other extractable matters from the polymer samples. The compounds found in the three different extracts were compared with mass spectra of compounds in National Institute of Standard and Technology (NIST) libraries which can be applied as data-base software.

Identification of polymer components from the $CHCl_3$ extract of HDPE polymer

A total of twelve compounds were found in the gas chromatogram of chloroform extract of polyethylene polymer that can be divided into three main groups (Figures 5 and 6 and Table 2), namely: (1) aromatic hydrocarbon compound (2) long chain hydrocarbon compound and (3) fatty alcohol and methyl ester of long chain fatty acid(both saturated and unsaturated).

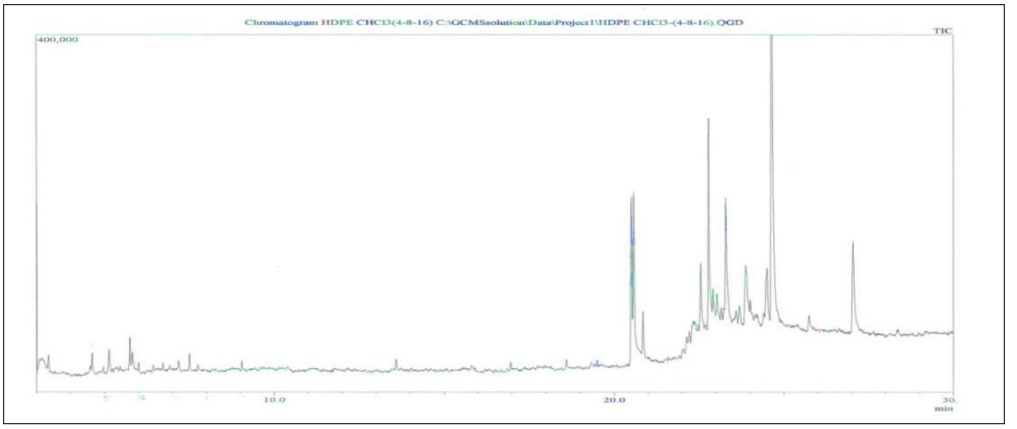

Figure 5: Gas chromatogram of $CHCl_3$ extract of HDPE sample

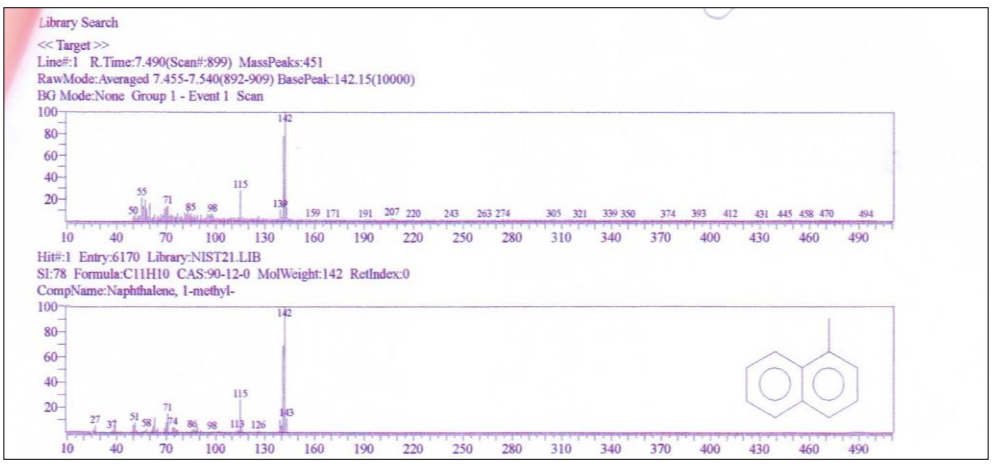

Figure 6: Mass spectrum of compound (retention time 7.49 min)from $CHCl_3$ extract

Long chain hydrocarbon found in the chloroform extract of polyethylene polymer was dotriacontane, $C_{32}H_{66}$. This compound is a normal alkane present in a typical middle range wax. This compound is used in polymer additives for diffusivity purpose. This type of long chain hydrocarbons compounds are also used for flexibility of polymer as the plasticizer or external lubricant in polymerization process (Fulmer,2000). Some of the migrant compounds in the chloroform extract are likely to be the oligomer components which come from the degradation product of polymer backbone. Therefore, this type of migrant compounds may be intentionally

added plasticizer or oligomer migrant compound. But, its relative percent area is very little (0.72%) among all of additives. Sometime this type of compound also occurs in some food such as butter, vinegar, and coffee for aroma carrier when taken into body serve to nourish and supply body heat (Dorland, 2007). Therefore, the health problem due to this compound is not considerable.

The fatty alcohol in chloroform extract was 2-hexadecanol. The fatty alcohols are obtained from the natural fats and oil or petrochemical sources. They are also used in the polymer production as the internal lubricant (semi-soluble plasticizer). Typical lubricants are fatty alcohols (C_{12}–C_{22}) or fatty acids (C_{14}–C_{18}). Therefore, these compounds might be leached out as product of polymeric lubricant, plasticizer.

Table 2: Identification of Polymer Components from the Chloroform Extract of HDPE Polymer

No.	Name of Compound	Retention time (min)	Base m/z	SI	A%
1.	1,2,4,5-tetramethyl Benzene	5.12	119.10	78	1.49
2.	Naphthalene	5.73	128.10	94	1.63
3.	1-ethyl-4-(1-methyl ethyl)- Benzene	5.80	133.15	82	0.43
4.	2-methyl Naphthalene	7.49	142.15	78	0.33
5.	Dotriacontane	13.58	57.10	84	0.72
6.	2-Hexadecanol	16.97	57.10	80	0.34
7.	9,12-Octadecadienoic acid methyl ester	20.50	67.05	95	8.80
8.	Methyl hexadecadienoate	20.57	55.10	89	7.87
9.	Eicosanoic acid methyl ester	22.79	74.05	84	10.75
10.	6,9,12,15-Docosatetra-enoic acid, methyl ester	23.30	93.10	82	6.87
11.	20-methyl-heneicosanoic acid methyl ester	24.64	74.05	92	45.62
12.	Heneicosanoic acid methyl ester	27.04	74.05	78	7.14

m/z- mass to charge ratio, SI- similarity index, A %-relative area percent

Six methyl esters of long chain fatty acid found in chloroform extract of PE polymer were 9,12-octadecadienoic acid methyl ester, methyl hexadecadienoate, eicosanoic acid methyl ester, etc.. All of these compounds are biodiesel components. According to chromatogram, these fatty acid methyl ester (FAME) compounds are most abundance compared to all of additives found. Among all FAME compounds, heneicosanoic acid methyl

ester, a type of saturated fatty acid ester is the highest in relative content. The migration of these compounds may have a worse effect on cholesterol level because "low in saturated fat" and "low in cholesterol".

Then, fatty acids are frequently used in food packaging products as antistatic agents and ester of fatty acid, fatty acid methyl ester (FAME) can be formed trans-esterification of fatty acid with methanol. Sometime, these FAME compounds are usually come from vegetables oil and used in polyethylene production as lubricants to ensure proper mold release, processing aid (Fulmer, 2000). Therefore, these substances are assumed to be the intentionally added substances.

The other leachable compounds found from the chloroform solvent are aromatic hydrocarbon compound, 1,2,4,5-tetramethyl benzene, naphthalene, 1-ethyl-4-(1-methyl ethyl)- benzene, 1-methyl naphthalene and their relative percents of total chromatogram are 1.49%, 1.63%, 0.43% and 0.33% respectively.1,2,4,5-tetramethyl Benzene is used for curing agents, adhesives, coating materials or cross-linking agent in polymer production. The LD_{50} value of this compound is 6989 mg/kg (oral, rat) and thus it is not listed as a carcinogen by any association such as IARC (2002) .

Naphthalene is used as a secondary plasticizer in plastic and resin and also in fuels and dyes. It is usually made from crude oil or coal tar. This compound had been defined a possibly human carcinogenic compound based on the results of animal studies (IARC,2002). A large amount of naphthalene may damage or destroy some of red blood cells and can cause hemolytic anemia (PubChem, 2005).1- Methyl naphthalenes are also used to make dyes, and resins. Naphthalene and naphthalene related compounds are same toxic manner according to ATSDR, (2005).Therefore, it can be concluded that these aromatic hydrocarbon compounds are assumed to be intentionally added substances that are not appropriate for human health. But their percent migrations found in this study were very low.

Identification of polymer components from the water extract of polyethylene polymer

In the gas chromatogram of water extract of polyethylene polymer, only five small speaks were observed (Figure 7). According to library mass

spectral analysis, most of the components in water extract are fatty acid methyl ester (FAME) compounds and only one component is one kind of medium chain aldehyde, nonanal(Figure 8 and Table 3). Nonanal is used as processing aid in industrial and lubricants and greases for commercial usage. Most aldehyde compounds are relatively reactive compound and has significant genotoxic effect at higher concentrations and mutagenicity for mammalian cells was observed with concentrations of 0.1-0.3 mM (Pub Chem, 2005). But relative abundance of this compound is very small and the content is at about 5.44%(of total migration percent into water, 0.11 %) compared to other components.

These FAME compounds in water extract were fatty acid derivatives of natural sources, such as vegetable oil, wax or animals' fat. But, the molecular ion peaks of every compound found from these extract are very small intensities when compared to others two extracts, therefore, the relatives concentrations of migrant compound will be very low levels. So, the adverse health effect due to the presence of these compounds will be very low. From this finding, the food containers of PE polymer were appropriate for watery food types.

Figure 7: Gas chromatogram of water extract of HDPE sample

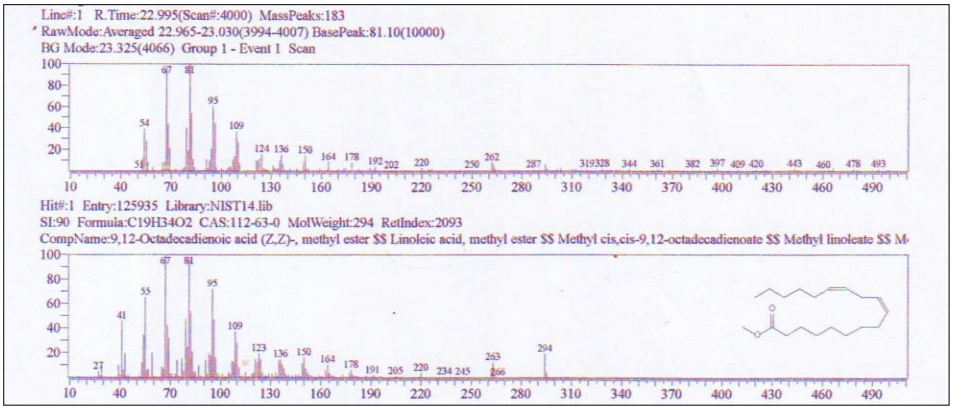

Figure 8: Mass spectrum of compound (retention time 22.99 min)from water extract of HDPE sample

Table 3: Identification of Polymer Components from the Water Extract of HDPE Polymer

No.	Name of Compound	Retention time (min)	Base m/z	SI	A%
1.	Nonanal	7.01	57.10	86	5.44
2.	Palmitic acid, methyl ester	21.09	74.05	92	16.45
3.	Linoleic acid, methyl ester	22.99	67.05	90	17.49
4.	9-octadecenoic acid(oleic acid), methyl ester	23.06	55.05	92	34.33
5.	Lignoceric acid, methyl ester	29.50	74.05	83	26.30

m/z - mass to charge ratio, SI - similarity index, A %-relative area percent

Identification of polymer components from the oil extract of HDPE polymer

The polymer components found in the oil extract of polyethylene polymer can be categorized into five main groups (Figures 9 and 10 and Table 4) namely: (1) long chain fatty alcohol, aldehydes and acids, (2) bicyclic compound (2-vinylbicyclo[2,1,1] hexan-2-ol), (3) epoxy compound, (4) thio compounds and (5) ether compound.

The usage of long chain fatty compounds in polymer production and their health effects were discussed in the previous section. Very long-chain fatty alcohols, fatty aldehyde, and fatty acid are reversibly inter-converted in a fatty alcohol cycle (Lunn and Theobald, 2006). Therefore, these compounds might be either intentionally added substances or inter-converted compounds of fatty alcohols.

The bicyclic compound found in the oil extract of polyethylene polymer is 2-Vinylbicyclo [2,1,1] hexan-2-ol. The various compounds that contain the vinyl (C_2H_3) group are used to make plastics, fabrics, phonograph recorder and paints for get tough, flexible, shiny plastics. The exact safety information of this compound is not available at the present although 4-Vinylcyclohexene is classified as a group2B (possible carcinogen) (IARC, 2002).

Another potential migrant compound found from the oil extract of PE polymer is epoxy compound, 2,3-epoxy-1-dodecyloxy propane. In the production of food packaging polymer, modified vegetable oil, alkyl aromatic sulfonate, polyol ester and cyclohexane diacid ester are also used as alternative plasticizers (Singh *et al.*, 2012). Epoxidised vegetables oil such as epoxidised soybean oil (ESBO) is used in a range of plastic, as a green plasticizer instead of phthalate plasticizer in food packaging materials (Hammarling *et al*., 1998). Generally, ESBO is also used in various food-packaging plastics as heat stabilizers, and also as lubricants and plasticizers (Boussoum *et al*., 2006). Therefore, the epoxy compound found in the oil extracts may be intentionally added substances.

The epoxidized oil and their derivatives are similarity in physicochemical properties, and absorbed and metabolized manner also similar to vegetable oils. There is no evidence concern with these compound groups to be carcinogenic, genotoxic or to have reproductive or developmental toxicity (OECD, 2006). It has been defined tolerable daily intake (TDI) for 1 mg/kg body weight and does not exceed 0.2 mg/kg from food package by the European Food Safety Authority (EFSA, 2006).

The thio compounds found in the oil extract of polyethylene polymer are N-(2-methyl-3-oxobutyl)-S-methyl dithiocarbamate and 3-methyl-4-(phenylthio)-2-prop-2-enyl-2,5-dihydro-thiophene 1, 1-dioxide. Actually,

dithiocarbamate compounds are one kind of pesticide which is used in farming of edible fruits that can produce thyroid cancer(USEPA, 2001). It has been shown to cause reproductive and birth defects in laboratory animals in long-term exposure. But, sulfur-containing antioxidants (such as dialkyl thiocarbamate, distearyl thiodipropionate) are added to various polymers (including PE) with phenolic antioxidants to get synergistic interaction between additives. This blend of phenolic antioxidants and divalent sulfur compound provides excellent combination for improving a polymer's long-term thermal stability.

Ether compound found in these extract is di-n-decyl ether, which may come from impurities of engineering machine or recycling process because polyether ether ketone polymers are used in engineering bearing (ball and roller) applications. Therefore, this type of migrant compounds may be non-intentionally added substances.

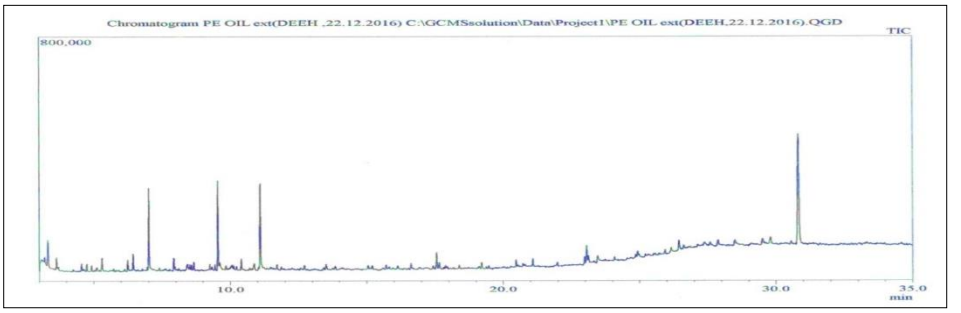

Figure 9: Gas chromatogram of oil extract of PE sample

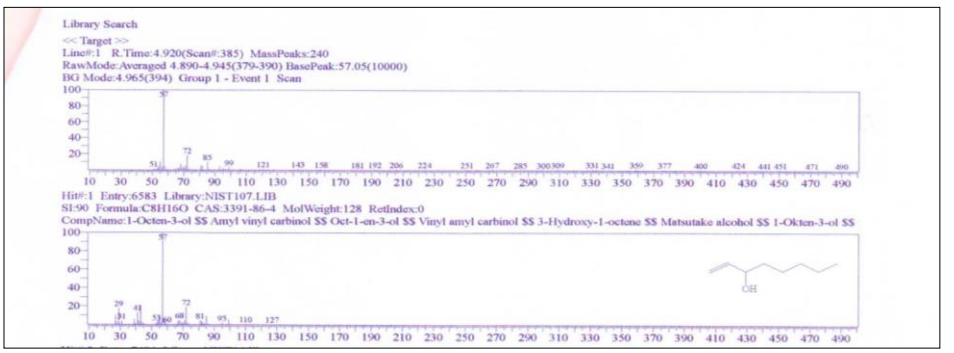

Figure 10: Mass spectrum of compound (retention time 4.92min) from oil extract of PE sample

Table 4: Identification of Polymer Components from Oil Extract of Polyethylene Polymer

No.	Name of Compound	Retention time(min)	Base m/z	SI	A%
1.	2-Vinylbicyclo[2,1,1] hexan-2-ol	3.64	91.05	92	1.19
2.	(E)-2-Heptenal	4.55	83.05	88	0.80
3.	1-Octan-3-ol	4.92	57.05	80	0.65
4.	Octanal	5.31	56.05	83	1.48
5.	(E)-2-Decenal	6.24	91.10	79	1.61
6.	E-11,13-Tetradecadiene-1-ol	6.43	56.05	85	1.81
7.	Nonenal	7.02	57.05	95	8.77
8.	2-hexyl Cyclopropanacetic Acid	8.43	58.05	80	1.20
9.	2,3-epoxy-1-dodecyloxy propane	8.58	57.05	81	0.48
10.	n-Decenal	8.66	57.05	83	0.91
11.	3-hydroxy Dodecanoic acid	9.25	71.10	79	0.54
12.	N-(2-methyl-3-oxobutyl)-S-methyl Dithiocarbamate	9.44	85.05	80	0.72
13.	(E)-2-Decenal	9.54	70.05	93	9.78
14.	9-Oxa bicyclo[6,1,0] nonan-4-ol	9.84	57.05	80	0.51
15.	di-n-Decyl ether	10.13	57.10	81	0.29
16.	(E,E)-2,4-Dodecadienal	10.40	81.05	82	1.33
17.	(E)-2-Tridecenal	11.10	70.05	90	10.43
18.	HeptadecanoicacidHeptadecyl ester	13.85	57.10	79	0.67
19.	3-methyl-4-(phenylthio)-2-prop-2-enyl-2,5-dihydrothiophene1,1-dioxide	15.05	57.05	79	0.55
20	12-Heptadecyn-1-ol	16.62	96.10	79	0.75
21	Z-5-Nonadecene	17.56	69.05	86	2.48
22	3-hydroxy-Dodecanoic acid	18.39	57.05	80	0.39
23	Z,Z-8,10-Hexadeca- diene-1-ol	20.42	71.10	83	0.87
24	(Z,Z)-9,12-Octadecadienoic Acid, methyl ester	22.99	67.10	91	0.84
25	Triolein	23.06	55.05	83	2.18

m/z - mass to charge ratio, SI - similarity index, A %- relative area percent

Identification of Polymer Components from the $CHCl_3$ Extract of PP polymer

GC spectrum and MS spectrum of the compounds from the chloroform extract of polypropylene polymer are shown in Figures 11 and 12 respectively. All of the compounds found from the chloroform extract were fatty acid methyl ester (Table 5). So, most of the potential migrant compounds were polymer lubricants. The highest migration percent (83.85%) of total migrants (1.35%) is FAME compound, intentionally added substances and the rest percent will be trace amount of NIAS or impurities.

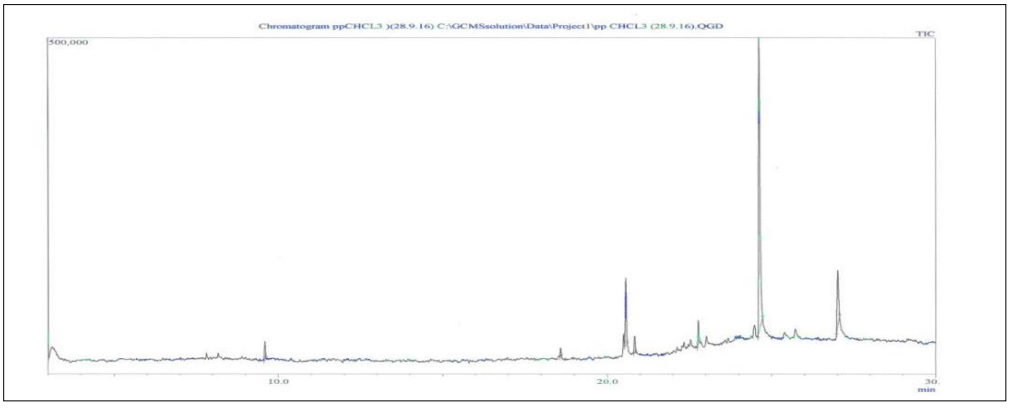

Figure 11: Gas chromatogram of $CHCl_3$ extract of PP sample

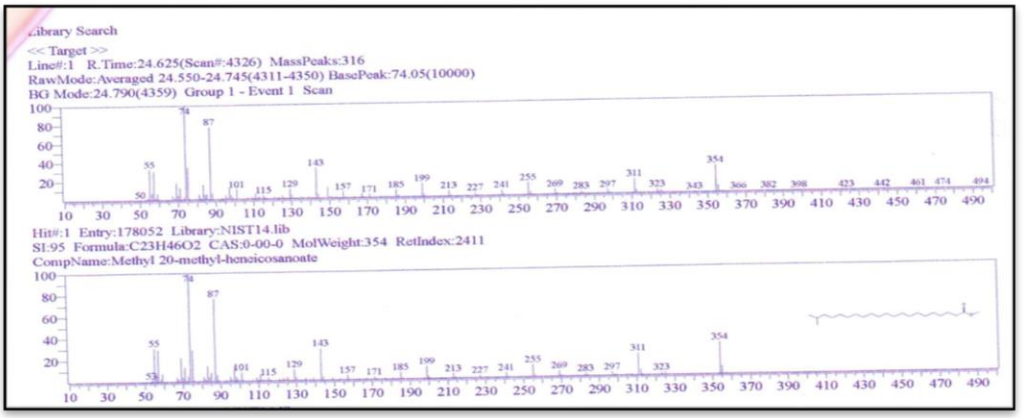

Figure 12: Mass spectrum of compound (retention time 24.63min) from $CHCl_3$ extract of PP sample

Table 5: Identified Polymer Components from the $CHCl_3$ extract of PP Polymer

No.	Name of Compound	Retention time (min)	Base m/z	SI	A%
1.	trans-Cyclopropanepentanoic acid, 2-undecyn-methyl ester	9.95	74.05	81	2.43
2.	12-methyl tetradecanoic acid methyl ester	18.58	74.05	82	1.02
3.	Hexadecanoic acid, methyl ester	20.49	67.05	89	11.25
4.	7-hexadecenoic acid, methyl ester	20.83	74.05	77	2.65
5.	Methyl 20-methyl-heneicosanoate	24.63	74.05	85	66.50
6.	Tetracosanoic acid, methyl ester	27.02	74.05	93	12.57

m/z - mass to charge ratio, SI - similarity index, A % - relative area percent

Identification of polymer components from the water extract of PP polymer

The gas chromatogram of polymer components from the water extract of PP polymer (Figure13).All identified compounds found from the water extract of polypropylene polymer are also FAME compounds (cyclic and straight chain), polymeric lubricants (plasticizers) (Table 6). But, the common used polymeric lubricants are not in the positive additive list. The safety assessment of saturated free fatty acids, the precursor of FAME compounds such as oleic acid, lauric acid, palmitic acid, myristic acid, and stearic acid shows that high intake has been associated with the incidence of atherosclerosis and thrombosis (Pub Chem, 2005). Chronic Exposure to palmitic acid is related to breast carcinomas and "leukemia-lymphoma" in animal study. These fatty acids are also related to insulin secreting function of islet beta-cells and CNS function (Warnotte *et al*., 1999).

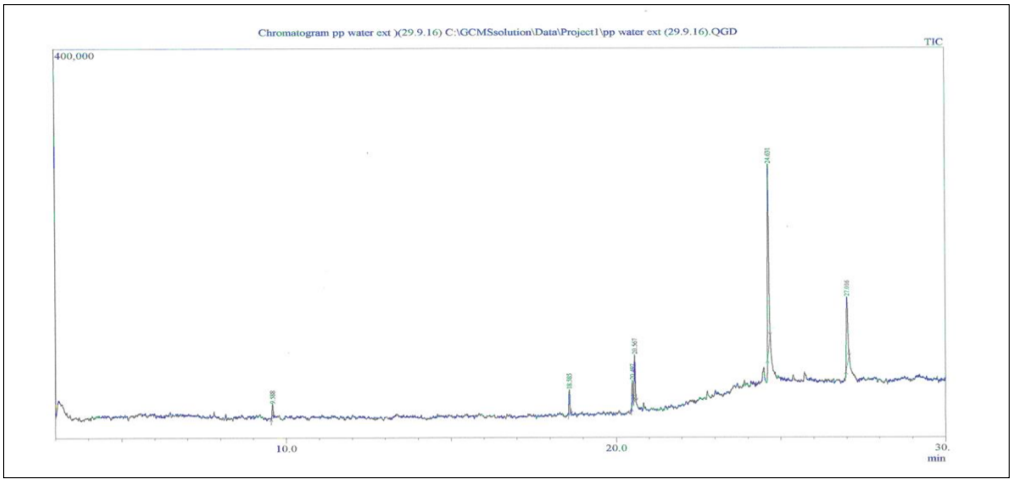

Figure 13: Gas chromatogram of water extract of PP sample

Table 6: Identification of Compounds from the Water Extract of PP Polymer

No.	Name of Compound	Retention time (min)	Base m/z	SI	A%
1.	Tras-2-Undecyl-cyclopropanepenoic acid, methyl ester	9.59	74.05	78	3.64
2.	Hexadecanoic acid, methyl ester	18.58	74.05	93	5.20
3.	9,12- Octadecenoic acid(Z,Z)-methyl ester	20.49	67.05	91	4.80
4.	7-octadecenoic acid, methyl ester	20.56	55.10	89	0.18
5.	Methyl 20-methyl-heneicosanoate	24.63	74.05	95	52.17
6.	Tetracosanoic acid methyl ester	27.01	74.05	90	24.02

m/z - mass to charge ratio, SI - similarity index, A % - relative area percent

Identification of polymer components from the oil extract of polypropylene polymer

The GC spectrum of the oil extract of PP polymer is shown in Figure 14 and MS spectrum of compound (retention time 18.59 min) is shown in Figure 15.

The oil extract of PP polymer contain the following groups of compound: long chain hydrocarbon compound (-ane, -ene, -ald, both cyclic and aliphatic) and fatty acid methyl ester and ketone (Table 7).

The polypropylene polymer is very closely similar to polyethylene polymer. The methyl branch group on polypropylene polymer makes it stronger and more flexible than polyethylene polymer. Their usage of additive may slightly different from each other in the amount and type of additives. From the results, most of the migrant compound groups from the PP polymer are similar to that of PE polymer. The constituents of olive oil (blank) were subtracted from the results.

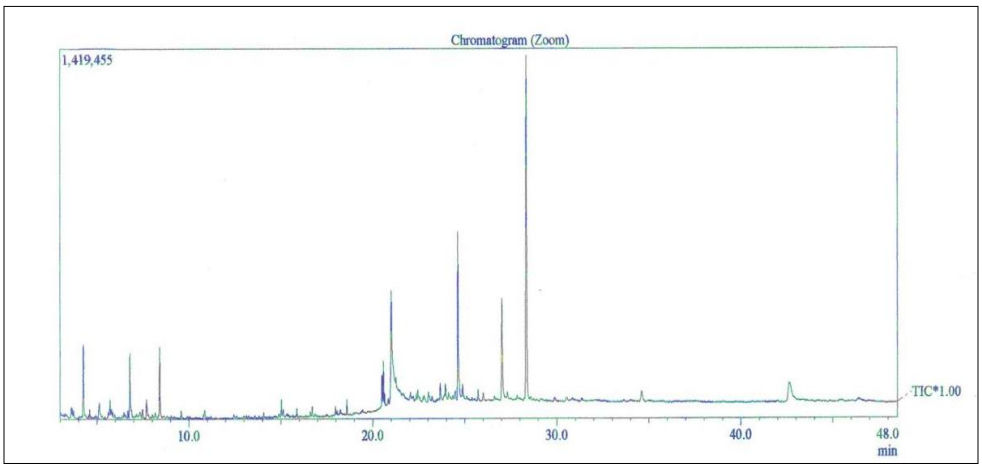

Figure 14: Gas chromatogram of oil extract of PP sample

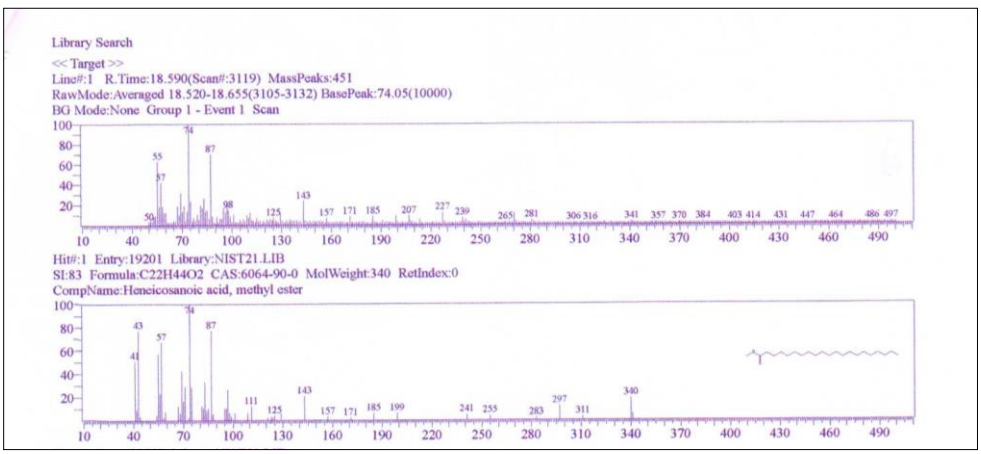

Figure 15: Mass spectrum of compound (retention time 18.59 min from oil extract of PP sample

The long chain hydrocarbon compound (-ane, -ene, -ald, both cyclic and aliphatic), methyl ester of fatty acid and ketone are also used in PP polymer. Their usages and possible health effect were discussed in the migrant compounds groups from PE polymer.

According to the findings, the migration percent of IAS and NIAS from PP polymer is more than that of PE polymer. The migrant compounds released into the organic solvent (chloroform) were more than those into water, nearly seven times in PE polymer (0.81% in chloroform and 0.11 % in water) and four times in PP polymer(1.35% in chloroform and 0.34% in water). This means that watery food have less chance to contain these migrant compounds than other food types, except oily food, because most of migrant compounds are fat soluble. Comparison of two types of polymer, migration amount of polymer additives from PP polymer is more than those from PE polymer. Therefore, it can be concluded that PE polymer is more appropriate for all types of food rather than PP polymer.

Table 7: Identification of Polymer Components from the Oil Extract of PP Polymer

No.	Name of Compound	Retention time (min)	Base m/z	SI	A%
1.	Nonanal	4.26	57.10	94	4.29
2.	(E)-2-Dacenal	6.79	70.05	90	3.30
3.	(E,E)-2,4-Dodecadienal	7.70	81.05	87	1.37
4.	(E)-2-Tridecenal	8.41	70.05	90	4.15
5.	(Z)-Hexadecenoic acid, methyl ester	9.59	74.00	80	0.36
6.	1-Pentadecene	10.86	69.05	87	0.46
7.	Z-5-Nonadecene	15.03	55.05	88	0.88
8.	Cyclooctane (methoxymethoxy)	15.87	56.10	83	0.42
9.	1-Pentadecene	16.70	55.10	87	0.46
10.	9-Octadecenal, (Z)	17.97	55.05	87	0.34
11.	Hexadecenoic acid, methyl ester	18.59	74.05	83	0.66
12.	7-hexadecenoic acid, methylester	20.57	55.05	86	1.87
13.	2-Hydroxy-Cyclo pentadecanone	21.00	55.05	87	14.38
14.	(E,E,E)9-Octadecenoic acid,1,2,3-propanetriyl ester	23.66	55.05	83	0.96
15.	Heneicosanoic acid, methyl ester	27.01	74.05	80	8.87

m/z - mass to charge ratio, SI - similarity index, A % - relative area percent

Elemental Analysis of Polymer Samples by WDXRF

Elemental analysis by WDXRF showed that the common elements found in both types of polymer samples were Ti, Zn, Ca, Fe, Cl, Si, K and Al. Pb and Cu were found only in PE polymer and Ru and S were only in PP polymer (Table 8).

Table8:Relative Abundance of Elements in HDPE and PP Polymer by WDXRF

Elements	Relative Abundance (%)	
	HDPE Polymer	PP Polymer
Al	0.0169	0.0126
Si	0.0291	0.0391
S	-	0.0133
Cl	0.0410	0.0516
K	0.0104	0.0156
Ca	0.1080	0.1230
Ti	1.5200	0.0133
Fe	0.0846	0.0656
Cu	0.0122	-
Zn	0.1380	0.2040
Ru	-	0.0929
Pb	0.0404	-

From the observation of WDXRF spectra, high concentration of Ti element and medium concentration of Pb were observed in PE polymer. Ti is used as catalyzing agent in initial polymerization process. The contamination of Pb can influence the effect of human metabolism. Therefore, Ti may be IAS for the polymerization reaction and Pb may be contaminated from the raw materials sources or engineering process. Therefore, Pb may be NIAS. The other elements found from both types of polymers are not health concern and relatively small in abundance.

Conclusion

According to the results obtained from the FT IR spectra, the type of polymer of the selected Yoghurt bottle was confirmed as polyethylene (PE) polymer and that of disposable plastic cup was polypropylene (PP) polymer. According to GC-MS analyses, most of the additives found in two types of polymer were same chemical nature. The plasticizers mostly found from the two types of polymers are fatty acid methyl esters (FAME) such as tetracosanoic acid methyl ester, hexadecanoic methyl ester and methyl 20-methyl-heneicosanoate. Non-intentionally added substances (NIAS) such as di-n-decyl ether and 2-hydroxy-cyclo pentadecanone which may come from impurities of engineering machine or recycling process were also detected in these types of polymers. The migration percents of HDPE polymer were found to be 0.11 %, 0.81% and 0.06% and those of PP polymer were found to be 0.34%, 1.35% and 0.07% in water, chloroform and oil respectively.This study provided that polypropylene (PP) polymer has more leachable probability of additives than high density polyethylene (HDPE) polymer. The polymer additives compounds of both polymers are more soluble in organic solvent, chloroform, than in water. The migrant compounds in polyethylene and polypropylene food packages were mostly found to be oil soluble compounds. So, the migration would enhance into the oil at the elevated temperature up to 110°C. According to migration manner from this study, it can be concluded that HDPE polymer is more appropriate for the food packaging than PP polymer.

Acknowledgements

The authors would like to thank Professor Dr. Yi Yi Myint (Head of the Department of Chemistry, University of Mandalay) and Board of Directors of Department of Medical Research for their kind permission and supports to do this research work. We are also grateful to the Myanmar Academy of Arts and Science to allow for submission of this research paper.

References

ATSDR.(2005). *Toxicological Profile for Naphthalene, 1-Methyl naphthalene, and 2-Methyl naphthalene*. Atlanta: U.S. Department of Health and Human Services, Public Health Service, Agency for Toxic Substances and Disease Registry

Boussoum, M.O., Atek, D. and Belhaneche-Bensemra, N. (2006).“Interactions between PVC Stabilised with Epoxidized Sunflower Oil and Food Simulants”. *Polymer Degradation and Stability*, vol. 91, pp.579-584

Cromptom, T.R. (2007). *Additive Migration from Plastics into Foods*: *A Guide for Analytical Chemist*. Shawbury, England: Smithers Rapra Publishing

Dorland, W.A.N. (2007). *Dorland's Illustrated Medical Dictionary*. Philadelphia, PA: 31st edition,Saunders

EFSA.(2006). **“**Opinion of the Scientific Panel on Food Additives, Flavourings, Processing Aids and Materials in Contact with Food Related to Exposure of Adults to Epoxidised Soybean Oil Used in Food Contact Materials (Question No EFSA-Q-2005-219)”. *The EFSA Journal*,vol. 293, pp. 1-15

Fulmer, M.S. (2000). *Introduction to Lubricants and Additives for Polymer Compounds*. Quality Additives for Performance.www.struktol.com/pdfs/Lubricants(Accessed 2 September 2017)

Hammarling, L., Gustavsson, H., Svensson, K., Karlsson, S. and Oskarsson, A.(1998). “Migration of Epoxidized Soya Bean Oil from Plasticized PVC Gaskets into Baby Food”. Food Addit-Contam.,vol.15(2),pp. 203-8

IARC.(2002). *Some Traditional Herbal Medicines, Some Mycotoxins, Naphthalene and Styrene*. Lyon, France: IARC Monographs on the Evaluation of Carcinogenic Risk of Chemicals to Humans, International Agency for Research on Cancer, vol. 82

Jung, M.R.,Horgen, F.D., Orski, S.V., Rodriguez, C.V., Beers, K.L., Balazs, G.H., Jones, T.T., Work, T.M., Brignac, K.C., Royer, S.J., Hyrenbach, K.D., Jensen, B.A. and Lynch, J.M.(2018). “Validation of ATR FT-IR to Identify Polymers of Plastic Marine Debris, Including those Ingested by Marine Organisms”. *Marine Pollution Bulletin*,vol. 127,pp.704–716

Kerry, J.P., O’Grady, M.N. and Hogan, S.A. (2006). “Past, Current and Potential Utilisation of Active and Intelligent Packaging Systems for Meat and Muscle-based Products: A Review”. *Meat Science,* vol.74 (1), pp. 113-130

Leivadara, S.V., Nikolaou, A.D. and Lekkas, T.D. (2008) “Determination of Organic Compounds in Bottled Waters*”*. *Food Chemistry*, vol. 108(1), pp. 277-286

Lunn, J. and Theobald, H.E.(2006).“The Health Effects of Dietary Unsaturated Fatty Acids”. Nutrition Bulletin,vol.31,pp. 178-224

OECD. (2006).*Epoxidized Oils and Derivatives*. Paris: Organisation for Economic Co-Operation and Development – Screening Information Data Set (OECD SIDS), UNEP Publications

Pub Chem. (2005). *Open Chemistry Database*. Rockville Pike: National Center for Biotechnology Information, U.S. National Library of Medicine

Singh, P., Saengerlaub, S., Wani, A.A. and Langowski, H.C.(2012). "Role of Plastics Additives for Food Packaging".*Pigment and Resin Technology*, vol.41 (6), pp.368 – 379

USEPA. (2001).*The Grouping of a Series of Dithiocarbamate Pesticides Based on a Common Mechanism of Toxicity* . Washington DC: Environmental Protection Agency

Warnotte, C., Nenquin, M. and Henquin, J.C. (1999).“Unbound Rather than Total Concentration and Saturation Rather than Unsaturation Determine the Potency of Fatty Acids on Insulin Secretion*”*. Molecular and Cellular Endocrinology, vol. 153(1-2),pp.147-153

XANTHONES DERIVATIVES FROM *Cratoxylum cochinchinense* BLUME. AND THEIR CYTOTOXICITIES

Zaw Min Thu[1], Hnin Thanda Aung[2], Rosamaria Lappano[3], Giovanni Vidari[3], Myint Myint Sein[5]

Abstract

Three cytotoxic xanthones (**1-3**), together with other ten known compounds, have been isolated from the barks of *Cratoxylum cochinchinense* Blume. (Mei-thanyo), collected from Kachin State, Northern Myanmar. These structures were established on the basis of extensive spectroscopic methods. Among the isolated compounds, six xanthones and one anthraquinone were evaluated for their cytotoxicities by using the MTT assay. Compound **1** showed a significant cytotoxicity against all tested human cancer cell lines with IC_{50} values in the range 3-9 µM, on average lower than the anticancer drug cisplatin. Compounds **2** and **3** exhibited, instead, high cytotoxicity only against some cell lines. In striking contrast, other compounds showed from moderate to no activity.

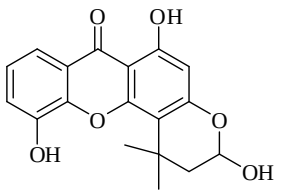

1

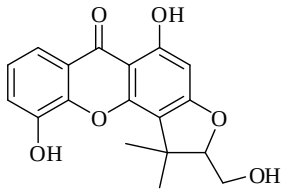

2

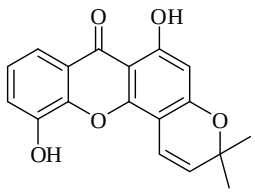

3

Keywords: cytotoxic xanthones, *Cratoxylum cochinchinense* Blume., human cancer cell lines, MTT assay, cisplatin

Introduction

Natural products and their derivatives have been recognized for many years as a source of therapeutic agents and of structural diversity. The relationships of natural products, traditional medicine, and health care seem to be the contemporary situation. Recent reviews have highlighted the continuing

1. Dr, Assistant Lecturer, Department of Chemistry, Kalay University
2. Dr, Lecturer, Department of Chemistry, Kalay University
3. Dr, Professor, Department of Pharmacy of Health and Nutritional Sciences, University of Calabria, Italy
4. Dr, Professor and Director (Retired), Department of Chemistry and CISTRE, University of Pavia, Italy
5. Dr, Professor and Head (Retired), Department of Chemistry, University of Mandalay

role that natural products and structures derived from or related to natural products continue to play in the development of new drugs (Ji *et al*., 2009; Newman and Cragg, 2007). Promising sources of novel bioactive compounds include plants growing in several third world countries where the local flora, is still largely uninvestigated. This is the case of Myanmar, especially in Kachin state.

Cratoxylum cochinchinense Blume. is a small genus belonging to the Clusiaceae (Guttiferae) family, which is found mainly in Southeast Asia. This plant is known as "Mei-thanyo" locally in Myanmar. The bark, roots, and leaves of this plant have been used in traditional medicine to treat fevers, coughs, diarrhoea, itches, ulcers, and abdominal complaints (Vo, 1997). In previous phytochemical studies this plant has been reported to be a rich source of xanthones, triterpenoids, tocotrienols, benzophenones, and bisanthraquinone, among which xanthones are the most abundant metabolites (Boonnak *et al.*, 2009; Duan *et al.*, 2012; Laphookhieo *et al*., 2008; Mahabusarakam *et al*., 2006; Sia *et al.*, 1995; Udomchotphruet *et al*., 2012; Nguyen and Harrison, 1998; Yu *et al*., 2009; Rattanaburi *et al*., 2014). It has also been reported that some of these xanthones possessed significant pharmacological properties, including antimalarial, cytotoxicity, and antibacterial activity (Boonnak *et al*., 2009; Laphookhieo *et al.*, 2006; Mahabusarakam *et al*., 2008). The use of this plant as a traditional medicine, and the earlier interesting results stimulated us to search bioactive compounds from a sample of the plant collected in Northern Myanmar, for which no phytochemical study exists. We have now analysed the MeOH extract of the bark of *C. cochinchinense*, collected from Kachin State, Myanmar. In this investigation, eight known xanthones (**1-8**) and one anthraquinone (**9**), as well as four common triterpenes were isolated. The structures were established by interpretation of their spectroscopic data (^{1}H, ^{13}C, COSY, HSQC and HMBC) analysis as well as comparison with those reported in the literature and some structures were also confirmed by X-ray crystallography. This report also describes the *in vitro* cytotoxic effects of some isolates.

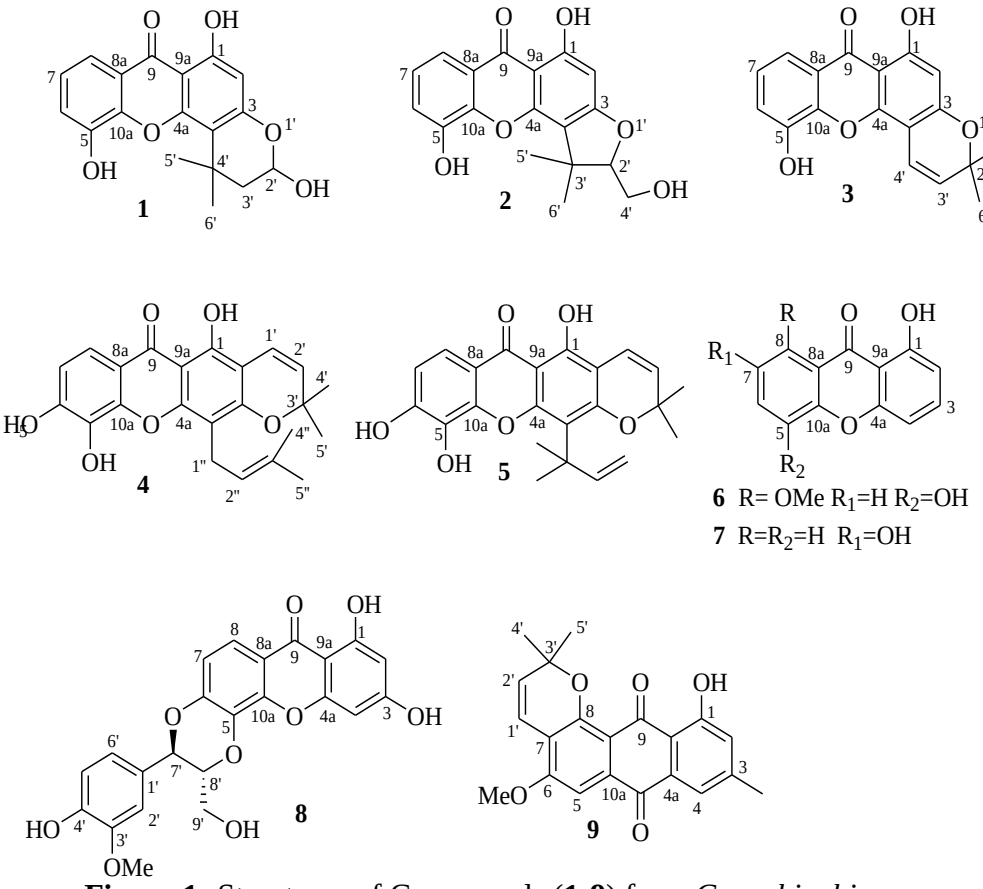

Figure 1: Structures of Compounds (**1-9**) from *C. cochinchinense*

Materials and Methods

Optical rotation was measured with a Perkin-Elmer 241 polarimeter. Infrared spectra were recorded on NaCl disks on an FT IR Perkin Elmer Paragon 100 PC spectrometer; ν in cm^{-1}. NMR experiments were performed on a Bruker AV 300 spectrometer, at 300 MHz (^{1}H) and 75.47 MHz (^{13}C) without TMS or a Bruker 600 MHz (^{1}H) and 150 MHz (^{13}C) with TMS. NMR chemical shifts are reported in ppm and solvent peaks were used as internal standards. The abbreviations s = singlet, d = doublet, dd = double doublet and t = triplet are used throughout; coupling constants (*J*) are reported in Hz. The multiplicity of each carbon atom was determined by DEPT and APT experiments. COSY, DEPT, HSQC, HMBC spectra were recorded using

standard pulse sequences. NMR spectra were recorded in in $CDCl_3$ and MeOH-d_4 (99.8 % deuterium atoms), purchased from Sigma-Aldrich. ESIMS data were recorded on a Thermo TSQ mass spectrometer, by flow injection analysis (FIA), with electron spray ionization source (ESI). High Resolution mass spectra were measured on a FT-ICR Bruker Daltonics Apex II mass spectrometer. For silica gel and reversed phase column chromatography, Merck Kieselgel 60 (40-63 μm) and Merck LiChroprep RP-18 (25-40 μm) were employed, respectively; for direct phase and reversed phase TLC, 0.25 mm silica gel 60 (GF_{254}, Merck) or RP-18 (F_{254}s, Merck), aluminium-supported plates were used. Compounds were visualized under UV light (254 and 366 nm) and, additionally, they were stained by exposure to a 0.5% solution of vanillin in H_2SO_4-EtOH (4:1) or dipping in $KMnO_4$ in acetone, followed by gentle heating at 100 °C. Preparative MPLC separations were performed on a *Isolera* instrument equipped with home-made silica gel and RP-18 filled cartridges and a UV detector. Reagent grade solvents from Aldrich were used for extraction and chromatographic separations.

Plants Materials

The barks of *C. cochinchinense* (Mei-thanyo) were collected near Nam-Pha Lake, about 2.5 km east of the Nam-Pha village, Banmaw Township, Kachin State, Myanmar in December 2012. The plant was analyzed and identified by Professor Dr Htar Htar Lwin, Department of Botany, Banmaw University, Myanmar.

Extraction and Isolation

Chopped, dried barks of *C. cochinchinense* (1 kg) were exhaustively extracted with methanol. Evaporation of solvent under vacuum produced a MeOH extract (29 g) which was partitioned between water and ethyl acetate to give an EtOAc soluble fraction (8.19 g). Subsequently, the EtOAc fraction (8.19 g) was partitioned between hexane and MeCN. Removal of solvents in vacuo (< 40 °C) produced a yellow-brown, viscous hexane fraction (3.24 g) and a dark-brown MeCN fraction (3.61 g), respectively. A sample of the MeCN fraction (1.12 g) was fractionated by column chromatography on RP-18. Elution with a gradient of MeCN in water (from 33 to 100 % MeCN) afforded 10 fractions (A1-A10). Fraction A3 (133 mg) was subjected to

further fractionation, using a silica gel CC. Elution with a gradient of hexane-EtOAc (from 0 to 100 % EtOAc) afforded twelve subfractions (A3.1 - A3.12). CC of fraction A3.2 (4.76 mg) over silica gel yielded 6-deoxyisojacareubin (**3**, 2.4 mg), upon elution with hexane-EtOAc, 9:1. CC of fraction A3.3 (6.4 mg) over silica gel gave pruniflorone N (**1**, 3.3 mg), upon elution with hexane-EtOAc, 4:1. CC of fraction A3.9 (5 mg) on silica gel yielded pruniflorone M (**2**, 2.5 mg), upon elution with hexane-EtOAc, 7:3. In addition, multiple chromatographic separations of the MeCN (2.40 g) and hexane (3.24 g) fractions gave xanthone V_1 (**4**, 3.4 mg), macluraxanthone (**5**, 16 mg), 1,5-dihydroxy-8-methoxyxanthone (**6**, 2.9 mg), 1,7-dihydroxyxanthone (**7**, 3.1 mg), 5'-demethoxycadesin G (**8**, 4.3 mg), vismiaquinone D (**9**, 2.8 mg), α -amyrin (10.7 mg), α -amyrenone (28.7 mg), lupeol (70.5 mg), and lupenone (47.5 mg).

MTT assay

Cell cultures

MCF7 breast and HepG2 hepatocellular cancer cells were maintained in DMEM/F-12 and DMEM, respectively, supplemented with 10 % fetal bovine serum (FBS), 100 mg/mL penicillin/streptomycin and 2 mM L-glutamine (*Life Technologies*, Milan, Italy). SkBr3 breast and BG-1 ovarian cancer cells were cultured in RPMI-1640 and DMEM medium respectively, without phenol red supplemented with 10 % FBS, 100 mg/mL penicillin/streptomycin and 2 mM L-glutamine (*Life Technologies*, Milan, Italy). Ishikawa endometrial cancer cells were maintained in MEM supplemented with 10 % FBS, 100 mg/ml penicillin/streptomycin, 2 mM L-glutamine and 1 % Non-Essential Amino Acids Solution (*Life Technologies*, Milan, Italy). Mesothelioma cancer cells IST-MES1 were maintained in Nutrient Mixture F-10 Ham (*Sigma-Aldrich*, Milan, Italy) supplemented with 20 % FBS, 100 mg/mL penicillin/streptomycin. All cell lines were obtained by ATCC and used less than 6 months after resuscitation, except IST-MES1 cells which were kindly provided by "*Istituto Nazionale per la Ricerca sul Cancro*, Genova, Italy".

Cell proliferation

The effects of each compound on cell viability were determined by using the MTT [3-(4,5-dimethylthiazol-2-yl)-2,5-diphenyltetrazolium bromide] assay, which is based on the conversion of MTT to MTT-formazan by mitochondrial enzyme. 24 Cells were seeded in quadruplicate in 96-well plates in regular growth medium and grown until 70 % confluence. Cells were washed once they had attached and then treated with increasing concentrations of each compound for 48 h in regular medium supplemented with 1 % FBS. The relative cell viability was determined by using the MTT assay according to the manufacturer's protocol (*Sigma-Aldrich*, Milan, Italy). The mean absorbance for each drug dose was expressed as percentage of the cells treated with vehicle absorbance and plotted versus drug concentration. Cisplatin was used as the positive control.

Results and Discussion

Extensive preparative chromatographic separation of the methanol extract of the bark of *C. cochinchinense* on silica gel and reverse phase columns, afforded the xanthones pruniflorone N (**1**), pruniflorone M (**2**) (Boonnak *et al*., 2010), 6-deoxyisojacareubin (**3**) (Sabphon *et al*., 2012), xanthone V_1 (**4**) (Botta *et al*., 1986), macluraxanthone (**5**) (Laphookhieo *et al.*, 2009; Botta *et al*., 1986), 1,5-dihydroxy-8-methoxyxanthone (**6**), 1, 7-dihydroxy xanthone (**7**) (Nagem and de Oliveira, 1997), 5'-demethoxycadesin G (**8**) (Sia *et al.*, 1995), and the anthraquinone vismiaquinone D (**9**) (Reyes-Chilpa *et al*., 2014). In addition, four common triterpenoids, α-amyrin (Chaturvedula and Prakash, 2013), α-amyrenone (de Oliveira *et al*., 2012), lupeol (Jash *et al*., 2013), and lupenone (Ahn and Oh, 2013) were isolated. 1,7-Dihydroxyxanthone (**7**), 1,5-dihydroxy-8-methoxyxanthone (**6**), pruniflorone N (**1**), pruniflorone M (**2**), α-amyrin, α-amyrenone, lupeol and lupenone were isolated for the first time from this plant, while 6-deoxyisojacareubin (**3**) and vismiaquinone D (**9**) were isolated from the genus *Cratoxylum* for the first time.

Structural Elucidation of Isolated Compounds (1-3)

Compound 1 (pruniflorone N)

Compound **1** was isolated as yellow small crystals and was assigned as the molecular formula $C_{18}H_{16}O_6$ on the basis of its ^{13}C NMR data (Table 1) and an ion at *m/z* 327.15 $[M-H]^-$ in the ESIMS spectrum (negative mode), indicating 11 degrees of unsaturation. The FT IR spectrum exhibited absorption bands for hydroxyl (3394 cm^{-1}), chelated aromatic carbonyl (1648 cm^{-1}) and aromatic ring (1578 cm^{-1}).

The presence of a hydroxyl-chelated carbonyl group in a xanthone nucleus was indicated by the quaternary carbon signal at δ_C 182.8 ppm in the ^{13}C NMR spectrum and the singlet at δ_H 13.0 ppm in the ^1H NMR spectrum in Me_2CO-d_6 (Boonnak *et al*., 2010), which was attributed to a phenolic OH group attached to the aromatic quaternary carbon C-1, resonating at δ_C 162.2 ppm in the ^{13}C NMR spectrum. The ^1H NMR spectrum showed a sharp singlet of an isolated aromatic proton at δ_H 6.20 ppm [1H, s (H-2)] and an ABM splitting pattern, attributed to a 1,2,3-trisubstituted benzene ring, at δ_H 7.63 ppm [1H, dd, *J* = 7.7 and 2.0 Hz (H-8)], δ_H 7.27 ppm [1H, dd, *J* = 7.7 and 2.0 Hz (H-6)] and δ_H 7.22 ppm [1H, t, *J* = 7.7 Hz (H-7)]. Characteristic protons resonances of a *gem*-dimethyl-substituted δ-lactol ring were evident at δ_H 5.43 ppm [1H, dd, *J* = 8.5 and 2.5 Hz (H-2')], 1.97 ppm [1H, dd, *J* = 11.2 and 2.5 Hz (H_b-3')], 1.91 ppm [1H, dd, *J* = 11.2 and 8.5 Hz (H_a-3')], 1.60 ppm [3H, s (H_3-5')], and 1.72 ppm [3H, s (H_3-6')]. These ^1H NMR (Table 1) data as well as COSY correlations (Figure 2) suggested for compound **1** a trioxygenated xanthone structure, sharing an oxygen atom with a fused δ-lactol ring.

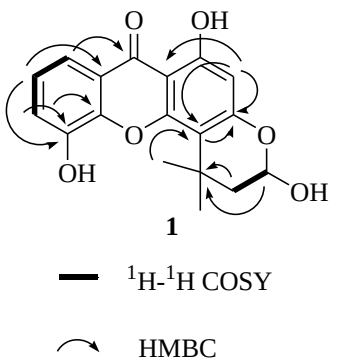

Figure 2: Selected COSY (bold bond) and key HMBC correlations of compound 1

In the HMBC spectrum (Figure 2), the most deshielded aromatic proton (δ_H 7.63) showed a correlation to the carbonyl carbon (δ_C 182.8), revealing its attachment to C-8. On the other hand, in the ^{1}H NMR spectrum, H-8 appeared as a double-doublet with *ortho*- and *meta*- coupling constants (J = 7.7 and 2.0 Hz), indicating that its *ortho*-coupled partner (δ_H 7.22, t, J = 7.7 Hz) and *meta*-coupled partner (δ_H 7.27, dd, J = 7.7 and 2.0 Hz) had to be positioned at C-7 and C-6, respectively. In addition to HMBC correlations with the *ortho*-protonated aromatic carbon (δ_C 115.8, C-8) and one oxygenated aromatic carbon (δ_C 148.3, C-5), the H-7 proton was correlated with a quaternary aromatic carbon (δ_C 122.5), which was then identified as C-8a. This pattern was confirmed by HMBC correlations of H-6 with C-8, C-5 and another oxygenated quaternary aromatic carbon resonating at δ_C 146.7, which was assigned to C-10a. These data firmly identified the carbon and hydrogen atoms of the C-ring of the xanthone nucleus, including an OH substituent at C-5.

The upfield shifted isolated aromatic proton, resonating at δ_H 6.20 in the ^{1}H NMR spectrum of **1**, was identified as H-2, on the basis of the resonance at δ_C 100.2 of C-2, identified in the HSQC spectrum. This value nicely corresponded to the chemical shifts determined for the C-2 carbons of 1,3-dioxygenated xanthones (Boonnak *et al*., 2010). Accordingly to this assignment, H-2 correlated to two oxygenated aromatic carbons, occurring at δ_C 162.2 and 161.9, respectively, which were identified as C-1 and C-3, and to two quaternary aromatic carbons, occurring at δ_C 105.3 and 111.0, respectively, which were identified as C-9a and C-4, respectively.

The 6-hydroxy-4,4-dimethyldihydropyran ring and its angular fusion to the C-3 and C-4 of the xanthone nucleus were established on the basis of HMBC correlations (Figure 2) of the hemiacetal methine proton (δ_H 5.43) to C-4' (δ_C 33.4) and C-3' (δ_C 47.2), the H_b-3' proton (δ_H 1.97) to C-4' (δ_C 33.4), and the methyl protons H_3-5' (δ_H 1.60) and H_3-6' (δ_H 1.72) to C-4 (δ_C 111.0), C-4' (δ_C 33.4), and C-3' (δ_C 47.2). The remaining oxygenated aromatic carbon (δ_C 157.1) was thus assigned to C-4a. The compound was therefore assigned the structure of 3,6,11-trihydroxy-1,1-dimethyl-2,3-dihydropyrano[2,3-*c*] xanthen-7(1*H*)-one, known in the literature with the trivial name of pruniflorone N (Boonnak *et al*., 2010).

Interestingly, although the configuration at C-2' could easily racemize, compound **1** showed a small but not-null positive optical rotation power. The vicinal coupling constants of H-2', J = 8.5 and 2.5 Hz, clearly indicated that this proton was axially oriented; however, the absolute configuration was not established for lack of material. Compound **1** showed potent nitric oxide inhibitory activity *in vitro*, with an IC_{50} value of 4.4 μM, better than that of the positive control indomethacin, which is a well-known non-steroidal anti-inflammatory drug (IC_{50} = 20.1 μM) (Boonnak *et al*., 2010).

Compound 2 (pruniflorone M)

Compound **2** was obtained as a yellow amorphous powder. The molecular formula $C_{18}H_{16}O_6$, was deduced from the NMR data (Table 1) and an ion peak at *m/z* 327.15 $[M-H]^-$ in the ESIMS spectrum (negative mode), indicating 11 degrees of unsaturation. The FT-IR spectrum showed hydroxyl, conjugated carbonyl and aromatic functionalities at 3448 cm^{-1}, 1648 cm^{-1} and 1581 cm^{-1}, respectively. Thus compounds **1** and **2** were isomeric.

Indeed, the NMR data of the protons and carbons of rings B and C and the oxygenation pattern of ring A of compound **2** were almost coincident with those of **1**, while the signals of the heterocyclic rings differ significantly. In fact, compound **2** contained a dihydrofuran instead of a dihydropyran ring. Accordingly, the ^1H NMR spectrum of **2** showed a triplet at δ_H 3.89, integrating for 2H, that was attributed to a hydroxymethyl group (H_2-4'), a doublet at δ_H 4.49, integrating for 1H, coupled (COSY) with a J = 6.0 Hz to the hydroxymethyl group and thus assigned to H-2', and two germinal methyl groups resonating at δ_H 1.44 (H_3-5') and 1.69 (H_3-6'), respectively. Moreover, the two methyl groups showed HMBC correlations (Figure 3) with the oxygenated methine carbon C-2' (δ_C 96.0) and with a quaternary aromatic carbon at δ_C 114.2 (C-4), that also showed a HMBC cross-peak with an isolated aromatic proton resonating at δ_H 6.23 (H-2). The last proton also showed HMBC cross- peaks with another quaternary aromatic carbon at δ_C 104.7, attributed to C-9a, and to oxygenated quaternary aromatic carbons at δ_C 167.6 and 165.5, assignable to C-1 and C-3.

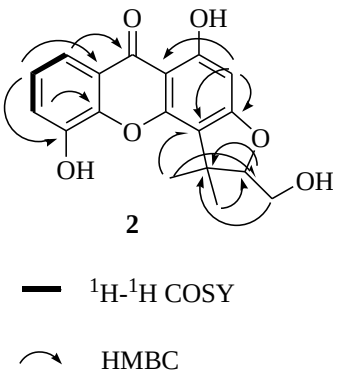

Figure 3: Selected COSY (bold bond) and key HMBC correlations of compound **2**

Consequently, the compound **2** was identified as 5,10-dihydroxy-2-(hydroxymethyl)-1,1-dimethyl-1*H*-furo[2,3-*c*]xanthen-6(2*H*)-one, known in the literature with the trivial name of pruniflorone M (Boonnak *et al*., 2010). Interestingly, the sign of the optical rotatory power of our sample of pruniflorone M was opposite to that reported in the literature (Boonnak *et al*., 2010). Compounds **1** and **2** are very rare in nature and, to the best of our knowledge, they have been isolated before only from another *Cratoxylum* species, namely *C. formosum* ssp *pruniflorum* (Boonnak *et al*., 2010).

Compound 3 (6-deoxyisojacareubin)

Compound **3** was a bright yellow amorphous solid, showed the molecular formula $C_{18}H_{14}O_5$ as determined by the ion peak at *m/z* 309 $[M-H]^-$ in the ESIMS spectrum (negative mode) and the ^{13}C NMR data, requiring 12 degrees of unsaturation. The FT IR spectrum showed the presence of hydroxyl (3417 cm^{-1}), conjugated carbonyl (1651 cm^{-1}) and aromatic ring (1574 cm^{-1}).

The presence of a chelated carbonyl group in a xanthone nucleus was indicated by the quaternary carbon signal at δ_C 182.5 ppm in the ^{13}C NMR spectrum and the singlet at δ_H 13.0 ppm in the ^{1}H NMR spectrum in Me_2CO-d_6 (Sabphon *et al.*, 2012). The ^{1}H NMR spectrum in MeOH-d_4 revealed the signals of an isolated aromatic proton at δ_H 6.19 ppm [1H, s (H-2)] and the ABM splitting pattern of a 1,2,3-trisubstituted benzene ring at δ_H 7.66 ppm [1H, dd, J = 7.7 and 2.0 Hz (H-8)], 7.28 ppm [1H, dd, J = 7.7 and 2.0 Hz

(H-6)] and 7.23 ppm [1H, t, J = 7.7 Hz (H-7)]. In addition, the presence of a dimethyl-substituted chromene ring was indicated by two doublets, each assigned to an olefinic proton, at δ_H 7.03 ppm [1H, d, J = 10.1 Hz (H-4')] and 5.72 ppm [1H, d, J = 10.1 Hz (H-3')], respectively, and one singlet at δ_H 1.48 ppm, integrating for 6H of two coincident methyl groups (H_3-5' and H_3-6'). The remaining atoms of the chromene ring were identified in the ^{13}C NMR spectrum as one oxygenated quaternary sp^3 carbon at δ_C 79.5 ppm (C-2'), carrying the geminal methyl groups H_3-5' and H_3-6', and two quaternary sp^2 carbons at δ_C 102.7 ppm (C-4) and 162.3 ppm (C-3), the latter bonded to the oxygen of the pyran ring. HMBC correlations (Figure 4) were fully consistent with these assignments.

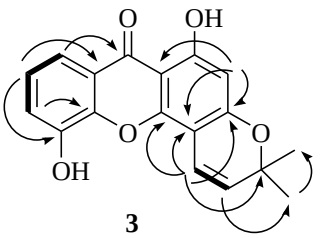

3

^1H-^1H COSY

HMBC

Figure 4: Selected COSY (bold bond) and key HMBC correlations of compound **3**

In the HMBC spectrum (Figure 4), the most deshielded aromatic proton (δ_H 7.66) correlated to the carbonyl carbon (δ_C 182.5), revealing its attachment to C-8. Its *ortho*-coupled proton (δ_H 7.23), bonded at C-7, showed correlations through three bonds with a phenolic carbon (δ_C 147.7, C-5) and a quaternary aromatic carbons (δ_C 122.6) which was assigned to C-8a. On the other hand, the H-6 proton gave a cross-peak with another oxygenated aromatic carbon (δ_C 146.9) which was assigned to C-10a. These data firmly identified the carbon and hydrogen atoms of the C-ring of the xanthone nucleus, including an OH substituent at C-5. The angular fusion of the pyran ring at C-3 (δ_C 162.3) and C-4 (δ_C 102.7) of the xanthone nucleus was clearly indicated by the HMBC correlation of H-4' (δ_H 7.03) with the oxygenated quaternary sp^2 carbon at δ_C 153.0, that was assignable to C-4a. As a further evidence of this attribution, the carbon bearing the most shielded

aromatic proton (δ_H 6.19) resonated at δ_C 99.9, consistent with the chemical shift expected for the C-2 of 1, 3-dihydroxyxanthones (Sabphon *et al.*, 2012), while the attached proton H-2 showed HMBC correlations with two oxygenated aromatic carbons (δ_C 162.3 and 164.2) which were C-3 and C-1. Compound **3** was thus assigned the structure of 6,11-dihydroxy-3,3-dimethylpyrano[2,2-*c*] xanthen-7(3H)-one, known in the literature with the trivial name of 6-deoxyisojacareubin (Sabphon *et al.*, 2012).

Table 1: ^{1}H NMR (300 MHz) and ^{13}C NMR (75.47 MHz) Spectroscopic Data for Compound 1-3 (in MeOH-d_4, □ in ppm, *J* in Hz)

Position	1		2		3	
	^{1}H NMR	^{13}C NMR	^{1}H NMR	^{13}C NMR	^{1}H NMR	^{13}C NMR
1	-	162.2, C[a]	-	167.6, C[a]		164.2, C
2	6.20, s	100.2, CH	6.23, s	94.4, CH	6.19, s	99.9, CH
3	-	161.9, C[a]	-	165.5, C[a]		162.3, C
4	-	111.0, C	-	114.2, C		102.7, C
5	-	148.3, C	-	148.0, C		147.7, C
6	7.27, dd (7.7, 2.0)	120.7, CH	7.26, dd (7.7, 2.0)	121.2, CH	7.28, dd (7.7, 2.0)	121.9, CH
7	7.22, t (7.7)	125.0, CH	7.20, t (7.7)	125.0, CH	7.23, t (7.7)	125.2, CH
8	7.63, dd (7.7, 2.0)	115.8, CH	7.64, dd (7.7, 2.0)	116.2, CH	7.66, dd (7.7, 2.0)	116.5, CH
9	-	182.8, CO	-	182.3, CO	-	182.5, CO
4a	-	157.1, C	-	154.0, C	-	153.0, C
10a	-	146.7, C	-	147.8, C[c]	-	146.9, C[c]
8a	-	122.5, C	-	122.7, C	-	122.6, C
9a	-	105.3, C	-	104.7, C[c]	-	104.3, C[c]
1'	-	-	-		-	-
2'	5.43, dd (8.5, 2.5)	94.2, CH	4.49, t (6.0)	96.0, CH	-	79.5, C
3'	1.97, dd (11.2, 2.5) 1.91, dd (11.2, 8.5)	47.2, CH_2		44.4, C	5.72, d (10.1) -	128.4, CH
4'	-	33.4	3.89, d (6.0)	61.7, CH_2	7.03, d (10.1)	164.2, C
5'	1.60, s[a]	28.9,CH_3[b]	1.44, s[a]	21.1, CH_3[b]	1.48, s	28.6, CH_3
6'	1.72, s[a]	29.1,CH_3[b]	1.69, s[a]	27.1, CH_3[b]	1.48, s	28.6, CH_3
1-OH	-	-	-	-	-	-
3-OH	-	-	-	-	-	-
5-OH	-	-	-	-	-	-

[a,b]Assignments in the same vertical column can be interchanged; [c]Chemical shift assigned from HMBC spectra.

Pruniflorone N (**1**): yellow crystals (MeOH); mp >300°C with decomposition, $[\alpha]_D^{20}$ = +2.14 (c = 0.0015, MeOH), Lit. (Boonnak *et al*., 2010): +5.2 (*c* 0.42, Me_2CO); ESIMS *m/z* 327 $[M-H]^-$ for $C_{18}H_{16}O_6$; FT IR (NaCl) ν_{max} 3394, 2958, 1648, 1578, 1420, 1171, 1058 cm^{-1}; ^1H NMR (300 MHz, MeOH-d_4) see Table 1; ^{13}C NMR (75.47 MHz, MeOH-d_4) see Table 1.

Pruniflorone M (**2**): yellow amorphous powder; $[\alpha]_D^{20}$ = -42.8 (c = 0.0012, MeOH), Lit. (Boonnak *et al*., 2010): +64.6 (*c* 0.04, $CHCl_3$); ESIMS *m/z* 327 $[M-H]^-$ for $C_{18}H_{16}O_6$; FT IR (NaCl) ν_{max} 3448, 2974, 2867, 1648, 1581, 1460, 1069, 911 cm^{-1}; ^1H NMR (300 MHz, MeOH-d_4) see Table 1; ^{13}C NMR (75.47 MHz, MeOH-d_4) see Table 1.

6-Deoxyisojacareubin (**3**): bright yellow amorphous powder; ESIMS *m/z* 309 $[M-H]^-$ for $C_{18}H_{14}O_5$; FT IR (NaCl) ν_{max} 3417, 2958, 1651, 1574, 1462, 1062, 761 cm^{-1}; ^1H NMR (300 MHz, MeOH-d_4) see Table 1; ^{13}C NMR (75.47 MHz, MeOH-d_4) see Table 1.

Xanthone V_1 (4): Yellow amorphous; ESIMS $[M-H]^-$ *m/z* 393 for $C_{23}H_{22}O_6$; FT IR (NaCl) ν_{max} 3350, 3054, 2970, 2929, 1651, 1589, 1463, 1265, 1188, 1133, 741 cm^{-1}; ^1H NMR Spectral Data (600 MHz, methanol-d_4): δ 13.18 (1H, s, 1-OH), 7.74 (1H, d, *J* = 8.5 Hz, H-8), 6.96 (1H, d, *J* = 8.5 Hz, H-7), 6.75 (1H, d, *J* = 10 Hz, H-1'), 5.60 (1H, d, *J* = 10 Hz, H-2'), 5.25 (1H, d, *J* = 6.7 Hz, H-2''), 3.50 (2H, d, *J* = 6.7 Hz, H-1''), 1.88 (3H, s, H-4''), 1.73 (3H, s, H-5''), 1.48 (6H, s, H-4' and H-5'); ^{13}C NMR Spectral Data (150 MHz, methanol-d_4): δ 180.9 (C-9), 158.3 (C-3), 156.6 (C-1), 154.3 (C-4a), 149.5 (C-6), 145.5 (C-4b), 130.8 (C-5), 127.7 (C-2'), 123.3 (C-2''), 118.6 (C-8), 116.5 (C-1'), 114.7 (C-8a), 112.9 (C-7), 107.4 (C-4), 105.3 (C-2), 103.3 (C-8b), 78.6 (C-3'), 28.7 (C-4' and 5'), 26.0 (C-4''), 22.1 (C-1''), 18.3 (C-5'').

Macluraxanthone (5): Yellow crystal ($CDCl_3$); mp. 181-182; ESIMS $[M-H]^-$ *m/z* 393.25 for $C_{23}H_{22}O_6$; ^1H NMR Spectral Data (300 MHz, $CDCl_3$): δ 7.69 (1H, d, *J* = 8.8 Hz, H-8), 6.95 (1H, d, *J* = 8.8 Hz, H-7), 6.77 (1H, d, *J* = 10.2 Hz, H-2'), 6.76 (1H, dd, *J* = 17.7 and 10.6 Hz, H-2''), 5.62 (1H, d, *J* = 10.2 Hz, H-1'), 5.22 (1H, d, *J* = 17.7 Hz, H-3a''), 5.05 (1H, d, *J* = 10.6 Hz, H-3b''), 1.65 (6H, s, H-4'' and H-5''), 1.52 (6H, s, H-4' and H-5'); ^{13}C NMR Spectral Data (75 MHz, $CDCl_3$): δ 181.1 (C-9), 159.3 (C-3), 157.2 (C-2''), 157.1 (C-4a), 154.4 (C-1), 149.3 (C-6), 144.9 (C-5a), 131.4 (C-5), 127.5 (C-2'), 117.8 (C-8),

116.4 (C-1'), 114.1 (C-4), 113.4 (C-9a), 113.1 (C-7), 105.9 (C-2), 103.6 (C-3''), 103.4 (C-8a) 78.6 (C-3'), 41.8 (C-1''), 28.3 (C-4' and 5'), 28.5 (C-4'' and C-5'').

1,5-dihydroxy-8-methoxyxanthone (6): Yellow powder ($CDCl_3$); ESIMS $[M+Na]^+$ *m/z* 258 for $C_{14}H_{10}O_5$; FT IR (NaCl) ν_{max} 3359, 2926, 2854, 1651, 1593, 1264, 1070, 739 cm^{-1}; ^1H NMR Spectral Data (600 MHz, $CDCl_3$): δ 12.98 (s, 1-OH), 7.56 (1H, t, *J* = 8.3 H-3), 7.32 (1H, d, *J* = 8.9 Hz, H-6), 6.74 (1H, d, *J* = 8.9 Hz, H-7), 3.99 (3H, s, OCH_3), 6.90 (1H, dd, *J* = 8.3 and 1.1 Hz, H-4), 6.81 (1H, dd, *J* = 8.3 and 1.1 Hz, H-2); ^{13}C NMR Spectral Data (150 MHz, $CDCl_3$): δ 182.9 (C-9), 162.8 (C-1), 155.0 (C-4a), 154.1 (C-8), 145.6 (C-5a), 138.2 (C-5), 136.8 (C-3), 121.3 (C-6), 111.6 (C-8a), 109.6 (C-9a), 111.8 (C-2), 106.3 (C-4), 105.8 (C-7), 56.9 (8-OMe).

1,7-dihydroxyxanthone (7): Yellow needle (MeOH); mp. 150-151°C (Lin *et al*., 1996); ESIMS $[M-H]^-$ *m/z* 257 for $C_{14}H_{10}O_5$; ^1H NMR Spectral Data (300 MHz, methanol-d_4): δ 7.65 (1H, t, *J* = 8.4, H-3), 7.55 (1H, d, *J* = 3.0 H-8), 7.47 (1H, d, *J* = 9.05, H-5), 7.34 (1H, dd, *J* = 9.05 and 3.0 Hz, H-6), 6.98 (1H, dd, *J* = 8.4 and 0.8 Hz, H-4), 6.76 (1H, dd, *J* = 8.4 and 0.8 Hz, H-2); ^{13}C NMR Spectral Data (75 MHz, methanol-d_4): δ 163.2 (C-1), 158.2 (C-4a), 155.9 (C-7), 151.8 (C-5a), 138.2 (C-3), 126.7 (C-6), 122.5 (C-8a), 120.6 (C-5), 110.9 (C-2), 109.5 (C-4), 108.4 (C-8).

5'-demethoxycadesin G (8): White amorphous; ESI-MS $[M-H]^-$ *m/z* 437 for $C_{23}H_{18}O_9$; FT IR (NaCl) ν_{max} 3350, 3054, 2928, 1651, 1574, 1455, 1265, 1103, 738 cm^{-1}; ^1H NMR Spectral Data (600 MHz, methanol-d_4): δ 7.68 (1H, d, *J* = 8.9 Hz, H-7), 7.06 (1H, d, *J* = 1.9 Hz, H-2'), 6.97 (1H, d, *J* = 8.9 Hz, H-8), 6.95 (1H, dd, *J* = 8.1 and 1.9 Hz, H-6'), 6.87 (1H, d, *J* = 8.1 Hz, H-5'), 6.39 (1H, d, *J* = 2.1 Hz, H-4), 6.18 (1H, d, *J* = 2.1 Hz, H-2), 5.10 (1H, d, *J* = 8.1 Hz, H-7'), 4.20 (1H, ddd, *J* = 8.1, 3.8 and 2.3 Hz, H-8'), 3.99 (3H, s, 3'-OCH_3), 3.91 (1H, dd, *J* = 12.7 and 2.3 Hz, H-9'), 3.57 (1H, dd, *J* = 12.7 and 3.8 Hz, H-9'); ^{13}C NMR Spectral Data (150 MHz, methanol-d_4): δ 181.3 (C-9), 167.4 (C-3), 164.7 (C-1), 159.3 (C-4a), 150.7 (C-6), 149.3, (C-3'), 148.7 (C-4'), 147.6 (C-5a), 133.2 (C-5), 128.1 (C-1'), 121.9 (C-6'), 118.1 (C-8), 116.4 (C-5'), 116.1 (C-8a), 114.7 (C-7), 103.4 (C-9a), 112.2 (C-2'), 99.4 (C-2), 95.3 (C-4), 80.1 (C-8') and 78.4 (C-7'), 61.8 (C-9'), 56.5 (3'-OMe).

Vismiaquinone D (9): Yellow powder; ESI-MS $[M+Na]^+$ *m/z* 373.17 for $C_{21}H_{18}O_5$; FT IR (NaCl) ν_{max} 3054, 2978, 1636, 1560, 1266, 1126, 738 cm^{-1}; ^1H NMR Spectral Data (300 MHz, $CDCl_3$): δ 13.20 (1H, s, 1-OH), 7.57 (1H, d, *J* = 1.1 Hz, H-4), 7.44 (1H, s, H-5), 7.07 (1H, d, *J* = 1.1 Hz, H-2), 6.73 (1H, d, *J* = 10 Hz, H-1'), 5.84 (1H, d, *J* = 10 Hz, H-2'), 4.02 (3H, s, 6'-OCH_3), 2.43 (3H, s, H-3), 1.57 (6H, s, H-4' and H-5'); ^{13}C NMR Spectral Data (75 MHz, $CDCl_3$): δ 187.4 (C-9), 182.9 (C-10), 162.8 (C-1), 158.9 (C-6), 156.5 (C-8), 146.9 (C-3), 135.6 (C-4a), 132.8 (C-5a), 132.3 (C-2'), 124.7 (C-2), 119.9 (C-4), 116.5 (C-7), 116.3 (C-1'), 115.6 (C-8a) and 114.9 (C-9a), 103.0 (C-5), 77.9 (C-3'), 56.4 (6-OMe), 28.2 (C-4' and 5'), 22.2 (C-3).

Cytotoxic Activity

The effects of compounds **1-5**, **7**, and **9** on the proliferation of tumor cells were evaluated in comparison with the well-known antitumor drug cis-diamminedichloroplatinum (II) (cisplatin) by using MTT assays. In particular, MCF7 and SkBr3 breast, endometrial Ishikawa, ovarian BG-1, mesothelioma IST-MES1 and hepatocellular HepG2 cancer cells were treated for 48 h with increasing concentrations of tested compounds. Macluraxanthone **(5)**, 1, 7-dihydroxyxanthone **(7)** and vismiaquinone D **(9)** were inactive on all cell lines, whereas xanthone V_1 **(4)** exhibited moderate effects on all cells (Table 2). The most active xanthones of the series were **1-3**. In particular, pruniflorone N (**1**) showed a stronger inhibitory activity than cisplatin on five of the six cell lines, while pruniflorone M (**2**) and 6-deoxyisojacareubin (**3**) were more active on four (MCF7, HepG2, Ishikawa, and BG-1) and two (MCF7 and BG1) types of cells, respectively (Table 2).

Table 2: Cytotoxic Activity of Tested Compounds on Breast MCF7 and SkBr3, Endometrial Ishikawa, Ovarian BG-1, Mesothelioma IST-MES1 and Hepatocellular HepG2 Cancer Cells, after 48 h Treatment, as Determined by Using the MTT Assay. IC_{50} values were calculated by probit analysis (P<0.05, □2 test).

Compound	IC_{50} (μ M)±S.D					
	MCF7	SKBR3	Ishikawa	BG-1	IST-MES1	HepG2
Pruniflorone N (**1**)	7 (±3.1)	9 (±2.4)	7 (±3.7)	3 (±1.6)	5 (±2.8)	6 (±2.4)
Pruniflorone M (**2**)	10 (±2.3)	12 (±2.8)	7 (±1.6)	6 (±1.7)	25 (±4.9)	7 (±1.3)
6-Deoxyisojacareubin (**3**)	6 (±2.2)	7 (±2.3)	>50	7 (±3.1)	>50	>50
Xanthone V_1 (**4**)	20 (±2.2)	19 (±1.9)	21 (±2.3)	25 (±1.7)	20 (±3.3)	18 (±1.6)
Macluraxanthone (**5**)	>100	>100	>100	>100	>100	>100
1,7-Dihydroxyxanthone (**7**)	>50	>50	>50	>50	>50	>50
Vismiaquinone D (**9**)	>50	>50	>50	>50	>50	>50
Cisplatin	19 (±3.2)	4 (±2.8)	8 (±1.4)	15 (±4.3)	7 (±2.7)	13 (±2.3)

Structure-Activity Relationship Study

Interestingly, compared to the other xanthones, compounds **1-3** have an additional oxygenated heterocyclic ring fused to the xanthone nucleus at C-3/C-4, that may play an important role in the cytotoxicity. Instead, an isoprenyl moiety, such as that occurring in compounds **4** and **5**, seems to reduce cytotoxicity.

Conclusion

In conclusion, the results confirmed that *C. cochinchinense* is a rich source of bioactive secondary metabolites and that xanthones are the most abundant and characteristic ones. Of the thirteen compounds isolated from this plant, nine were known aromatic substances while four were common triterpenoids. The structures of all metabolites were elucidated by spectroscopic data analysis and seven compounds (**1-5**, **7**, and **9**) were selected for cytotoxic activity. Their cytotoxic activities were measured against six human cancer cell lines, by using MTT assay. Pruniflorone N (**1**) showed the highest activity, which was even higher than the very well-known chemotherapy agent cisplatin on five tumor cell lines. On the other hand,

pruniflorone M (**2**) and 6-deoxyisojacareubin (**3**) resulted to be more potent cytotoxic than cisplatin on four and two lines, respectively. Cell viability mostly affected by all three compounds **1-3** were the MCF-7 breast and the BG-1 ovarian cancers. Macluraxanthone **(5)**, 1,7-dihydroxyxanthone **(7)** and vismiaquinone D **(9)** showed no effect (IC_{50} > 50 μM) on all cell lines, whereas xanthone V_1 **(4)** exhibited moderate effects on all cells. Vismiaquinone D (**9**) showed from low to no activity.

Acknowledgements

We express our thanks to Pro-Rector Dr Thar Tun Maung and Prof. Dr Myint Myint Khine (Head of the Department of Chemistry) of Kalay University for their kind permissions to submit this paper. The authors thank Prof. Mariella Mella of the Department of Chemistry, University of Pavia, for the 2D NMR measurements and Prof. Htar Htar Lwin for the identification of the plant material. One of the authors (Zaw Min Thu) thanks the European Commission for the ERASMUS MUNDUS (PANACEA) fellowship.

References

Ahn, E.K., and Oh, J.S. (2013). "Lupenone Isolated from *Adenophora triphylla* var. japonica Extract Inhibits Adipogenic Differentiation through the Downregulation of PPARγ in 3T3-L1 Cells". *Phytotherapy Research*, vol. 27, pp. 761-766.

Boonnak, N., Khamthip, A., Karalai, C., Chantrapromma, S., Ponglimanont, C., Kanjana-Opas, A., Tewtrakut, S., Chantrapromma, K., Fun, H.K. and Kato, S. (2010). "Nitric Oxide Inhibitory Activity of Xanthones from the Green Fruits of *Cratoxylum formosum* ssp. pruniflorum". *Aust. J. Chem.*, vol. 63, pp. 1550-1556.

Boonnak, N., Karalai, C., Chantrapromma, S., Ponglimanont, C., Fun, H.K., Kanjana-Opas, A., Chantrapromma, K. and Kato, S. (2009). "Anti-Pseudomonas aeruginosa Xanthones from the Resin and Green Fruits of *Cratoxylum cochinchinense*". *Tetrahedron*, vol. 65, pp. 3003-3013.

Botta, B., Delle Monache, G., Delle Monache, F., Marini Bettolo, G.B. and Menichini, F. (1986). "Vismione H and Prenylated Xanthones from *Vismia guinensis*". *Phytochemistry*, vol. 25, pp. 1217-1219.

Chaturvedula, V.S.P., and Prakash, I. (2013). "Ursane and Oleane Triterpenes from *Astragalus propinquus*". *International Journal of Research and Development in Pharmacy and Life Sciences*, vol. 2, pp. 503-506.

de Oliveira, P.V., Lemos, R.P.L. and Conserva, L.M. (2012). "Chemical Constituents of *Rourea doniana*". *Brazilian Journal of Pharmacognosy*, vol. 22, pp. 451-454.

Duan, Y., Dai, Y., Chen, L., Liu, M., Li, Y. and Yao, X. (2012). "Xanthones from the Stems of *Cratoxylum cochinchinense*". *MRC Letters*, vol. 50, pp. 642-645.

Jash, S.K., Gangopadhyay, A., Sarkar, A. and Gorai, D. (2013). "Phytochemical Investigation of the Hexane Extract of Stem Bark of *Peltophorum pterocarpum* (DC.) ". *Der Pharma Chemica*, vol. 5, pp. 49-53.

Ji, H.F., Li, X.J. and Zhang, H.Y. (2009). "Natural Products and Drug Discovery". *EMBO reports*, vol. 10, pp. 194-200.

Laphookhieo, S., Syers, J.K., Kiattansakul, R. and Chantrapromma, K. (2006). "Cytotoxic and Antimalarial Prenylated Xanthones from *Cratoxylum cochinchinense*". *Chem. Pharm. Bull.*, vol. 54, pp. 745-747.

Laphookhieo, S., Maneerat, W. and Koysomboon, S. (2009). "Antimalarial and Cytotoxic Phenolic Compounds from *Cratoxylum maingayi* and *Cratoxylum cochinchinense*". *Molecules*, vol. 14, pp. 1389-1395.

Laphookhieo, S., Maneerat, W., Buatip, T. and Syers, J.K. (2008). "New Xanthones from *Cratoxylum cochinchinense*". *Can. J. Chem*., vol. 86, pp. 757-760.

Lin, C. N., Chung, M. I., Liou, S. J., Lee, T. H. and Wang, J. P. (1996). "Synthesis and Anti-inflammatory Effects of Xanthone Derivatives". *J. Pharm. Pharmacol*., vol. 48, pp. 532-538.

Mahabusarakam, W., Rattanaburi, S., Phongpaichit, S. and Kanjana-Opas, A. (2008). "Antibacterial and Cytotoxic Xanthones from *Cratoxylum cochinchinense*". *Phytochemistry Letters*, vol. 1, pp. 211-214.

Mahabusarakam, W., Nuangnaowarat, W. and Taylor, W.C. (2006). "Xanthone Derivatives from *Cratoxylum cochinchinense* Roots". *Phytochemistry*, vol. 67, pp. 470-474.

Nagem, T.J. and de Oliveira, F.F. (1997). "Xanthones and other Constituents of *Vismia parviflora*". *Journal of the Brazilian Chemical Society*, vol. 8, pp. 505-508.

Newman, D.J. and Cragg, G.M. (2007). "Natural Products as Sources of New Drugs over the Last 25 Years". *Journal of Natural Product*, vol. 70, pp. 461-477.

Nguyen, L.H.D. and Harrison, L.J. (1998). "Triterpenoid and Xanthone Constituents of *Cratoxylum cochinchinense*". *Phytochemistry*, vol. 50, pp. 471-476.

Rattanaburi, S., Daus, M., Watanapokasin, R. and Mahabusarakam, W. (2014). "A New Bisanthraquinone and Cytotoxic Xanthones from *Cratoxylum cochinchinense*". *Natural Product Research*, vol. 28, pp. 606-610.

Reyes-Chilpa, R., Gómez-Cansino, R., Guzmán-Gutiérrez, S. L., Hernández-Ortega, S., Campos-Lara, M., Vega-Avila, E. and Nieto-Camacho, A. (2014). "Anthraquinones from *Vismia mexicana*". *Zeitschrift für Naturforschung C*, vol. 69c, pp. 29-34.

Sabphon, C., Sermboonpaisarn, T. and Sawasdee, P. (2012). "Cholinesterase Inhibitory Activities of Xanthones from *Anaxagorea luzonensis* A. Gray". *J. Med. Plants Res.*, vol. 6, pp. 3781-3785.

Sia, G.L., Bennett, G.J., Harrison, L.J. and Sim, K.Y. (1995). "Minor Xanthones from the Bark of *Cratoxylum cochinchinense*". *Phytochemistry*, vol. 38, pp. 1521-1528.

Udomchotphruet, S., Phuwapraisirisan, P., Sichaem, J. and Tip-pyang, S. (2012). "Xanthones from the Stems of *Cratoxylum cochinchinense*". *Phytochemistry*, vol. 73, pp. 148-151.

Vo, V.V. (1997). *Dictionary of Medicinal Plants in Vietnam*. Ho Chi Minh: Medical Publishing House, pp. 435.

Yu, H.Y., Jin, S.L., Zhang, X., Liu, Y., Ou, Y.F., Wang, N.L. and Yao, X.S. (2009). "Two New Benzophenone Glucosides from *Cratoxylum cochinchinense*". *Chinese Chemical Letters*, vol. 20, pp. 459-461.

ENCAPSULATION EFFICIENCY OF ROSELLE CALYCES FOOD COLOURANT USING DIFFERENT WALL MATERIALS

Kyaw Thu[1], San San Yu[2], Ah Mar Yi[3]

Abstract

Roselle calyces have the intense red colour due to the accumulation of anthocyanins. They could be extracted using distilled water and 2 % citric acid solution. Total anthocyanins content expressed as cyanidin – 3-glycoside in each extract was determined by pH differential method. Total anthocyanins content of 2 % citric acid extract was higher than that of watery extract. Some quantitative tests for anthocyanins extract were carried out by using ferric chloride, dilute hydrochloric acid and dilute sulphuric acid. Powders of anthocyanins were prepared using different wall materials : maltodextrin (MD), gum arabic (GA) and a combination of maltodextrin and gum arabic (MD + GA) with 1 : 1 ratio. Tween – 80 was used as emulsifier. Each of the wall materials was homogenized to the core material with the ratio of 1 : 1 and were micro encapsulated by microwave –assisted drying at 1100 W. The encapsulated powders were analysed for moisture, hygroscopicity, colour density and morphology. The stability of anthocyanins powder was evaluated under different temperature conditions (Refrigerator, room temperature, sunlight). The results indicated that encapsulated powder with the GA and MD combination gave the better quality of powder and it could be applied in colouring of jelly.

Keywords: Anthocyanins, roselle calyces, pH differential method, encapsulated powder

Introduction

Food dye or food colouring is a type of food additive that is added to food or drinks. It is a form of pigment, dye or substance that imparts colour when it is added. Food dye can be found in the form of powder, liquid and gel. In the current market, food dye can be divided into two types: natural food

[1.] Dr, Lecturer, Department of Chemistry, Taunggyi University
[2.] MRes, Student, Department of Chemistry, Taunggyi University
[3.] Dr, Professor (Head), Department of Chemistry, Taunggyi University

dye and synthetic food dye (artificial colourants). Natural colourants have been widely used in food and cosmetic products (Piyarat *et al*., 2014).

Artificial colourants are synthetic dyes derived from petroleum. These chemicals may have harmful side effects and could cause health problems in adults or children. Moreover artificial food dyes do not add nutritional value to the food. Their chemicals may have synthesized colours which are easier and less costly to produce and are superior in colouring properties. In the last 20 years synthetic colourants have been increasingly perceived as undesirable or harmful by consumers (Ni and Gong, 1997). Hence, most countries have limited the use of synthetic colourants. Natural dyes have been used for centuries to colour food. These dyes are produced from plant and animal sources. Natural food colours offer additional health benefits of biologically active compounds like vitamins, minerals, flavonoids, chlorophyll, and other cancer fighting antioxidants. But natural colourants are generally more sensitive to light, temperature, pH and redox agents (Macrae *et al*., 1993).

Roselle (*Hibiscus subdariffa* L.) is a tropical plant (Figures 1 and 2) which belongs to the family Malvaceae and is known in Myanmar as chin-baung. It is probably a native of West Africa and is now widely cultivated throughout the tropics and subtropcis e.g. Sudan, China, Thailand, Egypt, Mexico and the West India (Purseglove, 1974).

Botanical description of *Hibiscus sabdariffa* L. is as follows:

Botanical name	-	*Hibiscus sabdariffa* L.
Family	-	Malvaceae
Common name	-	Roselle
Myanmar name	-	Chin baung thee
Parts used	-	Calyces

Figure 1: Plant of roselle (Chin-baung)

Figure 2: Roselle calyces

Encapsulation is a technique that is used for protection, stabilization and slow release of core materials. There are several techniques and wall materials that are available for encapsulation of natural food colourants to overcome their instability, solubility and handling problems (Khazaei and Jafari, 2014).

In this research, anthocyanin was extracted from roselle calyces by using 2 % citric acid solution and then encapsulated with wall materials such as maltodextrin, gum arabic and combination of maltodextrin and gum arabic. The stability of encapsulated powder was evaluated under different light and temperature conditions.

Materials and Methods

Sample Collection

The roselle calyces were collected from Yat Sauk Township, Southern Shan State during August 2017. The roselle calyces were washed with distilled water and dried at room temperature for about two weeks and then ground into powder.

The encapsulating agents used were maltodextrin (DE 4-17), gum arabic and Tween-80. All reagents were analytical grade.

Phytochemical Investigation on Roselle Calyces

Phytochemical investigation on roselle calyces was carried out according to the reported methods (Harborne, 1984).

Preparation of the Anthocyanin Extracts from Roselle Calyces

Extraction of anthocyanin pigments from roselle calyces was carried out according to the procedure described by Spanga*et al*., (2003). The extracting solvents were: distilled water and 2 % citric acid solution. The extracts were kept in refrigerator until further analysis.

Determination of Total Monomeric Anthocyanins

Before the determination of anthocyanins content, maximum absorption of anthocyanins extract was detected by UV-VIS spectrophotometer. Total anthocyanin content was determined by using the spectrophotometric pH-differential method described by Wang and Xu (2007) using two buffer systems: potassium chloride buffer, pH 1.0 (0.025 mol/L) (125 mL of 0.2 mol/L KCl and 375 mL of 0.2 mol/L HCl) and sodium acetate buffer, pH 4.5 (0.4 mol/L) (400 mL of 1 mol/L sodium acetate, 240 mL of 1 mol/L HCl and 360 mL of distilled water). The absorbance was measured at 520 and 700 nm with distilled water as blank by using a UV–VIS spectrophotometer (Spectro UV 2550). The absorbance difference between the pH 1.0 and pH 4.5 was calculated:

Absorbance= (A_{520nm} pH1.0 – A_{700nm} pH1.0) – (A_{520nm} pH4.5 – A_{700nm} pH4.5).

The total anthocyanin content was calculated as cyanidin-3-glucoside according to the following equation:

$$\text{Total anthocyanin content (mg/100g)} = \frac{A \times MW \times DF \times 10^3}{\varepsilon l}$$

where, MW (molecular weight)

DF = the dilution factor; *l* = path length, A =Absorbance, ε=Molar absorptivity.

Choice of Solvent for Extraction of Anthocyanin

To choose the best solvent, pH and yield percent of both extracts were compared. 2 % citric acid extract with deep colour was chosen for the research work.

Qualitative Tests for Anthocyanins in 2 % Citric Acid Extract

The presence of anthocyanins in 2 % citric acid extract was tested by using three common reagents: (i) sulphuric acid (ii) ferric chloride and (iii) dilute hydrochloric acid (Spanga*et al*., 2003).

Preparation of Anthocyanins Encapsulated Powder

Anthocyanin extract (100 mL) was added to 100 mL of each wall material (gum arabic (GA) 40 % solution, maltodextrin (MD) 40 % solution and combination of maltodextrin (MD) and gum arabic (GA) with 1:1 ratio). This immiscible mixture was homogenized at 1000 rpm for 10 min by using magnetic stirrer until the anthocyanin dispersed completely. Two drops of Tween-80 was added to aid the emulsification process (Krishan *et al*., 2005). The mixture was placed inside crucible and placed in a domestic microwave oven. Each mixture was treated for up to 14 min at microwave power intensities (1100 W). They were ground into powder and immediately placed in brown bottle and stored in refrigerator.

Determination of some Physicochemical Properties of Encapsulated Powders

Some physicochemical properties such as pH, moisture content, hygroscopicity, colour density, dissolution time and solubility were carried out by the reported methods. Colour density was determined by densitometer and the surface morphology of the encapsulated powders was examined by scanning electron microscope (SEM, JEOL-JSM-5610LV, Japan) at Universities' Research Centre (URC). The presence or absence of artificial colours in encapsulated powder was determined at Food Chemical Control Laboratory, Department of Food and Drug Administration, Nay Pyi Taw.

Evaluation and Application of Encapsulated Anthocyanins Powder (III)

The stability of encapsulated powder (MD+G) was evaluated placing under different storage conditions (Refrigerator, Room and Sunlight) and it was applied in colouring of jelly.

Sample Preparation and Analysis of Colour by Paper Chromatography using Ascending Method

The Whatman No.1 paper was spotted with the sample solution. The sample spot was dried with a hair dryer. It was run in a chromatographic chamber containing solvent (I) (2 g trisodium citrate in 20 mL ammonia and 80 mL distilled water) by ascending method. Similarly, the same experiment was run in a chromatographic chamber containing solvent (II) (n-butanol: acetic acid: distilled water 12:3:5). At the end of the running, the paper was removed from the jar and hanged them to be dried. The results were compared with standard artificial colours such as Auramine O, Brilliant Bule (BB), Tartrazine (TT) and Curcumin.

Application of Encapsulated Anthocyanin Powder in Jelly Preparation

About 1 g of jelly powder was added to 50 mL of distilled water, then heated at 70^{o} C, stirred for about 15 min and cooled at room temperature. The boiled encapsulated anthocyanin powder solution (1 g in 20 mL of distilled water) was added to jelly solution. When the mixture was left for about 15 min, the coloured jelly was obtained.

Results and Discussion

Preliminary Phytochemical Tests for Roselle Calyces

The preliminary phytochemical tests on the dry powder sample revealed the presence of alkaloids, amino acids, carbohydrates, glycosides, phenolic compounds saponins, steroids, sugars, tannins, flavonoids, lipophilic group, proteins, polyphenols and starch. However, resin and cyanogenic glycoside were absent.

Extraction of Anthocyanin Pigments from Roselle Calyces

Distilled water and 2 % citric acid solution were used as solvents for extraction of anthocyanins. Material to solvent ratio was 1:25 w/v. The pH

values of red colour of watery extract of anthocyanins and 2 % citric acidextract of anthocyanin (Figure3) were found to be 2.7 and 2.5, respectively.

(a) (b)

Figure 3: Extracts of anthocyanin (a) watery extract (b) 2 % citric acid extract

Total Anthocyanin Pigment

Before determination of total anthocyanin pigment in both extracts, maximum absorption of both anthocyanin extracts were detected by uv-visible spectrophotometer. In both extracts, maximum absorption was found to be 520 nm (Figure 4). Therefore λ_{max} = 520 nm was used for the calculation of anthocyanin content in pH differential method.

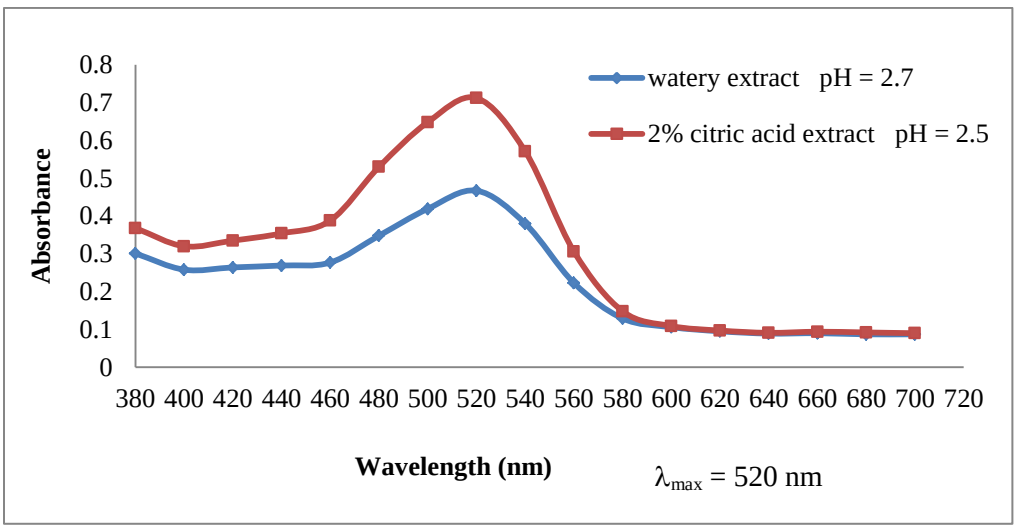

Figure 4: UV- visible absorption spectra of anthocyanin in watery extract and 2 % citric acid extract

Choice of Solvent for Extraction of Anthocyanins

The extraction efficiency of anthocyanin was affected by the type of solvents. The anthocyanin content of 2 % citric acid extract was higher than that of water (Table 1). At low pH value, anthocyanin content was found to be higher and the colour was more stable (Bronnum-Hansen *et al.*, 1985). Therefore, 2 % citric acid was chosen for the extraction of anthocyanins from roselle calyces.

Table 1: Extraction Efficiency of Anthocyanin Affected by the Type of Solvents

No.	Extraction Solvent	pH	Anthocyanin content (mg/100g)
1	Distilled Water	2.7	195
2	2 % citric acid	2.5	254

* Based on dry weight

Qualitative Tests for Anthocyanins in 2 % Citric Acid Extract

According to qualitative tests pelargonidin, cyanidin and malvidin were found to be present in anthocyanin extracts (Figure 5).

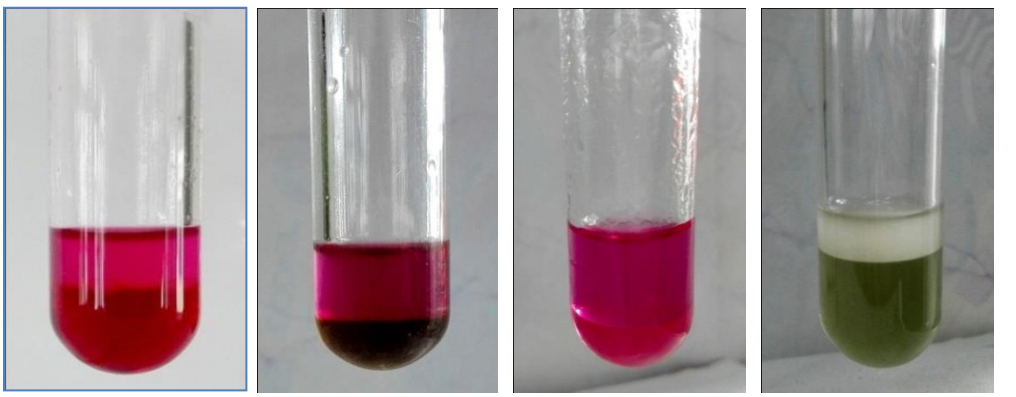

Anthocyanins Malvidin Pelargonidin Cyanindin

(i) Sulphuric acid test **(ii) Ferric chloride test** **(iii) Dilute hydrochloric acid test**

Figure 5: Qualitative tests for anthocyanins

Encapsulation of 2 % Citric Acid Anthocyanin Powder

In general, the coating agent alone does not offer all the properties required to ensure a good microencapsulation and a mixture of one or more components is frequently employed to enhance the encapsulation (Turchiuli and Fuchs, 2005).

To increase the stability of anthocyanins and protection from light, high temperature, pH and oxidation, encapsulation was carried out. In this research, anthocyanins pigment of 2 % citric acid solution extract for core material, a mixture of gum arabic and maltodextrin for wall materials and Tween-80 as emulsifier were used. The core to wall materials ratio was 1:1. The powders obtained from different wall materials are shown in Figure 6.

Powder I usingMaltodextrin (MD)

Powder II using Gum Arabic (GA)

Powder III usingMaltodextrin and Gum Arabic (MD+GA)

Figure 6: Encapsulated anthocyanins powders

Some Physicochemical Properties of Encapsulated Anthocyanin Powders

According to Table 2, powder encapsulated with a combination of gum arabic and maltodextrin has medium pH, moisture content, hygroscopicity, colour density and solubility in water. Moreover it showed the highest dissolution time, indicating that the time taken for the powder to reconstitute in water was longer than the others.

Table 2: Some Physicochemical Properties of Encapsulated Anthocyanin Powders with Different Wall Materials

Powder	Coating material	pH	Moisture (%)	Hygroscopicity (%)	Colour density (D)	Dissolution time (min)	Solubility in water (%)
I	Maltodextrin	2.9	4	11.9	0.36	1	96
II	Gum Arabic	3.4	7	15.2	0.53	4	93
III	Maltodextrin and Gum Arabic	3.0	5	13.8	0.42	8	95

SEM Analysis of the Encapsulated Anthocyanin Powder

The encapsulation efficiency of anthocyanin was evaluated by scanning electron microscope (SEM). The morphological structures of powder (I, II, III) are shown in Figure 7.

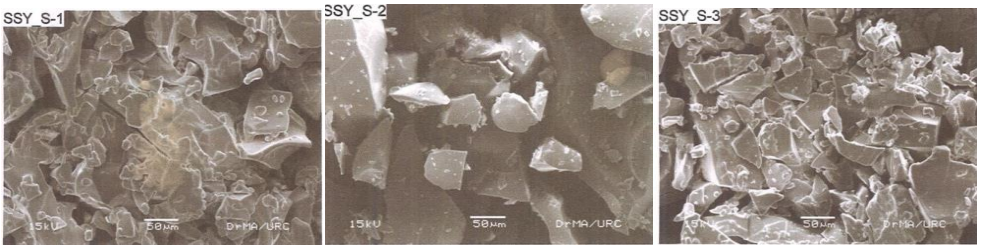

Powder I MD | Powder II GA | Powder III MD+GA

Figure 7: SEM images of the encapsulated powder with different wall materials(at 500 X magnification)

It was found that all particles produced had smooth surface and flake like structure. SEM image of combination of maltodextrin and gum arabic showed more dents surrounding the core materials whereas few dents appeared in micrograph of encapsulated maltodextrin alone and gum Arabic alone. According to a study carried out by Cano-Chauca *et al*., (2005), the addition of gum arabic to maltodextrin allows particles with better distribution and uniformity to be obtained. Therefore, combination of wall materials had higher encapsulation efficiency than the others.

Evaluation and Application of the Encapsulated Anthocyanins Powder(III)

Evaluation of encapsulated powder (III) (MD +GA)

Stability of anthocyanins in encapsulated powder III (MD +GA) was evaluated under different storage conditions (Refrigerator, Room and Sunlight). The decrease in absorbance implies the degradation of anthocyanins in storage conditions. The resultant data of absorbance and their related concentrations are tabulated in Table 3 and the degradation curves for various storage conditions are shown in Figure 8.

Table 3: The Absorbance and Concentration of the Encapsulated powder (III) in Various Storage Conditions

No.	Time (Days)	At 4 ± 1°C in the absence of light (Refrigerator)		At 25 ± 1°C in the of light		Sun light	
		Absorbance	Conc: (M)	Absorbance	Conc: (M)	Absorbance	Conc: (M)
1	0	0.562	2.089×10^{-5}	0.562	2.089×10^{-5}	0.560	2.082×10^{-5}
2	2	0.562	2.089×10^{-5}	0.562	2.089×10^{-5}	0.556	2.067×10^{-5}
3	4	0.562	2.089×10^{-5}	0.562	2.089×10^{-5}	0.550	2.045×10^{-5}
4	6	0.562	2.089×10^{-5}	0.560	2.082×10^{-5}	0.548	2.037×10^{-5}
5	8	0.562	2.089×10^{-5}	0.559	2.078×10^{-5}	0.540	2.007×10^{-5}

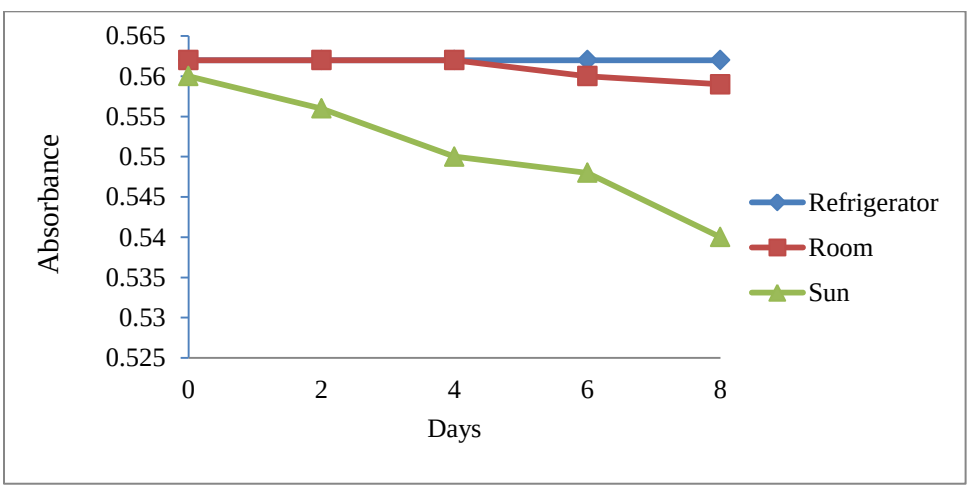

Figure 8: Degradation of the encapsulated anthocyanin powder with time

The anthocyanins were affected by the ambient conditions (light and temperature). Falcao *et al*., (2004) pointed out that light is an important accelerating factor in the degradation of anthocyanins. According to the Table 3 and Figure 8, the samples stored in refrigerator showed lower degradation than the samples stored at 25° C in room temperature and under sunlight. It was noted that when exposed to sunlight at ambient temperature, the sample showed a significant decrease of the absorbance on third day of exposure. These findings are in agreement with Janna *et al*. (2007). The visual colour changes of model samples in various storage conditions for 12 days period are shown in Figure 9. Thus, samples stored in refrigerator and at room temperature showed lower degradation of anthocyanins than the sample placed in sunlight.

4 ± 1°C Room Temperature Sunlight

Figure 9: Colour changes of the encapsulated powder (iii) under different conditions

Chromatographic Analysis of Artificial Colours

According to the chromatograms, the powder did not contain artificial colours such as Auramine O, Brilliant Blue (BB), Tartrazine (TT) and Curcumin (Figures 10 and 11). It confirms that the encapsulated powder is natural food colourant. Therefore it can be eaten safely for consumers.

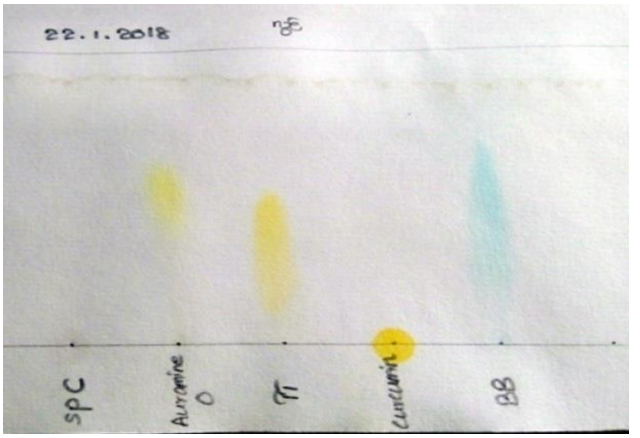

Figure 10: One Dimensional ascending paper chromatogram of the encapsulated powder (iii) in solvent I

Solvent I = Trisodium citrate + ammonia solution
SPC = Encapsulated powder sample Artificial colours
Auramine O
Tartrazine (TT)
Curcumin

Brilliant Blue (BB)

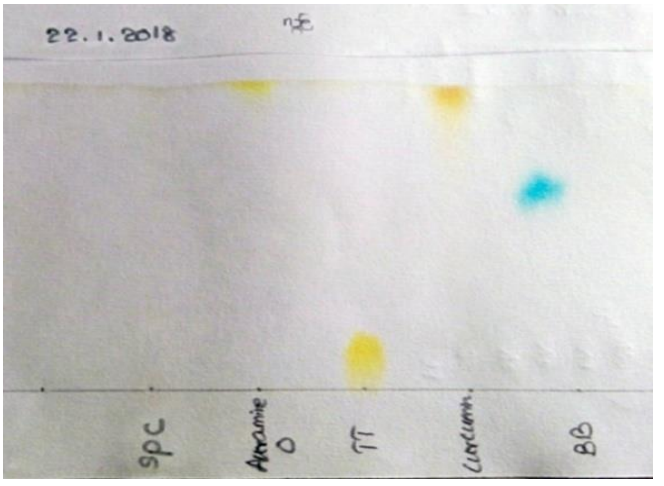

Figure 11: One dimensional ascending paper chromatogram of the encapsulated powder (iii) in solvent II

Solvent II = n-Butanol + acetic acid
SPC = Encapsulated powder sample Artificial colours
Auramine O
Tartrazine (TT)
Curcumin
Brilliant Blue (BB)

Application of encapsulated powder (III) (MD +GA)

Encapsulated anthocyanins powder (GA + MD) was used for colouring jelly. Material to ready made jelly powder ratio was 1:1. The resultant jelly is shown in Figure 12. The stickiness of the products could be reduced by using encapsulated powder.

Figure12: Colouring of jelly

Conclusion

An attempt has been made to extract anthocyanins as natural food colourant from Roselle calyces using 2 % citric acid solution and to prepare encapsulated powders (I, II, III) and to be applied in colouring of jelly. From the results of some physicochemical properties, the encapsulated powder III of (MD + GA) had medium moisture content, hygroscopicity value, solubility in water and colour density compared to other encapsulated powders of sample I and sample II. Moreover, SEM micrograph of MD + GA indicated the better quality microcapsules, which means higher encapsulation efficiency. It also had a longer dissolution time compared to others. According to FDA result, powder III (MD + GA) did not contain synthetic dyes. Due to perceived safety, this powder can be a good substitute for artificial colours causing harmful effects for consumers. Storage of the encapsulated powder (III) in

refrigerator in the absence of light was the best condition for its stability whereas sunlight was found to be unsuitable condition. Therefore the storage temperature and light conditions are very important for natural food colourant.

With regard to natural sources of the raw material for natural colourants, Myanmar is rich with coloured plants which are available year-round. It is believed that the simple and effective technology of this research work may initiate to produce the commercial availability of natural food dye in Myanmar.

Acknowledgements

The authors would like to thank the Myanmar Academy of Arts and Science for allowing to present this paper.

References

Bronnum-Hansen, K., Jacobsen F. and Flink. M. J. (1985). "Anthocyanin Colourants from Elderberry (*Sambucusnigra*, L.).1. Process Considerations for Production of Liquid Extract".*J. Food Technol*, vol. 20 (6), pp.703-711

Cano-Chauca, M., Stringheta, P.C., Ramos, A. M. and Cal-Vidal, J. (2005). "Effect of the Carriers on the Microstructure of Mango Powder Obtained by Spray Drying and its Functional Characterization". *Innovative Food Science and Emerging Technologies,* vol.6, pp.420-428

Falcao, L.D., Gauche, C. and Barros, D.M. (2004)."Stability of Anthocyanins From Grape (Vitisvinifera L.) Skins with Tannic Acid in a Model System". *Italian Journal of Food Science*, vol.16, pp. 323-332

Harborne, J.B. (1984). *Phytochemical Methods*: *A Guide to Modern Techniques of Plant Analysis*. New York: 2nd Ed., Chapman and Hall Ltd.

Janna, O., Khairul, A., &Maziah, M. (2007). "Anthocyanin stability studies in *Tibouchinasemidecandra*L. Food Chemistry". vol.1010 (4). pp. 1640-1646.

Khazaei, K.M. and Jafari, S.M. (2014)."Application of Maltodextrin and Gum Arabic in Microencapsulation of Saffron Petal's Anthocyanins and Evaluating Their Storage Stability and Colour". *Carbohydrate Polym*, vol.105, pp. 57-62

Krishnan, S., Bhosale, R. and Singhal, R.S. (2005)."Microencapsulation of *Cardamom oleoresin*: Evaluation of Blends Gum Arabic, Maltodextrin and a Modified Starch as Wall Materials". *Carbohydrate Polymers*, vol.61, pp. 95-102

Macrae, R., Robinson, R.K. and Sadler, M. J. (1993). *Encyclopaedia of Food Science, Food Technology and Nutrition*. San Diego: Academic Press

Ni, Y. and Gong, X. (1997)."Simutaneous Spectrophotometric Determination of Mixtures of Food Colourants". *Analytica Chimica Acta*, vol.354, pp.163-171

Piyarat, K., Walaisiri, M. and Pornpen, W. (2014).“ Comparison of Stability of Red Colourants from Natural Sources, Roselle and Lac in Micelles”. *International Food Research Journal*,vol.21(1),pp. 325-330

Purseglove, J.W. (1974). *Tropical Crops Dicotyledoms*. London: Longman Group Ltd, vol.2, pp.370-372

Spagna, G., Barbagallo, R.N. Todaro, A. Durantel, M.J. and Piffer, P.G. (2003).“A Method for

Anthocyanin Extraction from Fresh Grape Skin”.*Italian Journal of Food Sciences*, vol.3, pp.337-346

Turchiuli, C. and Fuchs, M. (2005).“Oil Encapsulation by Spray Drying and Fluidized Bed Agglomeration”. *Innovative Food Science and Emerging Technologies*, vol.6, pp.29-35

Wang, W.D. and Xu, S.Y. (2007).“Degradation Kinetics of Anthocyanins in Black Berry Juice and Concentrate ”. *J. Food Eng*.,vol.82, pp.271-275

COMPARATIVE STUDY ON THE CHARACTERISTICS OF EGGSHELL WASTES FOR PREPARATION OF CALCIUM ACETATE

Yu May[1], Ohn Mar Nyein[2],Nan Non Khan[3]

Abstract

Eggshells are a rich source of mineral salts mainly calcium carbonate. This work was aimed to study the elemental contents and to characterize the egg shell wastes such as chicken, duck and quail eggshells for the preparation of calcium acetate. Relative abundances of elements in eggshells were determined by using X-ray fluorescence technique. Results of X-ray diffraction showed that the crystalline phase present in the waste sample is calcium carbonate in the form of calcite ($CaCO_3$).The comparative analysis of calcium carbonate contents was carried out for the selected eggshells by using back titration method. Furthermore, preparations of calcium acetate were done from three eggshell samples by soaking calcium carbonate in vinegar. The yield percent of the prepared calcium acetate were 46.76 % for chicken eggshell, 33.00 % for duck eggshell and 32.27 % for quail eggshell. Melting point determinations of calcium acetate were also done for three eggshell samples. The functional groups present in calcium acetate prepared from three eggshell samples were confirmed by FTIR analysis. The prepared calcium acetate were also be examined by EDXRF and SEM analysis. Chicken eggshell waste is appropriate and cheap source for preparation of calcium acetate.

Keywords: Eggshells, calciumcarbonate, calcium acetate, melting point, back titration

Introduction

Nowadays, there is a great interest in finding new pure calcium carbonate sources (Daengprok *et al*., 2000). Calcium carbonate ($CaCO_3$) can be found in large quantities in nature, with applications mostly as raw material for the ceramic calcium carbonate development in rapidly growing technology and research, such as hydroxyl apatite material synthesis as an alternative to the teeth and bones of human. Calcium carbonate obtained from bones flour, does not contain the same bioavailability of calcium obtained from synthetic sources. Calcium carbonate from oyster shells contain lead vestige among the

[1.] Dr, Lecturer, Department of Chemistry, Taunggyi University
[2.] Candidate, MRes, Department of Chemistry, Taunggyi University
[3.] Dr, Associate Professor, Department of Chemistry, Taunggyi University

others potential toxical elements such as aluminium, cadmium and mercury (Schaafsma,1997). On the other hand, eggshells have an advantage for not containing toxical elements (Macneil,1997). The word eggshell is a general name given to the hard exterial cover of the egg which consists of several constituent with calcium carbonate is the major one. Egg products industries produce great amount of shells and their final destiny is an environmental impact challenge.

Calcium acetate is one of a number of calcium salts used to treat hyperphosphatemia (too much phosphates in the blood) in patients with end stage kidney disease who are on dialysis (Chan *et al*., 2017). Calcium acetate works by binding with the phosphate in the food in the body, so that it is eliminated from the body without being absorbed. Preparations of calcium acetate from littleneck clam shell (Park *et al*., 2015) and butter clam shell (Lee *et al*., 2015) have been reported. Calcium acetate has been used in the manufacture of metallic soaps and synthetic resins; in lubricants as a corrosion inhibitor and as a mordant in dyeing. On the basis of these facts the synthesis and characterization of calcium acetate from waste eggshells as calcium source were conducted in this study due to the high content of calcium carbonate in the eggshells.

Materials and Methods

Sample Preparation and Characterization

Three different types of eggshells *viz*.,chicken, duck and quail eggshell samples were collected from Myoma market, Taunggyi Township, Southern Shan State. After removing the dirt particles, the samples were dried, ground and finally sieved to prepare fine powder.

The relative abundances of elements in eggshells powder samples were determined by EDXRF (Shimadzu-8000). The surface morphology of eggshells were examined by SEM (JSM 5610 LV,JEOL Ltd), the crystal structures by XRD (Rigaku Co., Japan) with Cu Kα (λ =1.54056 Å) radiation over a range of 2θ angles from 10° to 70°) and thermal properties by TG-DTA by using DTG-60 H Detector, at temperature 30 to 600 °C with a scanning rate of 50 mL/min, under nitrogen.

Determination of Calcium Carbonate Content in Eggshells

Each of the sample(0.2 g) was put into a conical flask by adding several drops of ethanol as a wetting agent. After that, 25 mL of 0.1 M hydrochloric acid solution was added into each flask and swirled the flask to wet the solid. The solutions in the flask were heated until they began to boil for complete digestion and were allowed to cool. Next, 3 drops of phenolphthalein were added to each flask and titrated against sodium hydroxide solution to the first persistent pink colour. Then the titration for the other samples were repeated and the percentage of calcium carbonate in each shell was calculated.

Preparation of Calcium Acetate from Eggshell Samples

Eggshells samples (20 g each) were boiled with 100 mL of vinegar for 1 h. Then the solutions were filtered and the filtrate solutions were placed in a small beaker on a hot plate at 50 °C to yield calcium acetate via forced evaporation. The remaining solution was allowed to stand at room temperature and seeded with a cotton thread to initiate crystal growth.

Melting Point Determination for Calcium Acetate Prepared from Three Eggshell Samples

The melting points of the three eggshell samples were determined by MPA 100 Automated Melting Point Apparatus.

Functional Groups of Calcium Acetate from Three Eggshell Samples

The functional groups present in preparared calcium acetate samples were investigated by FT IR spectrometer measured at the Universities' Research Centre, Yangon University.

Energy Dispersive X Ray Fluorescence Analysis of Prepared Calcium Acetate from Three Eggshell Samples

The relative abundances of the prepared calcium acetate were determined by EDXRF spectrometer at the Universities' Research Centre, Yangon University.

SEM Analysis of Prepared Calcium Acetate from Three Eggshell Samples

SEM analysis of the prepared calcium acetate from three eggshell samples were conducted at the Universities' Research Centre, Yangon University.

Results and Discussion

Energy Dispersive X-Ray Fluorescence from Three Eggshell Samples

Relative abundances of elements present in eggshell samples were determined by EDXRF spectrometer. The EDXRF spectra obtained are shown in Figure1.

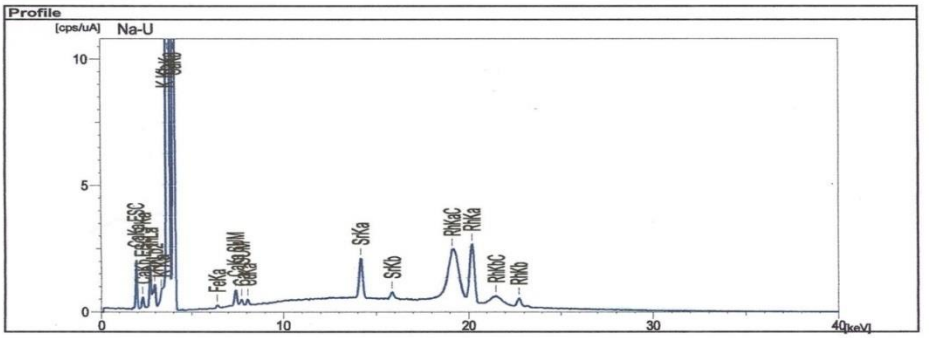

(a)

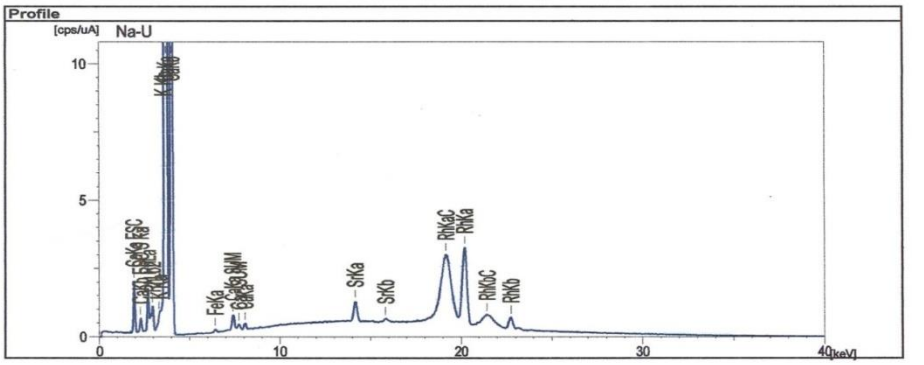

(b)

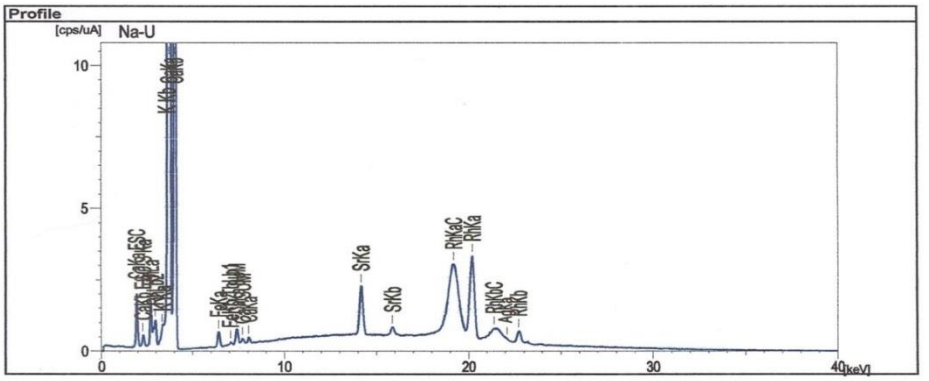

(c)

Figure 1: EDXRF spectra of eggshell samples (a) chicken (b) duck and (c) quail

Ca was found to be highest among the elements found in eggshell powder samples ranging from 26.189 % to 29.263 % (Table 1).Ca content in chicken eggshell was 29.263 %and found to be the highest. The high amount of calcium is associated with the presence of calcium carbonate which is the main component of eggshell (Leach, 1982). K and S were found as second and third abundant elements in the samples with minor amounts. Moreover, trace amounts of Sr (0.011 % to 0.027 %), Fe (0.007 % to 0.025 %) and Cu (0.006 % to 0.007 %) were also found in eggshell powder samples.

Table 1: Relative Abundance of Elements in Three Different Eggshell Samples

No	Elements	Relative abundance (%)		
		Chicken eggshell	**Duck eggshell**	**Quail eggshell**
1	Ca	29.263	28.559	26.189
2	K	0.239	0.230	0.263
3	S	0.102	0.171	0.102
4	Sr	0.025	0.011	0.027
5	Fe	0.007	0.007	0.025
6	Cu	0.007	0.007	0.006
7	Ag	-	-	0.006
8	COH	70.358	71.016	73.383

X-ray Diffraction Analysis of Eggshell Samples

The XRD patterns for different eggshell powder samples are shown in Figure 2. The XRD pattern of chicken eggshell powder exhibited the characteristic peaks at the Miller indices of (012), (104), (110), (113), (202) and (024) corresponding to the 2θ values of 22.840˚ , 29.227˚ , 35.803˚ , 39.271˚ , 43.014˚ and 46.997˚ respectively (Table 2). Similarly, duck eggshell sample showed peaks at Miller indices of (012), (104), (110), (113) and (202) corresponding to the 2θ values of 22.936˚ , 29.304˚ , 39.898˚ , 39.342˚ and 43.078˚ and quail eggshell powder showed diffraction peaks at the Miller indices of (012), (104), (110), (113), (202) and (204) corresponding to the 2θ values of 23.102˚ , 29.218˚ , 35.804˚ , 39.277˚ , 43.000˚ and 46.174˚ respectively. The peaks appeared in the diffractograms were found to be well-matched with both the peak location and the relative peak intensities of the diffraction data of the calcite phase. Similar reults were also found by Choudhary *et al*. (2015) and Freire and Holanda (2006). All the eggshell powder samples studied were indexed as hexagonal structure with lattice constants of equal ′a′ and ′b′ and longer ′c′ (Table 3).

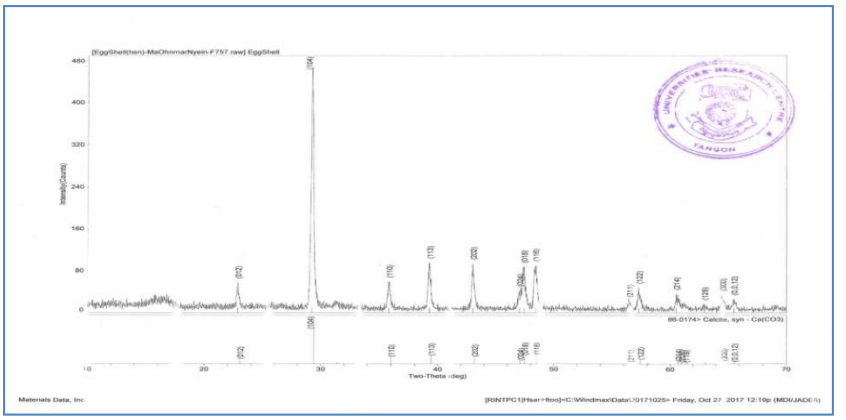

(a)

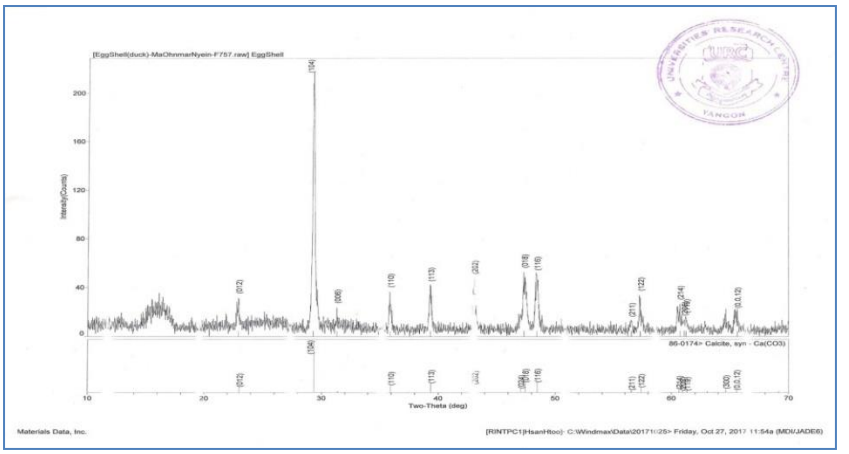

(b)

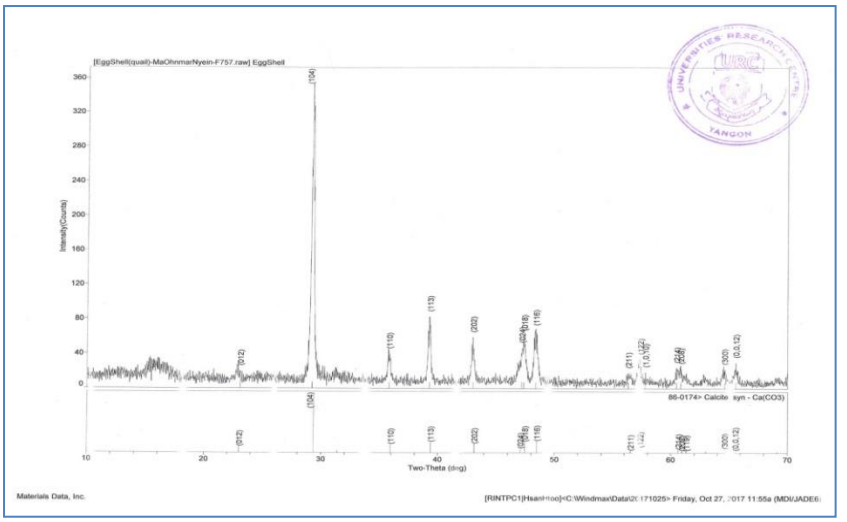

(c)

Figure2: XRD patterns of eggshell Samples (a) chicken (b) duck and (c) quail

Table 2: Miller Indices, Peak Position and Interplanar Spacing for Eggshell Samples

No	Miller indices			Eggshell Sample	Peak position 2θ (degree)	Interplanar spacing d (Å)
	h	k	l			
1.	0	1	2	Chicken	22.840	3.8903
				Duck	22.936	3.8743
				Quail	23.102	3.8467
2.	1	0	4	Chicken	29.227	3.0531
				Duck	29.304	3.0452
				Quail	29.218	3.0540
3.	1	1	0	Chicken	35.803	2.5059
				Duck	39.898	2.4995
				Quail	35.804	2.5059
4.	1	1	3	Chicken	39.271	2.2923
				Duck	39.342	2.2883
				Quail	39.277	2.2919
5.	2	0	2	Chicken	43.014	2.1011
				Duck	43.078	2.0981
				Quail	43.000	2.1017
6.	0	2	4	Chicken	46.997	1.9318
				Duck	-	-
				Quail	46.174	1.9250

Table 3: Lattice Constant and Structure of Eggshell Powder Samples

No	Eggshell powder	Lattice constant (Å)			Structure
		a-axis	b-axis	c-axis	
1	Chicken	4.9982	4.9982	17.7387	Hexagonal
2	Duck	4.9934	4.9934	17.4162	Hexagonal
3	Quail	5.0005	5.0005	16.8550	Hexagonal

SEM Analysis for Three Eggshell Samples

The morphology of the eggshell sample were investigated by SEM as shown in Figure 3. According to the SEM images, the eggshell samples comprise irregular shape of particles with various sizes and shapes. Small holes called pore canals were seen on the surface of the shell for gas-exchange.

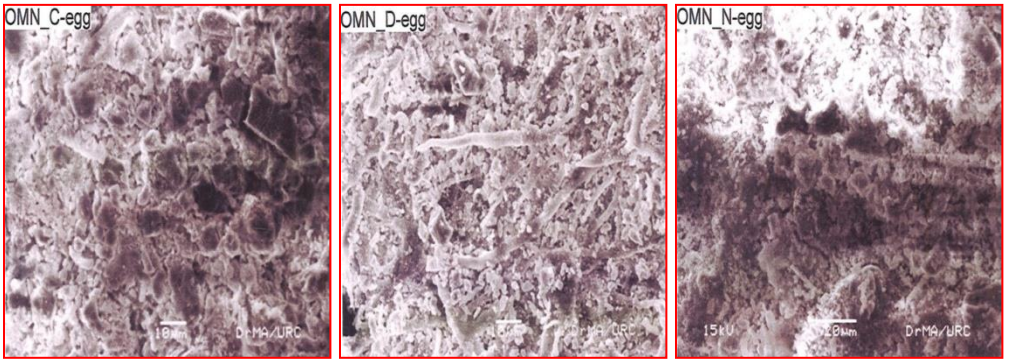

(a) (b) (c)

Figure 3: SEM images of eggshell samples (a) chicken (b) duck and (c) quail at 1000X magnification

Thermogravimetric Differential Thermal Analysis for Eggshell Samples

The thermal behaviour of the each eggshell waste sample was investigated by TG-DTA. The TG-DTA thermograms of eggshell waste samples are shown in Figure 4 and the results are summarized in Table 4. The results showed the presence of two thermal events. The first event below 140 ºC (75 ºC in chicken eggshell sample, 82 ºC in duck eggshell sample and 117 ºC in quail eggshell sample) is endothermic and is attributed to the removal of physically adsorbed water (moisture) on the particles of the waste sample. The second event between 140 and 600 ºC (327 ºC in chicken eggshell sample, 387 ºC in duck eggshell sample and 368 ºC in quail eggshell sample) is exothermic, and related to combustion of organic matter..

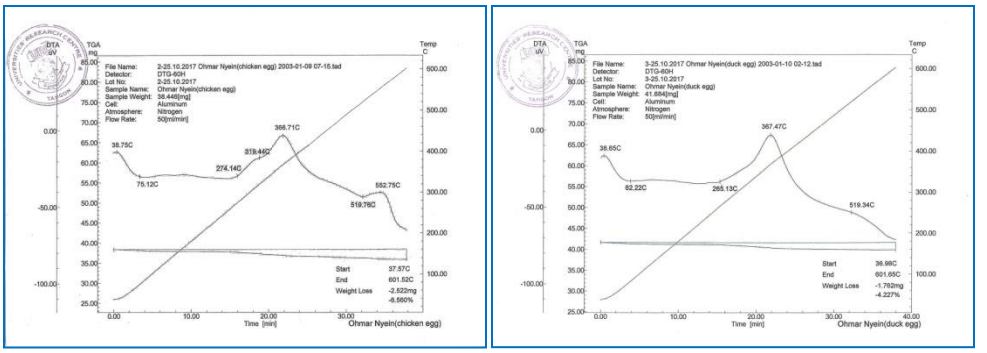

(a) (b)

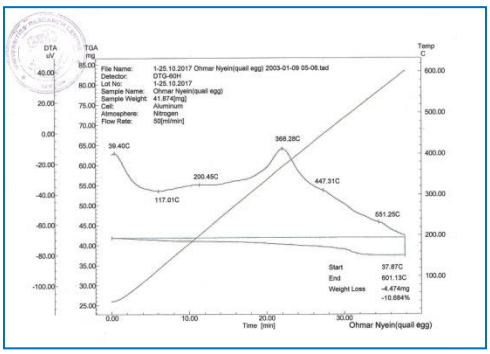

(c)

Figure 4:TG-DTA thermograms of eggshell samples (a) chicken (b) duck and (c) quail

Table 4: Thermal Analysis Data of Eggshell Samples

No	Sample	Peak's Temperature (°C)	Weight loss (%)	Nature of Peak	Remark
1	Chicken eggshell	75	1.73	Endothermic	Due to the removal of moisture
	Duck eggshell	82	1.71	Endothermic	
	Quail eggshell	117	1.49	Endothermic	
2	Chicken eggshell	327	4.83	Exothermic	Due to the combustion of organic matter
	Duck eggshell	387	2.52	Exothermic	
	Quail eggshell	368	9.19	Exothermic	

Calcium Carbonate in Eggshell Samples

In this experiment, the calcium carbonate content in eggshell was determined by back titration method. The percentages of calcium carbonate in three eggshell samples are tabulated in Table 5. According to the results obtained from experimental analysis, chicken eggshell contains the highest calcium carbonate content of 61.75 % followed by duck eggshell (60.30%) and quail eggshell (59.80 %).

Table 5: Calcium Carbonate Contents in Eggshell Samples

Samples	$CaCO_3$ content (%)
Chicken Eggshell	61.75
Duck Eggshell	60.30
Quail Eggshell	59.80

Prepared Calcium Acetate from Three Eggshell Samples

Eggshells are made up of calcium carbonate and vinegar is a mixture made up of very dilute acetic acid. The calcium carbonate in the eggshell and the acetic acid in vinegar interact setting off a chemical reaction. First, the acetic acid and calcium carbonate form carbonic acid and calcium acetate.

$$CH_3\,COOH + Ca\,CO_3 \rightarrow H_2\,CO_3 + Ca\,(CH_3\,COO)_2$$

Next, the carbonic acid breaks down to form carbon dioxide and water.

$$H_2\,CO_3 \rightarrow H_2O + CO_2$$

The overall reaction is

$$2CH_3\,COOH + Ca\,CO_3 \rightarrow H_2O + CO_2 + Ca\,(CH_3\,COO)_2$$

Needle shape crystals of prepared calcium acetate from three eggshell samples are clearly observed in Figure 5.

Figure 5: Crystallization of calcium acetate from (a) chicken eggshell(b) duck eggshell and (c)quail eggshell

The yield percentages of calcium acetate are tabulated in Table 6. Highest amount of calcium acetate (46.76 %) from chicken eggshell was obtained followed by 33.00 % from duck eggshell and 32.27 % from quail eggshell.

Table 6: The Amounts of the Calcium Acetate Prepared from Three Different Eggshell Samples

Samples	**$(CH_3COO)_2Ca$ (%)**
Chicken Eggshell	46.76
Duck Eggshell	33.00
Quail Eggshell	32.27

Melting Point of Calcium Acetate

The melting points of calcium acetate obtained from the three eggshell samples were determined by the melting point apparatus. The results are mentioned in Table 7. Melting points of calcium acetate samples were 160-161 ^{o}C, the literature value being 160 ^{o}C (NIOSH, 2015).

Table 7: Melting Points of Calcium Acetate from Different Eggshell Samples

Raw materials	Melting Point (□C)of Calcium Acetate
Chicken Eggshell	160-161
Duck Eggshell	160-161
Quail Eggshell	160-161

FT IR Analysis of the Prepared Calcium Acetate from Eggshell Samples

FT IR spectra of calcium acetate obtained from eggshell samples are shown in Figure 6 and band assignments are indicated in Table 8.

Each spectrum has been divided into three regions. The first region between 2700-3700 cm^{-1} which is dominated by stretching vibrations of O-H and C-H groups from calcium acetate monohydrate (Frost *et al*., 2004). The two weak bands at 3512 cm^{-1} and 3146 cm^{-1} in the spectrum of chicken eggshell sample, 3497 cm^{-1} and 3201 cm^{-1} in the spectrum of duck eggshell sample and 3348 cm^{-1} in the spectrum of quail eggshell sample are due to (O-H) stretching vibration. C-H stretching vibration of methyl group were observed at 2980 cm^{-1}, 2990 cm^{-1} and 2996 cm^{-1}, respectively, for chicken, duck and quail eggshell samples .

The second region of each spectrum from 1100-1600 cm^{-1} concerned with CH_3 bending and C-O stretching vibrations.The calcium acetate formed through forced evaporation showed some very weak bands at 1640, 1645 and 1645 cm^{-1} in FT IR spectra of chicken, duck and quail eggshell powder samples respectively, due to stretching of the carbonyl C=O bond present. The band appeared at 1537, 1539 and 1546 cm^{-1} and 1437, 1440 and 1454 cm^{-1} in the spectra of chicken, duck and quail eggshell samples respectively, due to the asymmetric and symmetric stretching vibrations of C-O.The in plane bending vibration of the methyl group appeared at 1024 cm^{-1} and the υ(C – C) stretching vibration of the acetate anion was observed at about 950 cm^{-1}.

The low wavenumber region of the FT IR spectrum from 600-500 cm^{-1} concerned with the vibrations of O − C − O. The calcium acetate prepared from chicken, duck and quail eggshell samples exhibited two poorly defined peaks at 690 cm^{-1} and 640 cm^{-1}, 690 cm^{-1} and 617 cm^{-1} and 673 cm^{-1} and

621 cm^{-1}, respectively, due to out of planestretching and bending vibrations of O − C − O fragment of the acetate anion (Frost *et al*., 2004).

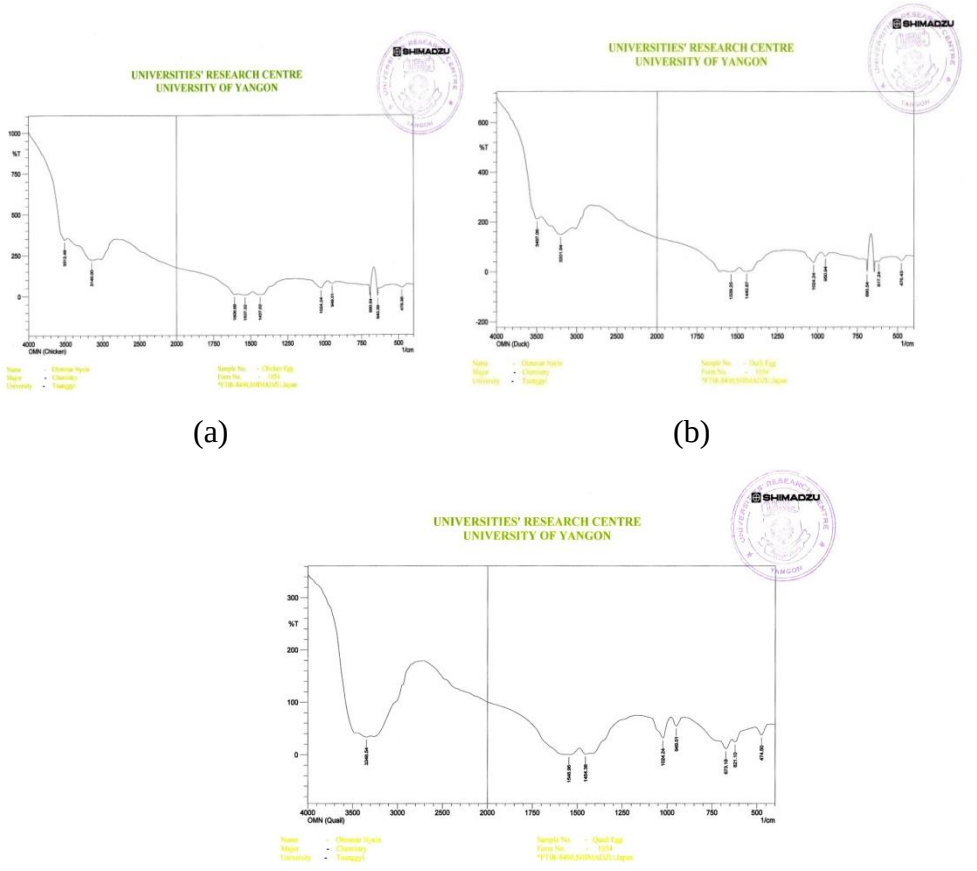

(a) (b)

(c)

Figure 6: FT IR spectra of calcium acetate from eggshell samples (a) chicken (b) duck and (c) quail

Table 7: FT IR Spectral Data for Prepared Calcium Acetate from Eggshell Powders

No	Observed wavenumber (cm^{-1})			*Reported wavenumber (cm^{-1})	Remark
	Chicken	Duck	Quail		
1	3512-3146	3497-3201	3348	3571-3147	O-H stretching vibration
2	2980	2990	2996	2927	C-H stretching of CH_3
3	1640	1645	1645	1648-1689	C=O stretching of carbonyl group in acetate anion
4	1537	1539	1546	1540 -1604	Asymmetric stretching vibration of C-O
5	1437	1440	1454	1442-1459	Symmetric stretching vibration of C-O
6	1024	1024	1024	1030	In plane bending vibration of the methyl group
7	949	950	949	925-951	Symmetric C-C stretching vibration
8	690	690	673	659-672	Out of plane stretching vibration of O-C-O group
9	640	617	621	616-623	Out of plane bending vibration of O-C-O group

*****Frost *et al*., 2007

Energy Dispersive X Ray Fluorescence of Calcium Acetate from Three Eggshell Samples

The relative abundances of elements in prepared calcium acetate were determined by EDXRF spectrometer. The results obtained are shown in Figure 7.

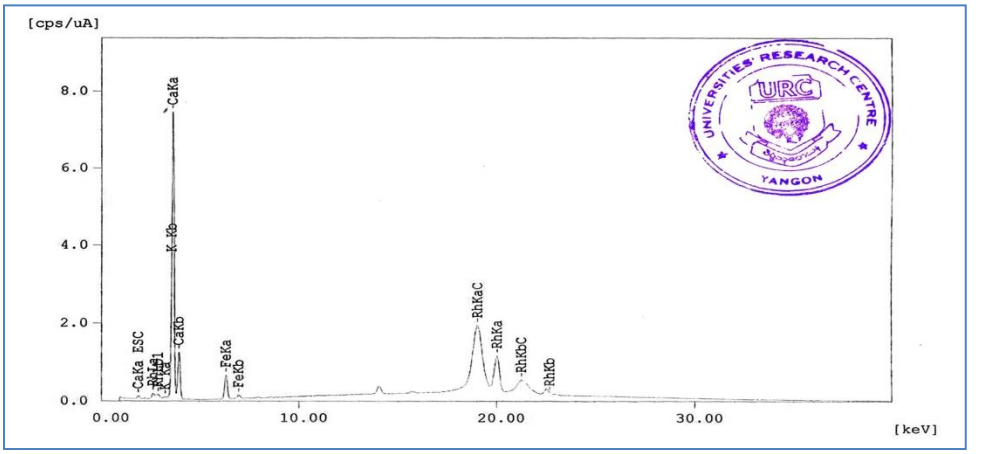

(a)

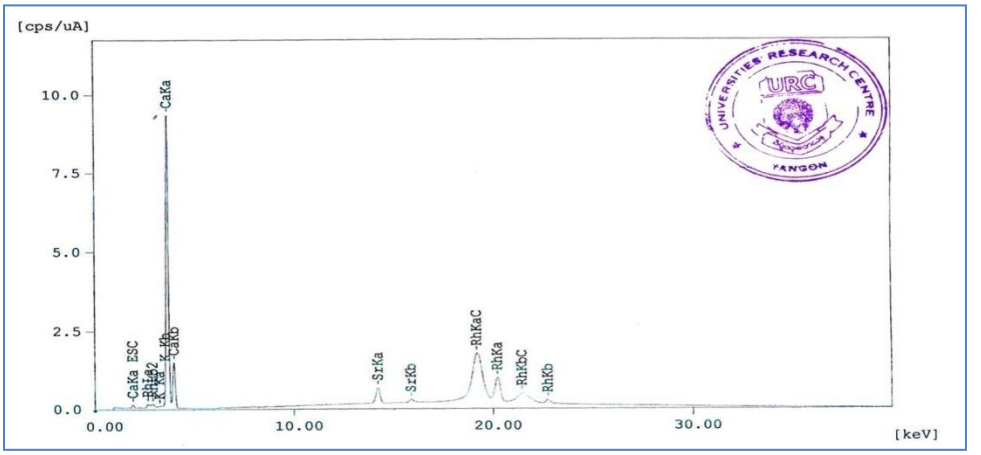

(b)

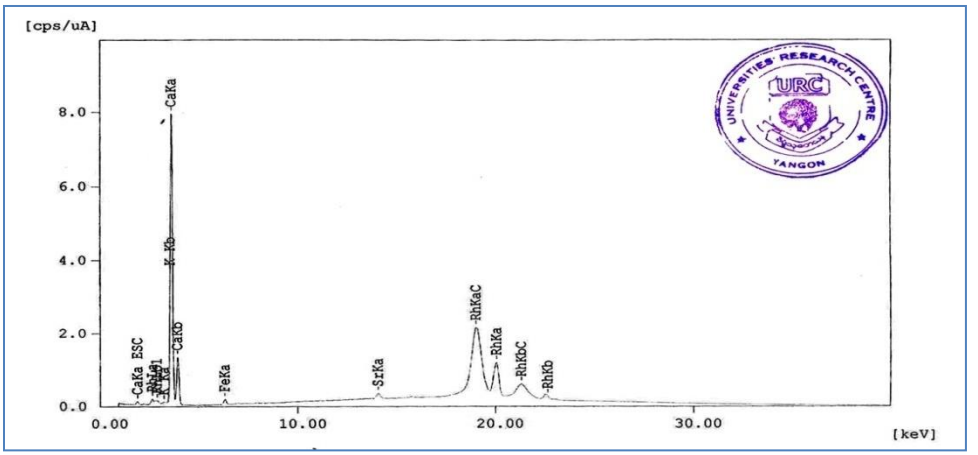

(c)

Figure 7: EDXRF spectra of calcium acetate from three eggshell samples (a) chicken (b) duck and (c) quail

Ca was found to be highest among the elements in calcium acetate ranging from 94.455 % to 98.615 %. Trace amount of Fe, K and Sr were also found. The highest percentage of calcium acetate was obtained from chicken eggshell.

Table 8: EDXRF Data for Prepared Calcium Acetate from Eggshell Samples

No.	Elements	Relative abundance (%)		
		Chicken eggshell	Duck eggshell	Quail eggshell
1.	Ca	98.615	97.797	94.455
2.	Fe	-	0.995	4.589
3.	K	0.713	0.973	0.956
4.	Sr	0.672	0.236	-

SEM Analysis of Prepared Calcium Acetate from Three Eggshell Samples

The surface morphology of resulting calcium acetate was analysed using Scanning Electron Microscopy. It was seen that the three crystal structures were seen to be needle like crystals (Figure 7).

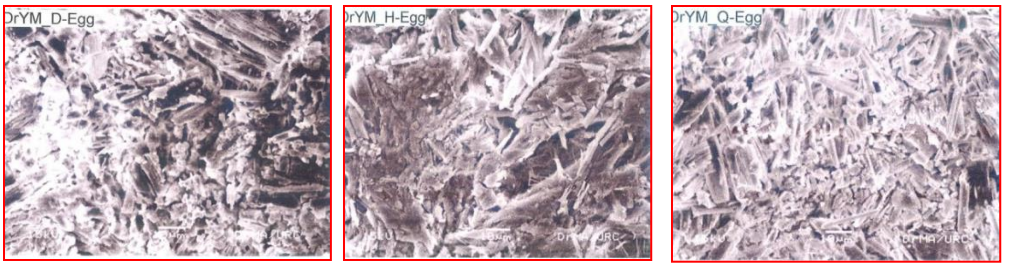

(a) (b) (c)

Figure 7: SEM images of calcium acetate from three eggshell samples (a) chicken (b) duck (c) quail at 1000 X magnification

Conclusion

In this study, the chemical, physical and morphological characteristics of the eggshell samples were investigated by using EDXRF, XRD and SEM. The results obtained from EDXRF spectrum showed that the most inorganic compounds in eggshell samples were calcium (29.26 % in chicken, 28.56 % in duck and 26.19 % in quail). XRD patterns of the three eggshell samples are identical with the calcite phase with hexagonal crystal system with lattice constant values of equal a and b axes and longer c axis. According to SEM micrographs, the eggshells were composed of calcium carbonate layer with small holes called pore canals on the surface of the shell for gas-exchange. Thermal behaviour of eggshell samples showed the presence of two thermal events, loss of moisture and combustion of organic matter accompanied by endothermic peaks and exothermic peaks respectively.The calcium carbonate content from three eggshell samples were found to be 61.75 % in chicken, 60.3 % in duck and 59.8 % in quail and thus these eggshell were good source of calcium. The shapes of the calcium acetate samples prepared form eggshell waste samples were needle like structure. The calcium acetate contents from eggshell samples were 46.76 % from chicken, 33.00 % from duck and 32.27 % from quail. The characteristic peaks of calcium acetate prepared from eggshell samples were found in corresponding FT IR spectra. Calcium acetate obtained from chicken eggshell gave the highest amount of calcium. From the results chicken eggshell waste contained the highest amount of calcium carbonate yielding the highest amount of calcium acetate.Thus, chicken

eggshell waste is appropriate for preparation of calcium acetate, a pharmaceutical excipient.

Acknowledgements

The authors would like to thank the Myanmar Academy of Arts and Science for allowing to present this paper and Professor and Head Dr Daw Ah Mar Yi, Department of Chemistry, University of Taunggyi, for her kind encouragement.

References

Chan,. S.,Au, K.,Francis, R. S.,Mudge, D.W., Johnson, D. W. and Pillans, P. I. (2017). "Phosphate Binders in Patients with Chronic Kidney Disease". Aust Prescr.,vol.40(1), pp.10–14

Choudhary, R., Koppala, S. and Swamiappan, S. (2015). "Bioactivity Studies of Calcium Magnesium Silicate Prepared from Eggshell Waste by Sol–gel Combustion Synthesis". *J. Asian Ceram. Soc*..vol. 7 (2), pp.1-5

Daengprok, W., Mine, Y.and Garnjanagoonchorn, W . (2000)."Fermented Pork Sausage Fortified with Commercial or Hen Eggshell Calcium Lactate". *Meat Sci.*, vol. 62(2), pp. 199-204

Freire, M. N. and Holanda, J. N. F. (2006). "Characterization of Avian Eggshell Waste Aiming its Use in a Ceramic Wall Tile Paste ". *Cerâmica*,vol. 52 ,pp. 240-244

Frost, L.R.,Musumeci, W. A. and Waclawik, E.R. (2007). "A Spectroscopic Study of the Mineral Paceite (Calcium Acetate)". *SpectrochimicaActa part A:Molecular and Biomolecular Spectroscopy* ,vol.67 (3-4), pp. 649-661

Leach,Jr. R.M. (1982). "Biochemistry of the Organic Matrix of the Eggshell".*Poultry Sci* .,vol. 61,pp.2040- 2047

Lee, H.J., Jung, N.Y., Park, S.H., Song, S.M., Kang, S.I., Kim, J.S.and Heu, M.S. (2015). "Characteristics and Preparation of Calcium Acetate from Butter Clam (*Saxidomuspurpuratus*) Shell Powder by Response Surface Methodology ". *J Korean Soc Food SciNutr*.,vol.44 (6), pp.888-895.

Macneil, J. (1997)."Composition of Egg Shell". *Egg Industry*, vol.102, pp. 15-17

NIOSH. (2015).*Calcium Acetate*.Atlanta: National Institute for Occupational Safety and Health.US Department Health and Human Service

Park, S.H., Jang, S. J., Lee, H. J., Lee, G.W., Lee, J.K., Kim, Y. J., Kim, J.S. and Heu, M. S. (2015)."Optimization of Calcium Acetate Preparation from Littleneck Clam (*Ruditapesphilippinarum*) Shell Powder and Its Properties ". *Korean J. Food Sci. Technol*. vol. 47 (3), pp. 321-327

Schaafsma, G. (1997)."Bioavailability of Calcium and Magnesium". *Eur. J. Clin. Nutr*., vol. 51, pp.S13-S16

PREPARATION AND CHARACTERIZATION OF $CaFeO_3$ POWDER AND ITS COAGULATION ACTIVITY IN TERMS OF REDUCING TURBIDITY

Mya Theingi[1], Thu Thu Hlaing[2]

Abstract

In recent years, materials with porous structure and high surface area are being developed for several applications in nanotechnology. The present research deals with a study on the preparation and characterization of $CaFeO_3$ nanocrystalline powder and its coagulation performance in a bentonite clay sample solution and river water. $CaFeO_3$ nanocrystalline powder was synthesized by citric acid sol-gel combustion method using citric acid and ethylene glycol as a fuel and the corresponding metal nitrates as oxidizers. The resulting xerogel was thermally treated in the muffle furnace at different temperatures (300 °C, 400 °C and 500 °C) for a maximum of 4 h each. The thermal behavior of samples was determined by Thermal-Gravimetric and Differential Thermal Analysis (TG-DTA). The prepared powder samples were characterized by X-ray powder diffraction (XRD), Scanning Electron Microscopy (SEM), Energy Dispersive X-ray Fluorescence (EDXRF), and Fourier Transform Infrared Spectroscopy (FT IR). X-ray diffraction (XRD) was used to study the transformation from precursor powders to rhombohedral crystals by calcination. Scanning Electron Microscopy (SEM) analysis showed the porous nature of the prepared powders. Physicochemical properties of the prepared nanocrystalline powder such as pH, moisture contact, bulk density and surface area also studied. Bentonite clay sample solution and river water sample were used to investigate the coagulation activity of the prepared $CaFeO_3$ nanocrystalline powder in terms of reducing turbidity.

Keywords: Sol-gel method, $CaFeO_3$, nanocrystalline powder, turbidity, coagulation

Introduction

In recent years, materials with porous structure and high surface area are being developed for several applications in nanotechnology (Bharat, 2010). Particular areas of interest include catalysis and separation science. The development of such materials is important for solving economic problems, which include the shortage of natural resources. Since the discovery of the

[1]. Dr, Lecturer, Department of Chemistry, University of Yangon
[2]. Demonstrator, Department of Chemistry, Yangon University of Distance Education

ordered mesoporous silica, a large number of porous materials have been made using surfactants as template. However, most of these materials are unstable on removal of the surfactant and the porous skeleton readily collapse when heated above 400 ºC. The collapse of mesostructure in mesoporous materials might be related to the structural rearrangement due to crystallization after removal of organic templates during calcination (Nagaraja *et al.*, 2012) Therefore, it is desirable to develop new methods of synthesis. Thermal stability, i.e., the ability of the material maintaining porous structure at high temperature is a key to both coagulation of ordered porous material and its practical applications (Emongor *et al.*, 2005, Tiwari *et al.*, 2008). This research deals with a study on preparation and characterization of calcium iron oxide ($CaFeO_3$) powder and its coagulation activity in terms of reducing turbidity (Jebun *et al.*, 2016).

In the present work, $CaFeO_3$ powder was prepared by sol-gel method. The thermal analysis on $CaFeO_3$ precursor powders were carried out at the temperature range of 30 to 600 ºC for 3 h by Thermogravimetry and Differential Thermal Analysis (TG-DTA). X-ray diffraction (XRD) was used to study the transformation from precursor powders into orthorhombic crystal structure. The Scherrer's formula was used to compute the average crystallite sizes of $CaFeO_3$ powders. The morphology of prepared powder was characterized by Scanning Electron Microscopic (SEM) analysis. Inorganic synthetic coagulants are commonly used in non-potable water and wastewater industries. The prepared $CaFeO_3$ nanocrystalline powder was first time used as coagulants and study the coagulation activity in terms of reducing turbidity from both collected river water and betonite clay sample suspension.

Materials and Methods

All the chemicals were analytical grade. Calcium nitrate $Ca(NO_3)_2.4H_2O$, iron nitrate $Fe(NO_3)_3.9H_2O$, citric acid $C_6H_8O_7$ were Merck product with a purity of 99.99 %. Ethylene glycol was product from Applichem, Germany. All solutions were prepared using distilled water during preparation procedures. Various conventional and modern instruments techniques were used throughout the experimental procedure. These include X-ray Diffractometry (XRD), Energy Dispersive X-ray Fluorescence (EDXRF), Scanning Electron Microscope (SEM), Thermogravimetry/

Differential Thermal Analysis (TG-DTA) and Fourier Transform Infrared Spectroscopy (FT IR). Physicochemical properties of prepared $CaFeO_3$ nanocrystalline powders such as free moisture contact, pH, bulk density and specific surface area were determined by conventional laboratory methods. Coagulation activity in terms of reducing turbidity from both collected river water and betonite clay suspension were carried out.

Preparation of $CaFeO_3$ Powders by Sol-Gel Method

Calcium nitrate, iron nitrate, citric acid and ethylene glycol were used as starting materials for synthesis of nanocrystalline $CaFeO_3$ powders. First calcium nitrates and iron nitrate were dissolved in deionized water and solution (I) was obtained. Citric acid was dissolved in distilled water and solution (II) was obtained. The solution (I) and (II) were mixed as the molar ratio of citric acid and metal ion in 1:2 and then 5 mL of ethylene glycol was added to the mixture solution. This mixture solution was stirred with magnetic stirrer and heated at 70 °C-80 °C for 7 h to get $CaFeO_3$ gels. The gels were dried oven at 110 °C for 4 h and ground with mortar and pestle to get dry as-prepared $CaFeO_3$ powder. A small part of the as-prepared powder was used for thermal analysis (TG-DTA). The prepared as-prepared $CaFeO_3$ powder was calcined at 300 °C, 400 °C and 500 °C for 4 h, and the samples were designated as CFO-300, CFO-400 and CFO-500 with their calcination temperatures. Finally, the samples were ground smoothly in an agate mortar and nanocrystalline $CaFeO_3$ powders were obtained (Mya Theingi 2013). Flowchart of the preparation procedure is shown in Figure 1.

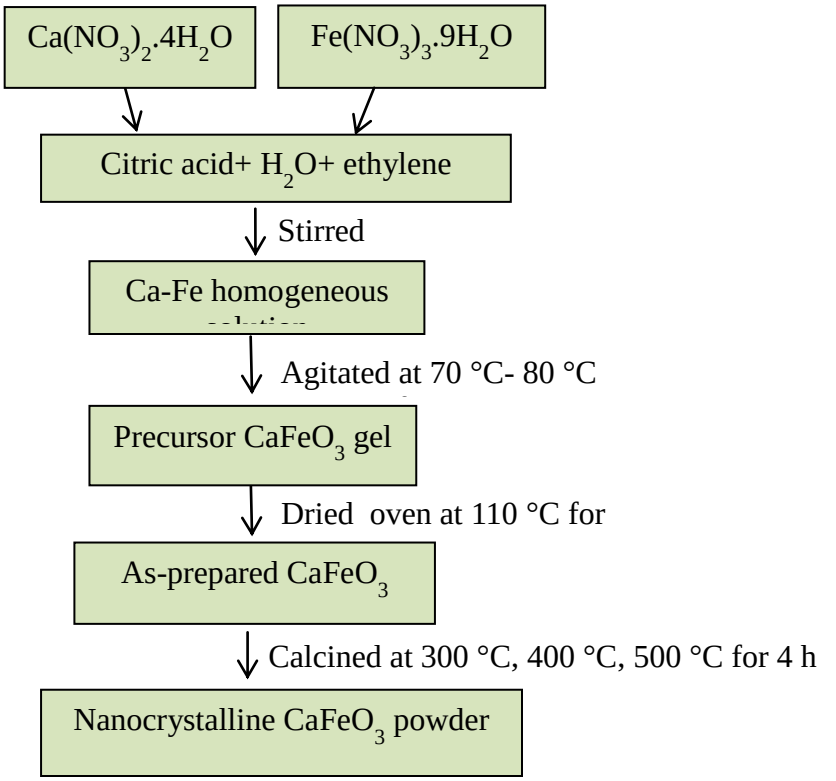

Figure 1: Flowchart of the preparation of $CaFeO_3$ by Sol-gel method

Characterizations of Prepared $CaFeO_3$

The thermal decomposition behaviours of the as-prepared and nanocrystalline $CaFeO_3$ powders were examined by means of thermal gravimetric and differential thermal analysis (TG-DTA) by using a Perkin Elmer in the range of 35–600 °C with heating rate 10 °C/min in static air and Al_2O_3 as a reference. Crystal structure and phase analyses were performed by X-ray diffraction (XRD) using Rigaku, D-Max 2200, Japan. Morphology of the powder and the elemental composition were recorded by scanning electron microscope, ZEISS Gemini SEM, Germany. Energy dispersive X-ray fluorescence (EDXRF) confirms the elemental compositions of the prepared sample by using Perkin Elmex 700, ED XRF spectrometer. FT IR transmission spectra in the region from 400-4000 cm^{-1} were measured using Shimadzu model IR 408, Japan. The physicochemical properties such as free

moisture contact, pH, bulk density and specific surface area of the prepared nanocrystalline $CaFeO_3$ powders were determined by conventional laboratory methods. For examples, moisture contact was measure by oven dry test; pH was measure by a pH meter, bulk density was measured by tapped method and specific surface area was determined by methylene blue adsorption test.

Coagulation Activity of the Prepared Nanocrystalline $CaFeO_3$ powders

Bentonite Clay ample Suspension was prepared by 0.7 g of bentonite clay was dissolved in 1L of water and river water was collected from Yangon River (Kyee Myindaing Kanner Road, Kyee Myindaing Township, and Yangon, Myanmar). The coagulation activity in terms of reducing turbidity from both collected river water and betonite clay sample suspension were investigate by effect of contact times of coagulants.

Effect of Contact Time

About 0.1 g of the prepared $CaFeO_3$ samples (coagulants) was taken into the conical flasks and then 50 mL of bentonite clay sample suspension or 50 mL of collected river water were added to each conical flask. The conical flasks were shaken in orbital shaker with 150 rpm in 30, 60, 90 minutes. The conical flasks were kept for 1 day. The top layer of water was collected from each conical flask with pipette and the turbidities were measured by turbidimeter. Coagulation activity was calculated by using the following equation: coagulation activity = $\frac{\mathrm{TB} - \mathrm{TS}}{\mathrm{TB}} \times 100$, where TB is the turbidity of blank and TS is the turbidity of the sample, (Ebeling *et al.*,. 2003).

Results and Discussions

Thermo Gravimetric and Differential Thermal Analysis (TG-DTA) of $CaFeO_3$ Powders

Thermal analysis was carried out on the as-prepared $CaFeO_3$ powder by sol-gel method and TG-DTA thermogram are show in Figure 2 and the interpretation data are summarized in Table 1. There are four weight loss steps in the TG curve accompanied with one endothermic and three exothermic peaks which are observed in DTA curve. The first step was found a small endothermic peak which at the temperature range of 30-100 ºC with the 8.255

% weight loss and this may be due to the evaporation of absorbed water or bound water. In the second stage, an exothermic peak in the temperature range of 200 °C and 300 °C with the weight loss percent was 30.958 % could be attributed to the decomposition of organic matters in the as-prepared powder like C-N, C-H and C-O. In the third stage, an exothermic peak in the temperature range 300 °C and 400 °C with the weight loss percent was 21.67 % and this may be due to the decomposition of nitrates (NO_3^-) and crystallization of $CaFeO_3$. In the fourth stage, an exothermic peak in the temperature range 400 °C and 500 °C with the weight loss percent was 15.48 % due to due to the formation of the expected perovskite phase of $CaFeO_3$. With respect to above result calcination temperatures of the samples were taken at 300 °C, 400 °C and 500 °C and these samples were designated as CFO-300, CFO-400 and CFO-500, respectively. Thermal analysis was also carried out on the prepared CFO-500 powders by TG-DTA and their curves are shown in Figure 3. There was no prominent weight loss on TG curve indicating that the prepared powder was almost stable (Heshem, 2004)

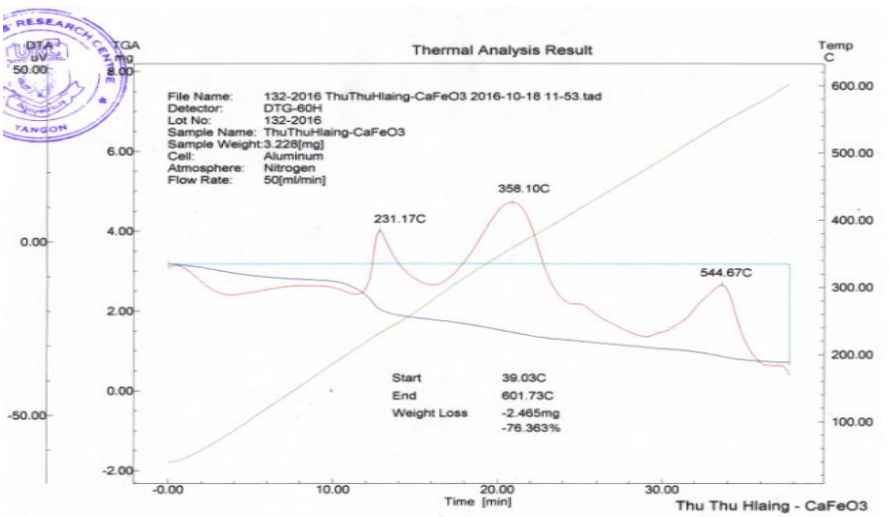

Figure 2: TG-DTA curves of the thermal decomposition of as-prepared $CaFeO_3$ powder

Table 1: Interpretation Data for the Thermal Decomposition of $CaFeO_3$ As-prepared Powder by TG-DTA Analysis

Temp. Range /°C	Weight loss (%)	Nature of peak	Peak's temp. /°C	Remark
80-100	8.255	endo	80	evaporation the absorbed water or bound water
200-300	30.958	exo	231	decomposition organic species
300-400	21.67	exo	358	decomposition of nitrate and crystallization
500-600	15.48	exo	544	formation of the expected perovskite phase of $CaFeO_3$

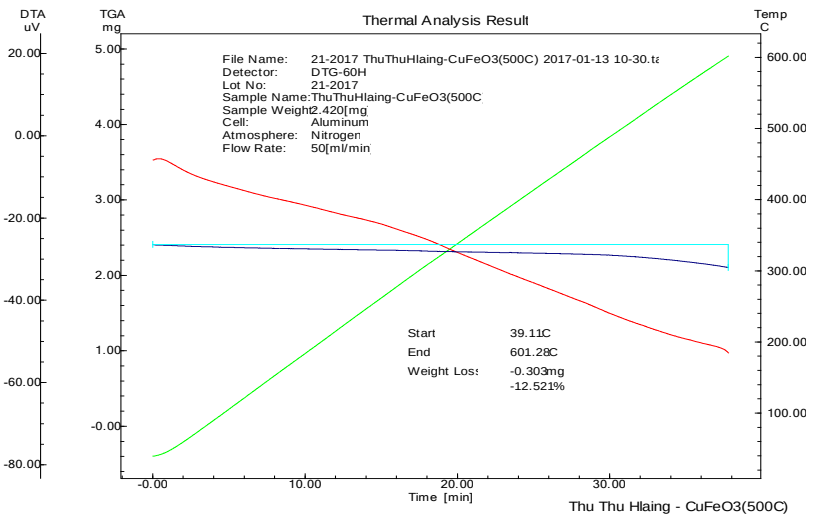

Figure 3: TG-DTA curves of the thermal decomposition of CFO-500

X-ray Diffraction Studies (XRD) of $CaFeO_3$ Powders

The formation of the crystalline structure and crystallite size of prepared samples were confirmed by XRD analysis. XRD diffractograms for as-prepared powder, CFO-300, CFO-400 and CFO-500 are shown in Figures 4 (a)-(d). From these analyses, the as-prepared powder is amorphous nature

and X-ray powder diffraction patterns of CFO-300, CFO-400 and CFO-500 confirm the crystalline forms of the samples. XRD pattern of CFO-300 matched with PDF card No. 84-08847 of calcium iron oxide ($CaFeO_3$) but some of the peaks is disappeared due to impurities and crystal structure of CFO-300 is tetragonal. XRD pattern of CFO-400 also matched with PDF card No. 84-08847 of calcium iron oxide ($CaFeO_{2.5}$) and it has pure phase and other secondary phases are not observed. Crystal structure of CFO-400 is orthorhombic. XRD pattern of CFO-500 also matched with PDF card No. 84-08847 of calcium iron oxide ($Ca_4Fe_{14}O_{25}$). Crystal structure of CFO-500 is hexagonal. The average lattice constants, the average crystallite sizes of the prepared samples that were calculated by using the Debye-Scherrer equation: $D = k\lambda/B \cos\theta$, (Zafar *et al.*, 2015) where D is the average size of crystalline particle, assuming that particles are spherical, $k = 0.9$, λ is the wavelength of X-ray radiation, B is full width at half maximum of the diffracted peak, and θ is angle of diffraction, are shown in Table 2. Crystallite size of CFO-300 has 46.18 nm, CFO-400 has 29.81 nm and CFO-500 has 35.27 nm. It was found that the crystallite size of $CaFeO_3$ decrease with increasing calcination temperature and the crystal structure of the prepared sample is mainly depended on calcination temperatures.

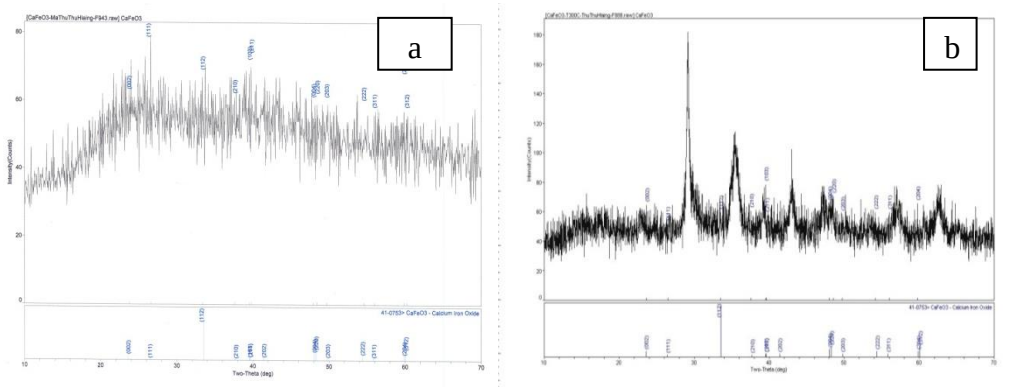

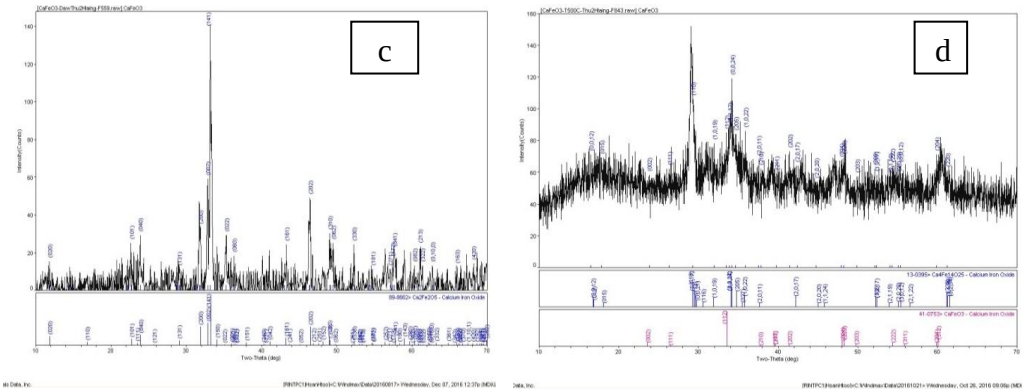

Figure 4: X-ray diffraction patterns of (a) as-prepared powder (b) CFO-300 (c) CFO-400 (d) CFO-500

Table 2: Average Lattice Constants, Crystal Structure and Average Crystallite size of CFO-300, CFO-400 and CFO-500

Samples	Average Lattice Constants /A°			Crystal structure	Crystallite Size/nm
	a	b	c		
CFO-300	5.3394	-	7.5511	Tetragonal	46.18
CFO-400	5.6224	14.9187	5.4532	Orthorhombic	29.81
CFO-500	6.0998	-	58.3881	Hexagonal	35.27

Scanning Electron Microscopy Studies (SEM) of $CaFeO_3$ Powders

The surface morphologies of the prepared CFO-300, CFO-400 and CFO-500 were studied by SEM and their micrographs are shown in Figures 5 (a)-(c). The SEM images reveal that all of the products look like low density, loose and porous materials that is favorable for filtration process. It was also found that agglomeration of the particles increased with increasing temperatures.

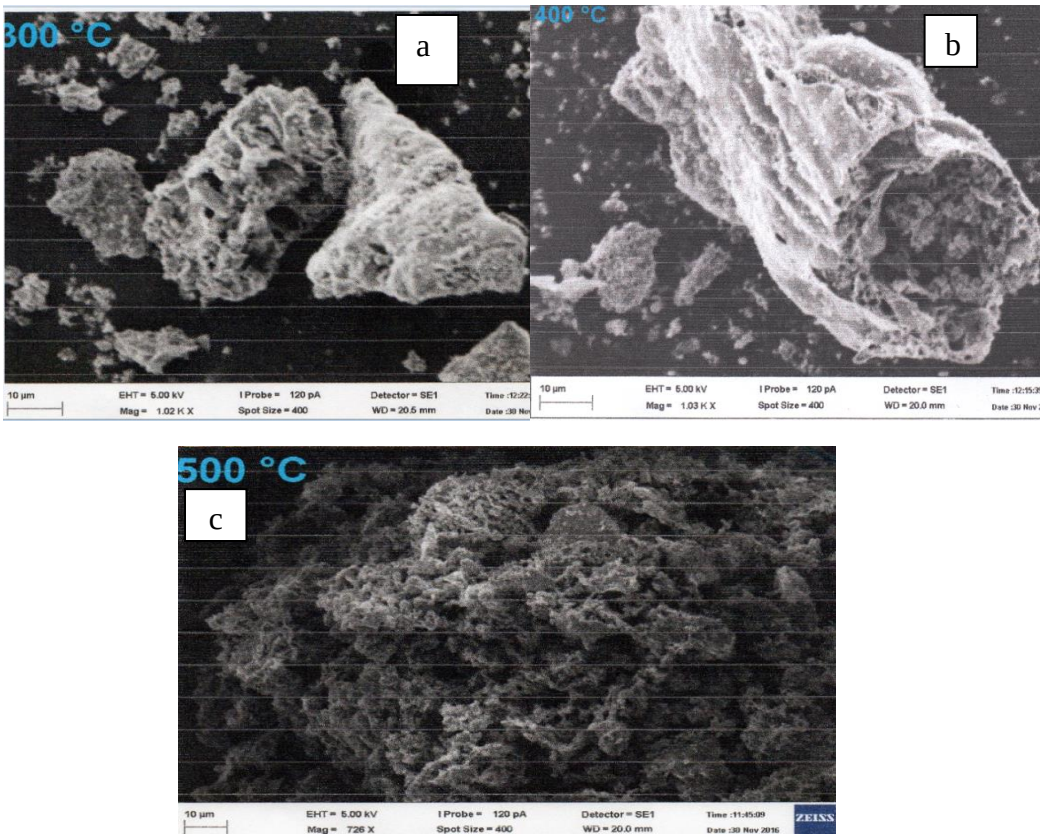

Figure 5: SEM micrographs of the prepared (a) CFO-300 at 1.0 kX magnification, (b) CFO-400 at 1.0 kX magnification and (c) CFO-500 at 0.75 kX magnification

Elemental Studies (ED XRF) **of $CaFeO_3$ Powders**

Figures 6 (a)-(c) show energy Dispersive X-ray Fluorescence (EDXRF) spectra of $CaFeO_3$ samples, which confirm the relative abundance of the elements in $CaFeO_3$ nanocrystalline powders. From the EDXRF spectra, it is further confirmed that no elements other than Ca and Fe were present hence it shows that the prepared samples were highly pure. The relative abundance of the elements (%) of the samples is listed in table 3.

Table 3: Relative Abundance of Elements of the prepared CFO-300, CFO-400 and CFO-500 by EDXRF Analysis

Elements	Relative Abundance of Elements in the Samples (%)			Molar mass ($gmol^{-1}$)
	CFO-300	CFO-400	CFO-500	
Ca	37.205	39.222	39.413	40
Fe	62.456	60.426	60.255	56

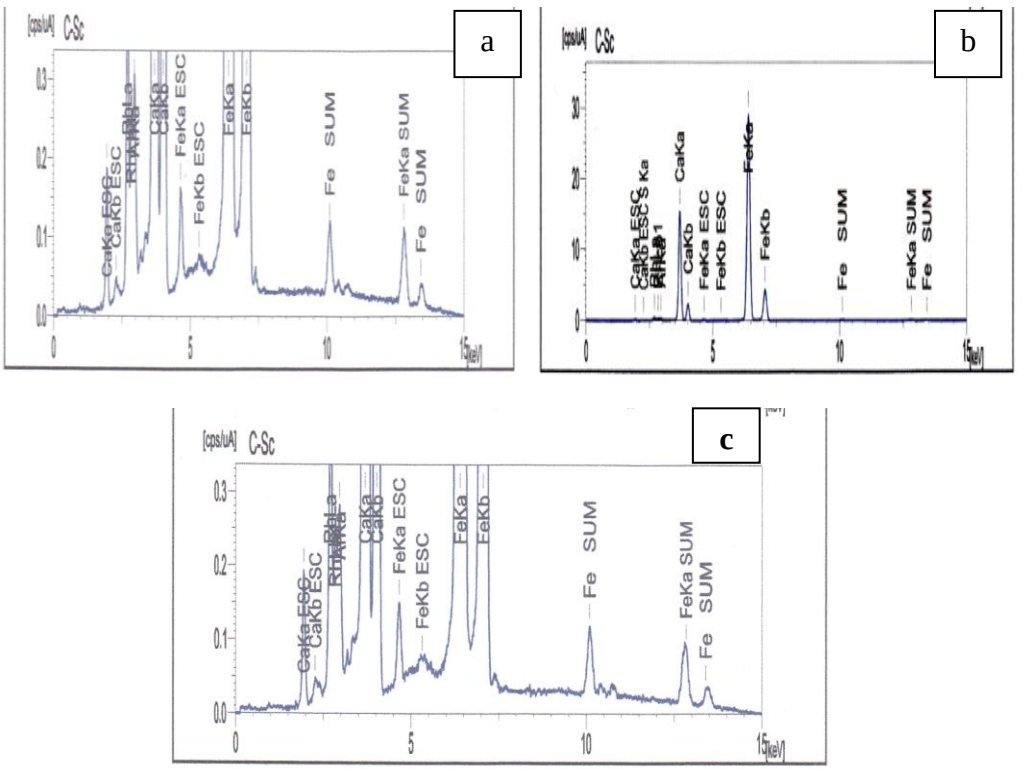

Figure 6: ED XRF spectra of the prepared $CaFeO_3$ nanocrystalline powders (a) CFO-300, (b) CFO-400 and (c) CFO-500

Fourier-transform Infrared Spectroscopy Studies (FT IR) of $CaFeO_3$ Powders

FT IR spectra of the prepared $CaFeO_3$ xerogel powder before calcination and after calcined (CFO-300, CFO-400 and CFO-500) are shown in Figures 7(a)-(d). In the FT IR spectrum of the prepared as-prepared $CaFeO_3$ powder, the band occurred at 3429 cm^{-1}, due to O-H stretching vibration and the band occurred at 1618 cm^{-1} due to N-O stretching vibration. The band at 1242 cm^{-1} shows C-O stretching vibration of chelating agent and the band at 661 cm^{-1} attribute the stretching of metal-oxygen vibration. The results suggested that the as-prepared gel consists of an intermediate/complex of citric acid, water, and metal ions. The FT IR spectra of the prepared CFO-300, CFO-400 and CFO-500 samples exhibit absorption bands between 3400-3000 cm^{-1} due to the O-H stretching vibration, a band between 1400-1500 cm^{-1} which represent the C-O stretching vibration from residual carbon, the band at 800-900 cm^{-1} shows C-H bending vibration from residual carbon and the bands between 400-750 cm^{-1} show stretching vibration of metal-oxygen bond. The observed FT IR data of the prepared $CaFeO_3$ powders were consistent with literature values, (Nakamoto1970).

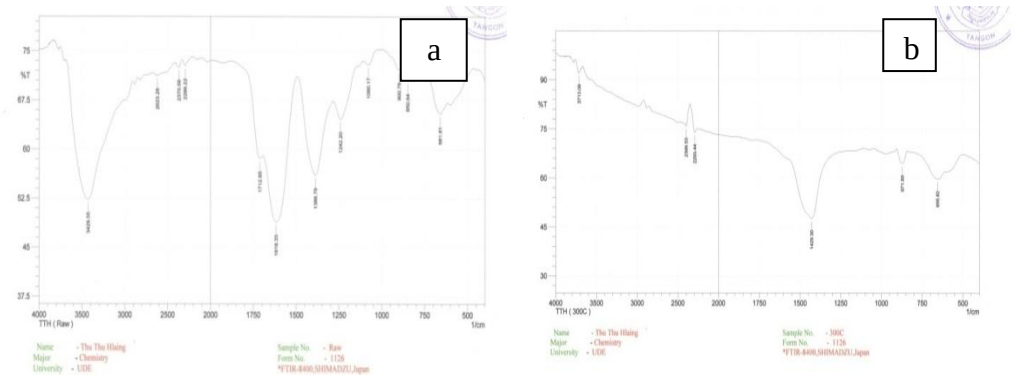

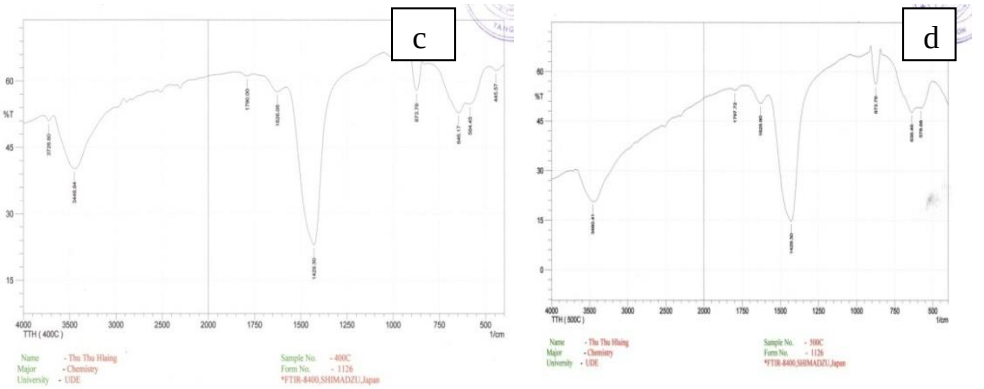

Figure 7: FT IR spectra of (a) as-prepared $CaFeO_3$ powder (b) CFO-300,(c) CFO-400 and (d) CFO-500

Physicochemical Properties of $CaFeO_3$ Powders

Physicochemical properties of prepared calcium iron oxide powders were determined by conventional laboratory methods. The physicochemical properties such as free moisture contact, pH, bulk density, specific surface area of prepared calcium iron oxide powder are presented in Table 4. It was found that pH of the prepared samples are almost neutral. Moisture contact decreases with increasing calcination temperature. Surface areas of the prepared CFO-300, CFO-400 and CFO-500 powders are 3.87 6 m^2/g, 5.612 m^2/g and 4.808 m^2/g, respectively. It was found that CFO-400 has the largest surface area among three prepared samples.

Table 4: Some Physicochemical Properties of the Prepared $CaFeO_3$ Nanocrystalline Powders

Sample	pH	Moisture Contact / %	Bulk Density/ gmL	Surface Area/ m^2/g
CFO-300	7.55	8	0.623	3.876
CFO-400	7.45	7	0.395	5.612
CFO-500	7.44	5	0.51	4.808

Coagulation Activity of $CaFeO_3$ Powders

The coagulation activity or removal percent of turbidity of $CaFeO_3$ powders were studied on river water as well as betonite clay suspension by varying contact time effect. The measurement of turbidity is a key test of water quality. WHO (2017) water quality standard is not exceeding 5 nephelometric turbidity units (NTU). Variation of reduced turbidity and removal percentages of turbidity from river water and betonite clay suspension with contact time are shown in Tables 5-8.

Table 5: Variation of Reduced Turbidity of Bentonite Clay Suspension by the Prepared Samples with Different Contact Time

Sample	Turbidity (NTU) at Different Shaking Time (minutes)			
	0	**30**	**60**	**90**
Bentonite Clay Suspension	77.20	26.60	23.60	23.80
CFO-300	-	7.83	10.00	13.30
CFO-400	-	1.25	2.42	1.42
CFO-500	-	1.62	1.45	0.91

Table 6: Variation of Coagulation Activity of the Prepared Samples on Bentonite Clay Suspension with Different Contact Time

Sample	Coagulation Activity (%) at Different Contact Time (minutes)		
	30	**60**	**90**
CFO-300	89.86	87.05	82.77
CFO-400	98.38	96.87	98.16
CFO-500	97.90	98.12	98.82

Table 7: Variation of Reduced Turbidity of River Water by the Prepared Samples with Different Contact Time

Sample	Turbidity (NTU) at Different Shaking Time (minutes)			
	0	**30**	**60**	**90**
River Water	83.5	26	23.4	21.9
CFO-300	-	9.23	8.42	9.96
CFO-400	-	1.44	1.46	1.24
CFO-500	-	1.41	1.43	1.43

Table 8: Variation of Coagulation Activity of the Prepared Samples on River Water with Different Contact Time

Sample	Coagulation Activity (%) at Different Contact Time (minutes)		
	30	**60**	**90**
CFO-300	88.95	89.92	88.07
CFO-400	98.28	98.25	98.51
CFO-500	98.31	98.29	98.29

Conclusion

$CaFeO_3$ nanocrystalline powders are of considerable interest due to their wide range of applications in fields such as magnetic storage, medicine, chemical industries and water purification. The present research deals with a study on preparation, characterization and coagulation activity of the prepared $CaFeO_3$ powders. By TG-DTA analysis the minimum crystalline temperature or required $CaFeO_3$ structure formation temperature was started from 400 °C. The XRD patterns of the three prepared powder samples, CFO-300, CFO-400 and CFO-500, $CaFeO_3$ described the tetragonal, orthorhombic and hexagonal phases with respect to their calcination temperatures. The average crystallite sizes of the CFO-300, CFO-400 and CFO-500 were found to be 46.18, 29.81, 35.27 nm, respectively. From SEM results, it was confirmed that the CFO-300 sample showed porous nature with less agglomerate, CFO-400 samples had porous and fibrous and porous nature and CFO-500 had porous and more

uniformly agglomerate. From EDXRF results, the main constituent elements of all three samples are Fe and Ca and all are approximately 1:1 molar ratio. According to FT IR, C-O stretching vibration at 1408 and 1033 cm^{-1}, C-H stretching vibration at 874 cm^{-1} and metal oxygen stretching vibration at 712 cm^{-1} are observed in all three prepared sample. Surface area of CFO-400 (5.612 m^2/g) is greater than that of other two samples. The coagulation activities of $CaFeO_3$ powders were studied in term of turbidity of bentonite clay suspension and river water. The coagulation activities of prepared samples from river water are 87.05 % by CFO-300, 96.87 % by CFO-400 and 98.12 % by CFO-500 powder with contact time 1h. The coagulation activities of prepared samples on the bentonite clay suspension are 89.92 % by CFO-300, 98.25 % by CFO-400 and 98.29 % by CFO-500 powder with contact time 1h. According to these removal percentages, CFO-400 and CFO-500 powders were found to be more efficient than CFO-300 for the removal of turbidity from both river water and bentonite clay suspension. This research mainly concerns with the preparation and characterization of $CaFeO_3$ nanocrystalline powders but only study coagulation activity of the prepared samples in terms of reducing turbidly of water and further characteristic factors of water are still needed to study.

Acknowledgements

The authors would like to express their profound gratitude to the Department of Higher Education, Ministry of Education, Yangon, Myanmar, for provision of opportunity to do this research and Myanmar Academy of Arts and Science for allowing to present this paper.

References

Bharat, B. (2010). *Introduction to Nanotechnology*, *Springer Handbook of Nanotechnology*. New York: 3rd Ed., Ie-tex Publishing Services, pp.1-12

Ebeling, J. M., Sibrell, P. L., Ogden, S. R. and Summerfelt, S. T. (2003). "Evaluation of Chemical Coagulation Flocculation Aids for the removal of Suspended Solids and Phosphorus from Intensive Recirculating Aquaculture Effluent Discharge". *Aquacultural Engineering*, vol. 29 (1), pp. 23-42

Emongor, V., Nkegbe, E., Kealotswe, B., Koorapetse, I., Sankwasa, S. and Keikanetswe, S. (2005). "Pollution Indicators in Gaborone Industrial Effluent". Journal of Applied Sciences, vol. 5, pp.147-150

Hesham, I.S. (2004). "Synthesis and Formation Mechanism of Calcium Ferrite Compounds". *J. Mater. Sci. Technol*., vol. 20 (5), pp. 530-534

Jebun, N., Mamun, A., Alam, A. M. and Ahand Raus, R. B. (2016). "Fungal Flocculants to Reduce Turbidity of River Water". *ARPM J. of Eng. and Applied Sciences*. Vol. 11 (6), pp. 4094-4099

Nagaraja, R., Girija, C. R. and Nagabhushan, H. (2012). "Removal of COD from Polluted River Water Using Nanocrysatalline $LaMnO_{3+\delta}$ Powder". *International J. of Science Research*, vol. 1 (2), pp. 87-90

Nakamoto, K. (1970). *Infrad Spectra of Inorganic and Coordination Compounds*. New York: 2nd Edition, Wiley Interscience Publication, pp. 436-445

Tiwari, D. K., Behari, J. and Sen, P. (2008). "Application of Nanoparticles in Waste Water Treatment". *World Applied Science Journal*, vol. 3 (3), pp. 417-433

Mya Theingi. (2013). *Study of Electrical Properties and Laser Induced Voltage Effect in* $La_{1-x}Ca_xMnO_3$ *Epitaxial Thin Films.* China: PhD Dissertation, Material Science, Kunming University of Science and Technology

Zafar, N. and khan, M. N.. (2015). Structural, Electric and Thermoelectric Studiues of $CaFeO_3$ System" *J. of Nucleus*. vol. 52 (1), pp. 25-28

CHEMICAL INVESTIGATION AND ANTIOXIDANT ACTIVITY OF *Piper betel* L. (KUN) AND ITS POSSIBLE USE IN DRUGS FOR DENTAL AND SKIN INFECTIONS

San San Aye[1], Zar Chi Soe[2], Myo Min[3]

Abstract

Today, there are various types of infections. Among them, dental infections and skin infections are very common in developing countries. Myanmar medicinal plant; *P.betel* (KUN) used for the treatment of dental infections and skin infections, was screened for antimicrobial activity by agar disc diffusion technique. Polar and non-polar solvents were employed for the extraction of leaves of *P. betel.* Essential oil was obtained from leaves by steam distillation. The antimicrobial activity of crude extracts and essential oil of *P. betel* was studied on seven species of *Staphylococcus aureus* cultured from plaque of gingivitis and five strains of organisms which usually cause skin infections. It was observed that extracts and essential oil of *P. betel* were effective against all the tested microorganisms (11 mm - 40 mm). The minimum inhibitory concentration (MIC) of the active extract was evaluated by agar disc diffusion method. Acute toxicity of 70 % ethanol and watery extracts of the leaves evaluated by the methods of Organization for Economic Cooperation and Development (OECD) guidelines showed no toxicity. Eugenol (0.1 %) was isolated from essential oil of *P. betel* and identified by UV, FT IR and EI-MS. In addition, an ointment was formulated with essential oil of *P. betel* and *in-vivo* test was performed on induced open wound infected with *Staphylococcus aureus* on rats. The ulcer healing was observed within 9 days. Moreover, *in-vitro* antioxidant activity of ethanol and watery extract were determined by Dot-Blot and DPPH staining method. The results thus indicated the possible uses of *P. betel* leaf in the formulations of drug for dental and skin infections.

Keywords: antimicrobial, essential oil, dental infection, skin infection, *Piper betel*

Introduction

In Myanmar, some herbal medicinal plants are effective against bacteria in oral cavity and are used in the treatment of oral diseases. Skin infections are treated by many antibiotic ointments, creams and other topical

[1]. Associate Professor, Department of Chemistry, Myingyan Degree College
[2]. Lecturer, Department of Pharmacology, University of Pharmacy
[3]. Associate Professor, Department of Chemistry, West Yangon University

applications. However, some bacteria are resistant to some antibiotics which may delay healing. Thus ointments and topical applications prepared by using extracts of medicinal plants that are very common and easily available is desirable (Mi Mi Htwe *et al*., 2001).

Piper betel L. belongs to the family Piperaceae and also known as KUN in Myanmar. It is a common plant cultivated in Asia countries. *P. betel* leaves are used in folk medicine for the treatment of various disorders and are commonly chewed among Asians (Arambewela, 2006). It is an indigenous medicinal plant and is relatively cheap, easily available and less expensive. Although antibacterial activities of petroleum ether (60 - 80 ℃), methanol and watery extracts of *P. betel* (KUN) were reported in Myanmar (Hnin Hnin Aye, 2002), no paper has been published regarding the evaluation of antimicrobial activity against infectious bacteria causing dental and skin infections. Thus the present study focused on the investigation of antimicrobial activity of the essential oil and solvent extracts of *P. betel* on microorganisms from dental infections and skin infections, with the aim of making economic production of antimicrobial and preparation of ointment for wounds and sores. Therefore, the present study is expected to provide valuable information in traditional and alternative medicine practice.

Materials and Methods

Sample

The plant sample, the leaves of *P.betel* (KUN) was collected from Tontay Township, Yangon Region, in January and February 2016. Botanical identification of plant sample was confirmed by Daw Khin Lay, Associate Professor and Head, Department of Pharmacognosy, University of Pharmacy, Yangon.

Preparation of crude extracts

Dried powders of leaves were extracted with petroleum ether (60 - 80 ℃), 95 % ethanol and water using Soxhlet apparatus. Extraction time with each solvent was 6 h. After removing each solvent by rotary evaporator, the crude extract was dried and kept in desiccator.

Extraction of essential oil from *P. betel* L.

Extraction of essential oil from *P. betel* was carried by steam distillation. The dried powder (100 g) and distilled water (500 mL) were placed in 1 L round bottomed - flask. The flask was fitted for steam distillation and heated. The steam was passed into the flask. The condensed oil and water were collected in the flask and the oil was extracted with petroleum ether (60 – 80 ℃) in a separating funnel. The PE extract was dried over anhydrous sodium sulphate. After filtration, the filtrate was evaporated to get the essential oil which was weighed and kept in air tight bottle for further analysis (Pauli, 2001).

Antimicrobial activity

A sterile cotton swab was dipped into the bacterial suspension and streaked evenly three times by rotating the plates through an angle of 60 ℃ onto the surface of the nutrient agar plate before the plates were seeded. After the inoculum has dried for a few minutes, the dried discs impregnated with plant extract were placed on the agar with a flamed forceps and gently pressed down to ensure contact. A control disc, impregnated with solvent only and clinical drug discs were also included. Plates were incubated at 37 ℃ in an incubator within 30 min after inoculation. After overnight incubation, the zone of inhibition diameters (including 6 mm disc) were measured (WHO, 2003).

Determination of minimum inhibitory concentration (MIC) of the active extracts by agar disc diffusion method

In order to determine the least concentration of extracts that inhibit the growth of microorganisms, the specific concentrations of extracts were prepared in serial dilution with respective solvents (e.g. ethanolic extract with ethanol). The crude extract (0.1 g) was dissolved in 1 mL of respective solvent as a stock solution. And then 500 mL was carried over from the stock solution and diluted with 500 mL of respective solvent to obtain the following concentrations: (10, 5, 2.5 and 1.25 mg/mL) and used to testing with micro-organisms. The bacterial broth suspension was streaked onto the surface of the medium. After the inoculum was dried for five minutes, the dried discs incorporated with plant extracts which were diluted into various concentrations. Then, these discs were placed on the agar with a flamed

forceps and gently pressed down to ensure contact. The plates were incubated at 37 ℃ in an incubator within 30 min after inoculation. After overnight incubation, the lowest dilution of the plant extracts where organisms could not grow was taken as the MIC (Stokes *et al*., 1993).

Acute toxicity study of both 70 % ethanol and watery extracts on albino mice

To determine the consequence of utilization of the plant, the acute toxicity test was done to determine the nature and degree of toxicity produced by the plant extracts as the medium lethal doses (LD50). In this study, acute toxicity of 70 % ethanol and watery extracts of P. betel leaves were determined on albino mice, at Laboratory Animal Services Division, Department of Medical Research (DMR), and Yangon. Acute toxicity of different doses of the extracts was evaluated by the methods of OECD (Organization for Economic Cooperation and Development) Guidelines. They were fasted for 18 h before giving the extracts. Group (A) mice were orally administrated with ethanol extract of 2000 mg/kg dose. Group (B) mice were given orally with ethanol extract of 5000 mg/kg dose. Group (C) mice were orally administrated with watery extract of 2000 mg/kg dose. Group (D) mice were also given orally with watery extract of 5000 mg/kg dose. Group (E) mice performed as a control group and they were treated with clean water and normal animal food. All groups of mice were kept in the three mouse cages in the separated room at the room temperature of 26 ± 1 ℃. After administration of extract on each group of animals were observed first 6 hours continuously for mortality and behavior changes. Then check the animals each 24 h for fourteen days. The mortality during this period was noted (OECD, 2000).

***In- vivo* evaluation the healing activity of *Staphylococcus aureus* induced open wounds**

Both sexes of adult rats (154 g to 225 g), comprising four animals per group were used in the experiments: open wounds to be infected were made, using a modified method (Skerman, 1967). Inoculation of the wounds with *Staphylococcus aureus* was done as described above method. The flanks were chosen for the sites of operation. The areas were initially shaved with a razor blade and then sterilized by applying serially with methylated sprit.

Longitudinal incisions of three centimeters length was made in each sterilized area, the depth incision cutting through some fibers of the muscular layer. The bacterial suspension of *Staphylococcus aureus* 0.2 mL was induced into the incision by the syringe. The wounds were daily observed and dressed with either the test drug or just sterile dressing. Estimation of wound healing was made by measuring the length of unhealed portion of the wound, in centimeter. At the same time, evidence of induration, erythematous area and the presence of pus were checked and noted.

Rapid screening of antioxidant activity by Dot-Blot and DPPH staining method

In this study, the antioxidant potential of ethanol and watery extracts of *P. betel* leaves was evaluated by Dot-Blot and DPPH staining method (Soler-Rivas *et al*., 2000). Drops of each sample were carefully loaded on TLC plate and allowed to dry (3 min). Drops of each sample were loaded in order of decreasing concentration along the row. The sheet bearing the spots was placed upside down for 10 s in a DPPH solution. The stained silica layer revealed a purple background with white spots at the location of the drops, which showed radical scavenger capacity. Tested amounts were 400, 200,100, 50, 25, 12.5, 6.25 µg for each extracts.

Isolation and characterization of eugenol from *P. betel* L.

Eugenol was isolated from the essential oil of *P. betel* by column chromatographic method using toluene and ethyl acetate (9:1). It is clear to pale yellow oily liquid. It is slightly soluble in water and organic solvents. It has a pleasant spicy, clove-like odour.

Results and Discussion

Dental infection

Antimicrobial activity of petroleum ether, 95 % ethanol, watery extract and essential oil of *P. betel* was tested on seven species of *Staphylococcus aureus* isolated from plaque of gingivitis (Figures 1, 2 and Table 1). It was observed that all the extracts showed antimicrobial activity on the tested

bacteria strains (11 mm - 40 mm). Among them, essential oil (40 mm) has higher antimicrobial activity than the other extracts.

Skin infection

The screening of antimicrobial activity of crude extracts (PE, 95 % ethanol, water) and essential oil of *P. betel* was also tested on five strains of bacteria (*Candida albicans*, *Escherichia coli*, *Klebsiella aerogenes*, *Pseudomonas aeruginosa* and *Staphylococcus aureus*) which caused skin infection. From the experimental results, all the extracts showed antimicrobial activity against all tested organisms (11 mm - 40 mm) (Figures 3, 4 and Table 2). It is clearly seen that essential oil also shows significant antimicrobial activity against the organisms which can cause skin infections.

Minimum inhibitory concentration (MIC)

Minimum inhibitory concentrations of crude extracts (PE, 95 % ethanol, water) of *P. betel* were determined by agar disc diffusion method. It was found that MIC of PE extract on *S. aureus* from plaque of gingivitis was 5 mg/mL. It was also observed that the MICs of petroleum ether extract of *P. betel* were 5 mg/mL for *C. albicans*, 2.5 mg/mL for *K. aerogenes* and *S. aureus*. It did not give inhibition zone in concentration of 10 mg/mL on *P. aeruginosa*. Alcoholic extract and watery extract were 5 mg/mL for *P.aeruginosa* and *C. albicans* and 2.5 mg/mL for *K. aerogenes*. From the above data, the crude extracts of *P. betel* leave were more effective on *K. aerogenes* and *C. albicans*. These two organisms are the most common bacteria which can cause skin infections (Figures 5, 6 and Table 3).

Acute toxicity

Acute toxicity screening of 70 % ethanol and watery extract of P. betel leaves were done with the dosage of 2000 mg/kg and 5000 mg/kg body weight in each group of albino mice. The condition of mice groups was recorded after fourteen days' administration. The results showed no lethality of the mice was observed up to fourteen days' administration. Each group of animals were also observed still alive and did not show any visible clinical

symptoms of toxicity like restlessness, respiratory disorders, convulsion, aggressive activities, coma and death.

Wound healing activity

From the antimicrobial results, ointment was formulated by the fusion of essential oil of *P. betel* leaves and was tested on rats because of its strong activity against bacterial infection. The effect of ointment with the essential oil of *P. betel* leaves on open wound is shown in Figure 7. By *in - vivo* test, the oil of *P. betel* accelerated the rate of wound healing in infected rats when compared with the controls. In the control group of infected rats which did not receive any drug treatments, the healing activity was not observed after 9 days. Treatment with the ointment of oil of *P. betel* showed the complete healing in 9 days.

Antioxidant activity

To make a semi-quantitative visualization possible, ethanol and watery extracts were detected on the TLC plate by Dot - Blot and DPPH staining method. The appearance of white colored spots has a potential value of antioxidant activity. After staining with DPPH solution, white spots were appeared from 400 µg down to 6.25 µg of ethanol and watery extracts (Figure 8). From the experimental results, *P. betel* leaves extract were found to possess the antioxidant activity.

Identification of compound

The antimicrobial active oil of *P. betel* was separated on silica gel by using toluene: ethyl acetate (9:1). Eugenol (0.1 %) was obtained and the purity of compound was checked on TLC. It was identified by spectroscopic methods namely UV and FT IR and EI - MS. The EI - MS data clearly showed the molecular ion peak of eugenol at m/z 164 as well as the diagnostic fragments for eugenol at m/z 149, 137, 131 and 121.

Eugenol: UV λ_{max}^{PE} 280 nm (Figure 9), FT IR υ_{max}^{KBr} cm^{-1}: 3514 (ν_{O-H}), 1637 ($\nu_{C=C}$), 1268, 1234 (ν_{C-O-C}), 1634 (ν_{C-O-H}) (Figure 10), EI-MS m/z: 164, 149, 137, 131,121 (Figure 11)

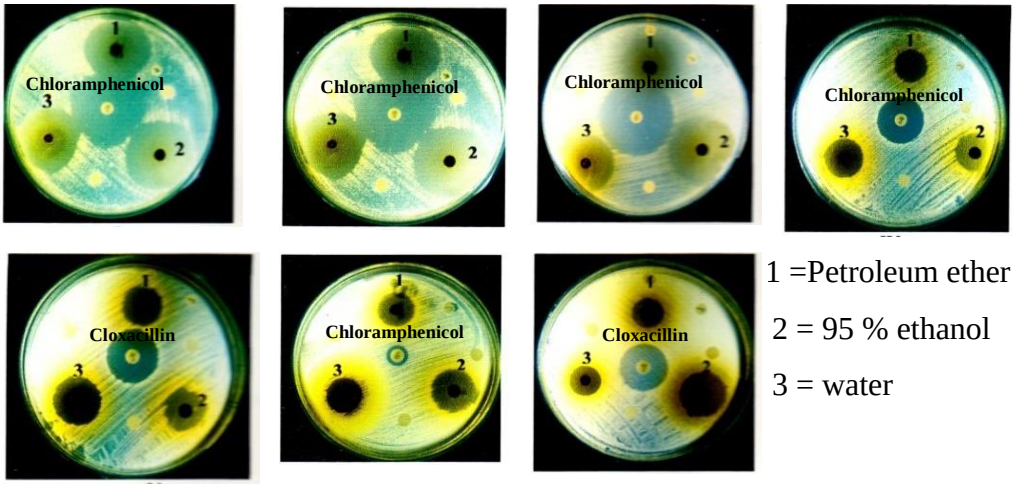

Figure 1: Sensitivity of crude extracts of *P. betel* on 7 species of *Staphylococcus aureus* from plaque of gingivitis

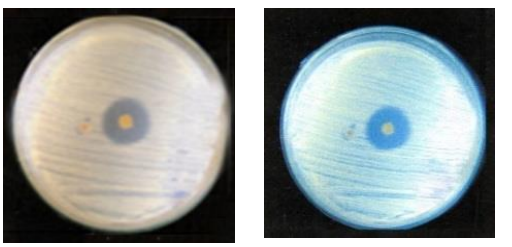

Figure 2: Sensitivity of essential oil of *P. betel* on *Staphylococcus aureus* from plaque of gingivitis

Table 1: Antimicrobial Activity of Different Extracts and Essential Oil of *P. betel* on *Staphylococcus aureus* from Plaque of Gingivitis

Tested Organisms	Diameter of zone of inhibition (mm)				
	PE	95 % Ethanol	Water	Essential oil	Antibiotic
S. aureus 1	35	33	33	11	42 (C)
S. aureus 2	20	20	23	20	45 (C)
S. aureus 3	30	33	30	40	40 (C)
S. aureus 4	32	33	30	20	28 (C)
S. aureus 5	15	15	20	16	35 (OB)
S. aureus 6	19	22	19	17	13 (C)
S. aureus 7	19	22	19	18	28 (OB)

C = Chloramphenicol, OB = Cloxacillin, disc diameter = 6 mm

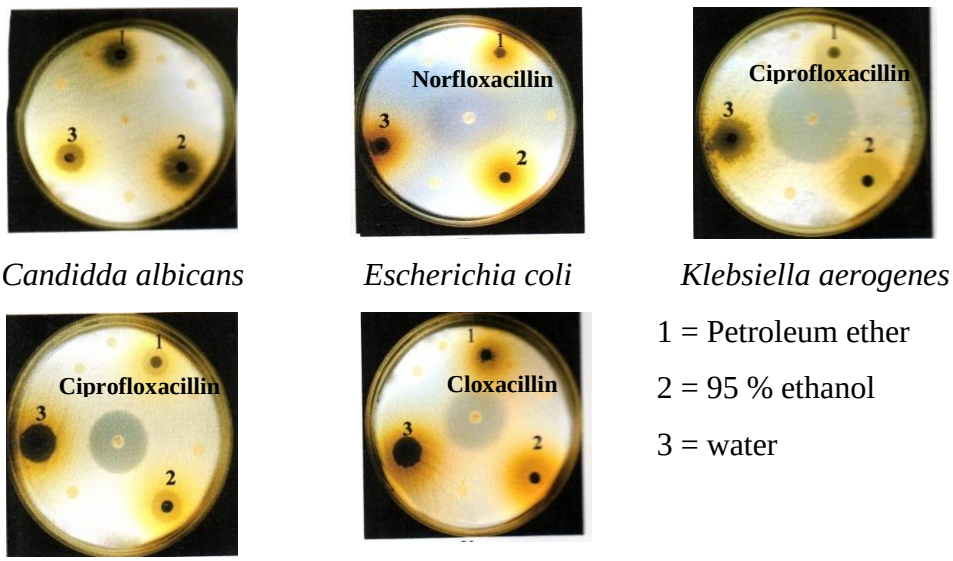

Candidda albicans *Escherichia coli* *Klebsiella aerogenes*

Pseudomonas aeruginosa *Staphylococcus aureus*

Figure 3: Sensitivity of crude extracts of *P. betel* on micro-organisms which cause skin infection

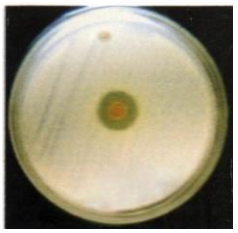

Candidda albicans

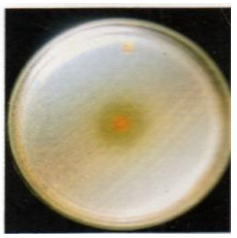

Escherichia coli

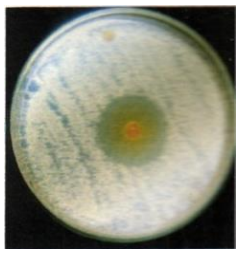

Klebsiella aerogenes

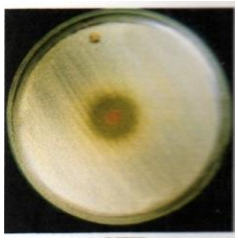

Pseudomonas aeruginosa

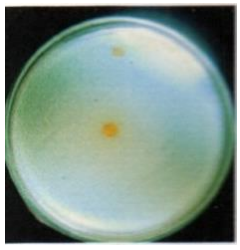

Staphylococcus aureus

Figure 4: Sensitivity of essential oil of *P. betel* on micro-organisms which cause skin infection

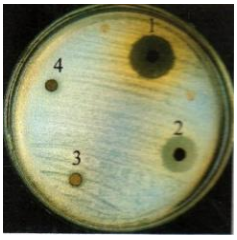

Petroleum ether

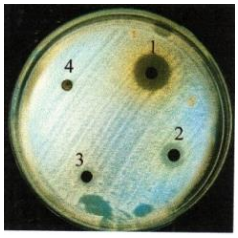

95 % ethanol

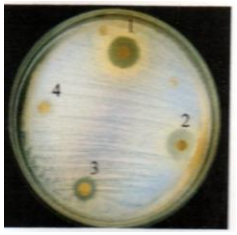

Water

1=10 mg/mL

2=5 mg/mL

3=2.5 mg/mL

4=1.25 mg/mL

Figure 5: Minimum inhibitory concentrations of crude extracts of *P. betel* on *Staphylococcus aureus* from plaque of gingivitis

Table 2: Antimicrobial Activity of Different Extracts and Essential Oil of *P. betel* on Micro-organisms of Skin Infections

Tested Organisms	Inhibition zone diameter (mm) of different extracts and control				
	PE	**95 % Ethanol**	**Water**	**Essential oil**	**Antibiotic**
Candida albicans	35	33	33	11	42 (C)
Escherichia coli (ATCC)	20	20	23	20	45 (C)
Klebsiella aerogenes	30	33	30	40	40 (C)
Pseudomonas aeruginosa	32	33	30	20	28 (C)
Staphylococcus aureus	15	15	20	16	35 (OB)

disc diameter = 6 mm, C = Chloramphenicol, OB = Cloxacillin

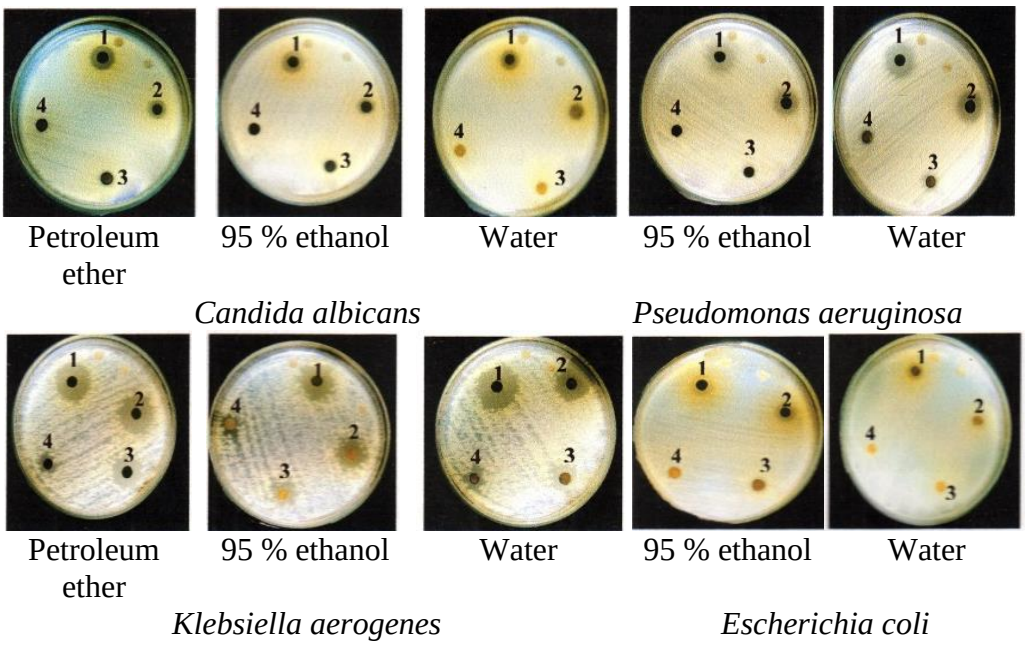

Figure 6: Minimum inhibitory concentrations of crude extracts of *P. betel* on microorganisms which cause skin infection

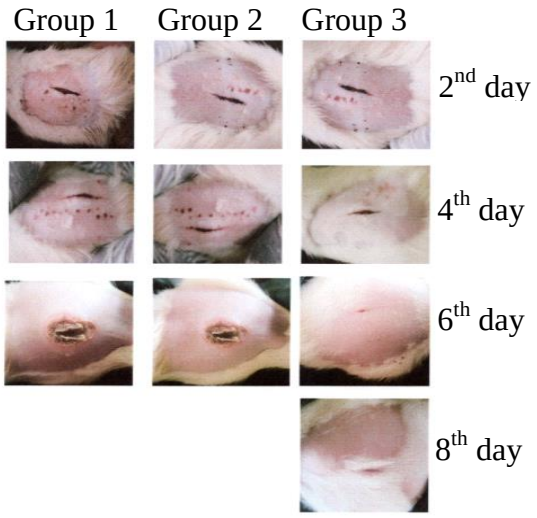

Figure 7: Process of the rate of wound healing of essential oil of *P. betel* on rats

Table 3: Minimum Inhibitory Concentration of Different Extracts of *P. betel*

Tested Organisms	Zone Inhibition Diameters (mm) of different extracts (mg/mL)											
	PE extract				95 % ethanol extract				Watery extract			
	10	5	2.5	1.25	10	5	2.5	1.25	10	5	2.5	1.25
**Staphylococcus aureus*	12	10	-	-	15	13	7	-	9	-	-	-
***Pseudomonas aeruginosa*	-	-	-	-	10	9	-	-	8	-	-	-
***Candida albicans*	12	8	-	-	13	9	-	-	11	7	-	-
***Klebsiella aerogenes*	20	21	17	-	24	17	14	-	17	15	13	-
***Escherichia coli*	-	-	-	-	9	10	-	-	9	-	-	-

disc diameter = 6 mm, * dental infections, ** skin infections

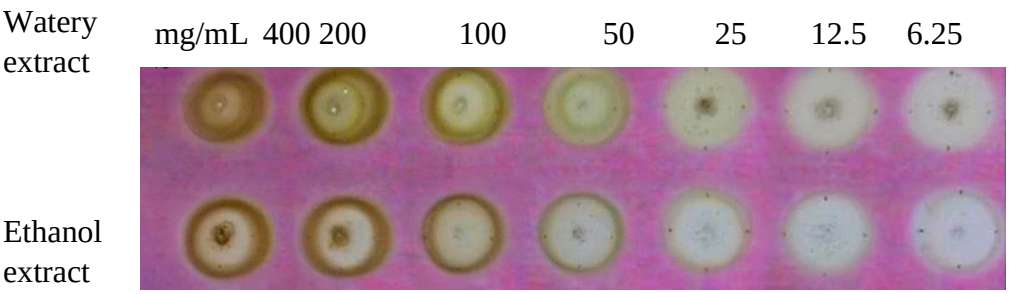

Figure 8 : Antioxidant activity of water and ethanol extract of *P. betel* by Dot-Blot and DPPH staining method

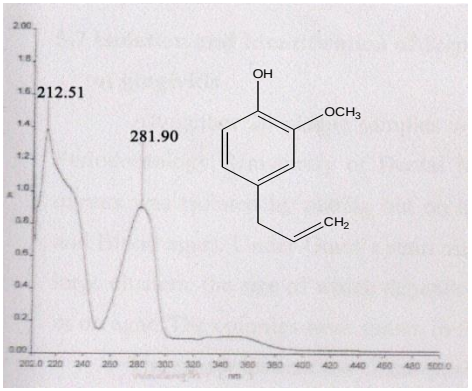

Figure 9: UV spectrum of isolated eugenol from *P. betel*

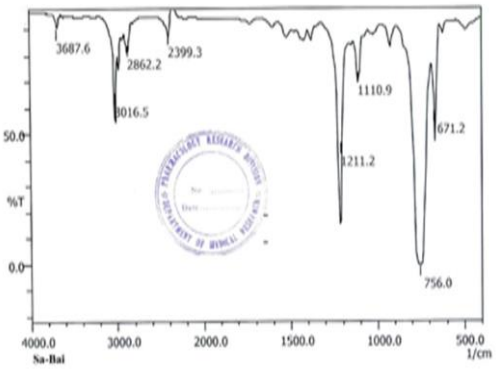

Figure 10: FT IR spectrum of the isolated eugenol from *P. betel*

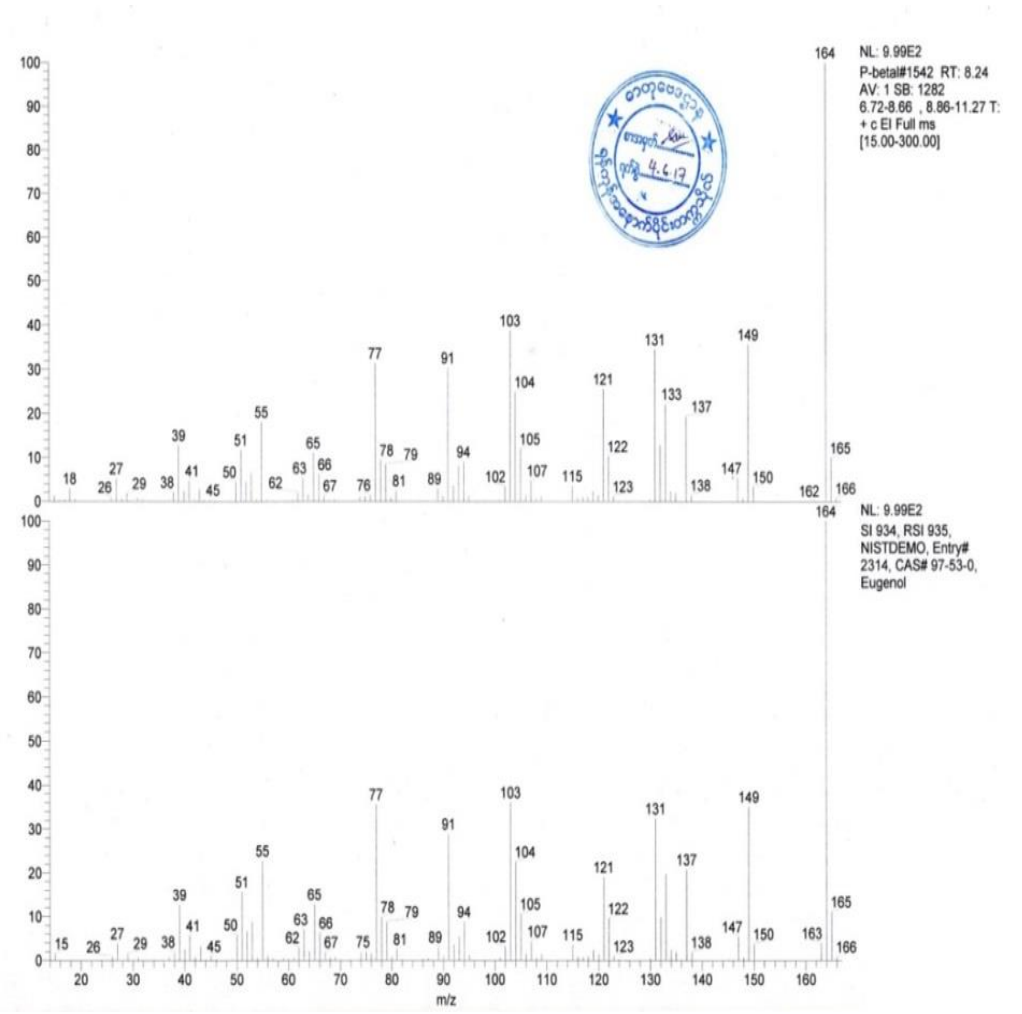

Figure 11: EI -MS spectrum of the isolated eugenol from *P. betel*

Conclusion

From the present research work, the following conclusions can be drawn.

Crude extracts have been prepared from *P. betel* by using polar and nonpolar solvents. Antimicrobial activity of crude extracts and essential oil were screened by agar disc diffusion technique on seven species of

Staphylococcus aureus isolated form plaque of gingivitis and five strains of organisms which usually cause skin infections. The minimum inhibitory concentration (MIC) of the 95 % ethanol extracts was 2.5 mg/mL for *Staphylococcus aureus* (dental infection) and 5 mg/mL for *Candida albicans* (skin infection).

Even with the dose up to 2000 mg/kg and 50000 mg/kg body weight administration, there was no lethality at the day fourteen. The ointment preparation with the essential oil of *P. betel* leaves promoted healing of wounds infected with *Staphylococcus aureus* in rats.

The evaluation of *in - vitro* antioxidant activities of extracts (ethanol, water) showed up to 6.25 µg/mL. Based on this information, it could be concluded that *P. betel* leaf is natural source of antioxidant of high importance. The essential oil of *P. betel* was fractionated by column chromatography to give eugenol (0.1 %). The isolated compound was confirmed by spectroscopic method (UV, FT IR and EI - MS).

From the experimental results, the extracts of *P. betel* leaves are suitable for economic production of antimicrobial agent for oral preparations. Moreover, the crude extracts are also more useful in skin infections caused by bacteria. The essential oil from *P. betel* will be useful medicament in wounds and sores as an alternative use in rural area especially where expensive antibiotics are not available.

Acknowledgements

The authors would like to express their profound gratitude to the Department of Higher Education, Ministry of Education, Yangon, Myanmar, for provision of opportunity to do this research and Myanmar Academy of Arts and Science for allowing to present this paper. We also wish to express our grateful thanks to Dr Maung Maung, Principal of Myingyan Degree College. We would like to extend my gratitude and deep appreciation to Dr Wynn Wynn Yi, Professor and Head of Chemistry Department, Myingyan Degree College for her encouragement and invaluable suggestion.

References

Arambewela, L. (2006). "A Potential Natural Antioxidant". *International Journal of Food Science & Technology*, vol.41, pp. 10-14

Hnin Hnin Aye. (2002). *Antituberculosis Activities and Chemical Investigation of Myanmar Traditional Medicine Used for the Treatment of Tuberculosis*. PhD Dissertation, Department of Chemistry, University of Yangon

Mi Mi Htwe, Mar Mar Nyein, Khin Chit, Mu Mu Sein Myint and Aye Than. (2001). "*In vitro* Antibacterial Activity of Some Indigenous Plants and Effect on *in vivo Staphylococcal* Induced Wounds". *Myanmar Health Science Research Journal*, vol.13 (1-3), pp. 32-37

OECD (2000). *Guidance Document on Acute and Toxicity*. Environmental Health and Safety Monograph Series on Testing and Assessment, No 24 (Organization for Economic Cooperation and Development).

Pauli (2001). "Antimicrobial Properties of Essential Oil Constituents". *J. Aromatherapy*, vol. 11(3),
pp. 126-133

Skerman. V. B. D. (1967). *A Guide to the Identification of Bacteria*. Baltimore: 2nd Ed, Williams and Wilkins Co

Soler – Rivas. C., Espin, J.C. and Wichers, H.J. (2000). "An Easy and Fast Test to Compare Total Free Radical Scavenger Capacity of Food Stuffs", *Phytochem. Annal*; **11,** p. 330

Stokes, E. J, Ridgway, G. L. and Wren, M. W. D. (1993). *Laboratory Control of Antimicrobial Chemotherapy, In: Clinical Microbiology*. London: 7th Ed, Edward Arnold, pp. 258-263

WHO. (2003). *Staining Techniques In: Guideline on SOP for Microbiology*. New Delhi: pp. 19-22

ANTIOXIDANT ACTIVITIES ON *Picrasma javanica* BL. (NANN-PAW-KYAWT) BY USING DPPH AND NITRIC OXIDE ASSAYS

Zin Thu Khaing[1], May Zin Phyo[2], Daw Hla Ngwe[3]

Abstract

Picrasma javanica Bl. (Nann-paw-kyawt) bark is one of the well known traditional medicinal plants. Since it has an invaluable medicine purpose, the bark of *P. javanica* was chosen for this research work. This study was designed to examine the phytochemicals, mineral contents, antioxidant activity and total phenol contents of *P. javanica* bark. In the present work, the preliminary phytochemical tests revealed that alkaloids, α-amino acids, carbohydrates, flavonoids, glycosides, phenolic compounds, reducing sugars, saponins, starch, steroids, tannins, terpenoids and organic acids were present and cyanogenic glycosides were not found in *P. javanica* bark. The mineral contents (Ca, K, Si, Fe, S, Mn, Ti, Zn, Cu, Sr and Rb) of *P. javanica* bark powder sample were determined by EDXRF. Among them, the calcium content of this sample was the highest (66.904 %). A compound Des-4-methyl-19-hydroxyquassin (0.013 %, white solid) was isolated from chloroform extract of *P. javanica* bark. *In vitro* antioxidant activities of ethanol and watery extracts of *P. javanica* bark were also assessed by 2, 2 diphenyl-1-picrylhydrazyl (DPPH) and Nitric Oxide free radical scavenging (NO) assays. By using DPPH assay the IC_{50} values of ethanol and watery extracts of *P. javanica* bark were 23.28 μg/mL and 17.47 μg/mL respectively. And also IC_{50} values of ethanol and watery extracts of *P. javanica* bark were 271.80 μg/mL and 105.28 μg/mL by using nitric oxide assay. The total phenol contents were determined by Folin-Ciocalteu Reagent (FCR) method and watery extract (19.67 μg GAE/mg) was found to be higher than ethanol extract (18.97 μg GAE/mg).

Keywords*:* *Picrasma javanica* Bl., phytochemicals, antioxidant activity, total phenol content, authentic compound, free radical

Introduction

Traditional herbal medicines are naturally occurring, plant-derived substances with mineral or no industrial processing that have been used to treat illness within local or regional healing practices. Traditional herbal

1. Dr, Lecturer, Department of Chemistry, University of Yangon
2. Candidate, MRes. (2016-2017), Department of Chemistry, University of Yangon
3. Dr, Professor and Head (Retd.) Department of Chemistry, University of Yangon

medicines are getting significant attention in global health debates. In China, traditional herbal medicine played a prominent role in the strategy to contain and treat severe acute respiratory syndrome. Many hope traditional herbal medicine will play a critical role in global health. China, India, Nigeria, the United States of America (USA) and WHO have all made substantial research investments in traditional herbal medicines (WHO, 2003).

Plants have long been serving mankind as sources of useful drugs, food, additives, flavoring agents, colorants, binders and lubricants (Falodun *et al.*, 2006). Medicinal plants are sources of important drugs used in the treatment of diseases either alone or in combination with other plants. Chemical substances found in plants include alkaloids, glycosides, essential oil, saponins, tannins, steroids, terpenoids, resins, flavonoids, proteins and others. These substances are potent bioactive compounds found in medicinal plant parts that can be used for therapeutic purposes (Nwachukwu, 2010). These inherent bioactive principles differ from plant to plant as a result of their biodiversity and they produced a definite physiological effect on human body. Several authors have screened different medicinal plants for the presence of these active principles. The knowledge of medicinal plants is important in pharmaceutical industry. *Picrasma javanica* Bl. (Nann-paw-kyawt) extract was chosen for evaluation of phytochemical test, antimicrobial activity, antioxidant activity, total phenol contents, antitumor activity. It has been found to be useful for treatment of malaria, antitumor, antiplasmodia, antibacterial, and skin diseases (Koike *et al*., 1991, Ohmoto *et al*., 1989).

Picrasma javanica (Nann-paw-kyawt) (Figure 1) is known as bitter plant and from Java (Christophe, 2006). In Myanmar, it is commonly known as Nya-bo-jaw (Poe Kayin) and Nann-paw-kyawt (Sagaw Kayin). It is a rainforest tree which grows to a height of 24 m and has a girth of 150 cm. The plant is found spanning Southeast Asia, Papua New Guinea and the Solomon Island. In Myanmar, it is only found in the border area of Kayin and Thailand, Myaing-Gyi-Ngu Special Region. The bowl is fluted, and the bark is dark, smooth, and brittle with bitter, with the inner bark, yellowish with brownish spa-wood. Leaves: compound, stipule and fragrant. The stipules are leafy. The blade comprises of 5-7 medium-sized and very thin follicles attached to 7 mm long petioles. The flowers are four and numerous and

whitish, and comprise of a thick nectar disc and few free carpel, each containing a single ovule. The fruits are green, red or blue drupes (Phokaew, 2005). The aim of this research is to study on the Myanmar traditional herbs that play a very important role in the development of new drugs. The objective of this research is to find out the elemental contents and antioxidant activity of *Picrasma javanica* (Nann-paw-kyawt). The isolation of new compound Des-4-methyl-19-hydroxyquassin from *Picrasma javanica* (Nann-paw-kyawt) bark and its anti-malaria activity had been explored in Department of Chemistry, University of Yangon (Yi Yi Win,2004).

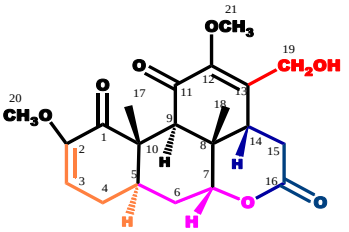

Des-4-methyl-19-hydroxyquassin

Botanical Description of *Picrasma javanica* BL. (Nann-paw-kyawt) Bark

Kingdom	:	Plantae
Phylum	:	Tracheophyta
Class	:	Magnolipsida
Family	:	Simaroubaceae
Genus	:	*Picrasma*
Species	:	*P.javanica*
Myanmar Name	:	Nann-paw-kyawt

Figure 1:Photographs of *Picrasma javanica* BL. (Nann-paw-kyawt)

Materials and Methods

Sample Collection and Preparation of *P. javanica* BL. (Nann-paw-kyawt)

Bark of *P. javanica* Bl**.** (Nann-paw-kyawt) was collected from Myaing-Gyi-Ngu Special Region on October; 2016. The sample was identified at the Department of Botany, University of Yangon. After cleaning the sample, it was dried at room temperature followed by making into powder and stored in an air-tight container.

Preliminary Phytochemical Investigation of *P. javanica* Bl. (Nann-paw-kyawt) Bark

In order to find out the types of phyto-organic constituents such as alkaloids, α-amino acids, carbohydrates, cyanogenic glycosides, flavonoids, glycosides, organic acids, phenolic compounds, reducing sugars, saponins, starch, steroids, tannins, and terpenoids in the sample, preliminary phytochemical tests were carried out according to the appropriate methods. Various crude extracts (PE, EtOH, EtOAc) of *P. javanica* were prepared for TLC investigation, which were loaded on the precoated TLC silica gel plate and the chromatography was carried out by using an appropriate standard solvent system for *P. javanica*. The developed chromatograms were first inspected under UV-254 nm and 365 nm light and then sprayed with detecting reagents to classify the compounds present and their functional groups.

Qualitative Elemental Analysis by Energy Dispersive X-ray Fluorescence (EDXRF) Spectrometry

The relative abundance of elements present in Nann-paw-kyawt bark was determined by (EDXRF) Spectrometer (Shimadzu-EDX-700) Department of Chemistry, West Yangon University. Each sample was run for a counting time of 100 seconds and the spectrum obtained was stored using EDX-700 software (Griken and Markowitch, 1993).

Isolation of Bioactive Organic Constituent from Bark of *P. javanica* (Nann-paw-kyawt)

The dried powder sample (300 g) was percolated with 95% ethanol (1000 mL) one week and filtered. This procedure was repeated for three times. The combined filtrate containing plant constituents were evaporated under reduced pressure by means of a rotary evaporator. Consequently, 95% ethanol soluble extract was obtained. The 95% ethanol extract was then partitioned with pet-ether (60-80 °C) (1000 mL) by using separatory funnel. The pet-ether fraction was removed under reduced pressure in a rotary evaporator. The pet-ether extract was obtained. The defatted alcohol soluble portion was then partitioned between chloroform and water by using separatory funnel. The solvent of chloroform fraction was removed under reduced pressure in a rotary evaporator. The chloroform extract was obtained.

Isolation and Purification of Bioactive Organic Constituents from Chloroform Extract of *P. javanica* (Nann-paw-kyawt) Bark

The chloroform extract (3 g) was dissolved in a volume of 10 mL of $CHCl_3$ and made slurry with silica gel. The resulting slurry was separated by column chromatography on a silica gel column (45 cm × 1.5 cm) using silica gel 40-60 μ m as stationary phase and $CHCl_3$ and MeOH (gradient elution) as mobile phase. The fractions were monitored by TLC. The fractions gave the similar appearance on TLC were combined and finally 4 main fractions FI to FIV were collected. Fraction II (0.580 g) was chromatographed by using precoated TLC silica gel with toluene: chloroform: ethyl acetate (1:1:1, v/v) solvent system. The seven detectable bands were collected by scraping from the TLC chromatogram after being checked under UV_{254}. Then the individual

component was eluted from gel by eluting with $CHCl_3$: MeOH (7:3) as eluent. The compound "A" was collected as white solid residue after evaporating the solvent.

Characterization and Identification of the Isolated Compound "A"

The isolated compound "A" was characterized by determination of some physical properties such as R_f value and melting point. The isolated compound A was subjected to TLC analysis and the R_f value of spot was determined. GF_{254} silica gel pre-coated aluminium plate (Merck) was employed and the chromatogram was developed in the appropriate solvent for the isolated compound. After the plate was dried, the R_f value of isolated compound was determined. Localization of spots was made by viewing directly under UV (254-365) or using spraying agents. For the identification of isolated compound, its ultra violet absorption spectrum was also recorded and examined by using UV-visible spectrophotometer at Universities' Research Centre, Yangon University. The infrared spectrum of the compound "A" was recorded by Shimadzu Perkin Elmer GX FT IR spectrophotometer at Chemistry Department, Yangon University.

Determination of Antioxidant Activity of Crude Extracts of *P. javanica* (Nann-paw-kyawt Bark) by DPPH Free Radical Scavenging Assay

The free radical scavenging activity of crude extracts of *P. javanica* (Nann-paw-kyawt) bark was measured by using DPPH free radicals scavenging assay. The activities of ethanol and water extracts of *P. javanica* (Nann-paw-kyawt) bark were determined by using UV-visible spectrophotometer (GENESYS 10S UV-Vis) (Marinova and Batchvarov, 2011). The control solution was prepared by mixing 1.5 mL of 0.002 % DPPH solution and 1.5 mL of ethanol in the brown bottle. The sample solution was prepared by mixing 1.5 mL of 0.002 % DPPH solution and 1.5 mL of test sample solution. These bottles were incubated at room temperature and were shaken on a shaker for 30 min. After 30 min, the absorbance values of these solutions were measured at 517 nm and the percentage of radical scavenging activity (% RSA) was calculated by the following equation.

$$\% \text{ RSA} = [\{(A_{DPPH} - A_{sample}) - A_{blank}\} / A_{DPPH}] \times 100$$

Where, %RSA = %radical scavenging activity of test sample

A_{DPPH} = absorbance of DPPH in EtOH solution

A_{sample} = absorbance of sample+ DPPH solution

A_{blank} = absorbance of sample + EtOH solution

The antioxidant power (IC_{50}) is expressed as the test substance concentration (μ g/mL) that results in a 50 % radical scavenging property of the sample. The standard deviation was also calculated by the following equation.

$$\textbf{Standard Deviation (SD)} = \sqrt{\frac{(\bar{x}-x_1)^2+(\bar{x}-x_2)^2+\ldots(\bar{x}-x_n)^2}{(n-1)}}$$

$\bar{x}$ = Average % Inhibition,

n = number of times

$x_1, x_2, \ldots, x_n$ = % inhibition of test sample solution

Determination of Antioxidant Activity of Crude Extracts of *P. javanica* (Nann-paw kyawt) Bark by Nitric Oxide Assay

The free radical scavenging activity of crude extracts of *P. javanica* (Nann-paw-kyawt) bark was measured by using Nitric Oxide method. Nitric oxide generated from sodium nitroprusside interacts with oxygen to produce nitrite ions which was measured by the Griess reaction (Marcocci *et al*., 1994). The reaction mixture containing 3.0 mL of 3 mM sodium nitroprusside in phosphate buffered saline (pH 7.4) and various concentrations of (400, 200, 100, 50, 25 μ g/mL) were incubated at 25 °C for 180 min. The NO° radical thus generated interacted with oxygen to produce the nitrite radical (NO°) which was assayed at 30 min intervals by mixing 1.0 mL of incubation mixture with an equal amount of Griess reagent (1% sulphnilamide in 5 % phosphoric acid and 0.1 % naphthyl ethylene diamine dihydrochloride). The absorbance of the chromophore (purple azo dye) formed during the diazotization of nitrite ions with sulphanilamide and subsequent coupling with naphthyl ethylene diaminedihydrochloride was measured at 546 nm. Each experiment was carried out at least three times and the data presented as an average of three independent determinations. The percentage of NO° radical

scavenging activity (% RSA) was calculated by the similar formula as mention in DPPH free radical rcavenging assay.

Determination of Total Phenolic Content of *P. javanica* (Nann-paw-kyawt) Bark by FCR Method

One of the anti-oxidative factors, total phenolic content (TPC) was measured by spectrophotometrically according to the Folin-Ciocalteu method. A 0.2 mL of each sample solution was mixed with 1.5 mL of Folin-Ciocalteu Reagent in a test tube covered with aluminum foil. After 5 min, 1.5 mL of 10 % Na_2CO_2 was added to each test tube. The sample was then incubated for 90 min at room temperature. The absorbance was measured at 765 nm spectophotometrically (KWF UV-7504). A standard curve of Gallic acid solutions (ranged from 0 - 250 μg mL^{-1}) was used for calibration. The experiment was done in triplicate. Concentrations of Gallic acid equivalent (GAE) in the plant extracts were calculated from the linear regression equation explored from standard curve construction for Gallic acid. TPC in the plant samples were expressed as (μg GAE/mg) (Reynertson, 2007).

Results and Discussion

Phytochemical Constituents of *P. javanica* (Nann-paw-kyawt) Bark

According to the phytochemical tests in order to know their types present in the selected sample, alkaloids, α-amino acids, carbohydrate, flavonoids, glycosides, phenolic compound, reducing sugars, saponins, starch, steroids, tannins, terpenoids, and organic acids were found to be present, however, cyanogenic glycosides was absent.

Elements Present in *P. javanica* (Nann-paw-kyawt) Bark by EDXRF Method

X-ray spectroscopy permits simultaneous analysis of light elements to heavy elements. In this work, relative abundance of elements present in the bark of *P. javanica* was determined by EDXRF spectrometer. It was observed that Ca and K are the major elements present in the barks of Nann-paw-kyawt. In addition the trace elements such as Si, Fe, S, Mn, Ti, Zn, Cu, Sr and Rb were also found in Nann-paw-kyawt bark. Among them, the

calcium content was the highest (66.90 %) in this bark (Table 1). Calcium is a mineral that is an essential part of bones and teeth. The heart, nerves and blood-clotting systems also need calcium work.

Table 1: Relative Abundance of Elements in *P. javanica* (Nann-paw-kyawt) Bark

Elements	Relative Abundance (%)
K	24.239
Si	3.413
Fe	3.183
S	1.272
Mn	0.294
Ti	0.227
Zn	0.178
Cu	0.105
Sr	0.080
Rb	0.050

Separation, Isolation and Purification of Compound "A" from Chloroform Extract of *P.javanica* (Nann-paw-kyawt) Bark

The chloroform extract (3 g)of Nann-paw-kyawt bark was separated column chromatographically on silica gel GF_{254} adsorbent by increasing the polarity of eluent, chloroform, chloroform : methanol (20:1, 15:1, 10:1 v/v) solvents, followed by TLC chromatographic separation. It was purified by washing with PE followed by crystallization from PE and EtOAc to give compound "A" 0.013 % as a white solide. After purification, compound "A" was stored for further pharmacological investigation.

The melting point of compound "A" was found to be 148 °C. Its R_f value was 0.17 (PE: EtOAc = 1:3 v/v). A purple spot on TLC after spraying and heating with 10 % H_2SO_4 reagent confirmed that the isolated compound A was a terpenoid compound. These physical properties of compound "A" are shown in Table 2. The melting point and R_f value of compound "A" were consistent to those of authentic Des-4-methyl-19-hydroxyquassin (148 °C). It is soluble in moderately polar solvents. It is UV active under 254 nm. It was

also inferred that compound "A" may not include phenolic group because no coloration was observed when it was treated with 5 % $FeCl_3$ solution. In the UV spectrum of compound "A", (Figure 2), the absorption maxima at 259 nm and 346 nm in MeOH indicates the presence of π→π* and n→π* transitions. It also agreed with the presence of double bond conjugation. conjugated with carbonyl group in compound A (Table 3). In FT IR spectrum of compound "A" (Figure 3), the –OH stretching of aliphatic alcoholic group appeared at 3533, 3479 and 3433 cm^{-1}. The strong =CH stretching band at 3070 cm^{-1} and =CH out of plane bending at 800 cm^{-1} indicated the presence of alkenic group. The absorption bands at 2970, 2931 and 2850 cm^{-1} indicated the presence of CH_3- and -CH_2- groups. The C = O stretching absorption band at 1735 cm^{-1} and C-O-C stretching band at 1190 cm^{-1} for ester. The stretching of α, β-unsaturated carbonyl group at 1690 cm^{-1} and C-O-C stretching of alcohol at 1034 cm^{-1} were also observed (Table 3). According to spectral data, melting point and Co-TLC chromatogram of isolated compound "A" and authentic Des-4-methyl-19-hydroxyquassin, the isolated compound "A" can be assigned as Des-4-methyl-19-hydroxyquassin.

Table 2: Some Physicochemical Properties of the Isolated Compound "A" from *P.javanica* (Nann-paw-kyawt) Bark

Experiments	Observations	Remarks
Melting point	148 °C	Similar to 148 °C (authentic Des-4-methyl-19-hydroxyquassin)
R_f value	0.17 (PE:EtOAc), (1:3 v/v)	Similar to R_f (authentic Des-4-methyl-19-hydroxyquassin
10 % H_2SO_4, Δ	Brown on TLC	-
H_2SO_4-Anisaldehyde, Δ	Purple	Terpenoid
H_2SO_4-Valine, Δ	Blue	Terpenoid

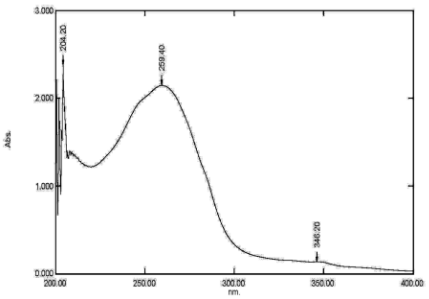

Figure 2: The UV spectrum of the isolated compound A (MeOH)

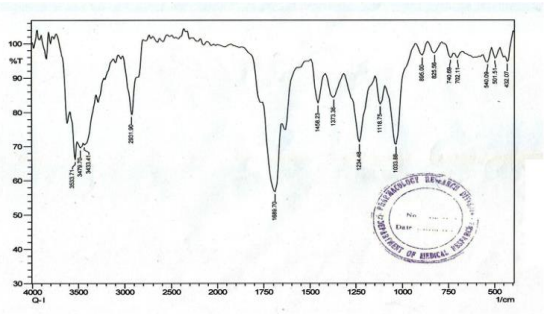

Figure 3: The FT IR spectrum of the isolated compound A (KBr)

Table 3: The FT IR Spectrum of the Isolated Compound "A"

Wave number (cm^{-1})	**Band Assignment**
3533,3479, 3433	υ_{OH} of OH group
3070, 3085	$\upsilon_{=C-H}$ of alkenic group
2970, 2931, 2850	$\upsilon_{C-H\ asym}$ and $\upsilon_{C-H\ sym}$ of CH_2 and CH_3 group
1735	$\upsilon_{C=O}$ of lactone ring
1690	$\upsilon_{C=O}$ of α , β -unsaturated C=O
1620	$\upsilon_{C=C}$ of alkenic group
1450	δ_{C-H} of CH_2 group
1380	δ_{C-H} of CH_3 group
1230	υ_{-C-O} of = C-O group
1190	υ_{C-O} of –C-O-C group
1034	υ_{C-O} of CH_2-OH group
800	δ_{oop} =C-H of alkenic group

Antioxidant Activity of *P.javanica* (Nann-paw-kyawt) Bark by DPPH Method

Antioxidants are essential and important for plants and animals' sustenance that protect cells from the damage caused by unstable molecules known as free radicals. The antioxidant activity of water and ethanol extracts of Nann-paw-kyawt bark were evaluated by DPPH free radical scavenging assay (Marinova and Batchvarov, 2011) and ascorbic acid was used as standard. The absorbance values of different concentrations (40, 20, 10, 5, 2.5, 0.625μg/mL) of tested samples were measured at wavelength of maximum absorption 517 nm by using UV-7504 spectrometer. It shows percent inhibition increased with increasing the concentration of crude extracts. The IC_{50} values of ethanol and water extracts were 23.28 μg/mL and 17.47 μg/mL respectively (Table 4 and Figure 4). So water extract was more potent in antioxidant activity than ethanol extract. However, antioxidant potency of both extracts were very weak when comparing with that of standard ascorbic acid (IC_{50} = 2.25 μg/mL).

Table 4 Oxidative Percent Inhibitions and IC_{50} Values of Crude Extracts of *P.javanica* (Nann-paw-kyawt) Bark by DPPH Method

Test samples	**% Inhibition of different concentrations (mean ±SD) (□g/mL)**						**IC_{50}(□g/mL)**
	1.25	**2.5**	**5**	**10**	**20**	**40**	
EtOH	10.32 ± 0.00	14.09 ± 0.01	15.83 ± 0.03	33.39 ± 0.03	47.78 ± 0.03	61.29 ± 0.00	23.28
H_2O	13.99 ± 0.01	20.46 ± 0.01	29.63 ± 0.01	39.19 ± 0.03	51.67 ± 0.01	59.56 ± 0.00	17.47
Ascorbic Acid	34.36 ± 0.00	53.86 ± 0.00	62.38 ± 0.00	66.87 ± 0.00	72.75 ± 0.01	82.5 ± 0.00	2.25

IC_{50} = 50 % Inhibition Concentration

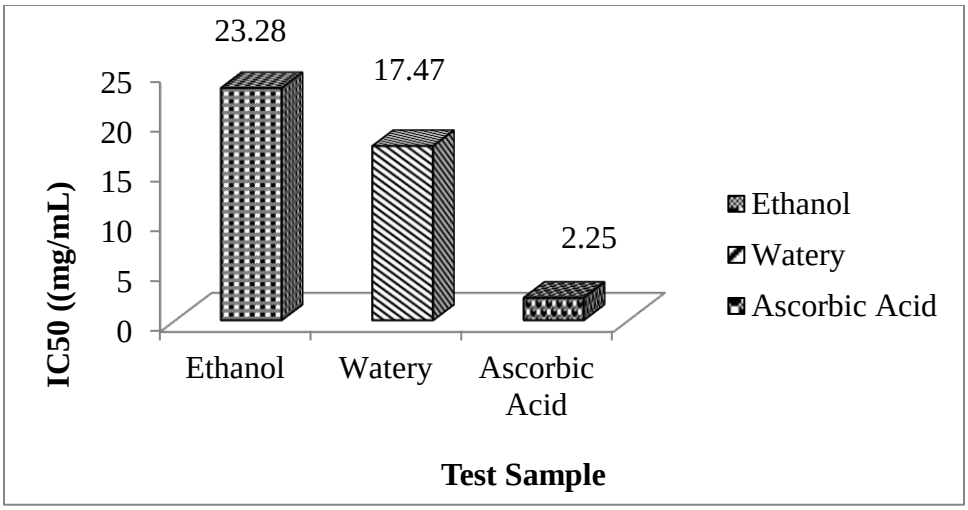

Figure 4: A bar graph of IC_{50} values of water and ethanol extracts of *P.javanica* (Nann-paw-kyawt) bark and standard ascorbic acid by DPPH method

Antioxidant Activity of *P. javanica* (Nann-paw-kyawt) Bark by Nitric Oxide Method

In this study the antioxidant activity of ethanol and watery extracts of (Nann-paw-kyawt) bark was evaluated by nitric oxide radical scavenging assay (Marcocci *et al*., 1994). Nitric oxide (NO°) is an important chemical mediator generated by endothelial cells, macrophages, neurons, etc. and is involved in the regulation of various physiological process (Lata and Ahuga 2003). NO° is generated in biological tissue by specific nitric oxide synthesis (NOSs), which metabolizes arginine to citralline with the formation of NO° via a five electron oxidative reaction (Ross, 1993). NO° scavenging capacity is determined by the decrease in the absorbance at 550 nm, induced by antioxidant. The absorbance values of different concentrations (400, 200, 100, 50, 25μ g/mL) of tested samples were measured at 550 nm by using UV-7504 spectrometer. The NO° scavenging activity of crude extracts are expressed in terms of % RSA and IC_{50} (50 % inhibitory concentration) and these values are calculated by linear progressive excel program. The IC_{50} values of ethanol and watery extracts were 271.80μ g/mL and 105.28μ g/mL respectively (Table 5 and Figure 5). So the antioxidant activity of watery extract possessed higher

potency than ethanol extract. Their antioxidant activity were very weak when comparing with that of ascorbic acid (IC_{50} = 34.51 μ g/mL).

Table 5 Oxidative Percent Inhibitions and IC_{50} Values of Crude Extracts of *P.javanica* Nann-paw-kyawt Bark by Nitric Oxide Method

Test samples	**% inhibition(mean ± SD) of different concentrations (μg/mL)**					**IC_{50} (μg/mL)**
	25	**50**	**100**	**200**	**400**	
EtOH	33.42 ± 0.04	42.83 ± 0.00	44.17 ± 0.00	48.33 ± 0.02	53 ± 0.02	271.80
H_2O	34.95 ± 0.01	42.39 ± 0.01	49.37 ± 0.02	61.12 ± 0.01	65.28 ± 0.00	105.28
Ascorbic acid	44.61 ± 0.01	58.77 ± 0.06	61.27 ± 0.06	62.65 ± 0.00	63.90 ± 0.03	34.51

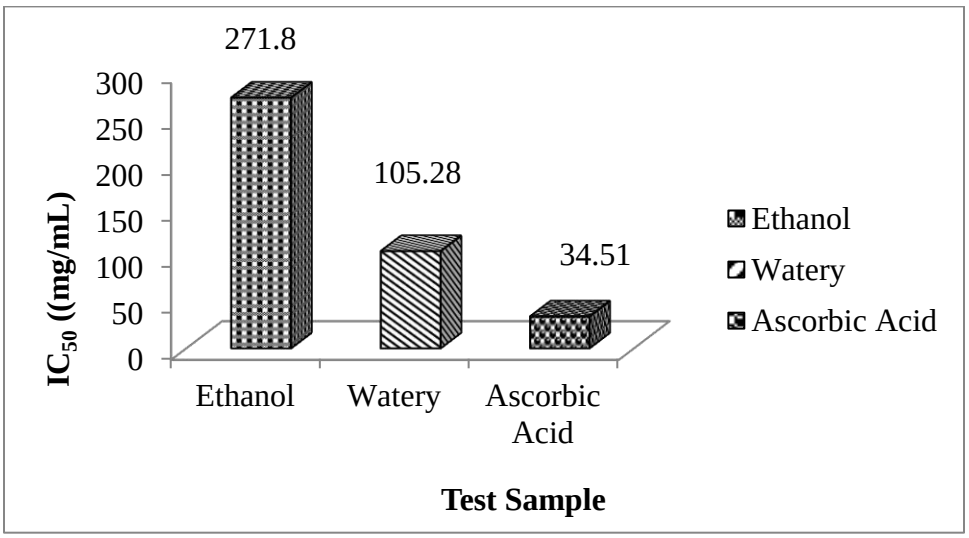

Figure 5: IC_{50} Values of standard ascorbic acid, EtOH and H_2O crude extracts of *P.javanica* (Nann-paw-kyawt) bark by using NO method

Total Phenolic Contents of Ethanol and Watery Extracts of *P.javanica* (Nann-paw-kyawt) Bark

In this study, the total phenolic content of *P.javanica* (Nann-paw-kyawt) bark was estimated by Folin-Ciocalteu method. Phenols react with an oxidizing agent phosphomolybdate in F-C reagent under alkaline conditions and result in the formation of blue coloured complex, the molybdenum blue which is measured at 765 nm colorimetrically. According to the results, the total phenolic content (TPC) (µg GAE/mg) of watery extract (19.67±1.96) was higher than that of ethanol extract (18.97±1.25). The greater the total phenolic content, the higher the antioxidant activity. Therefore, watery extract of *P.javanica* (Nann-paw-kyawt) bark has more antioxidant activity than ethanol extract. These results are reported in Table 6 and Figure 6.

Table 6: Total Phenolic Content of Ethanol and Water Extracts of *P.javanica* (Nann-paw-kyawt) Bark

No.	Test Samples	TPC (µg GAE/mg ± SD)
1.	Watery	19.67± 1.96
2.	Ethanol	18.97± 1.25

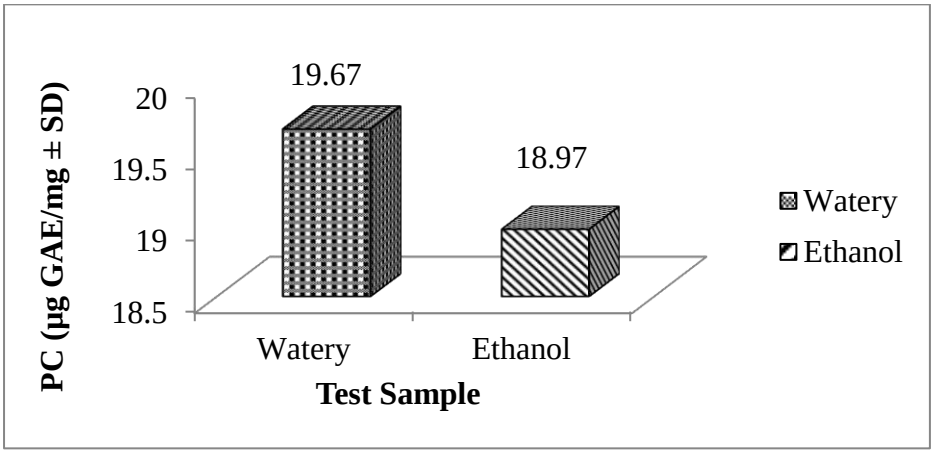

Figure 7: A bar graph of total phenolic contents of ethanol and watery extracts of *P.javanica* (Nann-paw-kyawt) bark

Conclusion

This research was intended to study some phytochemical constituents and antioxidant activities of *P.javanica* (Nann-paw-kyawt) bark.

Preliminary phytochemical tests showed the presence of the secondary metabolites such as α-amino acids, carbohydrates, flavonoids, glycosides, organic acids, phenolic compound, reducing sugar, saponins, starch, steroids, tannins, and terpenoids in *P. javanica* bark however cyanogenic glycosides were absent. Some elements such as Ca, K, Si, Fe, S, Mn, Ti, Zn, Cu, Sr and Rb were observed in the bark of *P. javanica* bark determined by EDXRF method. Among them, the calcium content of this sample was the highest (66.904 %).

A terpenoid, Des-A- methyl–19 – hydroxyquassin (0.013 % , based on chloroform extract, white solid , mpt. 148 °C) was isolated from chloroform extract.

DPPH assay method showed the antioxidant activity of ethanol and wateryextracts of *P. javanica* bark as 23.28 μg/mL and 17.47μg/mL of IC_{50} values, respectively. In addition, ethanol and watery extracts of *P. javanica* bark also respectively showed the antioxidant activity in 271.80 μg/mL and 105.28 μg/mL of IC_{50} values assessed by Nitric Oxide radical scavenging assay. Their antioxidant potency was concluded to be very weak when comparing with the potency of standard ascorbic acid (IC_{50}= 2.25 μ g/mL for DPPH assay and IC_{50} = 34.51 μ g/mL for NO° assay).

In the determination of the total phenol contents (TPC) of ethanol and watery crude extracts, it was observed that ethanol extract (52.31 ± 8.70 μg GAE/mg) was found to be higher than watery extract (16.92 ± 0.20 μg GAE/mg). It is a positive correlation between the total phenolic content and antioxidant activity in the selected plant sample. The results indicated that high phenolic content provided more potent antioxidant activity.

The findings from the present work will contribute to the scientific development of Myanmar traditional medicine, specifically in the areas concerned with oxidative stress.

The bark of *P. javanica* (Nann-paw-kyawt) could be applied as the local health remedy for the treatment of the diseases due to the oxidative stress.

Acknowledgements

The authors would like to thank the Department of Higher Education, Ministry of Education, Yangon, Myanmar, for the permission of doing this research and also to the Myanmar Academy of Arts and Science for allowing the present of this paper.

References

Christophe, W. (2006). *Medicinal Plants of the Asia-pacific Drugs for the Future?* Singapore: 1st Ed., World Science Publishing Co. Pte. Ltd., pp. 357 – 447

Falodun, A., Usifoh, C.O. and Nworgu, Z. A. M. (2006). "Smooth Muscle Relaxant Activity of 3-carbomethoxylpridine from *Pyrenucantha Staudtii* Leaf on Isolated Rat Uterus". *African Journal of Biotechnology*, vol 5(12), pp. 1271 – 1283

Griken, R. E. and Markowictz, A. A. (1993). Quantification in XRF Analysis of Intermediate Thickness Samples, New York: 1st Ed., Marcel Dekker Inc., pp 339 – 358

Koike, K., Ishii, K. Mitsunaga, K. and Ohmoto,T. (1991). "New Quassinoids from *Picrasma javanica*.Structures of Javananicins U, V, W, X and Y", *Chem. Pharm. Bull*., vol 39(8), pp. 2021 – 2023

Lata, H. and Ahuja, G. K. (2003). "Role of Free Radicals in Health and Disease" *Ind. J. Physiol. Allied Sci.*, vol 57, pp. 124 – 128

Marcocci, L., Maguire, J. J., Droy-Lefaix, MT. and Packer, L. (1994). "The Nitric Oxide Scavenging Properties of *Ginkgo biloba* Extract EGb 761", *Biochem. , Biophys. , Res. Commun*., vol 201, pp. 505 – 515

Marinova, G. and Batchvarov,V. (2011). "Evaluation of the Methods for Determination of the Free Radical Scavenging Activity by DPPH". *Bulgarian Journal of Agricultural Science*, vol 17, pp. 11 – 24

Nwachukwu , C.U., Umeh, C.N. and Kalu , I.G. (2010). "Identification and Traditional Uses of Some Common Medicinal Plants in Ezinihitte Mbaise L. G. A., of Imo State, Nigeria", Rep. Opinion , vol 2 (6), pp. 1-8

Ohmoto,T., Koike, K., Mitsunaga, K., Fukuda, H. and Kagei, K. (1989). "Studies on some Constituents of Indonesian *Picrasma javanica* III. Structures of New Quassinoids, Javanicins A, C and D", *Chem. Pharm. Bull*., vol 37(11), pp. 2991 – 2994

Phokaew, S. (2005). "Diversity Degrade Vulnerability of Cultural and Natural Diversity in Northern Karen State, Burma". *Karen Environmental and Social Action Network, Thailand*, pp. 65

Reynertson, K. A. (2007). "*Phytochemical Analysis of Bioactive Constiuents from Edible Myrtaceal Fruits*". PhD (Dissertation), New York, The City University, pp. 98

Ross, R. (1993). "The Pathogenesis of Atherosclerosis". *Free Rad. Res*., vol 362, pp. 801 – 804

Thomas, J., Joy, P. and Skaria, P. (1998). *Medicinal Plants. India:* 1st Ed., Kerala, pp. 3-4

WHO. (2003). "Clinical Trials on Treatment using a combination of Traditional Chinese Medicine and Western Medicine". *Traditional Medicine Strategy*, pp. 53 – 61

Yi Yi Win. (2014). *Antimalarial Activity of Stem Barks of Picrasma javanica Bl. (nann-paw-kyawt) and Alstonia scholaris L. (taung-mayoe) and Isolation and Identification of Active Compounds*. Phd (Dissertation), Myanmar: Department of Chemistry, University of Yangon

REMOVALOF METHYLENE BLUE USING ACTIVATED CHARCOAL OF *POLYALTHIALONGIFOLIO* (THIN-PAW TE)LEAVES

Hnin Yu Wai[1], Kaung Htet Swe[2]

Abstract

Removal of Methylene Blue (MB) from aqueous solution is carried out using carbonized material prepared from leaves of *Polyalthialongifolia* (PL) commonly called as Ashoka. The dried leaves samples were carbonized at 150° C for 2 h. The carbonized sample was heated at 175 °C for 1 h in muffle furnace to give the heated *Polyalthialongifolia* leaves charcoal (HPL). The activated carbon was prepared from *Polyalthialongifolia* leaves (APL) by chemical activation with $ZnCl_2$ as activation agent.The HPL and APL were characterized by FT IR and SEM. Batch sorption study has been carried out to investigate the effect of various parameters such as initial concentration of dye solution, contact time and amount of biosorbent. It was observed that the dye removal efficiency and adsorption capacity depended upon initial concentration of dye solution, contact time and amount of biosorbent. The equilibrium data were described by Freundlich and Langmuir isotherms. The resulting activated carbons were tested for their ability to sorb methylene blue in aqueous solution. The removal percent of methylene blue by HPL was 79.58 % and that by APL was 70.17 %.From Freundlich isotherm studies, the sorption capacity of HPL was 0.3716 mg g^{-1} and that of APL was 0.2773 mg g^{-1} for methylene blue and from Langmuir isotherm studies, the removal capacity of HPL was 232.55 mg g^{-1} and that of APL was 126.58 mg g^{-1} for methylene blue.The removal of methylene blue by HPL fits both Langmuir and Freundlich isotherms better than APL. The sorption capacity of *Polyalthialongifolia* leaves as found from the result suggests it to be a non-conventional and efficient biosorbent for the removal of MB from aqueous solution which can be used for the development of clean and cheap technology for effluent treatment.

Keywords: methylene blue, *Polyalthia longifolia* leaves, carbonized material, biosorbent

[1.] Dr, Lecturer, Department of Chemistry, University of Yangon
[2.] MSc Candidate, Department of Chemistry, University of Yangon

Introduction

Polyalthia longifolia is a large genus of shrubs and trees found in tropic and sub-tropic regions. It belongs to the family of Annonaceae. *Polyalthia longifolia* which is also known as false Ashoka, Buddha Tree, Green champa, Indian mast tree, and Indian Fire tree. It exhibits symmetrical pyramidal growth with willowy weeping pendulous branches and long narrow lanceolate leaves with undulate margins. The tree is known to grow over 30 ft in height(Parvin *et al*., 2013).

The leaves are used for ornamental decoration during festivals. The tree is a main attraction in gardens throughout India. The tree can be cut into various shapes and maintained in required sizes. The flexible, straight and light-weight trunks were used in the making of masts for sailing ships. The tree is mostly used for manufacturing small articles such as pencils, boxes, matchstick, etc,(Parvin *et al*., 2013).

Scientific classification

Kingdom	:	Plantae
Order	:	Magnoliales
Family	:	Annonaceae
Genus	:	*Polyalthia*
Species name	:	*Polyalthia longifolia*
Binomial name	:	*Polyalthia longifolia* Sonn.
English name	:	Ashoka tree, Buddha tree, Green champa
Myanmar name	:	Thin-Paw Te
Habital	:	Roadside tree

Coloured compounds are the most easily recognizable pollutants in the environment because of their appearance (Abudullah *et al*., 2005). Most of the industries such as textile, carpet, rubber, plastic, cosmetic, food and printing use dyes and pigments to colour their products. Among these various industries, textile ranks first in usage of dyes for colouration of fiber (Ladhe *et al*., 2011). Due to their good solubility, synthetic dyes are common water pollutants and they may frequent be found in trace quantities in industrial wastewater. However, the discharge of dye-bearing wastewater in natural

streams and rivers possess a severe problem, as dyes impart toxicity to aquatic life and are damaging the aesthetic nature of the environment. However, wastewater containing dyes is very difficult to treat, since the dyes are recalcitrant organic molecules, resistant to aerobic digestion, and is stable to light, heat and oxidizing agents due to their structure and molecular size (Tahir*et al*., 2008).

Different methods are available for the removal of dye and pollutants from waste water. Effluent is usually treated by either physical or chemical processes includes, chemical coagulation, ion exchange, membrane filtration, electrochemical destruction, irradiation, precipitation, floatation, membrane separation, chemical oxidation reverse osmosis, aerobic and anaerobic microbial degradation, hydrogen peroxide catalysis and ozonation. However, these processes are very expensive and could not be effectively used to treat the wide range of pollutants. The conventional biological treatment process is not very effective in treating a wastewater, due to low biodegradation of dyes (Velmurugan *et al*., 2011).

Among these adsorption method is the most effective and economical method. The process of adsorption has an edge over the other methods. It is potential alternative to conventional treatment techniques for the removal of pollutants from the contaminated effluent even from diluted solution. Adsorption is operative in most natural physical, biological, chemical system. It is widely used in industrial applications due to its sludge free clean operation, its simplicity of design, high removal capacity and ease of operation at large scale (Kalderis *et al*., 2008).

Activated carbon is the most widely used adsorbent as it shows excellent adsorption efficiency. The high adsorption capacity of activated carbon is associated with internal porosity and other properties such as, high surface area, pore volume, and pore size distribution. An attempt has been made to develop cheaper and effective adsorbents from low-cost waste material. In this situation, natural raw materials are possible biosorbents that could provide a successful solution.(Rengarag *et al*., 1996).

Methylene blue is not strongly hazardous but various harmful effects such as eye burns, irritation to the gastrointestinal tract and the skin, nausea, vomiting, profuse sweating, mental confusion, methemoglobine, mica by

ingestion. Tendency to change colour when touched by sweaty fingers, its toxicity. *P.longifolia* leaves are easily available, a garden waste and has no food value. In the present work an attempt has been made to investigate the adsorption potential of carbonized *P.longifolia* prepared from leaves of the said plant for the removal of MB.

Materials and Methods

The chemicals used in the experimental works were from British Drug House Chemical Ltd., England. In all the investigations, the recommended and standard procedures of both conventional and modern techniques were employed. The experiment was carried out in the Physical Chemistry Research Laboratory of the Department of Chemistry, and FT IR spectra was measured at the Department of Chemistry, University of Yangon and SEM micrograph was at West Yangon University.

Collection of Samples

In the experiments, healthy disease free mature fresh *P.longifolia* leaves were collected from University of Yangon Campus.

Preparation of Samples

P.longifolia leaves were cut into pieces. The cut pieces were washed thoroughly with distilled water to remove dust and impurities.After cleaning the sample; it was dried at room temperature. The dried sample was then ground in a mechanical grinder and screened through a sieve to obtain fine power of uniform particle size. The sieved material was then stored in an airtight plastic bottle for further experiment.

Preparation of Heated *Polyalthia longifolia* Leaves Charcoal Powder

The purified sample was ashed and sieved into 0.5 mm aperture size. The dried leaves samples were carbonized at 150˚C for 2 h. The carbonized sample was heated at 175˚C for 1 h in muffle furnace. The heated *longifolia* (HPL) was obtained.

Preparation of Activated *Polyalthia longifolia* Leaves Charcoal Powder

The dried samples were carbonized at 150°C for 2 h. Activated carbon was produced from carbonized samples soaked were in 10 % $ZnCl_2$ solution for 24 h. After soaking, the excess solution was decanted off and air dried. Then the samples were carbonized at 200°C for 4 h.The resultant activated carbon was washed several times with distilled water to obtain neutral pH.The sample was dried at 115°C and stored in a sealed bottle and the activated *Polyalthia longifolia* leaves charcoal powder was coated as APL.

Preparation of Stock Solution of Methylene Blue

A stock solution of 100 ppm for methylene blue solution was prepared by dissolving 0.1 g of dye in 1L of distilled water. By serial dilution the dye solutions methylene blue within the concentration range of 10 ppm to 60 ppm were prepared. Analyses were carried out by colorimetric method using Cary UV-Visible Spectrophotometer and calibration curves of methylene blue solution were plotted.

Physicochemical Properties of Powdered *Polyalthia longifolia* Leaves (PL), Heated *Polyalthia longifolia* Leaves Charcoal (HPL) and $ZnCl_2$ Activated *Polyalthia longifolia* Leaves Charcoal (APL)

The physicochemical properties (moisture content, ash content, bulk density, and pH) of prepared samples were determined by conventional method.

FT IR analysis

FT IR analysis was performed in order to characterize the functional groups of the sorbents HPL and APL.A Perkin-Elmer Spectrum GX, USA was used for FT IR analysis.

SEM analysis

The morphology of prepared adsorbents was studied by using scanning electron micrograph for analysing micro and macropores present on the surface of sorbents. The scanning electron micrographs of sorbents HPL and APL were obtained with the help of Scanning Electron Microscope (JSM-5160, JEOL Ltd., Japan).

Determination of Capacity of the Prepared Sorbents for the Removal of Methylene Blue

Optimization of process parameters such as the initial concentration of dye solution, contact time and dosage of sorbents on sorption were assessed by performing batch mode sorption experiments. Appropriate dosages of sorbents were added and the solution was stirred by using Orbital shaker at 150 rpm.The solutions, after adsorption were filtered by using filter paper. The absorbance was measured on UV–visible spectrophotometer at 665nm before and after adsorption to evaluate the initial concentration (C_0) and equilibrium concentration (C_e) of methylene blue.

Isotherm Studied

The adsorption capacities of heated *Polyalthia longifolia* leaves charcoal powder (HPL)and $ZnCl_2$ activated *Polyalthia longifolia* leaves charcoal powder (APL) were studied by Freundlich and Langumuir isotherm models.

Results and Discussion

Table 1 shows that the physicochemical properties (moisture content, ash content, bulk density, and pH) of the prepared samples (*Polyalthia longifolia* leaves powder (PL),heated *Polyalthia longifolia* leaves charcoal powder (HPL)and $ZnCl_2$ activated *Polyalthia longifolia* leaves charcoal powder (APL))were determined by conventional method. The pH values of samples were determined by pH meter. The pH value of samples were found to be 6.5,7.5 and 5.5 in PL, HPL and APL. The adsorption of methylene blue on adsorbent HPL increases with the increases of pH indicating favourable adsorption at alkaline medium which can be explained from the pH value of HPL.

Table1: Physicochemical Properties of Powdered *Polyalthia longifolia* Leaves (PL),Heated *Polyalthia longifolia* Leaves Charcoal (HPL) and Activated *Polyalthia longifolia* Leaves Charcoal (APL)

No.	Physical Properties	PL	HPL	APL
1.	Moisture content (%)	11.50	17.00	16.15
2.	Ash content (%)	6.12	12.07	9.40
3.	Bulk density (g mL^{-1})	38.54	36. 66	20.15
4.	pH	6.5	7.5	5.7

Plant based adsorbents have cellulosic nature. Several characteristic functional groups of cellulosic materials, which are capable of adsorbing dye, can be identified by using FT IR technique and SEM analyzer. The FT IR spectra show HPL and APL samples have especially hydroxyl and carbonyl stretching because of the presence of cellulose plays an important role in adsorption of dye were shown in Figures 1 (a) and (b). In the Figure 2(a), the surface morphology of HPL indicates that non uniform cavities and pores on surface of HPL which can be attributed to the adsorption of dye on HPL and the surface morphology of APL indicates spongy structure was shown in Figure 2(b). The pores were completely filled after adsorption of dye were shown in Figures 3(a) and (b).

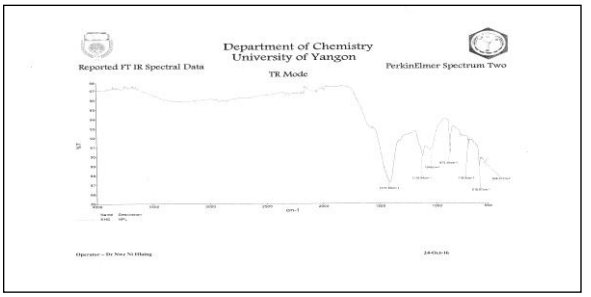

Figure 1:(a) FT IR spectrum of heated *Polyalthia longifolia* (HPL)

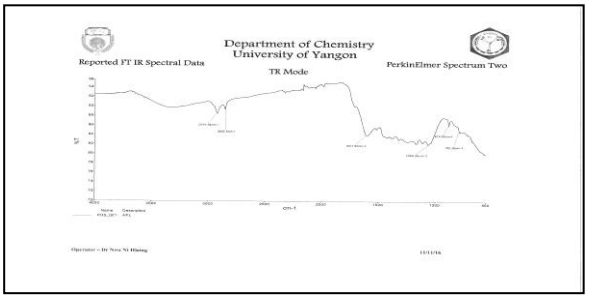

Figure 1:(b) FT IR spectrum of activated *Polyalthia longifolia* (APL)

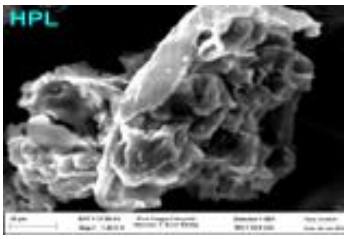

Figure 2:(a)SEM image of ofheated *Polyalthia longifolia* leaves charcoal (HPL) at 1.40 kx magnification

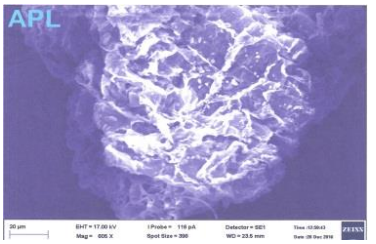

Figure 2: (b) SEM image of Activated *Polyalthia longifolia* leaves charcoal (APL)at 1.40 kx magnification

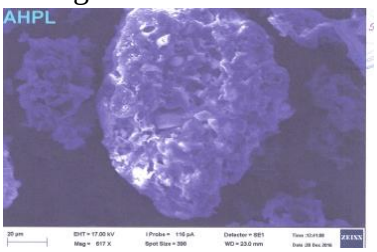

Figure 3:(a)SEM image of methylene blue sorbed of heated *Polyalthia longifolia* leaves charcoal (HPL)) at 1.40 kx magnification

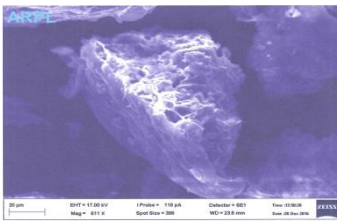

Figure 3: (b)SEM image of methylene blue sorbed Activated *Polyalthia longifolia* leaves charcoal (APL))at 1.40kx magnification

Effects of various parameters were studied and the results were recorded. Effect of initial concentration (C_0) was studied. The adsorption capacity (mg/g) decreased from 10 to 60 mg L^{-1} dose in all studied initial concentrations as indicated in Tables 2(a)and (b) and Figures 4 (a) and (b). It was observed that as the agitation time increased 60 min, percent removal and adsorption capacity increased in all initial concentrations used thereafter it remained constant. This may be due to higher rate of adsorption at low concentration were presented in Tables 3(a) and (b) and Figures 5(a) and (b).It was observed the as the amount of HPL is increased from 1 to 6 g L^{-1}, the percentage removal of methylene blue increased from 70.17 % to 93.23 % at C_0 = 30 mgL^{-1} of methylene blue. Increase in adsorbent dose increases surface area and availability of more adsorption sites, which results in increase in the removal of dye were shown in Tables 4(a) and (b) and Figures 6(a) and (b).

The removal effenciencies of adsorbents (HPL and APL) for sorption of dyes solution were calculated in equation (1)by the following:

$$R(\%) = \frac{(C_0 - C_e)}{C_0} \times 100 \qquad (1)$$

where, R is the removal percent (%), $C_0$and C_e are initial and equilibrium concentration of dye solution.

The results were shown Table 5. It indicated that the removal percent of dye solution was found to be 79.58 % and 70.17 % for removal of methylene blue by HPL and APL respectively. This result found that heated *Polyalthia longifolia* leaves charcoal (HPL)was more effective adsorbent for the sorption of methylene blue solution compared to $ZnCl_2$ activated *Polyalthia longifolia* leaves charcoal (APL) .

Tables 6(a) and (b) represented the data and Figures 7(a) and (b) were shown the sorption data for Freundlich equation is

$$\text{Log } x/m = 1/n \log C_e + \log K \quad (2)$$

where, x/m is the amount adsorbed per unit mass of the adsorbent

C_e is the equilibrium concentration

Tables 7(a) and (b) corresponding Figures 8(a) and (b) were shown the sorption data for Langmuir isotherms pertaining to Langmuir sorption equation 3. The Langmuir sorption equation 3 was used to fit the experimental sorption.

$$(1/x/m) = (1/b\ X_m C_e) + (1/X_m) \quad (3)$$

where, b is the adsorption coefficient or Langmuir constant

X_m is the monolayer capacity

Where, slope is $1/b\ X_m$ and intercept is $1/X_m$, regarding to the above equation 3, Figures 8(a) and (b) give linear plot. From the linear plot, Langmuir constant 'b' and 'X_m' were evaluated. The resulting data were shown in Table 8.

The calculated results of Langmuir and Freundlich isotherm constants were presented in Table 8. From Freundlich isotherm studies, the adsorption capacity of HPL was 0.3716 mgg^{-1} and that of APL was 0.2773 mgg^{-1} for methylene and from Langmuir isotherm studies, the removal capacity of HPL was 232.55 mgg^{-1} and that of APL was 126.58 mgg^{-1} for methylene blue. The removal of methylene blue by HPL fits both Langmuir and Freundlich isotherms as better than APL.

Table 2: (a) Effect of Initial Concentration on Percent Removal of Methylene Blue Using Heated *Polyalthia longifolia* Leaves Charcoal (HPL)

No.	Initial concentration(mg/L)	Final concentration(mg/L)	Removal	Percent (%)
1.	10	0.384	0.062	96.16
2.	20	2.768	0.447	86.16
3.	30	6.087	0.983	79.71
4	40	9.653	1.559	75.86
5.	50	13.486	2.178	73.03
6.	60	17.771	2.870	70.38

Dosage of HPL = 2 g/L, contact time = 1 h

Table 2: (b) Effect of Initial Concentration on Percent Removal of Methylene Blue Using Activated *Polyalthia longifolia* Leaves Charcoal (APL)

No.	Initial concentration(mg/L)	Final concentration(mg/L)	Adsorbance	Removal Percent (%)
1.	10	1.504	0.243	84.96
2.	20	5.089	0.822	74.56
3.	30	7.839	1.266	73.87
4	40	11.226	1.813	71.94
5.	50	14.804	2.391	70.39
6.	60	18.705	3.021	68.83

Dosage of APL = 2 g/L, contact time = 1 h

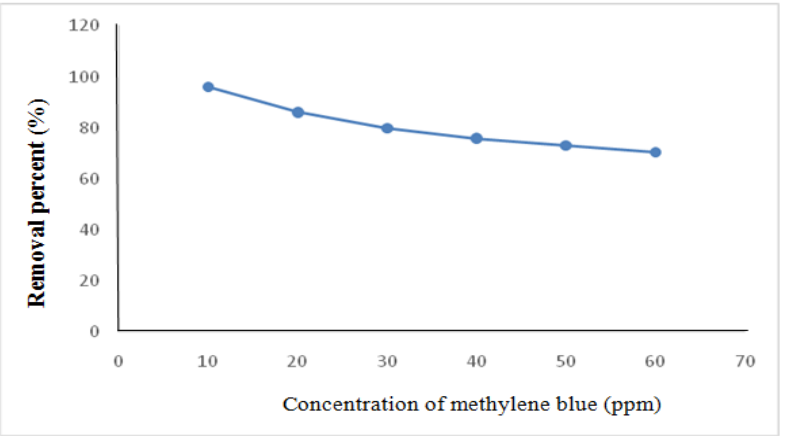

Figure 4:(a) Effect of concentration on removal percent of methylene blue by heated *Polyalthia longifolia* leaves charcoal (HPL)

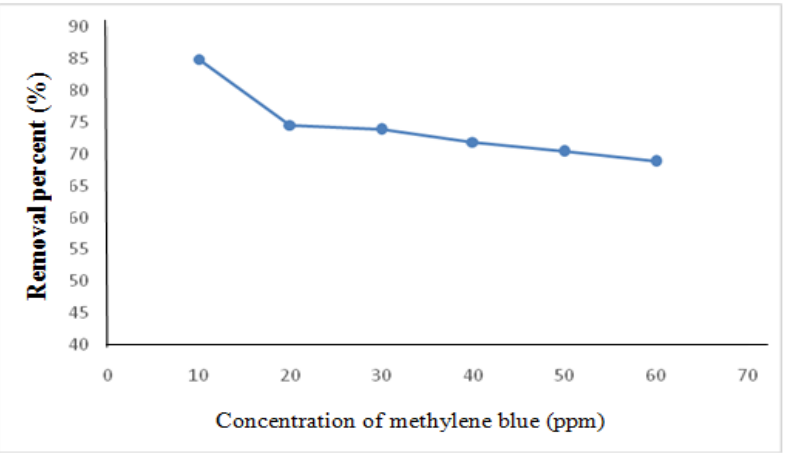

Figure 4: (b) Effect of concentration on removal percent of methylene blue by Activated *Polyalthia longifolia* leaves charcoal (APL)

Table 3: (a) Effect of Contact Times on Percent Removal of Methylene Blue Using Heated *Polyalthia longifolia* Leaves Charcoal (HPL)

No.	Contact time (min)	Final concentration (mg/L)	Absorbance	Removal Percent (%)
1.	30	7.963	1.286	73.46
2.	60	6.124	0.989	79.58
3.	90	4.663	0.753	84.46
4	120	2.266	0.366	92.45
5.	150	1.901	0.307	93.66
6.	180	1.616	0.261	94.61

Initial concentration = 30 mg/L, Dosage of HPL = 2 g/L

Table 3: (b) Effect of Contact Times on Percent Removal of Methylene Blue Using Activated *Polyalthia longifolia* Leaves Charcoal (APL)

No.	Contact time (min)	Final concentration (mg/L)	Absorbance	Removal Percent (%)
1.	30	9.715	1.569	67.61
2.	60	8.978	1.450	70.07
3.	90	8.458	1.366	71.81
4	120	8.359	1.350	72.14
5.	150	7.672	1.239	74.43
6.	180	7.622	1.231	74.59

Initial concentration = 30 mg/L, Dosage of APL = 2 g/L

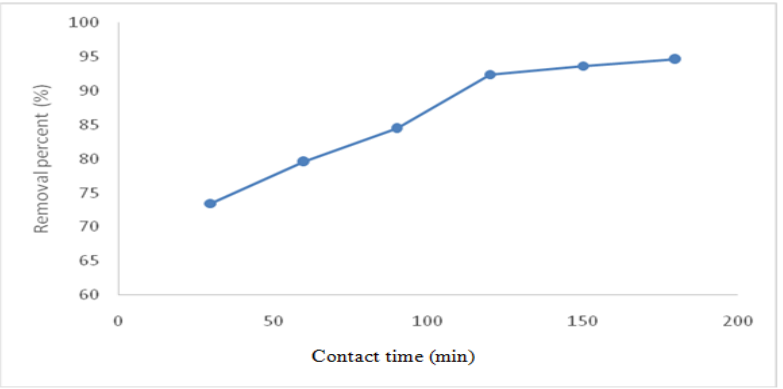

Figure 5: (a) Effect of contact times on removal percent of methylene blue by heated *Polyalthia longifolia* leaves charcoal (HPL)

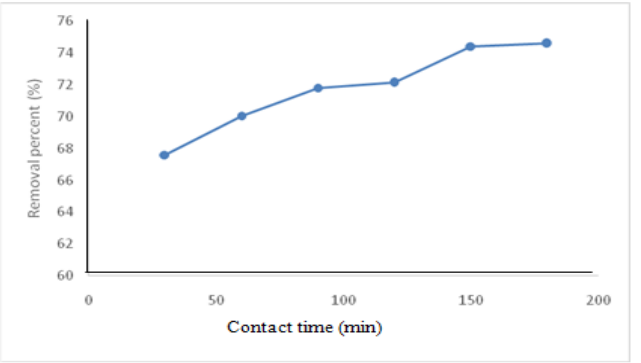

Figure 5: (b) Effect of contact times on removal percent of methylene blue by activated *Polyalthialongifolia* leaves charcoal (APL)

Table 4: (a) Effect of Adsorbent Dose on Percent Removal of Methylene Blue Using Heated *Polyalthia longifolia* Leaves Charcoal (HPL)

No.	Dosage (g /L)	Final concentration (mg/L)	Absorbance	Removal Percent (%)
1.	1	8.947	1.445	70.17
2.	2	5.888	0.951	80.37
3.	3	3.820	0.617	87.26
4	4	2.910	0.470	90.30
5.	5	2.359	0.381	92.13
6.	6	2.030	0.328	93.23

Initial concentration = 30 mg/L, contact time = 1 h

Table 4: (b) Effect of Adsorbent Dose on Percent Removal of Methylene Blue Using Activated *Polyalthia longifolia* Leaves Charcoal (APL)

No.	Dosage(g /L)	Final concentration (mg/L)	Adsorbance	Removal Percent (%)
1.	1	11.244	1.816	56.62
2.	2	6.588	1.064	77.19
3.	3	5.188	1.838	82.71
4	4	3.678	0.594	87.74
5.	5	2.953	0.477	90.15
6.	6	2.563	0.414	91.45

Initial concentration = 30 mg/L, contact time = 1 h

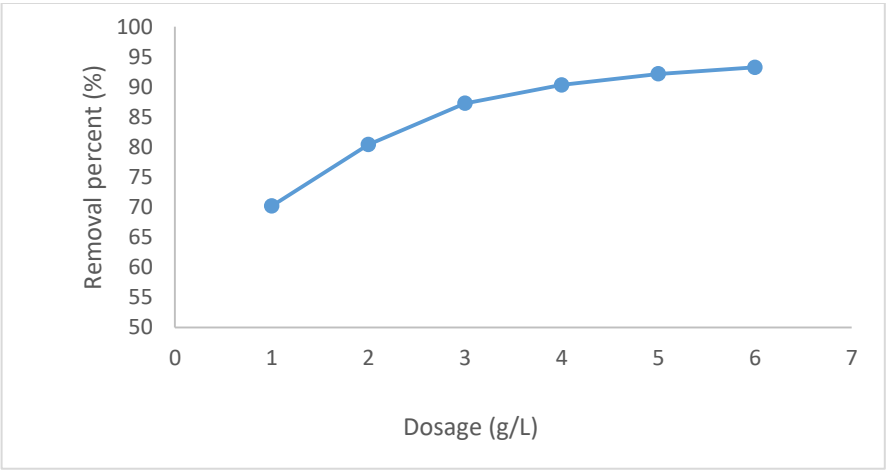

Figure 6:(a) Effect of adsorbent dosage on removal percent of methylene blue by heated *Polyalthia longifolia* leaves charcoal (HPL)

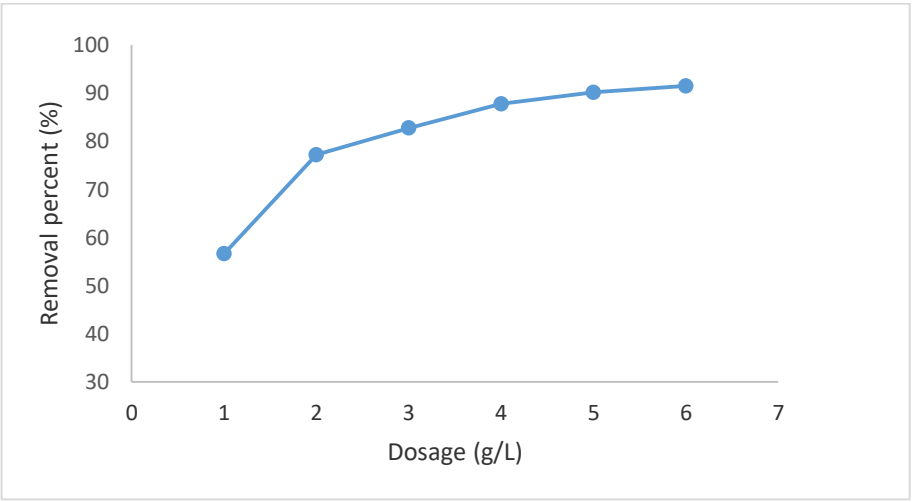

Figure 6:(b) Effect of adsorbent dosage on removal percent of methylene blue by activated *Polyalthia longifolia* leaves charcoal (APL)

Table 5: Comparison of Removal Percent of Methylene Blue by Heated *Polyalthia longifolia* Leaves Charcoal (HPL)and Activated Polyalthia *longifolia* Leaves Charcoal (APL)

Adsorbent	Removal percent of methylene blue (%)
HPL	79.58
APL	70.17

HPL = Heated *Polyalthia longifolia* Leaves Charcoal
APL = Activated *Polyalthia longifolia* Leaves Charcoal
Initial concentration = 30 mg/L
Dosage = 2 g/L
Contact time = 1 h

Table 6: (a) Freundlich Isotherm Adsorption of Methylene Blue by Heated *Polyalthia longifolia* Leaves Charcoal (HPL)

Wt of Sample (g/L)	Final Conc: C_e(mg/L)	Amount of MB adsorbed, x (mg/L)	x/m	Log C_e (mg/ g)	Log x/m
1	8.947	21.053	21.053	0.951	1.323
2	5.888	24.112	12.056	0.769	1.081
3	3.820	26.180	8.726	0.582	0.940
4	2.910	27.090	6.772	0.463	0.830
5	2.359	27.641	5.528	0.372	0.742
6	2.030	27.970	4.661	0.307	0.668

Initial concentration = 30 mg/L, contact time = 1 h

Table 6: (b). Freundlich Isotherm Adsorption of Methylene Blue by $ZnCl_2$ Activated *Polyalthia longifolia* Leaves Charcoal (APL)

Wt of Sample (g/L)	Final Conc: C_e(mg/L)	Amount of MB adsorbed, x (mg/L)	x/m (mg /g)	Log C_e	Log x/m
1	11.244	18.756	18.756	1.050	1.273
2	6.588	23.412	11.706	0.818	1.068
3	5.188	24.812	8.270	0.714	0.917
4	3.678	26.322	6.580	0.565	0.818
5	2.953	27.047	5.409	0.470	0.733
6	2.563	27.437	4.572	0.408	0.660

Initial concentration = 30 mg/L, contact time = 1 h

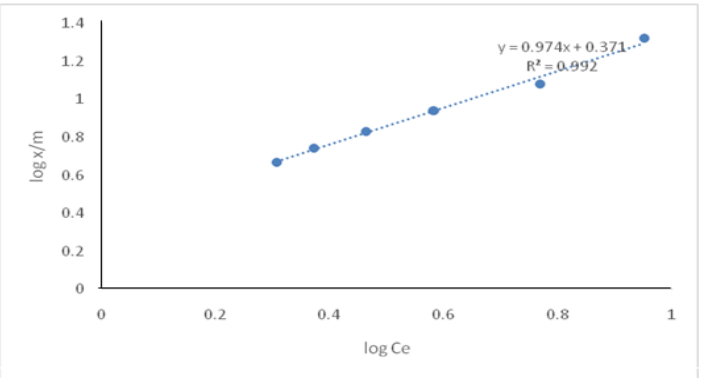

Figure 7: (a) Freundlich model of methylene blue on heated *Polyalthia longifolia* leaves charcoal (HPL)

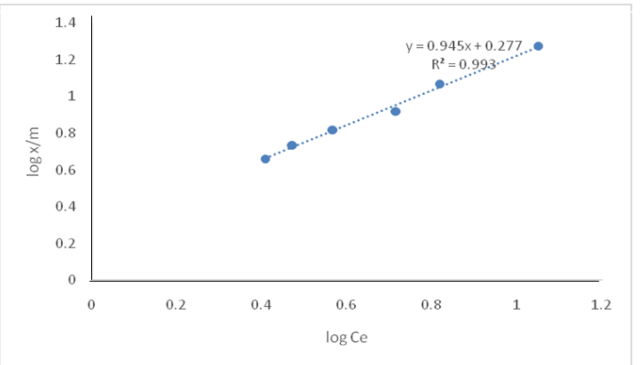

Figure 7: (b) Freundlich model of methylene blue on activated *Polyalthia longifolia* leaves charcoal (APL)

Table 7: (a) Langmuir Isotherm Adsorption of Methylene Blue by Heated *Polyalthia longifolia* Leaves Charcoal (HPL)

Wt of Sample (g/L)	Final Conc: C_e(mg/L)	$1/C_e$ (L/mg)	Amount of adsorbed, x (mg/L)	x/m (mg /g)	m/x (g/mg)
1	8.947	0.111	21.053	1.053	0.047
2	5.888	0.169	24.112	12.056	0.082
3	3.820	0.261	26.180	8.726	0.114
4	2.910	0.343	27.090	6.772	0.147
5	2.359	0.423	27.641	5.528	0.180
6	2.030	0.492	27.970	4.661	0.214

Initial concentration = 30 mg/L, contact time = 1 h

Table 7: (a) Langmuir Isotherm Adsorption of Methylene Blue by $ZnCl_2$ Activated *Polyalthia longifolia* Leaves Charcoal (APL)

Wt of Sample (g/L)	Final Conc: C_e(mg/L)	$1/C_e$ (L/mg)	Amount of adsorbed, x (mg/L)	x/m (mg/g)	m/x (g/mg)
1	11.244	0.088	18.756	18.756	0.053
2	6.588	0.151	23.412	11.706	0.085
3	5.188	0.192	24.812	8.270	0.121
4	3.678	0.271	26.322	6.580	0.151
5	2.953	0.338	27.047	5.409	0.185
6	2.563	0.390	27.437	4.572	0.219

Initial concentration = 30 mg/L, contact time = 1 h

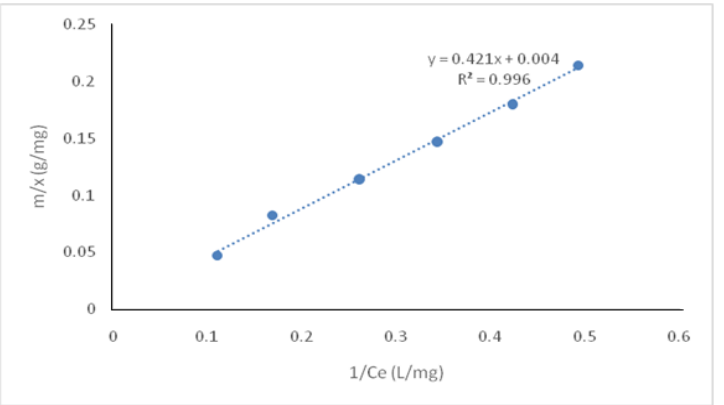

Figure 8:(a) Langmuir model of methylene blue on heated *Polyalthia longifolia* leaves charcoal (HPL)

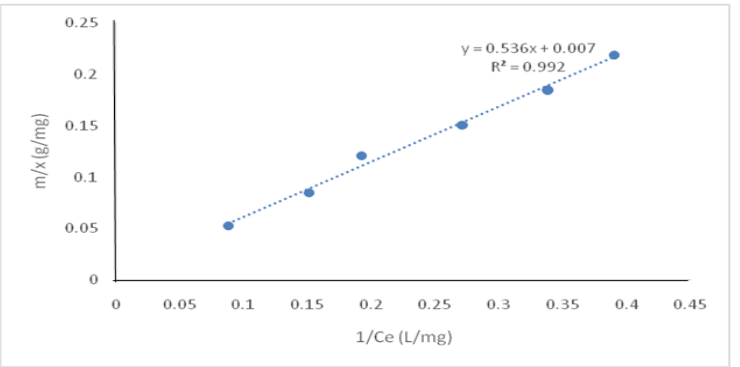

Figure 8:(b) Langmuir model of methylene blue on activated *Polyalthia longifolia* leaves charcoal (APL)

Table 8: **Adsorption Parameters for Monolayer Species by Two Types of Sorbents**

Sorbent	sorbat	Langmuir model			Freundlich model			
		X_m (mg g^{-1})	b (Lm g^{-1})	R^2	K (mg g^{-1})	1/n	n (Lm g^{-1})	R^2
HPL	MB	232.55	0.0102	0.9960	0.3716	0. 9740	1.0260	0.9920
APL	MB	126.58	0.0147	0.9920	0.2773	0.9454	1.0570	0.9930

HPL = Heated *Polyalthia longifolia* Leaves Charcoal
APL = Activated *Polyalthia longifolia* Leaves Charcoal
MB =Methylene Blue

Conclusion

This study reveals that the heated *Polyalthia longifolia* leaves charcoal (HPL)and activated *P. longifolia* leaves charcoal (APL) were tested with regards to decolourization nature of methylene blue in aqueous solution. *P.longifolia* leaves was collected at the Yangon University Campus, Yangon Region. The physicochemical properties of *P. longifolia* leaves powder (PL), heated *P.longifolia* leaves charcoal (HPL) and activated *P.longifolia* leaves charcoal (APL) were determined by conventional methods. FT IR analysis confirms the presence of active functional groups on the surface of sorbent and SEM analysis shows the presence of large cavities on the surface of HPL. The effect of initial concentration, dosage and contact time, were also investigated for the removal of dye (methylene blue) by HPL and APL samples. It was deduced that the percent removal of dye increased with the increasing time. The removal percent of methylene blue by HPL was 79.58 % and that by APL was 70.17 % by using 30 mg/L concentration of dye, 2 g of dosage and 1 h contact time. From Freundlich isotherm studies, the adsorption capacity of HPL was 0.3716 mgg^{-1} and that of APL was 0.2773 mgg^{-1} for methylene and from Langmuir isotherm studies, the removal capacity of HPL was 232.55 mgg^{-1} and that of APL was 126.58 mgg^{-1} for methylene blue. The removal of methylene blue by HPL fits both Langmuir and Freundlich isotherms was better than APL. This natural adsorbent has several advantages, such as low cost, environmental friendliness, high uptake capacity, and non-toxicity. Thus, it can be considered as an effective biosorbent on the removal of MB dye from aqueous solutions.

Acknowledgements

The authors would like to express their profound gratitude to the Department of Higher Education (Lower Myanmar), Ministry of Education, Yangon, Myanmar, for provision of opportunity to do this research and Myanmar Academy of Arts and Science for allowing to present this paper.

References

Abudullah, A.G., Salleh, M.A., Mazlina, M.K. and Sobri, S.V. (2005). "Azo Dye Removal by Adsorption Using Waste Biomass Sugarcane Bagass". *International Journal of Engineering and Technology*, vol. 2**,** pp.8-13

Kalderis, D., Koutoulakis, D., Paraskeva, P.andDiamadopoulos, E. (2008). "Adsorption of Polluting Substances on Activated Carbons Prepared from Rice Husk and Sugarcane Bagasse". *Journal of Chemical Engineering*,vol.144**,** pp.42-50

Ladhe, U.V., Wankhed, S. K., Pati, V. T. andPati, P. R.(2011). "Removal of Erichrome Black T from Synthesis Wastewater by Activated Nilgiri Leaves". *Journal of Chemical and Pharmaceutical Research*, vol.3**,** pp.670-675

Parvin, A., Akter, J., Hasan, M. and Biswas, N.(2013). "Study on the Comparative Antibacterial Activity of *Polyalthialongifolia* Leaf Extracts to Some Selective Pathogenic Bacterial Strains". *Journal of Science and International Research*, vol.57**,** pp. 129-132

Rengarag, S., Arabindoo, B.andMurugesan, V. (1996). "Activated Carbon from Ruber Seed and Pant Seed Coat, Preparation and Characterization". *Journal of Science and International Research*, vol.50**,** pp**.** 40-85

Tahir, H., Sultan, M. andJahanzeb, Q. (2008). "Removal of Basic Dye Methylene Blue by Using BioabsorbentsUlvaLactuca and Sargassum".*African Journal of Biotechnology*, vol.15, pp. 2649-2655

Velmurugan, P., Rathina, V. and Dhinakaran, G.(2011). "Dye Removal from Aqueous Solution Using Low Cost Adsorbent". *International Journal of Environmental Sciences*, vol.1**,** pp. 5-18

ASSESSMENT OF BRACKISH WATER QUALITY FROM LETKHOKKON AREA IN YANGON REGION, MYANMAR

Jue Jue Khin[1], Aye Khaing Soe[2]

Abstract

Eutrophication is the most studied form of coastal marine pollution. Eutrophic waters are characterized by excessive algae growth as a consequence of nutrient enrichments of coastal surface waters. In this research, totally 9 brackish water samples were collected from Letkhokkon area, seasonally in 2017. The aim of this research work is to study the water quality criteria of brackish water samples around Letkhokkon area and to identify eutrophication level of the studied area. Physicochemical and microorganisms investigations have been carried out by conventional and modern instrumental techniques and compared with the acceptable levels of ASEAN and EPA standards for human health and aquatic life protection. Sampling sites were recorded with GPS detector. According to the research, the eutrophic level (high nutrient-enrichment) was found in the hot season and the mesotrophic level (medium nutrient-enrichment) was found in the cold and rainy seasons.

Keywords: ASEAN, brackish water, EPA, eutrophication, eutrophic waters, mesotrophic level

Introduction

Brackish water is a type of water which has less salt in its water than in sea water. Brackish water is comprised of both seawater and fresh water as well. And it can be found in areas where lakes and rivers meet the ocean. Brackish water cannot be used as drinking water because tons of organisms which carry diseases thrive best in this type of water environment. Brackish water has a lower salinity than regular sea water. The saltiness of the sea water helps to eliminate these organisms. Brackish water usually takes on a brownish murky color. Swamps are made up of brackish water. An example of a type of swamp is the Mangrove swamps. Theses swamps act as a buffer which helps to separate the sea water from the brackish water. Technically, brackish water contains between 0.5 and 30 g of salt per liter more often expressed as 0.5 to 30 parts per thousand (ppt or %). Table 1 shows the water salinity based on the dissolved salts.

[1]. Dr, Demonstrator, Department of Chemistry, Maubin University
[2]. Demonstrator, Department of Chemistry, Maubin University

Table 1: Water Salinity Based on Dissolved Salts in Parts Per Thousand (ppt)

No	Water	Dissolved Salt (ppt)
1	Fresh water	<0.5
2	Brackish water	0.5-30
3	Saline water	30-50
4	Brine water	>50

Materials and Methods

Study Area

There are many beautiful beaches in Myanmar, such as Ngapali, Chaung Tha, Ngwe-saung, Maungmagan, Kanthaya, Setse' and Letkhokkon beaches. The studied area, Letkhokkon beach is situated less than 100 km to the south of Yangon. This is the nearest beach resort to Yangon, a distance of just under three hours drive after ferry-crossing the Yangon river. Although most of Myanmar's beaches feature crystal-clear water and powdery white sands, the Bago River flows into this area, turning it into a dark mud flat. The beach is certainly not tempting for swimming due to mud. It is however idyllic and little visited (Figure 1) (Wikipedia, 2014).

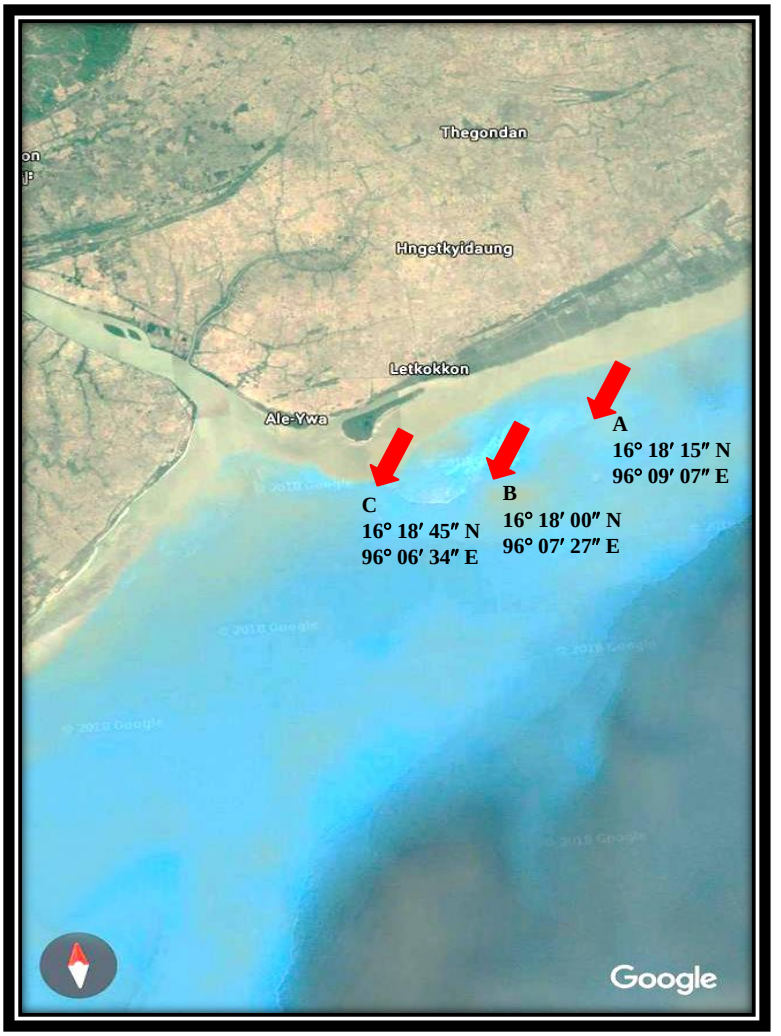

Figure 1: Satellite image of Letkhokkon beach
Sampling site – A (Near Seal Eain Tenn village)
Sampling site – B (Near Khanyein Kone Village)
Sampling site – C (Near Ahlae Village)

Table 2: Sampling Stations and Sampling Dates of Brackish Water Samples

Sample	Sampling Station		Sampling date
	Longitude (E)	Latitude (N)	
A	96° 09′ 07″	16° 18′ 15″	(30.3.17)
B	96° 07′ 27″	16° 18′ 00″	Hot Season
C	96° 06′ 34″	16° 18′ 45″	
A	96° 09′ 07″	16° 18′ 15″	(12.8.17)
B	96° 07′ 27″	16° 18′ 00″	Rainy Season
C	96° 06′ 34″	16° 18′ 45″	
A	96° 09′ 07″	16° 18′ 15″	(3.12.17)
B	96° 07′ 27″	16° 18′ 00″	Cold Season
C	96° 06′ 34″	16° 18′ 45″	

Sampling and Analytical Methods

In 2017, 9 brackish water samples were seasonally i.e, hot season (march), rainy season (August) and cold season (December) collected from 3 different sites A, B and C at Letkhokkon area, Yangon region (Table 2). Brackish water samples was taken 1 mile away from the bank and 1 meter depth from the surface water level. Polyethylene bottles were used for samples collection and storage. Physicochemical and microorganism detections were done by conventional methods and modern instrumental techniques.

Physicochemical parameters such as – temperature, pH, total alkalinity, total hardness, turbidity, total suspended solid, chlorinity, salinity, biochemical oxygen demand, chemical oxygen demand, dissolved oxygen, orthophosphate and total nitrogen contents in brackish water samples were analyzed along the Letkhokkon in order to monitore the quality of the brackish water. The pH of brackish water samples was determined by pH meter. The total alkalinity of brackish water samples were determined by titrating the sample with a standard solution of sulphuric acid using methyl orange as indicator. The total hardness of brackish water samples were determined by EDTA titrimetric method. Chlorinity and salinity of brackish water samples were determined by Mohr's modified method. The turbidity of brackish water samples was determined by turbidity meter. Total suspended

solid of brackish water samples were determined as the residue left after evaporation of the filtered water samples. Biochemical oxygen demand (BOD) of brackish water samples was measured by incubating the samples at 20 ^{o}C for 5 days. Chemical Oxygen demand (COD) of brackish water samples was measured by the permanganate oxidation method. The DO of brackish water samples was measured by DO meter. The content of orthophosphate was determined by UV-visible spectrophotometer. Total nitrogen contents in brackish water samples were determined by azo-dye method. Concentrations of some metal (Pb, Cd, Hg and As) in brackish water samples were determined by using Atomic Absorption Spectrophotometer (AAS) and microorganism indicators (total coliforms and *E. coli*) of brackish water samples were determined by multiple tube method.

Results and Discussion

The physicochemical properties of brackish water samples are shown in Tables 3, metal content in Table 7 and the microbiological properties in Table 8. The resultant data are illustrated in Figure 2 to 17. All of these results were observed in hot, rainy and cold seasons in 2017.

Temperature

The temperature of surface water is influenced by latitude, altitude, season, time of day, air circulation, cloud cover and the flow and depth of the water body. In this research, the temperature fluctuate seasonally in the range of between 28.34 ^{o}C and 30.54 ^{o}C. The minimum temperature 28.34 ^{o}C was found at sampling site A in rainy season due to the strong wind and rain (Table 3 and Figure 2).The maximum temperature 30.54 ^{o}C was found at sampling site C in hot season due to the intensity of solar radiation and evaporation. According to the resulting temperature range, the aquatic organisms which they can live normally in this study area.

pH

pH is an important parameter in water quality assessment as it influences many biological and chemical process within the water body. From the seasonal sample collection, the pH values of brackish water samples were

found in the range of between 7.70 and 8.00. The minimum pH value 7.70 was found at sampling sites B and C in rainy season. The maximum pH value 8.00 was found at sampling site C in hot season, because of the photosynthesis and respiration cycles of algae in eutrophic water (Strickland and Parsons, 1972) (Table 3 and Figure 3). In water body, point source pollution is a common cause that can increase or decrease pH depending on the chemicals involved. These chemicals can come from agricultural runoff, wastewater discharge or industrial runoff (Waterman, 2005). In the study areas, the observed pH values did not exceed the ASEAN standard (2010) (6.5-8.5) and EPA standard (2010) (6.0-8.0). However, these values were found to be slightly alkaline. pH can indirectly affect aquaculture species through its effect on other chemical parameters. So, the resulting pH value is good for aquatic life and fisheries.

Total Alkalinity

Total Alkalinity were attributed to the presence of hydroxide, carbonate and bicarbonate ion in the water sample. pH and alkalinity are directly related when water is at 100 % air saturation. Due to the presence of carbonates, alkalinity is more closely related to hardness than to pH (though there are still distinct differences). However, changes in pH can also affect alkalinity levels (as pH lower, the buffering capacity of water lowers as well). The total alkalinity of brackish water samples were observed in the range of between 100 ppm and 140 ppm. The lowest total alkalinity value 100 ppm was found at sampling sites C and B in rainy season and cold season. The highest total alkalinity values 140 ppm was found at sampling site C in hot season. It indicates that the concentration of basic compounds were higher in this sampling site C. These values are higher than the human health protection of ASEAN (2010) permissible guidelines (< 120 ppm) but within EPA standard (2010) of 30-150 ppm. Highly alkaline waters are usually unpalatable. Excess alkalinity in water is harmful for irrigation which leads to soil damage and reduce crop yields (Table 3 and Figure 4). Total alkalinity is not usually of concern for brackish water aquaculture. The desirable total alkalinity range is between 100 and 400 ppm is sufficient for aquaculture purpose.

Total Hardness

Total hardness of water is characterized with high mineral contents that are usually not harmful for humans. It is often measured as calcium carbonate ($CaCO_3$) because it consist mainly of calcium carbonate, the most dissolved ions in hard water (Chapman, 1996). In this research, the total hardness of brackish water samples were observed in the range of between 8890 and 9860 ppm. ASEAN and EPA standards (2010) values for total hardness in brackish water were not of concern (NC). The lowest total hardness value 8890 ppm was found at sampling site B in rainy season. The highest total hardness value 9860 ppm was found at sampling site A in hot season, due to the present of dissolved salts and the extensive geological formation of limestone in these area (Table 3 and Figure 5).

Chlorinity

Chloride is one of the major anions to be found in water and sewage. In this study, the chlorinity of brackish water samples was found in the range of 18.00 to 20.00 ppt. The lowest chlorinity value 18.00 ppt was found at sampling site C in rainy season due to the dilution effect of rain water. In hot season, concentration of the chlorinity value of 20.00 ppt was found in sampling site A. The chlorinity are of concern in water supplies used for aquaculture because the anion of chloride are essential for osmotic, ionic and water balance in all fish. These observed values were within the allowable limit of ASEAN standard (2010) for human health protection (Table 4 and Figure 6).

Salinity

Salinity measures dissolved inorganic content in water and usually expressed as parts per thousands (ppt). Salinity directly affects the level of dissolved oxygen, the higher the salinity, the lower the DO level at a given water temperature. The salinity of brackish water samples was found in the range of between 19.00 and 26.00 ppt. The lowest salinity value 19.00 ppt was found at sampling sites B and C in rainy season due to the dilution effect of rain water. The highest salinity value 26.00 ppt was found at sampling site A in hot season due to the high rate of evaporation, low rain fall and absence of river discharge. These values were agreed with the permissible level of

ASEAN standard (2010) (Table 4 and Figure 7). So, the water quality is good for the survival of brackish water fish.

Turbidity

Turbidity is a measure of cloudiness in water. In this study, the turbidity of brackish water samples was observed in the range of 5.90 to 8.30 FTU. These observed turbidity values was within the allowable limit of ASEAN standard (2010) and EPA standard (2010) for human health and aquatic life protection. The lowest turbidity value 5.90 FTU was found at site B in cold season. The highest turbidity value 8.30 FTU was found at sampling site A in hot and rainy seasons and it was noticed that the decrease in water clarity. In this sample, turbidity is related to the total suspended solid. Increase total suspended solid (TSS) has a similar effect to turbidity in that water. The highest turbidity can be caused the water clarity is reduced, water temperature can rise, oxygen level can fall as a result of less photosynthesis, and soil can bind to toxic compounds and heavy metal (Strickland and Parson,1972) (Table 4 and Figure 8).

Total Suspended Solid (TSS)

Total suspended solids (TSS) include a wide variety of material, such as silt decaying plant and animals matter, industrial wastes and sewage (APHA, 1992). The TSS of brackish water samples were found in the range of between 240 and 290 ppm. These values exceeded the ASEAN standard (2010) (< 75). The minimum turbidity value 240 ppm was found at sampling site B in cold season. The maximum TSS value 290 ppm was found in sampling site A in hot and rainy seasons, due to the high flow rate, soil erosion, urban and fertilizer run-off, waste water and septic effluents, decaying plants and geological features in these area. High level of TSS can cause gill irritations and tissue damage, with increase the stress levels of aquatic animals. In terms of water quality, high levels of total suspended solids will increase water temperatures and decrease dissolved oxygen (DO) levels (Table 4 and Figure 9).

Biochemical Oxygen Demand (BOD)

Biochemical oxygen demand (BOD) denotes the amount of oxygen needed by microorganisms for stabilization of decomposable organic matter under aerobic conditions. In this study, the BOD values of brackish water

samples was found in the range of between 1.00 and 2.00 ppm. The lowest BOD value 1.00 ppm was found at sampling site C in hot and rainy season. The highest BOD value 2.0 ppm was observed at sampling site A in hot and cold season. Unpolluted water typically has biochemical oxygen demand values of 2 ppm O_2 or less. These observed BOD values were within the ASEAN standard (2010) of < 15 ppm and EPA standard (2010) of 5 ppm for human health and aquatic life protection (Table 5 and Figure 10). So, the water quality is good for the brackish water fish.

Chemical Oxygen Demand (COD)

The chemical oxygen demand (COD) is a measure of the oxygen equivalent of the organic matter in a water sample. In this research, COD of brackish water samples was found in the range of 2.00 to 3.52 ppm. The lowest COD contents 2.00 ppm was found at sampling site C in rainy season probably due to the rainfall and run off. The highest COD contents 3.52 ppm was found at sampling site A in hot season. There is no major industries in the studies area, however, small scale industries like coconut husk retting are well established near the banks of the sea. It has negative impact such as the sharp rise and fall of pH, DO and also released toxic chemicals on the aquatic life and their sustainability. These values were within the allowable limits for human health and aquatic life protection of ASEAN standard (2010) and EPA Standard (2010) (Table 5 and Figure 11).

Seasonal Variation of Nutrient Level in Brackish Water Samples

Dissolved Oxygen (DO)

DO is an important indicator of water quality. The dissolved oxygen (DO) values of brackish water samples was found in the range of 2.00 to 3.50 ppm. The lowest DO value 2.00 ppm was found at sampling sites A and B in hot and cold seasons. Physical condition such as temperature, altitude and salinity can also affect oxygen level. The temperature and salinity increase, the solubility of oxygen in the water decreases. The highest DO value of 3.50 ppm was found at sampling site A in rainy season. In rainy season, heavy rainfall in the sea because of its churning dissolves more oxygen than still water, such as that in a reservoir behind a dam (Chapman, 1996). The resulting data are lower than the human health and aquatic life protection of ASEAN standard (2010) and EPA standard (2010) (Table 6 and Figure 12).

Orthophosphate

Phosphorus is usually present in natural water as phosphates (orthophosphates, polyphosphate, and organically bound phosphate). Soluble reactive phosphorus is a measure of orthophosphate (inorganic phosphate) that is dissolved or suspended in water. Excess phosphorus causes extensive algal growth called "blooms", which are the classic symptom of cultural eutrophication and lead to decrease oxygen levels in water body. In this research, the orthophosphate of brackish water samples was found in the range of 0.10 to 0.30 ppm. The lowest orthophosphate value 0.10 ppm was found at sampling sites B and C in hot season. The highest orthophosphate value 0.30 ppm was found at sampling sites A and C in rainy seasons and sampling site A in hot season. This may be due to the land runoff contaminated with super phosphate and from soap and detergents used by the public for bathing and washing clothes near water body. These values exceeded the ASEAN standard (2010) value 0.015 ppm (Table 6 and Figure 13).

Total Nitrogen

Nitrogen occurs in natural waters as nitrate, nitrite, ammonia and organically bound nitrogen. In this research, the total nitrogen of brackish water samples were observed in the range of 0.20 to1.00 ppm. The lowest total nitrogen value 0.20 ppm was found at sampling site B in hot season. The highest total nitrogen value 1.0 ppm was found at sampling site A in hot and rainy seasons. This may be due to the land runoff contaminated with fertilizer from the surrounding coconut gardens and vegetation (Table 6 and Figure 14).

In surface waters, phosphorus concentration exceeding 0.05 ppm may cause eutrophic conditions. If excessive amounts of phosphorus and nitrogen are added to the water, algae and aquatic plants can grow in large quantities. When these algae die, they are decomposed by bacteria. The decomposer use up the dissolved oxygen of the water body. The dissolved oxygen concentration often drop too low for fish to breathe, leading to fish kills (Waterman, 2005).

According to the evaluation degree of nutrient level, the studied areas around Letkhokkon Beach were identified as Mesotrophic level (medium nutrient enrichment) in rainy and cold seasons (Table 6). Eutrophic level (high nutrient enrichment) was found in hot season, due to the lesser amount

of fresh water inflow and high salinity. According to the results, it can be deduced that the studied areas are eutrophicated with nitrogen and phosphorus during the studied period within 2017.

Seasonal Variation of some Metals Contents in Brackish Water Samples

Most chemicals dissolved in brackish water are classified as some metals simply because so many ions and molecules are present at very low concentrations. Some metals in brackish water varied according to their locations and their depths. Some metals (Pb, Cd, Hg and As) contents of brackish water sample were determined by using Atomic Absorption Spectrophotometer (AAS). In this study, The Pb and Cd contents in brackish water sample were found in the range of 0.001 to 0.004 ppm and 0.005 to 0.009 ppm, respectively. The lowest Pb concentration of 0.001 ppm was found at sampling site C in rainy season and sampling sites A and C in cold season. The highest Pb concentration of 0.004 ppm was found at sampling site A in hot season. The minimum Cd concentration of 0.005 ppm was found at sampling site B in rainy season and the maximum Cd concentration of 0.009 ppm was found at sampling site A in hot season. The mercury and arsenic contents were not detected during the studied period of 2017. Industrial activity, anthropogenic activity and soil waste disposal may lead to increase some metal acidification of water bodies (Kyaw Naing, 2011). According to the results, some metal concentrations were within the allowable limits of ASEAN standard (2010) and EPA Standard (2010). Therefore, some metal pollution in Letkhokkon area is not at a level to affect the aquatic life and human health (Table 8 and Figures 15 and 16).

Seasonal Variation of Microorganisms Indicators (Total Coliform and *E.coli*) in the Brackish Water Samples

For the microbiological analysis of water samples in relation to human health, it is necessary to determine principally the pathogenic organism. Microbiological properties such as (Total coliforms and *E.coli*) of brackish water samples were determined by multiple tube method. In this research, total coliforms were found to be in the seasonal range of between 16 MPN/100 mL and 18 MPN/100 mL. The minimum total coliform value 16 MPN/100 mL was found at sampling sites A, B and C in cold season. The

maximum total coliform value 18 MPN/100 mL was found at sampling site A, B and C in hot season (Table 9 and Figure 17). These resultant values were within the allowable limits of the ASEAN standard (2010) for human health protection 100 MPN/100 mL. The number of Escherichia coli (*E.coli*) was not isolated in all brackish water samples during the studied period of 2017. ASEAN standard (2010) for *E.coli* value is Not of Concern (Table 9). According to the results, the studied regions were not polluted and adversely effect on aquatic life from the microorganism point of views.

Table 3: Seasonally Variation of Some Physicochemical Properties of Brackish Water Samples from Three Sampling Sites

Sampling sites	Season	Water Parameters			
		Temperature (^{o}C)	pH	Total alkalinity(ppm)	Total hardness(ppm)
A	Hot	29.64	7.90	110	9860
B		30.23	7.80	120	9840
C		30.54	8.00	140	9700
A	Rainy	28.34	7.80	120	9800
B		28.44	7.70	110	8890
C		28.42	7.70	100	9840
A	Cold	29.24	7.90	110	9800
B		29.46	7.80	100	9700
C		29.55	7.80	120	9600
ASEAN Standards (2010)		-	6.0-8.0	<120	NC
EPA Standards (2010)		-	6.5-8.5	30-150	NC

*NC – Not of Concern

Table 4: Seasonally Variation of Some Physicochemical Properties of brackish Water Samples from Three Sampling Sites

Sampling sites	Season	Water Parameters			
		Chlorinity (ppt)	Salinity (ppt)	Turbidity (FTU)	Total Suspended Solid (ppm)
A	Hot	20.00	26.00	8.30	290
B		18.65	24.00	7.50	250
C		18.40	25.00	7.60	260
A	Rainy	18.20	20.00	8.30	290
B		18.10	19.00	8.20	260
C		18.00	19.00	8.00	270
A	Cold	19.00	23.00	7.60	260
B		18.20	20.00	5.90	240
C		18.30	24.00	6.60	250
ASEAN Standards (2010)		>19	0.5-30	<700	<75
EPA Standards (2010)		-	-	15	NC

Table 5: Seasonally Variations of Some Physicochemical Properties of Brackish Water Samples from Three Sampling Sites

Sampling sites	Season	Water Parameters	
		BOD (ppm)	COD (ppm)
A	Hot	2.00	3.52
B		1.50	2.62
C		1.00	2.28
A	Rainy	1.50	2.20
B		1.10	2.10
C		1.00	2.00
A	Cold	2.00	3.00
B		1.50	2.40
C		1.40	2.20
ASEAN Standards (2010)		<15	<40
EPA Standards (2010)		5	-

Table 6: Seasonal Variation of Nutrient Level in Brackish Water Samples from Three Sampling Sites

Sampling sites	Season	Nutrient contents (ppm)			
		DO (ppm)	Orthophosphate (ppm)	Total Nitrogen (ppm)	Nutrient Enrichment
A	Hot	2.00	0.30	1.00	High
B		2.00	0.10	0.20	
C		2.50	0.10	0.30	
A	Rainy	3.50	0.30	1.00	Medium
B		2.50	0.20	0.80	
C		3.00	0.30	0.90	
A	Cold	2.50	0.20	0.30	Medium
B		2.00	0.15	0.30	
C		3.00	0.15	0.40	
ASEAN Standards (2010)		>5	0.015	-	
EPA Standards (2010)		-	-	-	

Table 7: Criteria for Evaluating Degree of Nutrient Over-Enrichment

Parameter	Low	Medium	High
N (ppm)	≤ 0.1	> 0.1 - < 1.0	≥ 1.0
PO_4^{3-} (ppm)	< 0.03	> 0.03 - < 0.3	≥ 0.3
DO (ppm)	≥ 5	> 2 – ≤ 5	0 - ≤ 2

(Tong and Deocadiz, 1999)

Table 8: Seasonal Variation of Some Metals Contents in Brackish Water Samples from Three Sampling Sites

Sampling sites	Season	Metal contents (ppm)			
		Pb	Cd	Hg	As
A	Hot	0.004	0.009	ND	ND
B		0.002	0.006	ND	ND
C		0.003	0.007	ND	ND
A	Rainy	0.002	0.007	ND	ND
B		ND	0.005	ND	ND
C		0.001	0.006	ND	ND
A	Cold	0.001	0.008	ND	ND
B		ND	0.006	ND	ND
C		0.001	0.007	ND	ND
ASEAN Standards (2010)		0.009	0.010	0.16	0.036
EPA Standards (2010)		-	-	-	-

*ND – Not Detected

Table 9: Seasonal Variation of Some Microorganism Indicators of Brackish Water Samples from Three Sampling Sites

Sampling sites	Season	Microorganisms	
		Total Coli form (MPN/100ml)	*Escherichia Coli* (MPN/100ml)
A	Hot	18	NI
B		18	NI
C		18	NI
A	Rainy	17	NI
B		17	NI
C		17	NI
A	Cold	16	NI
B		16	NI
C		16	NI
ASEAN Standards (2010)		100	NC
EPA Standards (2010)		-	NC

*NC – Not of Concern *NI- Not Isolated

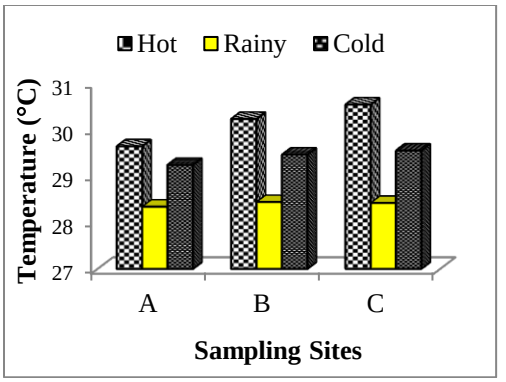

Figure 2: Bar graph of temperature in water samples from three sampling sites in three seasons

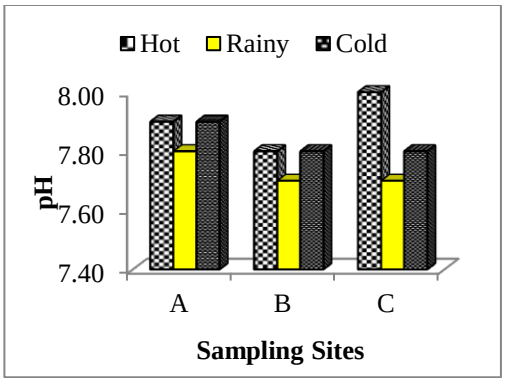

Figure 3: Bar graph of pH in water samples from three sampling sites in three seasons

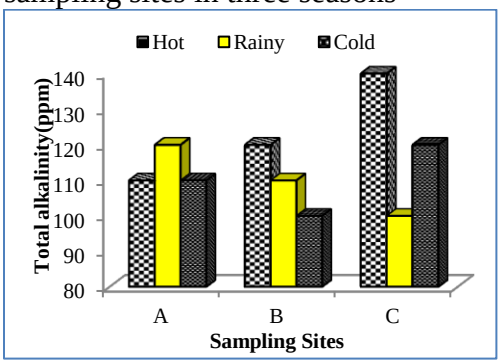

Figure 4: Bar graph of total alkalinity in water samples from three sampling sites in three seasons

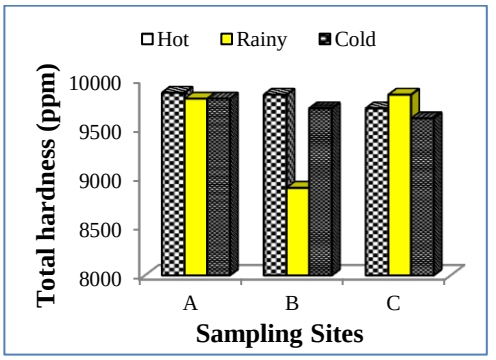

Figure 5: Bar graph of total hardness in water samples from three sampling sites in three seasons

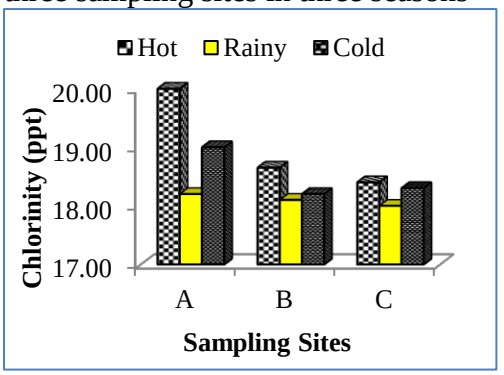

Figure 6: Bar graph of chlorinity in water samples from three sampling sites in three seasons

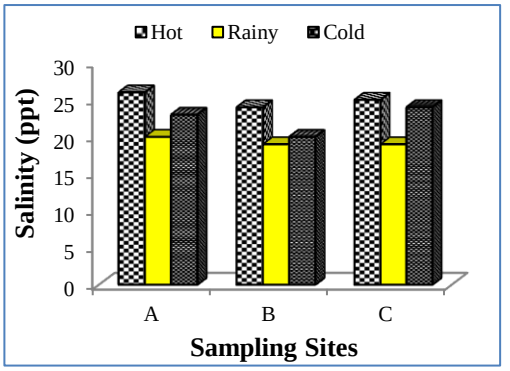

Figure 7: Bar graph of salinity in water samples from three sampling sites in three seasons

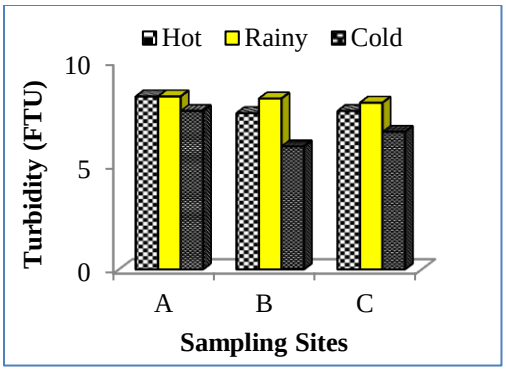

Figure 8: Bar graph of turbidity in water samples from three sampling sites in three seasons

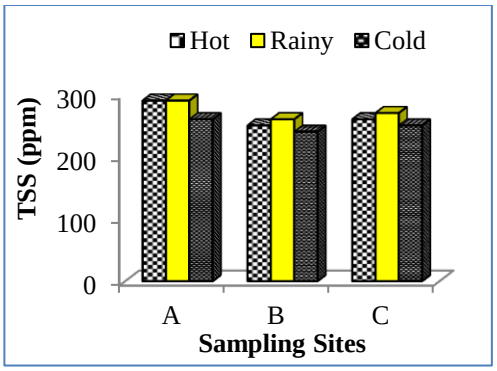

Figure 9:Bar graph of TSS in water samples from three sampling sites in three seasons

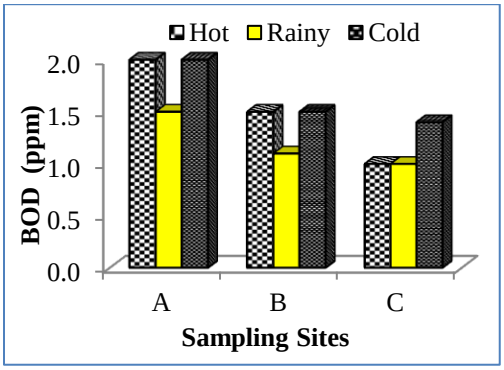

Figure 10: Bar graph of BOD in water samples from three sampling sites in three seasons

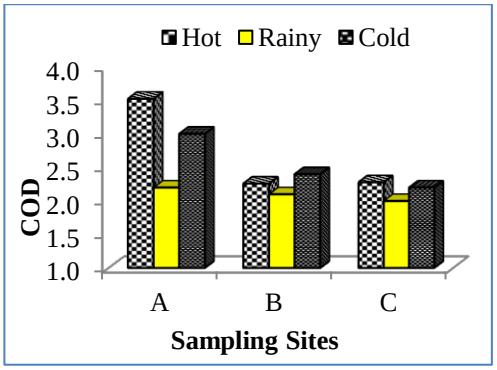

Figure 11: Bar graph of COD in water samples from three sampling sites in three seasons

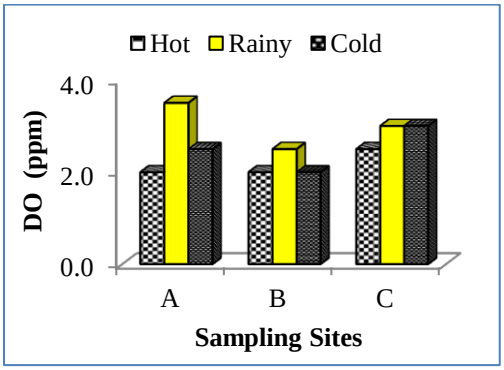

Figure 12: Bar graph of dissolved oxygen in water samples from three sampling sites in three season

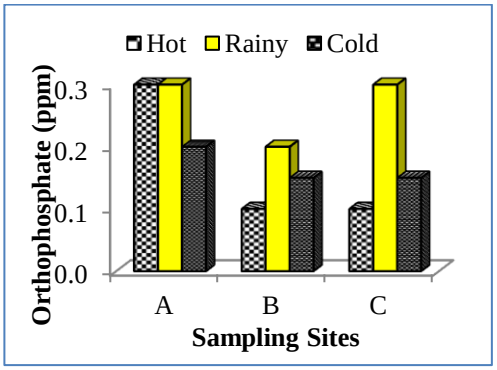

Figure 13: Bar graph of orthophosphate in water samples from three sampling sites in three season

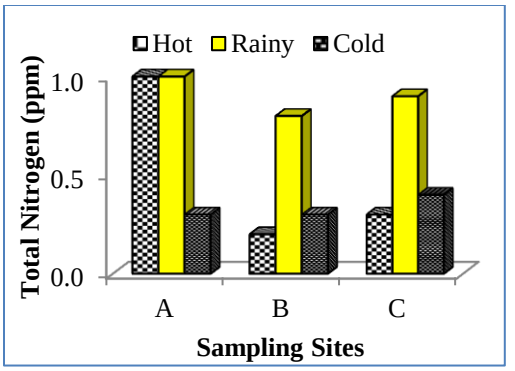

Figure 14: Bar graph of TN in water samples from three sampling sites in three seasons

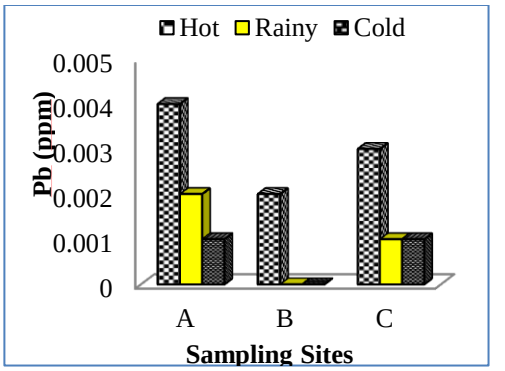

Figure 15: Bar graph of Pb in water samples from three sampling sites in three seasons

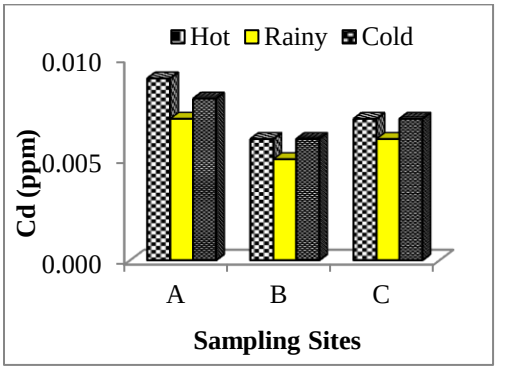

Figure 16: Bar graph of Cd in water samples from three sampling sites in three seasons

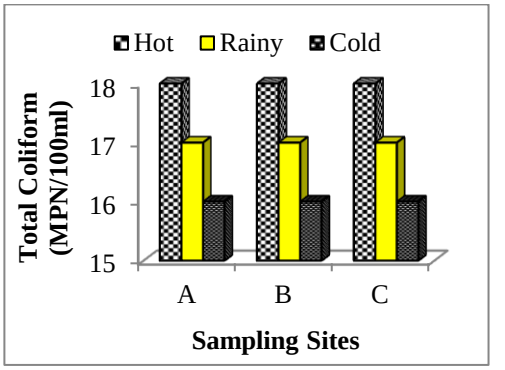

Figure 17: Bar graph of total coliform in water samples from three sampling sites in three seasons

Conclusion

Conclusively, the brackish water quality in terms of its physicochemical parameters, some metal concentrations and microorganism indicators in water from Letkhokkon area were assessed seasonally in 2017. The physicochemical properties of brackish water parameters-Temperature, pH, turbidity, DO, BOD, COD, chlorinity and total nitrogen concentrations were found within the range of ASEAN and EPA Standards for human health and aquatic life protection, however, total alkalinity, total suspended solid and orthophosphate contents were higher than the ASEAN and EPA standards (2010) for human health and aquatic life protection.

From the evaluation degree of nutrient level, the studied areas around Letkhokkon Beach were identified as Mesotrophic level (medium nutrient enrichment) in the rainy and cold seasons. Eutrophic level (high nutrient enrichment) was found in the hot season, it may be due to the lesser amount of fresh water inflow and high salinity. According to the results, it can be deduced that the studied areas were eutrophicated with nitrogen and phosphorus species during the studied period of 2017.

From the metal pollution point of views, some metal (Pb, Cd, Hg and As) concentrations of brackish water samples were within the allowable limits of ASEAN and EPA standards (2010) for human health and aquatic life protection. Therefore, metal pollution in Letkhokkon area were not at a level to affect the aquatic life and human health.

From the microorganism analysis of brackish water samples, the resultant data were within the allowable limits of ASEAN and EPA standards (2010) for human health and aquatic life protection.

According to the overall assessment of brackish water parameters, it can be concluded that the water quality of studied region might be used for aquaculture and agriculture purpose.

Acknowledgements

The authors would like to express their profound gratitude to the Department of Higher Education (Yangon Office), Ministry of Education, Yangon, Myanmar, for provision of opportunity to do this research and Myanmar Academy of Arts and Science for allowing to present this paper.

References

APHA. (1992). Standard Methods for the Examination of Water and Waste Waters. *Washington DC: 18th Edition. American Public Health Association, pp.121-129*

ASEAN Marine Environmental Management. (2010). *Water Quality Criteria and Standards for Freshwater and Marine Aquaculture*. North Vancouver : EVS Environmental Consultants Ltd., pp.171-189

Chapman, D. (1996). *A Guide to the Use of Biota Sediments and Water in Environmental Monitoring in Water Quality Assessment*. London : 2nd Edition, E & FNSPON, pp.8-91

EPA. (2010). *Nutrient Water Quality Standards.* Washington DC: Office of Water Research

Kyaw Naing. (2011). *National Report of Myanmar on the Costal Pollution Loading and Water Quality Criteria (Land-based Sources of Marine Pollution).* Rome: Bay of Bengal Large Marine Ecosystem Project to the Food and Agriculture Organization of the United Nations, FAO, pp. 1-53

Strickland, J. D. H. and Parsons, T. R. (1972). *A Practical Handbook of Sea Water Analysis*. Fisheries Research Board of Canada, pp.21-29

Tong, S. L. and Deocadiz, E.S. (1999). *Principles for developing ASEAN Marine Water Quality Criteria*. Malaysia: ASEAN Marine Water Quality Criteria, Department of Fisheries, pp. 1-12

Waterman, (2005). *Chemical and Physical Properties of Water*. http:// www.62.co.za/ index.html (Accessed 9 September 2013)

Wikipedia, the Free Encyclopedia. (2014). *Letkhokkon Beach*. http://en.wikipedia. org/wiki/ Letkhokkon. html (Accessed 30 May 2013)

SCREENING OF PHYTOCHEMICALS AND ANTIOXIDANT ACTIVITY OF THE RHIZOMES AND LEAVES OF *Hedychium coronarium* J.Koenig (Ngwe-Pan)

Pyae Phyoe Nwe[1], Myo Min[2], Hnin Hnin Aye[3]

Abstract

In the present study, the rhizomes and leaves of *Hedychium coronarium* J.Koenig (Ngwe-pan) were collected from Hmawbi Township, Yangon Region. The relative abundance of elemental composition was determined by ED-XRF method resulting the major mineral elements such as potassium, sulphur, calcium and phosphorus in the Ngwe-pan rhizomes and potassium, chlorine, calcium, sulphur in the Ngwe-pan leaves. In addition, the nutrient values of Ngwe-pan rhizomes and leaves were determined by AOAC method showing the moisture (13.08 %), ash (7.34 %), protein (3.36 %), crude fiber (14.81 %), crude fat (4.27 %), carbohydrates (25.17 %) and energy value (152.55 kcal/100 g) in Ngwe-pan rhizomes and moisture (13.89 %), ash (8.21 %), protein (7.46 %), crude fiber (35.42 %), crude fat (4.10 %), carbohydrates(12.93 %) and energy value (118.46 kcal/ 100g) in Ngwe-pan leaves. The preliminary phytohchemical constituents of both samples were examined by using the Test Tube method. According to the phytochemical tests, Ngwe-pan rhizomes and leaves extracts showed the presence of alkaloids, carbohydrates, flavonoids, glycosides, organic acids, phenolic compounds, reducing sugars, starch, saponins, steroids, terpenoids and tannins. However, cyanogenic glycosides were not found in these samples. The screening of antioxidant activities of Ngwe-pan rhizomes and leaves was carried out by DPPH method. Ascorbic acid was used as the standard. From the screening, among the extracts of rhizomes and leaves samples, the EtOH and H_2O extract of Ngwe-pan leaves showed the more potent antioxidant activity than that of the rhizome extracts.

Keywords: *Hedychium coronarium*, nutrient values, elemental composition, phytochemical constituents, antioxidant activity

Introduction

Hedychium coronarium is a monocotyledon perennial herb which belongs to family Zingiberaceae. It is commonly known as white ginger or butterfly ginger because its flower looks like a flying butterfly. *H. coronarium*

[1]. Candidate, 2 PhD, Department of Chemistry, University of Yangon
[2]. Dr, Associate Professor, Department of Chemistry, West Yangon University
[3]. Dr, Professor and Head, Department of Chemistry, University of Yangon

is an aromatic rhizomatous plant which possesses important medicinal properties and its various parts are used in traditional as well as modern medicine (Vaidyaratnam, 2006).

The medicinal value of this plant in the therapeutic field is mentioned in Ayurveda, Charaka Samhita and Sushruta Samhita. The all parts of this plant are utilized as medicine as well as other daily uses, although its applications varies by region. In the Ayurvedic system of Indian traditional medicine it has used as a febrifuge, tonic and excitant and also used as medicine in the treatment of tonsillitis, infected nostrils and tumor. In Chinese medicine it has been prescribed in treatment of headache, lancinating pain, contusion, inflammatory and intense pain due to rheumatism etc (Mishra, 2013). *H. coronarium* is also reported for its anti-cancerous, antioxidant, anti-hypertensive, diuretic, and leishmanicidal, anti-malarial activities it is also used in irregular menstruation, piles bleeding and stone in urinary tract. The essential oil extracted from leaves, flowers and rhizome of this plant possesses cercaricidal properties, molluscicidal activity, potent inhibitory action, antimicrobial activities, anti-inflammatory and analgesic effects. The paste prepared from rhizome is applied externally in cases of snakebite (Ray *et al*., 2011). The flowers and stems are also stand for Commercial importance as used in the manufacturing of perfume and paper respectively. Both of the flowers and rhizomes are also consumed as vegetables (Sarangthem *et al.*, 2012).

Aim

To perform the phytochemical constituents, elemental composition, evaluation of nutrient values and the determination of antioxidant activities of *H.coronarium* (Ngwe-pan) rhizomes and leaves.

Materials and Methods

Collection and Preparation of Plant Samples

The Ngwe-pan rhizomes and the leaves were collected from Hmawbi Township, Yangon Region, Myanmar, in the month of September-October, 2017. The plants were identified and authenticated at the Department of Botany, West Yangon University.

After collection, the rhizomes and the leaves were cleaned thoroughly with distilled water to remove any type of contamination. The washed rhizomes and leaves were air dried in shade for about two weeks and ground into the coarse powder with the help of a mechanical grinder. The powders of the samples were separately stored in air tight bottles.

Qualitative Elemental Analysis by Energy Dispersive X- Ray Fluorescence Method

Shimadzu EDX-8000 spectrometer can analyze the elements from Na to U under vacuum condition. In this research work relative abundance of elements present in Ngwe-pan rhizomes and leaves was determined by EDXRF spectrometer.

Determination of Nutritional Values

The nutritional values such as moisture, ash, crude protein, crude fiber, crude fat, carbohydrate contents and energy value of Ngwe-pan rhizomes and leaves were determined according to AOAC method (AOAC, 2000) at the Department of Research and Innovation Analysis Department (DRI), The Government of the Republic of the Union of Myanmar Ministry of Education (GRUMME), Yangon, Myanmar.

Preliminary Phytochemical Screening

The Ngwe-pan rhizomes and leaves were subjected to qualitative phytochemical tests for the identification of various bioactive constituents. Phytochemical screenings were carried out by using standard procedures to detect the presence of alkaloids, carbohydrates, glycosides, flavonoids, organic acids, phenolic compounds, reducing sugars, steroids, saponins, starch, terpenoids and tannins. After the addition of specific reagents to the test solution presence of phytoconstituents was examined by virtual observation of colour change or by precipitate formation.

Screening of Antioxidant Activity by DPPH Radical Scavenging Assay

The crude extracts of Ngwe-pan rhizomes and leaves were prepared by extracting the sample with different solvents like ethanol and water by cold percolation method. All of these extracts were kept for the determination of antioxidant activity. The antioxidant activity of 95 % EtOH and H_2O extracts was studied by DPPH Assay Method. DPPH radical scavenging activity was determined by spectrophotometric method. The control solution was prepared by mixing 1.5 mL of 60 µM DPPH solution and 1.5 mL of 95 % ethanol with vortex mixer. The sample solution was also prepared by mixing thoroughly 1.5 mL of 60 µM DPPH solutions and 1.5 mL of test sample solution with concentrations of (3.125, 6.25, 12.5, 25 and 50 µg/mL). The solutions were allowed to stand at room temperature for 30 min. After 30 min, measurement of absorbance at 517 nm was made by using spectrophotometer UV1800, Shimadzu, Japan. Absorbance measurements were done in triplicate for each solution and the mean value was obtained, and then used to calculate % inhibition of oxidation by the following equation,

$$\% \text{ oxidative inhibition } = \frac{A_c - (A - A_b)}{A_c} \times 100\ \%$$

% oxidative inhibition = % oxidative inhibition of test sample

A_c = absorbance of the control (DPPH alone)

A_b = absorbance of the sample + ethanol

A = absorbance of the DPPH radical + sample extract

Then IC_{50} (50 % inhibitory concentration) values were also calculated by linear regressive excel program (Brand-Williams *et al.,* 1995).

Results and Discussion

Relative Abundances of some Elements in Ngwe-pan Rhizomes and Leaves

As shown in Tables 1 and 2, by EDXRF data, the mineral elements such as K, S, Ca and P are major constituents in the rhizomes and the K, Cl, Ca and S are contained as main constituents in the leaves. Moreover, the

organic compounds are contained as predominant composition between (94-97%).

Table 1: Relative Abundance of Some Elements in Ngwe-pan Rhizomes

Element	Relative Abundance Percent (%)
K	1.222
S	0.283
Ca	0.251
P	0.184
Mn	0.101
Fe	0.005
Zn	0.002
Cu	0.001
Sr	0.001
Br	0.001
COH	97.948

Table 2: Relative Abundance of Some Elements in Ngwe-pan Leaves

Element	Relative Abundance Percent (%)
K	1.222
Cl	0.283
Ca	0.251
S	0.184
Mn	0.101
P	0.005
Fe	0.002
Zn	0.001
Cu	0.001
COH	94.788

Nutritional Values of Ngwe-pan Rhizomes and Leaves

The nutrient values of Ngwe-pan rhizomes and leaves such as moisture, ash, crude protein, crude fiber, crude fat, carbohydrates and energy value were determined by using standard methods for food analysis (AOAC, 2000) and the nutritional composition of the samples are described in Table 3.The rhizomes powdered samples were found to have higher energy values than in the leaves powdered samples.

Table 3: Nutritional Compositions of Rhizomes and Leaves of Ngwe-pan

Parameter	Nutritional Composition (%)	
	Rhizomes	Leaves
Moisture	13.08	13.89
Ash	7.34	8.21
Crude protein	3.36	7.46
Crude fiber	14.81	35.42
Crude fat	4.27	4.10
Carbohydrate	25.17	12.93
Energy value (kcal/100g)	152.55	118.46

Preliminary Phytochemical Screening of Ngwe-pan Rhizomes and Leaves

Phytochemical screening of the extracts of Ngwe-pan rhizomes and leaves were carried out to identify the secondary metabolites such as alkaloids, carbohydrates, flavonoids, glycosides, organic acid, phenolic compounds, reducing sugars, saponins, steroids, starch, tannins and terpenoids according to standard phytochemical methods. The phytochemical analysis revealed that alkaloids, carbohydrates, flavonoids, glycosides, organic acid, phenolic compounds, reducing sugars, saponins, steroids, starch, tannins and terpenoids were present in Ngwe-pan rhizomes and leaves. Cyanogenic glycoside was not detected in both samples (Table 4).

Table 4: Results of Phytochemical Investigation of Ngwe-pan Rhizomes and Leaves by Test Tube Method

Chemical Constituents	Test Reagent	Observation	Inference	
			R	L
Alkaloids	(i) Dragendorff's	Orange red precipitate	+	+
	(ii) Wagner's	Yellow ppt	+	+
	(iii) Mayer's	Creamy white precipitate	+	+
	(iv) Hager's	Yellow ppt	+	+
Carbohydrates	10% α-naphthol and Conc: H_2SO_4	Dull violet precipitate	+	+
Cyanogenic glycosides	Sodium picrate and Conc: H_2SO_4	No change	-	-
Flavonoids	Mg turning and Conc: HCl	Orange to red colour sol[n]	+	+
Glycosides	10% Lead acetate solution	yellow precipitate	+	+
Organic Acids	Bromocresol green indicator	Deep blue colour solution	+	+
Phenolic Compounds	5% Ferric chloride solution	Brown colour ppt	+	+
Reducing Sugars	Benedict's solution	Light green colour solution	+	+
Steroids	Liberman Burchard	red colour solution	+	+
Saponins	Foam test	Marked frothing	+	+
Starch	Iodine solution	Deep violet solution	+	+
Tannins	Ferrous sulphate	Greenish black precipitate	+	+
Terpenoids	Liberman Burchard	Brown ppt	+	+

(+) = present, (-) = absent, R = Rhizomes, L = Leaves, ppt = precipitate

Antioxidant Activity of Ngwe-pan Rhizomes and Leaves

Antioxidant activity was studied by DPPH free radical scavenging property by using UV spectroscopic method. Absorbance measurements were done in triplicate for each sample solution. Absorbance values obtained were used to calculate % inhibition, 50 % inhibitory concentration and standard deviation. The DPPH assay has been largely used as a quick, reliable and reproducible parameter to search for the in *vitro* general antioxidant activity of pure compounds as well as plant extracts. The decrease in absorbance by the DPPH radical indicates increase in concentration of the extract which manifested in the rapid discoloration of the purple DPPH.

In the present work, the free radical scavenger activity of ethanol and water extracts of Ngwe-pan rhizomes and leaves and the standard ascorbic acid were assessed on the basis of the radical scavenging effect on the 1, 1-diphenyl-2-picrylhydrazyl (DPPH). The various concentrations of each extract (50, 25, 12.5, 6.25 and 3.125 µg/mL) were prepared by dilution with

ethanol as the solvent. Ascorbic acid was used as standard in 3.125-50 μ g/mL solution. The absorbance of these solutions was measured at 517 nm by using UV spectrophotometer.

In the rhizomes extracts, the % free radical scavenging activities of ethanol and water extracts and ascorbic acid are presented in Table 5 and Figure 1. The % inhibition of ethanol extracts was 48.46 % and 56.29 % respectively at the concentration of 12.5 and 25 μ g/mL. And also, the % inhibition of water extract was 49.73 % and 52.46 % at 12.5 and 25 μ g/mL. The IC_{50} values of two extracts and standard ascorbic acid were calculated using linear regression method. Among two extracts tested for the in *vitro* antioxidant activity using the DPPH method, the water and ethanol extracts of rhizomes showed the highest antioxidant activities, with IC_{50} values of 14.06 and 20.11 μ g/mL. The IC_{50} value of standard ascorbic acid was 12.42 μg/mL. The IC_{50} value of Ngwe-pan rhizomes water and ethanol extracts were found to be higher than that of standard ascorbic acid.

In the leaves extracts, the % free radical scavenging activities of ethanol and water extracts are presented in Table 5 and Figure 2. The % inhibition of ethanol extracts was 44.64 % and 56.83 % at the concentration of 6.25 and 12.5 μ g/mL, respectively. And also, the % inhibition of water extract was 48.63 % and 50.82 % at 6.25and 12.5 μ g/mL, respectively. Among two extracts tested, the ethanol and water extracts of leaves showed the highest antioxidant activity, with IC_{50} values of 10.33 and 12.48 μ g/mL, respectively.

It indicates that the water and ethanol extracts of Ngwe-pan rhizomes and leaves have the potency of scavenging free radicals in *in vitro* and may provide leads in the ongoing search for natural antioxidants from medicinal plants to be used in treating diseases related to free radical reactions.

Table 5: Percent Oxidative Inhibition and IC_{50} Values of Crude Extracts of Ngwe-pan Rhizomes and Leaves

Test samples	%RSA±SD at Different concentration (µg/mL)					IC_{50} (µg/mL)
	3.125	6.25	12.5	25	50	
Rhizomes of Ngwe-pan (Ethanol)	23.66±0.001	39.93±0.002	48.46±0.003	56.29±0.001	78.08±0.004	20.11
Rhizomes of Ngwe-pan (H_2O)	46.56±0.002	48.08±0.005	49.73± 0.001	52.46±0.003	61.20±0.001	14.06
Leaves of Ngwe-pan (Ethanol)	42.98±0.002	44.64±0.003	56.83±0.011	90.93±0.001	67.49±0.006	10.33
Leaves of Ngwe-pan (H_2O)	46.88±0.001	48.63±0.002	50.82±0.004	53.55±0.002	57.63±0.001	12.48
Standard Ascorbic acid	35.26±0.217	40.35±0.218	50.12±0.150	66.61±0.122	80.71±0.070	12.42

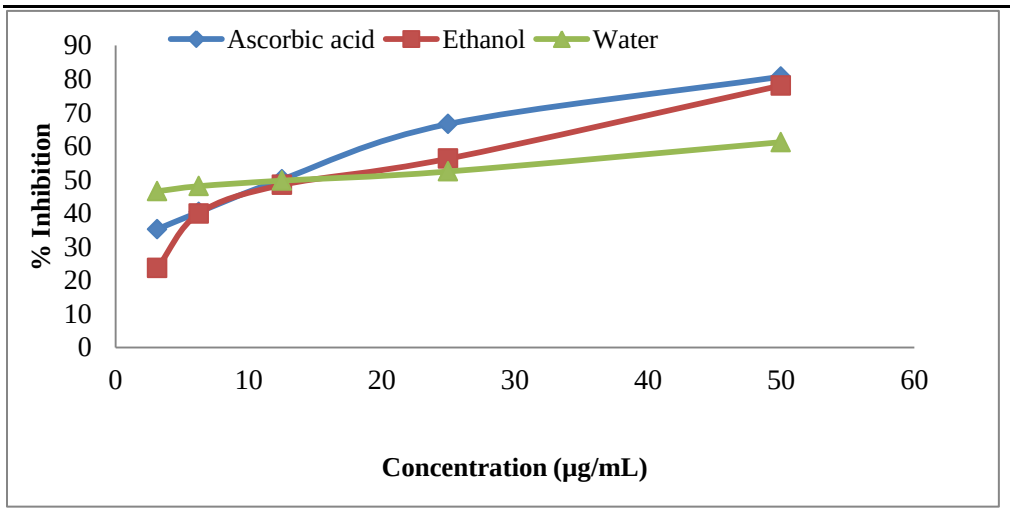

Figure 1: Antioxidant activity of ascorbic acid and different concentrations of Ngwe-pan rhizomes extract

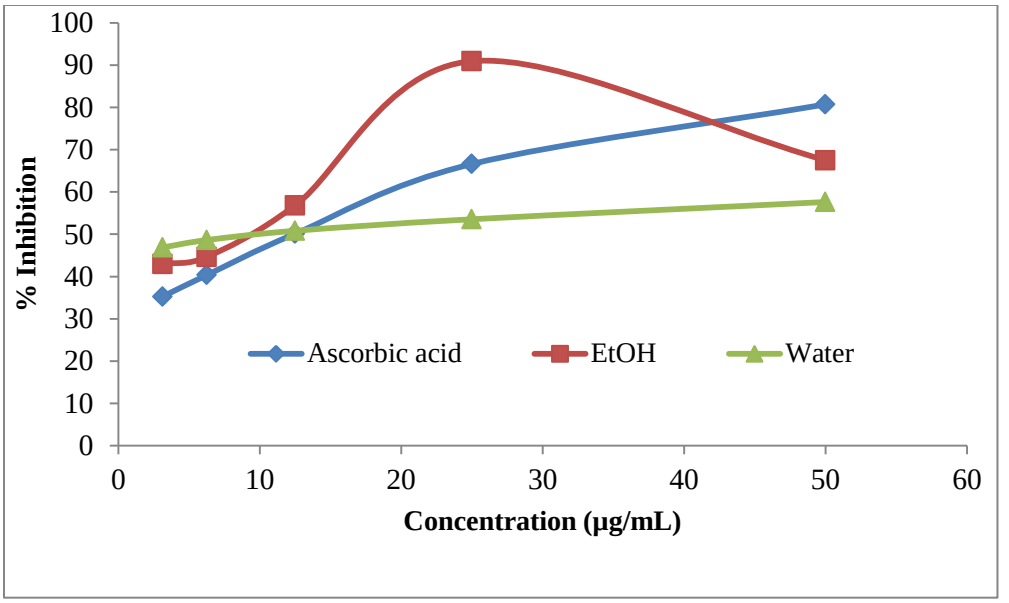

Figure 2: Antioxidant activity of ascorbic acid and different concentrations of Ngwe-pan leaves extract

Conclusion

In the present work, phytochemical analysis, nutritional values, EDXRF analysis and antioxidant activity of the Ngwe-pan rhizomes and leaves were studied. The phytochemical analysis of Ngwe-pan rhizomes and leaves powdered sample showed the presence of alkaloids, carbohydrates, glycosides, flavonoids, organic acids, phenolic compounds, reducing sugars, steroids, saponins, starch, terpenoids and tannin. Cyanogenic glycosides were absent both in the two samples. The presence of secondary metabolites in the rhizomes and leaves suggests that their consumption could have a preventive effect on human body and help to treat related diseases by providing indicated properties to the plant. By ED-XRF data, the mineral elements such as K, S, Ca and P are major constituents in the rhizomes and the K, Cl, Ca and S are also contained in the leaves. Therefore, Ngwe-pan rhizomes and leaves contained nutritionally important minerals. These mineral contents were well within permissible range for human consumption, therefore, recommended for safety and nutritious food. In addition, some nutrient values of rhizomes sample was found to contain of 13.08 % moisture, 7.34 % of ash, 3.36 % of

protein, 14.81 % of crude fiber, 4.27 % of crude fat, 25.17 % of carbohydrates and 152.55 kcal/100g of energy value, whereas the leaves sample was also contained of 13.89 % moisture, 8.21 % of ash, 7.46 % of protein, 35.42 % of crude fiber, 4.10 % of crude fat, 12.93 % of carbohydrates and 118.46 kcal/ 100g of energy value. These nutrient values of the sample support the diet supplement for the human health. *In vitro* antioxidant potential by DPPH free radical scavenging assay using ascorbic acid as the standard. The 95% EtOH and H_2O extracts of plant rhizomes and leaves were analyzed. Antioxidant activities in terms of IC_{50} values of H_2O and EtOH extracts of rhizomes were 14.06 µg/mL and 20.11 µg/mL respectively. Moreover, the IC_{50} values of leaves extract of H_2O and EtOH were 12.48 and 10.33 µg/mL, respectively. The smaller the IC_{50} values will greater the antioxidant activities. Therefore, the EtOH extract (10.33 µg/mL) and H_2O extract (12.48 µg/mL) of Ngwe-pan leaves and H_2O rhizome extract (14.06 µg/mL) have the highest antioxidant activity than the rhizome EtOH extract (20.11 µg/mL). The study revealed that *H.coronarium* rhizomes and leaves contained appreciable amounts of mineral elements, nutrients such as energy, protein and phytochemicals. According the findings, the water and ethanol extracts of *H.coronarium* leaves have more potent antioxidant activities than the *H.coronarium* rhizomes. Therefore, *H.coronarium* rhizomes and leaves possess the reasonable antioxidant activities and bioactive organic constituents will be beneficial for further studies on pharmacology activities.

Acknowledgements

The authors would like to thank the Department of Higher Education, Ministry of Education, Myanmar, for the permission of doing this research and Myanmar Academy of Arts and Sciences allowing the writing of this paper.

References

A.O.A.C. (2000). *Official Methods of Analysis of the Association of Official Analytical Chemists*. Washington DC: 17th Ed.

Brand-Williams,W., Cuvelier, M. E. and Berse, C. (1995). "Use of a Free Radical Method to Evaluate Antioxidant Activity". *Lebensm.-Wiss. u.-Technol*., vol. 28, No. 1, pp. 25-30.

Mishra, M. (2013). "Current Status of Endangered Medicinal Plant *Hedychium coronarium* and Causes of Population Decline in the Natural Forests of Anuppur and Dindori Districts of Madhya Pradesh, India". *International Research Journal of Biological Sciences*, vol. 2(3), pp.1-6.

Ray, S., Sheikh, M. and Mishra, M. (2011). "Ethnomedicinal Plants used by Tribal of East Nimar Region, Madhya Pradesh". *Indian J. Tradi Knowl*., vol, 10(2**)**, pp. 367-371

Sarangthem, N., Talukdar, N.C. and Thongam, B. (2013). "Collection and Evaluation of *Hedychium* Species of Manipur, Northeast India". vol, 60(1), pp.13-21

Vaidyaratnam, P.S. (2006). Indian Medicinal Plants-A Compendium of 500 Species. Kottakkal, India: Orient Longman Publishing House; p.146

ISOLATION OF A BIOACTIVE SESQUITERPENOID COMPOUND AND EVALUATION OF SOME BIOLOGICAL ACTIVITIES OF STEMS AND ROOTS OF *ALLAMANDA CATHARTICA* L. (SHWEWA-PAN)

Yin Yin Tun[1],[2], Khine Zar Wynn Lae[3], Nwet Nwet Win[4], Daw Hla Ngwe[5]

Abstract

This research focused on the screening of phytochemical constituents, nutritional values and biological activities such as antioxidant, antimicrobial and anti-tumor activities of the stems and roots of *Allamanda cathartica* L. (Shwewa-pan). These samples were collected from Bago University Campus and identified at Botany Department, Bago University. According to the phytochemical tests, alkaloids, flavonoids, terpenoids, steroids, glycosides, organic acids, phenolic compounds, saponins, tannins and carbohydrates were found to be present in both samples. The nutritional values were determined by AOAC method resulting 6.91 and 18.64 % of proteins, 2.04 and 3.04 % of moisture, 2.71 and 3.06 % of ash, 62.42 and 38.65 % of fiber, 10.33 and 16.15 % of fat in stems and roots of *A. cathartica*, respectively. By thin layer and silica gel column chromatographic methods, one compound, plumericin (1.51 %, m.pt 210°C) was isolated from ethyl acetate extract of the roots. The antioxidant activity of ethanol and watery extracts of the stems and roots determined by DPPH radical scavenging activity assay was found to be in the order of stem ethanol extract (IC_{50}= 65.89 µg/mL) > root ethanol extract (IC_{50}= 110.46µg/mL) > root watery extract (IC_{50}>200 µg/mL) ≈ stem watery extract (IC_{50}> 200 µg/mL) . The antimicrobial activity of PE, EtOAc, EtOH and H_2O extracts of stems and roots were screened on six microorganisms such as *Bacillus subtilis*, *Staphylococcus aureus*, *Pseudomonas aeruginosa*, *Bacillus pumilus*, *Candida albicans* and *Escherichia coli* by agar well diffusion method. All of the extracts from the roots have more pronounced antimicrobial activity with inhibition zone diameters ranged between 14 mm ~ 35 mm than stems extracts (12 mm ~ 18 mm). Among them EtOAc extract of the roots has the highest activity against *B. pumilus.* Antitumor activity of various crude extracts such as PE, EtOAc and EtOH extracts of stems and roots in different concentrations (0.5, 1.0, 1.5g/mL) and plumericin (10, 20, 30 mg/mL) were also determined on tumor producing bacteria by using PCG (Potato Crown Gall) test. It was found that EtOAc extract of roots, PE and EtOH extracts of both samples and plumericin exhibited the inhibition of tumor formation.

[1] Assistant Lecturer, Department of Chemistry, Bago University
[2] Fourth Year PhD Student, Department of Chemistry, University of Yangon
[3] Dr, Lecturer, Department of Chemistry, University of Yangon
[4] Dr, Associate Professor, Department of Chemistry, University of Yangon
[5] Dr, Professor and Head (Retd.,), Department of Chemistry, University of Yangon

Keywords **:** *Allamanda cathartica* L. Antioxidant activity, Antimicrobial activity, Antitumor activity, plumericin

Introduction

Plants based drugs have been used worldwide in traditional medicines for the treatment of various diseases. Shwewa-pan scientifically known as *A.cathartica* is of the plant family Apocynaceae. Genus is *Allamanda* and species is *cathartica.* Myanmar name is Shwewa-pan and also called Shwe-pan-nwe. Other common names are Golden trumpet, Yellow bell, Buttercup flower and Angle's trumpet (Chandrasekhar *et al*., 2012). Allamanda species are apparently native to northern Brazill Guyana, Surinam and probably French Guiana. It is a genus of climbing shrubs. The distribution of this species is global but is mainly presented in subtropical to tropical (Uduak and Esther, 2015). In Myanmar it is cultivated as ornamental garden plants. *A.cathartica* has long been used in traditional medicine for treating malaria and jaundice. The leaf extract was found to promote wound healing. The flower is also used as a laxative. The chemical constituents are allamandin, allamandicin, allamdin, plumericin, isoplumericin, plumieride, ursolic acid, beta-amyrin, beta-sitosterol, fluvoplumeirin, lupeol, quercetin, kaempferol, glabridin and naringenin (Fah, 2013).

A. cathartica (Shwewa-pan) has been chosen for this research because it has various biological activities and bioactive chemical constituents, and also due to the lack of scientific report on the locally grown *A. cathartica*. In this research work, screening of phytochemical constituents and investigation of antioxidant, antimicrobial and antitumor activities of stems and roots of *A.cathartica* (Shwewa-pan) are carried out on the respective various crude extracts. Furthermore one of the organic compound, plumericin is isolated as a major constituent from the roots and studied on its antitumor property.

Materials and Methods

Plant materials

The stems and roots of *A. cathartica* were collected from Bago University Campus, Bago Township, Bago Region, during October, 2015. Some pharmacological activities such as antimicrobial activity, antioxidant

activity and antitumor activity of various crude extracts of the stems and roots were determined in *in vitro*.

Phytochemical Screening

Preliminary phytochemical tests such as alkaloids, flavonoids, terpenoids, steroids, glycosides, organic acids, starch, phenolic compounds, saponins, tannins, carbohydrates, cyanogenic glycosides, reducing sugars and α - amino acids tests on the two samples were carried out according to the appropriate reported methods (Sofowora, 2000).

Determination of Nutritional Values

The nutritional values such as moisture, ash, fiber, protein and fat contents of the stems and roots of *A. cathartica* were determined by the respective AOAC method.

Isolation and Identification of Phytochemical Constituent from EtOAc Extract of Roots of *A. cathartica* by Column Chromatography

Dried powdered root sample (1000 g) were percolated in EtOH (70 %) (1000 mL) for one week and filtered. This procedure was repeated for three times. Then the filtrate was concentrated by using a vacuum rotatory evaporator to get EtOH extract (25 g). Then the EtOH extract was defatted by using pet-ether and the defatted EtOH extract was successively partitioned with between EtOAc and water. The EtOAc layer was concentrated under reduced pressure using vacuum rotatory evaporator. The EtOAc extract (8 g) was then separated by silica gel column chromatographic method successively eluting with n-Hexane:EtOAc in the ratios of 4:1, 2:1, 1:3 and 1:5 v/v solvent systems. On chromatographic separation, seven combined fractions (F-I to F-VII) were collected after examining on percoated TLC plates. Among the seven fractions, fraction (F-III) gave a white crystal (1.51 %, 121.1 mg, based on EtOAc extract).

The isolated compound was then identified by using joint application of its physicochemical properties and modern spectroscopic techniques such as UV, FT IR, NMR and Mass spectroscopies, and compared with the reported data. The NMR and Mass spectra of the isolated compound were measured at Division of Natural Product Chemistry, Institute of Natural Medicine, University of Toyama, Japan.

Screening of Antioxidant Activity of Ethanol and Watery Extracts of the Stems and Roots of *A. cathartica*

In this experiment, DPPH (2 mg) was thoroughly dissolved in EtOH (100 mL). This solution was freshly prepared in the brown coloured reagent bottle and stored in the fridge for no longer than 24 h. Each tested sample (2 mg) and 10 mL of EtOH were thoroughly mixed by shaker. The mixture solution was filtered and the stock solution was obtained. By adding with EtOH, the sample solutions in different concentrations of 200, 100, 50, 25, 12.5 and 6.25μ g/mL were prepared from the stock solution. The effect on DPPH radical was determined using the method by Marinova and Batchvarov (2011). The control solution was prepared by mixing 1.5 mL of 50 μM DPPH solution and 1.5 mL of EtOH using shaker. The test sample solution was also prepared by mixing thoroughly 1.5 mL of 50 μM DPPH solution and 1.5 mL of each sample solution. The mixture solutions were allowed to stand at room temperature for 30 min. Then, the absorbance of each solution was measured at 517 nm by using UV-1650 spectrophotometer. Absorbance measurements were done in triplicate for each concentration and then mean values so obtained were used to calculate percent inhibition of oxidation, the capability to scavenge the DPPH radical was calculated by using the following equation:

$$\% \text{RSA} = \frac{A_c - (A - A_b)}{A_c \times 100}$$

Where, %RSA = Radical Scavenging Activity

A_c = absorbance of the control (DPPH only) solution

A_b = absorbance of the blank (EtOH + Test sample solution) solution

A = absorbance of the test sample solution

Screening of Antimicrobial Activity of Various Crude Extracts from the Stems and Roots of *A. cathartica* by Agar Disc Diffusion Method

The screening of antimicrobial activity of various crude extracts such as PE, EtOAc, EtOH, watery extracts from the stems and roots of *A. cathartica* were carried out by agar disc diffusion method at Fermentation Laboratory, Pharmaceutical Research Department, Ministry of Industry, Yangon, Myanmar. Six microorganisms namely *Bacillus subtilis*,

Staphylococcus aureus, *Pseudomonas aeruginosa*, *Bacillus pumilus*, *Candida albicans* and *Escherichia coli* were used for this test.

Screening of Antitumor Activity of the Various Crude Extracts from the Stems and Roots of *A. cathartica*

The antitumor activity of ethanol, ethyl acetate and petroleum ether extracts from the Stems and Roots of *A. cathartica* was examined by Potato Crown Gall (PCG) or Potato Disc Assay (PDA) method (Coker *et al.,* 2003) at the Fermentation Laboratory, Pharmaceutical Research Department, Ministry of Industry, Yangon, Myanmar.

Fresh disease-free potatoes were purchased from a local market. Tubers of moderate size were surface sterilized by immersion in 0.1 % sodium hypochlorite for 20 min. Ends were removed and the potatoes were soaked an additional 10 min. A core of the tissue was extracted from each and discarded. The remainder of the cylinder was cut into 1.0 cm thick discs with a surface sterilized scalpel. The discs were then transferred to agar plates (1.5 g of agar dissolved in 100 mL deionized distilled water, autoclaved for 20 min at 121 ºC, 20 mL poured into each Petridish). Each plate contained four potato discs and 4 plates, were used for each of the sample solution.

Sample (0.05, 0.10, 0.15 g) was separately dissolved in DMSO (1 mL) and filtered through Millipore filters (0.22 μ m) into sterile tube. This solution (0.5 mL) was added to sterile distilled water (1.5 mL), and broth culture of *A. tumefaciens* in PBS (2 mL) was added. Controls were made in this way; DMSO (0.5 mL) and sterile distilled water (1.5 mL) were added to the tube containing 2 mL of broth culture of *A. tumefaciens.* By using a sterile disposal pipette, 1 drop (0.05 mL) each from these tubes was used to inoculate each potato disc by spreading it over the disc surface. After inoculation, Petri dishes were sealed by film and incubated at 27~30 ºC for 3 days. Observation was made on appearance of tumors on potato discs after 3 days under stero-microscope followed by staining with Lugol's iodine (10 % KI and 5 % I_2) after 30 min and compared with control. The antitumor activity was examined by observation of tumor produced or not on the potato discs. The results are shown in Table 4.

Results and Discussion

Types of Phytochemicals Present in the Stems and Roots of *A. cathartica*

In order to find out the types of phytochemical constituents present in the stems and roots of *A. cathartica*, the phytochemical tests were preliminary carried out according to the reported procedure. From the data findings, it was observed that various secondary metabolites such as alkaloids, flavonoids, terpenoids, steroids, glycosides, organic acids, starch, phenolic compounds, saponins and tannins together with starch and carbohydrates were present, however cyanogenic glycosides, reducing sugars and α - amino acids were not detected in both of the stems and roots samples. According to these results, it can be seen that the stems and roots samples might contain potent bioactive secondary metabolites.

These secondary metabolites contribute significantly towards the biological activities of medicinal plants such as hypoglycemic, antidiabetic, antioxidant, antimicrobial, antiinflammatory, anticarcinogenic, antimalarial, anticholinergic, antileprosy activities etc. These two samples for screening were found to possess tannins. Tannins have amazing stringent properties. They are known to hasten the healing of wounds and inflamed mucous membranes. Flavonoids are also present in two samples as a potent water-soluble antioxidant and free radical scavengers, which prevent from the oxidative cell damage and also have strong anticancer activity. It also helps in managing diabetes induced oxidative stress. Terpenoids have been found to be useful in the prevention and therapy of several diseases, including cancer. Terpenoids are also known to possess antimicrobial, antifungal, antiparasitic, antiviral, anti-allergenic, antispasmodic, antihyperglycemic, antiinflammatory and immune modulatory properties. In addition, terpenoids can be used as protective substances in storing agricultural products as they are known to have insecticidal properties as well (Yadav *et al*., 2014).

Some Nutritional Values of the Stems and Roots of *A. cathartica*

The nutritional values were determined by AOAC method resulting 6.91 and 18.64 % of proteins, 2.04 and 3.04 % of moisture, 2.71 and 3.06 % of ash, 62.42 and 38.65 % of fiber and 10.33 and 16.15 % of fat in the stems and roots of *A. cathartica*, respectively. According to these results, both of the samples were found to be high in fiber content. Fiber is a type of carbohydrate

that the body cannot digest. Though most carbohydrates are broken down into sugar molecules, fiber cannot be broken down into sugar molecules, and instead it passes through the body undigested. Fiber helps to regulate the body's use of sugars, helping to keep hunger and blood sugar in check.

Identification of the Compound Isolated from the EtOAc Extract from the Roots of *A. cathartica*

From the silica gel column chromatographic separation of EtOAc extract of the roots, a compound was isolated in 1.51 % of yield based on EtOAc extract as a white crystal. Its melting point was found to be 210 ~ 211°C and its R_f value was observed to be 0.4 (PE: EtOAc, 4:1 v/v). It is soluble in chloroform, methanol and ethanol but insoluble in pet-ether, ethyl acetate, acetone and water. Since the melting point of the isolated compound was observed to be identical with the reported melting point (m.pt. 205-206 ºC) of plumericin (Maged *et al.,* 1997), a major constituent of *A. cathartica*, this isolated compound can be assigned as plumericin. It was confirmed by using modern spectroscopic methods.

It is UV active and the band with maximum absorption at λ_{max} 230 nm was observed in the UV spectrum (Figure 1), indicating the presence of conjugated double bonds in the compound. It could be also confirmed by FT IR spectral data. In the FT IR spectrum (Figure 2) the absorption band appeared at 3084 cm^{-1} was due to the =C-H stretching indicating the presence of alkenic =C-H groups and these alkenic groups were defined to be *trans*- and *cis*- disubstituted according to the bands occurred at 950 and 762 cm^{-1}. The absorption bands observed at 2950 and 2910 cm^{-1} were due to the asymmetric and symmetric C-H stretching vibrations indicating the presence of –CH, CH_2 and CH_3 alkyl groups and their respective C-H bending vibration were observed at 1647, 1616 and 1437 cm^{-1}. The absorption band at 1757 cm^{-1} was appeared due to the C=O stretching of cyclic ester and lactone and the absorption band occurred at 1714 cm^{-1} the C=O stretching of ester. These observations indicate that the compound might possess two ester groups, *ie.*, a lactone ring and an ester. The absorption band at 1083 cm^{-1} was due to the C-O-C stretching of ether. Therefore from UV and FT IR spectral data assignment, it can be inferred that the isolated compound is bearing the conjugated double bonds, alkyl groups, lactone ring, ester group and ether

functional groups and it indicates that the isolated compound must have the plumericin skeleton as follows.

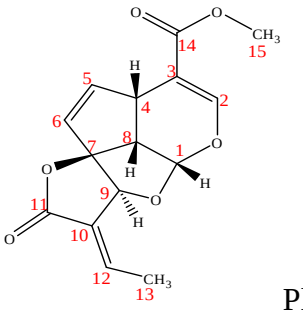

Plumericin

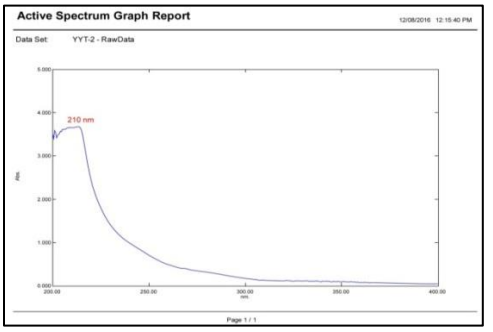

Figure 1: UV spectrum of the isolated compound (Methanol)

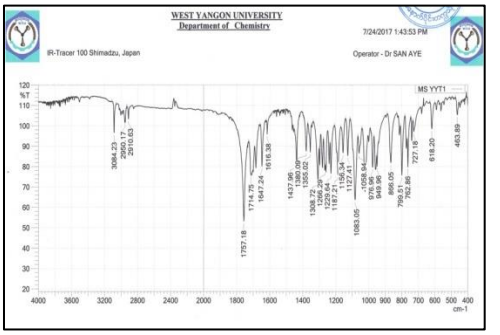

Figure 2: FT IR spectrum of the isolated compound

In addition, the structure of the isolated compound was identified by 1 D and 2 D NMR spectra. The integration of ^{1}H NMR (500 MHz, $CDCl_3$) spectrum (Figure 3) indicated the presence of fourteen protons which further supported the suggested molecular formula. The doublet signal with coupling constant of 7.25 Hz appeared at δ_H 2.1ppm (J =7.25 Hz) and a singlet signal at δ_H3.7 ppm were assigned to be two methyl groups: a aliphatic –CH_3 and a methoxy methyl group (-O-CH_3). The signals appeared at δ 5.55 ppm (1H, d, J = 5.85 Hz), δ 7.4 ppm (1H, s), δ 4.02 ppm (1H, ddd, J = 9.45, 2.25, 2.15 Hz), δ 6.05 ppm (1H, dd, J =2.2, 5.5 Hz), δ 5.65 ppm (1H, dd, J =2.2, 5.5 Hz), δ 3.4 ppm (1H, dd, J = 5.85, 9.45 Hz), δ 5.11 ppm (1H, s) and δ 7.2 ppm (1H, dq, J =7.25, 1.5 Hz) were assigned to be eight methine protons.

The ^{13}C NMR (125 MHz, $CDCl_3$) spectrum of the isolated compound is shown in Figure 4. The spectrum revealed the presence of fifteen carbon signals including two methyl carbons at the chemical shifts of δ_C 16.07 and δ_C 51.64 ppm, eight methine carbons at δ_C152.67, 145.26, 141.05, 126.35, 102, 80.27, 53.66 and 38.38 ppm, three quartenary carbons at δ_C 127.41, 109.33 and 104.57 ppm and two carbonyl groups at δ_C 168.15 and 166.64 ppm.

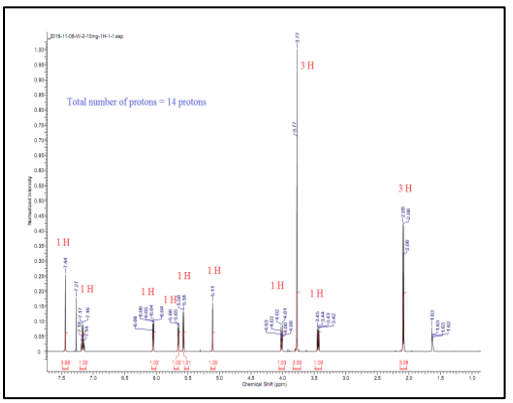

Figure 3: ^{1}H NMR (500 MHz, $CDCl_3$) spectrum of the isolated compound

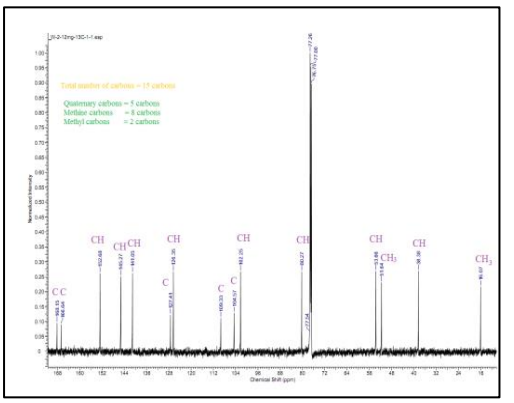

Figure4: ^{13}C NMR (125 MHz, $CDCl_3$) spectrum of the isolated compound

The correlation between the protons directly attached to the carbons, *ie.*, types of carbons (methyl, methine and quarternary carbons) was studied by HMQC spectrum (Figure 5) and proton-proton correlation stduied by ^{1}H-^{1}H COSY spectrum (Figure 6). Furthermore, the long range proton-carbon correlation was also examined by using 2 D HMBC spectrum (Figure 7). The resultant data are shown in Table 1. It was found that the observed data of the isolated compound were similar to the reported data of plumericin (Maged *et al.*, 1997).

Finally, the structure of the isolated compound was confirmed by using EI-LRMS mass spectrum (Figure 8). According to FT IR and NMR spectral data, there were two ester groups, 15 carbons, 14 protons indicating the partial structural formula might be $C_{15}H_{14}O_4$ with molecular weight of m/z 258. The molecular weight of the isolated compound was found to be 290 as observed in MS spectrum. Consequently, the isolated compound must contain

another two oxygen atoms as two ether groups and the complete structural formula of this isolated compound must be assigned as $C_{15}H_{14}O_6$ with the molecular weight 290 and it was identified as plumericin.

Table 1: 1 D and 2 D NMR Spectral Data of the Isolated Compound and the Reported Data of Plumericin

Carbon Position	Isolated Compound				Plumericin *	
	δ_H(ppm)	δ_C(ppm), HMQC	COSY	HMBC	δ_H(ppm)	δ_C(ppm)
1	5.55 (1H, d, 5.85)	102.25,CH	H-8	C-3, C-7, C-8	5.55(1H, d, 5.9)	102.49, CH
2	7.4 (1H, s)	152.67,CH		C-1, C-4	7.42 (1H, s)	152.94,
3		109.33,C				109.58, C
4	4.02, (1H, ddd, 9.45, 2.25, 2.15)	38.38, CH	H-8	C-3, C-14	4.00(1H, ddd, 9.5, 2.2, 2.1)	38.63, CH
5	6.05(1H, dd, 2.2, 5.5)	141.05, CH	H-6	C-6, C-7, C-8	6.03(1H, dd, 5.4, 2.2)	141.31, CH
6	5.65 (1H, dd, 2.2, 5.5)	126.35, CH	H-5	C-5, C-7	5.63(1H, dd, 5.4, 2.1)	126.61, CH
7		104.57, C				104.83, C
8	3.4 (1H, dd, 5.85, 9.45)	53.66, CH	H-4, H-1	C-3, C-7	3.42(1H,dd, 9.5, 5.9)	53.91, CH
9	5.11(1H, s)	80.27, CH		C-11	5.09(1H, s)	80.53, CH
10		127.41, C				127.68, C
11		168.15, C				168.42, C
12	7.2 (1H, qd, 7.25, 1.5)	145.26, CH	H-13	C-9, C-11	7.15 (1H, qd, 7.2, 1.4)	145.54, CH
13	2.1 (3H, d, 7.25)	16.07,CH_3	H-12	C-10, C12	2.07 (3H, d, 7.2)	16.33, CH_3
14		166.64, C				166.90,C
15	3.7 (3H, s)	51.64, CH_3		C-14	3.75 (3H, s)	51.90, CH_3

*Jutamas, 2015

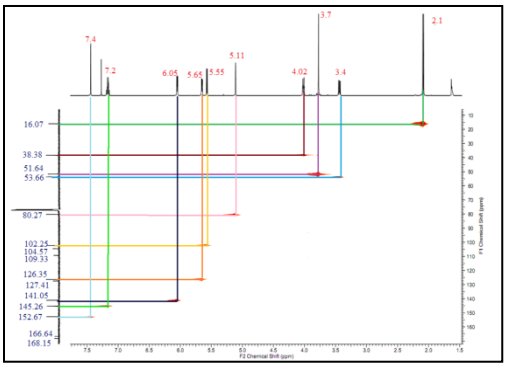

Figure 5: HMQC (500MHz, $CDCl_3$) spectrum of the isolated compound

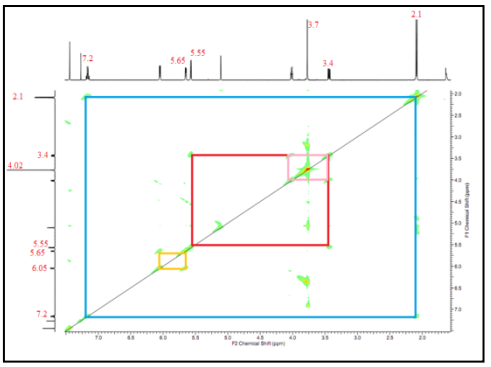

Figure 6: ^1H ^1H COSY (500MHz, $CDCl_3$) spectrum of the isolated compound

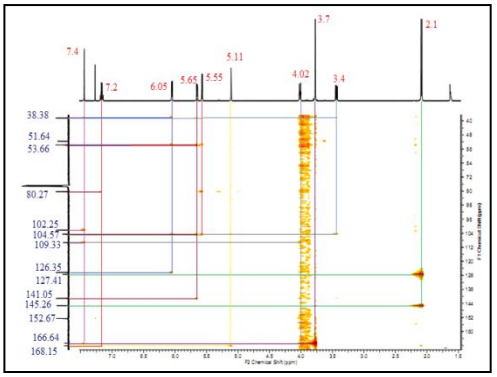

Figure 7: HMBC (500MHz, $CDCl_3$) spectrum of the isolated compound

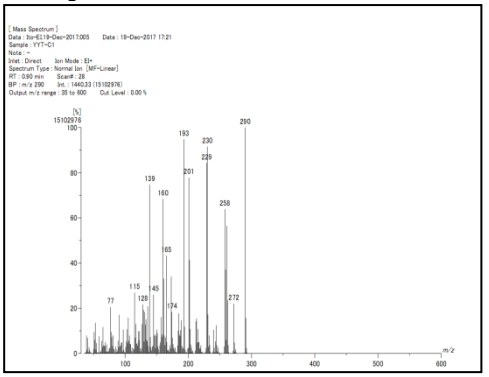

Figure 8: EI-LRMS spectrum of the isolated compound

Antioxidant Activity of the Stems and Roots of *A. cathartica*

The antioxidant activity was measured in terms of hydrogen donating or radical scavenging ability of the EtOH and watery extracts of the samples by using the stable radical DPPH. The results are shown in Table 2 and Figure 9. From these observations, the radical scavenging activity of EtOH extracts was found to be greater than watery extracts in both samples. EtOH extracts of the roots inhibited 50% of free radical scavenging at the concentrations (IC_{50}) of 110.46 μ g/mL and that of the stems was 65.89 μ g/mL. Watery extracts of the both samples did not show antioxidant activity up to optimum dose of 200 μ g/mL.

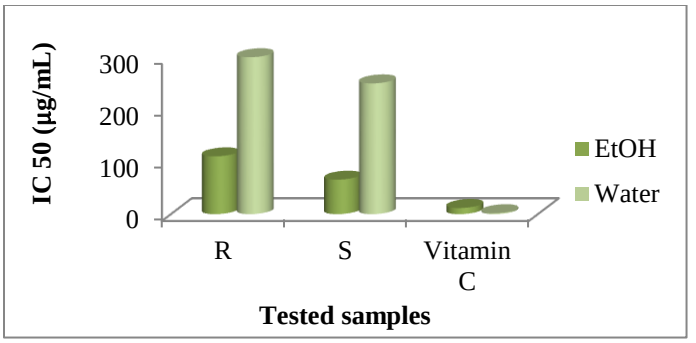

Figure 9: A bar graph of IC_{50} (µg/mL) of EtOH and watery extracts of the roots and stems of *A. cathartica*

Table 2: Percent Radical Scavenging Activity of Crude Extracts of Roots of *A. cathartica*

Sample	% Radical Scavenging Activity at Different Concentrations (µg/mL) ± SD of the sample						IC_{50} (µg/mL)
	6.25	12.5	25	50	100	200	
R-EE	21.70 ± 0.32	26.62 ± 0.95	28.64 ± 0.00	35.46 ± 0.48	48.43 ± 1.11	61.75 ± 0.95	110.46
S-EE	4.25 ± 0.63	12.64 ± 1.42	23.15 ± 3.32	39.26 ± 0.16	68.68 ± 1.58	101.5 ± 0.95	65.89
R-WE	7.54 ± 0.00	8.85 ± 0.02	10.95 ± 0.00	15.68 ± 0.00	26.81 ± 0.00	33.06 ± 0.10	>200
S-WE	28.35 ± 0.00	27.65 ± 0.00	28.39 ± 0.02	31.41 ± 0.00	38.15 ± 0.00	45.62 ± 0.00	>200
Vitamin C	25.20 ± 1.40	53.58 ± 0.88	65.53 ± 1.13	74.82 ± 0.59	83.32 ± 0.78	91.21 ± 0.48	11.7

R-EE = Shwewa Root EtOH Extract
S-EE = Shwewa Stem EtOH Extract
R-WE = Shwewa Root Watery Extract
S-WE = Shwewa Stem Watery Extract

Antimicrobial Activity of Crude Extracts of the Roots of *A. cathartica*

Four crude extracts such as PE, EtOAc, EtOH and water extracts from the stems and roots of *A. cathartica* were subjected to screening of antimicrobial activity against six different pathogenic microbes such as *Bacillus subtilis, Staphylococcus aureus, Pseudomonas aeruginosa, Bacillus pumilus, Candida albicans and Escherichia coli* using agar well diffusion method. This method is based on zone diameter including the well diameter, in millimeter (mm). The larger the zone diameter, the higher theactivity is. According to the results, watery extract of the stems did not show any antimicrobial activity against *P. aeruginosa* and *E. coli.* Moderately significant antibacterial activities were possessed by PE and watery extracts of both samples. Moreover, EtOAc and EtOH extracts of the roots inhibited significantly all strains of bacteria with the zone of inhibition ranged from 20 to 35 mm (Table 3). Hence in general, the extracts from the roots of *A. cathartica* were found to be high in antimicrobial activity against all tested microorganisms.

The results of present research highlight the fact that the organic solvent extracts exhibited greater antimicrobial activity because the antimicrobial principles were either polar or non-polar and they were extracted only through the organic solvent medium (Britto, 2001). The present observation suggested that the organic solvent extraction was suitable to verify the antimicrobial properties of medicinal plants and they supported by many investigators (Krishna *et al.*, 1997; Singh and Singh 2000; Natarajan *et al*., 2003 & 2005).The present study justifies the claimed uses of *A. cathartica* in the traditional system of medicine to treat various infectious diseases caused by the microbes.

Table 3: Inhibition Zone Diameters of Various Extracts of the Roots of *A. cathartica* against Six Microorganisms by Agar Well Diffusion Method

No.	Microorganisms	Samples	Inhibition Zone Diameters (nm) of Different Crude Extracts			
			PE	EtOAc	EtOH	Watery
1	*Bacillus subtilis*	I	15 (++)	30 (+++)	33 (+++)	24 (+++)
		II	13 (+)	14 (+)	16 (++)	13 (+)
2	*Staphylococcus aureus*	I	14 (+)	30 (+++)	30 (+++)	20 (+++)
		II	13 (+)	15 (++)	14 (+)	14 (+)
3	*Pseudomonasaeruginosa*	I	15 (++)	20 (+++)	20 (+++)	14 (+)
		II	18 (++)	18 (++)	15 (++)	-
4	*Bacillus pumilus*	I	16 (++)	35 (+++)	34 (+++)	24 (+++)
		II	12 (+)	13 (+)	14 (+)	15 (++)
5	*Candida albicans*	I	15 (++)	32 (+++)	30 (+++)	24 (+++)
		II	12 (+)	14 (+)	15 (++)	15 (++)
6	*Escherichia coli*	I	15 (++)	33 (+++)	33 (+++)	21 (+++)
		II	14 (+)	14 (+)	14 (+)	-

I = roots, II = stems
Agar well – 10mm, 10mm ~ 14mm (+), 15mm ~ 19 mm(++), 20mm and above (+++)

Antitumor Activity of the Stems and Roots of *A. cathartica*

Antitumor activity in this study was investigated by potato crown gall (PCG) assay as it is a valuable tool that indicates antitumor activity of the tested samples by their inhibition of the crown gall formation that was induced in wounded potato tissues by *Agrobacterium tumefaciens*.

Table 4:Tumor Inhibition by the Crude Extracts and Ioslated Plumericin from the Stems and Roots of *A. cathartica*

Test Samples	Extracts/Compound	Concentrations of Samples (g/mL/disc)	Tumor Inhibition
Control	-	0.00	+
Roots	PE	0.05	-
	PE	0.10	-
	PE	0.15	-
	EtOAc	0.05	-
	EtOAc	0.10	-
	EtOAc	0.15	+
	EtOH	0.05	-
	EtOH	0.10	-
	EtOH	0.15	-
Stems	PE	0.05	-
	PE	0.10	-
	PE	0.15	+
	EtOAc	0.05	+
	EtOAc	0.10	+
	EtOAc	0.15	+
	EtOH	0.05	-
	EtOH	0.10	-
	EtOH	0.15	-
Plumericin	-	10, 20, 30 mg/mL/disc	-

(+) Tumor appeared, (-) No tumor appeared

It could be clearly seen from the Table 4 that except EtOAc extracts of stems, all of the samples inhibited tumor growth in a concentration dependent manner. Significant tumor inhibition was observed at the concentrations of 0.05, 0.10 and 0.15 g/mL/disc. Plumericin showed antitumor activity at the concentrations of 10, 20 and 30 mg/mL/disc.

Since, tumor inhibition significantly occurred by the extracts of *A. cathartica* on potato discs, it could be concluded that the plant might be used as a potential source of antitumor agent.

Conclusion

From the overall assessment concerning with the investigation of phytochemicals and biological activities on the stems and roots of *A. cathartica*, the following inferences could be deduced. The various types of phytochemical constituents such as alkaloids, flavonoids, terpenoids, steroids, glycosides, organic acids, starch, phenolic compounds, saponins, tannins and carbohydrates were present in the stems and roots of *A. cathartica*, except cyanogenic glycosides, reducing sugars and α - amino acids. The approximate nutritional compositions were observed to be 6.91 and 18.64 % of proteins, 2.04 and 3.04 % of moisture, 2.71 and 3.06 % of ash, 62.42 and 38.65 % of fiber and 10.33 and 16.15 % of fat in stems and roots of *A. cathartica*, respectively. One organic compound, plumericin (1.51 %, mpt. 210 °C) was isolated as a major bioactive chemical constituent from ethyl acetate crude extract of the roots by using silica gel column chromatographic separation technique. The isolated compound was characterized by some physical and chemical properties and structurally identified by the combination of UV, FT IR, ^{1}H NMR, ^{13}C NMR, 2D NMR and EI-LRMS spectroscopic methods and also by comparing with the reported data.

The ethanol extract of stems possesses higher antioxidant activity than that of the roots. Although watery extract of the stems showed low activity and PE and watery extracts of the stems and roots showed medium activity, EtOAc and EtOH extracts of roots were found to possess high antimicrobial activity against all strains of microorganisms tested (inhibition zone ranged between 20 ~ 35 mm). Furthermore EtOAc extract of the roots, PE and EtOH extracts of roots and stems were also found to inhibit the formation of tumor. Plumericin has pronounced antitumor activity.

In conclusion, antimicrobial, antioxidant and antitumor activities of different extracts obtained from the stems and roots of *A. cathartica* grown in Myanmar could be evaluated. Strong antimicrobial activity was found in all tested samples. However the antioxidant activity of tested samples were very weak compared with the potency of standard vitamin C (IC_{50} = 1.17 μg/ mL). In addition, strong antitumor activity was also observed. With these results, the tested plant has some scientific justification as a medicinal plant that might be useful for the treatment of bacteria infected diseases and be used as antitumor agent.

Acknowledgement

The authors would like to express their profound gratitude to the Department of Higher Education (Lower Myanmar), Ministry of Education, Yangon, Myanmar, for provision of opportunity to do this research and Myanmar Academy of Arts and Science for allowing to present this paper.

References

A.O.A.C. (2000). *Official and Tentative Methods of Analysis,* Association of Official Analytical Chemists, USA: 17th Ed., Gaithersburg, Maryland, AOAC International, pp. 63-67.

Britto, J. S. (2001). "Comparative Antibacterial Activity Study of *Solanum incanum* L. "*J. Swamy Bot. Club*., vol. 18, pp. 81-82.

Chandrasekhar, N., V. Siddartha, and Venkateswarlu, B. (2012). "Evaluation of Antimicrobial Activity of Flower extracts of *Allamanda cathartica* L." *International Journal of Pharma World Research*., vol. 3, (2), pp. 1-20.

Coker, P.S., J. Radcke, C.Guy, and N. D. Camper, (2003). "Potato Tumor Induction Assay: A Multiple Mode of Action Drug Assay". *Phytomedicine*, vol. 10, pp. 133-138.

Fah, W. K. (2013). "Tissue Culture Studies, Secondary Metabolites and Pigment Extraction from *Allamanda cathartica* L.". MSc Thesis, University of Malaya, Kuala Lumpur, pp. 13-14.

Jutamas, S.K.H, Sumonthip, Y., Nuttawan, K. Kummalue, and Weena, J. (2015). "Antibacterial and Antiprokicerative Activities of Plumericin, an Iridoid Isolated from *Momordica charantia* Vine". *J. Complementary and Alternative Medicine., vol.* 15, pp. 1-10.

Krishna, K. T., Ranjiniand, C. E. and Sasidharan, V. K. (1997). "Antibacterial and Antifungal Activity of Secondary Metabolities from some Medicinal and other Common Plant Species". *J. Life Sci.*, vol. 2, pp. 14-19.

Maged, S. A. K.,W Jan, E., Randy, W. Hendrikvander, and David, G. I. K. (1997). "Bioactive Iridoids and a New Lignan from *Allamanda cathartica* and *Himatanthusfallax* from the Suriname Rainforest". *J. Nat. Prod.,* vol. 60,pp. 1294-1297.

Marinova, G. V. and V. Batchvarov, (2011). "Evaluation of the Mehthods for Determination of the Free Radical Scavenging Activity of DPPH". *Bulgarian Journal of Agricultural Science*, vol. 17, pp. 11-24.

Natarajan, D., J. S Britto, J. S., K., Srinivasan, N., Nagamurugan, C. Mohanasundari, and Perumal, G. (2005). "Anti-bacterial activity of Euphorbia fusiformis- a rare medicinal herb", *J. Ethnopharmacol*., vol. 102, pp. 123-126.

Natarajan, E., S. Senthilkumar, S. X., Francis, T. and Kalaiselvi, V. (2003). "Antibacterial Activities of Leaf Extracts of *Alangium salviifolium*". *J. Trop. Med. Plants*, vol. 4, pp. 9-13.

Singh, I. and V. P. Singh, (2000). "Antifungal Properties of Aqueous and Organic Solution Extracts of Seed Plants against *Aspergillus flavus* and *A. niger*". *Phytomorphol*, vol. 50, pp. 151-157.

Sofowora, E. E. (2000). "Phytochemical Screening of Nigerian Medicinal Plants". *J. Intergrative Med*., vol. 41, pp. 234-24.

Uduak, A. E. and S. U. Esther, (2015). "Comparative Phytochemical Screening and Nutritional Potentials of the Stems, Leaves and Flowers of *Allamanda cathartica* (Apocynaceae)". *International Journal of Science and Technology.*, vol. 4 (6), pp. 284-253.

Yadav, M., S., Chatterji, Gupta, S. K. and Watal, G. (2014). "Preliminary Phytochemical Screening of Six Medicinal Plants used in Traditional Medicine", *International Journal of Pharmacy and Pharmaceutical Sciences*, vol. 6 (5), pp. 539-542.

INVESTIGATION OF PHYTOCHEMICAL CONSTITUENTS AND SOME BIOCHEMICAL PROPERTIES OF THE BARK OF *Schleichera oleosa* (Lour.) Oken. (GYO)

Chan Myae Kyaw[1,2], Khine Zar Wynn Lae[3],Nwet Nwet Win[4], Hla Ngwe[5]

Abstract

Locally cultivated *Schleichera oleosa*(Lour.) Oken (Ceylon oak, Gyo) was chosen for the present study to investigate the phytochemicals and some biochemical properties of its bark.The preliminary phytochemical screening indicated that α-amino acids, carbohydrates, flavonoids, glycosides, phenolic compounds, reducing sugars, steroids, saponins, tannins and terpenoids were present while alkaloids was absent in the bark. The physico-chemical analysis revealed that the bark contained 2.14% of ash, 9.32% of moisture, 6.25% of protein, 22.78% crudefiber, 0.83% of crude fat and58.68% of carbohydrate. The elemental analysis carried out by EDXRF method showed some elements such as Ca, K, S, Fe, Sr, Mn and Cu were present in the sample. The extractable matters (% w/w)in different polarity of solvents such as methanol, ethanol, acetone, ethyl acetate and petroleum ether were respectively observed to be 5.8, 5.0, 2.0, 1.6, 1.0 % (w/w) and water soluble matter was 3.6 % (w/w) in the sample. The ethanol extract was found to have higher total phenol content (158.67±6.76 mg GAE /g of extract) and total flavonoid content (190.0 ± 8.5 mg QE/g of extract) than the watery extract containing 148.32 ± 4.73 mg GAE/g extract of total phenol content and 143.33±7.8 mg QE/g extract of total flavonoid content. Six different extracts (PE, EA, EtOH, MeOH, $CHCl_3$ and H_2O)exhibited mild antimicrobial activity against some microorganisms, determined by agar well diffusion method. The antioxidant activities of ethanol extract (IC_{50} = 0.56 μg/mL) and watery extracts (IC_{50} = 0.69 μg/mL) determined by DPPH radical scavenging assay were higher than that of standard gallic acid significantly. Some crude extracts such as MeOH, EtOH and watery extracts exhibited the inhibition of tumor formation at the dose of 0.2 g/disc, determined on tumor producing bacteria by using Potato Crown Gall test.The ethanol extract (LD_{50} = 2.69 μ g/mL) and watery extract (LD_{50} = 8.85μ g/mL) also showed significant cytotoxic effect against brine shrimp (24 h).Furthermore, ethanol extract possessedhigher antiproliferative

1. Assistant Lecturer, Department of Chemistry, University of Yangon
2. PhD Student, Department of Chemistry, University of Yangon
3. Dr, Lecturer, Department of Chemistry, University of Yangon
4. Dr, Associate Professor, Department of Chemistry, University of Yangon
5. Dr, Professor and Head, (Retd.), Department of Chemistry, University of Yangon

activity than watery extract against Hela (cervical) and MCF-7 (breast) human cancer cell lines determined by using CCK-8 Assay (Cell Counting Kit-8).

Keywords: *Schleicheraoleosa* (Lour.) Oken. (Gyo), total phenol content, total flavonoid content, antioxidant activity, antitumor activity, cytotoxic effect, antiproliferative activity

Introduction

At present, there are many researches in natural products which are interesting. Plant is important and necessary to dive into life, due to the fact that it is a source of food, traditional until modern medicine. Plants are natural source of producing a wide number of bioactive chemical constituents in most efficient way and precise selectivity (Ikram *et al.*, 2009). *Schleicheraoleosa* (Lour.) Oken is a plant in the family of Sapindaceae. In Myanmar, *S. oleosa* named Gyo is found in the Central regions. It is used in the wood industry. The wood is suitable for fuel wood and charcoal, the bark is used as dye and the young leaves are eaten as vegetable. Different parts of *S. oleosa*, such as fruits, leaves, barks and seeds are used as tribal food, animal feed, seed-oil and timber. The tree also serves as important source for traditional medicines for curing pruritus, malaria, inflammation and ulcers (Bhat *et al*., 2009). Most exoticpast research has studied the properties of *S. oleosa* extracts from the bark and stems, and it was found to reduce the free radicals that cause the death of cancer cells (Thind *et al*., 2010). Antimicrobial activities were also performed against some fungal and bacterial species (Ghosh *et al*., 2011). Oil extracted from seeds can be used for the cure of itch, acne, skin burns and used as massageoil for rheumatic pains (Palanuvej and Vipunngeun, 2008). The water extract of the bark of *S. oleosa* was used to treat menstrual pain as well (Mahaptma and Sahoo, 2008).

However, there is still lack of reports from the research on locally cultivated *S. oleosa*. Hence in this study, the bark of *S. oleosa* is chosen for the investigation of some phytochemical composition and some biological activities from its ethanol and watery extracts.

Materials and Methods

The bark samples were collected from Pyay Township, Bago Region, Myanmar. The plant was identified and authenticated at the Department of Botany, Pyay University. After collection, the washed barks were air-dried in shade for about two weeks and ground into the coarse powder with the help of a mechanical grinder. The powders of the samples were used to extract with solvents of various polarities by using ultrasonic effect and to analyze phytochemical composition.

Phytochemical Analyses

The selected bark powders were subjected to qualitative phytochemical tests for the classification of various bioactive constituents present (Harborne, 1973). Phytochemical screenings were carried out by using standard procedures to detect the presence of alkaloids, glycosides, carbohydrates, α-amino acids, phenolic compounds, flavonoids, steroids, terpenoids, saponins, tannins, starch, reducing sugars and organic acids. After addition of specific reagents to the test solution, the observation of colour change or precipitate formation was noted and recorded.

Some Physicochemical Analyses

In this study, the nutritional values such as moisture, ash, crude protein, crude fiber and crude fat of the selected bark powder was determined at Food Industries Development Supporting Laboratory (FIDSL), Myanmar Food Processors and Exporters Association (MFPEA), Yangon, Myanmar. In addition, the relative abundance of elements present in the bark sample was determined by EDXRF spectrometer at the Universities' Research Center, Yangon.

The crude extracts of the sample were prepared by extracting the sample with different solvents such as petroleum ether, ethyl acetate, ethanol, methanol and water by percolation method. All of these extracts were kept for the determination of total phenol contents, total flavonoid contents, antimicrobial activity, antioxidant activity, antitumor activity, cytotoxicity and antiproliferative activity.

Determination of Total Phenol Contents

The total phenol contents (TPC) in ethanol and watery extracts were estimated by the Folin-Ciocalteu method according to the procedure described by Saxena *et al.* (2013) and gallic acid was used as a standard. The sample solution (50 ppm) was prepared by dissolving 0.005 g of extract in methanol making up to 100 mL solution. Firstly, 0.5 mL of the prepared sample was mixed with 0.5 mL methanol. Then, 0.5 mL of Folin-Ciocalteu reagent (FCR: H_2O, 1:10) was added to the mixture and incubated for 5 min. 4 mL of 1 M sodium carbonate solution was added to each tube and the tubes were kept at room temperature for 2 h and the UV absorbance of each reaction mixture was recorded at λ_{max} 765 nm. The control solution was prepared as the above procedure by using distilled water instead of sample solution. Total phenolic content was estimated as mg gallic acid equivalents per g of EtOH/water extract.

Determination of Total Flavonoid Contents

The total flavonoids contents of the ethanol and watery extracts were measured by employing the method involving aluminium trichloride ($AlCl_3$) reagent and quercetin was used as standard(Kalita *et al.,* 2011).In the determination of total flavonoid contents, quercetin was used to construct the calibration curve. Quercetin (0.01 g) was dissolved in methanol and then diluted to various concentrations of 6.25, 12.50, 25, 50 and 100μ g/mL. A calibration curve was made by measuring the absorbance of the above different solutions at 415nm (λ_{max} of quercetin) with a Shimadzu UV-1800 spectrophotometer. Ethanol/watery extract solution in 50 ppm was prepared by dissolving 0.005 g of each extract in 100 mL of methanol solution. Each extract stock solution (0.5 mL), 1.5 mL methanol, 0.1 mL of aluminium chloride, 0.1 mL of potassium acetate solution and 2.8 mL of distilled water were added and mixed well. The blank solution was prepared in similar way by replacing aluminium chloride with distilled water. Their absorbance was measured at 415 nm.

Screening of Antimicrobial Activity

Antimicrobial activity of different crude extracts (PE, EA, EtOH, MeOH, $CHCl_3$ and water) of the sample was screened *in vitro* by agar well diffusion method (Perez *et al*., 1990). Bacterial cultures used in the research involved three strains of gram positive bacteria (*Bacillus subtilis, Staphyloccous aureus* and *Bacillus pumilus*), two strains of gram negative bacteria (*Pseudomonas aeruginosa* and *Escherichia coli*) and one strain of fungi (*Candida albicans*). This experiment was carried out at Pharmaceutical Research Department, Insein Township, Yangon Region, Myanmar.

Determination of Antioxidant Activity

The antioxidant activity of EtOH and H_2O extracts were spectrophotometrically determined by DPPH radical scavenging assay method (Brand-Williams *et al.*, 1995). The control solution was prepared by mixing 1.5 mL of 60 µM DPPH solution and 1.5 mL of 95 % ethanol with vortex mixer. The sample solution was also prepared by mixing thoroughly the 1.5 mL of 60 µM DPPH solution and 1.5 mL of test sample solution. The solutions were allowed to stand for 30 min at room temperature. After 30 min, absorbance was measured at 517 nm by using a spectrophotometer UV 1601 PC (P\N 206-6750), Shimadzu corporation. Absorbance measurements were done in triplicate for each solution and the mean values obtained were used to calculate % inhibition of oxidation by the following equation,

$$\% \text{ oxidative inhibition} = \frac{A_c - (A - A_b)}{A_c} \times 100\ \%$$

% oxidative inhibition = % oxidative inhibition of test sample

A_c = absorbance of the control (DPPH alone)

A_b = absorbance of the blank (EtOH + Test samplesolution)

A = absorbance of test sample solution

Then IC_{50} (50 % inhibitory concentration) values were also calculated by linear regressive excel program.

Screening of Antitumor Activity

The antitumour activity of methanol, ethanol and watery extracts of the sample was examined by Potato Discs Assay Method (Ali *et al.*, 2016). This experiment was carried out at Pharmaceutical Research Department, Insein Township, Yangon Region, Myanmar. Tumor producing bacteria, *Agrobacterium tumefaciens*, isolated from *Sandoricum koetjape* Merr. (Thitto)leaves were used in this study. This bacterial strain has been maintained as solid slants under refrigeration. For inoculation on the potato discs, 48 h broth cultures containing 5×10^7~5×10^9 cell / mL were used. Fresh, disease free potato tubers were obtained from local markets and were transferred within 48 h to the laboratory.

Tubers of moderate sizes were surface-sterilized by immersionin 50 % sodium hypochlorite (Clorox) for 20 min. The ends were removed and soaked for 10 min more in Clorox. A core of the tissue was extracted from each tuber by using surface-sterilized (ethanol and flame) 2.5 cm wide cork borer and 2 cm pieces were removed from each end and discarded and the remainder of the cylinder was cut into 1.0 cm thick discs with a surface-sterilized cutter. The discs were then transferred to 1.5 % agar plates (1.5 g of Difco agar was dissolved in 100 mL of distilled water, autoclaved and 20 mL poured into each petri dish). Each plate contained three discs. This procedure was done in the clean bench in the sterile room. The sample (0.1, 0.15 and 0.2 g) was filtered through Millipore filters (0.22 μm) into a sterile tube. A 0.5 mL of this solution was added to 1.5 mL of sterile distilled water and 2 mL of broth culture of *A.tumefaciens* strain (48 h culture containing 5×10^7~5×10^9cells/mL) were added aseptically.

Controls were made in this way; 0.5 mL of DMSO and 1.5 mL of sterile distilled water were added to the tube containing 2 mL of broth culture of *A. tumefaciens* (from the same 48 h culture). Using a sterile disposable pipette, 1 drop (0.05 mL) from these tubes was used to inoculate each potato disc, spreading it over the disc, surface. The process of cutting the potatoes and incubation must be conducted within 30 min. The plates were sealed with tape to minimize moisture loss and incubated at room temperature and counted with microscope and compared with control. The antitumor activity was examined by observation if tumor is produced or not.

Determination of Cytotoxicity

The cytotoxicity of crude ethanol and watery extracts of the sample was investigated by using brine shrimp lethality bioassay according to the procedure described by Dockery and Tomkins, 2000. The brine shrimp (*Artemiasalina*) was used in this study for cytotoxicity bioassay (Ali *et al*., 2016). Brine shrimp cysts (0.5 g) were added to the 1.5 L of artificial sea water bottle. This experiment was carried out at the Department of Chemistry, Yangon University, Myanmar. The suspension was aerated by bubbling air into the funnel and kept for 24 h at room temperature. After aeration had been removed, the suspension was kept for 1 h undisturbed, whereby the remaining unhatched eggs dropped. In order to get a higher density of larvae, one side of the separating funnel was covered with aluminium foil and the other illuminated with a lamp, whereby the phototropic larvae were gathering at the illuminated side and could be collected by pipette. The shrimp larvae were transferred to an agar well filled with 9 mL of salt water and the dead larvae counted (number N). A solution of crude extract (31.25 ~ 1000 ppm) (1 mL each) was added and the plate kept at room temperature in the dark. After 24 h, the dead larvae were counted in each well under the microscope (number A). The still living larvae were killed by addition of ca. 0.5 mL methanol so that subsequently the total number of the animals could be determined (number G).The control solution was prepared as the above procedure by using distilled water instead of sample solution. The mortality rate M was calculated in %. Each test row was accompanied by a brine solution (number B). The mortality rate M was calculated by using the following formula:

$$M = \left[\frac{(A - B - N)}{(G - N)} \right] \times 100$$

Where, M = percent of the dead larvae after 24 h
A = number of the dead larvae after 24 h
B = average number of the dead larvae in the brine solution after 24 h
N = number of the dead larvae before starting of the test.
G = total number of brine shrimps

Determination of Antiproliferative Activity

Antiproliferative activity of ethanol and watery extracts were investigated in*vitro* by using cancer cell lines at Division of Natural Product Chemistry, Institute of Natural Medicine, University of Toyama, Japan. The cell lines used were Hela (human cervix cancer) and MCF 7 (human breast cancer).K562 α-Minimum essential medium with L-glutamine and phenol red (α-MEM, Wako) were used for cell cultures. All media were supplemented with 10 % fetal bovine serum (FBS, sigma) and 1 % antiobiotic antimycotic solution (Sigma). For MCF 7 cell, 1 % 0.1 M non-essential amino acid (NEAA, Gibco) and 1 % 1 mM sodium pyruvate (Gibco) were also supplemented. The *in vitro* antiproliferative activity of the crude extracts was determined by the procedure described by Win *et al.* (2015). Briefly, each cell line was seeded in 96-well plates (2×10^3 per well) and incubated in the respective medium at 37 °C under 5 % CO_2 and 95 % air for 24 h. After the cells were washed with PBS (Nissui Pharmaceuticals), serial dilutions of the tested samples were added. After 72 h incubation, the cells were washed with PBS and 100 μL of medium containing 10 % WST-8 cell counting kit (Dojindo; Kumamoto, Japan) solution was added to the wells. After 2 h incubation, the absorbance was measured at 450 nm. The concentrations of the crude extracts were 200, 100, 10 μg/ mL and 10, 1, 0.1 mM for positive control were prepared by serial dilution. Cell viability was calculated from the mean values of the data from three wells using the equation below and antiproliferative activity was expressed as the IC_{50} (50 % inhibitory concentration) value. 5-fluorouracil (5FU) was used as positive control.

$$(\%)\ \text{Cell viability} = 100 \times \frac{\left\{\text{Abs}_{(\text{test samples})} - \text{Abs}_{(\text{blank})}\right\}}{\left\{\text{Abs}_{(\text{control})} - \text{Abs}_{(\text{blank})}\right\}}$$

Results and Discussion

Phytochemicals Present in the Bark of *S. oleosa*

The bark sample of *S. oleosa* collected from Pyay Township, Bago Region was found to contain some of the secondary metabolites such as steroids, glycosides, phenolic compounds and terpenoids (Table 1) according

to preliminary phytochemical screening. According to the nutritional composition of the sample (Table 2),the bark sample was found to contain higher crude fiber content (22.78 %) but lower protein content (6.25 %) and fat content(0.83 %).It was also observed to contain 2.14 % of inorganic matters (ash).

Some Physicochemical Properties of the Bark of *S. oleosa*

As shown in Table 3, it can be seen that organic compounds are predominant in the sample, and other elements such as Ca, K and S are also present in reasonable composition but Fe and Mn were present in medium amount and Cu was present in very little amounts based on the relative abundance of elements.

The soluble matter contents of the bark powder of *S. oleosa* in solvents of different polarities were observed to be 5.8 % in methanol, 5.0 % in ethanol, 2.0 % in acetone, 1.6 % in ethyl acetate, 1.0 % in pet-ether and 3.6 % in water (Table 4). Therefore, it indicated that the phytochemicals present in bark sample were mostly the polar organic compounds.

Table 1: Results of Phytochemical Screening of the Bark of *S. oleosa*

Types of compounds	Extracts	Test reagents	Observation	Remark
Alkaloids	1% HCl	Dragendroff's reagent Mayer's reagent Wagner's reagent	No orange ppt No white ppt No reddish brown ppt	- - -
α-Amino acids	H_2O	Ninhydrin	purple spot	+
Carbohydrates	H_2O	10% α -naphthol, conc: H_2SO_4	red ring	+
Flavonoids	EtOH	Mg turning, conc: HCl	pink colour	+
Glycosides	H_2O	10% Lead acetate solution	White ppt	+
Phenolic compounds	H_2O	5% $FeCl_3$ solution	Green solution	+
Reducing sugars	Dil H_2SO_4	Benedict's solution	Brick-red ppt	+
Steroids	PE	Acetic anhydride, conc: H_2SO_4	Green colour	+

Types of compounds	Extracts	Test reagents	Observation	Remark
Saponins	H_2O	Distilled water	Frothing	+
Tannins	H_2O	2% gelatin solution	white ppt	+
Terpenoids	$CHCl_3$	Acetic anhydride, conc: H_2SO_4	Pink colour	+

(+) = Presence, (−) = absence

Table 2: Approximate Nutritional Composition of the Bark of *S. oleosa*

Nutrition Values	% (w/w, based on dry weight)
Ash content	2.14
Moisture content	9.32
Protein content	6.25
Crudefiber content	22.78
Crude fat content	0.83
Carbohydrate content	58.68

Table 3: Relative Abundance of Elements in the Bark of *S.oleosa* by EDXRF Spectrometry

Macro and Micronutrients	Relative aundance(%)
Ca	4.714
K	0.472
S	0.177
Fe	0.091
Sr	0.019
Mn	0.004
Cu	0.001
COH	94.521

Table 4: Extractable Matter Contents in the Bark of *S.oleosa*

Solvents	Weight of extractable matter (% w/w)
Water	3.6
Methanol	5.8
Ethanol	5.0
Acetone	2.0
Ethylacetate	1.6
Petroleum Ether	1.0

Total Phenol and Total Flavonoid Contents in the Bark of *S. oleosa*

Total phenol and total flavonoid contents in the bark of *S. oleosa* are shown in Figure 1 and Table 5. Total phenol contents of the extracts were calculated from the regression equation of calibration curve (Y = 0.0638 x + 0.0169; R^2 = 0.9941) and expressed as mg gallic acid equivalents (GAE) per gram of sample in dry weight. To perform the calculation of the total flavonoid contents in the samples by using Kiranmai *et al.* (2011) method, a standard curve is needed which is obtained from a series of absorbance of different quercetin concentrations (Y = 0.0019x +0.0115; R^2 = 0.9955). It can be seen that the total phenol of the ethanol extract (158.67±6.76 mg GAE/g of extract) was slightly higher than that of watery extract (148.32 ± 4.73 mg GAE/g of extract. In the case of total flavonoid content, total phenol content of ethanol extract (190 ± 8.5 mg QE/g of extract) is significantly higher than that of water extract (143.33 ± 7.8 mg QE/g of extract). The ethanol extract showed higher total phenol content and total flavonoid content than water extract, indicating that phenolic and flavonoids compounds were more soluble in organic solvent than water. Generally, extracts with a high amount of phenolic compounds might exhibit high antioxidant activity.

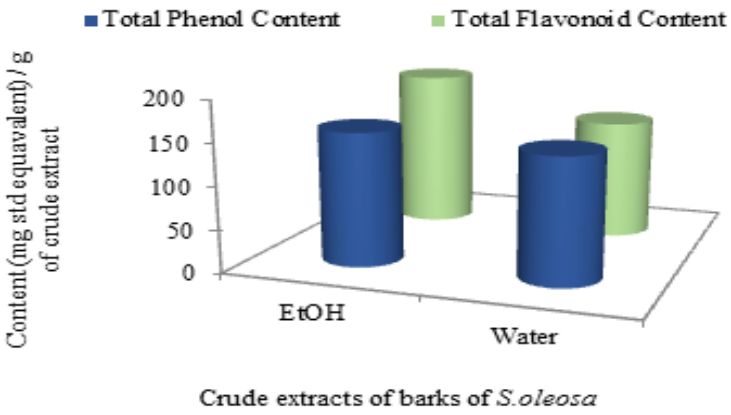

Figure 1: Total phenol and total flavonoid contents of *S. oleosa* Bark

Table 5: Total Phenol Content (TPC) and Total Flavonoid Content (TFC) of Crude Extracts

Types of compounds	EtOH extract	Water extract
TPC (mg GAE ± SD)/g of extract	158.67±6.76	148.32±4.73
TFC (mg QE ± SD)/g of extract	190.00 ±8.5	143.33±7.8

Antioxidant Activity of the Bark of *S. oleosa*

Most of the medicinal plants possess phytochemicals and antioxidant activity. Flavonoids and tannins are phenolics which are a major group of compound in plants. These compounds act as primary antioxidant or free radical scavengers (Ayoola*et al*., 2008). The antioxidant activity of watery and ethanol extracts of the sample was studied by DPPH free radical scavenging assay (Marinova and Batchvarov, 2011). Gallic acid was used as standard. The DPPH (2, 2-diphenyl-1-picrylhydrazyl) assay is widely used to investigate the free radical scavenging activities of several natural compounds such as crude extracts of plants. DPPH radical is scavenged by antioxidant through the donation of electron forming the reduced DPPH. Sample's colour change from purple to pale yellow which can be quantified by its decrease of absorbance at wavelength 517 nm (Maw *et al*., 2011). The radical scavenging activity of crude extracts were expressed in term of % RSA and IC_{50} (50% inhibition concentration). The results are shown in Table 6. From these observations, the larger DPPH radical scavenging activity was observed in ethanol extract, which inhibited 50% of free radicals at the concentration of 0.56 μg/mL (IC_{50}) than the water extract which inhibited 50% of free radicals at the concentration of 0.69 μg/mL (IC_{50}). It can be inferred that the antioxidant potency of the ethanol extract was found to be stronger than that of the watery extract, and both extracts were observed to be significantly higher than standard gallic acid (IC_{50} = 5.07 μg/mL) in antioxidant property.

Table 6: DPPH Free Radical Scavenging Activity (%RSA) and IC_{50} of Crude Extracts of the Bark Sample and Standard Gallic Acid

Samples	% RSA ± SD at Different Concentrations (μg/mL)						IC_{50} (μg/mL)
	0.3125	0.625	1.25	2.5	5	10	
EtOH extract	22.08 ± 0.38	57.62 ± 1.75	58.94 ± 1.75	61.59 ± 5.17	70.42 ± 4.69	80.13 ± 0.66	0.56
Water extract	43.49 ± 5.63	46.14 ± 1.38	82.29 ± 0.86	84.37 ± 2.65	85.46 ± 3.23	86.67 ± 3.09	0.69
Standard Gallic Acid	27.06 ± 13.01	33.12 ± 5.15	34.42 ± 10.45	41.13 ± 3.33	49.35 ± 1.12	97.40 ± 0.65	5.07

Antimicrobial Activity of the Bark of *S. oleosa*

The antimicrobial activity was assessed by agar well diffusion method which is equally suited to the screening of antibiotics or the products of plant evaluation and is highly effective for rapidly growing microorganisms and the activities of the test extracts are expressed by measuring the zones (mm) of inhibition. Generally, the more susceptible the organism, the bigger is the zone of inhibition. Antimicrobial activities of six different extracts (PE, EA, EtOH, MeOH, $CHCl_3$, H_2O) of the sample were also determined against some fungal and bacterial species. The observed data are tabulated in Table 7. Generally, ethyl acetate and ethanol extracts have medium activities on the gram positive bacteria: *B. subtilis*and *B. pumilus* and low activity against two gram negative bacteria *S. aureus*and *P. aeruginosa*. Although ethyl acetate extract showed medium activity on *C. albicans*, ethanol extract did not inhibit well. Ethanol extract was found to possess medium antimicrobial activity against *E. coli*,however, ethyl acetate exhibited low activity. Methanol, chloroform and water extracts were observed to exhibit low antimicrobial activities against all tested microorganisms whereas pet-ether extract showed low activity against only *B. subtilis*, *P. aeruginosa*, *C. albicans* and *E. coli*.

Table 7: Inhibition Zone Diameters of some Crude Extracts against Six-Microorganisms by Agar Well Diffusion Method

Organisms	Inhibition Zone Diameters (mm) of Crude Extracts						
	PE	**EA**	**EtOH**	**MeOH**	**$CHCl_3$**	**Water**	**Control**
B. subtilis	11 (+)	16(++)	15 (++)	14 (+)	12(+)	12(+)	-
S. aureus	-	13 (+)	13 (+)	14(+)	12(+)	12(+)	-
P. aeruginosa	11(+)	11(+)	14(+)	12(+)	12(+)	13(+)	-
B. pumilus	-	16(++)	15(++)	12(+)	12(+)	12(+)	-
C. albicans	11(+)	15(++)	14(+)	12(+)	12(+)	13(+)	-
E. coli	11(+)	13(+)	15(++)	11(+)	11(+)	13(+)	-

Agar Well – 10 mm ; control - solvent used; 10 mm ~ 14 mm (+) (low activity); 15 mm ~ 19 mm (++) (medium activity) ; above 20 (+++) (high activity)

Antitumor Activity of the Bark of *S. oleosa*

The antitumor activity of ethanol and watery extracts of the bark sample was investigated by using PCG test with the isolated tumor forming bacterium *A. tumefaciens*. The 48 h broth cultures containing 5 x 10^9 cells/mL were used to inoculatethe potato disc. The tested samples were dissolved in DMSO to dilute and the diluted samples were mixed with the bacterial culture for inoculation. After preparing the inoculums, the bacterial suspension was inoculated on the cleaned and sterilized potato discs, and incubated at room temperature for 3 days. Then the tumors appeared on potato discs and checked by staining the knob with Lugol's (I_2-KI) solution. In the control, the formation of white knob on the blue background indicated tumor formation. The active test samples did not form any tumor on the potato discs and its surface remained blue. This experiment revealed that all of the tested samples exhibited the inhibition of tumor formation at the dose of 0.2 g/disc after 5 days and 7 days treatment (Table 8).

Table 8: Observation of Tumor Inhibition by Different Concentrations of Crude Extracts of the Bark Sample

Extracts	Days	Observation of Tumor Formation by Different Concentrations of Crude Extracts		
		0.10 g/disc	0.15 g/disc	0.20 g/disc
MeOH		+	+	-
EtOH	5	+	+	-
H_2O		+	+	-
MeOH		+	+	-
EtOH	**7**	+	+	-
H_2O		+	+	-
Control	++			

(+) Tumor formation (-) No Tumor formation

Cytotoxicity of the Bark of *S. oleosa*

The cytotoxicity of water and ethanol extracts fromthe sample was evaluated by brine shrimp cytotoxicity bioassay. This bioassay is general toxicity screening for bioactive phytoconstituents and their derivatives. A model animal that has been used for this purpose is the brine shrimp, *Artemiasalina* (Tawaha, 2006). The cytotoxicity of crude extracts was expressed in term of mean ± SEM (standard error mean) and LD_{50} (50% Lethality Dose) and the results are shown in Table 9. In this experiment, standard potassium dichromate ($K_2Cr_2O_7$) and caffeine were chosen because $K_2Cr_2O_7$ is well-known toxic in this assay (Salinas and Fernendez, 2006) and caffeine is a natural product. As shown in Table 9, the ethanol extract of the selected sample was more toxic to brine shrimp than the watery extract. The LD_{50} values of EtOH and watery extracts were 2.69 µg/mL and 8.85 µg/mL, respectively. On the other hand, the ethanol and watery extracts were less toxic than standard $K_2Cr_2O_7$(LD_{50} 1.5 µg/mL) and more toxic than caffeine(LD_{50} >1000 µg/mL) to brine shrimp. These results revealed that the plant extracts possessed cytotoxic activity and can be used as a source of cytotoxic compounds. The selected plant sample can be used in traditional medicine to treat many kinds of diseases. The reported cytotoxic plants in this study are worth of further pharmacological and phytochemical studies in order

to define what kind of bioactivity they have and to isolate the natural active constituents, which are responsible for the activity.

Table 9: Cytotoxicity of Ethanol and Watery Crude Extracts of the Bark Sample

Crude extract	Dead % by using different concentrations (μg/mL) of samples				LD_{50} (μg/mL)
	1	10	100	1000	
EtOH	44.7±1.7	73.1±1.1	85.5±7.8	87.9±7.4	2.69
Water	36.4±2.7	51.9±8.7	77.6±2.5	80.5±6.4	8.85
*$K_2Cr_2O_7$	48.63±19.19	73.13±4.076	74.67±11.8	100±0	1.50
*Caffeine	0 ± 0	0 ± 0	9.582±0.917	12.73±4.103	>1000

*****standard

Antiproliferative Activity of the Bark of *S. oleosa*

Cancer is a malignant tumor or malignant neoplasm, is a group of diseases involving abnormal cell growth with the potential to invade or spread to other parts of the body. Many traditional plant treatments for cancer are used throughout the world, and some of these plants have been scrutinized while a good number of them are yet to receive scientific scrutiny. Among them, the bark of *S. oleosa* was selected for this study since they are widely distributed in Myanmar. Antiproliferative activity is the activity relating to a substance used to prevent or retard the spread of cells, especially malignant cells, into surrounding tissues. Antiproliferative activity was studied in vitro using human cancer cell lines.Screening of antiproliferative activities of ethanol and watery extracts from the bark of *S. oleosa*was done by using two human cancer cell lines such as Hela (human cervix cancer) and MCF7 (human breast cancer). Antiproliferative activity was expressed as the IC_{50} (50 % inhibitory concentration) value. 5-Fluorouracil was used as positive control. The antiproliferative activity of crude extracts are summarized in Table 10. From the results, the IC_{50} values were found to be 142.58 μg/mL againstcervix cancer and 135.63 μg/mL against breast cancer by ethanol extract and 150.31 μg/mL against cervix cancer and 178.18 μg/mL against

breast cancer by watery extract, respectively. Since the lower the IC_{50} values, the higher the antiproliferative activity, ethanol extract was more potent than watery extract in antiproliferative activity on the selected cell lines.

Table 10: Antiproliferative Activity of Crude Extracts against Two Types of Cancer Cell Lines

Samples	IC_{50} (μg/mL) of various samples against tested cell lines	
	Hela	**MCF 7**
EtOH Extract	142.58	135.63
Water Extract	150.31	178.18
5FU*	3.102	4.821

Hela - human cervical cancer cell lines
MCF 7 - human breast cell lines
5FU* - Fluorouracil (drug for cancer)

Conclusion

From the overall assessment concerning with investigation of phytochemicals and some biological activities on the bark of*S. oleosa* (Lour.) Oken. (Gyo), ethanol extract was observed to possess higher antimicrobial, antioxidant and antiproliferative activities than watery extract, it might be due to its higher contents of total phenols and total flavonoids. According to the observations, since the ethanol and watery extract of Gyo bark showed these activities, these extracts may be effectively used for the treatment of skin disease, wound infections, diarrhea and also as antioxidant for curing the oxidative stress related diseases, some forms of cancer and some age-related disorders. The quantitative and qualitative phytochemical analytical data are also expected to be applicable to some extent in the medicinal formulation by using the bark of *S. oleosa*.

Acknowledgements

The authors would like to express our gratitude to the Department of Higher Education, Ministry of Education, Myanmar, for their permission to do this research and also to the Myanmar Academy of Arts and Science for allowing to read this paper.

References

Ali, N., Zada, A., Ali, M. and Hussain, Z. (2016).“Isolation and identification of *Agrobacterium tumefaciens* from the Galls of Peach Tree”.*Journal of Rural Development and Agriculture*, vol. 1(1), pp. 39-48.

Ayoola, G. A., Coker, H. A. B., Adesegun, S. A., Bello, A. A. A., Obaweya, K., Ezennia, E. C., and Atangbayila, T. O. (2008). “Phytochemical Screening and Antioxidant Activities of Some Selected Medicinal Plants Used for Malaria Therapy in Southwestern Nigeria”.*Tropical Journal of Pharmaceutical Research*, vol. 7, pp. 1019–1024.

Bhat, S. V., Nagasampagi, B. A. and Meenakshi, S. (2009). *Natural Products:Chemistry and Applications*. Oxford: 1st Ed., Alpha Science International Ltd., 1-242.

Brand-Williams, W., Cuvelier, M. E.andBerse, C. (1995). "Use of a Free Radical Method to Evaluate Antioxidant Activity".*Lebensm.-Wiss. u.-Technol*., vol. 28 (1),pp. 25-30.

Dockery, M. and Tomkins, S. (2000). *Brine Shrimp Ecology*.London : 1st Ed., The British Ecology Society, pp. 92-93.

Ghosh, P., Chakraborty, P., Mandal, A., Rasul, M. G., Chakraborty, M. and Saha, A.(2011). “Triterpenoids from Schleicheraoleosa of Darjeeling Foothills and their antimicrobial activity”.*Indian Journal of Pharmaceutical Science*, vol.73, pp. 231-233.

Harborne, J. B. (1973). *Phytochemical Methods : A Guide to Modern Techniques of Plant Analysis*.London: 2nd Ed., pp. 37-38.

Ikram, E. H. K., Eng, K. H., Jalil, A. M. M., Ismail, A., Idris, S., Azlan, A., Nazri, H. S. M. , Diton, N. A. M. and Mokhtar, R. A. M. (2009). “Antioxidant capacity and total phenolic content of Malaysian underutilized fruits”. *Journal of Food Composition and Analysis*,vol. 22, pp. 388-393.

Kalita, S., Kumar, G., Karthik, L. and Rao, K. V. B. (2011)."Phytochemical Composition and *In Vitro* Hemolytic Activity of *Lantana camara* L.(Verbenaceae) Leaves".*Pharmacology*,vol.1, pp. 59-67.

Kiranmai, M., Mahender, K. C. B., and Ibrahim, M. D. (2011). “Free Radical Scavenging Activity of Neem Tree (*Azadirachta indica* A. Juss Var., Meliaceae) Root Bark Extract”.*Asian Journal of Pharmaceutical and Clinical Research*,vol.4 (4), pp.134-136.

Mahaptma, S. P. and Sahoo, H.P. (2008). “An Ethano-medico-botanical Study of Bolangi, Orissa, India: Native plant remedies against Gynaecological diseases”. *International Journal of Ethanobotanical Research*, vol. 12, pp. 846-854.

Marinova, G. and Batchvarov, V.(2011). "Evaluation of the Methods for Determination of the Free Radical Scavenging Activity by DPPH", *Bulgarian Journal of Agricultural Science*.vol.17, pp. 11–24.

Maw, S. S., Mon, M. M. and Oo, Z. K. (2011)."Study on Antioxidant Activities of Some Herbal Extracts".*World Academy of Science, Engineering and Technology,* vol.51, pp. 450–452.

Palanuvej, C. and Vipunngeun, N. (2008). "Fatty Acid Constituents of Schleicheraoleosa(Lour) Oken. Seed Oil".*Journal of Health Research*,vol. 22(4), pp. 203.

Perez, C., Paul, M. and Bazerque, P. (1990). "Antibiotic Assay by Agar Well Diffusion Method.". *Alta BioMed Group Experiences,*vol. 15, pp.113-115.

Salinas, M. M. G. and Fernandez, S. S. (2006). "A Modified Microplate Cytotoxicity Assay with Brine Shrimp Larvae (*Artemiasalina*)".*Pharmacology*, vol.3, pp. 633–638.

Saxena, M., Saxena, J., Nema, R., Singh, D. and Gupta, A. (2013)."Phytochemistry of Medicinal Plants".*Journal of Pharmacognosy and Phytochemistry*,vol. 1(6), pp.168-172.

Tawaha, K. A. (2006). "Cytotoxicity Evaluation of Jordanian Wild Plants Using Brine Shrimp Lethality Test". *J. Appl. Sci*., vol. 8, pp. 12–17.

Thind, T. S., Rampal, G., Agrawal, S. K., Saxena, A. K., and Arora, S. (2010). "Diminution of Free Radical Induced DNA Damage by Extracts/Fractions from bark of *Schleicheraoleosa* (Lour.) Oken". *Drug and Chemical Toxicology*, vol. 33, pp. 329-336.

Win, N. N., Ito T., Aimaiti, S., Kodama, T., Imagawa, H., Ngwe, H., Asakawa, Y., Abe, I., Morita, H. (2015). "Kaempulchraols I-O: New Isopimarane Diterpenoids from *Kaempferiapulchra* Rhizomes Collected in Myanmar and their Antiproliferative Activity". *Tetrahedron*, vol. 71, pp. 4707-4713.

SYNTHESIS OF ZINC OXIDE NANOPARTICLES USING *Aloe vera* LEAF AQUEOUS EXTRACTS AND ITS CHARACTERIZATION

Kyaw San Min[1], Ohn Ohn Soe[2] and Daw Hla Ngwe[3]

Abstract

The aim of this research was to synthesize zinc oxide nanoparticles via green routes using *Aloe vera* leaf aqueous extracts as well as via chemical method and to study its characteristics. In biosynthesis of zinc oxide nanoparticles, zinc acetate was used as a precursor and *A. vera* leaf hot and cold aqueous extracts used as reducing and stabilizing agents. On the other hand, zinc oxide nanoparticles were synthesized chemically from zinc acetate in the presence of sodium hydroxide. The synthesized zinc oxide nanoparticles were characterized by X-ray diffraction (XRD), FT IR, scanning electron microscopy (SEM) and thermogravimetric /differential thermal analysis (TG-DTA) techniques. The amount of yield percents of the synthesized ZnO NPs obtained by biosynthesis method were higher than those of the chemical method at the same temperature. The zinc oxide nanoparticles were observed as particles agglomeration studied by the morphology using SEM images and had hexagonal wurtzite structure with the lattice constants of a = b = 3.2511 Å and c = 5.2076 Å in average crystallite size about 18 ~ 19 nm, according to XRD analysis. FT IR spectrum showed the Zn-O absorption bands in range between 600 ~ 400 cm^{-1}. TG-DTA analysis resulted the weight loss about 4 ~5 % of the synthesized zinc oxide nanoparticles at nearly 250 °C. Small weight losses of zinc oxide samples indicated the thermal stability of the synthesized zinc oxide nanoparticles.

Keywords*:* Biosynthesis, ZnO nanoparticles, *Aloe vera* leaf aqueous extracts, wurtzite structure, SEM, XRD, FT IR, TG-DTA

Introduction

The term “nano” is derived from the Greek word “nanos” which means small and it is used as the prefix for one billionth part (10^{-9}). "Nano" is now a popular label for much of modern science, and many “nano” words have recently appeared in dictionaries, including: nanometer, nanoscale, nanoscience, nanotechnology, nanotube, nanowire, and nanorobot (Sovan,

1. 2 PhD candidate, Department of Chemistry, University of Yangon
2. Dr, Associate Professor, Department of Chemistry, Loikaw University
3. Dr, Professor and Head (Retd.), Department of Chemistry, University of Yangon

2011). Nanochemistry is a branch of nanoscience, deals with the chemical applications of nanomaterials in nanotechnology. Nanochemistry involves the study of the synthesis and characterization of materials of nanoscale size. Nanotechnology is emerging as a rapidly growing field with its application in science and technology for the purpose of manufacturing new materials at the nano scale level (Rana *et al.,* 2010).

Metal oxides play a very important role in many areas of chemistry, physics, and materials science. The increases surface area and smaller size of these particles make them an ideal antibacterial agent. The zinc oxide nanoparticles are of significant interest as they provide many practical applications in worldwide (Mayekar *et al.,* 2013).

Particles are further classified according to diameter. Coarse particles cover a range between 2,500 and 10,000 nanometers. Fine particles are sized between 100 and 2,500 nanometers. Ultrafine particles, or nanoparticles are between 1 and 100 nanometers in size.

Synthesis Approaches and Techniques

To prepare these nanomaterials, novel synthesis procedures have been developed that can be described as physical and chemical methods. In general, there are two approaches to the synthesis of nanomaterials and the fabrication of nanostructures: top-down and bottom-up. Top-down approach refers to slicing or successive cutting of a bulk material to get nanosized particles. Bottom-up approach refers to the build-up of a material from the bottom. Both approaches play very important roles in nanotechnology (Zheng**,** 2009).

Currently, a large number of physical, chemical and biological methods are available to synthesize different types of nanoparticles. The chemical synthesis involves toxic solvents, high pressure, energy and high temperature conversion and microbe involved synthesis is not feasible industrially due to its lab maintenance (Ayodeji and Olabisi, 2013). Organic chemical solvents are toxic and require extreme conditions during nanoparticle synthesis (Parthasarathy *et al.,* 2016). The development of safe eco-friendly methods for biosynthesis production is now of more interest due to simplicity of the procedures and versatility (Vishwakarma, 2013). Plant

extracts function as stabilizing, capping or hydrolytic agents. These plant extracts also allow a controlled synthesis (Mohammed Osman and Mustafa, 2015).

Physical and Chemical Properties of Zinc Oxide

Zinc oxide is an inorganic compound with the formula ZnO. It usually appears as a white powder known as zinc white. It is usually crystallizes in three different forms: hexagonal wurtzite (Figure 1), cubic zinc blende and cubic rocksalt (rarely). Among them, the hexagonal wurtzite is most stable at ambient conditions. In zinc oxide, zinc and oxide centers are tetrahedral, except rocksalt (Behera, 2013).

In nature, zinc oxide is usually orange or red in colour due to manganese impurity and other elements. Crystalline zinc oxide is thermochromic, which changes from white to yellow colour when heated and reverting to white colour on cooling. This change in colour is caused by a very small loss of oxygen at high temperatures. Zinc oxide is amphoteric oxide. It is nearly insoluble in water and alcohol, but it is soluble in (degraded by) most acids, that is it reacts with both acids and alkalis (Behera, 2013).

Type of Compound - Inorganic Compound

Molecular Formula - ZnO
Molar Mass - 81.408 g/mol
Appearance - White Solid
Odour - Odourless
Relative Density - 5.607
Melting Point - 1975 ^{o}C
Refractive Index - 2.004

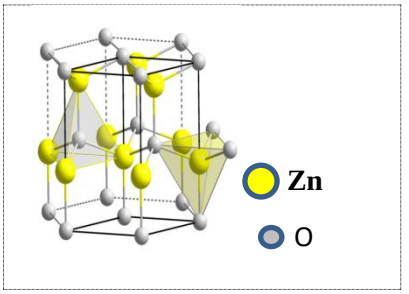

Figure 1: Hexagonal wurtzite structure model of ZnO

Advantages of Nanoparticles Synthesis

ZnO nanoparticles can be prepared on a large scale at low cost by simple solution methods, such as alkali precipitation, thermal decomposition, hydrothermal synthesis, sol-gel methods, spray pyrolysis and other routes.

Among all these different methods, the precipitation is one of the most important methods to prepare nanopowder, due to its excellent advantages such as low cost, low temperature, non-toxic operation and environmental friendliness. It is suitable for industrial, technical and medical applications due to its diverse properties which have been found to strongly depend on their morphology. So, it is necessary to confirm by techniques employ for nanoparticles characterization.

So, the biosynthesis method is the best option for the synthesis of nanoparticles by using *A. vera* leaf aqueous extracts. In this present work, *A. vera* leaf extracts were used as reducing agent for synthesis of zinc oxide nanoparticles and the characteristics of the prepared zinc oxide nanoparticles were studied by XRD, SEM, FT IR and TG-DTA analyses.

Materials and Methods

The experiments were carried out at Department of Chemistry, University of Yangon. All of the chemicals used in the present work were analytical reagent grade. Fresh *Aloe vera* leaves were purchased from the local market in Hledan, Kamayut Township, Yangon. The samples were identified by authorized botanist of Department of Botany, University of Yangon.

Preparation of *Aloe vera* Leaf Aqueous (Hot and Cold) Extracts

The fresh *A. vera* leaf (100 g) were thoroughly washed with distilled water, dried and then boiled in 150 mL of deionized water (solution changed from watery to light green) for half an hour. The resulting solution was cooled and filtered to get the *A. vera* aqueous hot extracts (AHE).

On the other method, *A. vera* leaf (100 g) were thoroughly washed with distilled water, dried and then percolated in 150 mL of deionized water for 24 h. The resulting solution was filtered to get the *A. vera* aqueous cold extracts (ACE) (Parthasarathy *et al.,* 2016).

Preliminary Phytochemicals Screening of *A. vera* Leaf Aqueous Extracts

Preliminary phytochemical tests were performed to know the different types of compounds present in *A. vera* leaf aqueous extracts. Phytochemicals screening for alkaloids, α-amino acid, carbohydrates,

coumarins, cyanogenic glycosides, flavonoids, glycosides, phenolic compound, quinones, saponins, steroids, tannins and terpenoids were carried out by the reported methods.

Biosynthesis and Chemical Synthesis of ZnO Nanoparticles

In biosynthesis method, 2.00 g, 2 %, w/v of zinc acetate was dissolved in 100 mL of distilled water. Each of (10 mL) *A. vera* leaf aqueous extracts in the ratio of 1:10, v/v was added drop-wise and the resulting mixtures were stirred for 10 min by using a magnetic stirrer at temperature 120 °C. In order to adjust the pH-12 of the solution with sodium hydroxide (2 M) was added drop-wise while stirring. A white crystalline precipitate of zinc hydroxide was obtained, which was washed repeatedly with distilled water and ethanol, filtered and then dried on an oven at 120 °C for 3 h to obtain the zinc oxide nanoparticles (Elizabeth and Mary, 2015).

In chemical method, 2.00 g, 2 %, w/v of zinc acetate was also dissolved in 100 mL of distilled water. 2 M Sodium hydroxide in the ratio of 1:10, v/v was added drop-wise into the 2 % zinc acetate solution with stirring for 10 min by using a magnetic stirrer at temperature 120 °C. A white crystalline precipitate of zinc hydroxide was obtained, which was washed repeatedly with distilled water and ethanol, filtered and then dried on an oven at 120 °C for 3 h to obtain the ZnO nanoparticles (Mayekar *et al.*, 2013).

Characterization of the Prepared Zinc Oxide Nanoparticles

XRD analysis

Zinc oxide nanoparticles were examined by X-ray diffractometer (Rigaku D/max, Japan) for 2θ values ranging from 10° to 70° using (Cu / K-α) radiation at λ = 1.5406 Å. The average crystallites size (D) of the synthesized zinc oxide nanoparticles were calculated by using the well-known Scherrer formula.

SEM analysis

The surface morphological features of synthesized zinc oxide nanoparticles were studied by scanning electron microscope (EVO - 18, Brand

ZEISS, Germany). SEM is a type of electron microscope that produces images of a sample by scanning it with a focused beam of electrons.

FT IR analysis

The prepared zinc oxide nanoparticles were characterized by fourier transform infrared spectroscopy. FT IR infrared radiation refer to the part of electromagnetic spectrum between the visible and microwave regions. The FT IR spectrum recorded in the range 4000–400 cm^{-1} by using FT IR spectrometer (8400-SHIMADZU, Japan) at universities research centre (URC).

TG-DTA analysis

TG-DTA measures both heat flow and weight changes in a material as a function of temperature or time in a controlled atmosphere (Coats, 1963). The stability of the synthesized zinc oxide nanoparticles was studied with the TG-DTA thermogram measured by using Perkin-Elmer thermogravimetric-differential analyzer.

Results and Discussion

Phytochemicals Present in *Aloe vera* Leaf Aqueous Extracts

Preliminary phytochemical screening revealed that alkaloids, α-amino acids, coumarins, flavonoids, glycosides, tannins and terpenoids were found to be present in *A. vera* leaf aqueous extracts. All of these secondary metabolite phytoconstituents could support to reduce zinc acetate to zinc oxide nanoparticles.

Biosynthesis and Chemical Synthesis of Zinc Oxide Nanoparticles

In the biosynthesis, zinc oxide nanoparticles were prepared from zinc acetate in the presence of *A. vera* leaf aqueous hot extracts (AHE) and in *A. vera* leaf aqueous cold extracts (ACE) at 120 °C. The pH of the reaction mixture was controlled at pH-12 by using 2 M sodium hydroxide solution. The ZnO nanoparticles were respectively obtained as a light brown crystalline powder (ZnO-AHE) and as a pale yellow crystalline powder (ZnO-ACE) in 41.17 % and 41.01 % of yields by using *A. vera* leaf aqueous hot extracts and *A. vera* leaf aqueous cold extracts as reducing agent (Figures 2 (a) and 2 (b)).

Zinc oxide nanoparticles were also chemically synthesized from zinc acetate by reducing agent with 2 M soidum hydroxide solution (1:10, v/v) at 120 °C (Jeeva Lakshmi, 2012). The zinc oxide nanoparticles (ZnO-CM) were obtained as white crystalline powder in 38.21 % of yield (Figure 2 (c)).

The yield percents of zinc oxide nanoparticles synthesized by green route and chemical synthesis are listed in Table 1. The yield percents obtained in biosynthesis were slightly higher than that obtained in chemical synthesis (38.21 %). The yield percents of zinc oxide by using *A. vera* leaf aqueous hot extracts (41.17 %) was found to be similar that obtained by using *A. vera* leaf aqueous cold extracts (41.01 %).

Figure 2: Photographs of the synthesized zinc oxide powders by using (a) *A. vera* aqueous hot extracts, ZnO-AHE (b) *A. vera* aqueous cold extracts, ZnO-ACE and (c) chemical method, ZnO-CM

Table 1: Yield Percents of the Synthesized Zinc Oxide Nanoparticles

No.	Methods used	ZnO nanoparticles	Weight of ZnO nanoparticles (g)	Yield of ZnO nanoparticles (%)
1.	Biosynthesis	ZnO-AHE	0.82	41.17
2.	Biosynthesis	ZnO-ACE	0.83	41.01
3.	Chemical synthesis	ZnO-CM	0.76	38.21

Zinc acetate = 2.0 g
ZnO-AHE = ZnO nanoparticles prepared by using *A. vera* leaf aqueous hot extracts
ZnO-ACE = ZnO nanoparticles prepared by using *A. vera* leaf aqueous cold extracts
ZnO-CM = ZnO nanoparticles prepared by using chemical method

Characteristics of Zinc Oxide Nanoparticles

XRD analysis

The x-ray diffraction patterns of ZnO nanoparticles prepared by biosynthesis and chemical synthesis are shown in Figures 3, 4 and 5 for the results of ZnO-AHE, ZnO-ACE and ZnO-CM, respectively. The purity and crystallite size were characterized by studying the x-ray diffraction patterns. It is evident from the diffractograms that, the 7 peaks observed in all of the diffractograms are similar and their peak positions coincide with that of reference values. The 7 peaks noticed are in accordance with ZnO phase. The x-ray diffractograms of ZnO samples obtained at 120 ^{o}C showed well-defined peaks with Miller indices (100), (002), (101), (102), (110), (103) and (112) corresponding to Bragg angles, 31.57^{o}, 34.22^{o}, 36.10^{o}, 47.30^{o}, 56.39^{o}, 62.70^{o} and 67.89^{o} in AHE, 31.66^{o}, 34.30^{o}, 36.18^{o}, 47.46^{o}, 56.47^{o}, 62.76^{o} and 67.84^{o} in ACE and 31.80^{o}, 34.40^{o}, 36.26^{o}, 47.54^{o}, 56.67^{o}, 62.89^{o} and 67.96^{o} in CM, respectively. All diffraction peaks can be readily indexed to hexagonal wurtzite zinc oxide structure with the average crystallite size about 18 ~ 19 nm. X-ray diffraction patterns indicated that the obtained ultrafine nanoparticles are in good crystallinity which exhibited in the range of nano scale (< 100 nm).

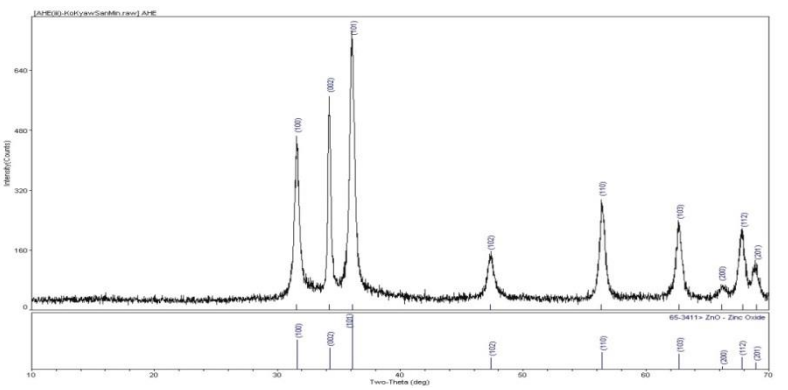

Figure 3: XRD diffractogram of zinc oxide nanoparticles prepared by using *Aloe vera* leaf aqueous hot extracts (10 mL) at 120 ^{o}C

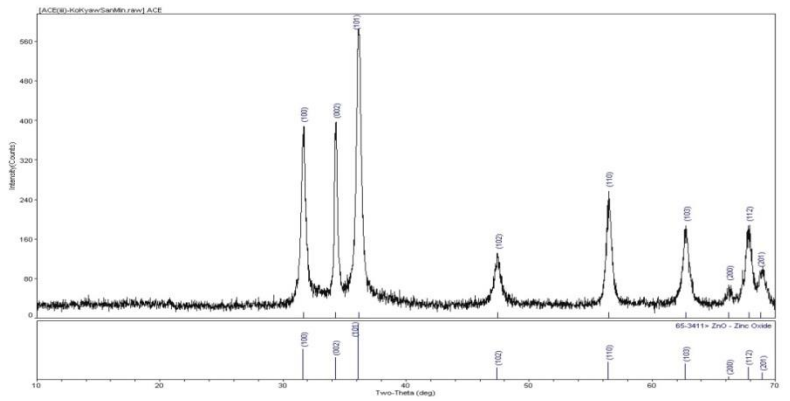

Figure 4: XRD diffractogram of zinc oxide nanoparticles prepared by using *Aloe vera* leaf aqueous cold extracts (10 mL) at 120 ^{o}C

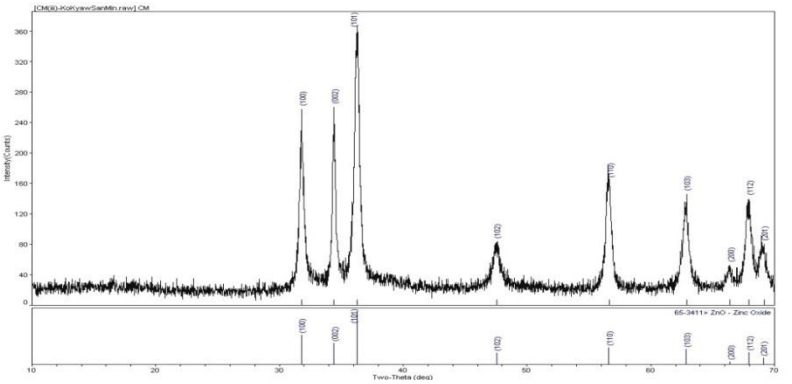

Figure 5: XRD diffractogram of zinc oxide nanoparticles prepared by using sodium hydroxide (10 mL) at 120 ^{o}C

SEM analysis

The SEM analysis was used to identify the size and shape of the zinc oxide nanoparticles. According to the SEM analysis, the morphology of the synthesized all ZnO nanocrystals (Figures 6, 7 and 8) were found to be observed as agglomerated particles at temperature 120 ^{o}C in both of biosynthesis and chemical synthesis.

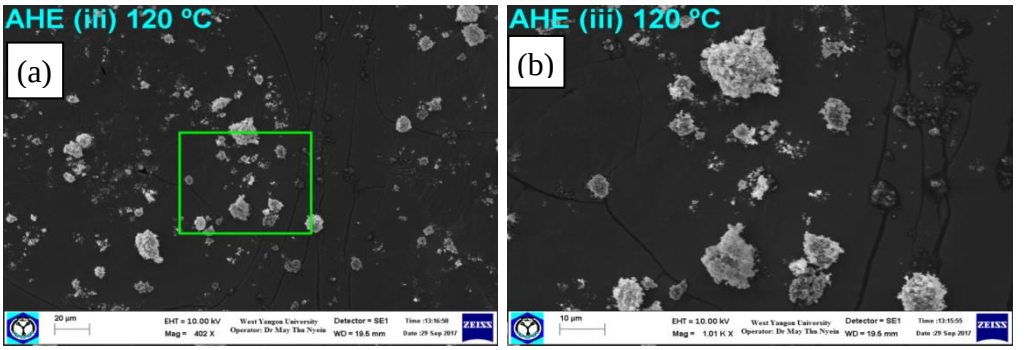

Figure 6: SEM images of the synthesized ZnO nanoparticles (ZnO-AHE) prepared at 120 ^{o}C (a) 402 X magnification and (b) 1000 X magnification

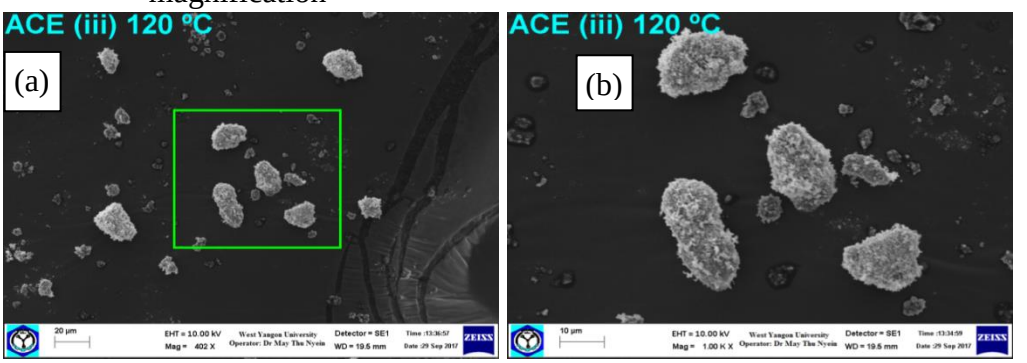

Figure 7: SEM images of the synthesized ZnO nanoparticles (ZnO-ACE) prepared at 120 ^{o}C (a) 402 X magnification and (b) 1000 X magnification

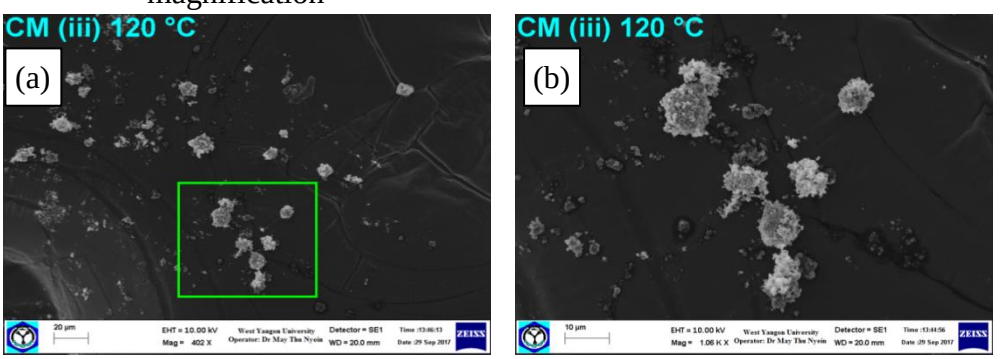

Figure 8: SEM images of the synthesized ZnO nanoparticles (ZnO-CM) prepared at 120 ^{o}C (a) 402 X magnification and (b) 1000 X magnification

FT IR analysis

Fourier Transform Infrared Spectroscopy was used to identify the presence of biomolecules which plays an important role in the biosynthesis of nanoparticles**.** In all of the synthesized ZnO-AHE, ZnO-ACE and ZnO-CM at temperature 120 ^{o}C, the absorption bands observed at 3455, 3431 and 3472 cm^{-1} are due to the O-H stretching vibration of water (Figure 9). The peaks at 1414 and 1383 cm^{-1} which correspond to the O-H bending vibration of water for ZnO-ACE and ZnO-CM (Willard *et al.*, 1965). Similarly, the absorption peaks at 916, 903 and 897 cm^{-1} are also due to the formation of tetrahedral coordination of Zn in all samples. The main absorption peaks at 426, 421 and 419 cm^{-1} which indicated the formation of (Zn-O linkage) zinc oxide nanoparticles (Elizabeth and Mary, 2015).

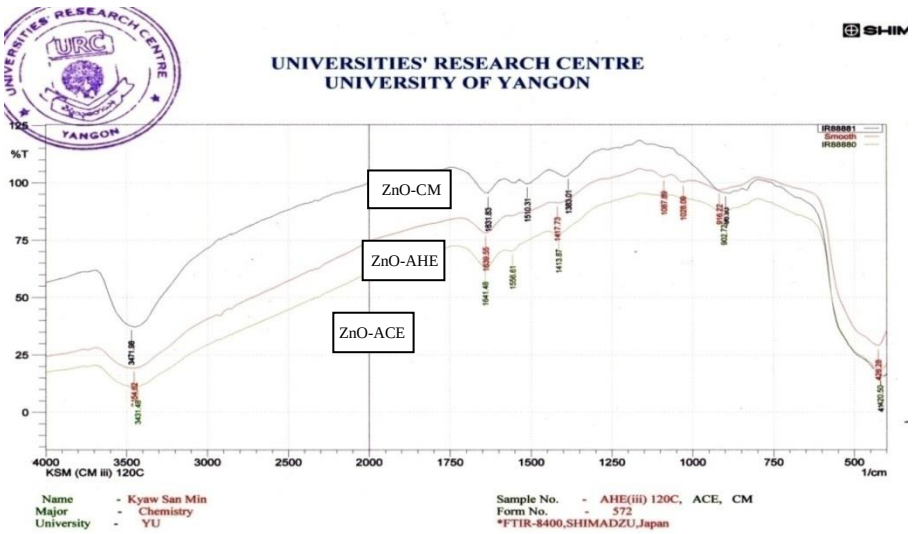

Figure 9: FT IR spectra of zinc oxide nanoparticles [ZnO-AHE, ZnO-ACE and ZnO-CM] prepared at 120 ^{o}C

TG-DTA analysis

The thermogravimetric analysis of the synthesized zinc oxide nanoparticles was performed on Perkin-Elmer thermogravimetric-differential analyzer. It showed that the small endothermic peaks (Figures 10, 11 and 12) for loss of weight (5.10 % in ZnO-AHE, 3.23 % in ZnO-ACE and 2.85 % in ZnO-CM) at nearly 200 ^{o}C due to the loss of water. In TG-DTA thermogram

of ZnO-ACE nanoparticles (Figure 11), a small exothermic peak was continuously observed at nearly 370 ^{o}C, indicating the loss of weight in 1.94 % due to the loss of other organic residues components in the plant extracts. On the other hand, the weight loss (1.19 %) in ZnO-CM nanoparticles, a small exothermic peak (Figure 12) occurred at 370 ^{o}C might be due to the decomposition of precursor leads to the formation of zinc oxide (Zhaol *et al.*, 1998).

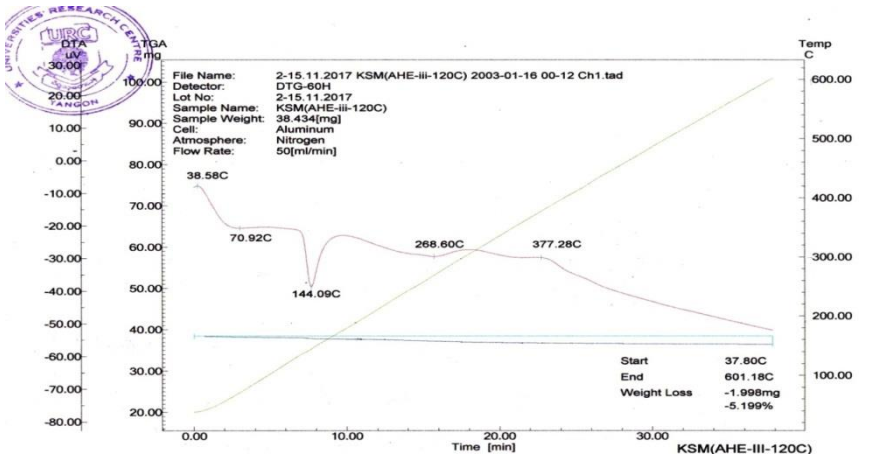

Figure 10: TG-DTA thermogram of the synthesized zinc oxide nanoparticles (ZnO-AHE) prepared at 120 ^{o}C

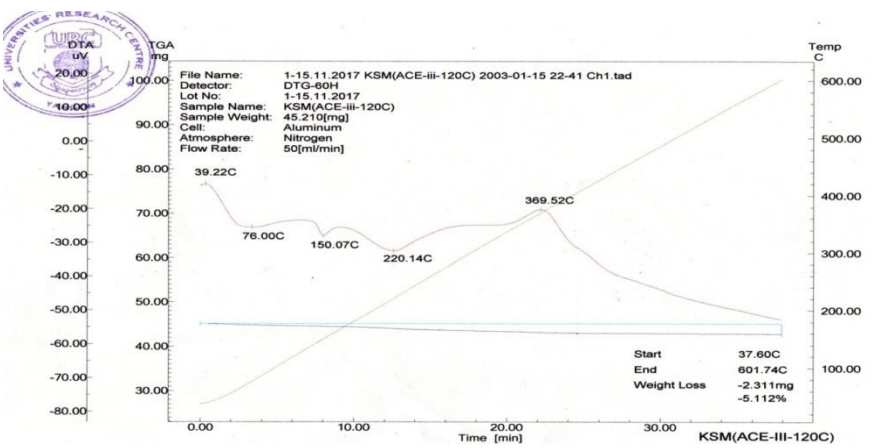

Figure 11: TG-DTA thermogram of the synthesized zinc oxide nanoparticles (ZnO-ACE) prepared at 120 ^{o}C

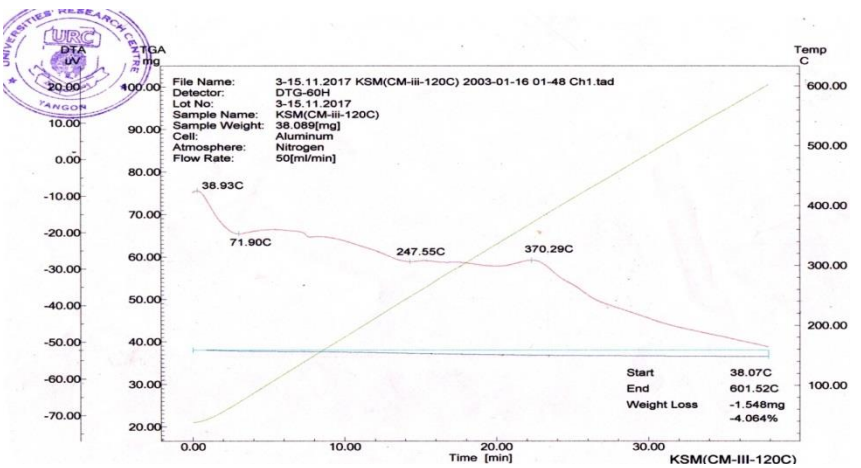

Figure 12: TG-DTA thermogram of the synthesized zinc oxide nanoparticles (ZnO-CM) prepared at 120 ^{o}C

Conclusion

The zinc oxide nanoparticles were synthesized by using zinc acetate as metal ion precursor materials and *Aloe vera* leaf aqueous extracts as reducing and stabilizing agents. Zinc oxide nanoparticles have been successfully synthesized by using *Aloe vera* leaf extracts (hot and cold) and also by chemical method. Preliminary phytochemical constituents in *Aloe vera* leaf aqueous extracts were investigated. In this study, alkaloids, α-amino acid, coumarins, flavonoids, glycosides, tannins and terpenoids were found to be observed while the other compounds (carbohydrates, cyanogenic glycosides, phenolic compound, quinones, saponins and steroids) were not present in *Aloe vera* leaf aqueous extracts. The zinc oxide nanoparticles were respectively obtained as a light brown crystalline powder (ZnO-AHE) and as a pale yellow crystalline powder (ZnO-ACE) while obtained as white crystalline powder (ZnO-CM). The synthesized zinc oxide nanoparticles were characterized by using several techniques such as XRD, SEM, FT IR and TG-DTA. The synthesized zinc oxide nanoparticles with average crystallite size about 18 ~ 19 nm had hexagonal wurtzite structure with the lattice constants of a = b = 3.2511 Å and c = 5.2076 Å, according to XRD analysis. The SEM analysis of ZnO exhibited the morphology of the samples to be networked with some agglomeration. The FT IR studies exhibited a characteristic

absorption peaks of the synthesized ZnO NPs nearly at 450 cm^{-1} (Zn-O linkage) which indicated the formation of zinc oxide nanoparticles.

In this research, according to the XRD and SEM analyses of the synthesized zinc oxide nanoparticles are not different between the two methods used : biosynthesis and chemical methods. However, the amount of yield percents of the synthesized ZnO NPs obtained by biosynthesis method was higher than those of the chemical method at the same temperature. Since, from the results of XRD and FT IR analyses, there was no significant impurity present in all samples synthesized by these two methods at temperature 120 ^{o}C. From the results of TG-DTA analysis, the weight loss of all samples were in the range of 4.064 % to 5.199 % and it was also observed no significantly changed by the temperature affect, except a little amount of weight loss due to removal of water absorbed. The zinc oxide nanoparticles obtained from chemical method were slightly more stable than those of the biosynthesis method. Small weight losses of zinc oxide samples indicated the thermal stability of the synthesized zinc oxide nanoparticles.

Therefore, these two methods used in this study have advantages to prepare zinc oxide nanoparticles that might be due to the lack of toxicity, less expensive, easy and faster process.

Acknowledgements

The authors would like to express their profound gratitude to the Department of Higher Education (Yangon Office), Ministry of Education, Yangon, Myanmar, for provision of opportunity to do this research and Myanmar Academy of Arts and Science for allowing to present this paper.

References

Ayodeji, O. and Olabisi, A. M. (2013). "Synthesis and Characterization of ZnO Nanoparticles with Zinc Chloride as Zinc Source". *Asian Journal of Natural & Applied Sciences*, vol. 2 (2), pp. 41-44

Behera, O. (2013). *Synthesis and Characterization of ZnO Nanoparticles of Various Sizes and Applications in Biological Systems*. Thesis (B.Tech), Deptartment of Biotechnology and Medical Engineering. pp. 1-36

Coats, A. W., and Redfern, J. P. (1963). "Thermogravimetric Analysis: A Review". *Analyst*, vol. 88, pp. 906-924

Elizabeth, V. and Mary, G. (2015). "Green Synthesis of Zinc Oxide Nanoparticles". *International Journal of Advanced Research in Sciences and Engineering*, vol. 4 (1), pp. 307-314

Jeeva Lakshmi, V., Sharath, R., Chandraprabha, M. N., Neelufar, E., Abhishikta, H. and Malyasree, P. (2012). "Synthesis, Characterization and Evaluation of Antimicrobial Activity of Zinc Oxide Nanoparticles". *Journal of Biochemistry Technology*, vol. 3 (5), pp. 151-154

Mayekar, J., Dhar, V. and Srinivasan, R. (2013). "To Study the Role of Temperature and Sodium Hydroxide Concentration in the Synthesis of Zinc Oxide Nanoparticles". *International Journal of Scientific and Research Publications*, vol. 3 (11), pp. 1-5

Mohammed Osman, D. A. and Mustafa, M. A. (2015). "Synthesis and Characterization of Zinc Oxide Nanoparticles using Zinc Acetate Dihydrate and Sodium Hydroxide". *Journal of Nanoscience and Nanoengineering*, vol. 1 (4), pp. 248-251

Parthasarathy, G., Saroja, M., Venkatachalam, M., Gowthaman, P. and Evanjelene, V. K. (2016). "Synthesis of Nanoparticles from *Aloe vera* Extracts – Review Paper". *Imperial Journal of Interdisciplinary Research (IJIR)*, vol. 4 (10), pp. 1570-1575

Rana, S. B., Singh, P., Sharma, A. K., Carbonari, A. W. and Dogra, R. (2010). "Synthesis and Characterization of Pure and Doped ZnO Nanoparticles". *Journal of Optoelectronics and Advanced Materials*, vol. 12, pp. 257-261

Sovan, L. P. (2011). "Nanoparticle : An Overview of Preparation and Characterization". *Journal of Applied Pharmaceutical Sciences*, vol. 1 (6), pp. 228-234

Vishwakarma, K. (2013). *Green Synthesis of ZnO Nanoparticles Using Abrus precatorius Seeds Extract and their Characterization*. M.Sc Thesis, National Institute of Technology, pp. 1- 36

Willard, H. H., Merrit, L. L. and Dean, J. A. (1965). *Instrumental M ethod of Analysis*. New York: 4th Ed., D.Van Nostrand Company Inc., pp. 142-143

Zhaol, X., Zheng, B., Li, C. and Gu, H. (1998). " Acetate-Derived ZnO Ultrafine Particles Synthesized by Spray Pyrolysis ". *Jol. of Powder Technology*, vol. 100, pp. 20□23

Zheng, Z. (2009). *Synthesis and Modifications of Metal Oxide Nanostructures and their Applications*. Inorganic Materials Research Group, Queensland University of Tech. pp. 1-107

STRUCTURAL, OPTICAL AND ELECTRICAL PROPERTIES OF PEROVSKITE $LaCoO_3$ AND $LaFeO_3$ NANO CRYSTALLINE POWDERS

Kay Thi Tun[1], Mya Theingi[2], NweNweAung[3]

Abstract

Perovskite based transition metal oxides has been focused since the last few decades because of its wide range of applications in the environmental catalyst, gas sensors, oxygen permeation membranes, electrode materials in solid oxide fuel cells (SOFCs) etc. The aim of the research work is to study the structural, optical and electrical properties of perovskite type $LaCoO_3$ and $LaFeO_3$. These nanocrystalline powders were synthesized by citrate sol-gel method by using metal nitrates as starting materials and citric acid as the chelating agent. The dried precursor powders of $LaCoO_3$ and $LaFeO_3$ were amorphous and their thermal decomposition occurs stepwise upon heating to 600 °C by TG-DTA analysis. Pure perovskite type single phase $LaCoO_3$ and $LaFeO_3$ powders are formed after heating at 450 °C. The pellets prepared from calcined powders were sintered at 800, 900 and 1000 °C and crystalline pellets were characterized by XRD, FT IR, EDXRF, SEM, UV-Visible spectrometer and LCR meter. The XRD data confirms that the $LaCoO_3$ has hexagonal structure with space group R3c and $LaFeO_3$ has orthorhombic structure with space group Pnma. SEM micrograph shows that nanostructure and EDXRF analysis confirms that the all elements of the sample were present in good agreements with stoichiometric ratio. The optical properties of $LaCoO_3$ and $LaFeO_3$ were studied from UV-Visible spectrophotometer and the optical band gaps were also estimated by using Tauc's relation. The band gap values of these samples are 2.10eV and 2.40 eV respectively and these values are lie within semiconductor band-gap range. Frequency dependence of dielectric behaviour of the two perovskite samples was examined by LCR meter within the frequency range of 100 kHz- 1000 kHz. Dielectric loss tangent and dielectric loss were found to decrease with increase of frequency. The ac conductivity was dependent on the dielectric nature of the prepared samples and it was gradually increased with increase of frequency. The resistivity of $LaCoO_3$ sample is lower than that of $LaFeO_3$ sample. The dc and ac conductivities of $LaCoO_3$ are higher than that of the $LaFeO_3$ sample.

Keywords: Perovskite, $LaFeO_3$, $LaCoO_3$, citrate sol-gel method, optical properties, electrical conductivity

[1]. PhD Candidate, Department of Chemistry, University of Yangon
[2]. Dr, Lecturer, Department of Chemistry, University of Yangon
[3]. Dr, Lecturer, Department of Chemistry, University of Yangon

Introduction

Perovskiteis mixed oxide of transition metals with chemical formula ABO_3 where A is transition metal or lanthanide series cation B is transition metal cation and O is oxide anion. The structure of perovskite is a face-centered cubic cell of cation A and anion O. In the unit cell, cation A locates at the cubic corner and B at the center of the lattice. Several properties such as structure, electronics and magnetics of these compounds depend on the type of cations A and B. The property and use must be considered hand in hand, for example the perovskite for use as gas sensor should have A and B such that ABO_3 exhibits electronic property as semiconductor or if the aim is in fuel cell the selected ABO_3 should have dielectric (K) property. The La-based perovskite of $LaCoO_3$ and $LaFeO_3$ are very interesting compounds and their application can be found in many fields (Haron *et al*., 2016). The $LaCoO_3$ find application in the field of catalyst, fuel cell and gas sensor while the $LaFeO_3$ perovskite have been studied as photocatalyst, gas sensor and cathode for fuel cell (Haron *et al*., 2016). The efficiency of these materials depends on the synthesis methods. Many methods are available for the synthesis of perovskite oxide in the group of La-based perovskite such as solid state reaction, sol-gel method, solution combustion synthesis, hydrothermal synthesis and co-precipitation method etc. (Unikoth *et al*., 2014). In this paper, $LaCoO_3$ and $LaFeO_3$nanocrystalline samples were synthesized via a simple citrate sol-gel method and their structural, optical and electrical properties were investigated for further applications. This synthesis route has several advantages such as simplicity, low cost and no waste compared with other methods.

Materials and Methods

Synthesis of Perovskite$LaCoO_3$ and $LaFeO_3$ Powder

Perovskite$LaCoO_3$ and $LaFeO_3$nanocrystallite powders were prepared with some based modification on the citrate sol-gel method. All chemicals were analytical grade and used without further purification. They were procured from the British Drug House Chemical ltd., England (BDH). The deionized water was used throughout the experiment. La $(NO_3)_3$.$6H_2O$ and

Co $(NO_3)_2.6H_2O$ were used as starting materials for preparation of $LaCoO_3$. A specific amount of each salt was dissolved in deionized water and mixed together with vigorous stirring. And then citric acid solution was added in the mixture solution. Citric acid that was equivalent in gram mole with that of total cations (La^{3+}, Co^{2+}) (Anupama and Prasad, 2015).Subsequently, 5 mL of ethylene glycol was added to the mixture solution. Resulting purplecoloured solution was heated at 80 °C under continuous stirring. After being heated for about 6 h, the resulting solution became highly viscous and the purple transparent gel was formed. Finally, the xerogel was obtained after the gel was dried completely in an oven at 120 °C for 6 h. The xerogel was ground in the mortar and pestle (Khetre *et al*., 2010). The xerogeldried powder was calcined at 400 °C, 450 °C and 500 °C each for 4 h. The resulting calcined powders were compacted in a mortar driven uniaxial hydraulic press, using a mold 10 mm in diameter. The pellets thus obtained were sintered at 800, 900 and 1000 °Cfor 4 h. For perovskite$LaFeO_3$, the same procedure as above was applied but with Fe $(NO_3)_3.9H_2O$ as starting material. The citrate sol-gel synthesis occurs according to the following overall reaction (1) and (2) which give rise to perovskite powders and gaseous species.

$$La(NO_3)_3.6H_2O + Co(NO_3)_2.6H_2O + nC_6H_8O_7 + nC_2H_6O_2 \xrightarrow{\Delta} LaCoO_3 + nCO_2\uparrow + nN_2\uparrow + nH_2O \quad \text{----------} \quad (1)$$

$$La(NO_3)_3.6H_2O + Fe(NO_3)_3.9H_2O + nC_6H_8O_7 + nC_2H_6O_2 \xrightarrow{\Delta} LaFeO_3 + nCO_2\uparrow + nN_2\uparrow + nH_2O \quad \text{----------} \quad (2)$$

Characterization of the Prepared Perovskite$LaCoO_3$ and $LaFeO_3$

The thermal decomposition behaviours of the powders prepared by citrate sol-gel method were characterized by thermogravimetric and differential thermal analysis (TG-DTA) at a heating rate of 10°C/min in nitrogen. The phase identification of the as-prepared powder was performed using X-ray diffractometer with CuK_α radiation (λ =1.5405Å).The lattice parameters and the average crystallite size were calculated using PDXL-software. The crystallite size was also compared with the values obtained using Debye-Scherrer formula, $D = 0.9\,\lambda/\beta\cos\theta$, where λ is X-ray wavelength and β is peak width at half maximum.The FTIR measurements have been performed in the region of 400- 4000 $cm^{-1}$by using 8400

SHIMADZU, Japan FT IR spectrometer. The elemental compositions of $LaCoO_3$ and $LaFeO_3$ perovskite oxides prepared by citrate sol-gel method were investigated by using energy dispersive X-ray fluorescence spectrometer (EDXRF). The morphology of the prepared nano powders was characterized by scanning electron microscopy (SEM). The samples were characterized by UV-visible spectrophotometer (SHIMADZU UV-1800) for wavelength dependence absorption spectrum. The frequency dependence dielectric behavior was examined by LCR meter (GWInstek LCR- 8110 G).

Results and Discussions

The perovskite$LaCoO_3$ and $LaFeO_3$ were prepared by citrate sol-gel method. The precursor powders of two perovskite were calcined at different temperature 400, 450 and 500 °C for 4 h. The resulting calcined powders were compacted at 5 ton pressure in a motor driven uniaxial hydraulic press, using a mold 10 mm in diameter. The pellets were sintered at 800, 900 and 1000 °C for 4 h. Phase formation began at 450 °C and complete phase pure perovskite material was obtained on sintering the powders at 800, 900 and 1000 °C for 4h. The two perovskite samples were characterized by TG-DTA, XRD, FT IR, EDXRF and SEM analysis. The optimum sintering temperature was 900 °C and the average crystallite size was found 40.93 nm. The optical properties of perovskite$LaCoO_3$ and $LaFeO_3$ at 900 °C were studied by UV-visible absorption spectroscopy. Frequency dependence dielectric behavior of the pellet samples were determined by LCR meter.

Thermal Analyses

Thermal analysis can be utilized to identify the thermal stability and the decomposition temperature of the prepared perovskite. Figure 1 shows the TG-DTA thermogram of dried $LaCoO_3$xerogel powder. It was observed that two exothermic peaks at 170 °C and 412 °C formed in TG-DTA thermogram. The two exothermic peaks related to the combustion of organic residues and decomposition of metal nitrates due to the formation of expected perovskite $LaCoO_3$. It was found that the losses in weight were 12.49 % and 69.10 %. Above 450°C, there was no significant peak and the compound was thermally stable. Figure 2 shows the TG-DTA thermogram of dried $LaFeO_3$ xerogel powder. There were three exothermic peaks 261°C, 365°Cand 408°Cobserved

in the thermogram. The three exothermic lines related to the decomposition of metal nitrates, combustion of organic chelating and gelating agent, respectively, due to the formation of expected perovskite $LaFeO_3$. It was found that the weight losses percent were 35.75 %, 27.66 % and 17.30 %. Above 450°C, it was observed that there was no significant peak and the compound was thermally stable. From above results, it was concluded that the phase formation of $LaFeO_3$ and $LaCoO_3$ started at around 450 °C.

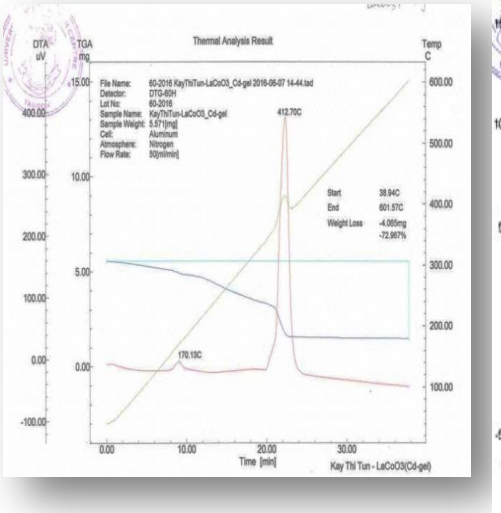

Figure 1: TG-DTA curve of the xerogel$LaCoO_3$ powder

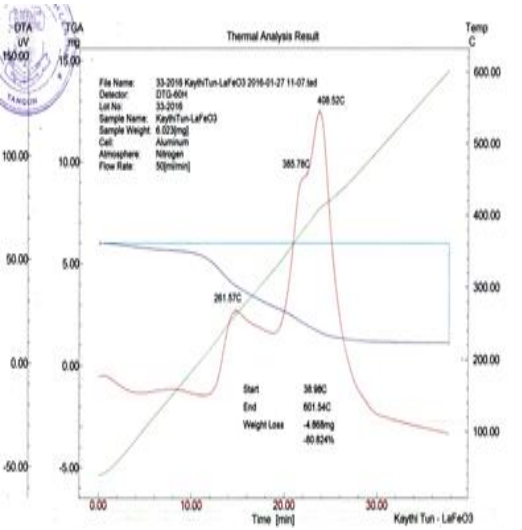

Figure 2: TG-DTA curve of the xerogel

XRD Analysis

From XRD analysis, the formation of perovskite phase was evidenced in the prepared samples of $LaCoO_3$ and $LaFeO_3$ obtained at various temperatures as shown in Figures 3(a-b) and 4(a-b).For $LaCoO_3$, the amorphous nature was found at calcination temperature 400 ˚C. The crystalline nature of $LaCoO_3$ nanoparticles was found at calcination temperatures of 450 ℃ and 500 ℃ and the crystallite sizes of $LaCoO_3$ found to be 19.37 nm and 26.08 nm respecively. The mixture of La_2O_3 and Co_2O_3 was obtained if the sintering temperature was lower than 900°C.The hexagonal $LaCoO_3$perovskite formed at 900 °C (matched with ICDD file no.

00-048-0123l) and the crystalline size was 40.93 nm.For$LaFeO_3$, the amorphous nature was found at the calcination temperature at 400 °C and the crystalline nature of$LaFeO_3$ nanoparticles was found at 450 ˚C and 500 ˚C. The crystalline size of $LaFeO_3$ found to be 27.87 nm and 28.92 nm, respectively. The effect of variation of sintering temperature on$LaFeO_3$ is shown in Figure 4(b). All of the peaks can be indexed to be $LaFeO_3$ structure of orthorhombic due to the lattice parameters aggrement with literature. The product obtained from sintering temperatures at 800 °C, 900 °Cand 1000 °C was orthorhombic perovskite $LaFeO_3$ (matched with ICDD file no.00-015-0148) with crystallite sizes of 51.28 nm, 49.76 nm and 66.73 nm respectively. It shows a trend that the average crystallite size is larger at higher calcination temperature, which is related to the grain growth (Theingi, 2013).The resultant data are presented in Table 1.

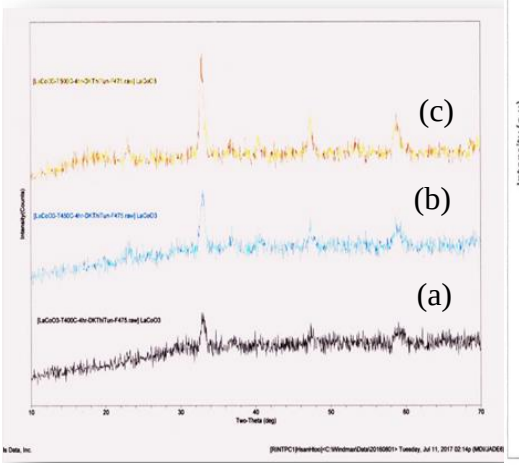

Figure 3:(a)XRD diffraction patterns of $LaCoO_3$powder at different calcined temperatures(a) 400 °C (b) 450 °C (c) 500 °C

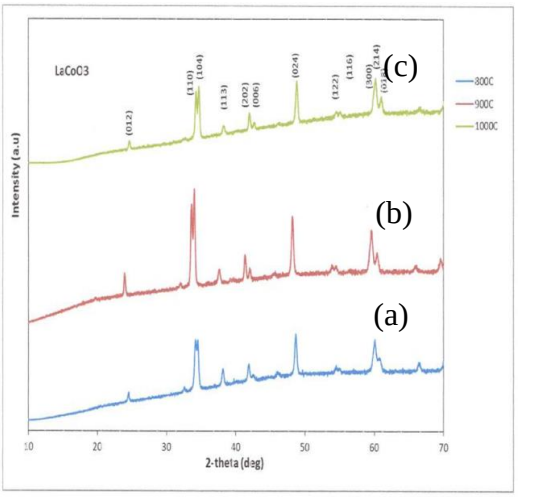

Figure 3: (b) XRD diffraction patterns of $LaCoO_3$ samples at sintered 4 temperatures at (a) 800˚ C (b) 900 °C (c) 1000 ˚ C

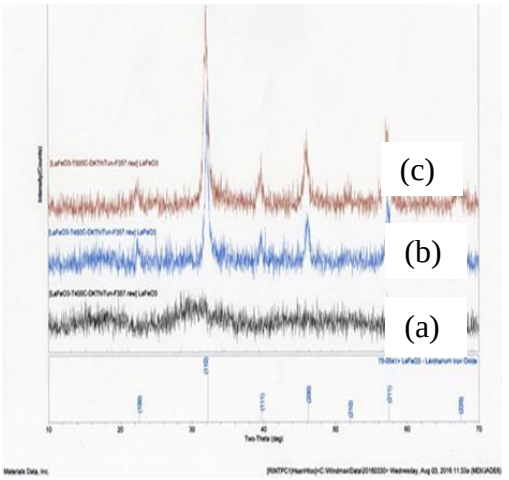

Figure 4: (a) XRD diffraction patterns of $LaFeO_3$ powder at different calcined temperatures(a) 400 °C (b) 450 °C (c) 500 °C

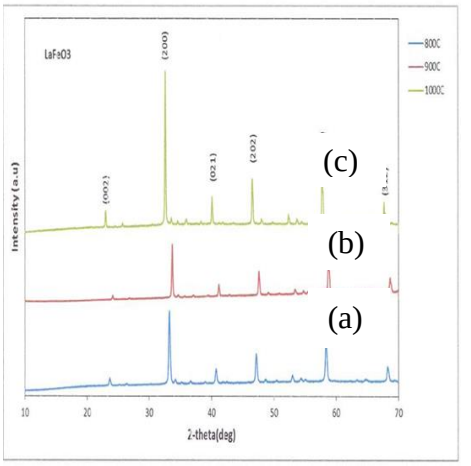

Figure 4: (b) XRD diffraction patterns of $LaFeO_3$ samples at sintered temperatures (a)800˚ C (b) 900 °C (c)1000 ˚ C

Table 1: Crystallite Size of $LaCoO_3$ and $LaFeO_3$ Nanoparticles Prepared by Citrate Sol-gel Method

Sample	Temperature (°C)	Crystallite size/D (nm)
$LaCoO_3$	450	19.37
	800	17.08
	900	40.93
	1000	37.17
$LaFeO_3$	450	27.68
	800	51.28
	900	49.76
	1000	66.73

FTIR Analysis

The $LaCoO_3$and $LaFeO_3$ nanopowder were mixed with appropiate amount of KBr salts to form pellets in order to observe FT IR spectra. FT IR spectra with wavenumber ranged from 400 – 4000 cm^{-1} are shown in Figures 5 and 6 for $LaCoO_3$ and $LaFeO_3$ prepared by citrate sol-gel method,

respectively. Both perovskites$LaCoO_3$ and $LaFeO_3$ showed an intense band around 550 cm^{-1} and 417 cm^{-1} due to metal-oxygen stretching vibration group and stretching vibration of La-O group. The low intense peak observed in $LaFeO_3$ at 3421cm^{-1} and 1629 cm^{-1} are respectively due to the stretching vibration and bending vibrationof O- H group in water molecules. But the hydroxyl group band was not observed in the FT IR data of $LaCoO_3$(Ghosh and Dasgupta, 2010).

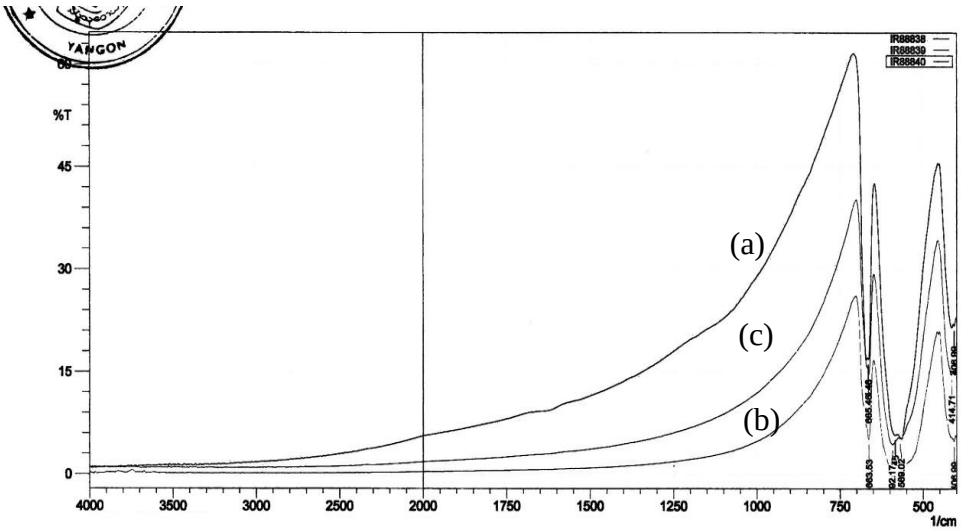

Figure 5: FT IR spectra of $LaCoO_3$ nanopowder synthesized by sintering at (a) 800˚C (b) 900˚C (c)1000 °C for 4 h

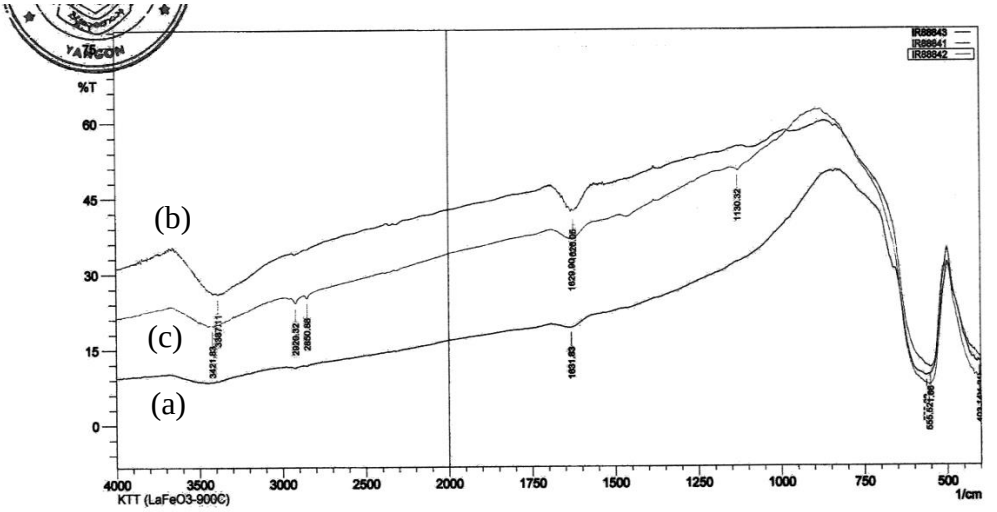

Figure 6: FT IR spectra of $LaFeO_3$ nanopowder synthesized by sintering at (a) 800 °C (b) 900 °C (c) 1000 °C for 4 h

EDXRF Analyses

The purity of all samples was also determined by usng EDXRF analysis. From the EDXRF pattern (Figures 7 and 8), all the elements detected were those that were expected to be present in the sample i.e., La, Co and Fe. In addition, all powder samples contain insignificant amounts of other contaminating elements. On the basis of the relative abundance in the matrix of the samples, the samlples contain high percentage of La, Co and Fe. These results confirmed the high purity of synthesized perovskite oxides.

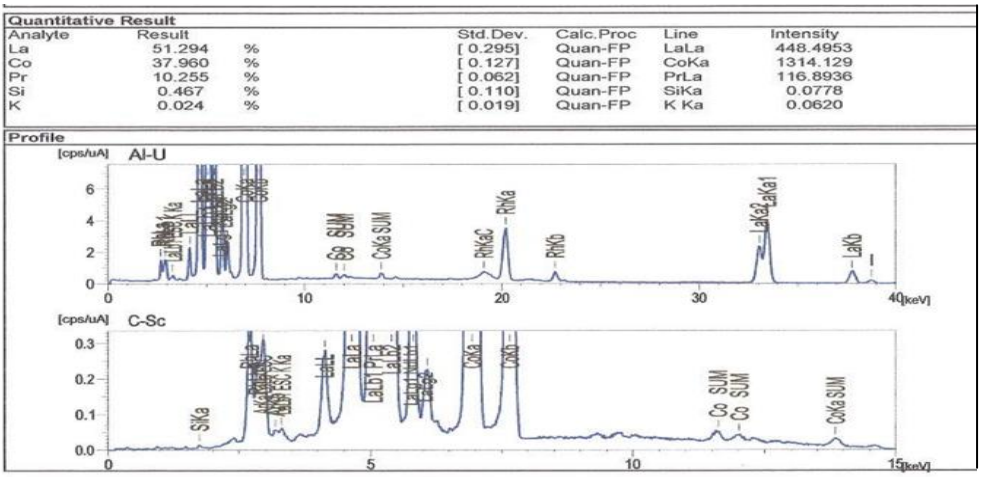

Figure7: EDXRF spectrum of $LaCoO_3$nanopowder synthesized by calcined at 450 °C for 4 h

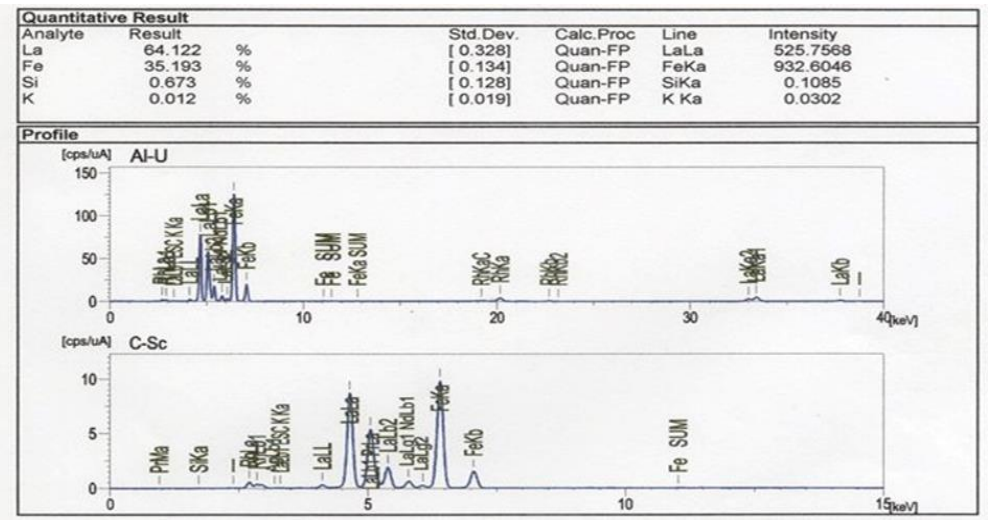

Figure 8:EDXRF spectrum of $LaFeO_3$ nanopowder synthesized by calcined at 450 °C for 4 h

SEM Analysis

The morphology of two perovskite samples was studied by using scanning electron microscope (SEM) with a magnification of 5500 times. Figure 9 and 10 show the SEM micrographs of the perovskite $LaCoO_3$ and

$LaFeO_3$.The highly dense structure was seen in perovskite $LaCoO_3$ and $LaFeO_3$ samples sintered at 900℃ for 4 h. Adjusting the sintering temperature improves the microstructure and the electronic conductivity. It can be seen that each sample has its own characteristic morphology (Haron*et al*., 2016). The particles morphology of $LaCoO_3$ was micron size with high degree of agglomeration composed of nanocrystallites with an average size of 40.93 nm at 900 °C(Ghasdi *et al*., 2010). The microstructure of $LaFeO_3$ powders were composed of small sized of grains with round shape and crystallite size was 49.76 nm at 900 °C.

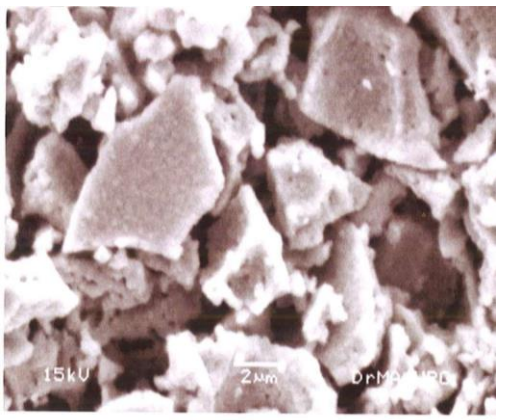

Figure 9: SEM micrograph of $LaCoO_3$sintered at temperature 900 °C for 4 h

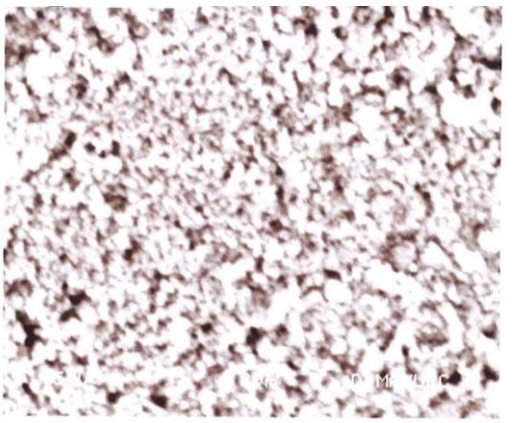

Figure10:SEM micrograph of $LaFeO_3$ sintered at temperature 900 °C for 4h

UV- Vis Spectroscopic Study

UV-visible absorption spectroscopic method is a powerful technique to explore the optical properties of semiconducting nanoparticles. The optical properties of perovskite $LaCoO_3$ and $LaFeO_3$ at 900 ℃ were studied by UV-Visible absorption spectroscopy in the range of 300-700 nm. The absorption coefficient (α) was calculated from the observed absorption spectra and the optical band gap of $LaCoO_3$ and $LaFeO_3$ were calculated from the Tauc'splots of $(\alpha h\nu)^2$ vs hν.Figures 11 and 12 show that the optical band gap of $LaCoO_3$ was found to be 2.15 eV and $LaFeO_3$ was found to be 2.40 eV. Band gap values of $LaFeO_3$ are larger than that of the $LaCoO_3$. These band gap values are also reliable within the semiconductor band gap ranges. The prepared

materials can be therefore used as gas sensor, cathode material for solid oxide fuel cell, solar cell and other optoelectronic devices.

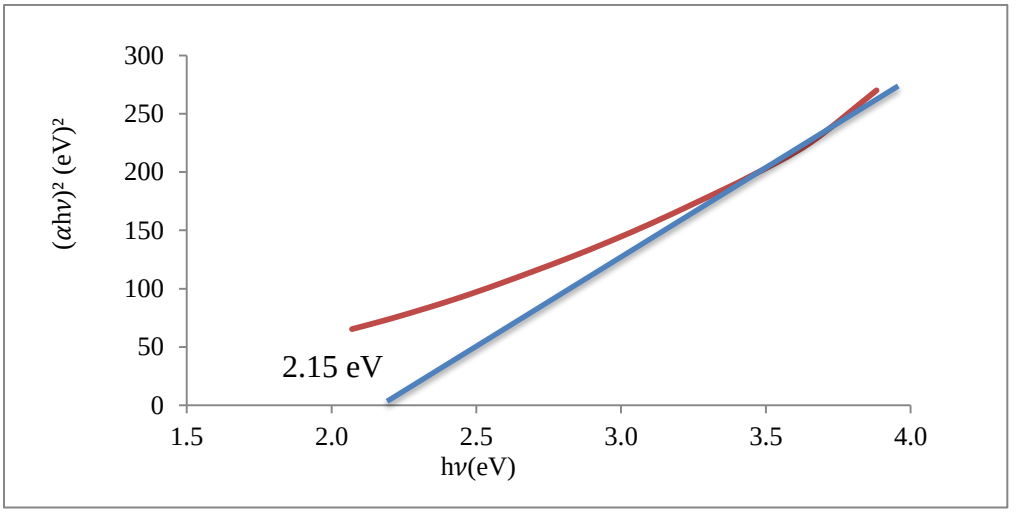

Figure 11: Plot of $(\alpha h\nu)^2$ against $h\nu$ for $LaCoO_3$ prepared by citrate sol-gel method at 900 °C

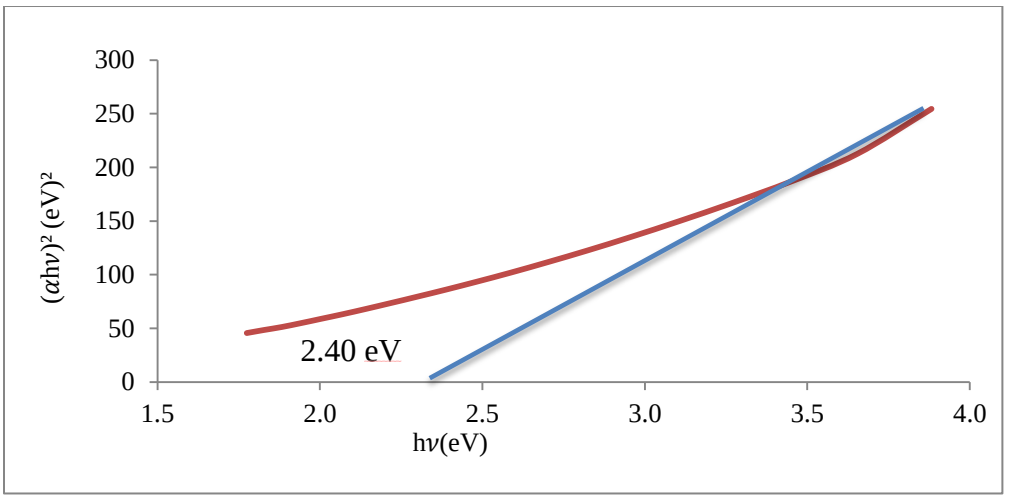

Figure 12: Plot of $(\alpha h\nu)^2$ against $h\nu$ for $LaFeO_3$ prepared by citrate sol-gel method at 900 ° C

Dielectric Studies

Dielectric measurements as a function of frequency in the range of 100-1000 kHz were performed by using LCR meter. The dielectric constant was calculated by using the formula $K = Cd/\varepsilon_0 A$ where C is the capacitance of pellet in μF, d is the thickness of the pellet; A is the cross sectional area of the flat surface of the pellet and ε_0 is the permittivity for free space. The ac conductivity (σ_{ac}) is obtained from the data of dielectric constant (ε_0) and loss tangent (tanδ) using the relation of $\sigma_{ac} = \varepsilon' \varepsilon_0 \omega \tan\delta$ where ω $(2\pi f)$ is the angular frequency. Thus σ_{ac} depends strongly on the frequency of the applied field (Priyanka *et al*., 2013). Figure 13(a) and (b) show that dielectric loss tangent (tan δ) and the dielectric constant decrease with frequency, which is a general ferroelectric behaviour (Unikoth *et al*., 2014). The higher value of dielectric constant measured at low frequencies can also be explained on the basis of interfacial space charge polarization due to inhomogeneous dielectric structure. The dielectric loss indicates the energy dissipation in the dielectric system (Asad Ali *et al*., 2015). The lower dielectric constant was found at higher frequencies in $LaCoO_3$ and $LaFeO_3$ perovskite samples. The frequency dependence of ac conductivity of $LaCoO_3$ and $LaFeO_3$ is shown in Figure13(c).It can be seen that the conductivity increases with increase in frequency. The resistivity of $LaCoO_3$ is lower than that of $LaFeO_3$ sample as shown in Figure 13(d).On the other hand, the higher dc conductivity was found for $LaCoO_3$ sample than the $LaFeO_3$ sample as shown in Figure 13(e). There is a correlation between the conductivity and the dielectric behaviour of the material. The conductivity is mainly due to the hopping of electrons and the decreasing function of frequency in the case of band conduction (Priyanka *et al*., 2013).

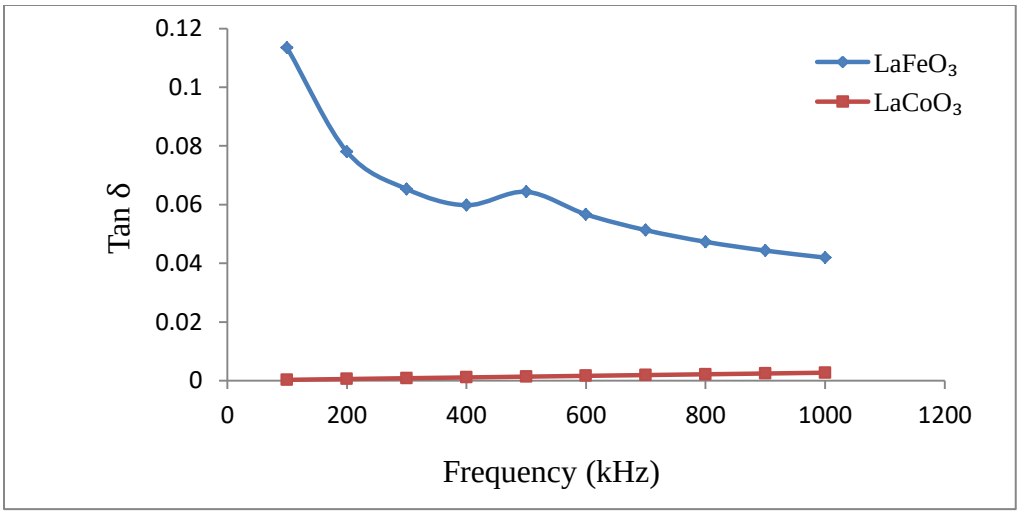

Figure 13:(a) Changes of dielectric loss tangent (tan δ) of $LaCoO_3$ and $LaFeO_3$ as a function of frequency at 2V

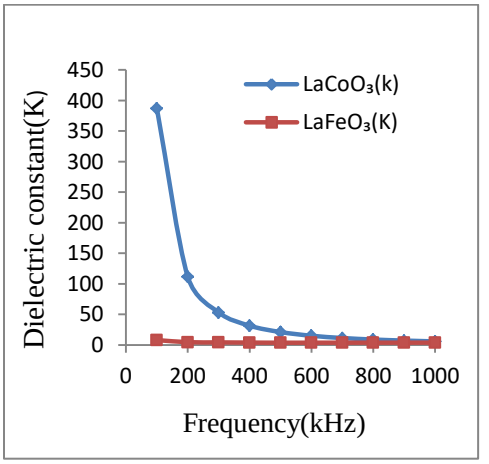

Figure 13:(b). Changes of dielectric constant of $LaCoO_3$ and $LaFeO_3$ as a function of frequency at 2V

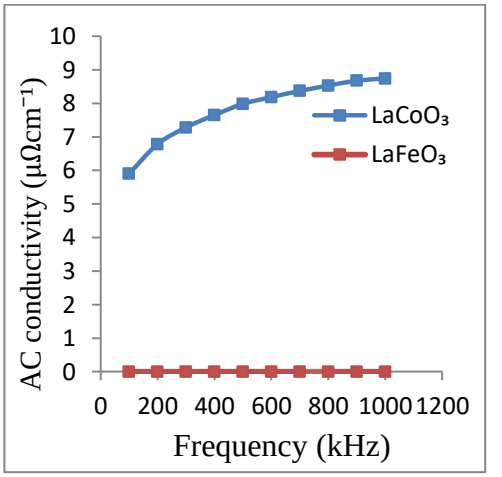

Figure 13: (c). Changes of ac conductivity of $LaCoO_3$ and $LaFeO_3$ as a function of frequency at 2V

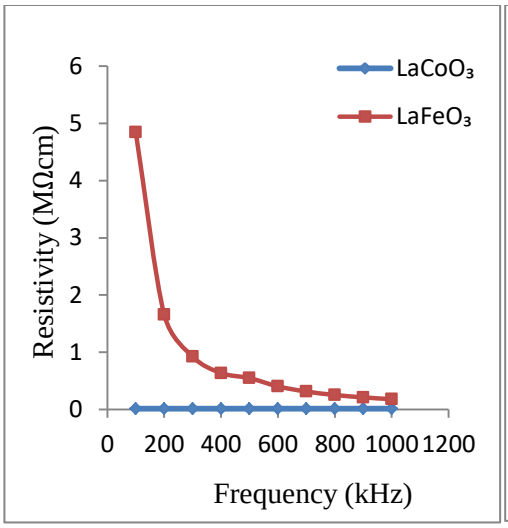

Figure13: (d). Changes of resistivity of $LaCoO_3$and $LaFeO_3$ as a function of frequency at 2V

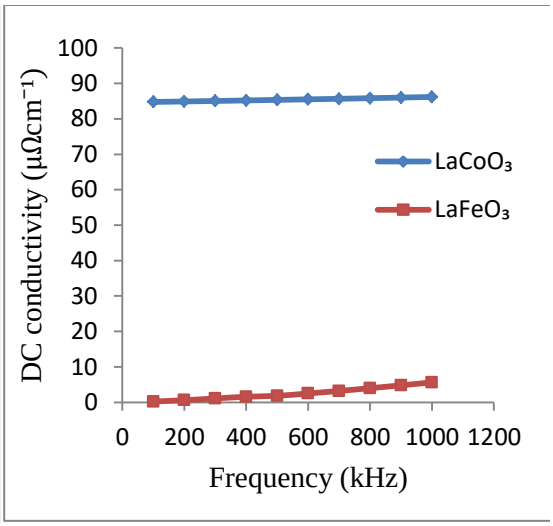

Figure13:(e).Changesofdc conductivity of $LaCoO_3$ and $LaFeO_3$ as afunction of frequency at 2V

Conclusion

Perovskite $LaCoO_3$ and $LaFeO_3$ samples have been successfully prepared by citrate sol-gel method. The crystalline pellets were obtained by sintering at 900 °C and its structural, optical and electrical properties were studied. From the study of structural properties showed that the $LaCoO_3$ has hexagonal crystal symmetry with R-3c space group having crystallite size of 40.93 nm and the $LaFeO_3$ has orthorhombic crystal symmetry with Pnma space group having crystallite size of 40.96 nm. The SEM image showed the nanostructure of the two samples and EDXRF spectra showed the presence of La, Co and Fe. From FT IR analysis, the Co-O and Fe-O stretching vibration mode band are observed at 550cm^{-1}. The band gap was calculated from UV-visible spectra which indicated the semiconducting nature of the materials. The optical band gap of $LaCoO_3$ and $LaFeO_3$were found to be 2.15 eV and 2.40 eV respectively. The ac conductivity and dielectric properties of $LaCoO_3$ and $LaFeO_3$perovskite samples were studied at the frequency range of 100-1000 kHz. The dielectric constant decreased in all samples with increase of frequency. The ac conductivity was high for higher frequencies at a given

temperature. The conductivity of perovskite $LaCoO_3$ sample have greater than the $LaFeO_3$ sample.

Acknowledgements

The authors would like to express their profound gratitude to the Department of Higher Education (Yangon Office), Ministry of Education, Myanmar, for provision of opportunity to do this research and Myanmar Academy of Arts and Science for allowing to present this paper.

References

Anupama, M. and Prasad, R. (2015). "Effect of Preparation Method and Calcination Temperature on $LaCoO_3$Perovskite Catalyst for Diesel Soot Oxidation".*J. Chem.*, vol. 3(1), pp. 95-107

Asad Ali, S., Naseem, S. andKhan, W.(2015). "Microstructural, Optical and Electrical Properties of $LaFe_{0.5}Cr_{0.5}O_3$Perovskite Nanostructures".*J. Mater. Sci*., vol. 5 (16), pp. 1-3

Ghasdi, M. and Almdari, H. (2010). "CO sensitive nanocrystalline$LaCoO_3$perovskite Sensor Prepared by High Energy Ball Milling". *J.Chem..*, vol. 148, pp. 478-485

Ghosh, S.andDasgupta, S.(2010). "Synthesis, Characterization and Properties of Nano Crystalline Peroskite Cathode Materials''.*J. Mater. Sci.*, vol.28 (2), pp. 427 - 438

Haron, W., Wisitsoraat, A. and Wongnawa, S. (2016). "A Simple Synthesis and Characterization of $LaMO_3$ (M= Al, Co, Fe) Perovskite via Chemical Co-precipitation Method". *J. Sci., Tech*. vol. 437, pp. 5-20

Khetre, S.M., Jadhav, H. V.and Bamane, S. R. (2010). "Synthesis and Characterization of Nano Crystalline $LaFeO_3$ by Combustion Route''.*J. Chem.*, vol.3(1), pp. 82-86

Priyanka, K. P., Sunny, J. and Varghese, T. (2013)."Dielectric Properties and AC Conductivity of Nanocrystalline Titania". *Journal of Basic and Applied Physics*, vol. 2(1), pp. 4-7

Theingi, M. (2013).*Study of Electrical Properties and Laser Induced Voltage Effect in* $La_{1-x}Ca_xMnO_3$ *Epitaxial Thin Films*. China:PhD Dissertation, Material Science, Kunming University of Science and Technology

Unikoth, M., Shijina, K. and Varghese, G. (2014)."Nano Sized $LaCo_{0.4}Fe_{0.6}O_3$PerovskiteSynthesized by Citrate Sol-Gel Auto Combustion Method''. *Processing and Application of Ceramic*s, vol.8(2), pp. 87-92

SCREENING OF *IN VITRO* ANTIDIABETIC EFFECT OF CRUDE EXTRACTS AND ISOLATION OF SOME TERPENOIDS FROM TUBERS OF *DIOSCOREABULBIFERA*L. (HPWUT-SA-U)

Kalya Cho[1], Yi Yi Win[2], Hnin Hnin Aye[3]

Abstract

*Diabetes mellitus*is a metabolic disorder characterized by chronic hyperglycemia. The management of the blood glucose level is a critical strategy in the control of diabetes complications. Low-cost herbal treatment is recommended due to their lesser side effect for treatment of diabetes. In this paper, tubers of *D. bulbifera* having significant traditional therapeutic potential were tested for their efficiency to inhibit α-amylase and α-glucosidase. *In vitro* α-amylase inhibitory activity of pet-ether, ethyl acetate, ethanol extracts as well as antidiabetic drugs, acarbose and metformin, were determined by starch iodine method and the 50 % inhibitory activity was found to be 172.50 μg/mL, 62.50 μg/mL, 65.00 μg/mL, 60.50 μg/mL and 42.50 μg/mL respectively. *In vitro*α-glucosidase inhibitory activity was measured by glucose oxidase method and the IC_{50} values of acarbose, metformin, pet-ether, ethyl acetate and ethanol were found to be 35.75, 67.75, 137.50, 80.00 and 115.25 μg/mL respectively. From ethyl acetate extract which revealed significant inhibitory activity on both enzymes, compounds A, B and C were isolated by column and thin layer chromatography and identified by modern spectroscopic methods. From these assessments, the isolated compounds were β-sitosterol (A) (0.0412 % yield, m.p 139 °C), diosbulbin B (B) (0.0012 % yield, m.p 217 °C) and 8-epidiosbulbin E-acetate (C) (0.0210 % yield, m.p 225 °C).

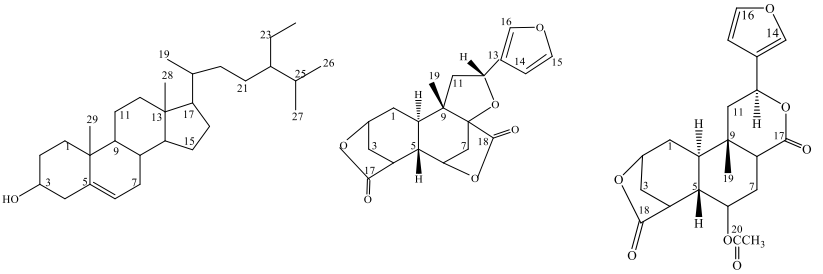

β-sitosterol (**A**) diosbulbin**B** (**B**) 8-epidiosbulbin E-acetate(**C**)

Keywords**:** antidiabetic**,** α-amylase, α-glucosidase, β-sitosterol, diosbulbin B,8-epidiosbulbin E-aceta

[1.] Lecturer, Department of Chemistry, Mawlamyine University
[2.] Dr, Lecturer, Department of Chemistry, University of Yangon
[3.] Dr, Professor and Head, Department of Chemistry, University of Yangon

Introduction

Diabetes mellitus is a chronic disorder of metabolism caused by an absolute or relative lack of insulin. It is characterized by hyperglycemiain postprandial and fasting state and its severe form is accompanied by ketosis and protein wasting. Evaluated postprandial hyperglycemia is one of the risk factors and it is elevated by the action of α-amylase and α-glucosidase. Inhibitions of these enzymes play a major role in managing postprandial hyperglycemia in diabetic patients. Inhibition of α-glucosidase enzyme activity leads to a reduction in disaccharide hydrolysis and inhibition of carbohydrate hydrolyzing enzyme such as α-amylase lowers blood glucose levels (Qaisar *et al.,* 2014). Many plants and their products have been widely prescribed and used for diabetic treatment all around the world. Thus, these natural products need to be evaluated scientifically in order to verify for their anti-diabetic properties (Bhutkar and Bhise, 2012).

Myanmar is rich in variety of medicinal plants and many people use these plants for their health care. *Diabetes mellitus*is one of the priority diseases in Myanmar. There are numerous indigenous medicinal plants which are reputed to be effective for the treatment of diabetes. Among them, *D. bulbifera* L. was selected from literature review (Gosh *et al.,* 2015). *D. bulbifera* belongs to the family Dioscoreaceae which is distributed in tropical and subtropical regions of Asia. This plant possesses profound therapeutic potential especially in the treatment of sore throat, gastric cancer, carcinoma of rectum and goiter. The various extracts of tubers of this plant have been reported to be antihyperlipidemic, antitumor, antioxidant, analgesic and anti-inflammatory and antihyperglycemic (Gao *et al.,* 2002). The present investigation was undertaken to study the ability of tubers of *D. bulbifera* to inhibit α-amylase and α-glucosidase activity and to isolate some phytoconstituents from it.

Figure 1: The photograph of plant of *D. bulbifera* L.

Figure 2: The photograph of tuber of *D. bulbifera* L.

Materials and Methods

Sample Collection and Preparation

Tubers of *D. bulbifera* used in this study were collected from Mawlamyine University campus. The collected sample was washed with water, air dried and peeled using a stainless knife. Then, the yam tissue was chopped into small cubes which were later air-dried to a constant weight at room temperature for one week. The dried sample was subsequently milled into coarse powder using a grinding mill and then stored in airtight plastic container for the experimental works.

Reagents

α-amylase (Jiangsu BoliBioproducts Co., Ltd), α-glucosidase (Cool Chemical Science and Technology Ltd., Beijing), Glucose oxidase (Hefei-Bomei Biotechnology Co., Ltd), Bicinchoninic acid (BCA), Metformin (DenkPharma GmbH Co., Munchon, Germany), Acarbose (Bayer Pharma AG, Kaiser-Wilhein-Allee, Leverkusen, Germany), Sucrose (BDH), Starch, Iodine, Pet ether, Ethyl acetate, Ethanol, n-hexane

Preparation of crude extracts

The dried powdered sample (300 g) was extracted with pet-ether, ethyl acetate and ethanol respectively by using maceration method. After 72 h

extraction at room temperature, each extract was filtered through Whatman's filter paper No.1 separately. This procedure was repeated for three times. The combined filtrates were evaporated under reduced pressure by means by a rotatory evaporator. Consequently, pet-ether, ethyl acetate and ethanol soluble extracts were obtained.

α-amylase inhibition assay

Alpha-amylase inhibitory activity of plant extracts was determined by starch iodine method (Ganapaty *et al.,* 2013). 10 μL of α-amylase solution (0.025 mg/mL) was mixed with 390 μL of phosphate buffer (40 mM containing 0.006 M NaCl, pH 7.0) containing different concentration of extracts and standard metformin and acarbose. After incubation at 37 °C for 10 min, 100 μL of starch (1 %) was added to the mixture and it was reincubated for 30 min. Then, 0.1 mL of 1 % iodine solution was added to this mixture. After adding 5 mL of distilled water, the absorbance was measured at 565 nm by UV spectrometer. Substrate and α-amylase blank determinations were carried out under the same conditions. The inhibitory activity was calculated by using the formula;

$$\% \text{ inhibition of enzyme activity} = \frac{A - C}{B - C} \times 100$$

where, A = absorbance of the sample

B = absorbance of blank (without α-amylase)

C = absorbance of control (without starch)

The concentration of test samples and standard which inhibited the hydrolysis of starch by 50 % (IC_{50}) were determined by linear regressive excel programme.

α - Glucosidase inhibition assay

α-glucosidaseinhibition activity can be measured *in vitro* by determining the reducing sugar (glucose) arising from hydrolysis of sucrose by α-glucosidase enzyme (Narkhede *et al.,* 2011). For estimating glucose concentration, a glucose oxidase method was used in which glucose-oxidase acts on glucose to produce hydrogen peroxide which directly reduced Cu (II)

complex of 2,-2' bicinchoninic acid (BCA) to Cu (I) complex (Warren, 1990). 75 μL of α-glucosidase solution (0.01 mg/L) was mixed with phosphate buffer (80 mM) containing different concentration of extracts and standard metformin and acarbose. After incubation at 37 °C for 30 min, 500 μL of 40 mM sucrose solution was added and reincubated for 20 min at 37 °C. Then the reaction mixture was kept in boiling water bath for 2 min and cooled at room temperature. After adding 300 μL of glucose-oxidase solution (1 mg/ 1 mL), it was reincubated at 37 °C for 10 min and 2 mL of colouring agent (BCA) was added. Then that solution was incubated for 20 min at 37 °C and the absorbance was measured at 565 nm by UV spectrophotometer. The percentage of inhibition was calculated from the following formula

$$\% \text{ inhibition of enzyme activity} = \frac{A - C}{B - C} \times 100$$

where, A = absorbance of the sample

B = absorbance of blank (without test sample)

C = absorbance of control (without BCA)

IC_{50} value was determined by linear regressive excel programme.

Isolation and identification of phytoconstituents

Among the three extracts, pet-ether, ethyl acetate and ethanol, ethyl acetate extract showed significant inhibition activity on both α-amylase and α-glucosidase enzymes. So part of the EtOAc extract (5 g) was subjected to column chromatography over silica gel using n-hexane:EtOAc as gradient elution to yield five sub-fractions; named I-V. Compounds A (0.0412 % yield) was directly isolated as solid material from fraction I and purified by washing with n-hexane and recrystallizing in chloroform and methanol. Fraction II which showed detectable sorts on TLC was further rechromatographed by using chloroform:methanol (19:1, 9:1 v/v) as eluents and afforded compounds B (0.33 % yield) and C (0.69 % yield).These isolated compounds were characterized by their physicochemical properties; melting point, R_f value and identified by modern spectroscopic methods; FT IR, ^{1}H NMR, ^{13}C NMR and EI-MS.

Results and Discussion

In vitro antidiabetic Effect of Tubers of *D. bulbifera*

The treatment goal of diabetic is to maintain near normal level of glycemic control in both fasting and post-prandial conditions. Many natural sources have been investigated with respect to suppression of glucose production from the carbohydrates in the gut or glucose absorption from the intestine. α-amylase catalyses the hydrolysis of α-1,4-glucosidic linkages of starch, glycogen and various oligosaccharides to disaccharide and α-glucosidase further breaks down these disaccharides to simple sugars for intestinal absorption. The inhibition of their activities in the digestive tract is considered to be effective tool to control diabetes (Genapaty *et al.*, 2013).

α-amylase inhibitory activity

α-amylase inhibitory activity was measured *in vitro* by hydrolysis of starch in the presence of α-amylase enzyme. The amount of starch remained was determined by using iodine which gave blue colour with starch. The reduced intensity of blue colour indicated the enzyme-induced hydrolysis of starch. In the other words, the more the intensity of blue colour, the higher the inhibitory activity of the test sample on α-amylase enzyme. The extracts exhibited IC_{50} less than 100 μg/mL will be considered active in comparison with standard metformin and acarbose (Ganapaty *et al.,* 2013). Table 1 shows the inhibitory of α-amylase by the extracts of tubers of *D. bulbifera*. All test extracts showed dose dependent inhibitory of enzyme. The IC_{50} values of pet-ether, ethyl acetate, ethanol as well as standard metformin and acarbose were found to be 172.50, 62.50, 60.00 and 42.50 μg/mL respectively. Among these extracts, ethyl acetate extracts showed significant α-amylase inhibitory activity, its IC_{50} value (62.50 μg/mL) was higher than acarbose (IC_{50} 42.50) but nearly the same as metformin (IC_{50} 60.00 μg/mL).

Table 1 : α-Amylase Inhibition % and IC_{50} Values of Various Crude Extracts of Tubers of *D. bulbifera* Compared with Standard Metformin and Acarbose

Sample	% Inhibition (mean ± SD) in different concentrations (μg/mL)					IC_{50} (μg/mL)
	25	50	100	200	400	
PE (extract)	14.75± 0.69	24.35± 1.84	30.44± 1.06	55.82± 1.53	69.26± 1.76	172.50
EtOAc (extract)	34.10± 1.38	44.71± 0.89	72.59± 1.95	78.11± 0.91	84.26± 0.61	62.50
EtOH (extract)	15.65± 0.73	28.37± 0.89	43.02± 0.65	55.34± 1.17	61.81± 1.00	165.00
Metformin (Standard)	21.85± 0.73	45.30± 1.01	66.76± 1.07	75.09± 0.85	86.61± 0.90	60.00
Acarbose (Standard)	25.98 ± 0.66	60.32 ± 0.21	79.86±0. 73	85.96 ± 1.11	95.06 ± 0.89	42.50

Data are expressed as means of triplicate determination ± standard deviation.

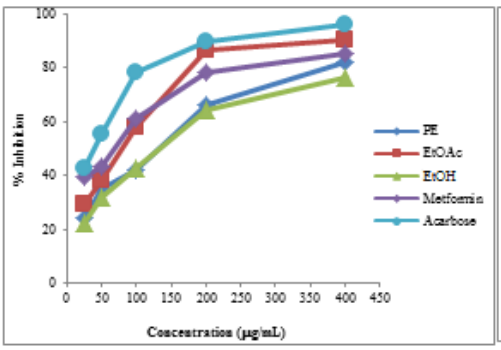

Figure 3: A plot of α-amylase inhibition activity and concentration of crude extracts of tubers of *D. bulbifera* compared with standard metformin and acarbose

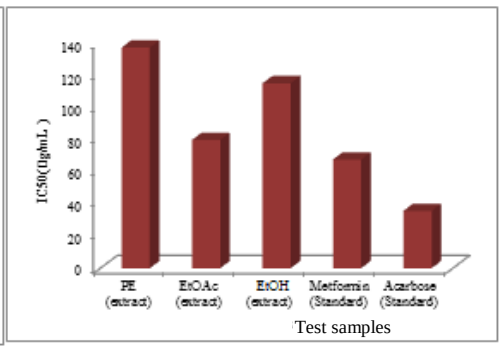

Figure 4: A bar graph of 50% α-amylase inhibitory concentration (IC_{50}) values of crude extracts of tubers of *D. bulbifera* compared with standard metformin and acarbose

α-glucosidase inhibitory activity

α-glucosidase inhibitory activity was determined by glucose oxidase method in which the green Cu (II) complex of BCA was reduced to the violet Cu (I) complex by hydrogen peroxide (Warren *et al.,* 1990). Table 2 shows the α-glucosidase inhibitory activity of extracts of tubers of *D. bulbifera*. The order of α-glucosidase inhibitory activities were found to be acarbose (IC_{50} 35.75 μg/mL) > metformin (IC_{50} 62.75 μg/mL) > ethyl acetate (IC_{50} 80.00 μg/mL) > ethanol (IC_{50} 115.25 μg/mL) > pet ether (IC_{50} 137.50 μg/mL). So ethyl acetate showed potent α-glucosidase inhibitory activity than pet-ether and ethanol extracts.

Table 2: α-Glycosidase Inhibition % and IC_{50} Values of Various Crude Extracts of Tubers of *D. bulbifera* Compared with Standard Metformin and Acarbose

Sample	% Inhibition (mean ± SD) in different concentrations (μg/mL)					IC_{50} (μg/mL)
	25	50	100	200	400	
PE (extract)	23.94 ± 0.78	35.27 ± 0.59	42.15 ± 1.13	66.03 ± 0.88	82.16 ± 1.40	137.50
EtOAc (extract)	29.46 ± 1.98	38.27 ± 1.33	58.02 ± 1.63	86.46 ± 0.49	90.25 ± 1.05	80.00
EtOH (extract)	22.36 ± 0.25	31.99 ± 1.06	42.83 ± 0.53	64.12 ± 0.88	76.45 ± 0.35	115.25
Metformin (Standard)	39.54 ± 6.28	43.58 ± 2.50	61.44 ± 0.66	78.19 ± 0.25	85.54 ± 0.35	62.75
Acarbose (Standard)	42.83 ± 1.05	55.31 ± 0.49	78.07 ± 1.63	90.06 ± 1.33	96.37 ± 1.98	35.75

Data are expressed as means of triplicate determination ± standard deviation.

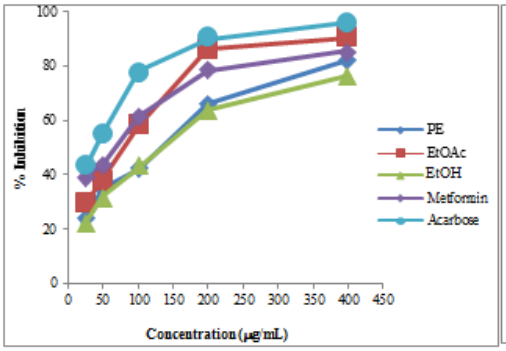

Figure 5:A plot of α-glucosidase inhibition activity and concentration of tubers of *D.bulbifera* compared with standard metformin and acarbose

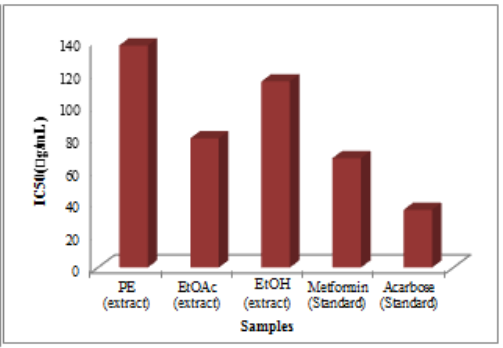

Figure 6:A bar graph of 50% α-glucosidase inhibitory concentration (IC_{50}) values of crude extracts of tubers of*D. bulbifera* compared with standard metformin and acarbose

Structure Elucidation of Isolated compounds

Three compounds; **A**, **B** and **C** were isolated from the active guided ethyl acetate extract by column chromatographic method and identified by spectroscopic methods. Photographs of isolated compounds and their TLC chromatograms are shown in Figure 7.

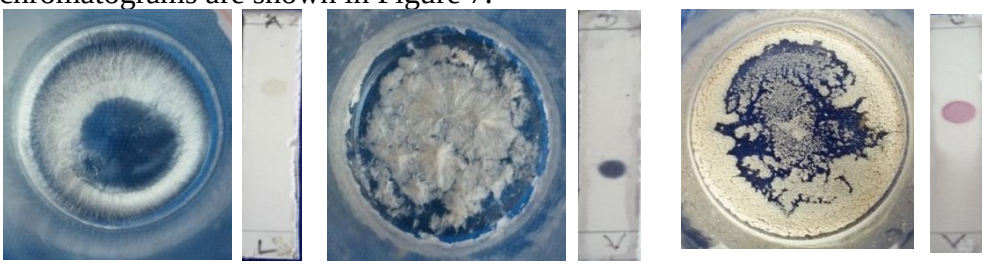

Compound A
Solvent = $CHCl_3$:MeOH, 19:1
Reagent = Liberman-Burchard,Δ
R_f= 0.72

Compound B
Solvent = $CHCl_3$:MeOH, 19:1
Reagent = H_2SO_4 - Anisaldehyde,Δ
R_f= 0.33

Compound C
Solvent = $CHCl_3$:MeOH, 19:1
Reagent = H_2SO_4 - Anisaldehyde,Δ
R_f= 0.69

Figure 7: Photographs and thin layer chromatograms of isolated compounds **A**, **B** and **C** from EtOAc extract of tubers of *D. bulbifera*

Compound A **(β- sitosterol)**

Compound **A** was also isolated as a white powder and the molecular ion in EI-MS of **A** appearing at *m/z* 414 suggested the molecular formula as $C_{29}H_{50}O$. Compound **A** also showed positive Liebermann-Burchard reaction indicated sterol nature. The ^{1}H NMR spectrum of compound **A** showed the presence of six methyl signals that appeared as two methyl singlets at δ 0.68, and 1.01; three methyl doublets that appeared at δ 0.81, 0.83, and 0.93; a methyl triplet at δ 0.84; and one olefinic proton at δ 5.36. The ^{1}H NMR spectra of compound **A** showed a proton corresponding to the proton connected to the C-3 hydroxy group which appeared as a triplet of doublet of doublets at δ 3.53. The ^{13} C NMR together with COSY, HMQC and HMBC showed twenty nine carbon signal including six methyl, eleven methylene, ten methane and three quaternary carbons. Thus, the structure of **A** was assigned as β-sitosterol that was consistent to the reported literature values (Chaturvedula and Prakash, 2012) and was further supported by the key COSY and HMBC correlations as shown below. Some respective NMR spectra of **A** are shown in Figures 8, 9,b10 and 11.

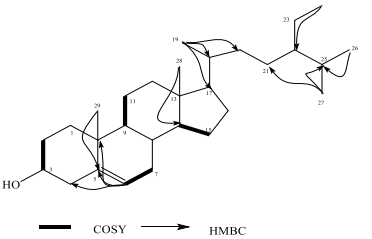

Key COSY and HMBC Correlation of compound A (β-sitosterol)

Compound B (Diosbulbin B)

Compound **B** was obtained as a white crystal. Its molecular formula was established as $C_{29}H_{20}O_6$ on the basis of EI-MS peak at *m/z* 344 (M^+ peak). Absorptions in the IR spectrum were attributable to *γ*- lactone (1773 and 1731 cm^{-1}) and a furan ring (1505 and 875 cm^{-1}).The ^{1}H, ^{13}C NMR and distortionaless enhancement by polarization transfer (DEPT) spectral data of **B** were the characteristic signals for a *β*- substituted furan ring (δ_C 145.0, 141.7, 126.6, and 109.7) and two *γ*- lactones (δ_C 176.9 and 178.8). The ^{1}H NMR spectrum, coupled with its ^{1}H-^{1}H correlation spectroscopy (^{1}H-^{1}H COSY)and heteronuclear single quantum coherence (HSQC) spectra, also

showed typical signals of a β-substituted furan ring at δ_H 7.62(1H, m, H-16),7.51(1H, m, H-15) and 6.55 (1H, m, H-14).The lactone carbonyl at δ_C 176.9 was assigned C-18 due to the HMBC correlations with proton signals at δ_H 1.75 (H-3) and 2.02 (H-5), and the correlation with oxymethine proton at δ_H 4.87 (H-2) indicated the lactone ring closure to C-2. Similarly the lactone carbonyl at δ_C 178.8 was assigned to C-17 due to the HMBC correlations with protons at δ_H 2.41 and 2.47 (H-7), while its ^{1}H-^{1}H COSY correlation with the proton at δ_H 4.79 (H-6) indicated the lactone ring closure to C-6. These NMR spectroscopic data of B similar to those of diosbulbin **B**, showing typical resonances for a norclerodanediterpenoid skeleton (Lin *et al.*, 2004) as below and some respective NMR spectra of **B** are shown in Figures 12, 13, 14 and 15.

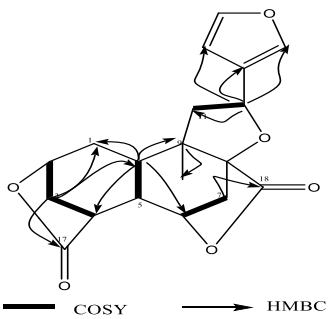

Key COSY and HMBC Correlation of Compound B (diosbulbin B)

Compound C

Compound **C** was obtained as a white amorphous with amolecular ion peak at *m*/*z* 388 in the EI-mass spectrum corresponding to molecular formula $C_{21}H_{22}O_7$.The^{13}C NMR analysis displayed 21 signals for all carbon atoms in the molecule, including three carbonyls, two non-protonated, ten methine, four methylene and two methyl carbons. The IR spectrum was consistent with the presence of the furan ring (1505 and 875 cm$-^1$),aγ-lactone(1781 and 1732 cm$-^1$). The absence of any vinyl proton resonance in the ^{1}H NMR spectrum, apart from the characteristic signals for a β- substituted furan ring, required the compound that contained one tertiary methyl group to be bicyclic. The γ-lactone ring was fused to ring A, the methane proton appeared at δ_H 4.88 (H-2) and showing coupling interactions with δ_H 1.88 (H-1), δ_H 2.53 (H-3)

and δ_H 2.60 (H-4) signals in its ^{1}H- ^{1}H COSY correlation. From the combination of ^{1}H- ^{1}H COSY, HSQC and HMBC, the structure of **C**was assigned as 8-epidiosbulbin E acetate that was consistent to the reported literature values(Shriram*et al.*, 2008). Some respective NMR spectra of **C** are shown in Figures 16, 17, 18 and 19.

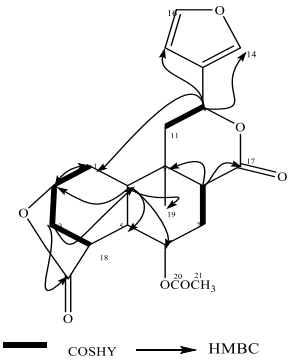

Key COSY and HMBC Correlation of Compound C (8-epidiosbulbin E acetate)

β-sitosterol (A): white crystal, m.p 139 °C, R_f 0.72 ($CHCl_3$:MeOH ,19:1 v/v), FT IR (υ_{max} cm^{-1}):3440 (υ_{OH}), 2935, 2867 (υ_{C-H}asym and sym), 1637 ($\upsilon_{C=C}$), 1465 (δ_{C-H}), 1063 (υ_{C-O}) and 958 ($\delta_{oop(C-H)}$), ^{1}H NMR (600 Hz, $CDCl_3$), δ_H : 0.68 (s, 3H, H-28), 0.81 (d, 3H, *J* = 6.4 Hz, H-27), 0.83 (d, 3H, *J* = 6.4 Hz, H-26), 0.93 (d, 3H, *J* = 6.5 Hz, H-19) 0.84 (t, 3H, *J* = 7.2 Hz, H-24),1.01 (s, 3H, H-29), 3.53 (tdd, 1H, *J* = 4.5, 4.2, 3.8 Hz. H-3),5.36 (t, 1H, *J* = 6.4 Hz. H-5),^{13}C NMR (150 Hz, $CDCl_3$), δ_C : 19.2 (C-19), 12.2 (C-24), 20.1 (C-26), 19.6 (C-27), 19.0 (C-28), 12.1(C-29), 37.5 (C-1), 31.9 (C-2), 42.5 (C-4), 32.1 (C-7), 21.3 (C-11), 40.0 (C-12), 24.5 (C-15), 28.5 (C-16), 34.2 (C-20), 26.3 (C-21), 23.3 (C-23), 72.0 (C-3), 121.9 (C-6), 32.1 (C-8), 50.4 (C-9), 57.0 (C-14), 56.3 (C-17), 36.3 (C-18), 46.1 (C-22), 29.9 (C-25), 140.9 (C-5), 36.7 (C-10), 42.5 (C-13). EI-MS m/z: 414 [M^+], 396, 381, 329, 303, 273, 255, 213, 159, 145, 95, 81, 55.

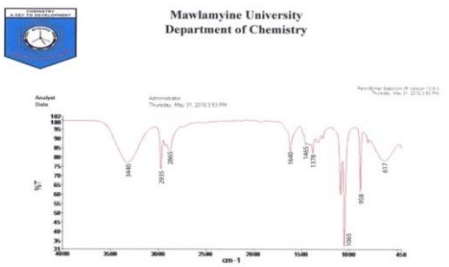

Figure 8: FT IR spectrum of the isolatedcompound **A**

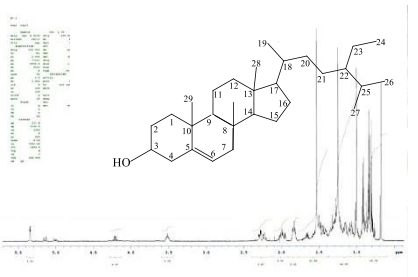

Figure 9: ^{1}H NMR spectrum of the isolated compound **A** (600 MHz, $CDCl_3$)

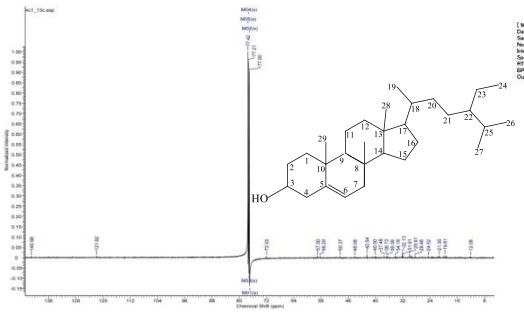

Figure 10: ^{13}C NMR spectrum of the isolated compound **A**(150 MHz, $CDCl_3$)

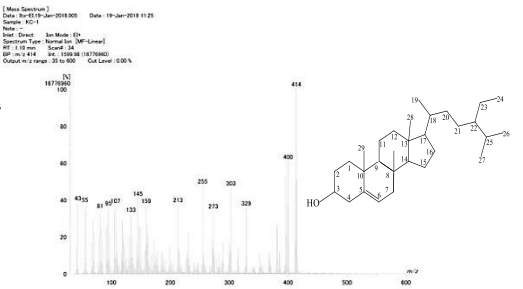

Figure11:EI-mass spectrum of the isolated compound **A**

Diosbulbin B (B): white crystal, m.p 217 °C, R_f0.33 ($CHCl_3$:MeOH, 19:1 v/v), FT IR (υ_{max} cm^{-1}); 2983, 2885 (υ_{CH}), 1773, 1731 ($\upsilon_{C=O}$), 1505 ($\upsilon_{C=C}$), 1463, 1371 (δ_{C-H}), 1252 (υ_{C-O}) and 875 ($\delta_{oop(C-H)}$), ^{1}H NMR (600 Hz, $CDCl_3$), δ_H: 7.66 (1H, s, H-16), 7.57 (1H, d, *J* = 1.8 Hz, H-15), 6.85 (1H, d, *J* = 1.8 Hz, H-14), 1.7 (3H, s, H-19), 4.84 (1H, ddd, *J* = 5.0, 5.5, 0.8 Hz, H-2), 4.76 (1H, d, *J* = 5.5 Hz, H-6), 5.24 (1H, dd, *J* = 5.0, 5.5 Hz, H-12), 2.71 (1H, d, *J* = 5.5 Hz, H-4), 2.16 (1H, d, *J* = 5.5 Hz,H-5), 1.63 (1H, m, H-10), 1.63 (H-1β), 1.86 (H-1α), 1.90 (H-3β), 2.38 (H-3α), 2.13 (H-7β), 2.43 (H-7α), 1.80 (H-11β), 2.00 (H-11α),^{13}C NMR (150 Hz, $CDCl_3$), δ_C: 176.1 (C-17) and 177.3 (C-18), 143.1 (C-15), 140.9 (C-16), 125.9 (C-13), 110.2 (C-14), 76.6 (C-2) 77.1 (C-6), 74.2 (C-12), 89.3 (C-8), 45.3 (C-9), 28.7 (C-1), 38.2 (C-3), 36.7 (C-7) and

41.5 (C-11), 40.9 (C-5), 41.3 (C-4), 38.5 (C-10), 46.1 (C-19). EI-MS m/z: 344 [M^+], 300 [$M^+ - CO_2$], 255 [M^+ m/z 300 – COOH], 206 [$M^+ - C_7H_6O_3$].

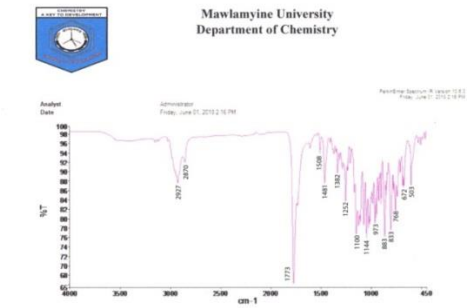

Figure 12:FT IR spectrum of the isolated compound **B**

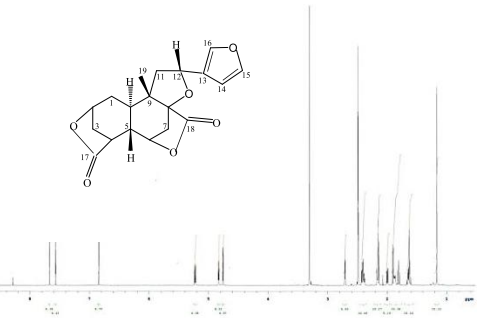

Figure 13:^{1}H NMR spectrum of the isolated compound **B** (600 MHz, $CDCl_3$)

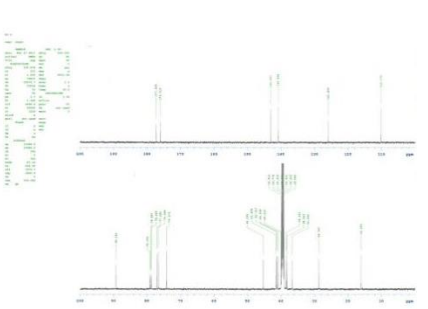

Figure 14:^{13}C NMR spectrum of the isolated compound **B** (150MHz, $CDCl_3$)

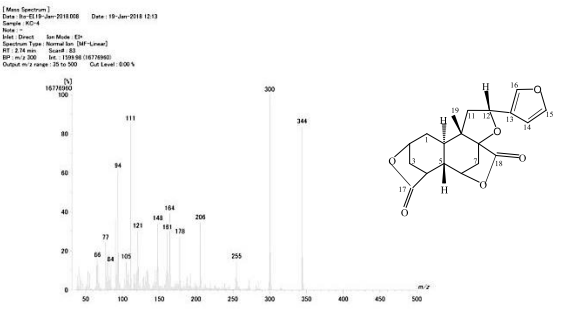

Figure 15:EI-mass spectrum of the isolated compound **B**

8-Epidiosbulbin E-acetate (C): white amorphous, m.p 255 °C, R_f0.69 ($CHCl_3$:MeOH, 19:1 v/v), FT IR ($\upsilon_{max}cm^{-1}$): 2962-2860 (υ_{CH}), 1783, 1769, 1701 ($\upsilon_{C=O}$), 1509 ($\upsilon_{C=C}$), 1460, 1330 (δ_{C-H}), 1252 (υ_{C-O}), 876 ($\delta_{oop(C-H)}$),^{1}H NMR (600 Hz, DMSO), δ_H: 7.66 (1H, s, H-14), 6.45 (1H, s, H-15), 7.70 (1H, s, H-16), 4.80 (1H, m, H-2), 4.75 (1H, dd, *J* = 5.5, 16.3 Hz, H-6), 2.60 (1H, m, H-4), 1.90 (1H, m, H-5), 3.05 (1H, m, H-8), 2.65 (1H, m, H-10), 1.88 (H-1α), 1.63 (H-1β), 2.53 (H-3α), 1.75 (H-3β), 3.01 (H-7α), 1.99 (H-7β), 2.14 (H-11α), 1.78 (H-11β), 1.16 (3H, s, H-19), 1.99 (3H, s, H-21),^{13}C NMR (150 Hz,

DMSO),δ_C: 170.1 (C-20), 174.1 (C-17), 176.7 (C-18), 109.2 (C-14), 124.6 (C-13), 140.1 (C-15), 143.9 (C-16), 69.4 (C-12), 69.5 (C-6), 76.7 (C-2), 36.7 (C-4), 41.2 (C-5), 41.6 (C-8), 41.6 (C-10), 27.7 (C-7), 28.8 (C-1), 38.1 (C-3), 41.1 (C-11), 16.2 (C-19), 21.0 (C-21), 35.5 (C-9). EI-MS m/z: 388 [M^+], 346 [M^+–(–CH_2=C=O)], 328 [M^+– $C_2H_4O_2$], 43 [M^+– $C_{19}H_{21}O_6$].

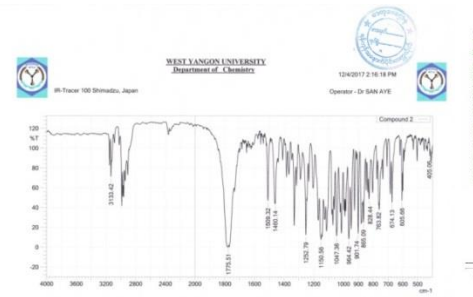

Figure 16:FT IR spectrum of the isolated compound **C**

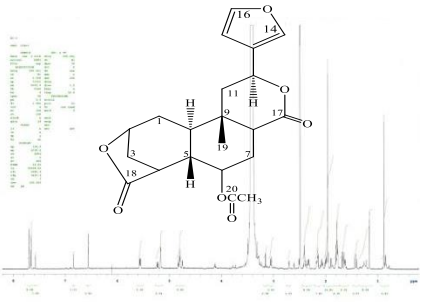

Figure 17:^{1}H NMR spectrum of the isolated compound **C** (600 MHz, DMSO)

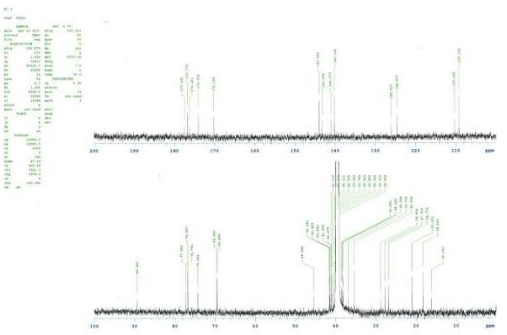

Figure 18:^{13}C NMR spectrum of the isolated compound **C** (150 MHz, DMSO)

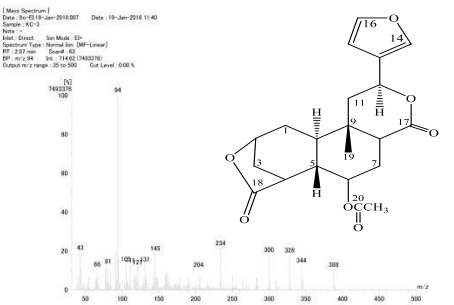

Figure 19:EI-mass spectrum of the isolated compound **C**

Conclusion

The present study deals with the investigation of antidiabetic activity of tubers of *D. bulbifera* and isolation of some phytoconstituents from it. *Invitro* α-amylase inhibitory activity was determined by starch iodine method and the resultant activities were compared with standard antidiabetic drugs; acarbose and metformin. The order of α-amylase inhibitory activities of crude

extracts were found as:acarbose(IC_{50} 42.50 μg/mL) > Metformin (IC_{50} 60.50 μg/mL) >EtOAc (IC_{50} 62.50 μg/mL)>MeOH (IC_{50} 165.00 μg/mL) > PE (IC_{50} 172.50 μg/mL).*In vitro* α-glucosidase inhibitory of crude extracts of tubers of *D. bulbifera*and standard acarbose and metformin were measured by glucose oxidase method. The IC_{50} values of acarbose, metformin, PE, EtOAc and MeOH extracts were found to be 35.75, 67.75, 137.50, 80.00 and 115.25 *m*g/mL respectively. These test results revealed that ethyl acetate extract showed potent inhibitory effect on both α-amylase and α-glucosidase enzymes.

Compounds **A**, **B** and **C** were isolated from activity guided ethyl acetate fraction by column chromatography and characterized by FT IR, ^{1}H NMR, ^{13}C NMR and EI-MS specroscopic methods. These isolated compounds were identified as β-sitostoral (**A**) (0.0412 % yield, m.p 139 °C), diosbulbin **B** (**B**) (0.002 % yield, m.p 217 °C) and 8-epidiosbulbin E-acetate (**C**) (0.0210 % yield, m.p 225 °C).

It is evident that ethyl acetate extract of tubers of *D. bulbifera* has significant antidiabetic effect and it is likely due to the presence of bioactive phytoconstituents, such as steroids and terpenoids. So, it can be inferred that tubers of *D. bulbifera* have invaluable medicinal use for the treatment of hyperglycemia in diabetes.

Acknowledgements

The authors would like to express their profound gratitude to the Department of Higher Education (Yangon Office), Ministry of Education, Yangon, Myanmar, for provision of opportunity to do this research and Myanmar Academy of Arts and Science for allowing to present this paper.

References

Bhutkar, A. M. and S. B. Bhise, (2012). "*In vitro* Assay of Alpha-Amylase Inhibitory Activity of some Indigenous Plant". *Int.J.Chem.Sci*, vol. 10(1), pp. 457-462

Chaturevedula, V.S.P. I. and Prakash, (2012)."Isolation of Stigmasterol and β-sitosterol from the Dichloromethane Extract of *Rubussuavissimus*".*International Current Pharmaceutical Journal*, vol. 1(9), pp. 239-242

Ganapaty, S.,R. Nandeesh,Veerapur, V.P.,Thippeswamy, B.S. and Shivasharan.D. (2013). "*In vitro* and *In vitro* Anti-Diabetic Effects of *Madhucaindica*; in Alloxan-Induced Diabetic rats". *IJAPBC*, vol.2(2), pp. 282-290

Gao, H., M.Kuroyanagi, Wu, L., Kawahara, N., Yasuno T. and Nakamura, Y. (2002). "Antitumor Promoting Constituents from *Dioscoreabulbifer*L. in JB6 Mouse Epidermal Cells". *Biol. Pharm. Bull*, vol. 25(9), pp. 1241-1243

Gosh, S., V.S. Parihar,P. More, D.Dhavale, and Chopade, B.A. (2015). "Phytochemistry and Therapeutic Potential of Medicinal Plant: *Dioscoreabulbifera*". *Med Chem*, vol5(4), pp. 160-172

Kuete, V., R. B,Tepono, Mbaveng, R. B.,Tapondjou, L. A., J. Meyer, J., Barboni, L. and Lall. N. (2012). "Antibacterial Activities of the Extracts, Fractions and Compounds from *Dioscoreabulbifera*", *Bio Med*, vol. 12, pp. 2-8

Liu, B., B. Shiren, Tu, Z., Wang, W. and Yang, C. (2004)."Isolation and Identification of Diterpene-B from *Dioscorea*of Gansu Loulu Decoction".*Journal of Beijing University of Traditional Chinese Medicine*, vol. 6, pp. 58-60

Narkhede, M. B., P.V. Ajimire, Wagh, A.E., Mohan. M. and Shivashanmugam, A.T. (2011)."*In vitro* Antidiabetic Activity of *Caesalpinadigyna*(R.) Methanol Root extract". *Asian Journal of Plant Science and Research*, vol. 1(2), pp.101-106

Qaisar, M. N., B. A. Chaudhary, M.U. Sajid, and Hussain, S. (2014). "Evaluation of α-Glucosidase Inhibitory Activity of Dichloromethane and Methanol Extracts of *Croton banplandianum* Baill".*Trop J Pharm Res*, vol. 13(11), pp. 1833-1836

Varsha, S., J.Sheetal, C.Latha, K, Vinay, P.Vedavatic, Supada, R., Prashant K.D. and Shitole, M.G. (2008). "A Potential Plasmid-Euring Agent, 8-Epidiosbulbin E Acetate from *Dioscoreabulbifera* L. against Multidrug-Ressistant bacteria". *International Journal of Antimicrobial Agents*, vol32**,** pp.405-410.

Warren, L. (1990). "Glucose Oxidase Reaction for Estimation of Glucose without Horseradish Peroxidase.Some Microbiology and Fermentation Application".*J. Inst. Brew*, vol. 97, pp. 457-462

SCREENING OF SOME BIOLOGICAL ACTIVITIES FROM LEAVES AND FLOWERS OF *Melastoma malabathricum* L. (NYAUNG-YE-O-PAN)

Hnin Htet Wai Nyunt[1], Khin Chaw Win[2], Ni Ni Than[3]

Abstract

The present study concerned with the determination of phytochemical constituents, nutritional values and biological activities such as antimicrobial, antioxidant, total phenol and flavonoid contents of leaves and flowers of *Melastoma malabathricum* L. (Nyaung-ye-o-pan, NYOP). The preliminary phytochemical results showed the presence of alkaloids, α-amino acids, carbohydrates, flavonoids, glycosides, organic acids, phenolic compounds, reducing sugars, saponins, starch, steroids, tannins and terpenoids in both leaves and flowers of NYOP. Some nutritional values such as the moisture contents (6.00 % and 8.00 %), the ash contents (7.53 % and 4.00 %), the fiber contents (13.81 % and 11.17 %), the fat contents (4.16 % and 2.44 %), the protein contents (4.55 % and 3.47 %), and the carbohydrate contents (63.95 % and 70.92 %) of leaves and flowers of NYOP were determined by using the respective methods. The screening of antimicrobial activity of crude extracts such as PE, EtOAc, EtOH and H_2O indicated that antimicrobial activity with inhibition zone diameters ranged between 13 mm~25 mm in NYOP (L) and 13 mm~27 mm in NYOP (F). The NYOP (F) showed higher activity than NYOP (L). The antioxidant activity of ethanol and watery crude extracts of Nyaung-ye-o-pan leaves and flowers was investigated by DPPH free radical scavenging assay. The IC_{50} values of NYOP (L) watery and ethanol crude extracts were17.14 µg/mL and 15.91 µg/mL, respectively, and those of NYOP (F) watery and ethanol extracts were 35.39 µg/mL and 21.95 µg/mL. Since the lower IC_{50} values, the higher antioxidant activity of the samples occurs. Thus, the ethanol extract of NYOP (L) was greater antioxidant activity than that of NYOP (F) whereas watery extract of NYOP (F) was greater than that of NYOP (L). The total phenolic contents in watery and ethanol extracts of NYOP (L) and (F) were found to be 416.2 and 212.2; 320.7 and 195.9 mg of GAE/g of extract respectively. Among these, watery extract of NYOP (L) contained the highest phenolic content. The total flavonoid contents in watery and ethanol extracts of NYOP (L) and NYOP (F) were 88.9 and 114.4; 125.6 and 112.2 mg of QE/g of extract respectively. Among these, watery extract of NYOP (F) has highest flavonoid content.

Keywords: *Melastoma malabathricum* L., phytochemical constituents, antimicrobial activity, antioxidant activity, phenolic content, flavonoid content

1. Candidate, 3 PhD, Assistant Lecturer, Department of Chemistry, University of Yangon
2. Dr, Lecturer, Department of Chemistry, University of Yangon
3. Dr, Professor, Department of Chemistry, University of Yangon

Introduction

Traditional medicinal plants contain various constituents which are very useful in both preventive and curative traditional medicine preparations for human beings. The plants which have been selected for medicinal use over thousands of years constitute the most obvious choice of examining the current search for therapeutically effective new drugs such as anticancer drugs and antimicrobial drugs(Munin, 2011).

In this study, our attention has been focused on *Melastoma malabathricum* L. that belongs to the family Melastomataceae and it is called Nyaung-ye-o-pan (NYOP) in Myanmar. It is native to India, China, Japan, Cambodia, Myanmar, Malaysia, Nepal, Philippines, Thailand and Vietnam (Nadkarni, 2000). It is an evergreen erect shrub and its average height is 1.5 to 5 m tall but may occasionally grow up to 5 m long. The stems are 4-sided to subterete, generally bristle, covered with small scales and reddish (Zakaria and Mohd, 1994). The leaves are 7 to 12 cm long, slightly rough and hairy on both surfaces. The flowers grow in 5 to 10 clusters and 5 petals. On rare occasions, *M.malabathricum* consists of 3 varieties, dark-purple petals, light pink-magenta petals and (the rare variety) white petals (Susanti *et al*., 2007). The fruits are classified as berries and when they are ripe, they split irregularly to reveal the soft, dark purple, sweet but rather astringent-tasting pulp and numerous orange seeds. The seeds are tasteless and can be eaten and they stain the tongue black (Koya, 2008). The young leaves are to treat diarrhea while the young premature leaves are consumed raw to cure dysentery. Other medicinally usesare to treat ulcers, gastric ulcer, scar, pimple and black spot at skin (Lohezic-Le Devehat *et al*., 2002). The flowers of *M.malabathricum* are also used as a nervous sedative and for hemorrhoidal bleeding. The leaves and flowers are useful for the treatment of cholera, diarrhoea, prolong fever, dysentery, leucohorrea, wounds and skin diseases and for the preparation of gargle (Perry, 1980).

Materials and Methods

Plant materials

The leaves and flowers of NYOP were collected from Hlar-ka-myin Village, Hpa-an Township in Kayin State. The plant was identifiedby the authorized botanist, at Botany Department, Hpa-an University, Myanmar. After cleaning and drying at room temperature, each of the dried samples was ground into powder and stored separately in air-tight containers. Each powder sample was used for determination of nutritional values and phytochemical constituents. The various crude extracts leaves and flowers of NYOP were used for some pharmacological activities such as antimicrobial and antioxidant activity. Each crude extract was used to determine total phenolic and total flavonoid contents.

Chemicals

Ferric chloride, potassium iodide, picric acid, sodium hydroxide, ninhydrin, α-napthol, sulphuric acid, lead acetate, acetic anhydride, iodine, bromocresol green, gelatin, ethanol, magnesium ribbon, hydrochloric acid, chloroform, petroleum ether, meat extract, peptone, sodium chloride, agar powder, DPPH (1,1 diphenyl-2-picrylhydrazyl), vitamin C, Folin-Ciocalteu reagent, sodium carbonate, standard gallic acid, aluminium chloride, potassium acetate and standard quercetin were used.

Instruments

Soxhlet extractor, water bath, Micro-Kjeldahl distillation apparatus, UV-spectrophotometer (UV- 7504 KWF, China), shaker and electric balance were required.

Phytochemical Investigation

The dried powdered samples were used for the chemical tests on the phytochemicalsby using standard procedure (M-Tin Wa, 1972; Trease and Evans, 1980; Shriner *et al*., 1980; Harborne, 1984; Marini-Bettolo *et al*., 1981; Robinson, 1983; Vogel, 1966).

Determination of Nutritional Values

Some nutritional values such as moisture, ash, fiber, fat, protein and carbohydrate contents were made by reported methods (Joslyn, 1970; Pearson, 1976; Steyermart, 1961; Anderson, 1984). The total energy value was determined from the sum of fat, protein and carbohydrate contents.

Screening of Antimicrobial Activity

The screening of antimicrobial activity of various crude extracts such as PE, EtOAc, EtOH and watery extracts of NYOP (L) and NYOP (F) were carried out by agar dics diffusion method at Pharmaceutical Research Department, Ministry of Industry, Yangon, Myanmar. Six microorganisms namely *Bacillus subtilis*, *Staphylococcus aureus*, *Pseudomonas aeruginosa*, *Bacillus pumilus*, *Candida albicans* and *Escherichia coli* were used for this test.

Screening of Antioxidant Activity

The antioxidant activity of each crude extract of NYOP leaves and flowers were screened by using DPPH Free Radical Scavenging Assay (Marinova and Batchvarov, 2011). 2 mg of DPPH powder was freshly prepared by dissolving in 100 mL of ethanol. Standard vitamin C was dissolved in 10 mL of ethanol to get the stock solution. Each respective crude extract of NYOP leaves and flowers (2 mg) was dissolved in 10 mL of ethanol to get the stock solution. Each stock solution of standard vitamin C and sample solution were two fold serially diluted with ethanol to get their respective solutions with the concentration of 200, 100, 50, 25, 12.5 and 1.625μg/mL. The blank solution was also prepared by mixing the sample solution 1.5 mL with ethanol. The control solution was prepared by mixing with 1.5 mL of DPPH solution and 1.5 mL of ethanol in brown bottles. These bottles are incubated at room temperature and were shaken on shaker for 30 min. After 30 min, the absorbance values of these solutions were measured at 517 nm.

Determination of Total Phenol Contents

The total phenol content in each sample was estimated by Folin-Ciocalteu method. Each extract (10 mg) was mixed with 10 mL of distilled water. Each extract solution (1 mL) was mixed with 5 mL of FCR solution and incubated for 5 min. To each tube, 4 mL of 1M sodium carbonate solution was added and the tubes were kept in room temperature for 2 h. The absorbance was measured spectrophotometrically at 765 nm. The concentrations of gallic acid equivalent of each of the plant extract were calculated by using linear regression equation from the standard curve of gallic acid. Total phenol content in the plant samples were expressed as mg gallic acid equivalent per 1 g dry plant extracts (Basma *et al*., 2011; Kaur and Poonam, 2014).

Determination of Total Flavonoid Contents

The total flavonoid content in each sample was estimated by Aluminium Chloride Calorimetric Assay. Each extract (10 mg) was mixed with 10 mL of distilled water. Each of this extract solution (0.5 mL) was mixed with 1.5 mL of methanol, 0.1 mL of 1 % $AlCl_3$ solution, 0.1 mL of 1 M potassium acetate and 2.8 mL of distilled water. The resultant mixture was allowed to stand for 30 minutes at room temperature. Absorbance of resulting blue solution was measured at 415 nm using spectrophotometrically (KWF UV-7504). In this method quercetin was used as a standard. The concentrations of quercetin equivalent (QE) in plant extracts were calculated by using the linear regression equation from standard calibration curve of quercetin. Total flavonoid content in the plant samples were expressed as mg quercetin equivalent per 1 g dry plant extracts (Basma *et al*., 2011; Kaur and Poonam, 2014).

Results and Discussion

Preliminary Phytochemical Investigation

According to the phytochemical test results, alkaloids, α-amino acids, carbohydrates, flavonoids, glycosides, organic acids, phenolic compounds, reducing sugars, saponins, starch, steroids, tannins, and terpenoids were present in both leaves and flowers of NYOP. However, cyanogenic glycosides were absent in both of these samples.

Investigation of some Nutritional Values

The moisture content was determined by oven drying method. The moisture contents of NYOP were found to be 6.00 % in leaves and 8.00 % in flowers. Since the moisture content is less than 12 %, the changes for the growth of microorganisms are greatly minimized. The ash content in leaves (7.53 %) was greater than that in flowers (4.00 %). The fiber content in leaves (13.81 %) was also higher than that in flowers (11.17 %). Moreover, the fat and protein contents of leaves of NYOP (4.16 % and 4.55 %) were much higher than that in flowers of NYOP (2.44 % and 3.47 %). However, the carbohydrate contents of leaves (63.95 %) are greatly less than that of flowers (70.92 %). The energy values were found to be (311.44 kcal/100 g) in leaves of NYOP which were also lesser than in flowers of NYOP (319.52 kcal/ 100 g). The results are shown in Table 1 and Figure 1.

Table 1: Some Nutritional Values of Leaves and Flowers of *M. malabathricum* (Nyaung-ye-o-pan)

No.	Nutritional parameters	NYOP (L)	NYOP (F)
1	Moisture (%)	6.00	8.00
2	Ash (%)	7.53	4.00
3	Fiber (%)	13.81	11.17
4	Fat (%)	4.16	2.44
5	Protein (%)	4.55	3.47
6	Carbohydrate (%)	63.95	70.92
7	Energy values (kcal/ 100 g)	311.44	319.52

*base on dry sample

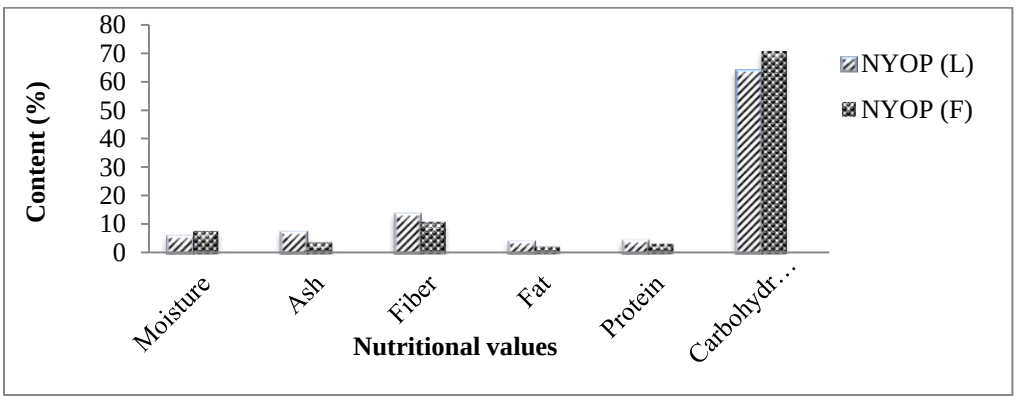

Figure 1: A bar graph diagram showing some nutritional values of leaves and flowers of *M. malabathricum* (Nyaung-ye-o-pan)

Screening of Antimicrobial Activity

Four crude extracts of such as PE, EtOAc, EtOH and H_2O were screened for antimicrobial activity against six different pathogenic microbes using agar well diffusion method. Larger the zone diameter, the more activity is on the test bacteria. According to the results in Figure 2 (a and b) and Table 2, PE and watery extracts of NYOP (L) did not show any antimicrobial activity against all of the microorganism tested. But PE extract of NYOP (F) showed antimicrobial activity except *Bacillus subtilis* and *Escherichia coli*. EtOAc and EtOH crude extracts of NYOP (L) showed antimicrobial activity against all the tested pathogenic microbes. Antimicrobial activity with inhibition zone diameters ranged between 13 mm~25 mm in NYOP (L) and 13 mm~27 mm in NYOP (F). The NYOP (F) showed higher activity than NYOP (L).

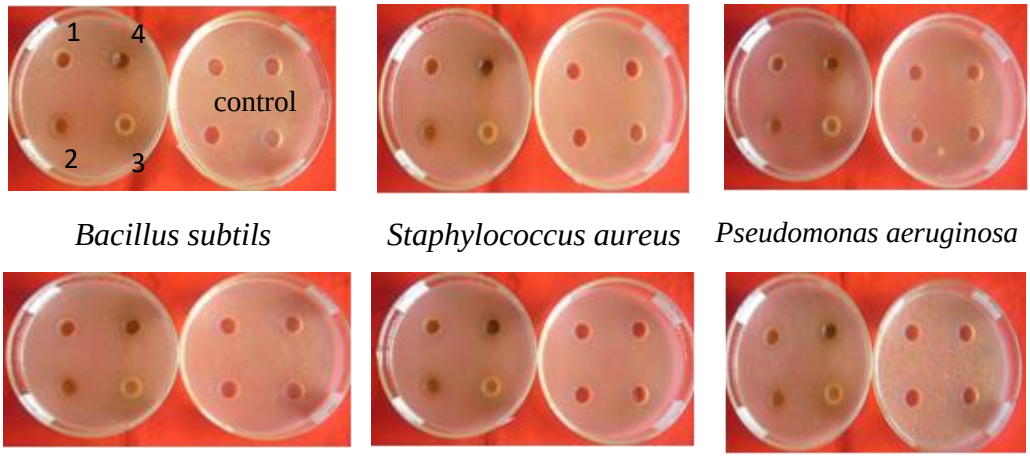

Figure 2(a): Screening of antimicrobial activities of varioucrude extracts from NYOP (L)

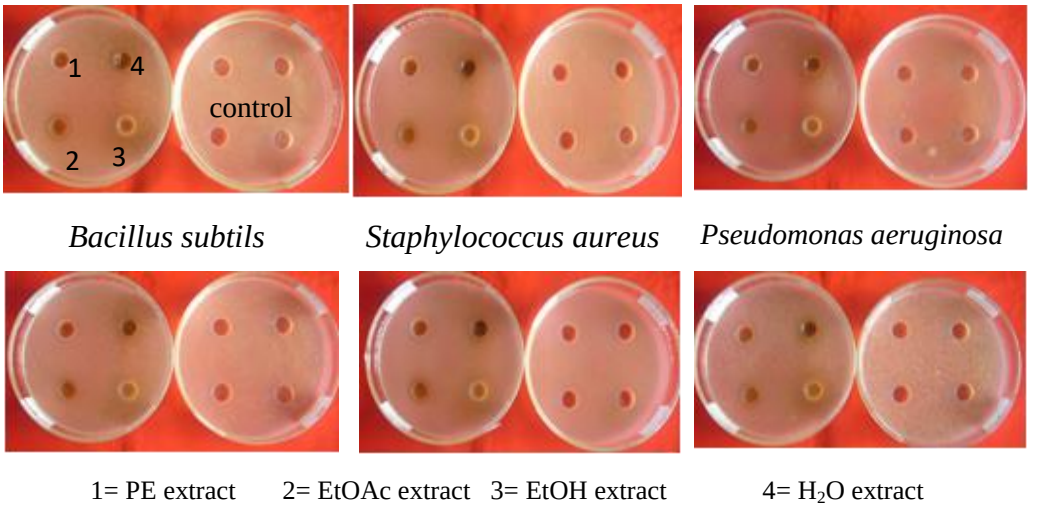

Figure 2(b): Screening of antimicrobial activities of various crude extracts from NYOP (F)

Table 2: Inhibition Zone Diameters of Various Crudes Extracts of Leaves and Flowers of NYOP against Six Microorganisms by Agar Well Diffusion Method

Samples	Solvents	Inhibition Zone Diameter (mm)					
		B. subtilis	***S. aureus***	***P. aeruginosa***	***B. pumilus***	***C. albicans***	***E. coli***
NYOP (Leaves)	PE	-	-	-	-	-	-
	EtOAc	15 (++)	15 (++)	25 (+++)	15 (++)	16 (++)	16 (++)
	EtOH	18 (++)	18 (++)	13 (+)	16 (++)	18 (++)	18 (++)
	H_2O	-	-	-	-	-	-
NYOP (Flowers)	PE	-	13 (+)	15 (++)	13 (+)	13 (+)	-
	EtOAc	15 (++)	15 (++)	20 (+++)	13 (+)	15 (++)	14 (+)
	EtOH	24 (+++)	24 (+++)	27 (+++)	26 (+++)	27 (+++)	25 (+++)
	H_2O	19 (++)	20 (+++)	20 (+++)	18 (++)	20 (+++)	20 (+++)

Diameter of agar well = 10 mm No activity = (-)
10 mm ~ 14 mm = (+) 15 mm ~ 19 mm = (++) 20 mm above = (+++)

Antioxidant Activity of some Crude Extracts from Leaves and Flowers of NYOP by DPPH Free Radical Scavenging Assay

The antioxidant activity was measured in terms of hydrogen donating or radicals scavenging ability using the stable radical DPPH at 517 nm. In this study, five different concentrations of 200 μg/mL, 100 μg/mL, 50 μg/mL, 25 μg/mL,12.5 μg/mL, 6.25 μg/mL of each crude extract were prepared by dilution with ethanol. The IC_{50} values watery and ethanol crude extracts of NYOP (L) were 17.14 μg/mL and 15.91 μg/mL.The watery and ethanol crude extracts of NYOP (F) were 35.39 μg/mL and 21.95 μg/mL. These results are shown in Table 3 and Figure 3. Since the lower IC_{50} values, the higher antioxidant activity of the samples occurs. Thus, the ethanol extract of NYOP (L) is greater antioxidant activity than that of NYOP (F) whereas watery extract of NYOP (F) is greater than that of NYOP (L).

Table 3: Radical Scavenging Activity (% RSA) and IC_{50} values of Crude extracts of Leaves and Flowers of NYOP

Test samples	% RSA ± SD at different concentration (μg/mL)						IC_{50} (μg/mL)
	6.25	12.5	25	50	100	200	
NYOP (L) Watery extract	27.36 ± 0.12	41.59 ± 0.81	64.26 ± 0.56	95.34 ± 0.09	101.91 ± 0.28	104.40 ± 0.09	17.14
NYOP (L) Ethanol extract	35.36 ± 0.23	43.36 ± 0.08	67.77 ± 0.05	75.32 ± 0.14	99.36 ± 0.18	112.92 ± 0.18	15.91
NYOP (F) Watery extract	28.36 ± 0.31	36.76 ± 0.61	42.66 ± 0.97	60.31 ± 1.70	70.88 ± 0.61	85.91 ± 0.24	35.39
NYOP (F) Ethanol extract	24.36 ± 0.24	30.68 ± 0.09	56.24 ± 0.19	99.74 ± 0.18	101.45 ± 0.19	103.29 ± 0.37	21.95
Standard Vitamin C	25.20 ± 1.40	53.58 ± 0.88	65.53 ± 1.13	74.82 ± 0.59	83.32 ± 0.78	91.21 ± 0.48	11.70

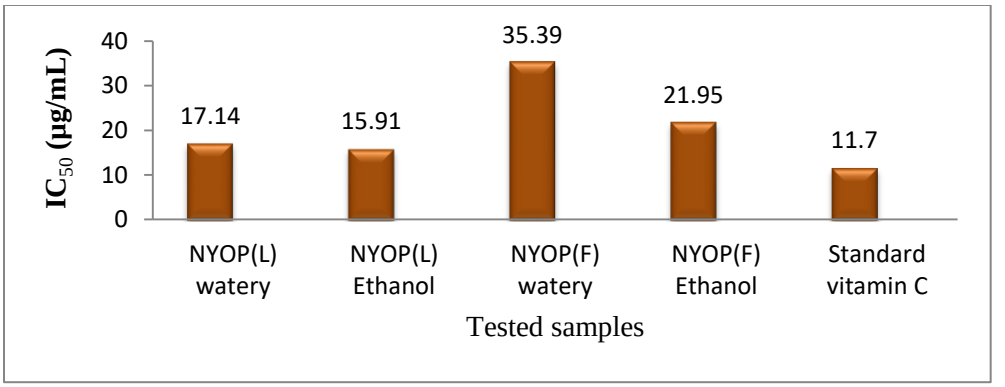

Figure 3: A bar graph of IC_{50} (µg/mL) of watery and ethanol extracts of leaves and flowers of NYOP

Determination of Total Phenolic and Total Flavonoid Contents of Leaves and Flowers of NYOP

The total phenolic contents and total flavonoid contents of NYOP leaves and flowers were estimated by Folin-Ciocalteau method and Aluminium Chloride Colorimetric method respectively. The total phenolic contents in watery and ethanol extracts of NYOP (L) and (F) were found to be 416.2 and 212.2; 320.7 and 195.9 mg of GAE/g of extract respectively. Among these, watery extract of NYOP (L)contained the highest phenolic content. The total flavonoid contents in watery and ethanol extracts of NYOP (L) and NYOP (F) were 88.9 and 114.4; 125.6 and 112.2 mg of QE/g of extract respectively. Among these, watery extract NYOP (F) has the highest flavonoid content. These results are shown in Table 4 and Figure 4.

Table 4: Total Phenolic and Flavonoid Contents of Leaves and Flowers of NYOP

Samples	TPC (mg GAE/g)	TFC (mg QE/g)
NYOP(L) Watery	416.2± 0.02	88.9± 0.01
NYOP(L) Ethanol	212.2± 0.02	114.4± 0.03
NYOP(F) Watery	320.7± 0.01	125.6± 0.01
NYOP(F) Ethanol	195.9± 0.01	112.2± 0.01

TPC = Total phenolic contents TFC = Total flavonoid contents

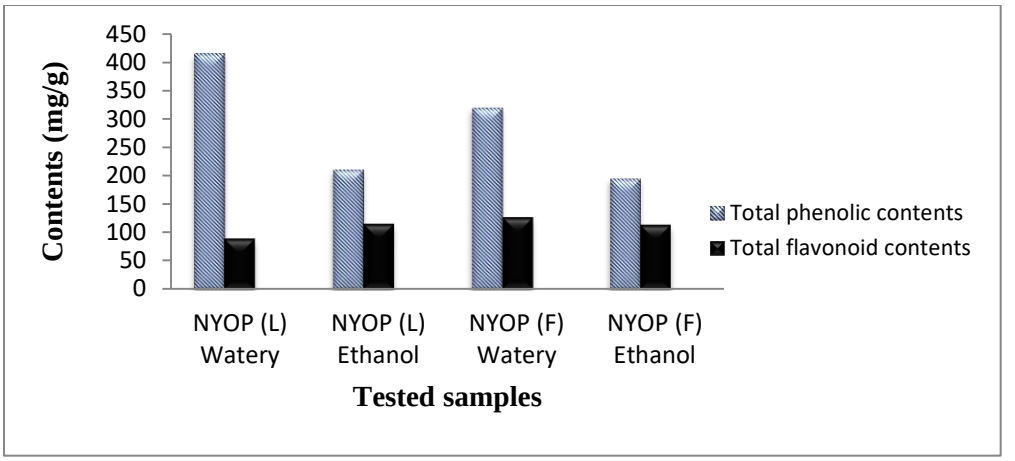

Figure 4: A bar graph of total phenol and flavonoid contents in watery and ethanol extracts of leaves and flowers of NYOP

Conclusion

The following inferences could be deduced from the overall assessment of the chemical investigation on the leaves and flowers of *M. malabathricum*(Nyaung-ye-o-pan).

The preliminary phytochemical tests investigated that alkaloids, α-amino acids, carbohydrates, flavonoids, glycosides, organic acids, phenolic compounds, reducing sugars, saponins, starch, steroids, tannins, and terpenoids were present in both leaves and flowers of NYOP. The harmful cyanogenic glycosides were absent in both of these samples indicating that these samples are free from toxic effect.

Some nutritional values such as moisture, ash, fiber, fat, protein and carbohydrate contents were observed in both of these samples. The leaves and flowers of NYOP exhibited interesting antimicrobial activities. This information provides a valuable clue for isolation of bioactive compound from leaves and flowers of NYOP.

The results indicated that leaves and flowers of *M. malabathricum* were found to berich in phenolic and flavonoid contents. Total phenolic and flavonoid contents had positive correlation with antioxidant activity. The finding of this study suggested that leaves and flowers of NYOP could be

potential source of natural antioxidant which are great important as therapeutic agents in preventing or slowing the progress of ageing and age associated oxidative stress related degenerative diseases.

Acknowledgements

I would like to acknowledge to Professor Dr. Hnin Hnin Aye (Professor and Head), Professor Dr. Ni Ni Than, Professor, Chemistry Department, University of Yangon, for their kind encouragement and supervisions, and Dr Khin Chaw Win, Lecturer, Chemistry Department, University of Yangon, for close supervisions, invaluable suggestions, helpful advice, patient guidance and encouragement. And I also would like to express profound gratitude to the Department of Higher Education (Lower Myanmar), Ministry of Education, Yangon, Myanmar, for provision of opportunity to do this research and Myanmar Academy of Arts and Science for allowing to present this paper.

References

AOAC. (2000). *Official and Tentative Methods of Analysis, Association of Official Analytical Chemists*.Washington D.C: 17th Ed., pp. 335-367

Anderson, J. (1984). "Effects of Dietary Carbohydrate and Fibre on Tilapia".*Aquaculture*, vol. 37,pp. 303-314

Basma, A. A., Zakaria, Z., Latha, L. Y. and Sasidharan, S. (2011). "Antioxidant Activity and Phytochemical Screening of the Methanol Extracts of *Euphorbia hirta*L.". *Asia Pacific Journal of Tropical Medicine*, vol. 4(5), pp. 386-390

Harborne, J.B. (1989). *Phytochemical Methods, A Guide to Modern Techniques of Plant Analysis*. New York: 2nd Ed., Chapman and Hall, New York, pp. 120-160

Joslyn, M.A. (1970). *Methods in Food Analysis*, New York: Academic Press, p. 405

Kaur, S.andPoonam, M.(2014). "Study of Total Phenolic and Flavonoid Content, Antioxidant Activity and Antimicrobial Properties of Medicinal Plants".*Journal of Microbiology and Experimentation*,vol. 1(1), pp. 1-6

Koya, S.S.(2008).*Establishment of Cell Suspension Culture of Melastoma malabathricum L. for the production of Anthocyanin*. Malaysia: Ph.D. (Dissertation), University Sians Malaysia

Lohezic-Le Devehat, F., Bakhtiar, A., Benzivin, C.,Amoros, M., and Boustie, J.(2002). "Antiviral and Cytotoxic Activities ofSome Indonesian Plants".*Fitoterapia*, vol. 73(5), pp. 400-405

Marini-Bettolo, G. B., Nicoletti, M., Patamia, M., Galeffi, C., and Messana, I. (1981). "Plant Screening by Chemical and Chromatography Procedure Under Field Conditions." *Journal of Chromatography*, vol. 231 (1), pp. 113-127

Marinova, G. and Batchvaros, V. (2011).“Evaluation of the Methods for Determination of the Free Radical Scavanging Activity by DPPH”.*Bulgarian Journal of Agricultural Science*, vol. 17(1), pp. 11-24

M-Tin Wa.(1972).“Phytochemical Screening, Methods and Procedures”. *Phytochemical Bulletin of Botanical Society of America*,vol. 5(3),pp. 4-10

Munin, A.(2011).“Phytochemical Analysis of Some Medicinal Plants”. *Journal of Phytology*, vol. 3(12), pp. 10-14

Nadkarni, A.K.(2000). *Indian Materia Medica*. Mumbai, India: 3rd Ed., Popular Press, pp. 45 – 49

Pearson, D. (1976). *The Chemical Analysis of Foods*. London: Churchill Livingstons, p. 16

Perry, L.M.(1980). *Medicinal Plants of East and Southeast Asia*., Cambridge;Harvest University, USA,pp. 258-260

Robinson, T.(1983).*The Organic Constituents of Higher Plants*. North America:5th Ed.,Cordus Press, pp. 63-68

Shriner, R. L., Fuson, R. C., Curtin, D. Y., and Morrill, T. C. (1980).*The Systematic Identification of Organic Compounds-A Laboratory Manual*, New York :John Willey and Sons Inc., vol. 4, pp. 113-121

Steyermark, A.I. (1961). *Quantitative Organic Macro Analysis.* London:2nd Ed., Academic Press, p. 188

Susanti, D., Sirat, H. M., Ahmad, F., Ali, R. M.,Aimi, N. and Kitajima, M. (2007). “Antioxidant and Cytotoxic Flavonoids from the Flowers of *Melastoma malabathricum* L.”*Food Chemistry*, vol.103 (3),pp. 710-716

Trease, G.E. and Evans, W. C. (1980).*Pharmacognosy*. London: 1st Ed., Spottiswoode Ballantyne Ltd., pp. 108, 529

Vogel, A. I.(1966). *A Text Book of Practical Organic chemistry*. London: 3rd Ed., Longmans, Green &Co. Ltd., p. 112

Zakaria, M. and Mohd, M.A. (1994). *Traditional Malay Medicinal Plants*.Kuala Lumpur: Fajar BaktiSdn. Bhd, p. 128

CHARACTERIZATION OF BANANA STEM FIBER AND EGG SHELL POWDER – NATURAL RUBBER COMPOSITES

Nyein Chan Aye[1], Nwe Nwe Aung[2], Nyo Nyo Myint[3], Thinzar Nu[4]

Abstract

This research work mainly concerned with the characterization of banana stem fiber(BSF) and egg shell powder(ESP)- natural rubber composites. Banana stem fiber and egg shell powder were used as fillers in the process of preparation of natural rubber composites. The banana stem fiber and egg shell powder-natural rubber composites were prepared by moulding method with various weight ratio (5 %, 10 %, 15 %, 20 %) of banana stem fiber and egg shell powder and were also characterized by modern technique such as SEM. The mechanical properties such as hardness, specific gravity, tensile strength, elongation at break and tear strength of banana stem fiber and egg shell powder- natural rubber composites were determined by standard rubber testing methods. From the experimental results, it was found that as the BSF and ESP loading increased, hardness and specific gravity also increased. Tensile strength of BSF and ESP composites decreased as BSF and ESP loading increased. Scanning electron micrograph results of both revealed that the distribution and adhesion interaction between the fillers and rubber matrix was good. It was generally observed that the egg shell powder presented better potentials for reinforcement than the banana stem fiber. These composites can be used as an alternative for various industrial applications.

Keywords: Natural rubber, banana stem fiber, egg shell powder, filler, mechanical properties

Introduction

Rubbers are widely used in various industrial applications, such as tires, seals and gaskets in automotive, aerospace, food and pharmaceutical industries, etc. credit to their highly non-linear elastic behaviour. Among all the rubbers available in the market, natural rubber which is obtained from the latex of the *Hevea brasiliensis* tree has good physical properties, such as high mechanical strength, low heat build-up and resistance to impact and tear.

[1.] PhD Student, Department of Chemistry, University of Yangon
[2.]Dr,Lecturer, Department of Chemistry, University of Yangon
[3.]Dr,Lecturer, Department of Chemistry, Mawlamyine University
[4.]Dr, Associate Professor, Department of Chemistry, University of Yangon

However, natural rubber has its drawback as well, such as low flame resistance, sensitivity to chemicals and solvents mainly due to its unsaturated hydrocarbon chain structure and its non-polar character, causing limitation in variety of applications. Hence, rubbers are reinforced by mixing with petroleum-based fillers, especially carbon black to enhance the mechanical properties of cross-linked rubbers. However, the petroleum reservoir is depleting due to its limited reserve and increasing demand from various industries. Furthermore, the world is facing environmental degradation due to excessive non-degradable waste rubber materials. Hence, developing alternative rubber composite materials which are cost effective, environmental friendly and biodegradable at the product end of life are amongst the most highly regarded research initiative. (Chai *et al*., 2016)

The advantage of composite material is that the high strength and stiffness of the filler can be incorporated into the soft, elastic rubber matrix. Among current biocomposites research works, food solid waste materials have been attractive bio-fillers for polymeric composites due to economic and environmental advantages. These bio-fillers are extracted from plants (e.g., oil palm, flax, jute, banana, hemp, etc.) and animals (e.g., eggshell, shellfish shell, shrimp shell, etc.) which are abundant and can be potentially used to replace the conventional reinforcing fillers. (Mohammed and Hadi, 2012)

Materials and Methods

Materials

Natural rubber (Grade 1) was obtained from Mudon Township, Mon State. The banana stems were collected from Mayangone Quarter, Mawlamyine Township, Mon State. To prepare eggshell powder used as the biofillers, chicken eggshell wastes were collected from various tea shops and home. The other compounding ingredients used were zinc oxide, stearic acid,N-cyclohexyl-2-dihydro-benzothiazolesulphonamide(CBS),2,6-di-tert-butyl-4-hydroxytoluene (BHT) and sulphur, which were supplied by Ministry of Agriculture, Livestock and Irrigation, Department of Agriculture, Rubber Research and Development Centre.

Preparation of Materials

Egg shell powder

The egg shell wastes (Figure 1) collected were washed thoroughly with water for several times. The egg shell membranes were removed and the egg shell pieces were dried under hot sun for three days (Figure 1). After the drying process, the egg shell pieces were grounded into powder form (Figure 2) by using domestic grinding machine.

Figure 1: Egg shell sample

Figure 2: Egg shell powder

Banana stem fiber

Banana stem was washed with water several times and dried under hot sun. And then, the dried stem was crushed and beaten by hand to obtain banana stem fiber. These fiber was ground by grinding machine (Figure 3).

Figure 3: (a) Banana stem (b) Banana stem fiber (c) Banana stem powder

Rubber composites

The formulation of the rubber is given in Table 1. The mixing of the rubber compounds were carried out by using a laboratory two roll open mixing millat Rubber Research and Development Centre. The nip gap, mill roll speed ratio, time, temperature of mixing, number of passes and sequence

of addition of ingredients during mixing were kept under same conditions for all compounds. The amount of fillers (egg shell powder and banana stem fiber) were varied 5-20 % in each composites.

Table 1: Formulation of Rubber Compounds

Ingredients	Amount (g)
Stearic acid	1.0
Zinc oxide	5.0
CBS	0.5
BHT	1.0
Sulphur	2.5
Fillers (BSF or ESP)	5-20

BSF - banana stem fiber	B_1 = 5 % BSF	E_1 = 5 % ESP
ESP - egg shell powder	B_2 = 10 % BSF	E_2 = 10 % ESP
g - gram	B_3 = 15 % BSF	E_3 = 15 % ESP
	B_4 = 20 % BSF	E_4= 20 % ESP

Methods

Some mechanical properties of composite such as hardness, specific gravity, tensile strength, elongation at break and tear strength were carried out by appropriated standard methods.

Determination of hardness

Hardness is a measure of the resistance to a reversible deformation of the rubber by a rigid indentor and widely used as a quality control measure. The hardness was measured using a Wallace Shore Adurometer according to ASTM D2240.

Determination of specific gravity

Specific gravity is a measure of the ratio of mass of a given volume of materials at 23 °C to the same volume of deionized water. The specific gravity was measured using a Wallace test equipment according to ASTM D792.

Determination of tensile strength

The fabricated composite was sized to obtain the required dimension and were made ready for testing as per ASTM: D638 standards. A universal testing machine was used to carry out the experiment at room temperature.

The standard dimension of tensile strength specimen is of length 165mm, 19mm breadth and 7 mm thickness. Test involved mounting the specimen and subjecting it to tension until fractures happened. The tensile load was recorded with respect to increase in gauge length. Each of 8 specimens namely B_1, B_2, B_3, B_4, E_1, E_2, E_3 and E_4 were prepared and experiment was repeated to obtain average values.

$$T_s = \frac{F}{W \times t}$$

T_s = tensile strength in Mega Pascal (MPa)
F = the maximum force recorded in Newton (N)
W = width of the narrow portion of the die in mm
T = thickness of the test length in mm

Study of surface morphology by scanning electron microscopy

The fracture behaviour of the specimens were observed using scanning electron microscope (Model - JOEL JSM- 5610) after sputter coating the samples with platinum for 45 seconds in a JOEL – JFC 1600 fine coater at a voltage of 12 kV. Photographs were taken at various magnifications.

Results and Discussion

Mechanical Properties

Hardness

Figure 4 shows that the hardness of composites increased as BSF and ESP % increased from 5 to 20 %. This is due to increasing the surface area of BSF and ESP in contact with rubber. The explanation of such behaviour agrees with the results of elasticity because hardness gives indication to modulus of elasticity for rubber under simple strain condition.

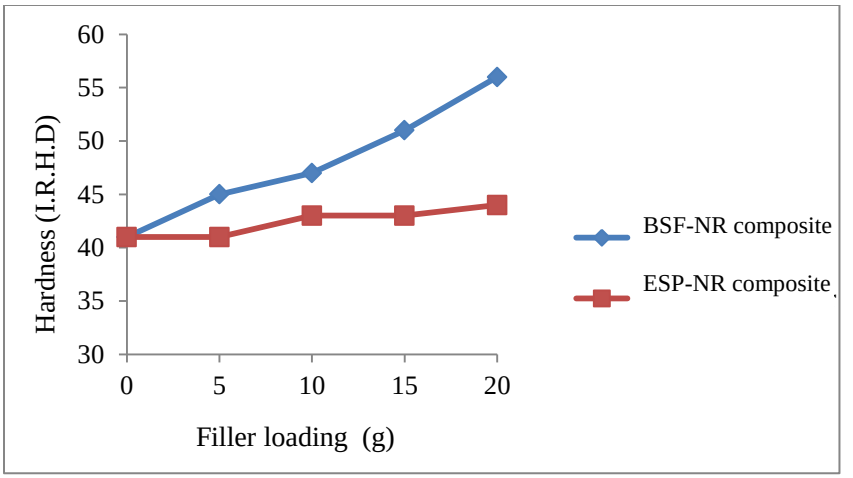

Figure 4: Hardness of prepared banana stem fiber-natural rubber composites and egg shell powder-natural rubber composites

Specific gravity

Figure 5 shows increasing of specific gravity of composites with increasing loading BSF and ESP %. This can be explained as follows that the particles interfere between rubber chains and make it denser per unit volume.

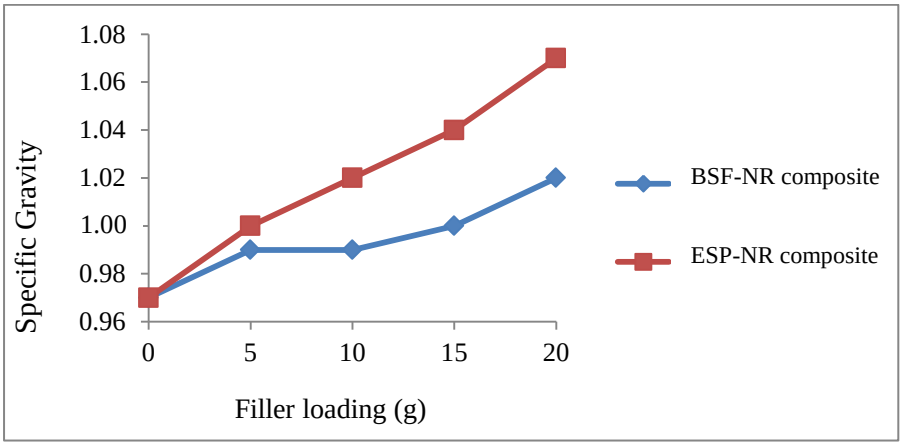

Figure 5: Specific gravity of prepared banana stem fiber-natural rubber composites and egg shell powder-natural rubber composites

Tensile strength

Figure 6 shows that the tensile strength of composites decreased as BSF and ESP % increased. The strength of particulate- filled polymer composites depends, to a great extent, on the interfacial adhesion between the matrix and the filler which will facilitate the transfer of a small section of stress to the filler particle during deformation. In this study, no coupling agent has been added into the BSF-NR and ESP-NR. In the absence of any coupling agent, the interfacial adhesion between the NR matrix and the BSF and ESP have obviously not been improved. Without the chemical modification, there is simply adhesion of the polymer to the filler through weak bonding, i.e., Vander Waals or induction interaction.

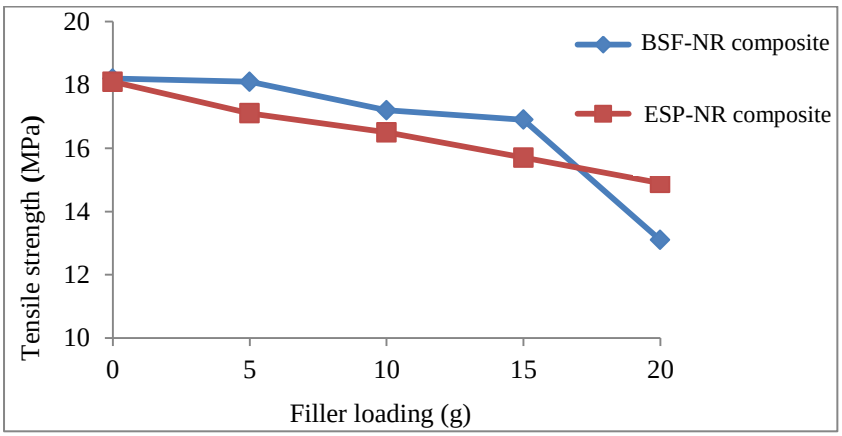

Figure 6: Tensile strength of prepared banana stem fiber-natural rubber composites and egg shell powder-natural rubber composites

Elongation at break

In Figure 7, it could be seen that the elongation at the break of composites decreased with increasing filler loading. Increased filler loading in the (NR) matrix resulted in the stiffening and hardening of the composite and the recipe take away from ductile.

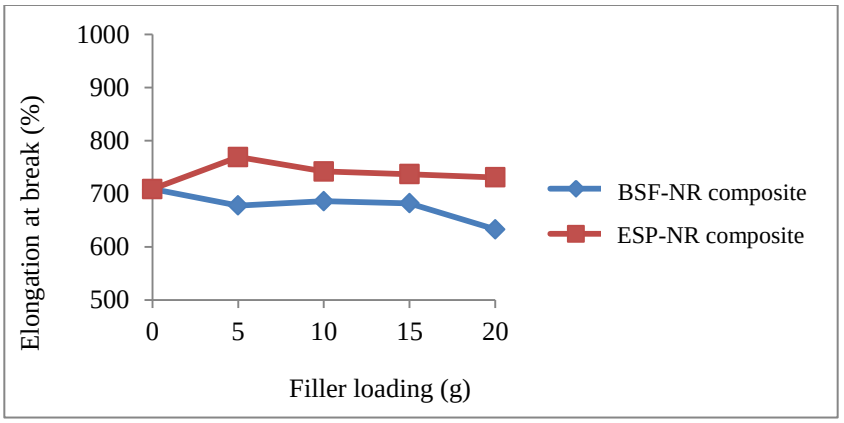

Figure 7: Elongation at break (%) of prepared banana stem fiber-natural rubber composites and egg shell powder-natural rubber composites

Tear strength

According to Figure 8, the tear strength results for ESP-NR composites decreased with increasing filler loading. On the other hand, the tear strength results for BSF-NR composites were fluctuated.

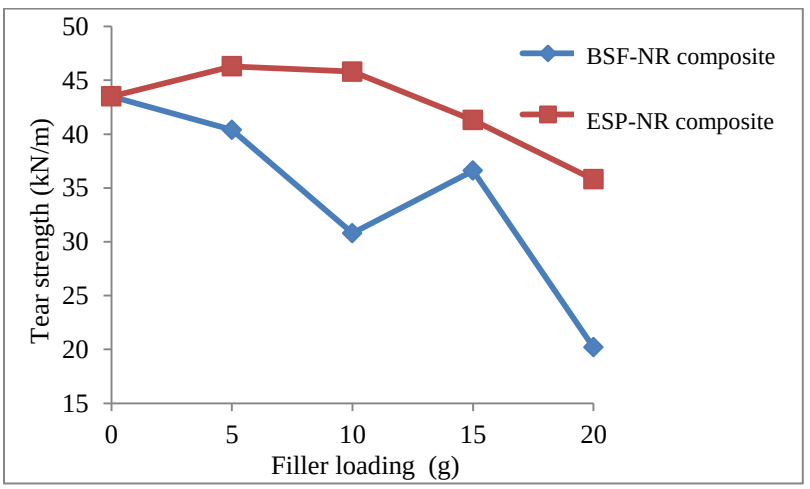

Figure 8: Tear strength of prepared banana stem fiber-natural rubber composites and egg shell powder-natural rubber composites

Morphological characteristics

Morphological characteristics of rubber composites obtained from banana stem fiber filled and egg shell powder filled natural rubber (Grade 1) with various fillers loading were investigated. Figures 9 (a), (b), (c) and (d) show the micrographs of B_1, B_2, B_3, B_4 composites. Among them, Figure 9 (c) shows the surface image of B_3 composite and it has uniform matrix with smooth interface having perfect regular shape of homogenous phase materials. Figures 10 (a), (b), (c) and (d) show the micrographs of E_1, E_2, E_3, E_4 composites. Among them, Figure 10 (b) indicated the surface image of E_2 composite which was more smoothand homogenously distributed through the particles on the composite, so the quality of it may be better than others.

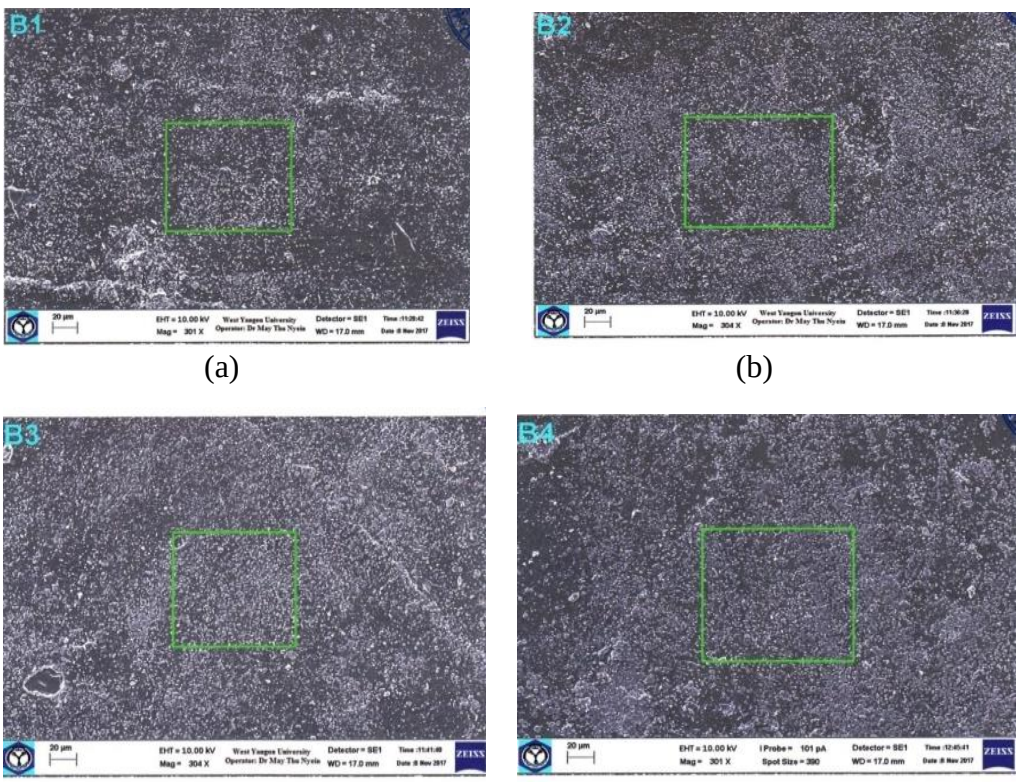

(a) (b)

(c) (d)

Figure 9: Scanning electron micrograph of B_1, B_2, B_3, B_4 composites

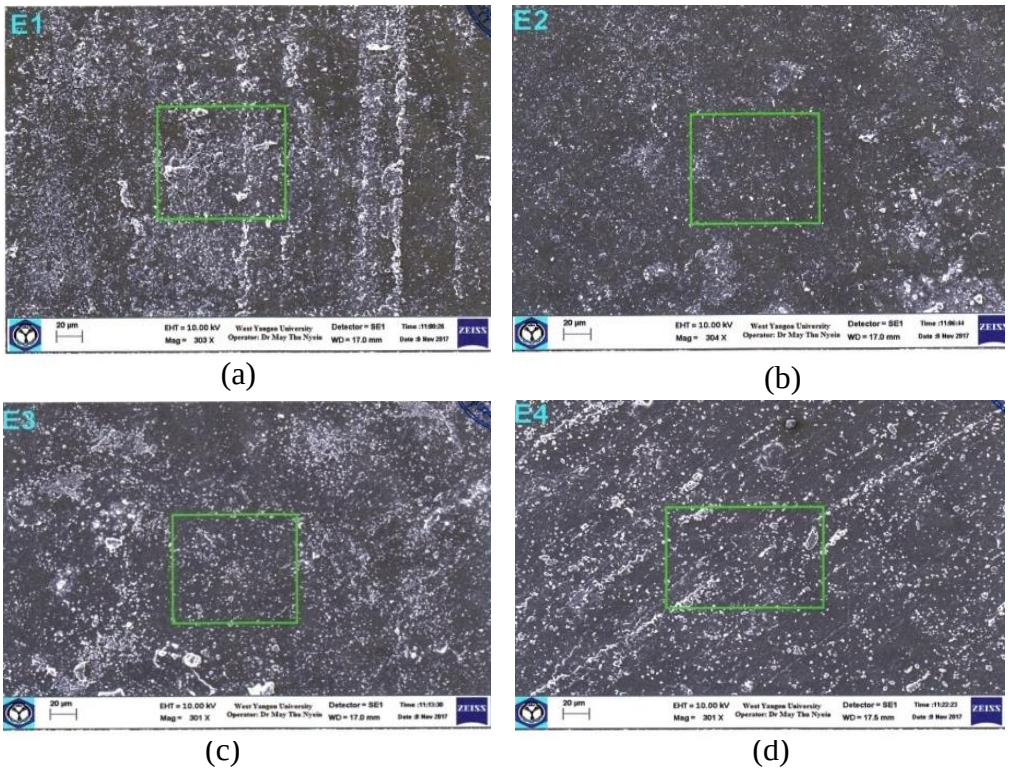

Figure 10: Scanning electron micrograph of E_1, E_2, E_3, E_4 composites

Conclusion

Banana stem fiber (BSF) and egg shell powder (ESP) were incorporated as biofillers in natural rubber composites. The mechanical properties and morphological properties of banana stem fiber and egg shell powder reinforced natural rubber composites have been investigated. As for the mechanical properties, it was concluded that as BSF and ESP loading increased, the hardness and specific gravity also increased. However, the tensile strength decreased as the filler content increased resulting in a poor dispersion of the filler on rubber matrix. The elongation at break and tear strength results for ESP-NR composites were decreased with increased filler percent in the rubber. The tear strength result for BSF-NR composites was fluctuated nature. The characteristics of composites were studied using scanning electron microscope. The results of this study was opened the

possibility to replace the use of existing fillers and decreased the cost of the products.

Acknowledgements

The authors wish to express their profound gratitude to the Myanmar Academy of Arts and Science for allowing to present this paper and to Professor Dr Hnin Hnin Aye, Head of the Department of Chemistry, University of Yangon for her kind encouragement.

References

Amal, S.M and Manusamy.Y. (2015).“Characterization of Raw Egg Shell Powder (ESP) as A Good Bio-filler”.*Journal of Engineering Research and Technology*, vol. 2(1), pp. 56-60

Blendzki, A. K and Gassan.J. (1999). “Composites Reinforced with Cellulose Based Fibers”. *Journal of Polymer Science*, vol. 24(2), pp. 221-274

Chai, A. B., Kamaruddin. S and Yeow.T.K. (2016). “The Effect of Oil Palm Fiber/ Egg Shell Powder Loading on The Mechanical Properties of Natural Rubber Composites”.*ARPN Journal of Engineering and Applied Sciences*, vol. 11(1), pp. 128-134

Ezema, I. C and Ravindranatha Mean. A. R. (2014). “Effect of Surface Treatment and Fiber Orientation on the Tensile and Morphological Properties of Banana Stem Fiber Reinforced Natural Rubber Composite”. *Journal of Minerals and Materials Characterization and Engineering*, vol.2, pp. 216-222

John, K. W and DeFilipps. R. F., Faff. Eand YinYinKyi. (2003). “A *Checklist of the Trees, Shrubs, Herbs and Climbers of Myanmar”.*Washington D.C: National Museum of United State, vol.45, pp. 1-590

Li, X., TabilL. G and Panigrahi. S. (2007).“Chemical Treatment of Natural Fiber for Use in Natural Fiber-reinforced Composites: A Review”. *J. polym.Envioron*,vol.15, pp. 25-33

Mohammed, R. M.,Hadi. A. N. (2012). “ Effect of Egg Shells Powder on Some Mechanical and Physical Properties of Natural Rubber (NR)”. *The Iraqi Journal For Mechanical and Material Engineering*, vol. 12(3), pp. 446-458

Mohanty, A. K.,Misra. M andHinrichsen.G. (2000).“Biofibers, Biodegradable Polymers and Biocomposites: An Overview”. *Journal of Macromolecular Material and Engineering*, vol. 3(4), pp. 1-24

NyoNyoMyint , Tin Tin Aye , KyawMyoNaing, Nyunt Wynn. (2008). “Performance study of the Natural Rubber Composites with Clay Minerals”.*Jou.Myan.Acad. Art &Sc*,vol. 6(1), pp. 151-159

Raghavendra,S.,Lingaraju, P.B. Shetty and Mukunda.P.G. (2013). " Mechanical Properties of Short Banana Fiber Reinforced Natural Rubber Composites". *International Journal of Innovative Research in Science, Engineering and Technology*, vol. 2(5), pp. 1652-1655

Santhosh, J., Balanarasimman. N.,Chandrasekar.R and Raja. S. (2014)."Study of Properties of Banana Fiber Reinforced Composites". *International Journal of Research in Engineering andTechnology*, vol. 3(11), pp. 144-150

Sonus, E. (2014). "Mechanical and Damping Properties of Rubber Reinforced with Natural Fiber". *The International Journal Engineering and Science*.,vol.3(5), pp. 17-24

EXTRACTION AND CHARACTERIZATION OF CHITOSANASE ENZYME FROM *Bacillus megaterium* UNDER LIQUID STATE FERMENTATION

Aye Aye Myat[1], Khine Zar Wynn Lae[2], Daw Hla Ngwe[3]

Abstract

The present research work focuses on the extraction of chitosanase enzyme from soil bacteria (*Bacillus megaterium*). In this research, the soil sample was collected from Htauk-kyant Township, Yangon Region for the isolation and cultivation of bacteria. In the isolation process, bacteria were isolated from the soil sample by serial dilution plate method, followed by culture in nutrient agar medium. Ten bacterial strains (A1 to A10) were isolated from the soil sample and were characterized by microscopic examination and gram staining methods. Among these bacterial strains, A1, A2, A3, A4, A6, A8, A9 and A10 were found to be gram positive, whereas only A5 and A7 were gram negative. According to the biochemical tests, out of eight gram positive bacterial strains, only A2 was observed to give the positive results on motility tests, methyl red tests, citrate utilization tests, starch hydrolysis tests, sugar fermentation tests and negative results on indole tests, nitrate tests, (VP) Voges-Proskauer tests that similar to the characteristics of chitosanase enzyme producing bacteria (*Bacillus megaterium*). Hence, A2 might be identified as *Bacillus megaterium.* For extraction of chitosanase enzyme, the isolated bacterial strain (A2) was cultured on chitosanase producing medium of 0.6 % poly peptone, 0.1 % K_2HPO_4, 0.05 % $MgSO_4.7H_2O$, 0.6 % yeast extract, 0.1 % glucose and 0.5 % colloidal chitosan and incubated at 30 °C. The optimum incubation time (3 days) of enzyme forming bacteria, inoculum sizes of bacteria (10 %), age of culture of bacteria (3 days), temperature of enzyme-catalyzed reaction (55 °C) and pH (7.0) of chitosanase producing medium were determined based on the chitosanase activities. Turbid enzyme bacterial solution was so prepared under above conditions for preparation of enzyme bacterial solution. The enzyme bacterial solution was centrifuged with 3000 rpm at room temperature and the supernatant enzyme solution was collected. The crude chitosanase solution was obtained and then partially purified by successive precipitation method by using 30 % and 70 % saturation of ammonium sulphate. Finally the total enzyme activity, protein contents and specific activity of crude enzymes obtained from each purification step were determined.

Keywords*:* chitosanase, *Bacillus megaterium*, biochemical tests, sugar fermentation tests, chitosanase enzyme activity

[1]. Ph.D, Student, Department of Chemistry, University of Yangon.
[2]. Dr, Lecturer, Department of Chemistry, University of Yangon.
[3]. Dr, Professor and Head, Department of Chemistry, University of Yangon.

Introduction

The enzyme found in numerous bacteria, fungi, insect, plant and animal involves in natural protection mechanism. Many bacteria and fungi containing the chitinolytic enzyme convert chitin into carbon and nitrogen that can serve as energy source. Chitinolytic bacteria are typically detected and screened through the production of clearing zones on chitin containing agar as selective medium. Chitinases have received attention because of their wide applications in the medicine, biotechnology, agriculture, biocontrol of plant pathogenic fungi, waste management and industrial applications such as food quality enhancer and biopesticide (Zarei and Aminzadeh, 2012).

Chitosanase or chitosan *N*-acetylglucosaminohydrolase (EC 3.2.1.132) catalyzes the hydrolysis of glycosidic bond of chitosan. Chitosanase has been found abundant in a variety of microorganisms, bacteria, including fungi, actinomycetes and a few in plants (Zakaria and Musa, 2012). It can be extracted from various types of bacteria such as *Bacillus megaterium*, *Bacillus cereus*, *Bacillus circulans*, *Bacillus coagulans*, *Bacillus licheniformis*, *Bacillus subtilis*, *Bacillus thuringiensis*, *Burkholderia gladioli*, *Matsuebacter chitosanotabidus*, *Streptomyces griseus*, *Trichoderma reesei*, *Pseudomonas aeruginosa* and these bacteria can be found in soil (Johnsen *et al.,* 2010). It has been used in the preparation of bioactive chitooligosaccharide, fungal protoplasts, biocontrol agent against pathogenic fungi and insects (Thadathin and Velappan, 2014).

Chitosan is a modified natural carbohydrate polymer derived from chitin consisting of 1, 4-β-linked d-glucosamine residues, partially substituted with *N*-acetyl groups to various degrees of acetylation and the chitin has been found in a wide range of natural sources such amycelial, sporangiophore walls of many fungi, the exoskeletons of insects, crustaceans, insects and some algae. In this study, *Bacillus megaterium* could be isolated from soil to produce chitosanase enzyme used to degrade chitosan into low molecular weight chitosan.

Materials and Methods

Sample Collection

The soil sample was collected from Htauk-kyant Township, Yangon Region. Dust and dead matters on the upper layer of the sampling site was removed followed by digging down to 6 inches depth. The collected soil sample was put into the sterilized plastic zipped bag and kept in refrigerator. The isolation of chitosanase enzyme producing bacteria *Bacillus megaterium* from soil sample was conducted in the Pharmaceutical Research Department, Insein, Yangon.

Isolation and Identification of *Bacillus megaterium* from the Collected Soil Samples

A 200 mL conical flask was filled with 99 mL of distilled water and four test tubes, each filled with 9 mL of distilled water were plugged with cotton wools and labeled as 10^2, 10^3, 10^4, 10^5 and 10^6 respectively and autoclaved at 121 ˚ C for 15 min.

About 1 g of the soil sample was put into 99 mL of distilled water in the 10^2 labeled conical flask. The flask was shaken gently for a few minutes and 1 mL of the above mixture was transferred into the 10^3 test tube and then 1 mL of mixture from the 10^3 test tube was transferred into the10^4 test tubes and so on.

After that, 1 mL of each of the prepared solutions (from 10^2, 10^3, 10^4, 10^5 and 10^6 conical flask and test tubes) was added to each of five nutrient agar plates and labeled. The inoculum was spread evenly over the entire surface of nutrient agar plates until the medium no longer appeared the moist. The spreader was returned to the alcohol and reap the flaming and spreading for each of the remaining four plates. Then all the plates were incubated in 37 ˚ C for 24 h.

The separate colonies were appeared and the different types of bacteria colonies were cultured in test. The colonies were found to be white to off-white in colour with smooth edges (Rampersad and Ammons, 2005) were selected and marked on Petri dish. The selected colonies with those characteristics were categorized as possible *Bacillus* colonies. Total of 10

colonies were chosen based on colony morphology. These selected colonies were repeatedly sub-cultured to obtain pure culture (Atlas and Synder, 2006).

The isolated bacterial strains were sub-cultured on nutrient agar slant cultures to check its purity and incubated at 37 °C for 24 h. Then the purified culture was maintained at refrigerator. The isolates were subjected to various physiological and biochemical tests. The isolates were identified by using conventional biochemical tests such as motility tests, methyl red tests, urease test, citrate utilization tests, indole tests, nitrate tests, (VP) Voges-Proskauer tests starch hydrolysis tests, sugar fermentation tests (Atlas and Synder, 2006; Garcia and Isenberg, 2007).

Determination of Optimal Conditions for Chitosanase Enzyme Production from the Selected Bacterial Strain

To find out the optimal conditions for producing chitosanase enzyme from the selected bacterial strain (A2), the effect of incubation time, pH, age of bacterial culture, inoculum size and temperature of enzyme catalyzed reaction on the chitosanase enzyme activity were studied.

(a) Effect of incubation time on chitosanase enzyme activity

Chitosan was used as the substrate in the chitosanase assay. Chitosanase activity was determined by quantitative estimation of the reducing sugars produced from chitosan. To prepare the culture medium for the production of chitosanase, the peptone (0.6 g), yeast extract (0.6 g), glucose (0.1 g), dipotassium hydrogen phosphate (0.1 g), magnesium sulphate (0.05 g) and colloidal chitosan (0.2 g) were used. The initial pH was adjusted to 7 with sodium hydroxide and the medium was put into a sterilized conical flask plugged with cotton wool and then sterilized by autoclaving autoclaved at 121 ºC for 15 min. The above medium was inoculated with 2 % inoculum size from 2 days age of culture in exponential growing phase and incubated on a shaker at 30 ºC and 180 rpm. To measure the enzyme activity, the content was centrifuged at 3500 rpm for 15 min and the cell free supernatant was used for analysis. For the optimum incubation time, the reaction temperature was used at 55 ºC.

(b) Effect of pH on chitosanase enzyme activity

The effect of pH on enzyme activity was determined by incubating the culture media at different pH values from 4 to 8 at optimized incubation period and 2 % inoculum size from 2 days age of culture. To study the optimum pH, the reaction mixture consisted of enzyme solution and 1 % colloidal chitosan between pH 4 to 8 at 55 ºC for 30 min. The reducing sugar was measured immediately at 540 nm by DNS method.

(c) Effect of age of culture on chitosanase enzyme activity

The effect of age of culture on enzyme activity was determined by incubation of five cultures on chitosanase producing agar at 30 ºC. The samples were taken every one day and stored for estimation of the optimum age of culture at 55 ºC for 30 min. The 1-5 days age of cultures were grown in chitosanase producing media using 2 % inoculums size at optimized incubation period and pH.

(d) Effect of inoculum size on chitosanase enzyme activity

The above medium (45 mL) in 250 mL of conical flask was inoculated with 2 %, 4 %, 6 %, 8 %, 10 % inoculum size of pre-culture in exponential growing phase and incubated on shaker at 30 ºC and 180 rpm. The effect of inoculum size on enzyme activity was determined by incubating the culture media at optimized incubation period, pH and age of culture.

(e) Effect of temperature on chitosanase enzyme activity

To determine the optimum temperature, the supernatant and 1 % colloidal chitosan were incubated at 35 ºC, 45 ºC, 55 ºC, 65 ºC and 75 ºC for 30 min at optimized incubation period, pH, age of culture and inoculum sizes.

Extraction and Partial Purification of Chitosanase Enzyme

Chitosanase enzyme solutions were extracted from the enzyme producing bacteria solution by precipitation method using 30 % and 70 % saturation with ammonium sulphate at 4 ºC. The mixture was allowed to settle down overnight. The bacterial cell pelleted out from precipitate was separated by centrifugation (3500 rpm, 30 min). Then the precipitate was

dissolved in 50 mL of 30 mM tris HCl buffer at pH 7.0. The solution was dialyzed overnight against the same buffer at 4 ºC (Sun *et. al*., 2009).

Determination of Protein Content in Partially Purified Chitosanase Enzyme

The concentration of protein content in supernatant obtained after precipitation with ammonium sulphate was determined by using Bovine serum Albumin (BSA) as standard. The reaction mixture was prepared by mixing 1 mL of sample and 4 mL of Biuret reagent solution at room temperature and allowed to stand for 30 min. It was followed by measuring the absorbance of the solution at 560 nm (Stoscheck, 1990).

Results and Discussion

Collection of Soil Sample

The soil sample was collected from the Htauk-kyant Township, Yangon Region. The soil sample was cultured on nutrient agar medium. Ten bacterial strains were isolated from the fresh soil sample.

Isolation and Culture of Bacterial Strain in Nutrient Agar Medium

Isolation plays a vital role for the identification of bacteria and this is the separation of pure culture (i.e., one species of bacteria) from mixed culture. During the process of taking bacteria from single by using a sterilized inoculating loop, the colony transfer was carried out in duplicate near the flame of spirit burner.

In the present work, nutrient agar medium was used as culture medium. Nutrient agar medium containing agar powder, nutrient broth with the combination of distilled water was found to be suitable for the culture of isolated ten bacterial strains (A1 to A10).

Identification of the Isolated Bacterial Strains

The morphology of ten isolated bacterial strains (A1 to A10) were examined under microscope. According to the microscopic examination, all of the isolated bacteria were found to be rod shape and motile.

Gram staining or Gram stain, also called Gram's method, is a method of staining used to distinguish and classify bacterial species into two large groups (gram-positive and gram-negative). The Gram stain is almost always the first step in the preliminary identification of a bacterial organism. According to the results from the characterization of the ten isolated bacterial strains (Table 1) by using gram staining tests, the bacterial strains A5 and A7 gave red colour and the remaining strains (A1, A2, A3, A4, A6, A8, A9 and A10) showed blue colour in this test.

Table 1: Characterization of the Isolated Bacterial Strains by Gram Staining Test

Isolated bacterial strains	Observed colour	Result
A1	Blue	+
A2	Blue	+
A3	Blue	+
A4	Blue	+
A5	Red	-
A6	Blue	+
A7	Red	-
A8	Blue	+
A9	Blue	+
A10	Blue	+

(+) = gram positive (-) = gram negative

Among ten bacterial strains, only 8 strains of gram-positive bacteria (A1, A2, A3, A4, A6, A8, A9 and A10) were selected to do further identification tests. The biochemical properties of that eight selected bacteria were studied by biochemical tests. In biochemical tests, bacterial strain A2 gave negative in indole test, nitrate reduction test and Voges-Proskauer and gave positive results in catalase, gelatin, urease, citrate utilization, starch hydrolysis, sugar fermentation, methyl red tests and motility tests. The results of biochemical tests for the eight selected bacterial strains are shown in Table 2 and that from sugar fermentation tests in Table 3. According to the biochemical tests and sugar fermentation tests, the results of the isolated bacterial strain A2 were found to be identical with the reported data of *B.*

megaterium (Beeseley *et al.*, 2010) as described in Tables 4 and 5. Consequently, the isolated bacterial strain A2 was identified as *B. megaterium*.

Table 2: Results of Biochemical Tests on the Eight Selected Bacterial Strains

Biochemical tests	Observation of the selected eight bacterial strains on biochemical tests							
	A1	**A2**	**A3**	**A4**	**A6**	**A8**	**A9**	**A10**
Motility	-	+	-	+	-	-	+	+
Gelatin liquefaction	+	+	+	+	+	+	+	+
Voges-Proskauer	-	-	-	-	-	-	-	-
Urease	+	+	-	-	-	+	-	-
Nitrate reduction	+	-	-	+	-	-	+	+
Starch hydrolysis	+	+	+	+	-	-	-	-
Citrate utilization	+	+	-	-	-	-	-	-
Methyl red	+	+	+	+	-	-	+	+
Indole	-	-	-	-	-	-	-	-

(+) = positive result, (-) = negative result

Table 3: Results of Sugar Fermentation Tests on the Eight Selected Bacterial Strains

Fermentation tests	Observation of the eight selected bacterias strains on sugar fermentation tests							
	A1	**A2**	**A3**	**A4**	**A6**	**A8**	**A9**	**A10**
Glucose	+++	+++	+++	+++	++	+++	+++	+++
Sucrose	++	++	++	+	++	++	+	++
Mannose	++	+	++	+	++	++	++	++

(+) = acid and gas liberate (slightly)
(++) = acid and gas liberate (moderately)
(+++) = acid and gas liberate (strongly)

Table 4: Comparison of the Results from Biochemical Tests on the Isolated Bacterial Strain A2 with the Reported Data of *B. megaterium*

Biochemical Tests	Observation on A2	**B. megaterium*
Motility	+ (Growth along the stab- line)	+
Gelatin liquefaction	+ (Liquefied)	+
Voges-Proskauer	- (Not appear pink colour)	-
Urease	+ (Pinkish- red)	+
Nitrate reduction	- (Not appear red colour)	-
Starch hydrolysis	+ (clear zone)	+
Catalase	+ (Bubble appeared)	+
Citrate utilization	+ (Blue colour)	+
Methyl red	+ (Red colour)	+
Indole	- (yellow layer)	-

* Beeseley *et al.,* 2010

Table 5: Comparison of the Results from Sugar Fermentation Tests on the Isolated Bacterial Strain A2 with the Reported Data of *B. megaterium*

Sugar tests	A2 (Isolated Bacteria)	* *B. megaterium*
Glucose	+++	+++
Sucrose	++	+++
Mannose	+	+

\+ = acid and gas liberate (slightly)
++ = acid and gas liberate (moderately)
+++ = acid and gas liberate (strongly)
\- = no gas
* Beeseley *et al.,* 2010

Producation of Chitosanase Enzyme Solution from the Isolated *B. megaterium*

Chitosan was used as the substrate in the chitosanase assay. Chitosanase activity was determined by quantitative estimation of the reducing sugars produced from chitosan. The reducing sugars formed in the supernatant were estimated spectrophotometrically by using the modified dinitrosalicyclic acid (DNS) method (Miller, 1959), using glucosamine hydrochloride as standard. Firstly, a standard calibration curve was constructed as a plot of absorbance vs concentrations of glucosamine solution (Table 6 and Figure 1).

Table 6: Relationship between Absorbance and Concentration of Standard Glucosamine Solution

Standard glucosamine solution	Glucosamine concentration (mg/mL)	Absorbance at 540 nm
1	1.00	0.064
2	2.00	0.140
3	3.00	0.206
4	4.00	0.276
5	5.00	0.339

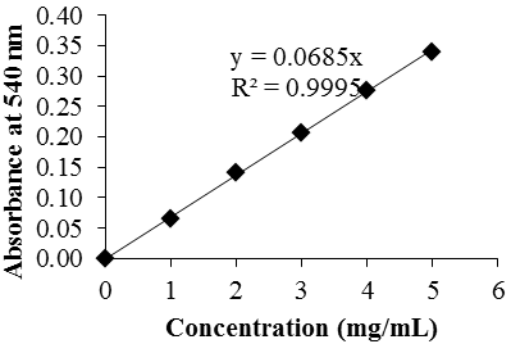

Figure 1: Standard calibration curve for glucosamine

Effect of different incubation times on enzymatic activity

The effect of incubation time on chitosanase production using pH 7, 2 % inoculum size from 2 days age of culture and reaction temperature 55 ºC is shown in Table 7. A2 bacterial strain produced the highest chitosanase activity on 3days (1.119 μmolmin^{1}mL^{1}). Enzyme production was gradually decreased after 3 days (Figure 2). One of the reasons for decreased production may be the lack of nutrients or production of toxic chemicals in the medium resulting in the inactivation of the enzyme production (Vanathia *et al*., 2016).

Table 7: Effect of Incubation Time of Chitosanase Forming Bacteria Solution on Chitosanase Activity by DNS Method

Incubation time (Day)	Absorbance at 540 nm	Chitosanase activity (μmol min^{-1} mL^{-1})
1	0.82	0.370
2	0.10	0.673
3	0.17	1.119
4	0.13	0.835
5	0.10	0.665

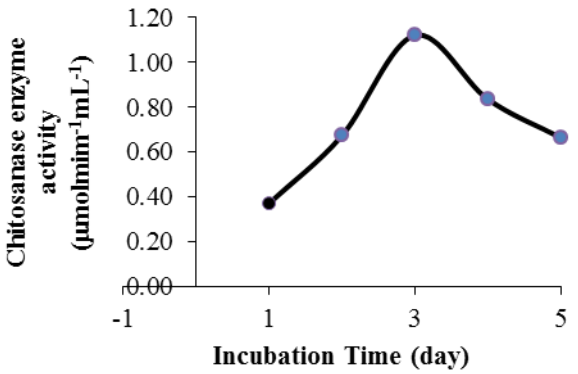

Figure 2: Plot of chitosanase enzyme activity as a function of incubation time of chitosanase enzyme forming bacteria solution

Effect of the different pH on enzymatic activity

The effect of pH of media on the chitosanase production was evaluated by bacterial cultures grown at different pH values (4 - 8) using optimum incubation time (3 days), 2 % inoculum size from 2 days age of culture and reaction temperature 55 ºC. Among the tested pH, pH 6 gave the maximum chitosanase activity (0.767 μmol mL^{-1} min^{-1}) (Table 8, Figure 3)

Table 8: Effect of pH of Chitosanase Production Medium on Chitosanase Activity by DNS Method

pH	Chitosanase activity (μmol mL^{-1} min^{-1})
4	0.709
5	0.718
6	0.767
7	0.682
8	0.639

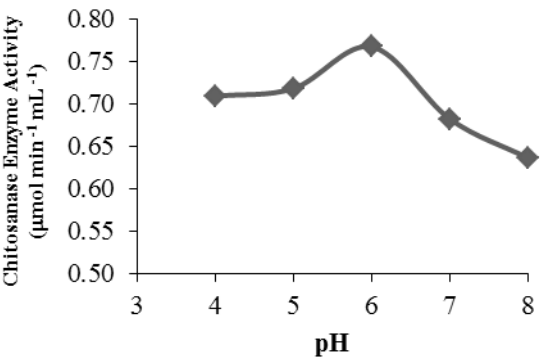

Figure 3: Plot of chitosanase enzyme activity as a function of incubation time of chitosanase enzyme forming bacteria solution

Effect of age of culture on enzymatic activity

The effect of the age of culture of media on the chitosanase production was studied up to 5 days using optimum incubation time (3 days), optimum pH 6, 2 % inoculum size and reaction temperature 55 ºC (Table 9). It indicated that chitosanase activity increased as the incubation time increased up to three days (0.840 μmol mL^{-1} min^{-1}) (Figure 4).

Table 9: Effect of Age of Culture of Bacterial Strain on Chitosanase Activity by DNS Method

Age of Culture (Days)	Chitosanase activity (μmol mL^{-1} min^{-1})
1	0.781
2	0.772
3	0.840
4	0.582
5	0.533

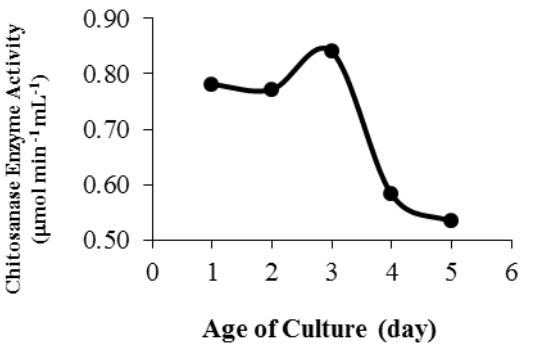

Figure 4: Plot of chitosanase enzyme activity as a function of age of culture of bacterial strain

Effect of inoculum sizes on enzymatic activity

The effect of inoculum size of media on the chitosanase production was evaluated by bacterial cultures grown at different inoculum size (2-10 %) using optimum incubation time (3 days), optimum pH 6, optimum 3 days age of culture and reaction temperature 55 ºC. Among the tested inoculum size, maximum inoculum size (10 %) gave the highest chitosanase activity (1.120 μmol mL^{-1} min^{-1}) (Table 10, Figure 5).

Table 10: Effect of Inoculum Sizes of Bacterial Solution on Chitosanase Activity by DNS Method

Inoculum Sizes (%)	Chitosanase activity (μmol mL^{-1} min^{-1})
2	0.569
4	0.605
6	0.745
8	0.840
10	1.120

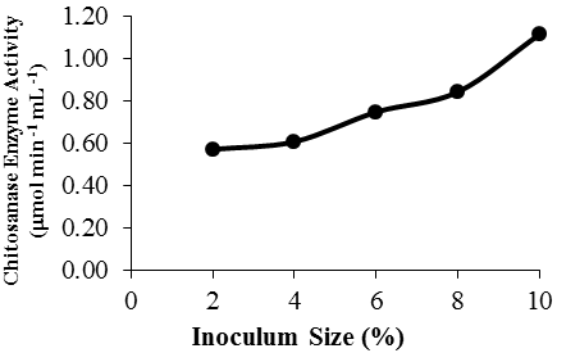

Figure 5: Plot of chitosanase enzyme activity as a function of innoculum sizes of bacterial solution

Effect of temperature on enzymatic activity

The effect of the temperature on the crude extract of chitosanase activity was studied in the range of 35 to 75 ºC using optimum incubation time (3 days), pH 6 and 10 % inoculum size from 3 days age of culture (Table 11). It was indicated that the maximum chitosanase activity (0.957 μmol $mL^{-1}min^{1}$) showed at the temperature 55 ºC (Figure 6).

Table 11: Effect of Temperature of Enzyme-catalyzed Reaction on Chitosanase Activity by DNS Method

Temperature (ºC)	Chitosanase activity (μmol mL^{-1} min^{-1})
35	0.682
45	0.827
55	0.957
65	0.890
75	0.740

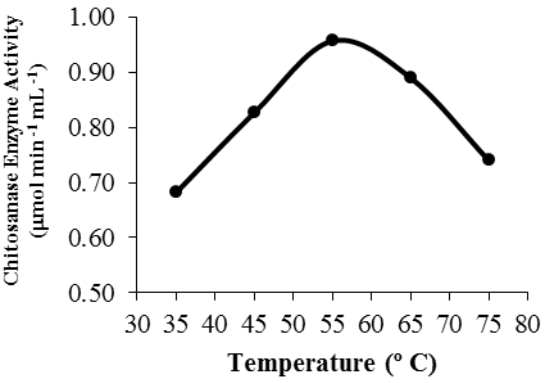

Figure 6: Plot of chitosanase enzyme activity as a function of temperature of enzyme catalysed reaction

The chitosanase activity (1.66 µ mol min^{-1}) was monitored by chitosanase assay method and the maximum activity of chitosanase was found under the condition for 3 days of incubation period of bacterial solution, pH 6 of chitosanase production medium, 10 % of inoculum size of bacteria and 3 days of age of bacterial culture and at 55 ºC of enzyme catalyzed reaction.

Partial Purification of Total Enzyme Activities of Crude Chitosanase Solution

The crude enzyme solution obtained from fermentation culture of *Bacillus megaterium* at optimum conditions was firstly purified by precipitating with 30 % saturation of ammonium sulphate solution. Then the collected supernatant enzyme solution in this step was also precipitated by using 70 % saturation of ammonium sulphate solution. The enzyme activities of the initial crude enzyme, the partially purified two enzymes by using 30 % and 70 % saturations of ammonium sulphate solutions were measured by DNS method. It was observed that the crude enzyme and two partially purified enzymes after precipitation with 30 % and 70 % saturation of ammonium sulphate solutions have 1.66 µ mol min^{-1}, 1.62 µ mol min^{-1} and 0.96 µ mol min^{-1} of enzyme activity, respectively. The degree of purity was 2.83 and 4.92 folds after 30 % and 70 % saturation of ammonium sulphate precipitation respectively (Table 12).

Total Protein Contents and Specific Enzyme Activities of the Isolated Chitosanase Enzymes

The crude chitosanase enzyme and two partially purified chitosanase enyzmes obtained by successive precipitation using 30 % and 70 % saturation of ammonium sulphate solutions were found to contain 6.43, 2.51 and 0.85 mg of protein contents, respectively. The protein contents of that enzymes were determined by Biuret assay method using bovine serum albumin (BSA) standard. It was found that the protein contents in enzymes decreased from 6.43 to 0.85 mg /mL after two steps purification.

Consequently, it leads to increase the total enzyme activity of the isolated enzymes and also to enhance the specific enzyme activity of crude enzyme from 0.26 μ mol min^{-1} mg^{-1} to 0.645 μ mol min^{-1} mg^{-1} after purified by 30 % saturation of ammonium sulphate solution and to 1.13 μ mol min^{-1} mg^{-1} after purified by 70 % saturation of ammonium sulphate solution. An increase in specific activity was observed after successively purified the crude enzyme by using 30 % and 70 % saturation of ammonium sulfate precipitation. The differences in specific activities observed at various purification steps while also comparing with that of the crude enzyme are shown in Table 12. According to the results described in the Table 12, the maximum specific activity was obtained after purified by using 70 % saturation of ammonium sulpahte precipitation.

Table 12: Total Enzyme Activity, Total Protein Content, Specific Enzyme and Degree of Purity Activity of the Isolated Chitosanase Enzymes

Purification steps	Total Enzyme activity (□mol min^{-1})	Total protein (mg)	Specific enzyme activity (□mol min^{-1} mg^{-1})	Degree of Purity (fold)
Crude enzyme solution	1.66	6.43	0.26	1.00
After 30 % $(NH_4)_2SO_4$ precipitation	1.62	2.51	0.65	2.83
After 70 % $(NH_4)_2SO_4$ precipitation	0.96	0.85	1.13	4.92

In each purification step, the total amount of chitosanase enzyme activity and protein decreased in order to salting out by high concentration of ammonium sulphate and removal of impurities. Purification of the crude chitosanase enzyme contained in the enzyme producing bacteria (*B. megaterium*) solution by 70 % ammonium sulphate precipitation resulted in increase in enzyme activity, which reflected in purification of 4.92 folds. Purification steps therefore resulted in elimination of interfering materials present in the crude cell- free extract thereby resulting in increased enzyme activity.

Conclusion

In this study, a gram-positive bacterial strain, *Bacillus megaterium* has been successfully isolated from the soil sample collected from Htauk-kyant Township, Yangon Region. The positive results were observed in biochemical tests such as catalase, methyl red, gelatin, urease, citrate utilization, starch hydrolysis, and sugar fermentation and negative results were observed in indole test, Voges-Proskauer test and nitrate reduction test.

The total enzyme activities of crude chitosanase having 1.66 μ mol min^{-1} and 6.43 mg of total protien content was produced from the isolated *B. megaterium* bacterial strain when 3 days of incubation period, pH 6 of chitosanase production medium, 10 % of inoculum size and 3 days age of bacteria culture at 55 ºC.

The crude chitosanase enzyme solution was partially purified by successive precipitation method using 30 % and 70 % saturation of ammonium sulphate solution giving 4.92 folds purity of chitosanase enzyme having 1.13 μ mol min^{-1} mg^{-1} of specific enzyme activity.

Acknowledgements

The authors would like to express their gratitude to the Department of Higher Education, Ministry of Education, Yangon, Myanmar, for provision of opportunity to do this research and Myanmar Academy of Arts and Science for allowing to submit this research paper.

References

Atlas, R. M. and Snyder, J. W. (2006). *Handbook of Media for Clinical Microbiology*. New York: 2nd Ed., CRC Publisher, pp. 278-339

Beesely, C. A., Vanner, C. L. and Helsel, L. O. (2010). "Isolation and Characterization of Clinical Bacillus Spp. Isolates Phenotypically Similar to *Bacillus anthracis*". *Federation of Europen Micrological Scocieties Microbiolol Lett*, vol. 313, pp. 47-53

Garcia, L. S. and Isenberg, H. D. (2007).*Clinical Microbiology Procedures Handbook.* Washington: 2nd Ed., DC American Society for Microbiology.

Johnsen, M., Hansen, O. and Stougaard, P. (2010). "Isolation, Characterization and Heterologous Expression of A Novel Chitosanase from Janthinobacterium sp. strain 4239". *Microbial Cell Factories*, vol. 9(1), pp. 5

Miller, G. L. (1959). "The Use of Dinitrosalicylic Acid Reagent for the Determination of Reducing Sugars". *Anal. Chem*. vol. 31, pp. 426–428

Prashanth, K. V. H and Tharanathan, R. N. (2007). "Chitin/Chitosan: modification and their unlimited application potential-an overview". *Trends in food Science & Technology*, vol. 18, pp. 117-131

Rampersad, J. and Khan, A. and Ammons, D. (2005). "A *Bacillus thuringiensis* Isolation Method Utilizing A Novel Stain Low Selection and High throughput Produced Atypical Results". *BMC Microbiol*. vol. 5, pp. 52-62

Stoscheck, C. M. (1990). "Quantitation of Protein Methods in Enzymology". *J. Boil. Chem*., vol. 18, pp. 61-65

Sun, Y., Zhang. J . and Wang, S. (2009). "Purification and Characterization of the Chitosanase from Aeromonas sp. HG08". *African journal of Biotechnology*, vol. 8(12), pp. 2830-2834

Thadathin, A. and Velappan, S. P. (2014). "Recent Developments in Chitosanase and Its Biotechnological Applications". *Journal of Food Chemistry*, vol. 150, pp. 392-399

Vanathia, P., Premasudha, P. and Rajendran, R. (2016). "Production and Characterization of Chitosanase Enzyme from Streptomyces sp Isolated from Biowaste Soil Samples". *Int. J. Pharm Bio Sci*, vol. 7(2), pp. 302-313

Zakaria, M. B. and Musa, M. (2012). "Identification of Chitosan-Degrading Microbes for the Production of Chitooligomer". *International Conference on Chemistry and Chemical Engineering IPCBEE*, vol. 38, pp. 127-131

Zarei, M. and Aminzadeh, S. (2012). "Chitinase Isolated from Water and Soil Bacteria in Shrimp farming Ponds". *Iranian Journal of Fisheries Science*, vol. 11 (4), pp. 911-925

ISOLATION AND GENOTYPIC IDENTIFICATION OF*ACIDITHIOBACILLUS FERROOXIDANS*

Khin Cho Lin[1], San Nwe Zin[2] and DawHla Ngwe[3]

Abstract

In this study, bioleaching of mineral pyrite ore collected from Moehti Moemi mining area, Yamethin Township, Mandalay Region was conducted by using *Acidithiobacillus ferrooxidans*. Two Soil samples were collected from two sampling areas, (Sakhangyi, SKG and Shwesin, SHN mining sites), Moehti Moemi, Yamethin, Mandalay Region. *A. ferrooxidans* was isolated from these two soil samples. The principal objective of the present investigation was to isolate and identify the acidophilic sulphur oxidizing *A. ferrooxidans* and to grow the isolates on selected 9K medium. The most commonly studied pyrite oxidizing bacteria are thermophilic *A. ferrooxidans*, which oxidizes ferrous iron and sulphur. The isolated bacteria were identified by phenotypic and genotypic identifications. In phenotypic identification, twelve biochemical tests such as motility test, hydrogen sulphide test, catalase test, urease test, starch hydrolysis test, indole test, methyl red test, gelatin liquefaction test, Voges- Proskauer test, nitrate reduction test, citrate utilization test and triple sugar iron test were performed. In genotypic identification, *A. ferrooxidans* was detected and confirmed by using specific primers for 16S rDNA PCR.

Keywords: *Acidithiobacillus ferrooxidans*, 9K medium, phenotypic identification, genotypic identification

Introduction

Acidithiobacillus ferrooxidans oxidizes iron(II) and recovers metals from low-grade sulphide ores and catalyses the oxidation of sulphur compounds to sulphuric acid. The acidiphilic microorganisms that take part in dissolution of metals from the sulphide ores are autotrophic in nature and can grow in inorganic medium having low pH values and can tolerate high metal ion concentrations. *A. ferrooxidans* species are rod-shaped, gram-negative, non-spore forming and thermophilic (Rawlings, 2002). These microbes have a number of features in common including; (a) they grow autotrophically by fixing CO_2 from the atmosphere, (b) they obtain their energy by using either ferrous iron or reduced inorganic sulphur compounds (some use both) as an

[1] Candidate, 3PhD Department of Chemistry, University of Yangon
[2] Dr, Associate Professor, Department of Chemistry, Bago University
[3] Dr, Professor and Head, (Retd.), Department of Chemistry, University of Yangon

electron donor, and generally use oxygen as the electron acceptor, (c) they are acidophiles and grow in low pH environments, (d) they are remarkably tolerant to a wide range of metal ions (Tuovinen, 1971). *A. ferrooxidans* have been isolated from different sources, most of the strains showed the following optimum growth conditions, i.e. pH 1.5-6 and a temperature range of 28–37 ^{o}C. Cells of *A. ferrooxidans* is ranging in length from 0.9 to 2 μm (Rawlings, 2002).

Bioleaching, a general term refers to the conversion of an insoluble metal into a soluble form by biological oxidation and by applying microbes. Metals for which this technique is mainly employed for recovery includes, copper, cobalt, nickel, iron, sulphur, zinc and uranium. For recovery of gold and silver the activity of leaching bacteria is applied only to remove interfering metal sulphides from ores bearing the precious metals prior to cyanidation treatment. The application of bacterial leaching to metal recovery from mineral ores has progressed steadily in the last 20 years (Rohwerder *et al*., 2003).Bioleaching has improved the efficiency of the mineral procession industry by lowering of the overall capital and procession costs and by diminishing environmental concerns associated with the pollution derived from emission of smelting operations (Quatrini and Holmes, 2005).

In the last few years, several molecular techniques for typing of *A. ferrooxidans* have been developed using PCR methodology such as 16S rDNA analysis. Many techniques are used to characterize and monitor microbial population. Molecular techniques have been employed to interrogate natural environment with great success. Many of these techniques have relied on the use of DNA sequence information. The polymerase chain reaction (PCR) has shown promise in detecting the presence of bioleaching microbes. The use of PCR allows for the detection of a specific organisms or groups. The 16S rDNA PCR used in this study is a rapid and specific tool for identification of microorganisms (Ilieva*et al*., 2011). In the present work, *A. ferrooxidans* were isolated from two soil samples collected from Moehti Moemi, Yamethin Township, Mandalay Region. It was characterized by using morphology and biochemical tests according to Bergey's Manual of Systematic Bacteriology (Bergey and Gibbons, 1974) and identified by PCR method using 16S rDNA analysis.

Materials and Methods

Collection of Soil Samples

Two soil samples from Sakhangyi(SKG) and Shwesin (SHN) were collected from Moehti Moemi, Yamethin Township, Mandalay Region. The collected soil samples were dried in air, ground and sieved through 200 mesh size and pH of the soil samples were determined.

Isolation of *A. ferrooxidans*

A. ferrooxidans was cultured on selected 9K medium, which mixed with solution A and solution B (Silverman and Ludgren, 1959). Solution A was prepared by adding 0.3 g of $(NH_4)_2SO_4$, 0.01 g of KCl, 0.05 g of K_2HPO_4, 0.05 g of ($MgSO_4$) $7H_2O$ and 0.001 g of $Ca(NO_3)_2$to 100 mL of distilled water. Solution B was prepared by 2.2 g of $FeSO_4$ in 50 mL of distilled water. In order to cultivate *A. ferrooxidans*, 50 mL of solution B was added to the prepared media. Two soil samples containing 9K medium were placed on a rotary shaker with 200 rpm for 8 days. After 8 days, bacteria were taken with a sterilized inoculation loop from the two conical flasks (9K medium) and streaked in Glucose Yeast Beef (GYB) medium plate by streak plate method. Then, it was incubated in an incubator at 37^{o}C for 7 days. After 7 days, single colonies of *A. Ferrooxidans* species were grown on GYB plate. Next, single colonies of *A. ferrooxidans* species were transferred to nutrient agar medium for culturing the pure colonies (Silverman and Ludgren, 1959). Five strains (two strains from SKG soil sample and three strains from SHN soil sample) of *A. ferrooxidans* subcultured on nutrient agar medium were stored in an incubator and transferred weekly for further studies.

The present research work was conducted at Myanmar Pharmaceutical Research Department and Microbiology Laboratory Department of Zoology, West Yangon University.

Phenotypic Identification of the Isolated *A. ferrooxidans*

The bacteria were identified by morphological examinations, gram staining and biochemical tests (Cruickshank, 1968).After confirming by microscopic examination, the isolated bacteria were identified by phenotypic method. Twelve biochemical tests such as motility test, hydrogen sulphide test, catalase test, urease test, starch hydrolysis test, indole test, methyl red

test, gelatin liquefaction test, Voges-Proskauer test, nitrate reduction test, citrate utilization test and triple sugar iron (TSI) test were conducted in accordance with Bergey's Manual of Determinative Bacteria. From phenotypic identification, among five isolated bacteria, one from SKG and one from SHN were identified as *A. ferrooxidans* (Shahroz *et al*., 2012).

Genotypic Identification of the Isolated *A. ferrooxidans*

The two selected bacteria were also characterized by genotypic identification. These bacteria were cultured in nutrient broth (NB) and laurain broth (LB) and allowed to stand for overnight. DNA was extracted from two A. *ferrooxidans*. Genomic DNA extraction was done by purelink genomic extraction kit according to protocol.DNA yield was checked by electrophoresis in 1 % agarose gel (35 min at 135 V and 60 mA) stained with 5μL dye (bromophenol blue and xylene cyanol). *A. ferrooxidans* was detected by using specific primers for 16S rDNA PCR. The nucleotide sequences of the primers used in PCR reactions for *A. ferroxidans* were F 5′ -AGA-GTT-TGA-TCM-TGG-CTC-AG-3′ and R 5′ -CGG-TTA-CCT-TGT-TAC-GAC-TT-3′ . Amplification conditions were carried out using Dream Taq PCR master mix, according to protocol. The volume of the reaction mixture was 25μL. The PCR program consisted of one cycle of DNA denaturation at 94 ^{o}C for 3 min, primer annealing at 50 ^{o}C for 3 min and a final extension at 72 ^{o}C for 8 min for 35 cycles gave a large number of products. The reaction were carried out in an Eppendorf Thermocycler. PCR products were separated by 1 % agarose gel and electrophoresis stained with 5 μL gel stain. Bands were visualized by illuminating ethidium bromide (Grigorii *et al*., 2003).

Results and Discussion

Sampling Sites

In this study**,** two soil samples: Sakhangyi (SKG) and Shwesin (SHN) collected from Moehti Moemi, Yamethin Township, Mandalay Region (Figure 1) were used to isolate *A. ferrooxidans*. The SKG soil was found to be moderately acidic (pH 5.7) and SHN soil was slightly acidic (pH 6.4).

Figure 1: Location of Moehti Moemi Gold Mine in Yamethin Township, Mandalay Region

Isolation of *A. ferrooxidans*

For isolation of acidophilic iron and sulphur-oxidizing bacteria(*A. ferrooxidans*), the collected two soil samples: SHN and SKG were activated in 9K acid medium. After shaking for 8 days, the cultured medium was observed by a change in colour to turbid brown (SHN soil sample) and reddish brown (SKG soil sample) due to the oxidation of Fe^{2+} to Fe^{3+} (Figures 2 and 3).

(a) SHN Soil (b) SKG Soil

Figure 2: Activation of soil samples in 9K acid medium (initial state)

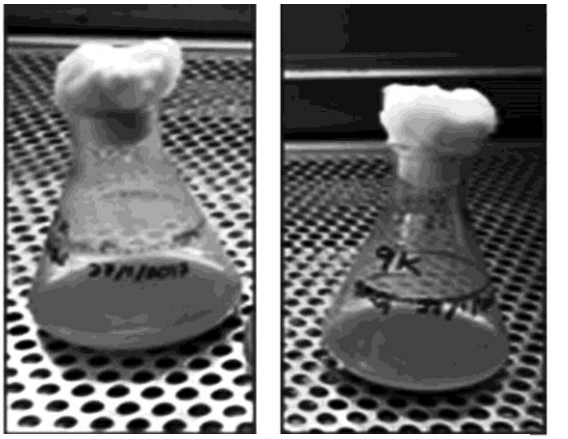

(a) SHN Soil (b) SKG Soil

Figure 3: Activation of soil samples in 9K acid medium (after 8 days)

It was streaked onto Glucose Yeast Beef medium (GYB). After 7 days of incubation at 37 °C, pale-yellow colonies of iron-oxidizing bacteria were developed on the GYB plate.

These pale-yellow colonies growing on GYB plates were picked, examined with microscope and cultivated separately on nutrient agar medium. Such ordinary procedures were repeated several times, finally pure cultured were obtained (Shahroz *et al*., 2012). From SKG soil samples, two strains of bacteria (SKG 1, SKG 3) and three strains of bacteria (SHN 2, SHN 4, SHN 5) from SHN soil sample were isolated.

Cell Morphology and Characterization of the Isolated Strains

According to microscopic observation, the five isolated strains (SKG 1, SHN 2, SKG 3, SHN 4 and SHN 5)were found to be motile and single rod-shape bacteria in pale yellow colour (Figure 4).

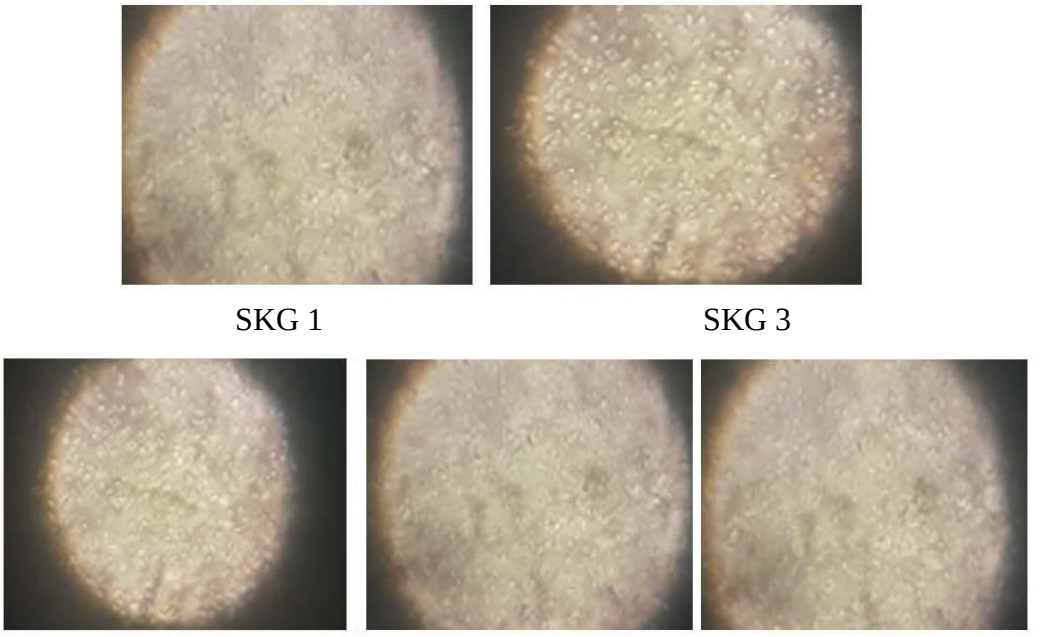

Figure 4: Morphology of five isolated bacterial strains

After the isolation of pure culture from nutrient agar medium, the bacteria were individually stained with 1 % crystal violet solution, gram's iodine solution, neutral red solution and then examined microscopically. It is the preliminary identification ofthe isolated strains. The strains gave red colour indicating to be Gram-negative.

Phenotypic and Genotypic Identification of *A. ferrooxidans*

Afterthegram's staining, different biochemical properties of the isolated bacteria were studied by motility test, hydrogen sulphide test, catalase test, urease test, starch hydrolysis test, indole test, methyl red test, gelatin liquefaction test, Voges-Proskauer test, nitrate reduction test, citrate utilization test and triple sugar iron test (TSI test) (Shahroz *et al*., 2012). In motility test, the growth of all organisms going out away from the stab line with surrounding medium was clearly transparent. So, all of the organisms gave positive results. In hydrogen sulphide test, black ferrous sulphide was not found so the bacteria can not produce hydrogen sulphide gas. The absence of

black precipitate was the sign of negative result. In the case of catalase test, formation of oxygen gas bubble were observed. This was positive in catalase test while the absence of bubble formation was a negative catalase test (Macfaddin, 2002).

In urease test, the organisms were grown in the urea broth medium containing the pH indicator phenol red (Jang *et al*., 1980). The colour did not turn into deep pink showing negative result. If the colour turned into deep pink it showed positive result (Cruickshank, 1968). In starch hydrolysis test, the medium colour was blue-black indicated the absence of starch-splitting enzymes and represented a negative result and a clear zone of hydrolysis around the growth of organisms, showed a positive result. In indole test, the absence of red colouration demonstrated the substrate tryptophan was not hydrolysed, giving negative result (Jang *et al*., 1980).

In methyl red test, the addition of methyl red caused the medium remained red indicating positive result. If the medium turns yellow it shows negative because pH of the medium increases. In gelatin liquefication test, the medium remained solid on refrigeration at 4 ^{o}C indicating the lack of gelatinase. In this test, the bacteria was not able to hydrolyse gelatin because the medium remained solid so gelatin liquefication test gave negative result. In the case of Voges-Proskauer test, it gave cherry red colour indicating positive result. In the study of nitrate reduction test, the colour did not turn into red indicating negative result. In citrate utilization test, the colour did not change which indicated that the citrate was not used as a carbon source and the result was negative. In triple sugar iron test (TSI test), the colour change showed the carbohydrate fermentation had not taken place and the result was positive (Shahroz *et al*., 2012).

According to the result from physiological, morphology and microscopic examinations, five isolated bacteria (SHN 2, SHN 4, SHN 5, SKG 1 and SKG 3) were selected. In biochemical test results, it was observed that bacterial strains SHN 2 and SKG 3 were generally in agreement with theoretical characters of *A. ferrooxidans*. The cell lengths of these bacteria were respectively found to be 1.2 µm and 2 µm. The results of biochemical tests for five isolated bacteria strains are described in Table 1.

Table 1:Results of Five Isolated Bacterial Strains by Biochemical Tests

Biochemical Tests	Observation	Results of observation of five isolated bacteria					*A. ferrooxidans*
		SKG 1	SHN 2	SKG 3	SHN 4	SHN 5	
Motility test	Growth of organisms	-	+	+	+	-	+
Hydrogen sulphide test	No precipitate	-	-	-	-	-	-
Catalase test	Bubble of O_2 gas	+	+	+	+	-	+
Urease test	No deep pink colour	+	-	-	+	-	-
Starch hydrolysis test	Blue to black	-	-	-	+	+	-
Indole test	No red colouration	-	-	-	-	-	-
Methyl red test	Yellow colour	+	-	-	+	+	-
Gelatin lique-Faction test	Remain solid	+	-	-	+	+	-
Voges-proskauer test	Red layer	+	+	+	+	+	+
Nitrate reduction test	No colour change	+	-	-	-	+	-
Citrate utilization test	No colour change	+	-	-	-	-	-
Triple sugar iron test	Colour change	+	+	+	+	+	+

(+) = positive, (-) = negative

* Shahroz*et al.,* 2012

The two isolated bacteria SHN 2 and SKG 3 were so further identified by partial nucleotide sequence of 16S rDNA. Amplification conditions were optimized using genomic DNA from pure cultures of two isolated strains. Total DNA fragments amplified from the genomic DNA of base pairs were revealed with the previous study (Ilieva *et al*., 2011).All of the base pairs were observed to be above the 950 level (Figure 5).

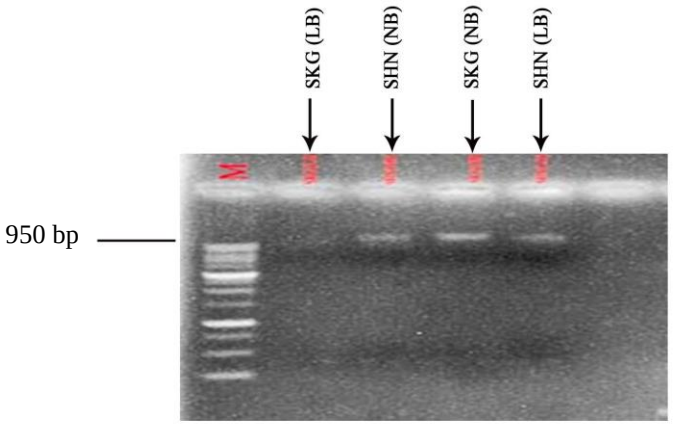

Figure 5:DNA fragments amplified from the genomic DNA of two isolated bacteria(SHN 2 and SKG 3)

Thus, the preliminary study of genomic DNA confirmed the isolated bacteria to be *A. ferrooxidans*. PCR was performed on the thermocycler. PCR under low stringency conditions gave a large number of products and several of which were of the anticipated size approx: 100 bp. This produced a few bands after gel electrophoresis. Each band were correspondedin size to the expected product of 118 bp which contained the desired sequences (Figure 6). PCR with 5′ -AGA-GTT-TGA-TCM-TGG-CTC-AG-3′ and R 5′ -CGG-TTA-CCT-TGT-TAC-GAC-TT-3′ primers gave single product of sizes upper the 100 bp (John *et al*., 1996). This is the first step in the molecular sequencing for the species identification. And also, this provide further impetus to study the commerical application of *A. ferrooxidans* in bioleaching process.

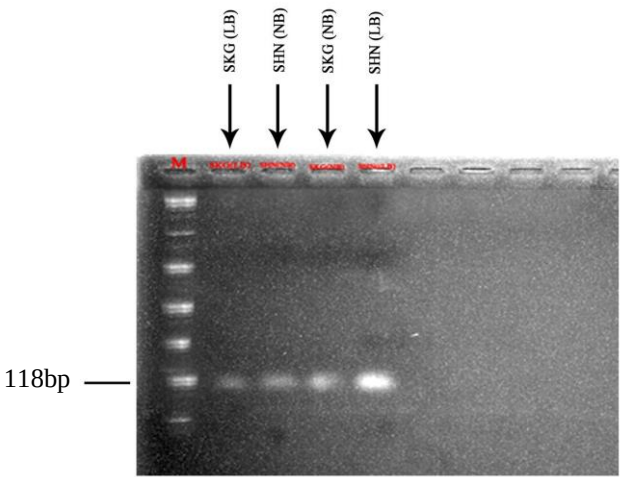

Figure 6: 16S rDNA amplification by PCR of two isolated bacteria (SHN 2 and SKG 3)

Conclusion

The results indicated that *A. ferrooxidans* was isolated from two soil samples collected from Sakhangyi and Shwesin mining sites, Moehti Moemi, Yamethin Township, Mandalay Region by 9K basal salt medium. The isolated *A. ferrooxidans* was identified phenotypically and genotypically. A. *ferrooxidans* is the main microbial species associated with the bioleaching process. Bioleaching is based on the ability of microorganisms to extract metal. The advantages of this technique are low cost, high efficiency and environmental friendliness.

According to molecular characterization, amplification conditions were optimized using genomic DNA from pure culture of the isolated bacteria (SHN 2 and SKG 3). The electrophoretic analysis of the PCR products showed that the size of the fragments amplified from the isolated bacteria matched with 118 bp. Also, no other amplification band was observed, which demonstrated the specificity of the chosen primers pairs. According to the result of this analysis, this extraction of genomic DNA could be done for molecular characterization and detection of sequencing for identification of *A. ferrooxidans*.

Acknowledgements

The authors would like to express their profound gratitude to the Department of Higher Education (Yangon Office), Ministry of Education, Yangon, Myanmar, for provision of opportunity to do this research and Myanmar Academy of Arts and Science for allowing to present this paper.

References

Bergey, D. H. and Gibbons, N. E. (1974).*BERGEY's Manual of Determinative Bacteriology.* United States of America : 8th ed., The Williams &Wilking Company, pp. 128-148

Cruickshank, R. (1968). *Medical Microbiology*. Edinburgh: 11th ed., E. and S. Livingstone Ltd., pp. 125-128

Grigorii, L., Tat'yana, P and Tamara, F.(2003). "Phylogenetic Heterogenetity of the Species *Acidithiobacillus ferrooxidans''*. *International Journal of Systematic and Evolutionary Microbiology*, vol. 53, pp. 113-119

Ilieva, R., Groudeva, V. and Iliev, M.(2011). "PCR Detection and 16S rDNA Squences Analysis of Different *Acidithiobacillus ferroxidans* Isolates". *Biotechnology and Biotechnological Equipment*, vol. 1, pp. 47-49

Jang, S.S., Biberstein, E. L. and Hirsch, D.C. (1988).*A Diagnostic Manual of Veterinary Clinical Bacteriology and Mycology*. University of California: 1th ed., Microbiological Diagnostic Laboratory, Veterinary Medical Teaching Hospital, pp. 112-113

John, F. H., Hasnain, S. and S and Ingledew, W. (1996). "The structural Gene for Rusticyanin from *Thiobacillus* ferrooxidans: Cloning and Sequencing of the Rusticyanin Gene". *Journal of Biological and Medical Sciences*, vol. 37, pp. 85-89

Macfaddin, J. F. (2000). *Catalase-Peroxidase Tests. Biochemical Tests for Identification of Medical Bacteria*. Philadelphia: 3rd Ed., Lippincott Williams and Wilkins, pp. 97

Quatrini, R. and Holmes, D. S. (2005)."Genomic Insights into the Iron Uptake Mechanisms of the Biomining Microorganism *A.ferrooxidans*". *Journal of Industrial Microbiol Biotechnol*, vol. 32, pp. 606-614

Rawlings, D.E. (2002). "Heavy Metal Mining using Microbes. Microbial".*Annual Review of Microbiology,* vol. 56 (1), pp. 65-91

Rohwerder, T., Gehrke, T. and Kinzler, K. (2003). "Bioleaching Review Part A". *Applied Microbiology and Biotechnology*, vol. 63(3), pp. 239-248

Shahroz, K., Farih, H. and Faizul, H. (2012) ."Growth and Biochemical Activities of *Acidithiobacillus thiooxidans* Collected from Black Shale". *Journal of Microbiology*, vol. 2(4),pp. 78-83

Silverman, M. P. and Lundgren, D. G. (1985). "Study on the Chemolithotrophic Iron Bacterium *Thiobacillus ferrooxidans*: An Improved Medium and a Harvestion Procedure for Securing High Cell Yields". *J. Bacteriol*, vol. 77, pp. 642-674

Tuovinen, O.H. (1971). "Tolerance of *Thiobacillus ferrooxidans* to Some Metals". *Antonieleeuwenhoek J Microbial*, vol. 37, pp. 489

ISOLATION AND CHARACTERIZATION OF FUNGAL LACCASE FROM *TRAMETES VERSICOLOR*

Khaing Khaing Myint[1], Ohn Ohn Soe[2], Daw Hla Ngwe[3]

Abstract

The present work focuses on screening, isolation, and partial characterization of the extracellular laccases from mushroom *Trametes versicolor*. Laccase-producing fungi were screened and isolated from the selected samples on Malt Extract Agar (MEA) medium. Laccase-producing fungi were detected by qualitative examination with guaiacol and tannic acid. The isolated fungal strain was identified by Lactophenol cotton blue dye method and microscopic examination. Laccase producing fungal strain was cultured under solid state fermentation using banana skin as support-substrate. The highest laccase activity was found on 12 days of incubation. Laccase was partially purified by ammonium sulphate fractionation (20 % and 70 %) and its activity was monitored by guaiacol assay method. Laccase was purified 6.4 fold over crude extract. The optimum pH and optimum temperature of fungal laccase was 5 and 40 ^{o}C, respectively.

Keywords: laccase, *Trametes versicolor,* guaiacol, solid state fermentation

Introduction

Laccases (benzenediol; oxygen oxidoreductase E.C. 1.10.3.2) are extracellular,multicopper enzymes that catalyze the oxidation of a variety of phenolic and inorganic compounds, with the concomitant reduction of oxygen to water (Stoilova *et al*., 2010). Laccase contains four copper atoms and is able to oxidize its substrates by using molecular oxygen as an electron acceptor (Thurston, 1994).These oxidative enzymes are particularly abundant in white-rot fungi. They have potential applications and used in many fields, including the environmental and industrial sectors such as pharmaceutical, nano-biotech, textile, paper and pulp, food-chemistry, cosmetic due to their low substrate specificities and high redox potentials (Madhavi and Lele, 2009; Upadhyay *et al.,* 2016; Akpinar and Urek, 2017).Fungal laccases have ability in the degradation of toxic fungal metabolite, such as aflatoxin B1, in ethanol production, manufacturing of cream and wine clarification. These

[1.] 3PhD Candidate, Department of Chemistry, University of Yangon
[2.] Dr, Associate Professor, Department of Chemistry, Loikaw University
[3.] Dr, Professor and Head (Retired), Department of Chemistry, University of Yangon

characteristics have led to laccases being qualified as ‘‘eco-friendly’’ enzymes (Alberts *et al*., 2009; Lu *et al*., 2007).

Laccases are widely distributed in nature and also been detected in plants (lacquer, mango, mung bean, peach, pin etc.), bacteria (*Bacillus subtilis*, *Escherichia coli*, *Pseudomonas syringae*) and especially in fungi (Majeau *et al*., 2010; Lui*et al*., 2017). Among them, white-rot fungi is the major laccase producer, and *Trametes versicolor* is an important representative of white-rot fungi. Many fungal laccases have been purified and characterized, such as *Trametes* sp. LAC-01, *Pleurotus* sp. MAK-II laccase and *Cerrena* sp. laccase (Manavalan *et al*., 2015 ; Ling *et al*., 2015; Yang *et al*., 2015).The genus *Trametes*, which belongs to the white-rot fungi, is assumed to be one of the main producers of laccases.

Two types of culture techniques are used for white-rot fungi to produce : solid-state fermentation (SSF) and submerged fermentation (SmF). The SSF occurs in absence or near absence of free liquid, using an inert substrate or a natural substrate as a solid support (Pandey *et al*., 1999). The former works as an attachment place for the microorganism, whereas the latter also acts as a carbon source, which considerably reduces the production costs (Ramana Murthy *et al*., 1999). SSF is advantageous in obtaining concentrated metabolites and subsequent purification procedures are economical.

This study is aimed to isolate laccases from white-rot fungi, *Trametes versicolor* using solid state fermentation and to partially characterize the enzyme.

Materials and Methods

Sample Collection

The mushroom (Figure 1) samples were collected in sterile plastic bags from the timber industry compound, Insein Township, Yangon Region, Myanmar. It was verified at Department of Agriculture, Ministry of Agriculture, Livestock and Arrigation.

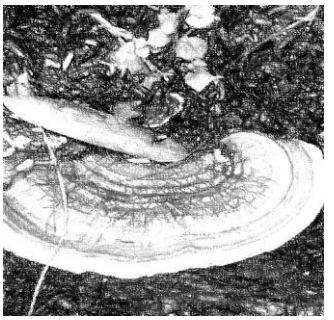

Figure 1: Mushroom (*Trametes versicolor*)

Screening of Fungal Strain

Mushroom sample (1 g) was extracted with 100 mL of sterile distilled water and then the aqueous extract was serially diluted (10^2, 10^3, 10^4, 10^5). After plating on Potato Dextrose Agar (PDA) and malt extract agar (MEA) media the petri dishes were incubated at 30°C for 5 days. The plates were marked as DMP-1, DMP-2, DMP-3 and DMP-4 for serially diluted mushroom samples in PDA media and DMM-1, DMM -2, DMM -3 and DMM -4 for diluted mushroom samples in MEA media (10^2, 10^3,10^4 and 10^5 dilutions respectively). Then white fungi were selected and sub-cultured on the PDA and MEA slant . Based on the heavy growth on MEA media it was chosen for further experiment. Then white fungi were selected and sub-cultured on the MEA media supplemented with 0.1% guaiacol and 0.1% tannic acid (Kiiskinen *et al.,* 2004). The fungi showing laccase activity were selected and then sub-cultured on the MEA slant. These strains were identified by Lactophenol dye method and observed under microscope. The fungal cultures were maintained by periodical sub-culturing on MEA slant at 30 °C and then stored at 4 °C.

Solid State Fermentation for Laccase Production

(a) Pretreatment of support – substrate, banana skin

Chopped banana skin (1 cm×1 cm) (70 g) was autoclaved at 120 °C for 20 min and then soaked in 200 mL of 83.17 mM potassium hydroxide solution for 1 h to neutralize the organic acid.The samples were thoroughly

washed with distilled water and dried at room temperature for one day. In this way the pretreated banana skin were obtained to be used as substrate for fermentation.

(b) Preparation of culture medium for solid state fermentation (SFF)

The composition of culture medium consisted of 3 g of peptone, 10 g of glucose, 0.6 g of potassium dihydrogenphosphate, 0.001 g of zinc sulphate, 0.4 g of dipotassium hydrogenphosphate, 0.0005 g of iron(II) sulphate, 0.05 g of manganese(II) sulphate and 0.5 g of magnesium sulphate in 1 L of distilled water. An inducer, copper(II) sulphate pentahydrate (0.0001 g) and one drop of Tween - 80 were added to the above culture medium.

(c)Preparation of crude laccase enzyme solution by solid state fermentation

Laccase was extracellularly excreted by *Trametes versicolor* during solid state fermentation. Three loops of fungal strain, 5 mL of culture medium and 30 g of the pretreated banana skin were inoculated in a 500 mL conical flask. This flask was incubated at 30 °C for 18 days.Fungal growth and enzyme activity were assayed periodically. To optimize the time for fungal growth,the fermented matter (2 g) of the specified period (3, 6, 9, 12, 15, 18 days) was obtained by adding 10 mL of distilled water to it. The flasks were mixed for 30 min at room temperature using a shaker (180 rpm). Solids were removed first by filtering and then by centrifuging at 2000 rpm for 20 min. The cell free supernatant obtained was used as crude enzyme extract for the determination of laccase activity.

(d) Purification of laccase by ammonium sulphate precipitation method

After 12 days of fermentation, the fermented matter of *Trametes versicolor* was dissolved in acetate buffer (pH 5) with 1:10 ratio and shaken on the shaker for 20 min. It was filtered to remove mycelia, followed by centrifugation at 2000 rpm for 30 min. The supernatant thus obtained was subjected to the total protein precipitation with ammonium sulphate in the range of 20–70 % saturation to obtain partially purified enzyme extract.

(e) Determination of laccase activity, protein content and specific activity in different purification steps

The laccase activities (guaiacol assay method) and protein contents (Biuret method) of the crude enzyme extract and the enzyme extract obtained after successive precipitation with 20 % and 70 % satuation of ammonium sulphate solutions.

(i) Determination of laccase activity of the crude enzyme extract by Guaiacol assay method

Guaiacol assay method was carried out according to the method of Desai *et al.* (2011).Guaiacol (2 mM) in sodium acetate buffer (10 mM pH 5.0) was used as substrate. The reaction mixture contained 3 mL of acetate buffer, 1 mL of guaiacol and 1 mL of the crude enzyme solution. For blank solution, 1 mL of distilled water was used instead of enzyme solution. The mixture was incubated at 30 ºC for 15 min and the absorbance was read at 450 nm. The laccase activity was calculated using the extinction coefficient of guaiacol (12,100 M^{-1} cm^{-1}) at 450 nm by the formula as shown below. E.A = (A x V) / (t x e x v) (Savitha *et al.,* 2011), where E.A = enzyme activity (U/mL), A = absorbance at 450nm, V = total volume of reaction mixture (mL), v = enzyme volume (mL), t = incubation time (min) and e = extinction coefficient (12100 M^{-1} cm^{-1}). One unit of enzyme was defined as the amount of enzyme required to oxidize 1 micromole of guaiacol per min.

(ii) Determination of protein content

Protein content was determined by Biuret method using Bovine Serum Albumin (BSA) as standard at 560 nm. Firstly, the calibration curve of BSA was constructed to determine the concentration of protein in the enzymes. Then 1 mL of standard protein solutions with concentrations of 1, 2, 3, 4 and 5 mg mL^{-1} was individually added to five test tubes, each containing 4 mL of Biuret reagent solution and the contents were mixed well. The solution mixture was kept for 30 min at room temperature. After that the absorbance values of the standard protein solutions were measured and the calibration curve was constructed. A blank solution and enzyme solution were prepared

by using 1 mL each of distilled water and enzyme solution, respectively, instead of standard protein solution.

(iii) Determination of specific activity

Specific activity was determined by the ratio of total activity to the total protein content. Specific activity is a measure of enzyme efficiency.

(f) Characterization of laccase

The optimum pH and optimum temperature of laccase- catalyzed reaction for the partially purified laccase enzyme obtained by 70 % ammonium sulphate precipitation were investigated by spectrophotometric method.

For the study on the effect of pH, the reaction mixtures contained 1mL each of guaiacol (2 mM) as substrate dissolved in 1 mL each of enzyme solution and 3 mL each of buffers of different pH values (acetate buffer pH 3, pH 4, pH 5, phosphate –citrate buffer pH 6 and pH 7). The mixtures were incubated at 40 ºC for 15 min and the absorbance values were recorded at 450 nm.

Similarly, for the study on the effect of temperature, the mixtures contained 1 mL each of guaiacol (2 mM) as substrate dissolved in 1 mL each of enzyme solution and 3 mL each of 10 mM acetate buffer (pH 5). The mixtures were then incubated at different temperatures of 25 ºC, 30 ºC, 35 ºC, 40 ºC, 45 ºC, 50 ºC, 55 ºC, and 60 ºC for 15 min and absorbance values were recorded at 450 nm.

Results and Discussion

Isolation of Laccase-producing Fungi from Mushroom, *Trametes versicolor*

The mushroom sample (1 g) (*T. versicolor*) collected from Timber Industry Compound near Gyogone, Insein Township, Yangon Region. It was firstly extracted with sterilized distilled water (100mL).And that extracted was then serially diluted($10^{2,}$ 10^3, 10^4, 10^5) and then the diluted solutions were inoculated in fungal selected Potato Dextrose Agar (PDA) and Malt Extract Agar (MEA) media. After 5 days of incubation, growth of fungi were seen on

the PDA and MEA media (Figure 2). Among 8 petridishes, 4 petridishes (DMP-3, DMP-4, DMM-3 and DMM-4) were selected due to the appearance of white fungi. Then the white fungi were sub-cultured in PDA and MEA slants and it was found that MEA slants gave purified fungi compared to PDA slants (Figure 3). Laccase – producing fungi was examined in the presence of guaiacol and tannic acid supplemented MEA media and the formation of reddish brown zones around the fungal colonies was observed after 6 days of incubation (Figure 4). The pure culture on MEA medium was rich with white aerial mycelium (Figure 5). The reverse of the mycelia was colourless, pigmentation was not found even after two weeks of cultivation. In the lactophenol cotton blue staining, spores were cylindrical to sub cylindrical and thin-walled (Figure 6). Hyphae (threadlike elements of the mycelium) have cross-walls called septa between cells. Therefore, Figures 4, 5, 6 stated the laccase - producing fungal character and showed isolated fungi.

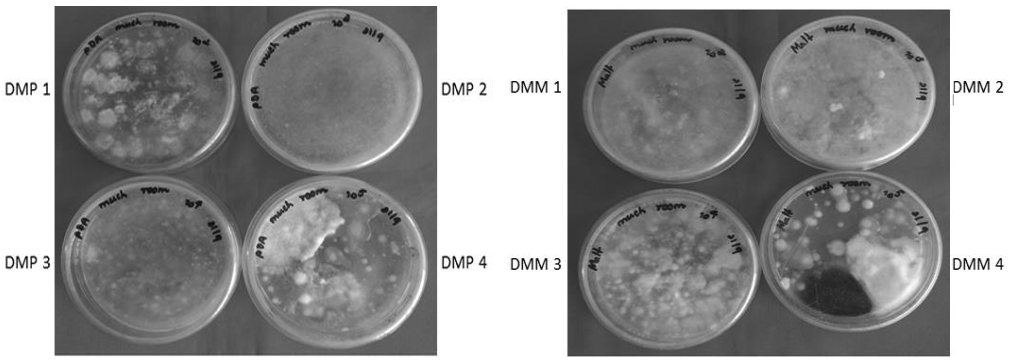

Figure 2: Growth of fungi from mushroom on (a) PDA media and (b) MEA media by serial dilution method

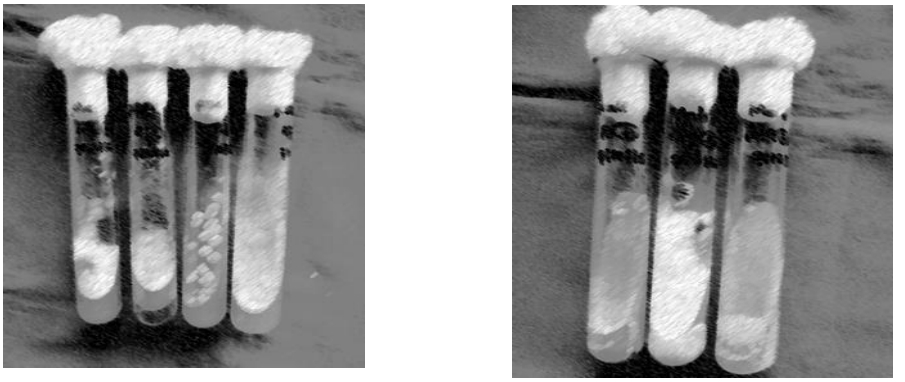

(a) (b)

Figure 3: Sub- culture of fungi in (a) PDA and (b) MEA slants

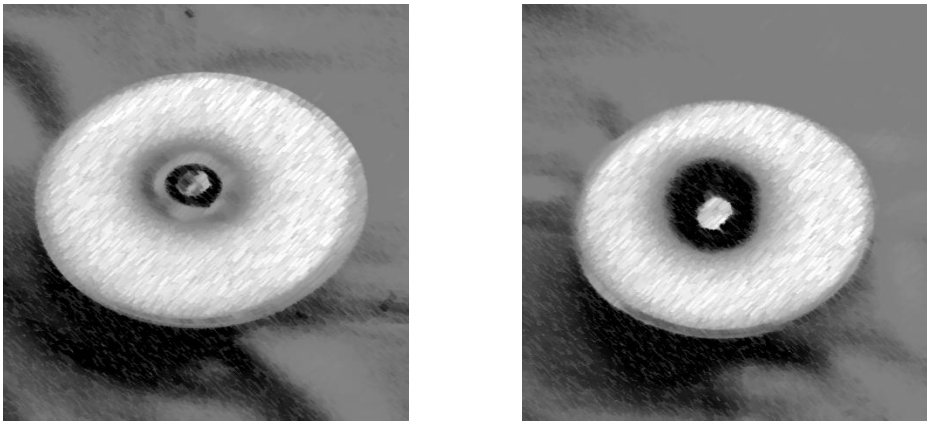

(a) (b)

Figure 4: Reddish-brown colonies zone on MEA media supplemented with (a) guaiacol and (b) tannic acid

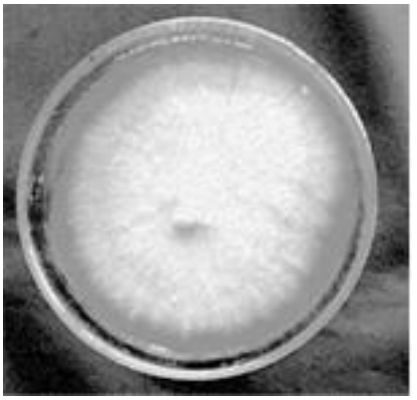

(a)

Figure 5: Pure culture of the isolated fungal strain

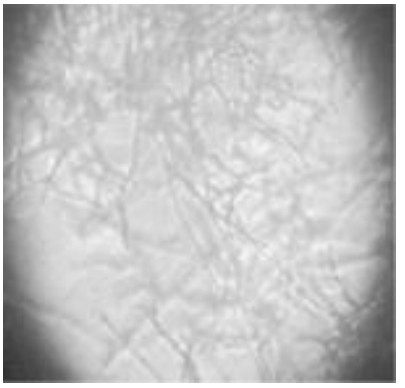

(b)

Figure 6: Mycelium structure of the strain under microscope at 40 X

Production of Laccase from the Isolated Fungus from *T. versicolor* under Solid State Condition

The result of the time course study for laccase production by using the pretreated banana skin as substrate by the isolated fungus is shown in Table 1 and Figure 7. In this study,Tween 80 was used as a surfactant which could modify the fungal membrane and promote laccase secretion by many fungal strains (Dekker *et al.*,2007). The laccase activity in the culture broth increased with increase in cultivation time and the production of laccase peaked at the late stage of cultivation,i.e., 12 days. However, the laccase activity decreased after further cultivation time. Maximum laccase activity was found after 12 days of solid state fermentation in this study.

Table 1: Activity of Laccase Produced at Various Incubation Times under solid State Fermentation (SSF)

No.	Incubation time (day)	Laccase activity ($\mu mol\ mL^{-1}\ min^{-1}$)
1	3	10.2
2	6	11.5
3	9	12.3
4	12	13.9
5	15	11.1
6	18	9.5

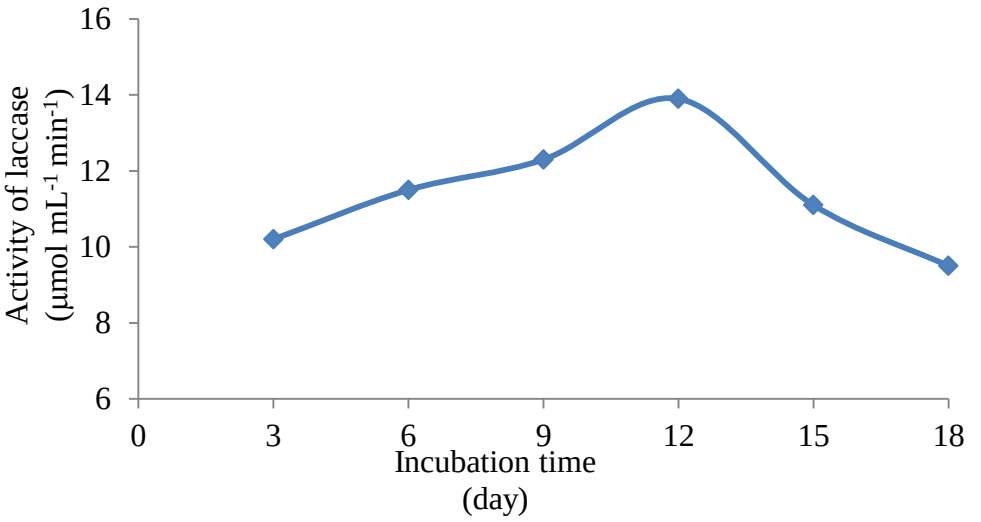

Figure 7: Activity of Laccase Produced at Various Incubation Times under solid State Fermentation (SSF)

Partial Purification of Laccase from*T. versicolor*

Laccase from *T. vesicolor* was partially purified by fractional ammonium sulphate precipitation method. Laccase activity in each purification step was determined by guaiacol assay method at 450 nm.For determination of specific activity of laccase, protein contents in enzyme extracts were determined by Biuret method using calibration curve of standard bovine serum albumin solution.

After 20 % ammonium sulphate precipitation, the specific activity of laccase increased from 0.25 µ mol $min^{-1}mg^{-1}$ in crude extract to 0.50 µ mol $min^{-1}mg^{-1}$ (Table 2). Furthermore, specific activity increased to 1.60 µ mol $min^{-1}mg^{-1}$ after 70 % ammonium sulphate precipitation and purification fold also increased to 6.4 fold over crude extract.

Table 2: Total Enzyme Activity, Total Protein and Specific Laccase Enzyme Activity Obtained at Different Purification Steps

Purification steps	Total activity (μ mol min^{-1})	Total protein (mg)	Specific activity (μ mol $min^{-1}mg^{-1}$)	Purification (fold)
Crude extract	6720	30000	0.25	1
After 20 %$(NH_4)_2SO_4$ precipitation	2590	5000	0.50	2
After 70 %$(NH_4)_2SO_4$ precipitation	3770	1600	1.60	6.4

Characterization of Purified laccase Enzyme

(a) Optimum pH

The pH optimum was determined over a range of pH 3–6 at 30 °C. The pH optimum of laccase was determined by using two different buffer systems comprising of 10 mM sodium acetate buffer (pH 3.0–5.0) and phosphate – citrate buffer (pH 6.0–7.0). Activity of laccase gradually increased from pH 3 to 5 and then abruptly increased when pH was reached at 5 (Table 3 and Figure 8). Beyond pH 5,laccase activity were found to decrease. In this study, the highest laccase activity was achieved at pH 5.Optimum pH value of laccase from both *Pleurotus ostreatus* and *Coprinusfriesii* was found as5.0 (Palmieri *et al*., 1997; Heinzkill *et al*., 1998).Stoilova *et al*. (2010) reported the optimum pH of laccase from *Trametes versicolor* as 4.5.The result in this study is in line with Holker *et al.* (2002) and Robles *et al.* (2002) who revealed that the optimal pH for fungal laccase was ranged from 4.0 to 6.0.

Table 3: Relationship between Laccase Activity and pH of Solutions

No.	pH	Buffer	Laccase activity (μmol mL^{-1} min^{-1})
1	3	Acetate	10.79
2	4	Acetate	12.40
3	5	Acetate	13.88
4	6	Phosphate - Citrate	11.75
5	7	Phosphate -Citrate	10.08

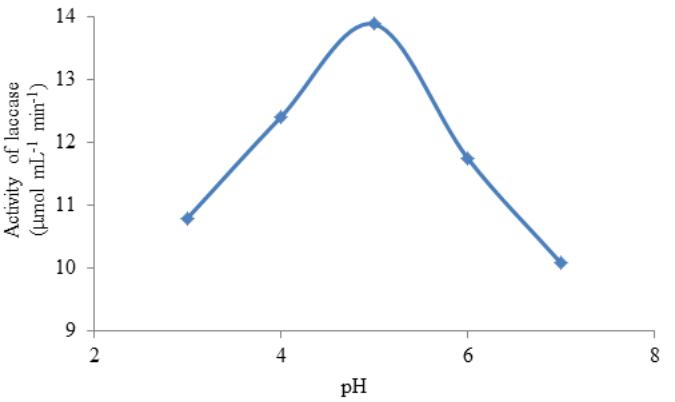

Figure 8: Plot of laccase activity as a function of pH of the solution

Optimum temperature

The effect of temperature on laccase activity was determined by oxidation of guaiacol for 30 min at temperature ranging from 25- 60 °C with an interval of 5 °C (Table 4 and Figure 9). Sodium acetate buffer (pH 5) was used for all the reactions, as optimum pH of laccase. The enzyme activity increased with increasing the temperature from 25 to 40 °C with the maximum activity at 40 °C and then gradually decreased from 40 °C to 60 °C. Rapid inactivation of the enzyme was observed at 70 °C.Thus the temperature optimum of the laccase from *Trametes versicolor* was 40^{o}C with guaiacol as a substrate in acetate buffer of pH 5.0. This result is in agreement with Kalra *et al.* (2013)who found that the optimum temperature for enzyme activity was

45-50°C.In general, laccases are stable at 30–50 °C and rapidly lose activity at temperatures above 60 °C.(Palonen *et al.*, 2003; and Xu *et al.*,1996).

Table 4: Relationship between Laccase Activity and Temperature

No.	Temperature (^{o}C)	Laccase activity (μmol mL^{-1} min^{-1})
1	25	9.45
2	30	10.03
3	35	11.57
4	40	13.30
5	45	13.80
6	50	12.85
7	55	10.10
8	60	8.81

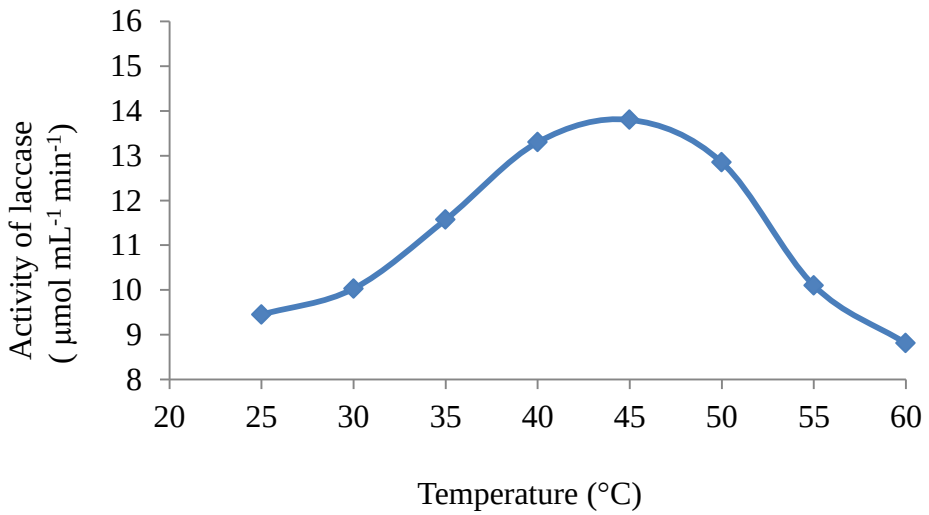

Figure 9: Plot of laccase activity as a function of temperature of the solution

Conclusion

This study revealed that interesting novel laccase producers can be discovered from the environments by very simple plate test methods using

Malt Extract Agar (MEA) as a screening medium. Banana skin , the main waste of banana plant, can be used as support-substrate for production of laccase at low cost by *Tramatese vesicolor* under solid state condition. Production of laccase under solid state condition showed that maximum laccase activity was attained after 12 days of fermentation. Partial purification of laccase by ammonium sulphate precipitation revealed that the specific activity of laccase was 1.60 μ mol $min^{-1}mg^{-1}$and it was purified by 6.4 fold over crude extract. The optimum pH and optimum temperature of fungal laccase was 5 and 40 ^{o}C, respectively.

Acknowledgements

The authors would like to express their profound gratitude to the Department of Higher Education, Ministry of Education, Myanmar for provision of opportunity to do this research and to the Myanmar Academy of Arts and Science for allowing to present this research paper.

References

Akpinar, M. and Urek, R. O.(2017).“Induction of Fungal Laccase Production under Solid State Bioprocessing of New Agroindustrial Waste and its Application on Dye Decolorization”. 3 Biotech.*,vol.7(2), p.98*

Alberts, J.F., Gelderbolm, W.C.A., Botha, A.,andVanzyl,W.H. (2009).“Degradation of Aflatoxin B1 by Fungal Laccase Enzymes”. *Int J Food Microbiol.*,vol.135,pp. 47-52

Dekker, R.F.H., Barbosa, A.M., Giese, E.C., Godoy, S.D.S. and Covizzi, L.G. (2007).“ Influence of Nutrients on Enhancing Laccase Production by *Botryosphaeriarhodina* MAMB-05”.*IntMicrobiol.*,vol.10,pp.177–185

Desai,S.S.,Tennali, G.B.,Channur, N.,Anup, A.C. ,Deshpande, D. and Murtuza, B.P.A .(2011). “Isolation of Laccase Producing Fungi and Partial Characterization of Laccase”. *Biotechnol. Bioinf. Bioeng.*,vol.1(4), pp.543-549

Heinzkill, M., Bech, L.,Halkier, T., Schneider, P. and Anke, T. (1998). “Characterization of Laccases from Wood - rotting Fungi (Family Coprinaceae)”. *Applied Environmental Microbiology*,vol.64 ,pp.1601 -1606

Holker, U., Dohse, J.,and Hofer, M., (2002). Extracellular Laccase in ascomycetes *Trichderma atroviride* and Trichoderma harziaman.Folia Microbiol.47, 423.

Kalra, K., Chauhan, R., Shavez, M. and Sachdeva, S. (2013).“Isolation of Laccase Producing *Trichoderma* spp. and Effect of pH and Temperature on its Activity”.*Int. J. Chem. Environ. Technol.*,vol. 5 (5), pp. 2229-2235.

Kiiskinen, L.L.,Rättö, M. and Kruus**,**K. (2004). “Screening for Novel Laccase-producing Microbes”. *Journal of Applied Microbiology*,vol.97 (3),pp. 640-646

Ling, Z.R., Wang, S.S., Zhu, M.J., Ning, Y.J., Wang, S.N., Li, B., Yang, A.Z., Zhang, G.Q. and Zhao, X.M.(2015).“An Extracellular Laccase with Potent Dye Decolorizing Ability from White Rot Fungus Trametes sp. Lac-01”. *International Journal of Biological Macromolecules*,vol.81 ,pp.785-793

Liu, L., Qin, Z.,Yue, Q. and Borras-Hidalgo, O. (2017). “Laccase Enzyme from *Trametesversicolor* with a High Decolorizing Ability on Malachite Green”. *EC Microbiology* ,vol.10 (3),pp.127-133

Lu, L., Zhao, M., Zhang, B. B., Yu, S. Y., Bain, X. J. and Wang, Y. (2017). “Purification and Characterization of Laccase from *Pycnoporussanguineus* and Decolorization of an Anthraquinone Dye by the Enzyme”. *Appl Microbiol Biotechnol.*, vol.74,pp.1232–1239.

Madhavi, V. and Lele, S.S. (2009).“Laccase: Properties and Applications ”. *Bioresources*,vol.4,pp.1694- 1717

Majeau, J. A., Brar, S. K. and Tyagi, R. D. (2010). “Laccases for Removal of Recalcitrant and Emerging Pollutants”. *Bioresour. Technol*.,vol. 101, pp. 2331–2350

Manavalan, A., Manavalan, T.,Murugesan, K.,Kutzner, A.,Thangavelu, K. P. and Heese, K. (2015).“Characterization of a Solvent, Surfactant and Temperature-Tolerant Laccase from Pleurotus Sp. Mak-Ii and Its Dye Decolorizing Property”.*Biotechnology Letters*,vol.37(12),pp.2403-2409

Murthy, M.V.R., Karanth, N.G. and RaghavaRao, K.S.M.S. (1993). “Biochemical Engineering Aspects of Solid-state Fermentation”. *Advances in Applied Microbiology*, vol.38, pp. 99-147

Palmieri, G., Giardina, P.,Bianco, C.,Scaloni , A.,Capasso, A. and Sannia, G. (1997). “A Novel White Laccase from *Pleurotusostreatus”. Journal Biochemistry* ,vol.272,pp.31301-31307

Palonen, H., Saloheimo, M., Viikariand, L. and Kruus, K. (2003). “Purification, Characterization and Sequence Analysis of a Laccase from the Ascomycetes *Mauginiella* sp.”.*Enzyme Microbiol. Technol.*vol. 33, pp.854–862

Pandey, A., Selvakumar, P., Soccol, C.R. and Nigam, P. (1999). “Solid State Fermentation for the Production of Industrial Enzymes”. *Current Science*, vol.77(1), pp.149-162

Robles, A., lucas, R., Martinez-Canamero, M., Omar, N.B., Perez, R.and Galvez, A..(2002). Characterization of laccase activity produced by hyphomycetes Chalara (syn. Thielaviopsis) paradoxa CH 32.Enzyme Microbiol. Technol.31, 516.

Savitha, S. and Gururaj, B. T.(2011). "Studies on Isolation of Laccase Producing Fungi and Partial Characterization of Laccase".*Society of Applied Biotechnology*, vol.1(4), pp.543-549

Stoilova, I.,Krastanov, A. and Stanchev.V. (2010)."Properties of Crude Laccase from *Trametes versicolor* Produced by Solid-substrate Fermentation". *Advances in Bioscience and Biotechnology*, vol.1, pp. 208-215

Thurston , C.F. (1994)."The Structure and Function of Fungal Laccase".*Microbiol.*,vol. 140, pp.19-26

Upadhyay, P., Shrivastava, R., and Agrawal, P.K. (2016).Bioprospectingand Biotechnological Applications of Fungal Laccase". *3 Biotech*.,vol.6,pp.189–199

Xu, F., Shin, W., Brown, S.H., Wahleitner, J.A., Sundaram, U.M. and Solomon, E.I.A. (1996). "Study of Recombinant Fungal Laccases and Bilirubin Oxidase that Exhibit Significant Differences in Redox Potential, Substrate Specificity, and Stability". *Biochem. Biophys. Acta*,vol.1292, pp.303-311

Yang, J., Yang, X.,Lin,Y., Ng, T. Z., Lin, J., Ye, X. and Hildén, K. (2015). " Laccase-Catalyzed Decolorization of Malachite Green: Performance Optimization and Degradation Mechanism". *PLoS One*,vol.10(5) , p. e 0127714

PHYTOCHEMICAL CONSTITUENTS, NUTRITIONAL VALUES AND ANTIMICROBIAL AND ANTIOXIDANT ACTIVITIES OF *SARACA INDICA* L. (THAWKA)

Khin Thandar Moe[1], Mya Thandar Aung[2], Saw Hla Myint[3]

Abstract

Plant materials have been used for the treatment of serious diseases throughout the world before the advent of modern clinical drugs. *Saracaindica* L. (Thawka) is an important indigenous plant with lots of traditional importance and has been claimed to possess various activities such as antioxidant, antimicrobial, anticancer, anti-diabetic etc. Therefore the leaf and bark of the plant has been chosen for the investigation of some biological activities. The samples were collected and identified. By phytochemical tests, carbohydrates, glycosides, organic acid, phenolic compounds, saponins, steroids and terpenoids were detected in the leaf; and alkaloids, carbohydrates, flavonoids, organic acids, saponins, starch, steroids, tannins and terpenoids, in the bark. Proximate analysis of the leaf showed ash (6.8 %), moisture (11.25 %), protein (13.24 %), fat (3.84 %), fiber (38.21 %), carbohydrates (26.66 %) and energy value (194 kcal/100 g); and for the bark, ash (12.96 %), moisture (15.96 %), protein (5.55 %), fat (4.15 %, fiber (25.71 %), carbohydrates (35.67 %) and energy value (202 kcal/100 g). Antimicrobial activity was screened by agar well diffusion method on six strains of bacteria. The highest inhibition zones were observed on *Pseudomonas aeruginosa* (32 mm) and *Bacilliuspumilus* (30 mm)for EtOAc extract of the bark, followed by *Bacilliuspumilus*and *Candida albicans*(16 mm each) for EtOAc extract of the leaf. No activity was found in the PE and watery extracts of both of the bark and leaf. According to the spectrophotometric DPPH assay, the antioxidant activity (IC_{50}) decreases in the order, ethanol extract of leaf (2.86 µg/mL), ethanol extract of bark (6.70 µg/mL), watery extract of bark (8.35 µg/mL) and watery extract of leaf (12.98 µg/mL), the reference used being vitamin C (1.17 µg/mL). Two compounds namely **A** (β-sitosteryl acetate), **B**(β-sitosterol) were isolated by SiO_2 column chromatography and identified by FT IR.

***Keywords*:** *Saracaindica* L., phytochemical constituents, antimicrobial activity, antioxidant activity

[1] PhD Candidate, Demonstrator, Department of Chemistry, University of Yangon
[2] Dr, Lecturer, Department of Chemistry, University of Yangon
[3] Dr, Part time Professor, Department of Chemistry, University of Yangon

Introduction

Plant materials have been used for the treatment of serious diseases throughout the world before the advent of modern clinical drugs. *Saracaindica* L. is an important indigenous plant with lots of traditional importance belonging to the family Caesalpinaceae. This plant possesses various activities such as analgesic, antipyretic, fungitoxic, anthelmintic, anti-diabetic, antimicrobial, antiulcer, anti-inflammatory activities etc. It is distributed in evergreen forests of India up to an elevation of about 750 m. It is found throughout Myanmar, India, especially in Himalaya, Kerala, Bengal and whole south region. The plant is perennial and woody throughout. The stems are erect or ascending, greater than 2 m tall, solid, glabrous or sparsely glabrate. Petals are separate which are orange-yellow in colour. Fruit is legume type, unilocular, freely dehiscent, ablong. Both leaf and bark contain epicatechin, catechin, gallic acid, kaempferol, leucopelargonidin, palmitic acid, stearic acid, oleic acid and β-sitosterol. The plant has therefore been chosen for the present work to validate some of its acclaimed bioactivities (Anshu*et al*, 2014).

Botanical Aspects of *Saracaindica* L.

Botanical name	:	*Saracaindica* L.
Myanmar name	:	Thawka
Family	:	Caesalpinaceae
Genus	:	*Saraca*
Species	:	*indica*
Parts used	:	leaf and bark

(a) Flowers (b) Bark (c)Plant

Figure 1: Thawka (a) flowers, (b) bark and (c) plant

Materials and Methods

Collection and Preparation of Plant Samples

The leaf and bark of Thawka were collected from University of Yangon Campus. The collected sample was identified by authorized botanist at the Department of Botany, University of Yangon.

The leaf and bark were dried for two weeks then the dried samples were made into powder by using electric grinder. The dried powdered samples were separately stored in air-tight containers to prevent moisture changes and contamination.

Preliminary Phytochemical Investigation

A few grams of dried powdered sample was subjected to the tests of alkaloids, amino acids, carbohydrates, cyanogenic glycosides, flavonoids, glycosides, organic acids, phenolic compounds, reducing sugars, saponins, tannins, starch, steroids and terpenoids (Harborne, J, 1984 ; M- Tin Wa, 1972).

Proximate Analysis

The analysis of the dried powdered sample were made such as moisture content by oven drying method, protein content by micro Kjeldahl distillation method, fat content by Soxhlet extraction, fiber content by fiber cap method, ash content by ashing in furnace method and carbohydrates content by calculation method (AOAC, 2000).

Investigation of Antimicrobial Activity

The antimicrobial activity of the extracts of the dried bark and leaf samples in solvents of different polarities, namely ethanol, ethyl acetate, petroleum ether (PE) and water was studiedon 6 strains of microorganisms, namely *Bacillus subtilis*, *Bacillus pumilus*, *Staphylococcus aureus*, *Pseudomonas aeruginosa*, *Escherichia coli* and *Candidaalbicans* by agar well diffusion method at the Central Research Development Center, Ministry of Industry (1), lower Myanmar, Yangon Region (Karthiheyan, 2012).

Investigation of Antioxidant Activity

DPPH (2,2-diphenyl-1-1-picryl hydrazyl) free radical scavenging assay was chosen to assess the antioxidant activity of the plant materials. This assay has been widely used to evaluate the free radical scavenging effectiveness of various flavonoids and polyphenols in food system.

In the present work, the antioxidant activity of ethanol and watery extracts of both of the leaf and bark of Thawka was studied by spectrometric DPPH free radical scavenging assay (Marinova and Batchvarov, 2011).

Isolation of Compounds A and B from bark of Thawka

The compounds **A** and **B** were isolated form the EtOAc extract of the bark by using column chromatographic method by gradient elution using PE, EtOAc and MeOH. Six fractions (F_1 to F_6) were obtained as mixtures. Successive fractions obtained were combined on the basis of their behaviors on TLC. The fraction F_1 was washed with EtOH and compound **A** was obtained as white crystals. The fraction F_2 was washed with EtOH and compound **B** was obtained as white needles.

Results and Discussion

Phytochemical Investigation of Thawka

Preliminary phytochemical investigation was carried out in order to know the types of phytochemical constituents present in leaf and bark of *Saracaindica* L.(Thawka). Carbohydrates, glycosides, organic acids, phenolic compounds, saponins, steroids and terpenoids were present in the leaf, whereas alkaloids, carbohydrates, flavonoids, organic acid, saponins, starch, steroids, tannins and terpenoids were present in the bark.

Nutritional Values of Thawka

Nutritional values of both of the leaf and bark were determined by standard AOAC methods, and the results are summarized in Table 1. The corresponding energy values calculated for the leaf and the bark, respectively, are 194and 202 kcal/100 g.

Table 1:Nutritional Values of Thawka (Leaf and Bark)

No	Parameters	Content (%)	
		Bark	Leaf
1	Ash	12.96	6.8
2	Moisture	15.96	11.25
3	Protein	5.55	13.24
4	Fat	4.15	3.84
5	Fiber	25.71	38.21
6	Carbohydrate	35.67	26.66

Screening of Antimicrobial Activity of Crude Extracts by Agar Well Diffusion Method

In the screening of antimicrobial activity by agar well diffusion method, the measurable clear zone diameter, including the well diameter, shows the degree of antimicrobial activity. The well diameter is 10 mm in the present study. The larger the zone diameter observed for an extract, the more active it is on the test organism.

The results of antimicrobial activity are shown in Table 2 and Figures 2, 3, 4 and 5. It was found that PE and watery extracts of both samples showed no activity on all tested microorganisms. The highest inhibition zones observed were 32 mm on *Pseudomonas aeruginosa* for barkand 16mm on *Bacillus pumilus* and *Candida albicans* for leaf, both for EtOAc extracts.

Table 2: Antimicrobial Activity Screening on Thawka (Leaf and Bark)

Types of Extracts	Types of Microorganisms and Diameter of inhibition zone (mm)					
	B.subtilis	*B.pumilus*	*S.aureus*	*P. aeruginosa*	*E.coli*	*C.albicans*
(Leaf)						
PE	-	-	-	-	-	-
EtOAc	14(+)	16(+)	13(+)	-	15(+)	16(+)
EtOH	-	11(+)	11(+)	-	11(+)	13(+)
H_2O	-	-	-	-	-	-
(Bark)						
PE	-	-	-	-	-	-
EtOAc	27(+++)	30(+++)	28(+++)	32(+++)	26(+++)	28(+++)
EtOH	14(+)	13(+)	14(+)	-	15(+)	14(+)
H_2O	-	-	-	-	-	-

Agar well	=	10 mm	15 mm ~19 mm	=	(++)
10 mm ~ 14 mm	=	(+)	20 mm above	=	(+++)

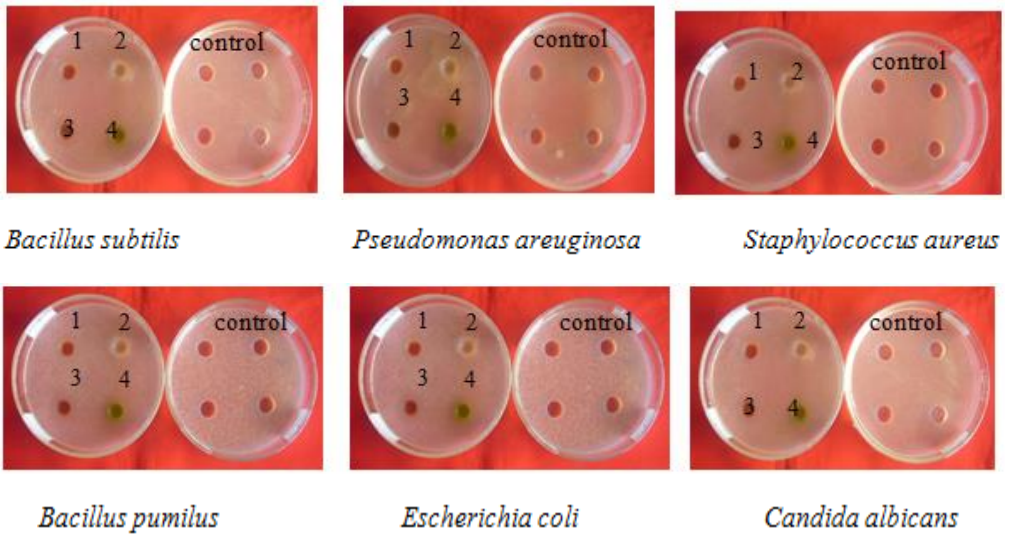

Figure 2: Screening of antimicrobial activities of different extracts of the leaf of Thawka

1 =PE extract 2 =H_2O extract
3 =EtOAc extract 4 =EtOH extract

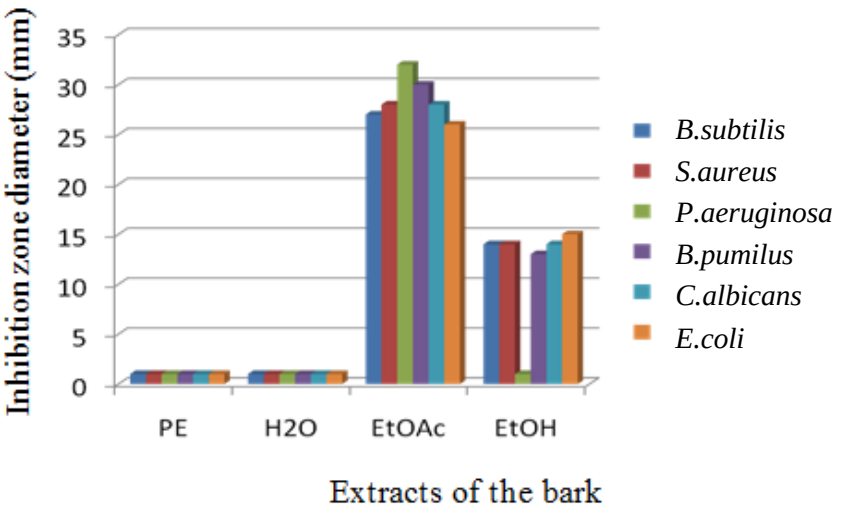

Figure 3: Bar graph of inhibition zone diameters of different leaf extracts on each type of microorganisms

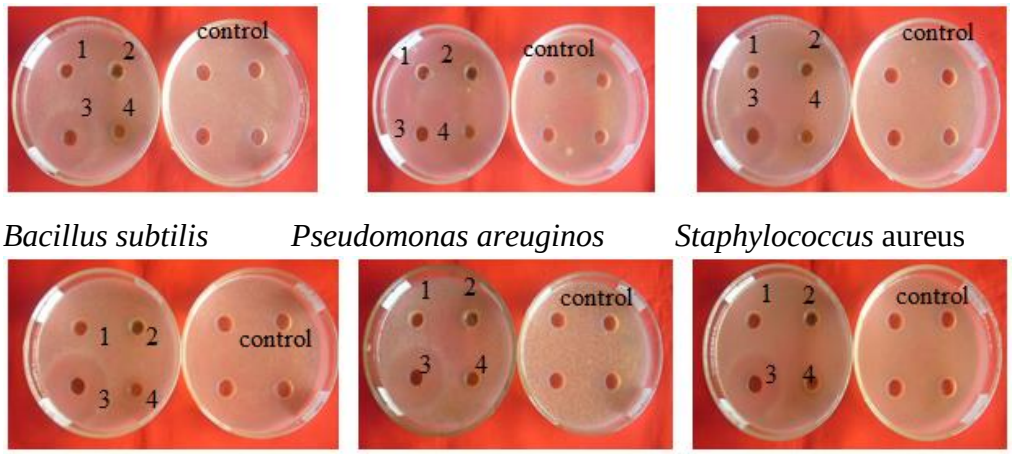

Bacillus subtilis *Pseudomonas areuginos* *Staphylococcus* aureus

Bacillus pumilus *Escherichia coli* *Candida albicans*

Figure 4: Screening of antimicrobial activities of different extracts of the bark of Thawka

1 = PE extract 2 = H_2O extract

3 = EtOAc extract 4 = EtOH extract

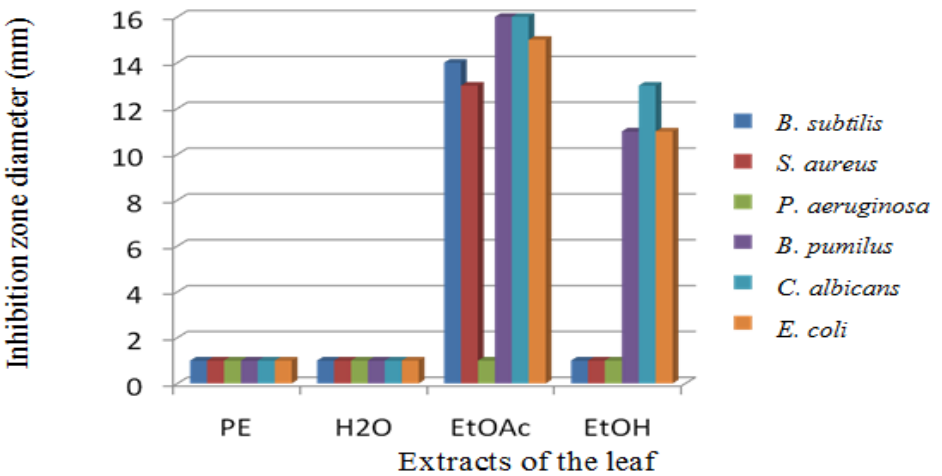

Figure 5: Bar graph of inhibition zone diameters of different bark extracts on each type of microorganisms

Investigation of Antioxidant Activity of Crude Extracts by DPPH Assay Method

The antioxidant activity of the EtOH and watery extracts of leaf and bark of Thawka was investigated by DPPH radical scavenging assay. There were different concentrations of each extract and vitamin C was used as standard. The extract was mixed with DPPH, decolorized due to hydrogen donating ability. The radical scavenging activity (RSA) of crude extracts was expressed in terms of % RSA and IC_{50}.The results are shown in Table 2 and Figure 6 and 7.

According to the results, among the extracts, the EtOH extract of leaf (2.86µg/mL) possessed highest antioxidant activity.

Table 2: % RSA (Radical Scanvenging Activity) and IC_{50} Values of Watery and Ethanol Extracts of Leaf and Bark of Thawka and Vitamin C

Test Samples	%RSA±SD at Different Concentration (µg/mL)						IC50(µg/mL)
	0.625	1.25	2.5	5	10	20	
Watery Leaf	7.89 ± 0.11	9.45 ± 0.33	12.73 ± 2.1	27.27 ± 0.11	43.75 ± 0.66	64.77 ± 7.84	12.98
Watery Bark	5.78 ± 0.44	9.61 ± 0.33	20 ± 1.1	31.48± 3.84	59.14± 0.99	65.86± 4.31	8.35
EtOH Leaf	9.50 ± 0.42	23.6 ± 0.57	46.6 ± 1.41	69.9 ± 0.41	71.4 ± 0.85	72.9 ± 0.56	2.86
EtOH Bark	4.3 ± 1.84	8.4 ± 1.98	22.7 ± 0.98	39.3 ± 0.98	70.8 ± 0.00	72.6 ± 0.57	6.70
*Vitamin C	25.20 ± 1.40	53.58 ± 0.88	65.53 ± 1.13	74.82 ± 0.59	83.32 ± 0.78	91.21 ± 0.48	1.17

SD- Standard Deviation

* Used as Standard

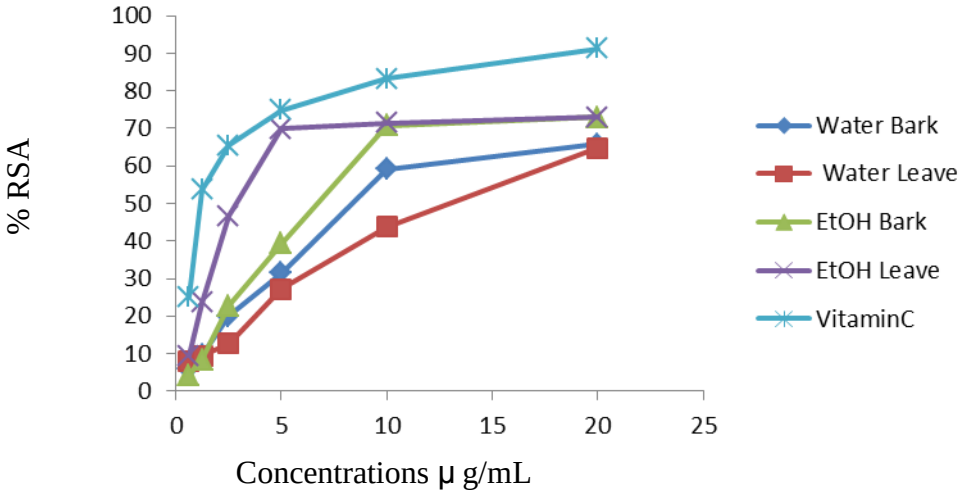

Figure 6: Radical scavenging activity (%RSA) of the EtOH and watery extracts of Leaf and Bark of Thawkavs concentrations

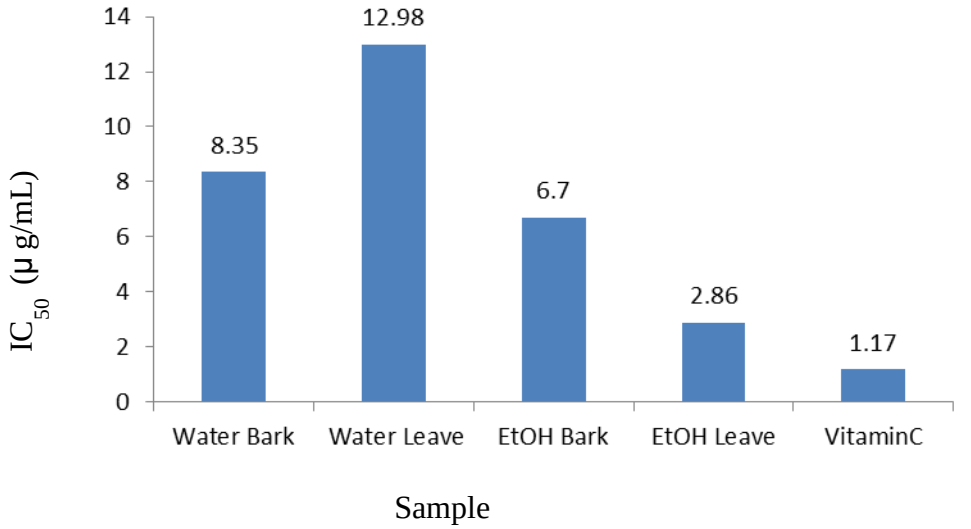

Figure 7: A bar graph of IC_{50} (µ g/mL) of the EtOH and watery extracts of Leaf and Bark of Thawka

Identification of isolated compounds

Compounds **A** and **B** were isolated from EtOAc extract of the bark by column chromatographic method as white crystals as UV inactive compounds. The isolated compounds **A**and **B** have very similar FT IR spectra (Figures 8 and 9), the main difference being the two additional ester bands at 1730 (C=O stretching) and 1272 (C-O stretching) cm^{-1} in **A**; whereas for **B**, it is the stronger band at 3478 cm^{-1} (O-H stretching).Other characteristic bands representing the olefinic group around 800cm^{-1} is present in both compounds. In fact the IR spectrum of **A** is almost superimposable with that of β-sitosteryl acetate (Figure 10), whereas the IR spectrum of **B** (Figure 11) is almost superimposable with that of β-sitosterol (Figure 12). Therefore **A** and **B** are β-sitosteryl acetate and β-sitosterol. The assignment of the IR bands of the two compounds is summarized in Table 3.

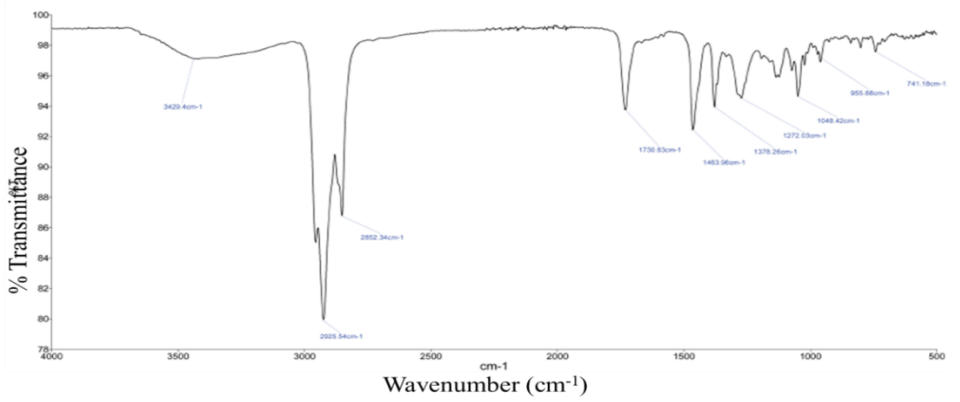

Figure 8: FT IR spectrum of isolated compound **A**

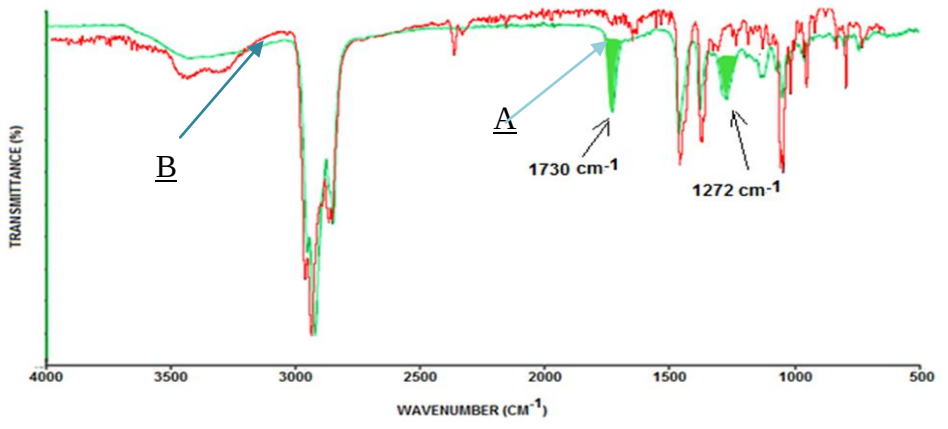

Figure 9: Comparison of the FT IR spectra of isolated compounds **A** and **B**

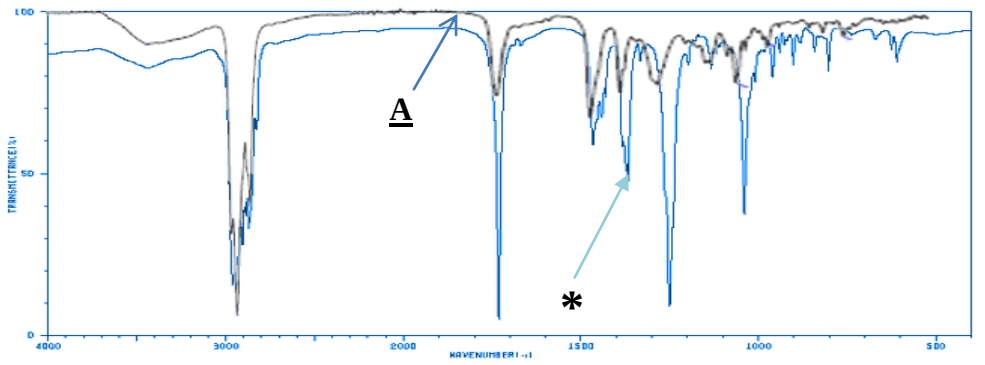

Figure 10: Comparison of FT IR spectrum of isolated compound **A** with the reference spectrum* of β sitosteryl acetate

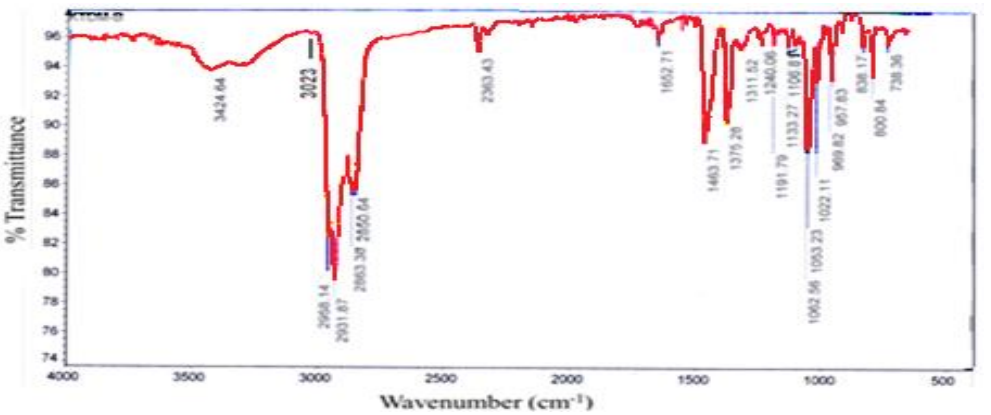

Figure 11: FT IR spectrum of isolated compound **B**

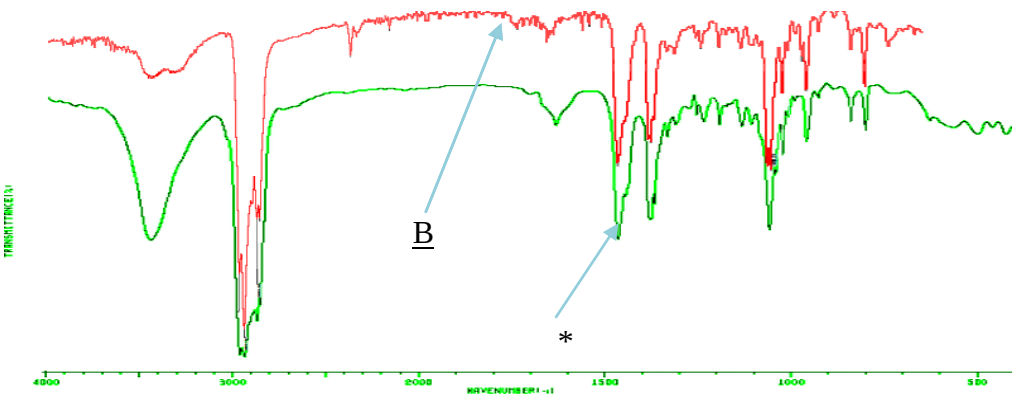

Figure 12: Comparison of FT IR spectra of the isolated compound **B** with the reference spectrum* of βsitosterol

*Spectral Database for Organic Compounds (SDBS), https://sdbs.db.aist.go.jp

Table 3 : Assignment of FT IR Spectral Data of Compound A and B

No	Wave number(cm^{-1})		Vibrational Mode	Band Assignment*
	Compound A	Compound B		
1	-	3424	ν O-H	OH
2	-	3023	ν =C-H	olefinic C-H
3	2953	2958	$\nu_{as}CH_3$	CH_3
4	2925	2931	$\nu_{as}CH_2$	CH_2
5	2866	2863	$\nu_{sy}CH_3$	CH_3
6	2852	2850	$\nu_{sy}CH_2$	CH_2
7	1730	-	$\nu_{C=O}$	carbonyl group of ester
8	1463	1463	δ CH_2, $\delta_{as}CH_3$	CH_3, CH_2
9	1378	1375	$\delta_{sy}CH_3$	$_{sy}CH_3$
10	1272,1043	1062,1053	ν C-O	C-O
11	787	800	δ_{oop}C-H	olefinic C-H out of plane bending

* Silverstein *et al.*, 2005; Pretsch *et al.*, 1989

Conclusion

In concluding the present work, the following inteferences can be deduced. Results of phytochemical investigations revealed that carbohydrates, glycosides, organic acids, phenolic compounds, flavonoids, saponins, steroids and terpenoids were present in the leaf;alkaloids, carbohydrates, flavonoids, glycosides, organic acids, saponins, starch, steroids, tannins and terpenoids were present in the bark.

Nutritional values were, ash(6.80%), moisture(11.25 %), protein (13.24 %), fat (3.84 %), fiber (38.21 %), carbohydrate(26.66 %) and energy value (194 kal/100g) in leaf and ash (2.96 %), moisture(15.96 %), protein (5.55 %), fat (4.15 %),fiber (25.71 %), carbohydrate(35.67 %) and energy value(202 kcal/100g) in bark.

From the screening of antimicrobial activity by agar well diffusion method on 6 strains of bacteria, the largest inhibition zone diameter of 32 mm was observed on *Pseudomonas aeruginos a* for the EtOAc extract of the bark; only half of this, *i.e.,* 16mm inhibition zone diameter was observed as the

highest activity for the EtOAc extract of the leaf on *Bacillus subtilis* and *Candida albicans*.

Antioxidant activity by spectrometric DPPH assay method indicated IC_{50} (µg/mL) values of standard, Vitamin C (1.17 µg/mL), ethanol extract of leaf (2.86 µg/mL), ethanol extract of bark (6.70 µg/mL), watery extract of bark (8.35 µg/mL) and watery extract of leaf (12.98 µg/mL).By the silica gel column chromatographic separation, five compounds were isolated from EtOAc extract of the bark and flower of Thawka.

Compound **A**and **B** were also isolated from the EtOAc extract of bark by using solvent system (PE:EtOAc; 3:7 v/v) as white needles crystals. Compound **A** was identified to be β-sitosteryl acetate by analysis of the FT IR spectral data and also by comparison with reference spectrum of β-sitosteryl acetate. Compound **B** was identified to be β-sitosterol by analysis of the FT IR and also by comparison with the reference FT IR spectral data of β-sitosterol.

Thus the ethyl acetate extract of the bark has good prospects for the formulation of antibacterial drugs; and for uses where antioxidant activity is desired, the ethanol extract of the leaf is more promising.

Acknowledgements

The author would like to thanks the Myanmar Academy of Art and Science for allowing to present this paper, and also thanks to Dr Hnin Hnin Aye (Professor and Head), Department of Chemistry, University of Yangon, for her kind encouragement. I would like to thanks Dr Saw Hla Myint (part-time professor) and Dr Mya Thandar Aung (Lecturer), Department of Chemistry , University of Yangon, for their kind encouragement and suggestions.

References

AOAC.(2000). "Official Methods of Analysis". *Association of Official Analytical Chemist International*, USA: pp. 7

Anshu, B. V., Saroj, A. and Gautam, B. (2014) . "Review on Ethnobotanical Importance of *Saracaindica*". *International Journal for Pharmaceutical Research Scholars (IJPRS).*Vol 3, pp.13-320

Harborne, J. B. (1984). *Phytochemical Methods; A Guide to Modern Techniques of Plant Analysis*. New York: 2nd Ed., Chapman and Hall, pp. 154

Karthikeyan, M., Mathews, J. A.and Annamalai, A. (2012). "Antibacteria Activity of *Phyllanthus maderaspatensis* leaves Extract". *Int. J. of Pharmaceutical Sciences*, Vol 3 (3), pp.1-10

Marinova, G and Batchvarov, V. (2011). "Evaluation of the Methods for Determination of the Free Radical Scavenging Activity of DPPH ". *Bulgarian Journal of Agricultural Science*.Vol 17,pp. 11-24

M-Tin Wa. (1972). "Phytochemical Screening, Methods Procedures". *Phytochemical Bulletin of Botanical Society of America*, Vol 5(3), pp. 4-10

Pretsch, E., W. Simon, J. Seibl and T. Clerc.(1989). *Tables of Spectral Data for Structure Determination of Organic Compounds*. Berlin: 2nded English translation of German 3rded, K. Biemann (Translator), Springer

Silverstein, R. M., F. X. Webster and D. J. Kiemle. (2005). *Spectrometric Identification of Organic Compounds*, New Jersey: 7thed, John Wiley and Sons, Inc., 72 -126

GASEOUS AIR POLLUTANTS AND PARTICULATES IN AMBIENT AIR OF AHLONE TOWNSHIP, YANGON CITY

Swe Swe Ohn[1], Ni Ni Sein[2], Daw Hla Ngwe[3]

Abstract

Rapid and unsystematic industrialization has become a major environmental concern for both developed and developing countries. Long-term and short-term effects on human health have been observed due to poor quality. In this study, a number of pollutants such as total suspended particulate matter (TSPM), particulate matter(PM-10), SO_2 and NO_2 affecting ambient air quality were measured for specified location in Ahlone Township, Yangon City. During study period from November 2015 to October 2017, variations of the pollutants have been monitored weekly, monthly and seasonally. On the basis of the monthly average, the statistical distribution parameters such as average, standard deviation (SD), minimum (Min) and maximum (Max) values for each of the pollutants were obtained. The average concentrations of TSPM, PM-10, SO_2 (24 h) and NO_2 (24 h) observed during the period of (2015-2017) were found to be 73.24 ± 43.44 μg m^{-3}, 38.43 ± 27.27 μg m^{-3}, 0.109 ± 0.271 μg m^{-3}, 6.38 ± 8.46 μg m^{-3} and 19.31 ± 33.41 μg m^{-3} respectively. All pollutants were observed to be high in concentration during summer as compared to winter and rainy, due to slow dispersion and dilution of pollutants. The results of this study identified the degree of air pollution in Ahlone Township, Yangon City. The data obtained will be statistically treated using SPSS (Statistical Package for the Social Science) software version 22.

Keywords : Pollutants, particulates, ambient air, TSPM, PM-10

Introduction

Air pollution results mainly from gaseous and particulates emission of industries, thermal power stations, automobiles, domestic combustion etc. which sources are natural as well as anthropogenic (Narayanan, 2009). Industrial pollution is one of the primary sources of environmental contamination. Factories pollute the air through fossil fuel emissions. Combustion creates toxic pollutants. Gases such as oxides of nitrogen (NO_x), oxides of sulphur (SO_2) and carbon monoxide (CO) may constitute some forms of pollutants. Presence of atmospheric air contaminants in such

[1]. Lecturer, Department of Chemistry, University of Yangon
[2]. Dr, Professor (Retired), Department of Chemistry, University of Yangon
[3]. Dr, Professor and Head (Retired), Department of Chemistry, University of Yangon

quantities and duration that many tend to be injurious to life or properties, health repose and safety constitute air pollution. High temperature combustion of hydrocarbon fuel sources such as gasoline, coal, and oil with air produce NO and smaller quantities of NO_2 from reactions between the oxygen and nitrogen present in the combustion air. Most of the NO in ambient air rapidly turns into NO_2. High temperature combustion of hydrocarbon fuel sources such as coal and oil can produce sulphur dioxide (SO_2) and sulphur trioxide (SO_3) from the oxidation of any sulphur in these fuels (Abdullahi *et al.,* 2017). Emissions of these sulphur compounds are associated with industrial operations and contribute to the majority of SO_2 emissions from man's activities. Long-term exposure to sulphur dioxide may cause respiratory symptoms and illness, and aggravate asthma (USEPA, 2014). All of the air pollutants are associated with a range of health impacts. Particulate matter is a major cause of all kinds of respiratory problems (Kumar and Kriti, 2016). The aim of this study is to achieve better understanding of the condition of atmosphere due to the air pollution.

Materials and Methods

General Description of Sample Collection Area

Sampling site was selected at the urban area in Yangon Region. Ahlone Township in the western part of Yangon is located between 16° 47.248′ N and 96° 07.793′ E. The township covers an area of 4 km^2 (1.4 sq. miles). The population was found to be 55428 in census 2014. The area which is very much close to Hteen Dan Port Jetty, Asia World Port Jetty, Kyee Myint Dine International Port, Myanmar Industrial Port, palm oil storage tank, white rice mill, CNG and LPG gas filling station, gas turbine plant, public transport station is surrounded by commercial complexes and residential area. Map of the study area is shown in Figure 1.

Samples, Study Area and Sampling Periods

The samples studied are airborne particulate matter (APM) samples including total suspended particulate matter (TSPM) and PM-10 and the gaseous air pollutants (GAPs) such as sulphur dioxide (SO_2) and nitrogen dioxide (NO_2). Sampling site is Occupational Health Department, Lower Kyee Myint Dine Road, Ahlone Township in Yangon (Figure 1). Air

sampling was conducted weekly for 2 years from November 2015 to October 2017. Samples were collected from November to February representing cold season, March to May representing hot season and June to October representing rainy season.

Sample Collection and Data Collection

The air sampling pump (High Volume Sampler (HVS), Envirotech APM 460 NL., New Delhi, India) was used to collect particulate matters (TSPM and PM-10) and the gaseous air pollutants (SO_2 and NO_2). Figure 2 depicts the HVS with gaseous sampling attachment and interior view of gaseous sampling attachment.PM-10 samples were collected on glass microfiber filter (460 x 570 mm) and pore size is 1.0 μm. Figure 3 shows the unloaded and loaded filters. TSPM was collected from the fiber container which was placed into the HVS. The average TSPM and PM-10 concentration were determined by dividing the net weight gain of the sample by the total volume of air sample. The gas-phase air pollutants (SO_2 and NO_2) were collected from impingers into the gaseous sampling attachment which was connected with HVS. All samples were collected for 24 h from 8.00 am first day to 8.00 am next day on every Thursday of the whole year. Temperature and pressure were also simultaneously measured hourly during the sampling period. Automatic air flow meter was set at a nominal flow rate of 1.5 Lm^{-1}. The HVS was placed about 5 m above the ground. The modified West and Gaeke Method IS 5218 Part II and Jacob and Hochheiser Method IS 5182 Part IV were used for absorbing the SO_2 and NO_2 contents respectively from the air which was analyzed with suitable spectrometer (Kamyotra and Saha, 2011).

Results and Discussion

In this study, four different numbers of pollutants (TSPM, PM-10, SO_2 and NO_2) affecting ambient air quality were measured for specified location of Occupational Health Department, Lower Kyee Myint Dine Road, Ahlone Township, Yangon City during the two-year period from November 2015 to October 2017. On the basis of the monthly average, the statistical distribution parameters such as average, standard deviation (SD), minimum (Min) and maximum (Max) values for each of the pollutants were determined.

Figure 1: Location of sampling site on the map of Ahlone Township

Figure 2: Photographs of high volume sampler (a) exterior view of HVS with gaseous sampling attachment (b) interior view of gaseous sampling attachment

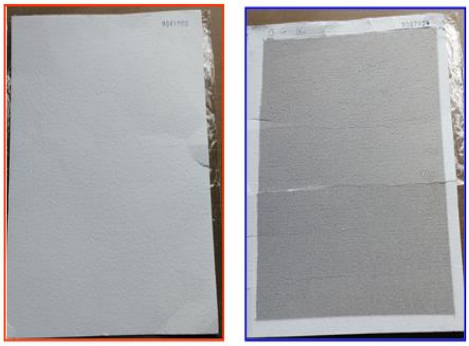

Figure 3: Filter papers (a) Unloaded filter paper and (b) loaded filter paper (460 x 570 mm)

The concentrations of TSPM were found to be in the range of 24.53 to 180.58 μg m^{-3} with the mean value of 89.15 ± 45.42 μg m^{-3} in the period of November 2015 to October 2016 and 10.46 to 152.31 μg m^{-3} with the mean level of 57.33 ± 34.45 μg m^{-3} in the periods of November 2016 to October 2017 (Table 1 and Figure 4). The concentrations of TSPM were lower than the permissible level of USEPA (1997) standard 150 μg m^{-3} except the month of January, February and May 2015 and September 2017. But, no significant difference in TSPM was observed during the study period ($p>0.05$).

The results of mean monthly concentrations of PM-10 are presented in Table 2 and Figure 5. It was observed that the mean monthly concentrations of PM-10 were found to be in the range of 2.48 to 120.41 μg m^{-3} with the mean value of 53.94 ± 29.37 μg m^{-3} in the periods of November 2015 to October 2016 and those of 2.06 to 63.60μg m^{-3} with the mean value of 22.91 ±12.28μg m^{-3}in the period of November 2016 to October 2017. In the period of November 2015 to October 2016 (except rainy season such as June, September and October), the level of PM-10 was found to be higher than the permissible level (50 μg m^{-3}) of WHO standard (2000).In the period of November 2016 to October 2017 (except rainy season such as July), PM-10 concentrations were found to be lower than the WHO standard (2000). PM -

10 concentrations were not significantly different to each other during the study period ($p>0.05$).

The mean monthly levels of SO_2 within24 h in ambient air that were found to be in the range of 0.006 to 1.930μg $m^{-3}$with the mean level of 0.103 ± 0.201 μg m^{-3} in the periods of November 2015 to October 2016 and 0.001 to 1.160μg $m^{-3}$with the mean value of 0.114 ± 0.228 μg m^{-3} in the periods of November 2016 to October 2017 (Table 3 and Figure 6). The mean monthly levels of SO_2 were lower than the WHO (2000)standard (20 μg m^{-3}). The mean monthly levels of SO_2 were significantly different during the study period ($p=0.001$).

The results of mean monthly concentrations of NO_2 within 24 h in ambient air were presented in Table 4 and Figure 7. It was observed that the mean monthly concentrations of NO_2 were found to be in the range of 0.49 to 17.51 μg m^{-3} with the mean value of 3.88 ±4.63 μg m^{-3} from November 2015 to October 2016 and those of 0.16 to 52.10μg m^{-3} with the mean level of 8.89 ± 10.83 μg m^{-3} from November 2016 to October 2017. All of the values in the periods of 2 years (except April 2017) were lower than the permissible limit(40 μg m^{-3}). The mean monthly concentrations of NO_2 were significantly different during the study period ($p< 0.001$).

Table 5 and Figures 8 -11 show the mean seasonal levels of PM (TSPM and PM-10) and GAPs (SO_2 and NO_2). The mean seasonal levels of TSPM, PM-10, SO_2 and NO_2 were found to be highest which were 120, 72.26, 0.19 and 5.76 μg m^{-3} respectively, in hot season 2016 and those were 67.02, 23.45, 0.33 and 17.35 μg m^{-3}respectively, in hot season 2017. During the study period (November 2015 – October 2017) in Ahlone Township, high concentrations of PM and GAPs were observed during hot season and low concentrations of pollutants were observed during rainy season. The ambient air PM and GAPs concentrations are within the acceptable limits of WHO (2000) and USEPA (1997) standard. Analysis of the data on seasonal basis revealed low concentration of particulate matter (TSPM and PM-10) in rainy season. In the rainy season, pollutants were dissolved and settle down on the earth due

Table 1: The Monthly Average, Standard Deviation (SD), Minimum (Min) and Maximum (Max) Values of TSPM (24h) Collected from Ahlone Township for the Period of 2 Years from November 2015 to October 2017

Sampling Periods	Mean monthly concentrations of TSPM (μg m^{-3})							
	2015- 2016 (Year one)				2016- 2017 (Year two)			
	Mean ± SD		Min	Max	Mean ± SD		Min	Max
November	61.47	± 22.27	31.57	94.32	47.22	± 29.69	18.15	87.57
December	96.64	± 50.99	60.58	132.70	107.8	± 34.10	72.68	140.78
January	139.66	± 33.06	107.54	168.98	47.04	± 15.01	30.39	61.46
February	132.13	± 21.29	100.12	159.84	64.26	± 42.39	34.70	125.00
March	120.99	± 35.09	69.65	148.97	94.2	± 30.19	61.93	128.94
April	91.12	± 41.87	46.18	129.03	54.69	± 31.86	33.53	91.34
May	147.91	± 40.87	125.34	180.58	52.16	± 27.10	24.78	85.49
June	49.66	± 10.55	39.34	61.59	41.35	± 13.71	20.80	58.45
July	75.32	± 26.47	41.41	131.41	51.12	± 25.73	28.27	76.23
August	65.01	± 8.41	50.24	96.77	21.98	± 14.13	10.46	42.24
September	53.14	± 26.67	24.53	86.60	58.75	± 53.49	18.37	152.31
October	36.73	± 7.91	24.62	44.03	47.39	± 13.51	37.10	62.69
	89.15	± 45.42	24.53	180.58	57.33	± 34.45	10.46	152.31
	(number of weeks) n = 50				n = 47			

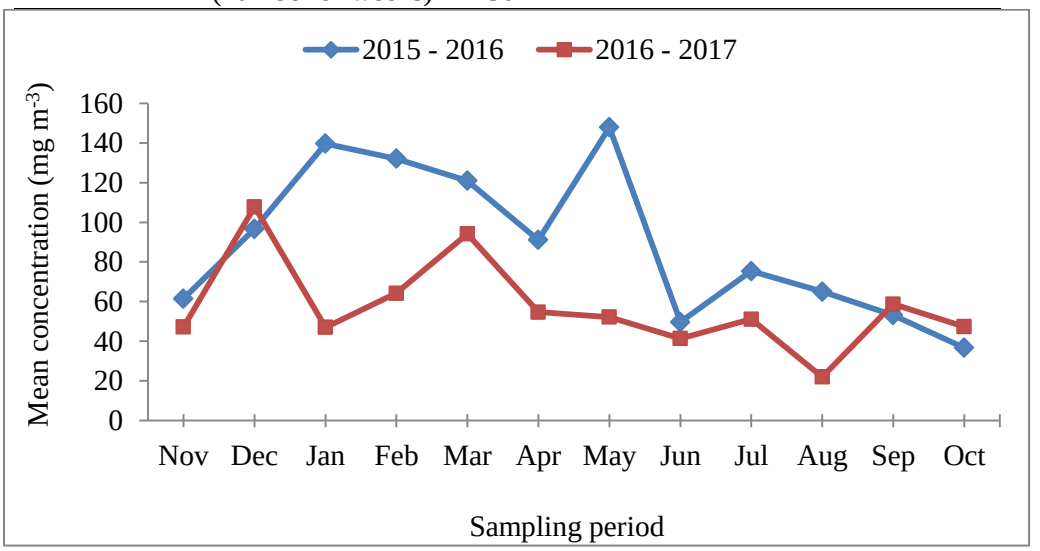

Figure 4: Variation of mean concentration of TSPM (24 h) collected from Ahlone Township for the period of 2 years

Table 2: The Monthly Average, Standard Deviation (SD), Minimum (Min) and Maximum (Max) Values of PM-10 (24h) Collected from Ahlone Township for the Period of 2 Years from November 2015 to October 2017

Sampling Periods	Mean monthly concentrations of PM-10 ($\mu g\ m^{-3}$)					
	2015- 2016 (Year one)			2016- 2017 (Year two)		
	Mean ± SD	Min	Max	Mean ± SD	Min	Max
November	36.90 ± 19.19	13.32	56.22	24.07 ± 14.59	11.45	43.55
December	70.32 ± 26.12	51.85	88.79	25.49 ± 9.62	17.96	36.34
January	78.34 ± 6.09	71.27	86.07	12.52 ± 9.68	5.16	26.79
February	81.56 ± 25.69	51.49	120.41	24.64 ± 4.91	20.43	30.50
March	75.27 ± 25.90	39.71	101.88	30.51 ± 3.56	27.60	35.04
April	56.05 ± 19.60	36.84	76.02	21.96 ± 6.25	16.40	28.73
May	85.45 ± 24.10	55.67	104.94	17.89 ± 12.76	6.37	34.74
June	28.25 ± 6.62	21.90	37.78	26.19 ± 12.48	15.42	40.29
July	41.35 ± 21.24	15.94	73.49	32.35 ± 21.07	17.45	63.60
August	51.65 ± 21.70	32.79	84.47	14.12 ± 15.03	2.06	36.00
September	28.14 ± 17.76	8.53	46.00	22.58 ± 15.10	8.44	48.24
October	14.01 ± 9.45	2.48	26.33	22.61 ± 7.00	15.16	29.06
	53.94 ± 29.37	2.48	120.41	22.91 ± 12.28	2.06	63.60
	(number of weeks) n = 50			n = 47		

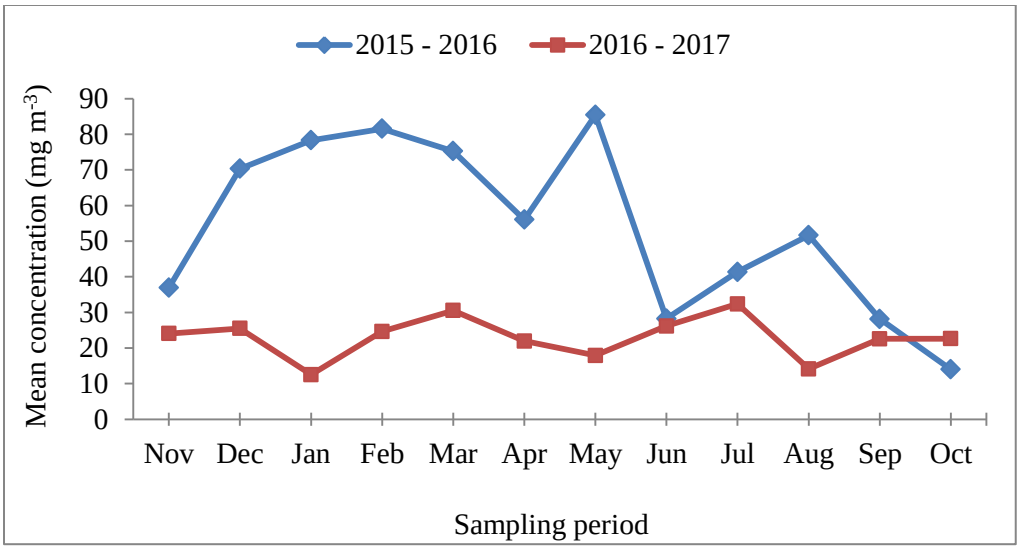

Figure 5: Variation of mean concentration of PM-10 (24 h) collected from Ahlone Township for the period of 2 years

Table 3: The Monthly Average, Standard Deviation (SD), Minimum (Min) and Maximum (Max) Values of SO_2 (24h) Collected from Ahlone Township for the Period of 2 Years from November 2015 to October 2017

Sampling Periods	Mean monthly concentrations of SO_2 (µg m^{-3})					
	2015- 2016 (Year one)			2016- 2017 (Year two)		
	Mean ± SD	Min	Max	Mean ± SD	Min	Max
November	0.010 ± 0.000	0.010	0.010	0.010 ± 0.001	0.009	0.010
December	0.010 ± 0.001	0.010	0.011	0.123 ± 0.076	0.070	0.201
January	0.020 ± 0.000	0.020	0.020	0.168 ± 0.178	0.020	0.380
February	0.160 ± 0.007	0.006	0.020	0.010 ± 0.000	0.010	0.010
March	0.010 ± 0.005	0.010	0.020	0.175 ± 0.100	0.070	0.300
April	0.010 ± 0.006	0.010	0.020	0.553 ± 0.541	0.120	1.160
May	0.540 ± 0.006	0.010	1.930	0.252 ± 0.479	0.007	0.970
June	0.010 ± 0.000	0.010	0.010	0.013 ± 0.006	0.007	0.020
July	0.010 ± 0.433	0.010	0.020	0.019 ± 0.027	0.004	0.060
August	0.088 ± 0.021	0.060	0.110	0.020 ± 0.135	0.004	0.008
September	0.075 ± 0.039	0.030	0.120	0.010 ± 0.008	0.001	0.005
October	0.303 ± 0.463	0.007	1.110	0.020 ± 0.004	0.003	0.010
	0.103 ± 0.201	0.006	1.930	0.114 ± 0.228	0.001	1.160
(number of weeks)	n = 50			n = 47		

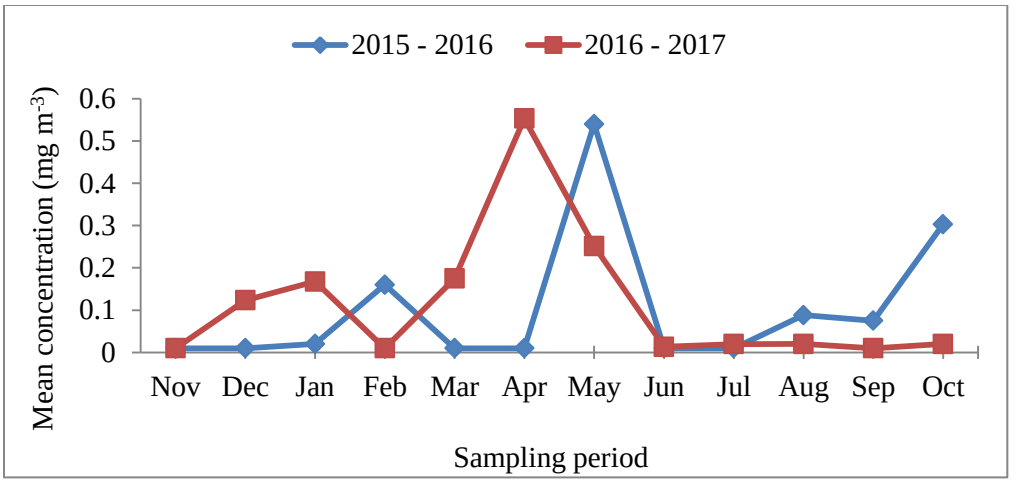

Figure 6: Variation of mean concentration of SO_2 (24 h) collected from Ahlone Township for the period of 2 years

Table 4: The Monthly Average, Standard Deviation (SD), Minimum (Min) and Maximum (Max) Values of NO_2 (24h) Collected from Ahlone Township for the Period of 2 Years from November 2015 to October 2017

Sampling Periods	Mean monthly concentrations of NO_2 (μg m^{-3})					
	2015- 2016 (Year one)			2016- 2017 (Year two)		
	Mean ± SD	Min	Max	Mean ± SD	Min	Max
November	1.06 ± 0.25	0.89	1.49	1.21 ± 0.22	0.98	1.50
December	0.85 ± 0.18	0.72	0.97	14.75 ± 6.60	10.92	22.38
January	1.35 ± 0.12	1.25	1.50	16.30 ± 9.66	8.85	30.50
February	1.52 ± 0.67	0.66	2.48	6.56 ± 4.11	3.30	12.54
March	7.09 ± 7.12	0.84	13.60	8.36 ± 16.18	0.16	32.64
April	1.03 ± 0.16	0.88	1.19	35.13 ± 14.70	26.31	52.10
May	9.17 ± 0.14	0.78	17.51	8.57 ± 8.33	3.70	20.98
June	0.75 ± 0.29	0.49	1.15	7.17 ± 4.94	3.32	13.12
July	1.16 ± 7.11	1.01	1.28	4.57 ± 2.99	2.20	8.90
August	9.39 ± 2.29	6.16	1.90	2.89 ± 2.54	1.03	6.40
September	7.72 ± 2.65	5.08	10.46	0.82 ± 1.11	0.31	2.60
October	5.43 ± 5.31	0.90	11.60	0.34 ± 1.25	0.26	0.43
	3.88 ± 4.63	0.49	17.51	8.89 ± 10.83	0.16	52.10
	(number of weeks) n = 50			n = 47		

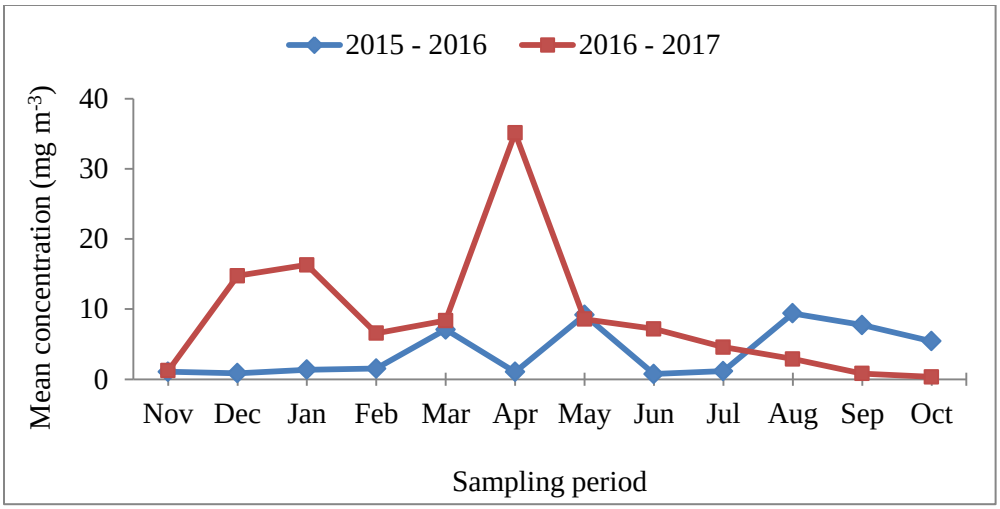

Figure 7: Variation of mean concentration of NO_2 (24 h) collected from Ahlone Township for the period of 2 years

Table 5: The Mean Seasonally Level of PM and GAPs Collected from Ahlone Township for the Period of 2 Years from November 2015 to October 2017

Sr No.	Season	Mean Levels of PM and GAPs (μg m^{-3})							
		TSPM		PM - 10		SO_2		NO_2	
		2015-2016	2015-2016	2015-2016	2015-2016	2015-2016	2015-2016	2015-2016	2015-2016
1	Cold	107.48	66.58	66.78	21.68	0.050	0.078	1.19	9.71
2	Hot	120.00	67.02	72.26	23.45	0.190	0.327	5.76	17.35
3	Rainy	55.97	44.12	32.68	23.57	0.097	0.017	4.89	3.16
Permissible level		150 **		50 *		20 *		40 *	

All were measured within 24 h
* WHO (2000)
** USEPA (1997)

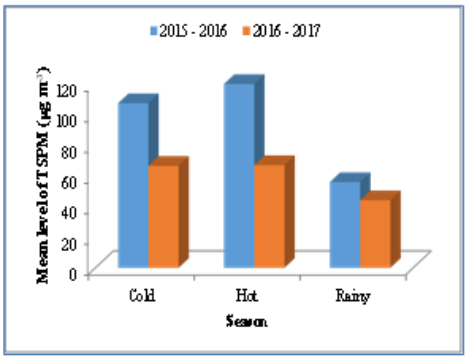

Figure 8: The histogram of the comparison of the mean levels of TSPM seasonally collected from Ahlone Township for the period of 2 years

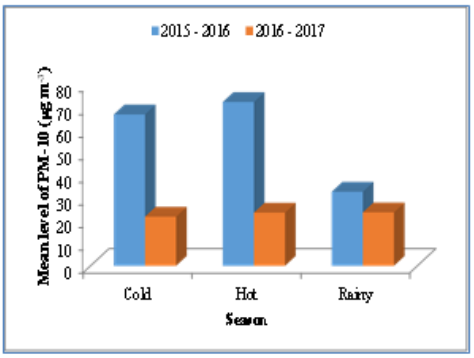

Figure 9: The histogram of the comparison of the mean levels of PM-10 seasonally collected from Ahlone Township for the period of 2 years

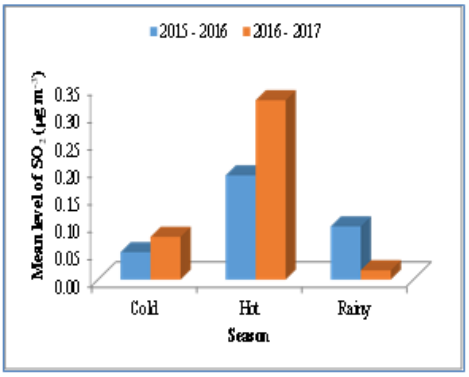

Figure10: The histogram of the comparison of the mean levels of SO_2 seasonally collected from Ahlone Township for the period of 2 years

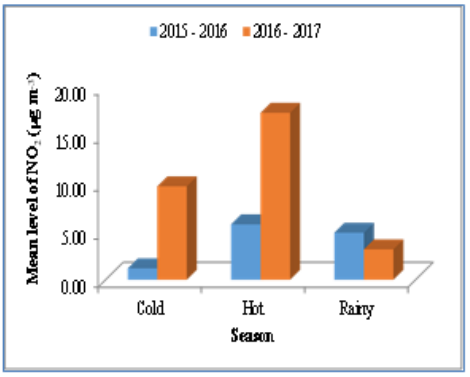

Figure11: The histogram of the comparison of the mean levels of NO_2 seasonally collected from Ahlone Township for the period of 2 years

to heavy rainfall and thunder, therefore, the quality of ambient air is good in this season. The concentration of PM was remarkably decreased in this season as compared to other seasons (Figures 8 and 9). This is significant as it establishes the correlation between the meteorological factors and pollutant concentrations. The high relative humidity, moderate temperature and heavy rains result in the decrease of concentration of PM. Low value of PM contents during cold season may be attributed to light wind and precipitation that prevails in cold season. These factors lead to dispersion of pollutants near the source resulting into less concentration of pollutants during the cold season.

Low value of pollutants during the cold season is also in line with the findings of Tripathy and Panigrahi (2000) and Sehra (2007). In addition, dry season is convenient for travelling, therefore traffic density is increased. So the large amount of exhaust emission and the PM-10 emission from vehicular sources (wear and tear of automobile tyres, clutch and brake ware, wiring of vehicles were increased. Construction works (building and road construction) were higher in dry season than in rainy season. So more GAPs and PM emission occurred in dry season than rainy season.

The summarized data of yearly average concentrations of PM and GAPs for the study periods are presented in Table 6 and Figure 12. The concentration of TSPM during the year one (2015-2016) was maximum (180.58 μg m^{-3}) in the hot season while a minimum was 24.53 μg m^{-3} in rainy season with the mean value of 89.15 ± 45.42 μg m^{-3} and during the year two (2016-2017) these values were 152.31 μg m^{-3} and 10.46 μg m^{-3} with the mean value of 57.33 ± 34.45 μg m^{-3}. The maximum and minimum values of PM-10 during the year one (2015-2016) were 120.41 μg m^{-3} and 2.48 μg m^{-3} respectively with the mean value of 53.94 ± 29.37 μg m^{-3} and during the year two (2016-2017), these values were 63.6 and 2.06 μg m^{-3} with the mean values of 22.91 ± 12.28 μg m^{-3}.The maximum and minimum values of SO_2 during the year one (2015-2016) were 1.930 and 0.006 μg m^{-3} respectively with the mean levels of 0.103 ± 0.201 μg m^{-3} and during the year two (2016-2017) these values were 1.160 and 0.001 μg m^{-3} with the mean value of 0.114 ± 0.228 μg m^{-3}. The concentration of NO_2 during the year one (2015-2016) was maximum (17.51 μg m^{-3}) in the hot season while a minimum was 0.49 μg m^{-3} in rainy season with a mean value of 3.88 ± 4.63 μg m^{-3} and during the year two (2016-2017) these values were 52.1 and 0.16 μg m^{-3} with a mean value of 8.89 ± 10.83 μg m^{-3} .

All of the particulates (TSPM and PM-10) were observed to be high in concentration during the year one (2015-2016) as compared to the year two (2016-2017). In the year one (2015-2016), high particulate concentration may be due to the fact that 24 h heavy transport activities in study area, construction activities, parking place for trucks in the vicinity, usage of generators during the frequent power cuts, narrow and poorly maintained

roads. In the year two (2016-2017), there was a drop in PM concentration. This was because all of the loading trucks were restricted to enter the urban area from 6 am to 8 pm, reducing the construction activities, parking place for trucks was transferred to the suburban and no electricity failures in urban area of Yangon City.

The concentration of SO_2 had been observed to be not much different between 2 years of study period and found to be within the acceptable limits of WHO (2000) air quality guideline. The concentration of NO_2 had been observed to be higher in the year two (2016-2017) than in the year one (2015-2016) but these values were found to be lower than the permissible level of WHO (2000) standard. The average concentration of SO_2 and NO_2 increased in the year two (2016-2017) as compared to the year one (2015-2016). It may be due to the fact that number of vehicles is increasing every year. Emission of pollutants from the vehicles depends upon the type of fuel used. Diesel engines have substantial emissions of which particulate matter and SO_2 is vital. Most particulate matter results from incomplete combustion of the fuel, petrol run vehicles emit CO, hydrocarbon, Pb and NO_2 in the atmosphere (Angelika and Raina, 2013). Most of the salon cars are petrol run vehicles. Therefore NO_2 emission increased during the latter period.

Table 6: The Comparison of the Yearly Average, Standard Deviation (SD), Minimum (Min) and Maximum (Max) Values of PM and GAPs Collected from Ahlone Township for the Period of 2 Years from November 2015 to October 2017

Sr No.	Pollutants	Concentration of PM and GAPs ($\mu g\ m^{-3}$)					
		2015-2016 (Year one)			2016-2017 (Year two)		
		Mean ± SD	Minimum	Maximum	Mean ± SD	Minimum	Maximum
1	TSPM	89.15 ± 45.42	24.53	180.58	57.33 ± 34.45	10.46	152.31
2	PM-10	53.94 ± 29.37	2.48	120.41	22.91 ± 12.28	2.06	63.60
3	SO_2	0.10 ± 0.20	0.00	1.93	0.11 ± 0.228	0.00	1.16
4	NO_2	3.88 ±4.63	0.49	17.51	8.89 ± 10.83	0.16	52.10

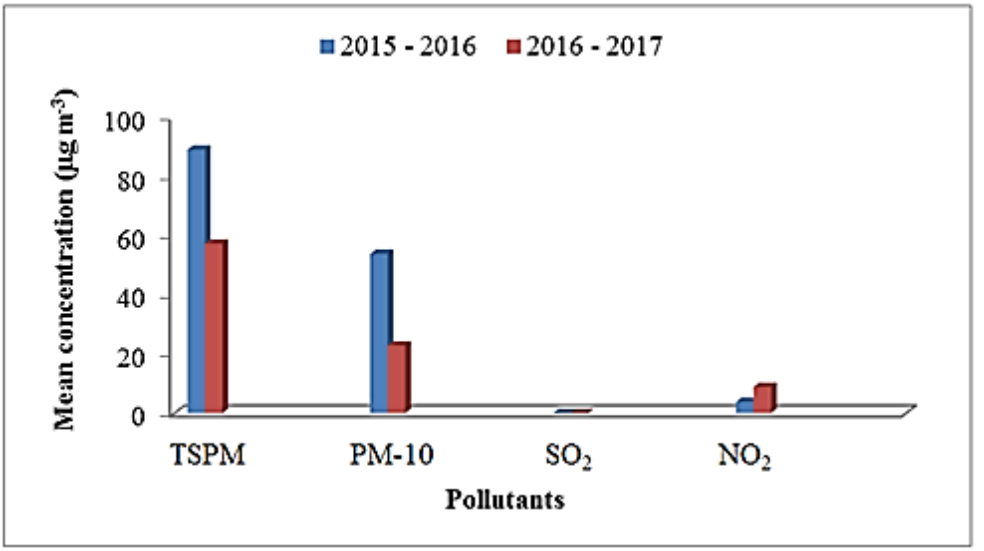

Figure 12: The histogram of the comparison of mean levels of pollutants collected from Ahlone Township for the period of 2 years

Conclusion

From the results of the present study, it was observed in the descending order of the concentrations of pollutants as: TSPM > PM-10 > NO_2> SO_2. This study reveals that both PM and GAPs are mostly below permissible limits of WHO (2000) and USEPA (1997) standards at the study site. Much is being done to control, monitor and rectify damage occurred by pollutants. The present study provides base line information and the results are useful for effective environmental pollution monitoring at Ahlone Township in Yangon City.

Acknowledgements

The authors thank the Occupational Health Department (Yangon), Ministry of Health and Sports for granting the use of research facilities for this research work. We would like to thank, Professor Dr Hnin Hnin Aye, Head of Department, Department of Chemistry, University of Yangon and Myanmar Academy of Arts and Science for allowing to present this paper.

References

Abdullahi, A. O., Maitera, O. N. Maina, H. M. and Yelw, J. M. (2017). "Determination of Some Pollutant Gases in Ambient Air of the Vicinity of a Kaolin Milling Plant in Alkaleri, Bauchi State, Nigeria". *IJARCS*., vol. 4 (12), p. 1-6

Angelika, S. and Raina, A. K. (2013). "Assessment of the Status of SPM in Jammu City and its Control Strategies". *Journal of Environmental Science,* vol.7 (1), pp. 8-12

Kamyotra, S. J. S. and Saha, D. (2011). *Guidelines for the Measurement of Ambient Air Pollutants.* India: Central Pollution Control Board, Ministry of Environmental and Forests, Govt. of India, vol.1, p. 1-7

Kumar, S.S. and Kriti, S. (2016)."Ambient Air Quality Status of Jaipur City, Rajasthan, India". *International Research Journal of Environment Science,* vol.5(1),p. 43-48

Narayanan, P.(2009). *Environmental Pollution : Principle, Analysis and Control.* India. CBS Publishers and Distributors Pvt Ltd., p. 47

Sehra, P. S. (2007). "Atmospheric Pollution :"A Case Study of Degrading Urban Air Quality over Punjab". *Indian J.Env.Prot.*, vol.27 (1), p. 32-38

Tripathy, A.K. and Panigrahi, G. P. (2000)."Assessment of Air Pollution due to SPM, SO_2, NO_x at IRE Ltd., Oscom Environment". *Indian J. Env. Prot.*, vol. 20 (1), p. 901 – 905

USEPA.(1997). *EPA Compendium of Methods for the Determination of Inorganic Compounds in Ambient Air, USA*

USEPA.(2014). *Air Quality Index- A Guide to Air Quality and Your Health*. North Carolina :US Environmental Protection Agency Office of Air Quality Planning and Standard Outreach and Information Division Research Triangle Park, p. 10

WHO.(2000). *Air Quality Guidelines for Europe*. Copenhagen: 2nd Ed., WHO Regional Publication, European Series, No. 91

EXTRACTION OF GLUCOSE ISOMERASE FROM *STREPTOMYCES* SP. AND ITS ACTIVITY

Kyaw Tun San [1], Khin Chaw Win [2] and Daw Hla Ngwe [3]

Abstract

The present study is concerned with the screening and isolation of glucose isomerase producing *Streptomyces* species from soil. Eleven soil samples were collected from the University of Yangon Campus (YU) and Pharmaceutical Research Department Campus (PRD), Yangon, Myanmar. A total of 29 strains of microorganisms were isolated and their glucose isomerase activites were screened by two different methods such as plate assay method by using three different media; X^+P^+, X^+P^- and wheat bran, and by fructose estimation method by using Seliwanoff's reagents. Among these 29 strains, only four strains: YU1-MAN3, YU3-PNI42, YU3-PNI44 and YU7-RCC3 showed glucose isomerase activity, and two strains YU3-PNI42and YU3-PNI44 were characterized as *Streptomyces* sp. according to the morphology, Gram's staining, spore staining, catalase test, gelatin test and nitrate test. The activities of glucose isomerase enzymes GI-PNI42 and GI-PNI44, extracted from *Streptomyces* sp. YU3-PNI 42 and YU3-PNI 44, were found to be 0.070 μmol min^{-1} mL^{-1} and 0.052 μmol min^{-1} mL^{-1}, respectively.

Keywords: *Streptomyces* sp., glucose isomerase, plate assay, wheat bran

Glucose isomerase (GI) enzyme is considered as one of the most important industrial enzymes (Sriprapundh *et al.*, 2003; Rao*et al.*, 2008) and it is the third highest value enzymes after amylase and protease (Srivastava *et al.*, 2010). The main practical application of this enzyme for its ability to isomerize D-glucose to D-fructose, and hence, it is widely used in industry for production of high-fructose corn syrup (HFCS) which is used all over the world as an alternative to sucrose or invert sugar in the food and beverage industry (Fenn *et al.*, 2004;Heo *et al.*, 2008; Brat *et al.*, 2009). Glucose isomerase (GI) can be isolated from a wide variety of bacteria such as Osmophillic *Aspergillus* sp. (Sayyed*et al.*, 2010), *Aerobacter aerogenes*, Strain HN-56 (Natake and Yoshimura, 1963), *Enterobacter agglomerans* (Nobel Surya Pandidurai *et al.*, 2011) and *Saccharamyces cerevisiae* (Brat *et al.*, 2009). Among them, *Streptomycetes* is one of the preferred categories of

[1] Demonstrator, Department of Chemistry, University of Yangon
[2] Dr, Lecturer, Department of Chemistry, University of Yangon
[3] Dr, Professor and Head, Department of Chemistry, University of Yangon

organisms for production of this enzyme. *Streptomycetes* are filamentous bacteria which possess extensive genes of primary and secondary metabolism. They are present in soil in abundance and are responsible for the degradation of all kinds of organic matter. This efficiency can be accounted by their capacity to produce different types of enzymes; amylase, protease, lipase, cellulase, glucose isomerase, xylanase, pectinase etc.

Some of the research for producing GI from *Streptomyces* sp. strain C (Bandlish *et al.*, 2002), *Streptomyces murinu* (Al-Tai *et al.*,1987), *Streptomyces phaeochromogenes* (Tsumura *et al.*, 1965), *Streptomyces albus* (Sanchez and Smiley, 1975), *Streptomyces* sp. (Takasaki, 1966), *Streptomyces cinnamonensis* (Joseph *et al.*, 1977), *Streptomyces flavovirens* (Sriprapundh *et al.*, 2003), *S. fradiae* (Mand *et al.*, 1977), *Streptomyces lividans* TK24 (Heo *et al*., 2008) and *Streptomyces* sp. (Chou *et al.*, 1976) had been published. However, the continuous studying of GI production from *Streptomyces* species is still being studied all around the world to achieve better GI producers.The present study is concerned with the screening and isolation of glucose isomerase producing *Streptomyces* species from soil.

Materials and Methods

Chemicals and Materials

All chemicals used in this research were from Merck, Germany. The materials are sterilizer (SM 310 Yomato), hot air sterilizer (GM-10E, DRWG No. YB-81051, Hawirawa Works LTD.), clean bench (CCV-1301EC, DRWG No. 4B-81048, Hitachi LTD.), medical freezer (Sanyo), microscope (Nicon, Japan), analytical balance (ATX224, Shimadzu), touch mixture (MT-11, Yomato), refrigerated centrifuge (5500, KuBoTa), incubator (Sanyo), homogenizer (HG-150, Wisetis), UV-Vis spectrophotometer (cenesys10s uv-vis, Thermo scientific), Shaking incubator (Jisico), digital water bath (ΔLab Tech, Dai Han lab tech Co. LTD.), loop, needle and, glasswares.

Soil Sample Collection and Isolation of Microorganisms

A total of 11soil samples were collected; 9 from the University of Yangon Campus (YU) and 2 from Pharmaceutical Research Department Campus (PRD), Yangon, Myanmar. One gram of each soil sample was 10 fold serially diluted in sterile water and 0.1 mL of each solution from dilutions

of 10^{-4} –$10^{-6}$was then spread on Peptone Yeast Agar medium plate (1 % peptone, 0.5 % yeast extract, 1 % xylose, 0.3 % K_2HPO_4, 0.1 % $MgSO_4$. $7H_2O$ and 2 % agar at pH 6.8–7 by the techniques of Dubey and Maheshwari (2009). Well grown colonies were picked and further purified by streaking onto the same agar medium plate. The pure strains were stored on Peptone Yeast Agar medium slant.

Preliminary Screening of Glucose Isomerase Producers

The isolates were screened qualitatively on xylose and wheat bran media. The organisms producing glucose isomerase can isomerise xylose to xylulose besides glucose to fructose. The organisms possessing very low or negligible GI activity might not grow on such a media. The screening strategy was designed according to the method described by Manhas and Bala(2004) and the modified method by Sheetal *et al.*(2013).Three different media, X^+P^+agar medium (1 % xylose 0.03 % peptone, 0.2 % KNO_3, 0.2 % K_2HPO_4,0.2 % NaCl, 0.05 % $MgSO_4.7H_2O$, 0.01 % $FeSO_4$, 0.02 % $CaCO_3$, 2 % agarat pH 7), X^+P^-agar medium (without peptone) and wheat bran agar medium (wheat bran was substituted for xylose as a carbon source) were used for preliminary screening. The cultures were spot inoculated on all the media and incubated at 30°C. The early developing isolates within 24 hron the plates were considered as higher GI producers.

Preparation of Enzyme Extracts

Peptone Yeast broth medium was used as a culture developing medium. The organism was grown in the medium at 30 °C for 4 days. The culture was harvested and centrifuged at 2000 rpm for 20 min at 4 °C. The cell was then collected and washed with potassium phosphate buffer (pH 7). After that, the cell was suspended with potassium phosphate buffer (pH 7). The cells were disrupted with the speed of 400 rpm for 5 minby Homogenizer. The cell free supernatant as crude intracellular enzyme extract was collected by centrifuging at 2000 rpm for 20 min at 4 °C.

Confirmation of Glucose Isomerase Extracted enzymes

The glucose isomerase activity was confirmed by Seliwanoff's reagent. The reaction mixture, according to Sathya and Ushadevi (2014)**,**

containing 0.4mL of crude enzyme and 0.6 mL glucose solution (0.1 M) was made up 2 mL with distilled water and incubated at 75 °C for 30min. Then, 2 mL of Seliwanoff's reagent was added into the reaction mixture and heated for 5min. The formation of cherry red colourindicated the occurrence of fructose due to the glucose isomerase activity of the test culture.

Identification of *Streptomyces* Sp.

The microorganism producing glucose isomerase enzyme was selected and further identified as a *Streptomyces* sp. The physiological and biochemical characteristics were determined. The colour and mycelium producing were detected on the growth of culture. Gram's staining, spore staining, citrate utilization, gelatin liquefaction, catalase and nitrate reduction were tested(Buchannan and Gibbons,1974).

Characterization of Glucose Isomerase Extracted from *Streptomyces* Sp.

The reaction mixture contained 0.2mL of 1 M glucose, 0.5 mL of potassium phosphate buffer, 0.1mL of 0.1M $MgSO_4.7H_2O$, 0.1mL of 0.01 M $CoCl_2$ and 0.2mL of enzyme extract. The final volume of assay mixture was made up to 2 mL with distilled water Isomerization was carried out at 70 °C for 30 min in water-bath. The reaction was stopped by adding 2 mL of 0.5 M perchloric acid. The fructose produced by isomerization was determined by the method described by Dische and Barnfoed (1951).To an aliquot of 0.1 mL of the above mixture, 0.9 mL of distilled water was added. 0.2 mL of 1.5 % cysteine hydrochloride, 6 mL of 70 % sulphuric acid and 0.2 mL of 0.12 % alcoholic carbazole were then added. The intensity of purple colour developed was determined at 560 nm using standard curve. One unit of glucose isomerase activity was defined as the amount of the enzyme that produced 1 μmol of D-fructose per minuteunder the assay conditions described.

Results and Discussion

Screening of Glucose Isomerase Activity of Isolated Microorganisms

A total of 29 culture strains were isolated from the soil. The glucose isomerase activity of isolated strains were primarily screening on three different media(X^+P^+ medium, X^+P^- medium and wheat bran medium). The

GI producers were characterized by two factors. One is the growth rate on the media; the higher growth of strains produced higher GI activity and the lower growth rate showed lower GI activity. And the other is the growth in X^+P^+ and X^+P^- media; the strain grown inonly $X^+P^+$was assumed as moderate GI producer and one grown inboth X^+P^+ and $X^+P^-$is good GI procedure. All strains grew in wheat bran medium but only 8 strains showed growth rate activity on X^+P^+ and X^+P^- media. The isolates giving early appearance on wheat bran medium also grew well on other two media. X^+P^+ and X^+P^- media gave a clear picture of isolates as GI producers (Sheetal *et al.*, 2013).The number of (+) signs is directly proportional to the growing capacity of the isolate on media. A comparison of growth on all the above media is shown in Table 1.This process indicated that 8 isolated strains were GI producers. The cultures selected by this method were further screened by Seliwinoff's reagent. The glucose isomerase enzymes were extracted from the selected culture.

Table 1: Growth Rate of Various Isolated Microorganisms on different Media

No.	Strains	Growth rate of microorganisms		
		X^+P^+	X^+P^-	Wheat Bran
1	YU1-MAN3	++	+++	+++
2	YU1-MAN21	+	–	+++
3	YU2-PNN3	+	+	+++
4	YU3-PNI42	+++	+++	+++
5	YU3-PNI44	+++	+++	+++
6	YU6-RCB5	+	–	+++
7	YU7-RCC3	++	+	+++
8	YU8-O7	+	–	+++

(+++) High growth rate, (++) Moderate growth rate, (+) Low growth rate and (–) No growth rate

The enzymatic reaction (isomerization of glucose to fructose) was performed using glucose as a substrate and fructose was identified by Seliwanoff's reagent. The cherry red colour development was identified against standard and blank test sample. In this process, among selected 8

strains, only 4 strains; YU1-MAN3, YU3-PNI42, YU3-PNI44 and YU7-RCC3showed higher growth rate inX^+P^+ and X^+P^- were found to be the similar colour forming as standard. The strains with very lower rate in screening plate media demonstrated negative glucose isomerase activity and the results are illustrated in Table 2. These methods are highly suitable for screening of glucose isomerase activity of microorganisms.

Table 2: Screening of Glucose Isomerase Activities of Enzymes Extracted from Various Isolated Microorganisms

No.	Strains	Extracted Enzymes	Glucose Isomerase Activities
1	YU1-MAN 21	GI-MAN 21	–
2	YU1-MAN3	GI-MAN3	+
3	YU8-O7	GI-O7	–
4	YU6-RCB5	GI-RCB5	–
5	YU7-RCC3	GI-RCC3	+
6	YU3-PNI42	GI-PNI42	+
7	YU3-PNI44	GI-PNI44	+
8	YU2-PNN3	GI-PNN3	–

(+) Glucose isomerase activity observed; (–) No glucose isomerase activity observed

Identification of *Streptomyces* Sp.

The four strains produced GI activity were selected and characterized based on their morphological, physical, cultural and biochemical properties with the help of Bergey's Manual of Determinative Bacteriology (Buchannan and Gibbons, 1974) and the Actinomycetes Vol. II (Selman and Waksman, 1961).Two of these species, YU1-PNI42 and YU1-PNI44 (Figure 1) were found to be Gram positive and spore positive, which is one of the important criteria of the *Streptomyces* sp.

(a) YU3-PNI42

(b) YU3-PNI44

Figure 1: Pure culture *Streptomyces* sp.

These strains were studied morphologically and microscopically. Microscopic observation revealed that only YU1-PNI42 and YU1-PNI44 showed better performance in the production of mycelia as well as sporulation (Figure 2). Other two strains, YU1-MAN3 and YU7-RCC3 could not produce mycelium but both were rod-shape. Therefore, according to the results and theoretical approach, it could say that YU1-MAN3 and YU7-RCC3 were not *Streptomyces* sp. and further consideration of the results of these strains could be neglected in the research. A biochemical characteristics of the selected isolates; such as catalase, gelatin, and nitrate had been considered for the identification of *Streptomyces* sp. analyzed (Table 3).

Table 3: Results of Characterization of *Streptomyces* Sp.

No.	Tests performed	Observation			
		YU3-PNI44	**YU3-PNI42**	**YU1-MAN3**	**YU7-RCC3**
1	Surface colour	watery	brown	Creamy	Creamy
3	Shape	mycelium	mycelium	Rod	Rod
5	Shape in liquid medium	pearl shaped	pearl shaped	–	–
6	Gram's stain	+	+	+	+
7	Spore stain	+	+	–	–
8	Gelatin	+	+	+	+
9	Catalase	+	+	+	+
10	Nitrate	+	+	+	+

+ = positive and– = negative

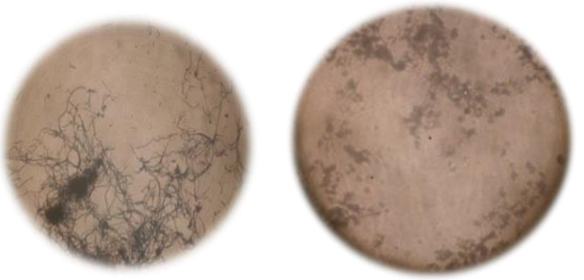

(a) (b)

Figure 2: Microscopic observation of *Sterptomyces* sp. (a) Mycelium (b) spore forming

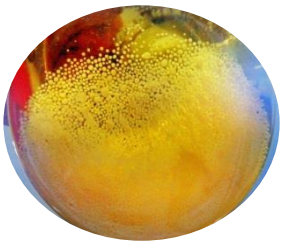

Figure 3: 4 day ages-*Sterptomyces* sp. in broth medium

Nitrate reduction, gelatin liquefaction and catalase tests were found to be positive in case of all strains. Other theoretical information was considered to this research to identify *Streptomyces* sp. In this research, the strain YU3-PNI42 and YU3-PNI44 was found that the growth rate was slow when they were incubated in at 37 °C butgrow well at 30 °C. Theoretical growth temperature range of *Streptomyces* sp. was 28 °C–30 °C. Streptomyces being a filamentous bacterium grew as pearl-shaped in the liquid medium.YU3-PNI42and YU3-PNI44 illustrated the pearl-shaped (Figure 3) in liquid medium and the beads grew in size and number with increase in incubation time.

Enzyme activity of Extracted GI from Isolated *Streptomyces* sp.

The activity of the glucose isomerase enzyme extracted from the strains of YU3-PNI42 and YU3-PNI44 was determined by isomerization of glucose substrate to fructose. The absorbance fructose formed was measured at 650 nm. The activities of glucose isomerase enzymes GI-PNI42 and GI-PNI44, extracted from respective strains were found to be 0.070 µmol $min^{-1}mL^{-1}$ and 0.052 µmol $min^{-1}mL^{-1}$, respectively. *Streptomyces* sp., YU3-PNI42 was found to be high glucose isomerase producer and the activity of enzyme of GI-PNI42 from YU3-PNI42 was higher than GI-PNI42 from YU3-PNI44 (Table 4).

Table 4: Activities of Glucose Isomerase Enzyme Extracted from the Isolated *Streptomyces* sp.

Enzyme Solutions	Enzyme Activity ($\mu mol\ min^{-1}\ mL^{-1}$)
GI-PNI42	0.070
GI-PNI44	0.052

Conclusion

The 11 soil samples were collected and cultured on PYA medium by serial dilution method. The pure colonies were isolated. Then the 29 pure cultures were screened on three different media plate such as X^+P^+, X^+P^- and wheat bran media. The 8 culture growth on these media was primarily selected and their GI activities were further confirmed by Seliwanoff's reagent. The strains grew with the very low growth rates in plate media did not show its GI activity when confirmed by Swellinoff's reagent. The four strains: YU1-MAN3, YU3-PNI42, YU3-PNI44 and YU7-RCC3 showed Glucose Isomerase activity. Only two strains: YU3-PNI42 and YU3-PNI44 could be characterized as *Streptomyces* sp. by assay methods. The activities of glucose isomerase enzymes GI-PNI42 and GI-PNI44, extracted from *Streptomyces* sp. YU3-PNI42 and YU3-PNI44, were found to be 0.070µmol $min^{-1}mL^{-1}$ and 0.052µmol $min^{-1}mL^{-1}$, respectively.

Acknowledgement

The authors gratefully acknowledge our sincere thanks to Member of Fermentation Department, Pharmaceutical Research Department (PRD) for provision to do this research and Myanmar Academy of Arts and Science for allowing to present this paper.

References

Al-Tai, A. M., Alit, Y. and Abdul-Razzak, S. H. (1987). "Isomerization of Glucose to Fructose: Production and Some Properties of Glucose Isomerase from *Streptomyces* sp. strain C". *Enzyme and Microbial Technology*, vol. 9(10), pp. 632–634

Bandlish, R. K., Hess, J. M., Epting, K. L., Vieille C. and Kelly, R. M. (2002)."Glucose-to-Fructose Conversion at High Temperatures with Xylose (Glucose) Isomerases from *Streptomyces murinus* and Two *Hyperthermophilic Thermotoga* species". *Biotechnology and Bioengineering*, vol. 80(2), pp. 185–194

Brat, D., Boles, E. and Wiedemann, B. (2009)."Functional Expression of a Bacterial Xylose Isomerase in *Saccharomyces cerevisiae*".*Appl. Environ. Microbiol.*, vol. 75(8), pp. 2304–11

Buchannan, R. E. and Gibbons, N. E. (1974).*Bergey's Manual ofDeterminativeBacteriology*.Baltimore:8th Ed, Williams and Wilkins Co. Ltd., pp. 581– 595

Chou, C. C., Ladisch, M. R. and Tsao, G. T. (1976)."Studies on Glucose Isomerase from a *Streptomyces* species". *Appl. Environ. Microbiol.*, vol. 32, pp. 489–493

Dische, Z. and Borenfreund, E. (1951)."A new spectrophotometric method for the detection and determination of keto sugars and trioses".*The Journal of Biological Chemistry*, vol. 192(2), pp. 583–587

Dubey, R. C. and Maheshwari, D. K. (2009).*Practical Microbiology*. New Delhi: S. Chand & Co. Ltd., pp. 37–79

Fenn, T. D., Ringe, D. and Petsko, G.A. (2004). "Xylose Isomerase in Substrate and Inhibitor Michaelis States: Atomic Resolution Studies of a Metal-Mediated Hydride Shift". *Biochemistry*, vol. 43, pp. 6464–6474

Heo, G.Y., Kim, W.C., Joo, G.J. and Kwak, Y.Y. (2008)."Deletion of xylR Gene Enhances Expression of Xylose Isomerase in *Streptomyces lividans* TK24".*J. Microbiol. Biotechnol.*, vol. 18(5), pp. 837–44

Joseph, R., Shonthamma, M. S. and Murthy, V. S. (1977)."Isolation of *Streptomyces* Having High Glucoseisomerase Activity and Assessment of their Efficiency in the Production of Fructose Syrup".*J. Food Sci. Technol.*, vol. 14, pp. 73–77

Mand, K., Srikanta, S., Joseph, R., Shanthamma, M. S. and Murthy, V. S. (1977). "Production of Glucose Isomerase by *Streptomyces fradiae*".*Indian J. Exp. Biol.*, vol. 15, pp. 668–669

Manhas, R. K. and Bala, S. (2004). "Thermostable Glucose Isomerase Production by some Bacteria and *Streptomyces*". *Indian Journal of Microbiology*, vol. 44(2), pp. 129–132

Natake, M. and Yoshimura, S. (1963).“Studies on Glucose Isomerase of Bacteria Part I. Formation of Glucose Isomerase by *Aerobacteraerogenes*, Strain HN-56, and its Relationship to Xylose Isomerase”.*Agr. Biol. Chern*., vol. 27(5), pp. 342–348

Nobel Surya Pandidurai, R., Kalaichelvan, P. T., Mukesh Kumar, D. J. and Gnanaraj, M. (2011). “Production of Extracellular Glucose Isomerase by *Enterobacter agglomerans* Isolated From Garden Soil”. *International Journal of Current Research*, vol. 3(7), pp. 21–25

Park, Y. K., and Toma, M. (1974).Some Interrelation between Microbial Xylanase and Glucose Isomerase Pro-duction”.*J. Gen. Appl. Microbiol.*, vol. 20, pp. 67–69

Rao, K., Chelikani, S., Relue, P. and Varanasi, S. (2008). “A Novel Technique that Enables Efficient Conduct of Simultaneous Isomerization and Fermentation (SIF) of Xylose”.*Appl. Biochem. Biotechnol*., vol. 146(1–3), pp. 101–17

Sanchez, S., and Smiley, K. L. (1975).“Properties of Dxyloseisomerase from *Streptomyces albus*”.*Appl. Microbiol.*, vol. 29, pp. 745–750

Sathya, R. and Ushadevi, T. (2014). “Isolation and Screening of GlucoseIsomerase Producing Marine *Streptomyces* species for Fructose Production”. *Der. Pharma. Chemica.*, vol. 6(5), pp. 215–219

Sayyed, R. Z., Shimpi, G. B. andChincholkar, S. B. (2010). “Constitutive Production of Extracellular Glucose Isomeraseby an *Osmophillic Aspergillus*sp. under Submerged Conditions”. *J. Food Sci. Technol.*,vol. 47(5), pp. 496–500

Selman, A. and Waksman. (1961). *The Actinomycetes Vol. II: Classification, Identification and Descriptions of Genera and Species*. Baltimore: 7th edition, The Williams and Wilkins Co. Ltd., pp. 61–297

Sheetal, B., Prachi, S., Pinkey, R. and Modi, H. A. (2013).“Comparative Study of Extraction Methods for Intracellular Produced Gsslucose Isomerase by *Streptomyces* sp. *SB–AII4”.Int. Res. J. Biological Sci.*, vol. 2(10), pp. 43–50.

Sriprapundh, D., Vieille, C. and Zeikus, J. G. (2003).Directed Evolution of Thermotoga neapolitana Xylose Isomerase: High Activity on Glucose at Low Temperature and Low pH”. *Protein Engng*., vol. 16, pp. 683–690

Srivastava, P., Shukla1, S., Choubey S. K. and Gomase, V. S. (2010). “Isolation, Purification &Characterization of Glucose Isomerase Enzyme form *Streptomyces* Species Isolated from Parbhani Region”. *Journal of Enzyme Research*, vol. 1(1), pp. 0976 –7665

Tsumura, N., Hagi, M. and Sato, T. (1965).“Enzymatic conversion of D-glucose to D-fructose.II. Properties of the Enzyme from *Streptomyces phaeochromogenes*”. *Agric. Biol. Chem.*, vol. 29, pp. 1129–1134

Takasaki, Y. (1966). “Studies on Sugar-Isomerizing Enzyme: Production and Utilization of Glucose Isomerase from *Streptomyces* sp.”.*Agric. Biol. Chem.*, vol. 30, pp. 1247–1253

BIS-NAPHTHO-γ-PYRONES FROM ENDOPHYTIC FUNGUS ISOLATED FROM THE LEAF OF *Andrographis paniculata* (Burn.f.) Wall. ex Nees AND THEIR BIOACTIVITIES

Tun Min Htet[1], Hnin Yu Win[2], Myint Myint Sein[3]

Abstract

In this research work, one of the Myanmar medicinal plants, *Andrographis paniculata* (Burn.f.)Wall. ex Nees was selected for chemical investigation of its endophytic fungus. The endophytic fungi from the leaf of the selected medicinal plant were cultivated on water-agar medium under sterile condition and isolation of pure culture was carried out. Selection of the target fungus was done based on chemical screening (spot pattern on TLC). The selected fungus was found to be *Alternaria* sp. according to morphological studies. After selecting the target fungus, up-scaled fermentation for pure isolated target fungus was performed on M_2 medium. After two weeks, the well-grown culture broths were exhaustively extracted with ethyl acetate. Then, the ethyl acetate extract was evaporated to dryness under reduced pressure to obtain brown crude extracts. The resulting microbial extracts were chromatographed to isolate the pure metabolites. The two pure yellow pigment organic compounds bis-naphtho-g-pyrones derivatives and ferulic acid were isolated from the extracts by using various chromatographic techniques. Furthermore, the structure of isolated compounds were deduced by NMR and mass studies.In addition, antimicrobial activities, cytotoxicity assay and the evaluation of antioxidant activitiy for the two pyrone derivatives compounds were also performed.

Keywords: *Andrographi spaniculata* (Burn.f.) Wall. ex Nees, Endophytic fungi, WA (water agar), M_2 (Malt extract, Glucose, Yeast extract), *Alternaria* sp., bis-naphtho-γ-pyrones

Introduction

People depend on plants because they provide compounds essential for human existence. Plants produce primary compounds such as sugars and proteins that are used in a plant's basic metabolism and form the base of our food web. Plants also produce an array of chemicals that are known as secondary compounds because they are not usually integral to basic

1. Dr, Assistant Lecturer, Department of Chemistry, Monywa University
2. Dr rer. nat., Lecturer, Department of Chemistry, University of Mandalay
3. Dr, Professor, Head of Department (Rtd.), Department of Chemistry, University of Mandalay

metabolism (Simpson and Ogorzaly, 1995). Medicinal plants and their endophytes are important resources for discovery of natural products (Huang *et al*., 2007). Endophytes are microorganisms that reside asymptomatically in the tissues of higher plants and are a promising source of novel organic natural metabolites exhibiting a variety of biological activities (Pimentel *et al*., 2011). Endophytic fungi are the main sources for the production of secondary metabolites. They live asymptomatically inside the tissues of higher plant (Bano*et al*., 2016). They have the ability to produce same or similar bioactive compounds as those originated from their host plant. Some endophytic fungi are rare; many of the biological active substances extracted from endophytic fungi are reported to be novel. Therefore, it is important to explore endophytic fungi in the medicinal plants (Singh *et al*., 2015).

In this research work, one Myanmar traditional medicinal plant, *Andrographi spaniculata* (Burn.f.)Wall. ex Nees (Kress *et al.* 2003) was selected for chemical analysis. *Andrographi spaniculata* is a herbaceous plant, commonly known as "King of Bitter", in the family Acanthaceae. It is widely distributed in Myanmar. It is locally known as Say-khar-gyi. The bioactive chemical constituents isolated from the endophytic fungus of the leaves of *A. paniculata* have been little explored. So, this drew our attention to investigate the chemical constituents of endophytic fungus isolated from the leaves of *A. paniculata.*

Materials and Methods

Sample Collection

The sample was collected form Monywa Township, Sagaing Region.

General Experimental Procedures

FT IR (Fourier Transform Infrared) spectrophotometer (Shimadzu, Japan), optical rotation was measured on a Perkin-Elmer polarimeter (model 241) (Perkin-Elmer, San Jose, CA, USA). NMR (Nuclear Magnetic Resonance) spectra were measured on a Varian Inova 600 (599.740 MHz) and a Varian Unity 300 (300.145 MHz) spectrometer. ESIMS were measured on a Quattro Triple Quadruple mass spectrometer with a Finnigan TSQ 7000 with nano-ESI API ion source. Column chromatography was carried out on MN silica gel 60, 0.05-0.2 mm; TLC (Thin Layer Chromatography) was

performed on Polygram SIL G/UV_{254}. All silica gel materials were purchased from Macherey-Nagel, Düren, Germany. Size exclusion chromatography was done on Sephadex LH-20 (Lipophilic Sephadex; Amersham Biosciences, Freiburg, Germany, purchased from Sigma-Aldrich Chemie, Steinheim, Germany). Micropipette (1000 mL), brown bottles, electric balance, shaker and UV-spectrophotometer (UV-7504, KWF, China) were also used.

Microbiological Materials

Autoclave: Abstell Hearson, Autoclave volume 119 L, working temperature 121 °C, working pressure 1.2 kg/cm^2. Esco Horizontal Laminar-Flow-Cabinet: EQU/ 03-EHC, Esco Micro Pte-Ltd, Singapore. Petridishes: 90 mm diameter, 16 mm height, China.

Nutrients

M_2 medium

Malt extract	10 g
Glucose	4 g
Yeast extract	4 g
Distilled water	1 L

The pH was adjusted to 7.8 using 2 N NaOH.

Water agar medium

Agar	20 g
Distilled water	1 L

All cultures media were autoclaved at 1.2 bar and 120 °C. Sterilization time for 1 L culture: 15 min.

Procedure

Preparation of M_2 Medium and WA (Water Agar) Medium

M_2 medium is the most widely used medium for growing fungi and bacteria which attack living plants or decay dead plant matter. Malt extract 10 g were mixed with 4 g of glucose and 4 g of yeast extract. Distilled water was added such that the total volume of the suspension is one liter. Then, the medium was sterilized by autoclaving at 121 °C for 15 min. After sterilization, chloramphenicol (50 mg/L) was added to the medium to suppress

bacterial contamination. Then, the medium was poured into petridish (Win, 2009).

Water agar medium is used to isolate individual fungal colonies. It was prepared by 20 g agar in 1 L distilled water. The procedure for sterilization and addition of antibiotic was the same as for M_2 medium.

Isolation of Endophytic Fungi

The fresh leaves were thoroughly washed in running tap water to remove dust and debris, and then air-dried on sterile filter paper and cut into small pieces using a blade. Sterile conditions were maintained for the isolation of endophytes and all the work was performed in a laminar flow hood to avoid contamination. Surface sterilization of the samples was achieved with 95 % EtOH for 30 s, 10 % sodium hypochlorite for 10 min, 70 % EtOH for 2 min, and then dried aseptically. The inner tissues were placed on isolation media (water agar; WA) in petridishes supplemented with 50 mg/L of chloramphenicol to suppress bacterial growth, and incubated at 25 °C until the outgrowth of endophytes was discerned. Individual fungal colonies were picked and transferred onto sterile WA medium and periodically checked for purity. A total of 7 strains were isolated and each strain was inoculated on 200 mL M_2 medium for pre screening (chemical screening) (Figure 1). The target fungus was selected for further studies due to its spot pattern on TLC (De, 1997; Larran, 2002; Radu and Kqueen, 2002).

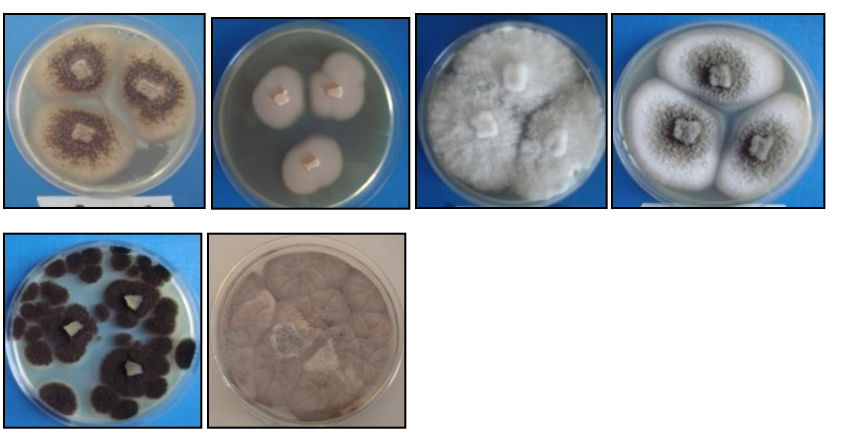

Selected fungus

Figure 1: Isolated fungi from *Andrographi spaniculata* (Burn.f.) Wall.exNees on M_2 medium

Up-scaled Fermentation for the Selected Fungus

The well grown agar cultures of the selected strain were used to inoculate 50 flasks of 1 L Erlenmeyer flasks containing 400 mL M_2 medium supplemented with antibiotic.

After two weeks, they were harvested and extracted with ethyl acetate. Then, the ethyl acetate was evaporated to dryness under reduced pressure. The resulting crude extract (11.25 g) was chromatographed to isolate the metabolites. Before harvesting, 1.5 mL of MeOH was added to each flask to kill fungus and left for 24 h.

Isolation of Metabolites from the Selected Fungus

EtOAc extracts were dissolved in the mixture of n-hexane and EtOAc and silica gel was added to that mixture and evaporated the solvents. The obtained crude extracts were homogenous adsorbed on silica gel.

Then, the crude extracts were subjected to silica gel using stepwise gradient of *n*-hexane:ethyl acetate. Totally 567 fractions were obtained. Each fraction was checked by TLC. Eleven combined fractions were obtained. Fraction VI was subjected to Sephadex LH-20 using MeOH to isolate TMH-3 (R_f = 0.31, 1:1 (*n*-hexane : ethyl acetate)) as pale yellow compound. It showed UV absorption band at 254 nm. After purification of fraction IX on Sephadex LH-20 using methanol and RP-18 (Reverse phase) using methanol and water, TMH-1 (R_f= 0.50, 2:1 (*n*-hexane : ethyl acetate)) and TMH-2 (R_f= 0.53, 1:2 (*n*-hexane : ethyl acetate)) were isolated as yellow compounds. They showed UV absorption band at 254 nm. The yield percents of pure compounds (TMH-1), (TMH-2) and (TMH-3) were found to be 0.15% (16.5 mg), 0.09 % (10.5 mg) and 0.04% (4.7 mg) upon ethyl acetate extracts (11.25 g) respectively.

Structure Elucidation of the Isolated Compounds

The structure elucidation of isolated compounds was determined by spectroscopic methods such as FT IR, ^{1}H NMR, ^{13}C NMR, DEPT, DQF-COSY, HMQC, HMBC, NOESY and ESI MS spectrometry respectively.

Screening of Antimicrobial Activities of Pure Compounds (TMH-1 and TMH-2)

Antimicrobial activities tests for pure compounds (TMH-1 and TMH-2) were performed at PRD (Pharmaceutical Research Department), Insein, Yangon.

Determination of Cytotoxicity of Pure Compounds (TMH-1 and TMH-2) by Brine Shrimp Lethality Bioassay

Pure compounds (TMH-1) and (TMH-2) were investigated by brine shrimp lethality bioassay according to the procedure described by Dockery and Tomkins, (2000).

Determination of Antioxidant Activity of Pure Compound (TMH-1) by DPPH Free Radical Scavenging Assay

The free radical scavenging activity of pure compound (TMH-1) was measured by using DPPH free radical scavenging assay (Marinovaand Batchvarov, 2011).

Results and Discussion

Structure Elucidation of Pure Compound (TMH-1)

In the aromatic region of ^{1}H NMR spectrum (Figure 6 (a)), two singlets at *d* 7.35 and *d* 7.23 ppm were ascribed to two aromatic methine protons. In the HMBC spectrum (Figure 8 (a)), these methine protons at *d* 7.35 and *d* 7.23 ppm showed *b* -correlation with sp^2 quaternary carbon at *d* 112.1 ppm.

Moreover, in the HMBC spectrum (Figure 8 (a)), sp^2methine proton at *d* 7.23 ppm showed *a*-coupling with one sp^2 quaternary carbon at *d* 161.5 ppm and *b*-coupling with sp^2 quaternary carbon at *d* 119.0 ppm and sp^2methine carbon at δ 103.1 ppm and small correlation with sp^2 quaternary carbon at *d* 159.4 ppm. In addition, one sp^2methine proton at *d* 7.35 ppm showed α-correlation with one sp^2 quaternary carbon at *d* 152.1 ppm which is probably attached to oxygen. Moreover, the proton at *d* 7.35 ppm showed *b*-correlations with sp^2 quaternary carbon at *d* 105.5 ppm and sp^2methine carbon at δ103.2 ppm. Therefore, fragment (a) could be confirmed (Figure 2).

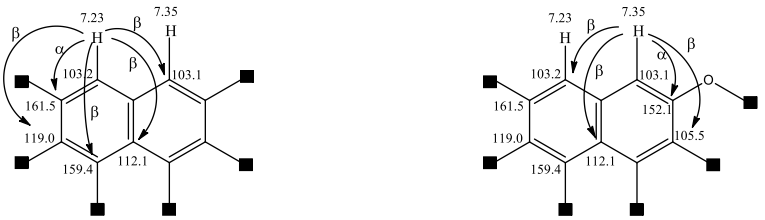

Fragment (a)

Figure 2:(→) HMBC correlation in fragment (a)

In the HMBC spectrum (Figure 8 (a)), there was the observation of *b*-coupling between singlet methoxy protons at *d* 3.80 ppm and aromatic sp^2 quaternary carbon at *d* 161.5 ppm and also the occurrence of *b*-coupling between singlet methoxy protons at *d* 3.45 ppm and aromatic sp^2 quaternary carbon at *d* 159.4 ppm.

Furthermore, in the HMBC spectrum (Figure 8 (a)), one sp^2methine proton at *d* 7.35 ppm showed *g*-correlations with carbonyl carbon at *d* 186.2 ppm and sp^2 quaternary carbon at *d* 154.7 ppm. The latter could be connected to hydroxyl group.

In the HMBC spectrum (Figure 8 (a)), the methine proton at δ6.15 showed α-coupling with one sp^2 quaternary carbon at δ 170.6 ppm and one carbonyl carbon at δ 186.2 ppm. Furthermore, it showed *b*-coupling with one sp^2 quaternary carbon at δ 105.5 ppm and methyl carbon at δ 20.6 ppm respectively. Moreover, methyl singlet at δ 2.43 ppm showed *a*-coupling with one sp^2 quaternary carbon at δ 170.6 ppm and *b* -coupling with one sp^2methine carbon at δ 107.9 ppm which implies the partial structure (I).

In the NOESY spectrum (Figure 9 (a)), there is a spatial correlation between sp^2methine proton at δ 7.23 ppm and methoxy protons at δ 3.80 ppm. Moreover, methine proton at δ 6.15 ppm showed NOESY with methyl protons at δ 2.43 ppm. Therefore, partial structure (I) could be confirmed (Figure 3).

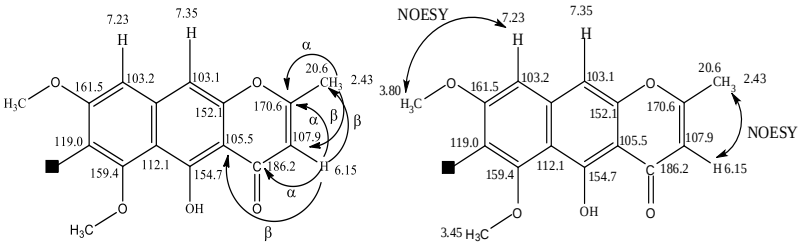

Figure 3: (→) HMBC correlation and (↔) H-H COSY correlation in Partial Structure (I)

In the aromatic region of ^{1}H NMR spectrum (Figure 6 (a)), one methine doublet at δ 6.50 ppm (J = 2.20 Hz) showed meta coupling with the doublet methine proton at δ 6.25 ppm (J = 2.15 Hz). Moreover, DQF-COSY spectrum (Figure 8 (b)) displayed the correlation between two methine protons at δ 6.50 and δ 6.25 ppm as expected in fragment (b) (Figure 4).

In the HMBC spectrum (Figure 8 (a)), one sp^2methine proton at δ 6.50 ppm showed *a*-coupling with two sp^2 quaternary carbons at δ 163.3 and 162.3 ppm and *b*-coupling with one sp^2 quaternary carbon at δ 109.4 ppm and one sp^2methine carbon at δ 97.5 ppm.

Moreover, one sp^2methine proton at δ 6.25 ppm showed α-coupling with one sp^2 quaternary carbon at δ163.3 ppm and β-coupling with sp^2methine carbon at δ98.3 ppm and sp^2 quaternary carbon at δ 109.4 ppm. From these data, the carbon atoms in the benzene ring could be assigned.

In the HMBC spectrum (Figure 8 (a)), there was the observation of *b*-correlation between singlet methoxy protons at δ 3.60 ppm and aromatic sp^2 quaternary carbon at δ 163.3 ppm. Moreover, *b*-correlation between singlet methoxy protons at δ 3.96 ppm and aromatic sp^2 quaternary carbon atδ162.3 ppm was also detected.

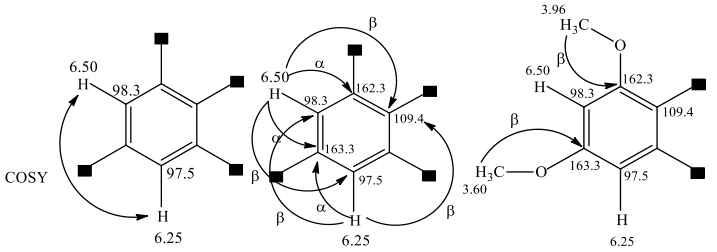

Fragment (b)

Figure 4: (→) HMBC correlation and (↔) H-H COSY correlation in fragment (b)

In the HMBC spectrum (Figure 8 (a)), sp^2methine proton at δ 6.08 ppm showed α-coupling with one sp^2 quaternary carbon at δ 170.3 ppm and *b*-coupling with one sp^2 quaternary carbon at δ 104.9 ppm and methyl carbon at δ 20.5 ppm respectively. In addition, the methyl singlet at δ 2.15 ppm showed α-coupling with one sp^2 quaternary carbon at δ 170.3 ppm and *b*-coupling with one sp^2 methine carbon at δ 107.8 ppm.

All HMBC correlations and chemical shifts of carbons showed similar structural feature of g-pyrone ring as in partial structure (I). Therefore, fragment (c) could be elucidated.

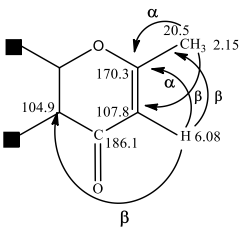

Fragment (c)

Fragments (b) and (c) could be connected by using HMBC spectrum. According to the spectrum, one sp^2methine proton at δ6.25 ppm showed *b*-coupling with one sp^2 quaternary carbon at δ 107.0 ppmand *g*-coupling with one sp^2 quaternary carbon at δ163.2 ppm and. Therefore, partial structure (II) could be elucidated.

In the NOESY spectrum (Figure 9 (a)), there is a spatial correlation between sp^2methine proton at δ6.50 ppm and methoxy protons at δ 3.96 ppm.

Moreover, methine proton at δ 6.25 ppm showed NOESY correlation with methoxy protons at δ 3.60 ppm, methine proton at δ6.08 ppm also showed NOESY correlation with methyl protons at δ 2.15 ppm. Therefore, partial structure (II) could be confirmed (Figure 5).

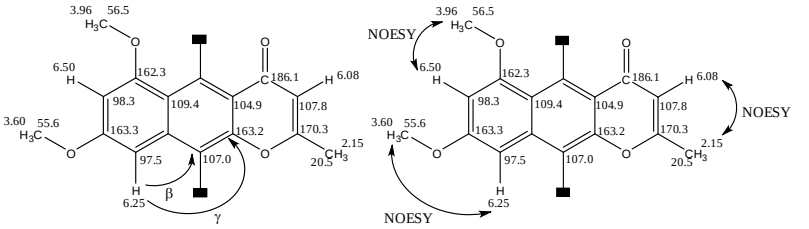

Partial Structure (II)

Figure 5: (→) HMBC correlation and (↔) H-H COSY correlation in Partial Structure (II)

The connections between the partial structures (I) and (II) were inferred mainly on the basis of NOESY spectrum (Figure 9 (a)). Therefore, complete structure of pure compound (TMH-1) could be elucidated (Figures 6-9). The partial molecular formula of pure compound (TMH-1) was assigned as $C_{32}H_{25}O_9$. Molecular formula of pure compound (TMH-1) was $C_{32}H_{26}O_{10}$. Therefore, the remaining molecular formula must be one hydroxyl group (-OH).

By logically, the chemical shift of C-5', C-9a and C-9'a could be assigned as δ162.2, 142.1 and 142.4 ppm.

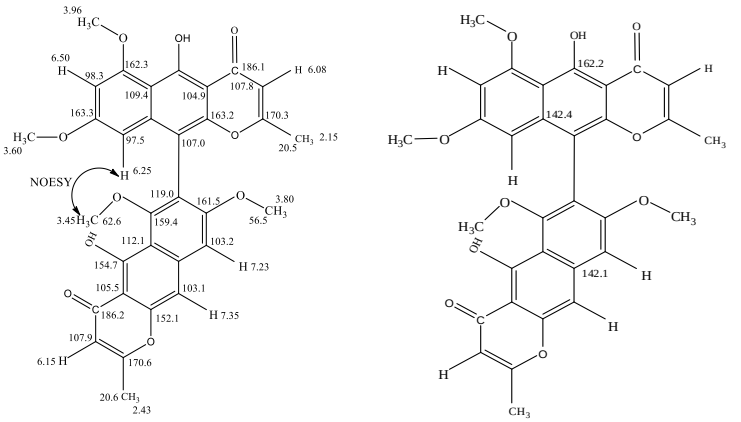

Complete Structure of Pure compound (TMH-1)

The high resolution (+) ESI MS gave pseudomolecular ion peak at *m/z* 593.1407 $[M + Na]^+$, and *m/z* 571.1590 $[M + H]^+$ (Figure 9 (b)). Thus, the molecular mass was deduced as 570 Daltons. The molecular formula was corresponded to $C_{32}H_{26}O_{10}$. The hydrogen deficiency index was 20.

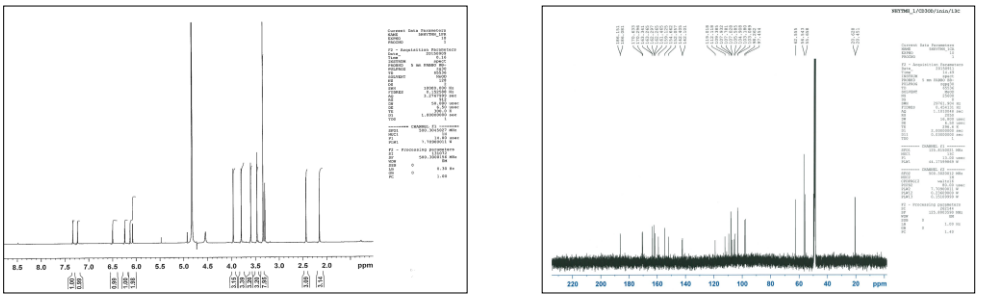

(a) **(b)**

Figure 6: (a) ^1H NMR and (b) ^{13}C NMR spectra of TMH-1

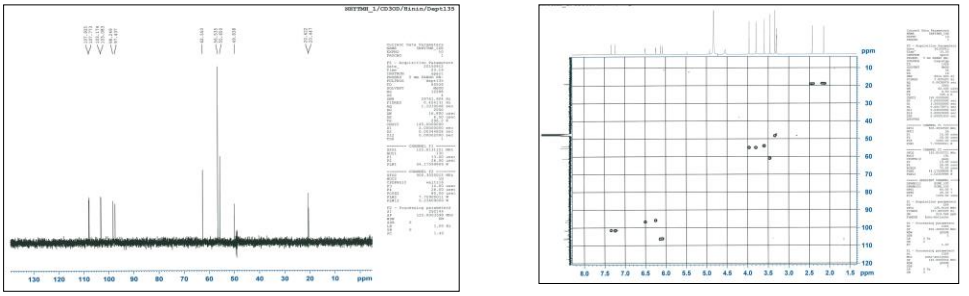

(a) (b)

Figure 7: (a) DEPT and (b) HMQC spectra of TMH-1

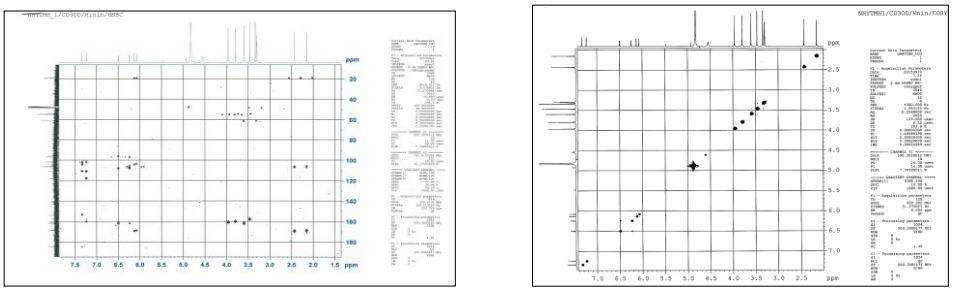

(a) (b)

Figure 8: (a) HMBC and (b) DQF-COSY spectra of TMH-1

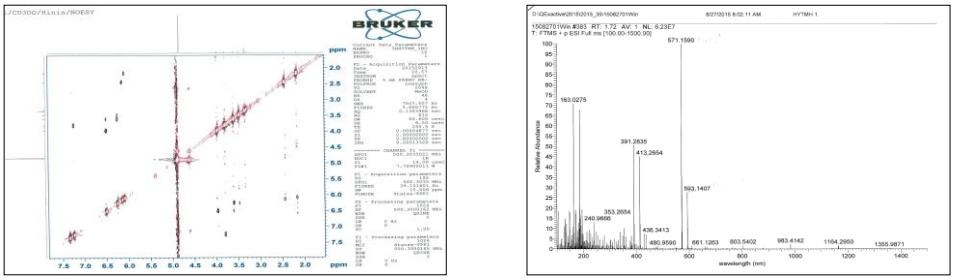

(a) (b)

Figure 9: (a) NOESY and (b) ESI-MS spectra of TMH-1

Structure Elucidation of Pure Compound (TMH-2)

Compounds TMH-1 and TMH-2 were not easily differentiated when they were analyzed by other spectroscopic methods such as FT IR, ESI MS and ^{1}H NMR which indicated that they had very similar molecular structures. The mass spectral data, obtained by electrospary ionization (ESI) in the positive ion mode, suggested them to be isomers of $C_{32}H_{26}O_{10}$ $[M+H]^{+}$ at *m/z* 571. Pure compound TMH-2 showed almost the same NMR data discussed above, but this isomer contains a different partial structure (I) (Figures 10-12).

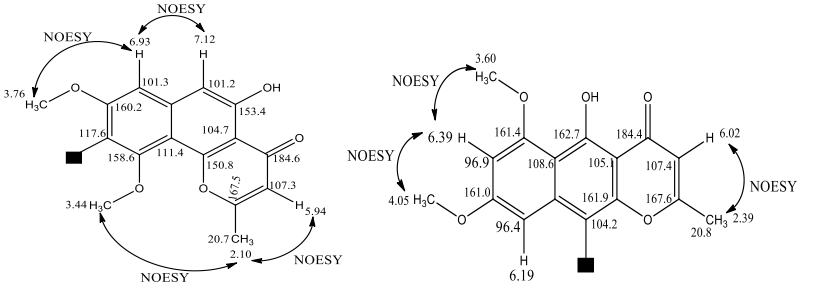

Partial Structure (I) Partial Structure (II)

The connections between the partial structures (I) and (II) were inferred mainly on the basis of NOESY spectrum (Figure 13 (a)). By logically, the chemical shift of C-9a' and 6a could be assigned as δ 140.5 and 140.7 ppm.

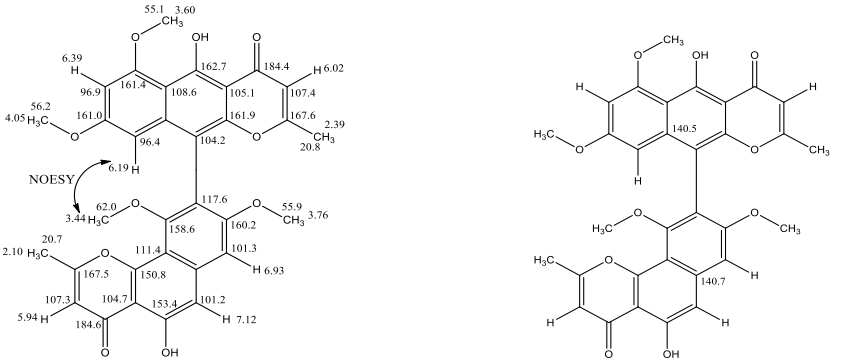

Complete Structure of Pure compound (TMH-2)

The complete isolated pure organic compounds (TMH-1) and (TMH-2) could be expressed as dimericnaphtho-g-pyrone derivatives. The chemical name of pure compounds (TMH-1) and (TMH-2) could be assigned as 5, 5'-dihydroxy-6, 6', 8, 8'-tetramethoxy-2, 2'-dimethyl-4H, 4'H-7,10'-bibenzo [g] chromene-4, 4'-dione and 5,5'-dihydroxy-6', 8, 8', 10'-tetramethoxy-2, 2'-dimethyl-4H, 4'H-9,10'-bibenzo[h, g]chromene-4, 4'-dione re

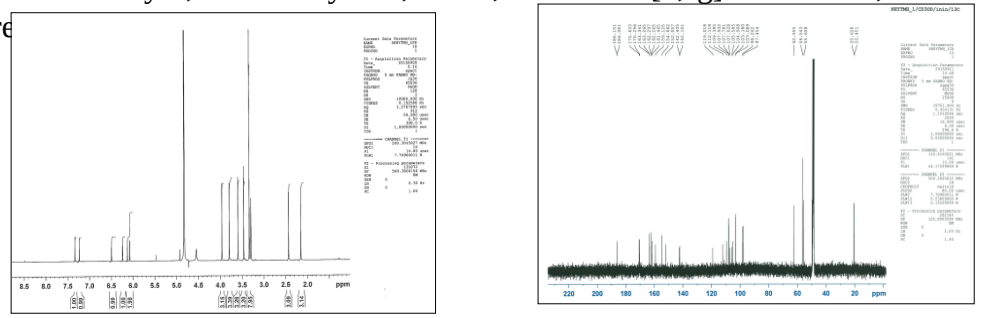

(a) (b)

Figure 10: (a) ^{1}H NMR and (b) ^{13}C NMR spectra of TMH-2

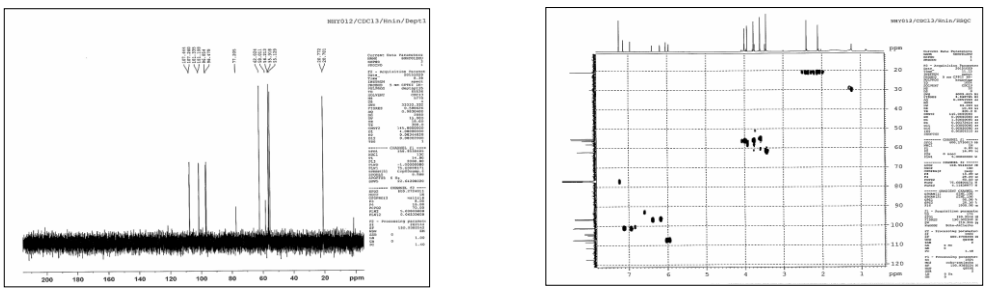

Figure 11: (a) DEPT and (b) HMQC spectra of TMH-2

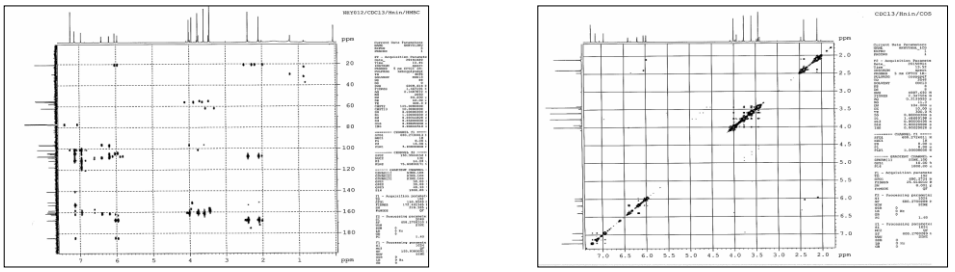

(a) (b)

Figure 12: (a) MHBC and (b) DQF-COSY spectra of TMH-2

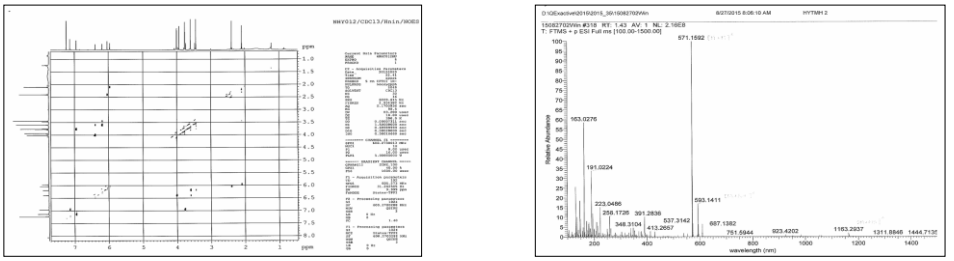

(a) (b)

Figure 13: (a) NOESY and (b) ESI-MS spectra of TMH-2

Structure Elucidation of Pure Compound (TMH-3)

The ^{1}HNMR spectrum (Figure 16 (a)) showed two doublets at δ 7.49 (J = 15.8 Hz) and δ6.32 ppm (J = 15.8 Hz) for a trans disubstituted α, b-unsaturated carbonyl group of ester, acid or amide. In DQF-COSY spectrum (Figure 18 (a)), the methine proton at *d* 6.32 ppm which is attached to carbon at *d* 118.8 ppm showed correlation with another methine proton at *d* 7.49 ppm (Figure 14).

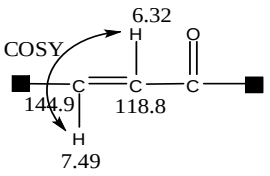

Fragment (a)

Figure 14:(↔) H-H COSY correlation in fragment (a)

In the aromatic region of ^{1}HNMR spectrum (Figure 16 (a)), doublet of doublet at *d* 7.02 ppm (*J* = 8.1, 1.7 Hz) showed ortho coupling to the proton at *d* 6.79 (*J* = 8.2 Hz) and meta coupling with the proton at *d* 7.15 ppm (*J* = 1.7 Hz). The pattern in the aromatic region was the ABX system of a 1, 2, 4-trisubstituted benzene ring. Moreover, DQF-COSY spectrum (Figure 18 (a)) displayed the correlation between two methine protons *d* 6.79 and *d* 7.02 ppm.

In the HMBC spectrum (Figure 17 (b)), sp^2 methine proton at δ 6.79 showed α-coupling with sp^2 quaternary carbon at δ 149.9 ppm and methine carbon at δ 123.5 ppm and *b*-correlations with two sp^2 quaternary carbons at δ 149.3 and δ 128.5 ppm. Moreover, sp^2 methine proton at δ 7.15 showed α-coupling with sp^2 quaternary carbon at δ 149.9 ppm and methine carbon at δ 123.5 ppm and *b*-correlations with two sp^2 quaternary carbons at δ 149.3 and δ 128.5 ppm (Figure 15).

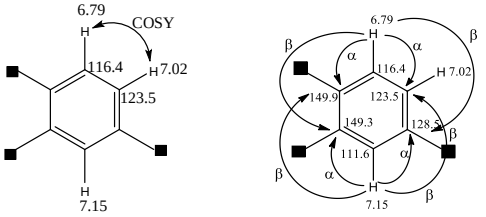

Fragment (b)

Figure 15:(↔) H-H COSY correlation and (→) HMBC correlations in fragment (b)

Moreover, there was the observation of *b*-correlation between singlet methoxy protons at δ 3.88 ppm and aromatic sp^2 quaternary carbon at δ 149.3 ppm which indicated fragment (b).

Fragments (a) and (b) could be connected by further HMBC correlation. One sp^2methine proton at *d* 7.49 ppm showed *b*-coupling with two sp^2methine carbons at *d* 123.5, *d* 111.6 ppm and carbonyl carbon at *d* 173.1 ppm. Furthermore, the proton at *d* 6.32 ppm indicated *b*-correlation with one sp^2quaternary carbon at *d* 128.5 ppm. The attachment of remaining one –OH group to one downfield quaternary carbon at *d* 173.0 ppm accomplished the complete structure of pure compound (TMH-3). The chemical name of

isolated pure compound (TMH-3) is 2(E)-3-(4-hydroxy-3-methoxy phenyl)-2-propenoic acid. So, pure compound (TMH-3) was assigned as ferulic acid.

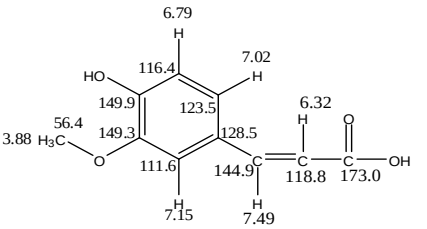

Complete Structure of Pure compound (TMH-3) (Ferulic acid)

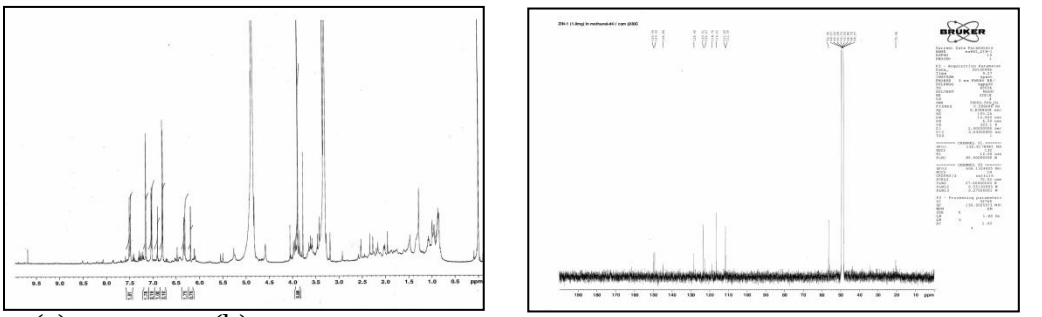

(a) (b)

Figure 16: (a) ^{1}H NMR and (b) ^{13}C NMR spectra of TMH-3

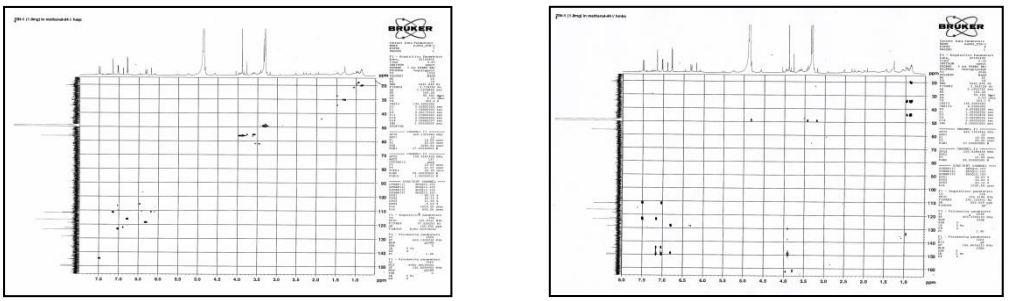

(a) (b)

Figure 17: (a) MHQC and (b) HMBC spectra of TMH-3

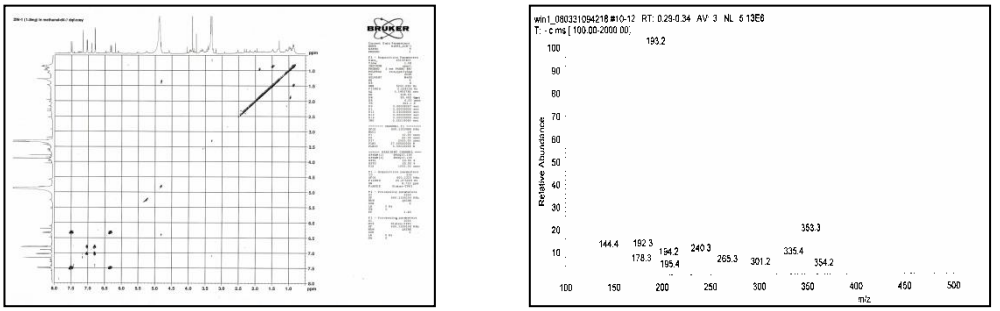

(a) (b)

Figure 18: (a) DQF-COSY and (b) (-) ESI spectra of TMH-3

Antimicrobial Activities of Pure Compounds (TMH-1 and TMH-2)

Due to the lack of appropriate test system or limitation of resources, the compounds (TMH-1 and TMH-2) could be tested against only six different microorganisms. The results are shown in Table 1.

Table 1: Results of Antimicrobial Activities of Pure Compounds (TMH-1 and TMH-2)

No.	Types of microorganisms	Diameter of Inhibition Zone (mm)	
		TMH-1	TMH-2
1.	*Bacillus subtilis*	11	11
2.	*Staphylococcus aureus*	-	12
3.	*Pseudomononas aeruginosa*	12	11
4.	*Bacillus pumilus*	11	11
5.	*Candida albicans*	12	11
6.	*E.coli*	12	12

Agar well ~ 10 mm
10 mm ~ 14 mm (+) weak activity
15 mm ~ 19 mm (++) medium activity
20 mm above (+++) high activity

Cytotoxicity of the Isolated Compounds (TMH-1 and TMH-2)

Pure compounds (TMH-1) and (TMH-2) were screened for cytotoxicity using brine-shrimp bioassay. The assay was based on the ability

of pure compounds to kill laboratory cultured brine shrimp. The results are shown in Table 2.

Table 2: Results of Brine Shrimp Lethality Bioassay

Test materials	% Mortality under the concentration studied (mg/mL)				LD_{50} (µg/mL)	Toxicity
(w/v)	0.1	1	10	100	0.26	Toxic
TMH-1	47.22	63.33	80	87.22		
(w/v)	0.3	3	30	300	0.38	Toxic
TMH-2	49.49	67.76	63.91	73.29		
(w/v)	1	10	100	1000	1.5	Toxic
$K_2Cr_2O_7$	48.63	73.13	74.67	100		
(w/v)	1	10	100	1000	50>1000	Non-toxic
Caffeine	0	0	9.58	12.73		

The LD_{50}-values of pure compounds (TMH-1) and (TMH-2) were 0.26 and 0.38 µg/mL which were considered toxic. Reference standard potassium dichromate showed LD_{50}-value (1.5 µg/mL). No mortality was found in negative control (caffeine) group.

Antioxidant Activity of the Isolated Compound (TMH-1)

The radical scavenging activity of pure compound (TMH-1) was determined by using DPPH assay method. The result is shown in Table 3.

Table 3: Mean % Inhibition of Pure Compound (TMH-1) in Different Concentrations and Its IC_{50} Value

Sample (µg/mL)	Mean % Inhibition in different concentrations						IC_{50} (µg/mL)
TMH-1	**0.78**	**1.56**	**3.13**	**6.25**	**12.50**	**25.0**	1.06
	47.77	54.02	77.23	80.80	84.97	85.57	

Table 4: Mean % Inhibition of Standard Gallic Acid in Different Concentrations and Its IC_{50} Value

Sample (µg/mL)	Mean % Inhibition in different concentrations						IC_{50} (µg/mL)
	0.31	**0.63**	**1.25**	**2.50**	**5.00**	**10.00**	
Gallic acid	27.06	33.12	34.42	41.13	49.35	97.40	5.07

From these results, the lower IC_{50} value indicates the higher antioxidant activity. The pure compound (TMH-1) exhibited lower IC_{50} value (1.06 µg/mL) than the standard gallic acid (5.07µg/mL). Therefore, the pure compound (TMH-1) responds higher antioxidant activity than the standard gallic acid.

Conclusion

In this research work, one of the medicinal plants, *Andrographis paniculata* (Burn.f.)Wall. exNees which was collected from Monywa Township, Sagaing Region, was selected for chemical investigation of its endophytic fungus due to its interesting medicinal uses.

Endophytes from *A. paniculata* were cultivated on water-agar medium. Selection of the target fungus from pure isolated cultures was performed based on chemical screening. The fermentation on large scale for the selected fungus was performed on M_2 medium. The well-grown solid cultures were extracted with EtOAc. In addition, pure compounds (TMH-1) and (TMH-2) were isolated as yellow pigments from extracts by applying modern separation techniques such as thin layer and column chromatography.

Structure elucidation of pure compounds (TMH-1) and (TMH-2) were done by using different types of NMR experiments such as ^{1}H NMR, ^{13}C NMR, DEPT, DQF-COSY, HMQC, HMBC, NOESY and ESI MS respectively. The pure compounds (TMH-1) and (TMH-2) were elucidated as bis-naphtho-g-pyrones derivatives**.** Together with pure compounds, other secondary metabolite namely, ferulic acid was isolated from the extracts. According to the results of antimicrobial activity, the isolated pure compound (TMH-1) showed weak activity on five selected organisms such as *Bacillus subtilis, Pseudomononas aeruginosa, Bacillus pumilus, Candida albicans* and *E.coli* and (TMH-2) showed weak activity on all tested organisms. In brine shrimp cytotoxicity test, the LD_{50}-value of pure compounds (TMH-1) and

(TMH-2) were found to be 0.26 and 0.38 µg/mL respectively. Then, the antioxidant activity of pure compound (TMH-1) was evaluated by using DPPH radical scavenging assay. Pure compound (TMH-1) showed the antioxidant activity with IC_{50} values of 1.06µg/mL.

Acknowledgements

The authors would like to thank the Myanmar Academy of Art and Science for allowing to present this paper and Professor and Head Dr Than Than Win, Department of Chemistry, Monywa University for her kind encouragement.

References

Bano, N., Rizvi, I. F., Sharma, N., Siddiqui, M. H., Khan, M.K.A. and Akhtar, S.(2016). "Production of Bioactive Secondary Metabolites from Endophytic Fungi". *International Research Journal of Engineering and Technology*, vol 3(6), pp. 1859-1866

De, K. K. (1997).An Introduction to*Plant Tissue Culture* (Repr.). Calcutta:, New Central Book Agency (P) Ltd., pp. 1-18

Huang, W.Y., Cai, Y-Z., Xing, J., Corke, H. and Sun, M. (2007)**. "**A Potential Antioxidant Resource: Endophytic Fungi from Medicinal Plants". *Economic Botany*, vol 61 (1), pp. 14-30

Kress, J.W., De Filipps, A.R., Farr, E. and Kyi, Y.Y.(2003)."*A Checklist of the Trees, Shrubs, Herbs, and Climbers of Myanmar*". Smithsonian Washington, vol 45, pp. 125

Larran, S., Perello, A., Simon, M.R. and Moreno, V. (2002)."Isolation and Analysis of Endophytic Microorganisms in Wheat (*Triticumaestivum* L.)Leaves". *World Journal of Microbiology*, vol. 18, pp. 683-686

Marinova, G. and Batchvarov, V. (2011)."Evaluation of the Methods for Determination of the Free Radical Scavenging Activity by DPPH". *Bulgarian Journal of Agricultural Science*, vol. 17, pp. 11–24

Pimentel, M. R., Molina, G., Dionisio, A. P., Marostica, M. R. Jr. and Pastore, G. M. (2011)**."**The Use of Endophytes to Obtain Bioactive Compounds and Their Application in Biotransformation Process". *Biotechnology Research International*, vol. 2011, pp. 1-11

Radu, S. and Kqueen, C. Y. (2002)."Preliminary Screening of Endophytic Fungi from Medicinal Plants in Malaysia for Antimicrobial and Antitumor Activity".*Malaysian Journal of Medical Science*, vol. 9(2), pp. 23-33

Simpson, B. B. and Ogorzaly.M.C. (1995).*Economic Botany: Plants in Our World*. New York: 2nd Ed., McGraw-Hill, p. 2

Singh, R., Singh, D., Rathod, V., Naaz, S.A., Kumar, A., Siddique, S. and Kainath, D.(2015)."Phytochemical Analysis and Antibacterial Studies of the Crude Extracts of Endophytic Fungi, *Colletotrichum* sp. and *Alternaria* sp. from the Medicinal Plant *Tridaxprocumbens* (L.)".*International Journal of Natural Products Research*.vol. 5(3), pp. 27-33

Win, H.Y. (2009). "Bioactive Mandalarpyrones, Their Derivatives and Further Novel Secondary Metabolites from Marine and Terrestrial Bacteria". PhD Dissertation, Göttingen, Germany.